THE BOOK WAS DRENCHED

TIGHT BINDING BOOK

UNIVERSAL
LIBRARY
OU_166695
UNIVERSAL
LIBRARY

OSMANIA UNIVERSITY LIBRARY

Call No. 532.8 L29F Accession No. 31928

Author Lapple, C.E.

Title Fluid and Particle mechanics

This book should be returned on or before the date last marked below.

FLUID AND PARTICLE MECHANICS

by

C. E. Lapple

With the assistance of G. E. Alves, O. P. Bergelin, D. F. Boucher, H. L. Bunker, M. G. Kershaw, M. S. Maleson and R. D. Morse

Based on a Graduate Chemical
Engineering Course given at the
University of Delaware

Published by
University of Delaware
Newark, Delaware
March, 1951

Lithoprinted in U.S.A.
EDWARDS BROTHERS, INC.
ANN ARBOR, MICHIGAN
1951

PREFACE

It is the aim of this publication to provide industrial and academic organizations with a readily usable critical review of recent developments in the field of Fluid and Particle Mechanics as they pertain to applications in the chemical industry. Progress during the past ten years has been extremely rapid. This is evidenced by the greatly accelerated pace of publication and by the pioneering of phases which heretofore had received but scant attention. Progress has indeed been so rapid that the practicing engineer has not had the time to usefully assimilate the results of the developments, because of their diversity and scatter in the literature.

In order to provide students and engineers in the Wilmington-Philadelphia area with a co-ordinated review of these developments and to stimulate their application in practice, the University of Delaware sponsored an extension course in Fluid Mechanics in the spring of 1948. The lectures were prepared and given by specialists from local industry, who were chosen for their experience and intimate familiarity with specific aspects of fluid and particle mechanics in the chemical industry. The course dealt with special topics, which are of great or growing importance in the chemical industry and which are not adequately covered elsewhere. Although fundamental and theoretical background information was presented, this was done only to the extent deemed necessary for a thorough understanding of the methods and limitations of application. Insofar as possible, the emphasis was on the presentation of a clear, concise, and critical review of available knowledge that could be utilized directly in industrial applications. Because of the vastness of the field and the limited time available, the entire field could not receive coverage. The topics included were determined by their relative industrial importance, as well as by the availability of qualified lecturers. In order to provide those taking the course with a permanent record for reference, detailed mimeographed notes were prepared and distributed by each lecturer. These were prepared as a comprehensive but concise summary of available information, with sufficient selected reference material to permit an individual to conduct an extensive study of a given topic should the need arise.

Because of the excellent reception of the course and the large number of requests for additional copies of the lecture notes, the University of Delaware has issued this Bulletin in order to make the information presented in the lectures more generally available. While the material represents a review of published material to a great extent, the co-ordination and interpretation of the results is in many cases novel, reflecting intuitive insight that comes with many years of specialized background and experience and with knowledge of unpublished information.

It is our sincere hope that this publication will serve its immediate function as an aid to industry in summarizing recent developments in a usable form and that it will act as a guide and stimulus for further work in academic and industrial research organizations. It is also our hope that this publication will find extensive use in graduate courses as a means for bridging the proverbial academic-industrial gap and thereby further one of the ends of professional education. To facilitate its classroom function in this respect, problems typical of those encountered in practice have been addended to each chapter.

Wilmington, Delaware
June, 1950

C. E. Lapple

TABLE OF CONTENTS

		Page
Chapter 1.	"Mass, Energy, and Momentum Balance"— D. F. Boucher	1
Chapter 2.	"Outline of Turbulence Theory and Boundary Layer Equations"—G. E. Alves	17
Chapter 3.	"Velocity Head Concept in Pressure Drop Calculations"— C. E. Lapple	29
Chapter 4.	"Flow of Compressible Fluids"—C. E. Lapple	51
Chapter 5.	"Ejector Design and Performance"—G. E. Alves	69
Chapter 6.	"Two-Phase Flow in Pipes"—G. E. Alves	95
Chapter 7.	"Non-Newtonian Flow"—G. E. Alves	115
Chapter 8.	"Fluid Metering"—D. F. Boucher	135
Chapter 9.	"Pipe Line Design"—H. L. Bunker	161
Chapter 10.	"Pumps"—M. S. Maleson	185
Chapter 11.	"Ventilation"—M. G. Kershaw	223
Chapter 12.	"Particle Technology"—C. E. Lapple	267
Chapter 13.	"Particle Dynamics"—C. E. Lapple	277
Chapter 14.	"Dust and Mist Collection"—C. E. Lapple	295
Chapter 15.	"Fixed and Fluidized Beds of Granular Materials"—R. D. Morse	325

Errata to "FLUID AND PARTICLE MECHANICS"
by C. E. Lapple et al.

31923

Chapter 1

MASS, ENERGY, AND MOMENTUM BALANCE

by

Donald F. Boucher
Engineering Research Laboratory
Engineering Department
E. I. du Pont de Nemours & Co., Inc.
Wilmington, Delaware

TABLE OF CONTENTS

		Page
I.	References	3
II.	Nomenclature	3
III.	Introduction	4
IV.	Equation of Continuity	5
V.	Energy Balance	5
	A. Over-All Energy Balance	5
	B. Mechanical Energy Balance	6
	C. System Pressure Drop Evaluation	7
	D. Example of Application of Mechanical Energy Balance	7
VI.	Momentum Balance	8
	A. Theory	8
	1. Conservation of Momentum	8
	2. Impulse and Momentum Equations	8
	B. Application	9
	1. Jet Impact	9
	2. Jet Deflected By a Fixed Surface	9
	3. Jet Deflected By a Moving Surface	9
	4. Jet Deflected By a Series of Moving Vanes	10
	5. Ejector Performance	11
	6. Abrupt Expansion	11
	7. Orifice Permanent Pressure Loss	12
	a. Special case for $A_1 = A_4$	13
	b. Special case for $A_2 = A_4$	13
	8. Flow in a Pipe	14
	a. Special case for straight circular pipe picking up fluid uniformly along its length	14
	b. Special case for straight circular pipe losing fluid uniformly along its length	15
	c. Special case for flow of a condensing vapor in straight circular pipe	15
VII.	Problems	16

LIST OF FIGURES

Page

Figure 1. Schematic Layout For Mechanical Energy Balance Example 7
Figure 2. Jet Impacting On a Stationary Flat Plate 9
Figure 3. Jet Deflected By a Fixed Surface 9
Figure 4. Jet Deflected By a Moving Surface 10
Figure 5. Draft-Tube Ejector 11
Figure 6. Abrupt Expansion 11
Figure 7. Flow Through An Orifice 12
Figure 8. Flow in An Inclined Pipe 14
Figure 9. Problem 1 16

I. REFERENCES

A. Energy Balance

1. Dodge, B. F., "Chemical Engineering Thermodynamics," 1st ed., New York, McGraw-Hill Book Co., 1944, pp. 308-14.
2. Dodge, R. A., and Thompson, M. J., "Fluid Mechanics," 1st ed., New York, McGraw-Hill Book Co., 1937, pp. 73-103.
3. McAdams, W. H., "Heat Transmission," 2nd ed., New York, McGraw-Hill Book Co., 1942, pp. 111-17.
4. O'Brien, M. P., and Hickox, G. H., "Applied Fluid Mechanics," 1st ed., New York, McGraw-Hill Book Co., 1937, pp. 39-57.
5. Perry, J. H., "Chemical Engineers' Handbook," 3rd ed., New York, McGraw-Hill Book Co., 1950, pp. 375-7.
6. Stodola, A., "Steam and Gas Turbines," 6th ed., Vol. 1, New York, McGraw-Hill Book Co., 1927, pp. 36-55.
7. Vennard, J. K., "Elementary Fluid Mechanics," 1st ed., New York, John Wiley and Sons, Inc., 1940, pp. 55-77.
8. Walker, W. H., Lewis, W. K., McAdams, W. H., and Gilliland, F. R., "Principles of Chemical Engineering," 3rd ed., New York, McGraw-Hill Book Co., 1937, pp. 41-8.

B. Momentum Balance

9. Dodge, R. A., and Thompson, M. J., "Fluid Mechanics," 1st ed., New York, McGraw-Hill Book Co., 1937, pp. 108-26.
10. O'Brien, M. P., and Hickox, G. H., "Applied Fluid Mechanics," 1st ed., New York, McGraw-Hill Book Co., 1937, pp. 57-82.
11. Vennard, J. K., "Elementary Fluid Mechanics," 1st ed., New York, John Wiley and Sons, Inc., 1940, pp. 77-92.

II. NOMENCLATURE

Any consistent set of units may be employed. English units are given here by way of illustration.

a = acceleration, ft./(sec.)^2

A = inside cross-sectional area of pipe, sq.ft.

b = perimeter, ft.

c_v = specific heat at constant volume, B.t.u./lb.

c_p = specific heat at constant pressure, B.t.u./lb.

C_c = contraction coefficient, dimensionless

C_v = velocity coefficient, dimensionless

d = differential operator, dimensionless

D = inside diameter, ft.

E_f = friction loss, (ft.)(lb.force)/lb.

f = friction factor, dimensionless

F = force, lb.force.

g_c = conversion factor, 32.17 (ft.)(lb.)/(lb.force)(sec.)^2

g_L = local acceleration due to gravity, ft./(sec.)^2

G = mass velocity, lb./(sec.)(sq.ft.)

h = enthalpy, B.t.u./lb.

J = conversion factor, 778 (ft.)(lb.force)/B.t.u.

k = ratio of specific heats, c_p/c_v, dimensionless

L = length, ft.

m = mass, lb.

M = molecular weight, dimensionless

p = pressure, lb.force/sq.ft.

P = power, (ft.)(lb.force)/sec.

q = volumetric flow rate, cu.ft./sec.

Q = heat supplied to system by surroundings, B.t.u./lb.

R = gas constant, 1546 (ft.)(lb.force)/(°R)(lb.mol)

S = entropy, B.t.u./(°R)(lb.)

t = time, sec.

T = absolute temperature, °R = °F + 460

u = internal energy, B.t.u./lb.

v = specific volume, cu.ft./lb.

V = linear velocity, ft./sec. (in a conduit, it is the average velocity, q/A)

w = flow rate, lb./sec.

W = work done on the system by the surroundings, (ft.)(lb.force)/lb.

W_e = work delivered by an external source such as a fan or pump, (ft.)(lb.force)/lb.

z = fraction condensed, dimensionless

Z = elevation, ft.

α = area ratio (always less than one), dimensionless

ρ = fluid density, lb./cu.ft.

τ = wall traction, lb.force/sq.ft.

Subscripts

1	corresponding to point 1
2	corresponding to point 2
3	corresponding to point 3
4	corresponding to point 4
a	refers to fluid entering through side walls of pipe
av	average
g	refers to vapor or gas flow
m	mixed fluids
max	maximum
M	of mass M
N	of mass N
opt.	optimum
p	primary fluid
r	relative
s	secondary fluid
v	of the moving vane
x	component in x direction
y	component in y direction

III. INTRODUCTION

A mass, energy, or momentum balance can be written across any given section of a fluid system. The mass balance, better known in fluid mechanics as the equation of continuity, has as its basis the well known law of conservation of mass. The energy balance in fluid mechanics is based on the first law of thermodynamics or the law of conservation of energy. The momentum balance in fluid mechanics is based on the well known Newton's law of motion.

IV. EQUATION OF CONTINUITY

Consider an item of equipment or a fluid stream whose boundaries are so constituted that there is no net flow across them. Under steady conditions of flow there will be no accumulation or depletion of fluid between any two sections of the apparatus and the mass flow rate across each section is thus constant. This is expressed by

$$w_1 = w_2 = \text{constant} \tag{1}$$

$$\text{or } \rho_1 V_1 A_1 = \rho_2 V_2 A_2 = \text{constant} \tag{2}$$

V. ENERGY BALANCE

A. Over-All Energy Balance

Consider the flow of a unit weight (1 lb.) of fluid in a system. The potential energy relative to a chosen reference level is Zg_L/g_C ft.-lb. force/lb. and the kinetic energy is $V^2/2g_C$ ft.-lb.force/lb. The total energy of the pound of fluid is $(Ju + Zg_L/g_C + V^2/2g_C)$ft.-lb.force/lb. For the steady flow of the fluid there will be no accumulation or depletion of fluid within the system and the total energy of the system can be altered only by permitting heat to flow into or out of the system or by having external work done on or by the system. This energy balance may be written in a differential form as follows:

$$Jdu + (g_L/g_C)dZ + d(V^2/2g_C) = JdQ + dW \tag{3}$$

The term W, which is the work done on the system by the surroundings, may be broken down into

$$dW = -d(pv) + dW_e \tag{4}$$

Where W_e is work delivered by external sources, such as a fan or pump. Combining equations 3 and 4 gives

$$Jdu + (g_L/g_C)dZ + d(V^2/2g_C) + d(pv) = JdQ + dW_e \tag{5}$$

The term g_L is the local acceleration due to gravity and has the dimensions ft./(sec.)^2, while the term g_C is a conversion factor equal to 32.17 ft.-lb./(lb.force)(sec.)^2. Thus, at normal elevations the ratio g_L/g_C is close to unity numerically but not dimensionally. For simplicity this ratio will be omitted in subsequent equations.

Equation 5 in the integrated form is

$$Ju_1 + Z_1 + p_1v_1 + V_1^2/2g_C + JQ + W_e = Ju_2 + Z_2 + p_2v_2 + V_2^2/2g_C \tag{6}$$

This expression is generally known as the over-all energy balance form of Bernoulli's theorem. It is to be noted that no friction term appears in this expression, inasmuch as friction, while it represents the conversion of mechanical energy into heat, does not change the over-all energy content of the system.

The kinetic energy terms in the foregoing equations apply strictly only for a uniform velocity across a given cross section. For turbulent flow in circular pipes, this term is 3-8% too low, while for streamline flow in circular pipes, the proper kinetic energy term is V^2/g_C which makes due allowance for the parabolic velocity distribution. For further details on velocity distribution, see Miller, B., Chem. and Met. Eng., 50, 90-1 (1943) Jan.

The relation between enthalpy and internal energy is given by

$$Jdh = Jdu + d(pv) \tag{7}$$

Substituting this into equation 5 and integrating gives

$$J(h_1 - h_2) + (Z_1 - Z_2) + JQ + W_e = (V_2^2 - V_1^2)/2g_C \tag{8}$$

This form is convenient for use with steam or other fluids for which the thermal properties are tabulated or calculable. One example is the adiabatic, ~~frictionless~~ flow of a gas through a nozzle, in which case equation 8 reduces to

$$J(h_1 - h_2) = (V_2^2 - V_1^2)/2g_c \tag{9}$$

where subscript 1 refers to conditions upstream from the nozzle and subscript 2 refers to conditions at the discharge of the nozzle. For a perfect gas

$$J(h_1 - h_2) = J\int_2^1 c_p dT = J(c_p)_{av}(T_1 - T_2) = \frac{k}{k-1}(p_1v_1 - p_2v_2) \tag{10}$$

Another example is the use of the throttling calorimeter in the determination of steam quality. For this case equation 8 reduces to

$$J(h_1 - h_2) + V_1^2/2g_c = 0 \tag{11}$$

where subscript 1 refers to conditions upstream from the throttling valve and subscript 2 refers to conditions in the calorimeter after throttling, where V_2 is considered to be zero. Further, the velocity V_1, ahead of the point of throttling, is generally small enough so that the term $V_1^2/2g_c$ is negligible compared to the enthalpy change, whereupon equation 11 reduces to $h_1 = h_2$. Thus, a temperature measurement within the calorimeter is all that is needed to determine the enthalpy of the steam before throttling. This value, together with the initial pressure, will enable the determination of the initial quality.

B. Mechanical Energy Balance

The internal energy of a pound of fluid is given by the following expression

$$Jdu = JTdS - pdv \tag{12}$$

Other forms of energy such as electrical and surface energy should be included in the right hand side of the equation but will be assumed to undergo no change and will be neglected in this presentation. The presence of friction loss renders the process irreversible, whence–

$$JTdS = JdQ + dE_f \tag{13}$$

Combining equations 5, 12, and 13 gives

$$dZ + d(V^2/2g_c) + d(pv) - pdv + dE_f = dW_e \tag{14}$$

$$dZ + d(V^2/2g_c) + vdp + dE_f = dW_e \tag{15}$$

The integrated form of equation 15 is

$$Z_1 + V_1^2/2g_c - \int_1^2 vdp - E_f + W_e = Z_2 + V_2^2/2g_c \tag{16}$$

Equation 16 is known as the mechanical energy form of Bernoulli's theorem. For liquids the integral $\int_1^2 vdp$ becomes simply $v(p_2 - p_1)$ where v is substantially constant. For gases, the exact value of the integral depends upon the path followed by the expansion. For isothermal flow of a perfect gas

$$\int_1^2 vdp = -(RT/M)\ \ln(v_2/v_1) = -(RT/M)\ \ln(p_1/p_2) \tag{17}$$

For most other cases, $(p_1 - p_2)v_{av.}$ may be used with an error no greater than the probable error in the friction factor for pressure ratios, p_2/p_1, as low as 1/2; where $v_{av.}$ is the arithmetic mean of the initial and final specific volumes. Note that $v_{av.}$ is equal to $(1/\rho)_{av.}$ but is not equal to $1/\rho_{av.}$

∴ The equation applies regardless of

p. 6, line 2: remove the word "frictionless". The equation applies regardless of whether or not the process involves friction. The magnitude of the friction simply determines the path taken or the final velocity and enthalpy relative to the initial.

C. System Pressure Drop Evaluation

There is a real distinction between pressure drop and friction loss. Pressure drop represents a conversion of pressure energy into any other form of energy, whereas friction loss represents a net loss in the total available work energy of the fluid. The two terms are related by equation 16. They are equal only for the flow of an incompressible fluid where the cross-sectional area and the elevation of the conducting equipment remain unchanged.

There are two methods of evaluating the over-all pressure drop for a system having a number of resistances in series. The first method involves the calculation of the pressure drop for each individual resistance with due regard for algebraic sign and then summing up all such items for the entire system. The second method involves the calculation of friction loss for each individual resistance, summing up all such items, and applying equation 16 to obtain the over all pressure drop. The pressure drop summation should be used in systems involving branching lines (combining or dividing flows). Also in the case of flow of compressible fluids at large pressure drops it is more convenient to employ the compressible flow equations which are set-up to give pressure drop directly (see C. E. Lapple, Trans. Am. Inst. Chem. Engrs., 39, 385-432 (1943)).

For liquids and for gases at low pressure drop, it is generally simpler to employ the friction loss summation since only the terminal values of elevation and kinetic energy need be considered and Bernoulli's theorem need only be used once. With the pressure drop summation, Bernoulli's theorem has to be used with each of the individual friction losses to give the individual pressure drops.

D. Example of Application of Mechanical Energy Balance

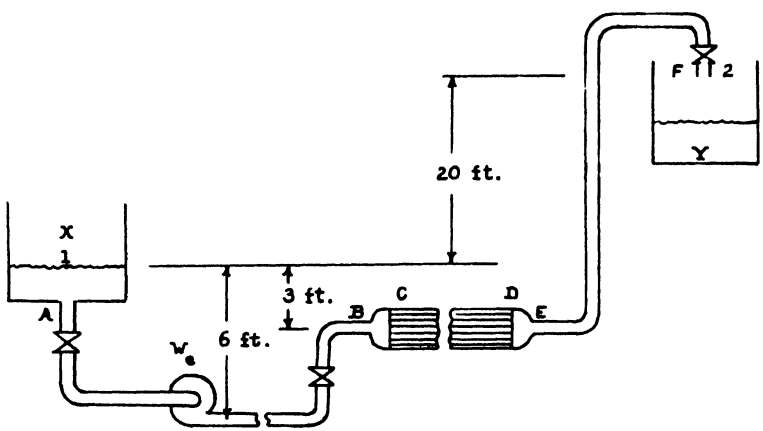


Figure 1. Schematic Layout for Mechanical Energy Balance Example

A centrifugal pump, W_e, is withdrawing a liquid from tank X, forcing it through a heat exchanger, and elevating it to tank Y. Find the maximum head to be supplied by the pump if the level in tank X never falls below point 1.

Given:

Velocity in lines AB and EF	= 3 ft./sec.
Velocity in heat exchanger tubes (CD)	= 4 ft./sec.
Contraction loss at A	= 0.07 ft. of fluid
Pipe-line friction for line AB	= 2.00
Expansion loss at B	= 0.14
Contraction loss at C	= 0.12
Friction loss in tubes CD	= 1.50
Expansion loss at D	= 0.25
Contraction loss at E	= 0.07
Pipe-line friction, line EF	= 1.50
	E_f = 5.65 ft. of fluid

Solution:

The head developed by the pump can be calculated using a friction loss summation and the mechanical energy form of Bernoulli's theorem as given by equation 16.

$$Z_1 + V_1^2/2g_c + p_1v - E_f + W_e = Z_2 + V_2^2/2g_c + p_2v$$

$V_1 = 0$, $p_1 = p_2 = 1$ atm., let $Z_1 = 0$ (reference plane)

Equation 16 then reduces to

$$-E_f + W_e = Z_2 + V_2^2/2g_c$$

$$W_e = 20 + (3)^2/64.4 + 5.65 = 25.8 \text{ ft. of fluid.}$$

The above problem illustrates the use of the friction loss summation. The use of a pressure drop summation would have been more time consuming since equation 16 would have had to be applied to each individual resistance.

VI. MOMENTUM BALANCE

A. Theory

1. Conservation of Momentum.

The total momentum within a system is unchanged by an exchange of momentum between two or more masses of the system. This is known as the principle of conservation of momentum and is illustrated mathematically as follows for the simple case of two bodies M and N, moving in the same direction, which collide or mix and then move together in the same direction as before with a common velocity V, after impact or mixing–

$$m_M V_M/g_c + m_N V_N/g_c = (m_M + m_N)\ V/g_c \tag{18}$$

The transfer of momentum in this case is accompanied by a loss in kinetic energy.

2. Impulse and Momentum Equations.

Newton's law of motion may be written thus –

$$F = \frac{m}{g_c} a = \frac{m}{g_c} \frac{dV}{dt} \tag{19}$$

For a body whose mass is constant –

$$F\Delta t = \frac{m}{g_c} \Delta V \tag{20}$$

This means that a force, F, acting on a body of mass m, over a time interval, Δt, will change its velocity by an amount ΔV. F and ΔV are vector quantities and must act in the same direction when defined by the above equation. The product $F\Delta t$ is known as the impulse of the force.

The equations of momentum are also readily applied to problems dealing with flowing fluids. In this case –

$$m = w\Delta t \tag{21}$$

and equation 20 becomes

$$F = w\Delta V/g_c = \rho q \Delta V/g_c \tag{22}$$

Where the fluid changes direction while under the action of a force, F, the equation can be written as above resolving the force and velocity change into components as follows:

$$F_x = w\Delta V_x/g_c \tag{23}$$

$$F_y = w\Delta V_y/g_c \tag{24}$$

$$F^2 = F_x^2 + F_y^2 \tag{25}$$

$$(\Delta V)^2 = (\Delta V_x)^2 + (\Delta V_y)^2 \tag{26}$$

where x and y represent reference axes at right angles.

B. Application

1. Jet Impact.

Consider an open jet impinging at right angles upon a stationary flat plate as shown in Figure 2. The force exerted by the fluid on the plate is designated as (-F), equal to but opposite in direction to the force exerted on the fluid. From equation 23 —

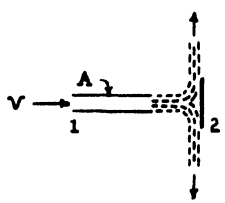


Figure 2. Jet Impacting on a Stationary Flat Plate

$$-F_x = -w\Delta V_x/g_c = -w(V_2 - V_1)_x/g_c \tag{27}$$

since $(V_2)_x = 0$

$$-F_x = wV_1/g_c = A\rho V_1^2/g_c \tag{28}$$

2. Jet Deflected By A Fixed Surface.

Consider an open jet which is deflected from its course by a fixed curved surface as shown in Figure 3. If it is assumed that the jet is tangent to the surface at the point of first contact so that there is no loss in shock and also that there is no friction loss and therefore no reduction in velocity ($V_2 = V_1$), the forces can be computed from the momentum equations. Thus it is assumed that the velocity is changed in direction only, the jet being deflected through an angle θ.

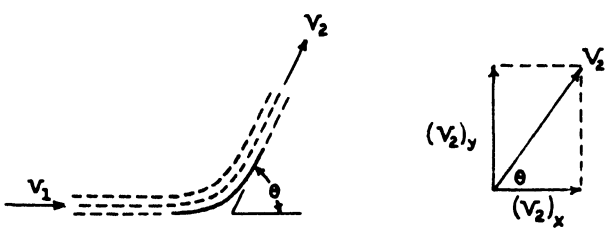


Figure 3. Jet Deflected by a Fixed Surface.

$$-F_x = w(V_1 - V_2)_x/g_c \tag{29}$$

$$(V_1)_x = V_1;\ \text{and}\ (V_2)_x = V_1 \cos\theta \tag{30}$$

$$-F_x = wV_1(1 - \cos\theta)/g_c \tag{31}$$

$$-F_y = w(V_1 - V_2)_y/g_c \tag{32}$$

$$(V_1)_y = 0;\ \text{and}\ (V_2)_y = V_1 \sin\theta \tag{33}$$

$$-F_y = -wV_1 \sin\theta/g_c \tag{34}$$

3. Jet Deflected By a Moving Surface.

Consider an open jet deflected from its course by a curved surface or vane under the same conditions as the preceding example except that the vane is moving with a velocity V_v in the same direction as the jet (see Figure 4). The jet fluid overtakes the moving vane with a relative velocity of

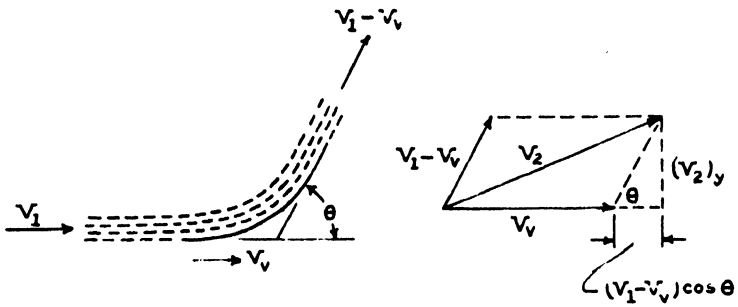


Figure 4. Jet Deflected by a Moving Surface

$V_1 - V_V$. The absolute velocity of the jet leaving the vane is the vector sum of its velocity relative to the vane and the velocity of the vane, as shown in the diagram. From the geometry of the figure, the components of V_2 are determined to be

$$(V_2)_x = V_V + (V_1 - V_V)\cos\theta \tag{35}$$

$$(V_2)_y = (V_1 - V_V)\sin\theta \tag{36}$$

Because of the motion of the vane, the rate at which the jet overtakes the vane, w_r, is less than the discharge rate of the jet. The relation between the two is given by the following—

$$w_r = w(V_1 - V_V)/V_1 \tag{37}$$

The forces acting on the moving vane can then be calculated from the momentum equations using the relative flow rate, w_r.

$$-F_x = w_r(V_1 - V_2)_x/g_c \tag{38}$$

$$-F_x = w_r(V_1 - \left[V_V + (V_1 - V_V)\cos\theta\right])/g_c \tag{39}$$

$$-F_x = \frac{w}{g_c}\frac{(V_1 - V_V)^2}{V_1}(1 - \cos\theta) \tag{40}$$

$$-F_y = w_r(V_1 - V_2)_y/g_c \tag{41}$$

$$-F_y = w_r(0 - \left[(V_1 - V_V)\sin\theta\right])/g_c \tag{42}$$

$$-F_y = -\frac{w}{g_c}\frac{(V_1 - V_V)^2}{V_1}\sin\theta \tag{43}$$

4. Jet Deflected By a Series of Moving Vanes.

In a closely spaced series of moving vanes of the above type, such as occurs in an impulse water turbine, all the fluid flowing is deflected by the vanes or blades and $w_r = w$. Thus the force exerted on the blades in the direction of motion may be calculated from

$$-F_x = w(V_1 - V_V)(1 - \cos\theta)/g_c \tag{44}$$

The power transferred from the jet to the blades is given by

$$P = (-F_x)V_V = wV_V(V_1 - V_V)(1 - \cos\theta)/g_c \tag{45}$$

The optimum velocity, $(V_V)_{opt.}$, can be determined by differentiating equation 45 with respect to V_V and setting the resultant expression equal to zero. This yields $(V_V)_{opt.} = V_1/2$. Combining this with equation 45 yields —

$$P = wV_1^2(1 - \cos\theta)/4g_c \tag{46}$$

For $\theta = 180°$

$$P_{max} = wV_1^2/2g_c \tag{47}$$

which is just equal to the power available in the jet.

5. Ejector Performance.
Consider the equipment shown schematically in Figure 5, known as the draft-tube ejector, in

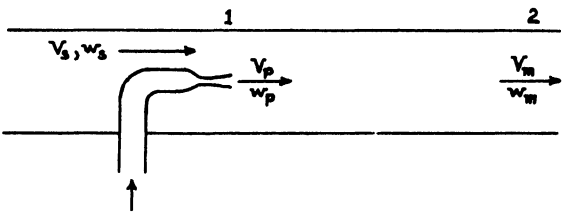


Figure 5. Draft-Tube Ejector

which a primary, high-velocity fluid enters at point 1 and mixes with a secondary fluid. The mixing is complete at point 2. A momentum balance yields:

$$F_p = w_p(V_{2m} - V_{1p})/g_c \tag{48}$$

$$F_S = w_S(V_{2m} - V_{1S})/g_c \tag{49}$$

$$F = F_p + F_S = \left[w_p(V_{2m} - V_{1p}) + w_S(V_{2m} - V_{1S})\right]/g_c \tag{50}$$

where F_p is the effective force acting on the primary fluid between points 1 and 2, F_S is the force acting on the secondary fluid between points 1 and 2, and F is the force acting on both streams. This force must be the result of a pressure difference between points 1 and 2, thus

$$F = (p_1 - p_2)\,A \tag{51}$$

Combining equations 50 and 51

$$g_c(p_1 - p_2)A = w_p(V_{2m} - V_{1p}) + w_S(V_{2m} - V_{1S}) \tag{52}$$

$$\text{or } g_c(p_2 - p_1)A = w_p(V_{1p} - V_{2m}) + w_S(V_{1S} - V_{2m}) \tag{53}$$

Thus $(p_2 - p_1)$ represents the pressure developed in the secondary fluid by the action of the primary jet.

6. Abrupt Expansion.
The pressure rise for an abrupt expansion as shown in Figure 6 can be calculated from a

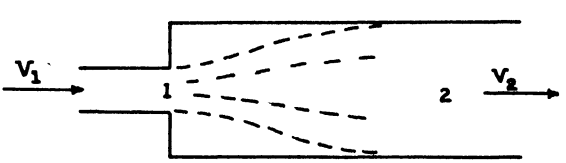


Figure 6. Abrupt Expansion

momentum balance using equation 23 as follows, assuming constant density:

$$F = (p_1 - p_2)A_2 = w(V_2 - V_1)/g_c \tag{54}$$

$$w = \rho V_2 A_2 \qquad V_2 = \alpha V_1 \tag{55}$$

$$(p_2 - p_1) = \rho V_1^2 \alpha(1 - \alpha)/g_c \tag{56}$$

The friction loss can be obtained by introducing the mechanical energy form of Bernoulli's theorem as follows (constant Z)

$$\frac{p_1}{\rho} + \frac{V_1^2}{2g_c} = \frac{p_2}{\rho} + \frac{V_2^2}{2g_c} + E_f \tag{57}$$

$$E_f = \frac{(p_1 - p_2)}{\rho} + \frac{V_1^2}{2g_c} - \frac{V_2^2}{2g_c} \tag{58}$$

$$E_f = \frac{V_2 A_2 (V_2 - V_1)}{g_c A_2} + \frac{V_1^2 - V_2^2}{2g_c} \tag{59}$$

$$E_f = \frac{2V_2^2 - 2V_1 V_2}{2g_c} + \frac{V_1^2 - V_2^2}{2g_c} \tag{60}$$

$$E_f = (V_1 - V_2)^2/2g_c \tag{61}$$

7. Orifice Permanent Pressure Loss.

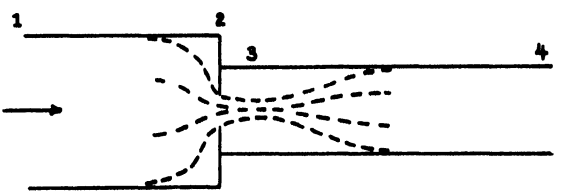


Figure 7. Flow Through an Orifice

Consider a fluid flowing from channel 1 through a restriction or orifice at 2, and reexpanding into channel 4 as shown. The stream, in passing from position 1 to position 4, increases in velocity and decreases in pressure. Position 3 represents the vena contracta or point of minimum cross section beyond which the stream again expands with an accompanying rise in pressure. Assuming no friction loss between points 1 and 3, an energy balance yields (for constant density and elevation)-

$$\frac{p_1}{\rho} + \frac{V_1^2}{2g_c} = \frac{p_3}{\rho} + \frac{V_3^2}{2g_c} \tag{62}$$

$$(\rho V_3^2/2g_c) = (p_1 - p_3) + (\rho V_1^2/2g_c) \tag{62a}$$

Actually a small loss occurs which can be allowed for by a velocity coefficient as follows -

$$(\rho V_3^2/2g_c) = C_V^2 \left[(p_1 - p_3) + (\rho V_1^2/2g_c) \right] \tag{63}$$

By definition the following relationships hold:

$$\alpha_1 A_1 = A_2 \tag{64}$$

$$\alpha_4 A_4 = A_2 \tag{64a}$$

$$C_C A_2 = A_3 \tag{64b}$$

It follows that for an incompressible fluid (constant ρ) -

$$V_1 = \alpha_1 V_2 \tag{65}$$

$$V_4 = \alpha_4 V_2 \tag{65a}$$

$$V_3 = V_2/C_C \tag{65b}$$

With the above conversions, equation 63 can be expressed in the following alternate forms

$$p_1 - p_3 = \left[(1/C_V^2C_C^2) - \alpha_1^2\right](\rho V_2^2/2g_C) \tag{66}$$

$$V_2 = \left[\frac{C_V C_C}{\sqrt{1 - \alpha_1^2 C_V^2 C_C^2}}\right]\sqrt{2g_C(p_1 - p_3)/\rho} \tag{66a}$$

$$w = A_2\left[\frac{C_V C_C}{\sqrt{1 - \alpha_1^2 C_C^2 C_V^2}}\right]\sqrt{2g_C(p_1 - p_3)\rho} \tag{66b}$$

Point 4 can be considered to be sufficiently far downstream so that the stream has expanded and filled the entire pipe cross section. Four pipe diameters downstream is usually sufficient. A momentum balance between points 3 and 4 can then be written as follows -

$$p_3 - p_4 = w(V_4 - V_3)/A_4 g_C \tag{67}$$

or

$$p_3 - p_4 = \rho V_2 A_2 (V_4 - V_3)/A_4 g_C \tag{67a}$$

Combining equations 65a, 65b, and 67a yields

$$p_4 - p_3 = (2\alpha_4 - 2\alpha_4^2 C_C)(1/C_C)(\rho V_2^2/2g_C) \tag{68}$$

Combining equations 66 and 68 gives

$$p_1 - p_4 = (1 - \alpha_1^2 C_V^2 C_C^2 - 2\alpha_4 C_V^2 C_C + 2\alpha_4^2 C_V^2 C_C^2)(1/C_V^2 C_C^2)(\rho V_2^2/2g_C) \tag{69}$$

a. Special Case For $A_1 = A_4$. This is the usual case for a metering orifice assembly. Here $\alpha_1 = \alpha_4$ and equation 69 becomes -

$$p_1 - p_4 = (1 - 2\alpha_1 C_V^2 C_C + \alpha_1^2 C_V^2 C_C^2)(1/C_V^2 C_C^2)(\rho V_2^2/2g_C) \tag{70}$$

Dividing equation 70 by equation 72 gives -

$$(p_1 - p_4)/(p_1 - p_3) = (1 - 2\alpha_1 C_V^2 C_C + \alpha_1^2 C_V^2 C_C^2)/(1 - \alpha_1^2 C_V^2 C_C^2) \tag{71}$$

Since C_V is usually close to unity, equation 71 can be closely approximated by -

$$(p_1 - p_4)/(p_1 - p_3) = (1 - \alpha_1 C_V C_C)/(1 + \alpha_1 C_V C_C) \tag{72}$$

The ratio $(p_1 - p_4)/(p_1 - p_3)$ represents the permanent pressure loss across the orifice expressed as a fraction of the orifice pressure differential measured with vena contracta taps. Generally satisfactory values will be given by equation 72 if the usual orifice coefficient, C, see equation 10 in Chapter 8, is employed as follows -

$$(p_1 - p_4)/(p_1 - p_3) = (1 - \alpha_1 C)/(1 + \alpha_1 C) \tag{72a}$$

b. Special Case for $A_2 = A_4$. This case corresponds to an abrupt entrance to a pipe. Here $\alpha_4 = 1$ and equation 69 becomes -

$$p_1 - p_4 = (1 - \alpha_1^2 C_V^2 C_C^2 - 2C_V^2 C_C + 2C_V^2 C_C^2)(1/C_V^2 C_C^2)(\rho V_2^2/2g_C) \tag{73}$$

In the case where A_1 is large compared to A_2, $\alpha_1 = 0$, and equation 73 reduces to -

p. 13, line following Equation 70 - "equation 72" should be "equation 66".

$$p_1 - p_4 = (1 - 2C_V^2C_C + 2C_V^2C_C^2)(1/C_V^2C_C^2)(\rho V_2^2/2g_C) \tag{74}$$

Assuming the values $C_V = 0.98$ and $C_C = 0.62$ as averages based on available sharp-edged orifice data, equation 74 reduces to

$$p_1 - p_4 = 1.49(\rho V_2^2/2g_C) \tag{74a}$$

Thus the contraction friction loss for this case is about 0.5 velocity heads based on the velocity in the smaller cross section.

8. Flow In A Pipe

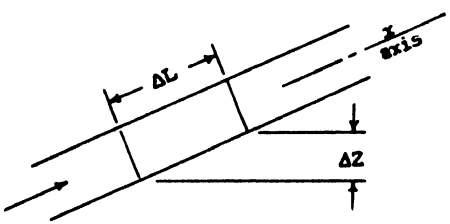


Figure 8. Flow in an Inclined Pipe

Consider an incremental length of pipe, ΔL, in which flow is taking place from left to right. It is more convenient in this case to sum up the forces acting in a left-to-right direction on the element (along the x-axis) and set the sum equal to zero.

The force in the left-to-right direction due to the accumulation of momentum in the element is given by

$$\frac{wV}{g_C} - \left[\frac{wV}{g_C} + \frac{d}{dL}\left(\frac{wV}{g_C}\right)\Delta L\right] = -\frac{d}{dL}\left(\frac{wV}{g_C}\right)\Delta L \tag{75}$$

The net force in the left-to-right direction due to a change in static pressure is given by

$$pA - \left(pA + \frac{d(pA)}{dL}\Delta L\right) = -\frac{d(pA)}{dL}\Delta L \tag{76}$$

The contribution due to a change in elevation is given by (omitting the ratio g_L/g_C)

$$\frac{A}{v}Z - \left(\frac{A}{v}Z + \frac{A}{v}\frac{dZ}{dL}\Delta L\right) = -\frac{A}{v}\frac{dZ}{dL}\Delta L \tag{77}$$

The traction on the wall has the effect of exerting a drag on the fluid which is a negative force in the left-to-right direction. For straight circular pipe

$$-\tau b\Delta L = -\frac{4fV^2A}{2g_CDv}\Delta L \tag{78}$$

Summing up the components given in equations 75, 76, 77, and 78

$$-\frac{d}{dL}\left(\frac{wV}{g_C}\right)\Delta L - \frac{d(pA)}{dL}\Delta L - \frac{A}{v}\frac{dZ}{dL}\Delta L - \frac{4fV^2A}{2g_CDv}\Delta L = 0 \tag{79}$$

Since $V = wv/A$, equation 79 becomes

$$\frac{v}{g_CA^2}d(w^2v) + vdp + dZ + \frac{4fw^2v^2}{2g_CDA^2}dL = 0 \tag{80}$$

$$\text{or } \frac{d(V^2)}{2g_C} + vdp + dZ + \frac{4fV^2}{2g_CD}dL = 0 \tag{81}$$

Equation 81 can be recognized as the differential form of the mechanical energy balance.

a. Special Case For Straight Circular Pipe Picking Up Fluid Uniformly Along Its Length. If auxiliary fluid enters the pipe at right angles to the flow it can ordinarily bring in no x-momentum. Assume, as an approximation, that the wall traction can be given by the same form of relation as for ordinary straight pipe. If w_a is the rate per foot of length (lb./(sec.)(ft.)) for the additive fluid, then

$$dw = w_adL \tag{82}$$

Equation 80 can be written as

$$\frac{2vwdw}{g_cA^2} + \frac{w^2dv}{g_cA^2} + dp + \frac{dZ}{v} + \frac{4fvw^2}{2g_cDA^2}dL = 0 \tag{83}$$

Combining equations 82 and 83

$$\frac{2vwdw}{g_cA^2} + \frac{w^2dv}{g_cA^2} + dp + \frac{dZ}{v} + \frac{4fvw^2}{2g_cDA^2w_a}dw = 0 \tag{84}$$

For a liquid, the integration is easy since v is constant and dv = 0. This gives

$$p_1 - p_2 = \frac{v(w_2^2 - w_1^2)}{g_cA^2} + \frac{(Z_2 - Z_1)}{v} + \frac{1}{3}\left[\frac{4fv(w_2^3 - w_1^3)}{2g_cDA^2w_a}\right] \tag{85}$$

For the case where all the fluid has entered through the wall, $w_1 = 0$ and $w_2 = w_aL$, and equation 85 reduces to

$$p_1 - p_2 = \frac{(Z_2 - Z_1)}{v} + \frac{V_2^2}{2g_cv}\left[2 + \frac{1}{3}\left(\frac{4fL}{D}\right)\right] \tag{86}$$

b. Special Case For Straight Circular Pipe Losing Fluid Uniformly Along Its Length. Assume that the openings in the pipe wall are sufficiently small so the fluid leaving through the walls has to effectively turn through 90° before leaving. In so doing it gives up its x-momentum to the surrounding fluid before leaving and there is thus no loss in x-momentum from this source. For this case

$$dw = -w_a\,dL \tag{87}$$

Combining equations 87 and 80 and integrating, for the case of liquids (dv = 0), yields

$$p_1 - p_2 = \frac{v(w_2^2 - w_1^2)}{g_cA^2} + \frac{(Z_2 - Z_1)}{v} - \frac{1}{3}\left[\frac{4fv(w_2^3 - w_1^3)}{2g_cDA^2w_a}\right] \tag{88}$$

For the case where all the liquid entering the pipe escapes through the side wall, $w_2 = 0$ and $w_1 = w_aL$, and equation 88 reduces to

$$p_1 - p_2 = \frac{Z_2 - Z_1}{v} + \frac{V_1^2}{2g_cv}\left[\frac{1}{3}\left(\frac{4fL}{D}\right) - 2\right] \tag{89}$$

c. Special Case For Flow of Condensing Vapor In Straight Circular Pipe. Equation 80, developed for flow in a straight, circular pipe, can be applied to the flow of a vapor-condensate mixture provided we assume that the condensate is carried as a spray and the spray and vapor move together without relative motion. If condensation is occuring in the section under consideration then another term must be added to allow for the momentum lost by the vapor when it condenses on the wall, the wall thereby receiving a forward push. This condensate is next reentrained by the vapor and is accelerated to the vapor velocity thereby exerting a drag on the vapor. Letting w_g be the flow rate of vapor, we have

$$w_g = w(1 - z) \tag{90}$$

and since w is constant

$$dw_g = -wdz \tag{91}$$

The rate of condensation in the length ΔL is given by

$$-\frac{dw_g}{dL}\Delta L = w\frac{dz}{dL}\Delta L \tag{92}$$

The momentum loss from condensation therefore becomes

$$\frac{wV}{g_c}\frac{dz}{dL}\Delta L$$

Incorporating this term into equation 79 gives

$$-\frac{d}{dL}\left(\frac{wV}{g_c}\right)\Delta L - \frac{d(pA)}{dL}\Delta L - \frac{A\,dZ}{v\,dL}\Delta L - \frac{4fV^2A}{2g_cDv}\Delta L - \frac{wV\,dz}{g_c\,dL}\Delta L = 0 \tag{93}$$

Since V = wv/A, and since w is constant

$$\frac{w^2}{g_cA^2}\frac{dv}{dL} + \frac{dp}{dL} + \frac{1}{v}\frac{dZ}{dL} + \frac{4fw^2v}{2g_cDA^2} + \frac{w^2v\,dz}{g_cA^2\,dL} = 0 \tag{94}$$

or

$$-\frac{dp}{dL} = \frac{G^2dv}{g_cdL} + \frac{dZ}{v\,dL} + \frac{4fG^2v}{2g_cD} + \frac{G^2vdz}{g_cdL} \tag{95}$$

This expression can be solved by combination with a heat balance over a differential length of pipe, utilizing the properties of the fluid to express all dependent variables in the resulting equation in terms of pressure and fraction condensed, and finally carrying out a step-wise integration.

VII. PROBLEMS

Problem 1.

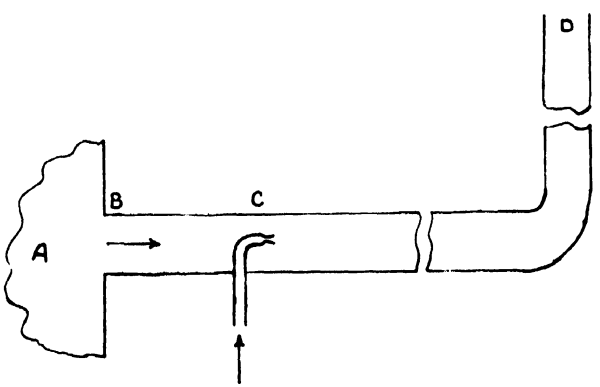


Figure 9. Problem Figure

Air at 70°F. is being exhausted from a hood (open to the atmosphere) at A through line BD to the atmosphere. Motive power is supplied by the draft-tube ejector at point C. The line is 4-in. i.d. There is an abrupt contraction at point B. Primary air is supplied to the ejector at 100 lb./sq.in. ga. It can be assumed that this primary air leaves the nozzle at a velocity (V_p) of 1680 ft./sec. Calculate the required primary air rate for the ejector in order to exhaust 250 cu.ft./min. (measured at 70°F. and 1 atm.) from the open hood. Neglect the pipe-line friction loss between B and C and assume it to be 2 velocity heads ($V_D^2/2g_c$) between C and D (including the bend). Assume that the gas temperature is the same before and after the ejector.

Problem 2. Prepare a plot of orifice permanent pressure drop, expressed as a fraction of the orifice differential pressure, versus the diameter ratio β. Assume a value of 0.61 for the usual orifice coefficient, C, for vena contracta taps. Compare with actual data as given on p. 404 of Reference 5.

Problem 3. Steam at 85 lb./sq.in. gage is checked for quality by expanding to one atmosphere in a throttling calorimeter. A temperature of 288°F. is obtained in the calorimeter. What velocity would theoretically be attained with this same 85 lb./sq.in. ga. steam expanding to one atmosphere through a De Laval nozzle. Assume frictionless, isentropic flow in the nozzle and neglect the approach velocity.

Problem 4. The cusped vanes on an impulse water wheel are curved through an arc of 160 degrees. The wheel is driven at its optimum speed by a 2-in. diameter jet of water having a velocity of 250 ft./sec. Compute the thrust on the vanes and the power developed.

Chapter 2

OUTLINE OF TURBULENCE THEORY AND BOUNDARY LAYER EQUATIONS

p. 17 - Author was George E. Alves.

by

Engineering Research Laboratory
Engineering Department
E. I. du Pont de Nemours & Co., Inc.
Wilmington, Delaware

TABLE OF CONTENTS

Page

I. References 18

II. Nomenclature 18

III. Outline of Turbulence Theory and Application to Flow in Pipes. 19

A. Theory 19

B. Application 22

1. Smooth Pipes 22
2. Rough Pipes 26

C. Notes 27

IV. Boundary Layer Equations for Flow over a Flat Plate 27

A. General 27

B. Laminar Boundary Layer 27

C. Turbulent Boundary Layer 28

V. Problems 28

LIST OF FIGURES

Figure 1. Velocity Profile 19
Figure 2. Velocity Profile (von Kármán) 21
Figure 3. Velocity Distribution Across a Pipe 24
Figure 4. Generalized Velocity Distribution Across a Pipe 26
Figure 5. Effect of Roughness on the Friction Factor 26
Figure 6. Flow over a Flat Plate 27

I. REFERENCES

1. Bakhmeteff, B. A., The Mechanics of Turbulent Flow, Princeton University Press, 1936.
2. Boelter, L. M. K., Martinelli, R. C., and Jonassen, Finn, "Remarks on the Analogy between Heat Transfer and Momentum Transfer," Trans. Amer. Soc. Mech. Engrs., 63, 447-455 (1941).
3. Goldstein, S., Modern Developments in Fluid Mechanics, (2 Vols.) Oxford Univ. Press, 1938.
4. O'Brien, M. P., and Hickox, G. H., Applied Fluid Mechanics, New York, McGraw-Hill Book Co., 1934.
5. Prandtl, L., "The Mechanics of Viscous Fluids," Vol. III, Durand, Aerodynamic Theory. Reprinted by Durand Reprinting Committee, Calif. Inst. of Tech., 1943.
6. Prandtl, L., and Tietjens, O. G., Applied Hydro- and Aero-Mechanics, New York, McGraw-Hill Book Co., 1934.
7. Rouse, H., Fluid Mechanics for Hydraulic Engineers, New York, McGraw-Hill Book Co., 1938.
8. Tetervin, Neal, "A Review of Boundary-Layer Literature," NACA Technical Note No. 1384, July 1947.
9. Vennard, J. K., Elementary Fluid Mechanics, 2nd Ed., New York, John Wiley & Sons, 1947.

II. NOMENCLATURE

b = width of plate, ft.

C = a constant

C_f = coefficient of skin friction, dimensionless

D_f = drag, lb.force

f = Fanning friction factor, dimensionless

g_c = conversion faction = $32.2 \left(\frac{\text{lb.}}{\text{lb.force}}\right) \left(\frac{\text{ft.}}{\text{sec.}^2}\right)$

k = turbulence universal constant

L = length of plate, ft.

L_M = a mixing length, ft.

L'_M = Prandtl's mixing length, ft.

N = a constant = y^+ for the intersection of the laminar film and turbulent core equations for u^+ and y^+.

N_{Re} = $\frac{u_{av.}\, 2r_o}{\nu}$, (for flow in pipes), or $\frac{u_o\, L \rho}{\mu}$, (in boundary layer equations)

= Reynolds number, dimensionless

r_o = inside radius of pipe, ft.

S = surface, sq.ft.

t = time, sec.

u = average velocity at a point, ft./sec.

$u_{av.}$ = average velocity across a section, ft./sec.

u_i = instantaneous velocity in the x direction, ft./sec.

$u_{max.}$ = maximum velocity, ft./sec.

u_w = velocity at edge of laminar layer, ft./sec.

u_o = free stream velocity, ft./sec.

u_* = $\sqrt{\frac{\tau_w g_c}{\rho}}$ = frictional velocity, ft./sec.

u' = instantaneous deviation from the average velocity, ft./sec.

u_1', u_2' = first derivative of velocity

u_1'', u_2'' = second derivative of velocity

$\bar{u}'$ = average instantaneous deviation from the average velocity, ft./sec.

$/\bar{u}'/$ = absolute value of the average instantaneous deviation from the average velocity, ft./sec.

$u^+ = \frac{u}{u_*}$ = dimensionless parameter

v_1 = instantaneous velocity in the y direction, ft./sec. Other velocities in y direction have same definitions as the corresponding velocity in the x direction.

y = distance from pipe wall, ft.

y_1 = distance to outer edge of laminar layer, ft.

y_2 = distance where turbulent core begins, ft.

$y^+ = \frac{u_* y}{\nu}$ = a dimensionless parameter

Z = a variable to assist in an integration

δ = thickness of boundary layer, ft.

δ_L = thickness of laminar layer, ft.

ϵ = characteristic dimension of roughness, ft.

μ = absolute viscosity, $\frac{\text{lb.}}{(\text{ft.})(\text{sec.})}$

μ_M = mechanical viscosity, $\frac{\text{lb.}}{(\text{ft.})(\text{sec.})}$

ν = kinematic viscosity, $\frac{\text{ft.}^2}{\text{sec.}}$

$= \frac{\mu}{\rho}$

ρ = density, $\frac{\text{lb.}}{\text{cu.ft.}}$

τ = tractive force per unit area, $\frac{\text{lb.force}}{\text{sq.ft.}}$

τ_w = tractive force per unit area at pipe wall, $\frac{\text{lb.force}}{\text{sq.ft.}}$

ψ = a function

III. OUTLINE OF TURBULENCE AND APPLICATION TO FLOW IN PIPES

A. Theory

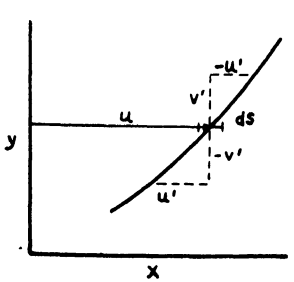


Figure 1. Velocity Profile

Turbulence causes the tangential stresses to be several times as large as the friction force if produced by purely viscous resistance. This increase in tangential stresses is caused by the change (loss or gain) of momentum due to the interchange of particles between one layer and another.

In this discussion the theories of Reynolds, Prandtl, and von Karman will be outlined. The details of the theories and a more complete discussion of their application can be obtained from the standard references (1, 3, 4, 7).

Consider Figure 1,

Reynolds stated that,

for the x direction:

$$u_i = u + u' \tag{1}$$

where: u = average velocity

u_i = instantaneous velocity

u' = instantaneous deviation from the average. The time average of u' is zero.

similarly for the y direction:

$$v_i = v + v' \tag{2}$$

but $v = 0$ and the time average of v' is zero.

The momentum transfer and tractive force are as follows: for the element dS (see Figure 1),

$dS \cdot v' \cdot \frac{\rho}{g_c}$ = mass rate of transfer

$-(v'\,dS)u_i \frac{\rho}{g_c}$ = instantaneous rate of transfer of x momentum.

$-v'\,u_i \frac{\rho}{g_c}$ = momentum transfer per unit area.

The time average of the momentum transfer must correspond to the tractive force per unit area,

$$\tau = -\frac{1}{t}\int_0^t v' u_i \frac{\rho}{g_c} dt \tag{3}$$

There is no net exchange of mass but there is a difference in momentum, since an element of mass moves from a low velocity level to a high velocity level and a corresponding element will move in the opposite direction.

Substituting Equation 1 for u in Equation 3,

$$\tau = -\frac{1}{t}\int_0^t \frac{\rho}{g_c} v' \,(u + u')\, dt \tag{4}$$

$$= -\frac{1}{t}\int_0^t \frac{\rho}{g_c} u\, v'\, dt - \frac{1}{t}\int_0^t \frac{\rho}{g_c} u'v'\, dt \tag{4a}$$

If the time interval, t, is taken large enough to include many fluctuations, the time average of the first term of Equation 4a is zero, because u is a constant and the time average of v' is zero. The second term can be integrated, assuming ρ is constant,

$$\tau = -\frac{\rho}{g_c}\frac{1}{t}\int_0^t u'\, v'\, dt \tag{5}$$

$$= -\frac{\rho}{g_c}\overline{u'\,v'} \tag{5a}$$

The expression $\overline{u'\,v'}$ is the time average of the product of the instantaneous fluctuating velocity components and is not necessarily zero even though the individual time average of u' and v' are zero.

It is now necessary to find the relation between u' and v'. From Figure 1, it should be noted that if v' is positive, particles move upward from regions of low velocity and if they originally have an x-component of velocity equal to u at their origin, the observed value of u' when they reach their destination will be negative; and if v' is negative, u' will be positive. Therefore, the product $u'v'$ is always negative.

Prandtl assumed that the elements of fluid moved in a manner similar to gas molecules and that they travel through a distance perpendicular to u'. This distance corresponds to the "mean free path"

in the case of gas molecules; this distance has been given the name "mixing length." Using this analogy and referring to Figure 1,

$$/\bar{u}'/ = CL_M\left(\frac{du}{dy}\right) \tag{6}$$

where $/\bar{u}'/$ is the average absolute value of u'. Prandtl also assumed that $/\bar{u}'/ \cong /\bar{v}'/$. Therefore,

$$\tau = - C^2 L_M'^2 \frac{\rho}{g_c}\left(\frac{du}{dy}\right)^2 \tag{7}$$

Let, $$L_M = CL'_M \tag{8}$$

Then, $$\tau = \frac{\rho}{g_c} L_M^2 \Big/\left(\frac{du}{dy}\right)\Big/\left(\frac{du}{dy}\right) \tag{9}$$

Just in passing, it may be well to mention Stanton's theory. Stanton introduced what is called the "mechanical viscosity," μ_M:

$$\tau = \frac{\mu_M}{g_c}\left(\frac{du}{dy}\right) \tag{10}$$

The "mechanical viscosity," μ_M, is also referred to as: mechanical factor, mechanical friction coefficient, turbulence factor, and austauschkoeffizient.

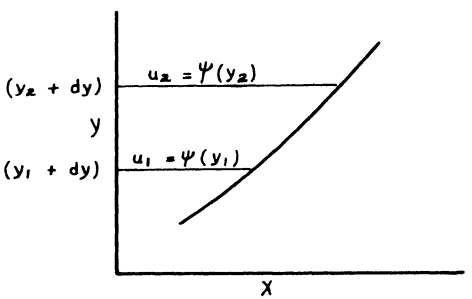


Figure 2. Velocity Profile (Von Kármán)

Von Kármán attacked the problem from the standpoint of the similarity of the local flow pattern. He assumed that:

(a) The mechanism of turbulent interchange is independent of the viscosity except in the immediate neighborhood of the walls.

(b) The principle of similarity can be applied to the mechanism of turbulent interchange in a sense analogous to molecular friction, i.e., the local flow pattern is statistically similar in the neighborhood of every point and only the time and length scale are variable.

Von Kármán expressed the variation of the velocity curve form by a Taylor's Series. Consider Figure 2,

$$u_1(y_1 + dy) = u_1(y_1) + u_1' dy + \frac{1}{2}u_1'' dy^2 + \frac{1}{6}u_1''' dy^3 + \ldots \tag{11a}$$

$$u_2(y_2 + dy) = u_2(y_2) + u_2' dy + \frac{1}{2}u_2'' dy^2 + \frac{1}{6}u_2''' dy^3 + \ldots \tag{11b}$$

The similarity pattern would suggest some regular proportionality relation:

$$\frac{u_2'}{u_1'} \sim \frac{u_2''}{u_1''} \sim \frac{u_2'''}{u_1'''} \sim \ldots \tag{12}$$

for the same points,

$$\frac{u_1'}{u_1''} \sim \frac{u_2'}{u_2''}\ ;\ \frac{u_1''}{u_1'''} \sim \frac{u_2''}{u_2'''};\ \ldots \tag{13}$$

The ratios in Equation 13 have dimensions of length and are proportional to the mixing length. That is,

p. 21 - Equation 6 should read:

$$/\bar{u}'/ = C\, L'_M\left(\frac{du}{dy}\right)$$

$$\frac{\left(\frac{du}{dy}\right)_1}{\left(\frac{d^2u}{dy^2}\right)_1} = \frac{\left(\frac{du}{dy}\right)_2}{\left(\frac{d^2u}{dy^2}\right)_2} = \text{const.} = \frac{L_M}{k} \tag{14}$$

Substituting Equation 14 into Equation 9,

$$\tau = k^2 \frac{\rho}{g_c} \frac{\left(\frac{du}{dy}\right)^4}{\left(\frac{d^2u}{dy^2}\right)^2} \tag{15}$$

The value of the constant, k, can be found as follows. Near the wall, a particular solution of Equation 14 may be obtained. In this case,

$$y \sim dy \text{ and } \frac{\left(\frac{du}{dy}\right)}{\left(\frac{d^2u}{dy^2}\right)} \sim dy \text{ and therefore,}$$

$$L_M = ky \tag{16}$$

From Nikuradse's data on flow in pipes,

$$\frac{L_M}{r} = 0.14 - 0.08\left(1 - \frac{y}{r}\right)^2 - 0.06\left(1 - \frac{y}{r}\right)^4 \tag{17}$$

now expanding Equation 17,

$$L_M = 0.4\ y - 0.44\ \frac{y^2}{r} + \ldots \tag{18}$$

near the wall, y approaches zero and

$$L_M \cong 0.4\ y \tag{19}$$

Therefore from Equations 16 and 19,

$$k = 0.40 \tag{20}$$

The above relations will now be applied to flow in both smooth and rough pipes.

B. Application

1. Smooth Pipes

Von Karman's universal relationship for the intensity of turbulent shear was given as Equation 15,

$$\frac{\tau g_c}{\rho} = k^2 \frac{\left(\frac{du}{dy}\right)^4}{\left(\frac{d^2u}{dy^2}\right)^2} \tag{15}$$

and for a pipe,

$$\tau = \tau_w \left(1 - \frac{y}{r_o}\right) \tag{21}$$

where: τ_w = shear stress at the pipe wall

Equation 21 is the law of linear stress distribution and is most general. It holds irrespective of the nature, type or origin of fluid resistance.

Substituting Equation 21 into Equation 15 and taking the square root,

$$\frac{\left(\frac{d^2u}{dy^2}\right)}{\left(\frac{du}{dy}\right)^2} = \left(\sqrt{\frac{-k}{\frac{\tau_w g_c}{\rho}}}\right)\left(\sqrt{\frac{1}{1-\frac{y}{r_o}}}\right) \tag{22}$$

The minus sign being used for the reason that throughout the range of integration the second derivative is negative.

Equation 22 may be integrated for $\left(\frac{du}{dy}\right)$, the constant of integration being determined by assuming an infinite velocity gradient at the boundary, that is,

$$\frac{du}{dy} = \infty \text{ for } y = 0$$

This results in,

$$\frac{du}{dy} = \frac{\sqrt{\frac{\tau_w g_c}{\rho}}}{2kr\left(1 - \sqrt{1 - \left(\frac{y}{r_o}\right)}\right)} \tag{23}$$

The velocity distribution can be obtained from the integration of Equation 23. The integration can be done by letting,

$$\left(1 - \frac{y}{r}\right) = Z^2$$

and noting that,

$$\text{for } y = r_o,\ u = u_{max}$$

The velocity distribution is then given as,

$$\frac{u_{max} - u}{\sqrt{\frac{\tau_w g_c}{\rho}}} = \frac{-1}{k}\left[\ln\left(1 - \sqrt{1 - \frac{y}{r_o}}\right) + \sqrt{1 - \frac{y}{r_o}}\right] \tag{24}$$

Equation 24 is the von Kármán equation for the velocity deficiency law in circular pipe

Prandtl assumed,

$$\tau = \tau_w = \text{constant} \tag{25}$$

Substituting Equation 25 into Equation 15 and integrating once, noting that,

$$\text{at } y = 0,\ \frac{du}{dy} = \infty$$

the velocity gradient is,

$$\frac{du}{dy} = \frac{\sqrt{\frac{\tau_w g_c}{\rho}}}{ky} \tag{26}$$

The velocity distribution is obtained by integrating Equation 26, noting that,

$$\text{at } y = r_o,\ u = u_{max}$$

$$\frac{u_{max} - u}{\sqrt{\frac{\tau_w g_c}{\rho}}} = \frac{1}{k}\ln\frac{r_o}{y} \tag{27}$$

Equation 27 is the Prandtl equation for the velocity deficiency law in circular pipes.

Equations 24 and 27, for k = 0.4, both agree with the results of Nikuradse's experiments.

p. 23 - line 16 from top of page should read:
"......deficiency law in circular pipes."

The term $(u_{max} - u)$ represents a so-called "velocity defect." The term $\sqrt{\frac{\tau_w g_c}{\rho}}$ has the dimensions of velocity and is commonly called the "friction velocity."

Equation 27, the simpler velocity deficiency equation, will be used throughout the remainder of the discussion.

Near the wall, altogether special conditions exist. The wall makes it impossible to have cross-current motions. Regardless of how much turbulence exists in the center of the pipe, near the wall the turbulence is reduced to zero and the tangential or shear stress is transferred by viscous action. This brings the concept of a "laminar layer" between the wall and the main core of turbulent motion. The region between the purely laminar layer and turbulent core is the transition region or "buffer layer."

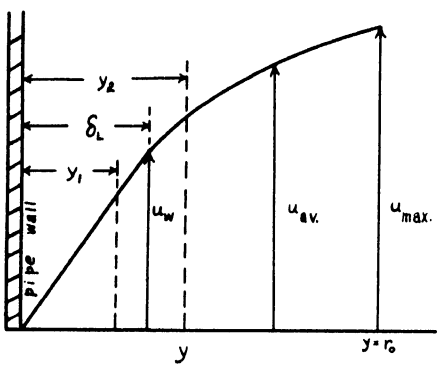


Figure 3.
Velocity Distribution Across a Pipe

The velocity gradient in the laminar layer is assumed as uniform; that is,

$$\left(\frac{du}{dy}\right)_{0 \to \delta_L} = \frac{u_w}{\delta_L} \tag{28}$$

In order to determine the thickness of the laminar layer, the following basic expressions should be noted.

The average tangential stress on a surface is,

$$\tau_w = f \frac{\rho}{g_c} \frac{u_{av}^2}{2} \tag{29}$$

and,

$$\tau_w = \frac{\mu}{g_c} \left(\frac{du}{dy}\right) \tag{30}$$

By the proper combination of Equations 28, 29, and 30, the following can be obtained,

$$\sqrt{\frac{\tau_w g_c}{\rho}} = u_{av} \sqrt{\frac{f}{2}} \tag{31}$$

and the thickness of the laminar layer,

$$\delta_L = \frac{\mu}{\rho} \frac{u_w}{\left(\sqrt{\frac{\tau_w g_c}{\rho}}\right)^2} \tag{32}$$

The following notation will now be used to simplify the equations,

$$u_* = \sqrt{\frac{\tau_w g_c}{\rho}} \tag{33}$$

$$u^+ = \frac{u}{u_*} \tag{34}$$

$$y^+ = \frac{u_* y}{\nu} \tag{35}$$

where,

$$\nu = \frac{\mu}{\rho} = \text{kinematic viscosity} \tag{36}$$

Within the film for $y \leq \delta_L$ and from Equations 28 and 30,

$$\tau_w = \frac{\mu}{g_c} \frac{u}{y} \tag{37}$$

Combining Equations 33 and 37,

$$\mu \frac{u}{y} = \rho u_*^2 \tag{38}$$

or,

$$\frac{u}{u_*} = \frac{u_* y}{\mu/\rho} \tag{38a}$$

and from Equations 34, 35, 36, and 38a,

$$y^+ = u^+ \tag{39}$$

It has been found that the parameter y^+ has a constant value for the passage from the laminar layer to the turbulent region; that is,

$$y^+ \text{ (at } y = \delta_L) = \text{constant} = N \tag{40}$$

From Nikuradse's experiments the value of N has been found to be,

$$N = 11.5 \tag{41}$$

The region between y_1 and y_2, Figure 3, is commonly called the "buffer layer." y_1 represents the region of the pure laminar film and y_2 represents the beginning of the purely turbulent core. Data has shown that for y_1, $y^+ = 5$ and for y_2, $y^+ = 30$. A paper by Boelter, et al (2) contains a good discussion of the buffer layer.

The velocity at the edge of the laminar layer and the thickness of the laminar layer can be obtained from Equations 32, 35, 38, and 40

$$\frac{u_w}{u_*} = N \tag{42}$$

$$\delta_L = N \frac{\nu}{u_*} \tag{43}$$

The above relations can be combined with the simple "velocity defect" equation, Equation 27, to give the velocity distribution in a smooth pipe.

With k = 0.4, Equation 27 becomes,

$$\frac{u}{u_*} = \frac{u_{max}}{u_*} - 5.75 \log \frac{r_o}{y} \tag{44}$$

$$= u^+$$

now,

$$u = u_w + (u_{max} - u_w) - (u_{max} - u) \tag{45}$$

and combining Equations 44 and 45,

$$u^+ = \frac{u_w}{u_*} + 5.75 \log \frac{r_o}{\delta_L} - 5.75 \log \frac{r_o}{y} \tag{46}$$

or

$$u^+ = \frac{u_w}{u_*} + 5.75 \log \frac{y}{\delta_L} \tag{46a}$$

By combining Equations 41, 42, and 46a, the velocity distribution in a smooth pipe is,

$$u^+ = 5.5 + 5.75 \log y^+ \tag{47}$$

and from Nikuradse's results,

$$\frac{u_{max} - u_{av}}{u_*} = 4.07 \tag{48}$$

where u_* is determined by Equation 31 and f from the following correlation of Nikuradse's results,

$$\frac{1}{\sqrt{4f}} = -0.8 + 2 \log \left(N_{Re} \sqrt{4f}\right) \tag{48}$$

$$N_{Re} = \frac{2r\, u_{av}}{\nu} \tag{50}$$

Equation 48 can also be written as,

$$\frac{u_{max}}{u_{av}} = 1 + 4.07 \sqrt{\frac{f}{2}} \tag{51}$$

Figure 4 is a sketch of the plot of Equations 39 and 47,

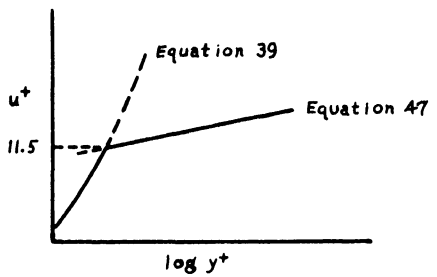


Figure 4. Generalized Velocity Distribution Across a Pipe

2. Rough Pipes

For the case of wall roughness of appreciable magnitude, the intensity of turbulence resulting from form drag will be so great as to render viscous shear relatively insignificant. Under such circumstances the velocity distribution should depend only upon wall roughness and distance from the wall. Assuming that roughness characteristics may be defined in terms of a linear dimension ϵ the general function for the velocity will become then,

$$u^+ = \psi \left(\frac{y}{\epsilon}\right) \tag{52}$$

von Karman obtained a velocity distribution of the form,

$$u^+ = C + \frac{1}{k} \ln \left(\frac{y}{\epsilon}\right) \tag{53}$$

From the data of Nikuradse, equation 53 becomes,

$$u^+ = 8.48 + 5.75 \log \left(\frac{y}{\epsilon}\right) \tag{54}$$

and

$$\frac{1}{\sqrt{4f}} = 1.74 + 2 \log \left(\frac{r_o}{\epsilon}\right) \tag{55}$$

Nikuradse in his experiments on roughness used artificial roughness. Sand grains of uniform diameter were cemented to the inner wall of the pipe. By the proper selection of grain size with respect to pipe diameter, he was able to vary the relative roughness, $\frac{r_o}{\epsilon}$, between the limits of 507 to 15; the grain diameter being used to represent the roughness dimension, ϵ . Nikuradse's results are sketched in Figure 5,

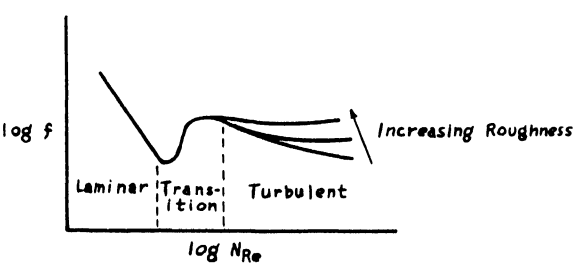


Figure 5. Effect of Roughness on the Friction Factor

It should be noted from Equation 55, that the Reynolds number does not appear, therefore, showing that the magnitude of f is totally independent of viscous influence. However, from Figure 5, it is indicated that for cases where the roughness projections are rendered ineffective by a surrounding laminar film, the friction factor remains the same as that for a smooth pipe; but with increasing Reynolds number, the laminar layer decreases in thickness, and must eventually yield to the roughness.

In the actual case ϵ will no longer represent a single linear dimension but becomes a parameter indicating relative performance rather than actual size of roughness.

The theoretical friction factor equation can be obtained from Equations 31, 48, and 54,

$$\frac{1}{\sqrt{4f}} = 1.56 + 2.03 \log \left(\frac{r_o}{\epsilon}\right) \tag{56}$$

The magnitude of the thickness of the laminar layer may be found from Equations 31, 43, and 50 and multiplying through by k,

$$\frac{\epsilon}{\delta_L} = \frac{0.0153\ N_{Re}\ \sqrt{4f}}{r_o/\epsilon} \tag{57}$$

c. Notes

1. In the 7th equation from the top of page 67, Bakhmeteff (1), a(-1) was omitted from the term within the brackets. The term should read, $[-1 + x + \ln(1 - x)]$.

2. On page 239, Rouse (7), the equation after Equation 164 should have a minus sign before the right hand term.

3. In the equation in Figure 118, page 243 and Equations 172 and 174, page 244, Rouse (7), the values 5.85 should be 8.48.

4. Benjamin Miller at the American Society of Mechanical Engineers annual meeting at New York City, December 1946, pointed out an apparent discrepancy in Nikuradse's y^+ values. Miller presented a paper on this subject at annual meeting of the American Society of Mechanical Engineers at Atlantic City, December 1947 and also at the Heat Transfer Symposium*, Oak Ridge, Tenn., December 1948.

IV. BOUNDARY LAYER EQUATIONS FOR FLOW OVER A FLAT PLATE

A. General

When a fluid of low viscosity flows with an initial uniform velocity over a flat plate, the velocity decreases until it is zero at the surface of the plate. This decrease in velocity takes place in a small layer of fluid called "the boundary layer." The boundary layer is of zero thickness at the leading edge and becomes thicker as the flow progresses along the plate. The flow in the layer is laminar at the leading edge of the plate and may become turbulent as the flow progresses along the plate. The transition between laminar flow in the layer (laminar boundary layer) and turbulent flow in the layer (turbulent boundary layer) may be determined from a Reynolds Number.

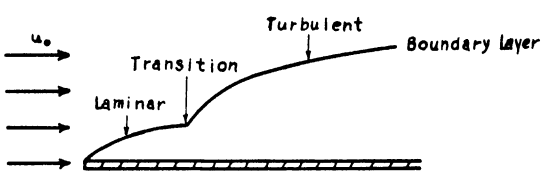


Figure 6. Flow over a Flat Plate

The above figure, Figure 6, is schematic for the flow over a flat plate.

The original theory on boundary layers was advanced by Prandtl. Only the final equations will now be presented. The mathematical theory can be obtained from several good sources (3, 5, 6, 7, 8, 9).

B. Laminar Boundary Layer

The drag on one side of a flat plate due to a laminar boundary layer is,

$$D_f = C_f(Lb)\frac{\rho u_o^2}{2g_c} \tag{58}$$

where

$$C_f = 1.328(N_{Re})^{-1/2} \tag{59}$$

and,

$$N_{Re} = \frac{u_o L \rho}{\mu} \tag{60}$$

*Miller, B., "Exploding a Heat Transfer Myth," Heat Transfer Lectures Vol. I, NEPA Division, Atomic Energy Commission, Oak Ridge, Tenn.

The thickness of the laminar boundary layer to a point where approximately 99 percent of the full velocity is attained is,

$$\delta = 5.19L(N_{Re})^{-1/2} \tag{61}$$

C. Turbulent Boundary Layer

The drag on one side of a flat plate due to a turbulent boundary layer is,

$$D_f = C_f(Lb)\frac{\rho u^2}{2g_c} \tag{58}$$

where,

$$C_f = 0.455(\log N_{Re})^{-2.58} \tag{62}$$

The thickness of the turbulent boundary layer to a point where approximately 99 per cent of the full velocity is attained is,

$$\delta = 0.37L(N_{Re})^{-0.2} \tag{63}$$

The Reynolds Number at which the transition between laminar flow and turbulent flow may be considered is,

$$N_{Re} = \frac{u_o L \rho}{\mu} = 500{,}000 \tag{64}$$

V. PROBLEMS

1. Draw the velocity distribution and compute the thickness of the laminar layer for the flow of water at 70°F. with an average velocity of 5 ft./sec. in a smooth 12-in. i.d. pipe.

2. Draw the velocity distribution for the same conditions as in problem 1 except the pipe is roughened to $\frac{\epsilon}{r_o} = 0.01$. Assume the same pressure gradient exists for this case as for problem 1.

Chapter 3

VELOCITY HEAD CONCEPT IN PRESSURE DROP CALCULATIONS

by

C. E. Lapple*
Engineering Research Laboratory
Engineering Department
E. I. du Pont de Nemours & Co., Inc.
Wilmington, Delaware

TABLE OF CONTENTS

Page

I. Reprint of paper "Using the Velocity Head Concept in Pressure Drop Calculations," Heating, Piping, and Air Conditioning, 17, 179-183, 262-267, 319-324 (1945) 31

A. Introduction 32

B. Definition of Velocity Head 34

C. Friction Loss and Pressure Drop 36

D. Friction Loss in Pipes 37

E. Pressure Drop Through Fittings and Valves 37

F. Friction Loss Across Tube Banks 38

G. Friction Loss Through Granular Beds 43

H. Friction Loss for Abrupt Expansion 43

I. Friction Loss for Abrupt Inlet 43

J. Differential Heads Across Metering Devices 43

1. Pitot Tube 45

2. Nozzle and Venturi Meters 45

3. Orifice Meters 45

K. Estimation of Pressure Drop or Friction Loss 46

L. Numerical Examples 47

M. Epilogue 48

N. References (pp. 40, 42, 47) 47

LIST OF FIGURES

Figure 1. Velocity Head Plot for Air at One Atmosphere Pressure 33
Figure 2. Velocity Head Plot for Water at Temperature of 4°C. 34
Figure 3. Chart for Determining Velocity in Conduits 35
Figure 4. Friction Factor - Reynolds Number Plot for Flow Through Straight, Circular, Smooth and Commercial Pipe 39
Figure 5. Friction Factor - Reynolds Number Plot for Flow Across Tube Banks 41
Figure 6. Friction Factor - Reynolds Number Plot for Flow Through Beds of Granular Solids . . . 44
Figure 7. Jacket Flow Distributor 46

*Present address: Associate Professor, Dept. of Chem. Engineering, Ohio State University, Columbus, Ohio.

LIST OF TABLES

Page

Table 1. Approximate Values of the Velocity Head. 34

Table 2. Values of $(L/D)_V$ for New Commercial Pipe. 40

Table 3. Pressure Drop Through Screwed Fittings and Valves (for Turbulent Flow Only). 40

II. Problems 49

Note: Another paper on this subject has recently been published in Chemical Engineering, 56, 96-104 (1949) May.

*

Using the Velocity Head Concept in

PRESSURE DROP CALCULATIONS

By C. E. Lapple

Reprinted from
Heating, Piping & Air Conditioning
April-June 1945
Printed in U. S. A.

Reproduced by permission of publisher.

Using the Velocity Head Concept in

PRESSURE DROP CALCULATIONS

By C. E. Lapple*

IN THE design of pipe lines, ventilation systems, and process equipment, it becomes necessary to estimate the overall pressure drop in order to specify the required fan, pump, blower, or compressor capacity. It may also be necessary to design adequate metering elements. In the operation of equipment, pressure drop estimates are often essential for purposes of locating possible plugged or corroded lines, checking on process performance, or determining "bottlenecks" for proposed capacity increases.

Conventional methods of calculation in the form of friction factors, orifice coefficients, or equivalent lengths of fittings and valves have been developed for many types of conduits and equipment commonly employed. Frequently, however, equipment is encountered for which no specific data are available, and it becomes necessary for the engineer, designer, or operator to be able to make a reasonable estimate. In order to make such estimates it is necessary to have available a clear physical concept of the mechanism that controls the pressure drop in a fluid. Fluid flow is often regarded as a complex phenomenon that can only be represented by intricate mathematical expressions which will yield the correct answer if proper substitutions and arithmetical solutions are applied. As a result, designers have developed "rules of thumb" as a guide or for purposes of checking the order of magnitude of such calculations. Such rules have been passed along and are accepted by some as approximate representations of practical experience and frowned upon by others who question their general validity. It is the purpose of this paper to furnish an insight into fluid flow mechanisms which will enable visualizing frictional or pressure drop processes and incorporating a physical conception into pressure drop equations, as well as to provide simplified equations for rapid estimating, for checking of more accurate calculations, or for use in the field where standard reference sources are not available.

DESIGN OF pipe lines, process equipment, ventilation systems, etc., requires estimation of pressure drops in order to specify the required pump, compressor, fan, or blower capacities. Pressure drop estimates are often necessary, too, in the operation of equipment for purposes of locating possible plugged or corroded lines, checking process performance, or determining bottlenecks for proposed capacity increases. The article of which this is the first part is intended as a guide to a physical conception or visualization of otherwise seemingly complex fluid flow phenomena. The approximations presented will be found to be entirely adequate for many purposes, and an attempt has been made by the author to point out their limits of accuracy.

The flow of a fluid may, in general, partake of one or both of two types of flow—streamline and turbulent. In streamline flow, adjacent layers of moving fluid slip over each other with no mixing or interchange of portions of fluid from one layer to the next. Turbulent flow is characterized by an eddying of the fluid within itself in addition to a specific motion of the fluid body in a given direction. In turbulent flow, adjacent layers do not shear smoothly over each other, but are continuously exchanging portions of fluid. In streamline flow, frictional losses are due directly to shearing between adjacent layers of fluid. In turbulent flow, frictional losses are due to random shearing and impact of fluid exchanged between the layers. Turbulent flow ensues when inertia forces predominate over the viscous forces within the fluid.

The nature of flow of a fluid is consequently characterized by the Reynolds number, *Re*, which represents a measure of the ratio of inertia to viscous forces. When this ratio exceeds a certain critical value (approximately 2000 for flow in straight round pipes), turbulent flow ensues, whereas for lower values the flow is streamline. Over 98 per cent of all fluid flow problems in practice are concerned with turbulent flow.

The velocity head concept visualizes pressure drop or friction loss in terms of the kinetic energy of the fluid and is thus valid where inertia forces or changes in kinetic energy of the fluid are concerned. Consequently, its utility is limited to turbulent flow conditions. The velocity head concept is not novel and has long been in actual use, particularly by ventilating engineers. Unfortunately, it is not adequately described in the literature or in textbooks, and its full physical significance and utility are not widely appreciated.

*Engineering Dept., Chemical Engineering and Metallurgical Laboratory, Experimental Station, E. I. du Pont de Nemours & Co., Inc.

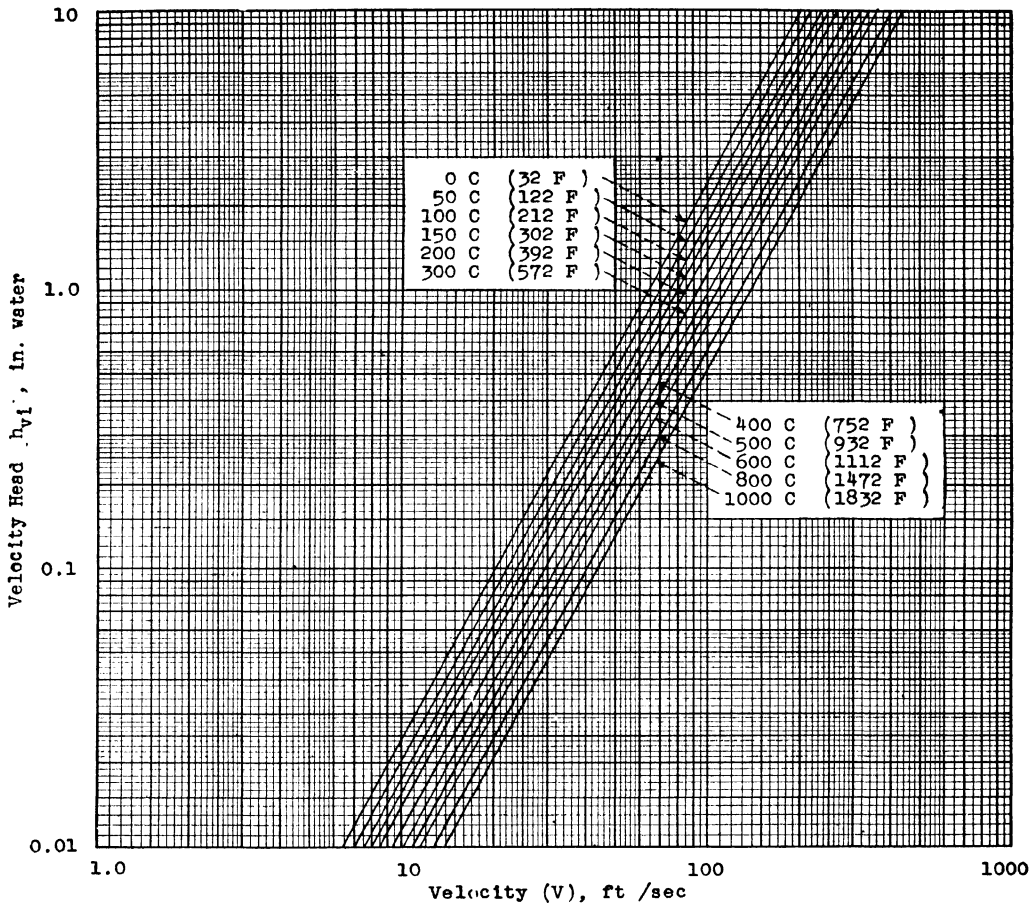


Fig. 1—Velocity head plot for air at one atmosphere pressure. (Note: For other pressures or gases, multiply h_{vi} by the absolute pressure, in atmospheres, and by the quantity, molecular weight ÷ 29)

Nomenclature

D = Inside diameter of circular pipe, ft;
D_c = Clearance between tubes in a tube bank, ft;
D_p = Diameter of granular particle, ft;
E_v = Kinetic energy of fluid (ft-lb force)/(lb mass);
F = Friction loss (lb force)/(sq ft)†
g_c = Conversion factor, 32.17 (lb mass/lb force) (ft/sec²);
g_L = Local acceleration due to gravity (ft/sec)/(sec);
h_v = Velocity head, ft of fluid flowing;
h_{vi} = Velocity head, in. of water;
p = Fluid pressure, (lb force)/(sq ft);
p_v = Velocity head (lb force)/(sq ft);
p_{vi} = Velocity head (lb force)/(sq in.);
Δp = Pressure drop (lb force)/(sq ft);
Re = Reynolds number, dimensionless = $(DV\rho/\mu)$ for flow through pipes, orifices, nozzles, or venturis; $(D_c V_{max}\rho/\mu)$ for flow across tube banks; $(D_p V\rho/\mu)$ for flow through beds of granular solids;
V = Average fluid velocity (ft/sec);
V_{max} = Maximum average fluid velocity in flow across tube banks (ft/sec);
Z = Elevation of fluid above arbitrary datum plane, ft;
ρ = Fluid density (lb mass)/(cu ft);
μ = Fluid viscosity (lb mass)/(ft) (sec) = centipoises ÷ 1488.

†Friction loss is often defined as an energy loss per unit mass of fluid, having the dimensions (ft-lb force)/(lb mass). This definition of friction loss is equivalent to the quotient F/ρ.

Definition of Velocity Head

A fluid flowing with a velocity, V, has associated with each pound of fluid a certain kinetic energy defined by

$$E_v = (V^2/2g_c) \quad \ldots\ldots\ldots\ldots [1]$$

Since pressure is a form of potential energy of the fluid, this kinetic energy can be expressed as an equivalent pressure differential which is known as the velocity head. For any fluid, the following alternate equations express this equivalent pressure or velocity head in various units:

$$p_v = (\rho V^2/2g_c) \quad \ldots\ldots\ldots [2]$$
$$p_{vl} = (\rho V^2/288g_c) \quad \ldots\ldots\ldots [3]$$
$$h_v = (V^2/2g_L) = (V^2/2g_c)(g_c/g_L) \quad \ldots\ldots [4]$$
$$h_{vl} = 0.00300\ \rho V^2 \quad \ldots\ldots\ldots [5]$$

The ratio (g_c/g_L) in Equation 4 is numerically equal to unity and is introduced only to maintain the equation correct dimensionally.* The term "velocity head" derives its name from the form given by Equation 4, which represents the fluid head equivalent to the kinetic energy per unit mass of fluid. It may also be interpreted as the height from which the fluid must fall to attain a velocity V in a vacuum.

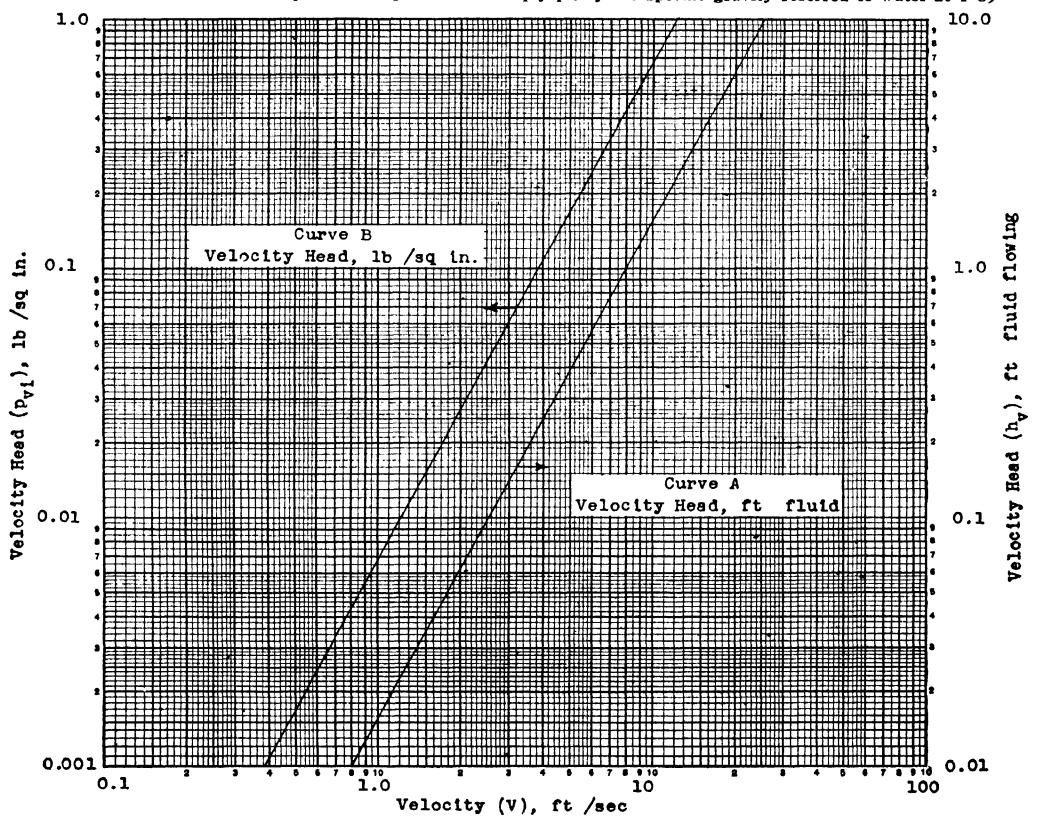
Figs. 1 and 2 give a plot of the velocity head for air and water, respectively, flowing at various temperatures and velocities. In Fig. 3 is given a plot for converting gal/min (Curve *A*) or cu ft/min (Curve *B*) to linear velocity for the case of flow in circular pipe. To obtain the velocity corresponding to a given volumetric flow rate in a given size pipe, multiply the volumetric flow rate by the abscissa corresponding to the pipe diameter. It should be noted that cu ft/min refers to the actual volumetric rate

*See Perry, J. H., Chemical Engineers Handbook, 2nd ed., section 6, p. 860, New York, McGraw-Hill Book Co., 1941.

Table 1—Approximate values of the velocity head

Fluid	Fluid Velocity ft/sec	Velocity Head
Air (1 atm, 125 F)	50	¾ in. water
	70	1 in. water
	100	2 in. water
Water	4	0.1 lb/sq in.
Any Fluid	8	1.0 ft fluid

Fig. 2—Velocity head plot for water at temperature of 4 C. (Note: Curve A—holds for any fluid as well as for water. Curve B—for other liquids or temperatures multiply p_{vl} by the specific gravity referred to water at 4 C)



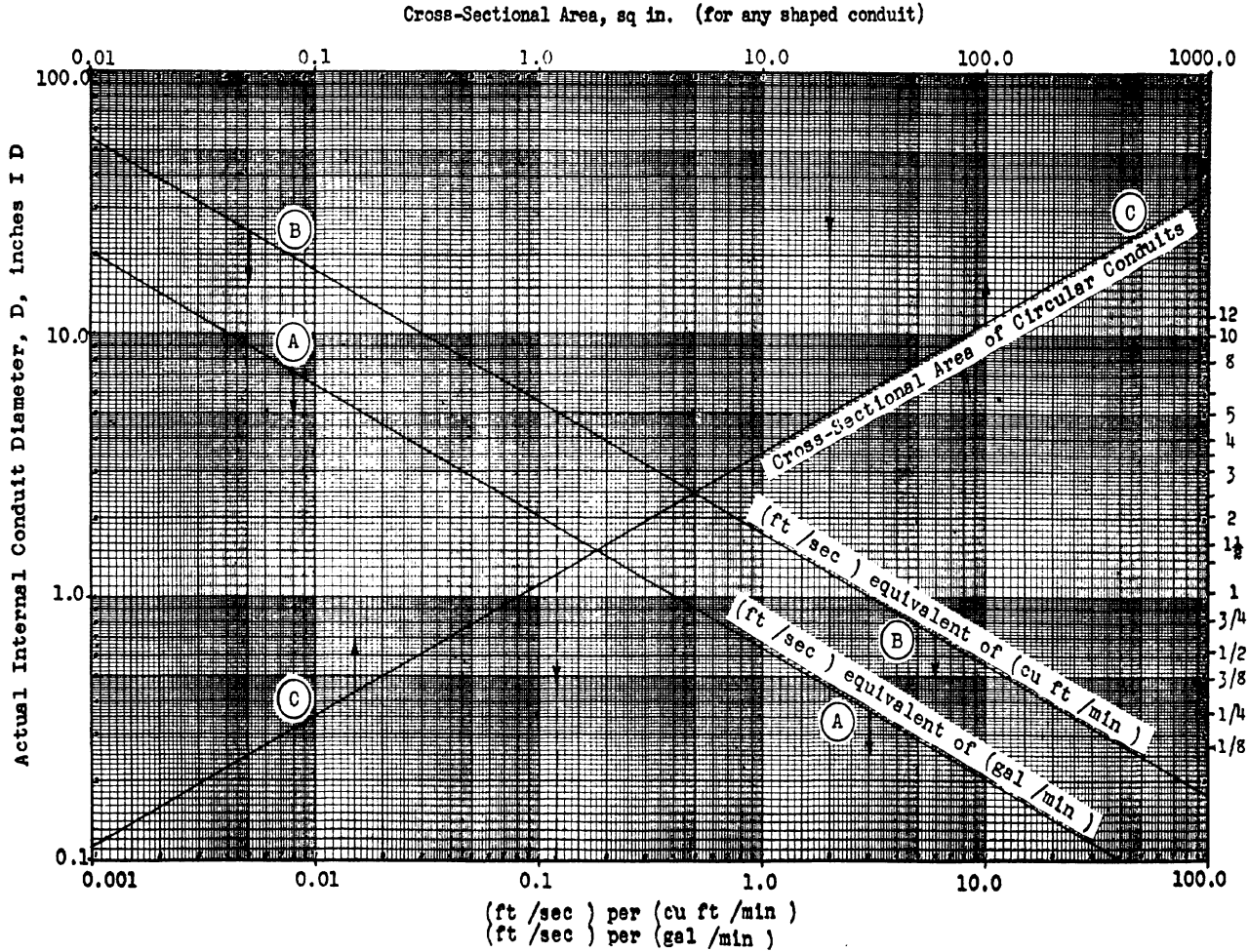


Fig. 3—Chart for determining velocity in conduits. Note: (cu ft/min) and (ft/sec) refer to the actual flow rate and velocity at the temperature and pressure in the conduit and do not refer to conditions at any standard temperature or pressure

at the conditions existing in the pipe and should not be confused with volumetric rates referred to any standard temperature or pressure conditions. For any shaped pipe, a plot (Curve *C*) is also given in Fig. 3 to indicate the equivalent circular pipe size having the same cross-sectional area. The dashed line shows the procedure for finding the ft/sec equivalent of cu ft/min for any shaped pipe having an area of 20 sq in.

Table 1 lists some values of the velocity head for specific fluids and velocities. These values are readily memorized and values of the velocity head for any other cases of fluid velocity or density can be readily obtained by mental cross-rationing. For other velocities, the corresponding velocity head is obtained by multiplying the value in the table by the square of the ratio of actual velocity to that given in the table. The velocity head is also directly proportional to fluid density. Thus, for other gases the value given in the table should be multiplied by the ratio of the actual molecular weight to that of air (29.0), as well as by the proper absolute pressure and temperature ratios to correct to other temperatures and pressures. For liquids, the value for water is to be multiplied by the specific gravity of the fluid. When expressed in terms of feet of fluid, of course, no density correction is needed. In practice, the unit, inches of water, is generally used in calculating pressure drops for low pressure gases; lb/sq in., for high pressure gases or liquids; and feet of fluid is often used for liquids.

Friction Loss and Pressure Drop

It is well to review at this point the distinction between friction loss and pressure drop. Pressure drop represents the difference in pressure of a fluid between two points in a system. This difference in pressure may be the result of a conversion of pressure energy into kinetic energy or potential energy resulting from a change in elevation, or it may be the result of a dissipation into heat by frictional losses. Friction loss represents only that portion of pressure energy lost as heat. The two items, pressure drop and friction loss, are related by Bernoulli's theorem, which applies where no mechanical work is done on or by the fluid,

$$\begin{aligned}\Delta p &= (p_1 - p_2) \\ &= (\rho V_2^2/2g_c) - (\rho V_1^2/2g_c) \\ &\quad + \rho(Z_2 - Z_1) + F \quad \ldots\ldots [6]\end{aligned}$$

where subscripts 1 and 2 represent conditions at the upstream and downstream locations, respectively. Thus, for horizontal equipment with the same inlet and outlet area, the overall friction loss and the pressure drop are identical, if the fluid density does not undergo any appreciable change.

Using the Velocity Head Concept in

PRESSURE DROP CALCULATIONS

IN THE calculation of pressure drops or friction losses, the utility of the velocity head concept lies in the fact that the pressure drop or friction loss can generally be expressed as a certain number of velocity heads, which is a dimensionless ratio. The actual pressure drop or friction loss can then be calculated from the velocity head and will have the same units as the velocity head. In turbulent flow, pressure drop represents largely a decrease in potential energy to develop a specific kinetic energy which may subsequently be dissipated as heat by impact or general turbulence or may be, at least partially, recovered as pressure if the fluid subsequently expands or decelerates. A small portion of the pressure drop may be directly due to frictional shearing between fluid layers. Where this is an appreciable factor, the pressure drop will be found to be a function of the Reynolds number. Where this is a negligible factor and pressure drop is due almost entirely to a deceleration or acceleration of the fluid, the pressure drop will be substantially independent of the Reynolds number. For conditions commonly encountered in practice, the flow through pipes, tube banks, and granular solids illustrates the first case, where frictional losses are appreciable even though the flow pattern is turbulent, while the flow through orifices and nozzles represents the latter case, where frictional losses are negligible. For the latter case, the pressure drop expressed as a number of velocity heads will be substantially constant and independent of the Reynolds number. Whereas the pressure drop expressed as number of velocity heads will vary somewhat with the Reynolds number for the first case, it can be approximated by a constant value within reasonable limits of accuracy over the usual Reynolds number range encountered in practice.

In the following paragraphs, the conventional pressure drop and friction loss equations will be presented in terms of velocity head together with an interpretation of their physical significance. It is assumed in these developments that the fluid density does not undergo any appreciable (more than 20 per cent) change in flowing through the pipe or apparatus under consideration so that an average density can be employed. When large density changes occur, such as are encountered in the flow of gases at high pressure drops, special methods of calculation are required. [See C. E. Lapple, Trans. Am. Inst. Chem. Engrs., *39*, 385-432 (1943).]

Friction Loss in Pipes

The friction loss or pressure drop in straight horizontal circular pipes is generally expressed in terms of the Fanning equation:

$$F = \Delta p = (4fL/D)\ (\rho V^2/2g_c) \quad \ldots.[7]$$

where f is a function of the Reynolds number as shown in Fig. 4. It will be observed that the second group of terms in parentheses represents the velocity head, so that Equation 7 may be rewritten as

$$\Delta p_v = \Delta p/(\rho V^2/2g_c) = (4fL/D) \quad \ldots\ldots\ldots.[8]$$

where the pressure drop is expressed as a certain number of velocity heads, given by $(4fL/D)$. From Equation 8 it is apparent that the length of pipe expressed as number of pipe diameters $(L/D)_v$, for which the pressure drop corresponds to one velocity head (i.e., for which $\Delta p_v = 1$) is given by

$$(L/D)_v = 1/(4f) \quad \ldots\ldots\ldots.[9]$$

In the process industries as well as in the ventilating field, actual designs will generally lie in the Reynolds number range of 5000 to 1,000,000. Inspection of Fig. 4 will show that in this range the friction factor, f, only varies over the range of 0.004 to 0.010 for clean commercial steel pipe. An average value of 0.0055 is a good approximation for rough estimates over the entire range and the corresponding value of $(L/D)_v$ as found from Equation 9 is 45. In other words, the pressure drop for 45 pipe diameters of clean commercial pipe is one velocity head within ± 40 per cent. This will be recognized as a common rule of thumb in the ventilation field. Water handling problems generally involve a range in Reynolds number of 10,000 to 100,000, while air handling problems usually fall in the range 50,000 to 1,000,000. It is apparent from Table 2 that, allowing for the maximum probable variation in f for new steel pipe, the length of pipe for which the pressure drop is equal to one velocity head may range from 25 to 65 pipe diameters, though, for most practical cases, it ranges from 30 to 45 pipe diameters for water lines and from 40 to 65 pipe diameters for air lines. Thus, within ± 25 per cent, $(L/D)_v$ may be taken as 40 and 50 for water and air handling, respectively.

While the previous discussion has dealt with flow through circular pipe, the same equations and friction factors will also apply to noncircular pipe for turbulent flow provided the diameter term, D, used in calculating (L/D) or Re is replaced by the hydraulic diameter, D_h. The velocity and velocity head, however, must be based on the actual cross-section of the pipe considered.

Pressure Drop Through Fittings and Valves

The pressure drop through fittings and valves in turbulent flow can be expressed either in terms of an equivalent length of straight pipe of the same nominal size or as a certain number of velocity heads in the pipe of the same nominal size as shown in Table 3. While

these two methods are not entirely comparable and will yield slightly different answers, both methods give results which are well within the accuracy of available data and within variations due to differences in specific structural details of commercial fittings and valves. For Reynolds numbers less than 100,000, the equivalent length values give a more accurate correlation of data on a specific fitting or valve, whereas for larger values of the Reynolds number the equivalent velocity head is more accurate. However, all the values of Table 3 are probably good to better than ± 30 per cent, and represent averages of the data reported in References 13-20.

Friction Loss Across Tube Banks

The friction loss or pressure drop across tube banks is commonly expressed as

$$F = \Delta p = (4 f_1 N)\ (\rho V^2_{max}/2g_c) \quad ..[10]$$

where f_1 is a form of friction factor which is a function of the Reynolds number. For tube banks the Reynolds number is usually expressed either as $(D_t V_{max} \cdot \rho/\mu)$ or $(D_c V_{max} \cdot \rho/\mu)$, the two being directly related in terms of the configuration of the tube bank. The maximum velocity between tubes, $V_{max.}$ is defined as the velocity based on the smallest free total area through which all the fluid must pass, whether this be between tubes in a row normal to the general flow direction (for all in-line and some staggered arrangements) or along the diagonal openings between tubes in adjacent rows (for staggered arrangements with very close row spacings). The term D_c is defined as the clearance between tubes corresponding to this minimum flow area. For all in-line arrangements and most staggered arrangements commonly encountered in practice, $V_{max.}$ and D_c will be based on the free area and clearance between tubes in a row normal to the general flow direction. In the subsequent discussion of tube banks, the Reynolds number will be defined as $(D_c V_{max} \cdot \rho/\mu)$.

*Engineering Dept., Chemical Engineering and Metallurgical Laboratory, Experimental Station, E. I. du Pont de Nemours & Co., Inc.

By C. E. Lapple*

DESIGN OF pipe lines, process equipment, ventilation systems, etc., requires estimation of pressure drops in order to specify the required pump, compressor, fan, or blower capacities. Pressure drop estimates are often necessary, too, in the operation of equipment for purposes of locating possible plugged or corroded lines, checking process performance, or determining bottlenecks for proposed capacity increases. The article of which this is the second part (the first was published in the April issue) is intended as a guide to a physical conception or visualization of otherwise seemingly complex fluid flow phenomena. The approximations presented will be found to be entirely adequate for many purposes, and an attempt has been made to point out their limits of accuracy.

Nomenclature

D = Inside diameter of circular pipe, ft;

D_c = Clearance between tubes in a tube bank, ft;

D_h = Hydraulic diameter = 4 × cross-sectional area ÷ "wetted" perimeter = D for circular pipe;

D_p = Diameter of granular particle, ft;

D_t = Outside diameter of tubes in a tube bank, ft;

E_v = Kinetic energy of fluid (ft-lb force)/(lb mass);

f = Fanning friction factor for flow in conduits, dimensionless;

f_1 = Friction factor for flow across tube banks, dimensionless;

f_2 = Friction factor for flow through beds of granular solids, dimensionless;

F = Friction loss (lb force)/(sq ft)†

g_c = Conversion factor, 32.17 (lb mass/lb force) (ft/sec²);

L = Length of straight horizontal pipe or depth of bed of granular solids in direction of flow, ft;

L_e = Equivalent length of straight pipe of same nominal size as valve or fitting, ft;

$(L/D)_v$ = Length of straight pipe, expressed as number of pipe diameters, for which pressure drop is one velocity head (i. e., for which $\Delta p_v = 1$), dimensionless;

N = Number of rows of tubes normal to general direction of flow, dimensionless;

p = Fluid pressure, (lb force)/(sq ft);

p_v = Velocity head, (lb force)/(sq ft);

Δp = Pressure drop, (lb force)/(sq ft);

Δp_v = Pressure drop, number of velocity heads, dimensionless;

R_e = Reynolds number, dimensionless = $(DV\rho/\mu)$ for flow through pipes, orifices, nozzles, or venturis; $D_c V_{max.} \rho/\mu)$ for flow across tube banks; $(D_p V \rho/\mu)$ for flow through beds of granular solids;

V = Average fluid velocity, (ft/sec);

$V_{max.}$ = Maximum average fluid velocity in flow across tube banks, (ft/sec);

ρ = Fluid density, (lb mass)/(cu ft);

μ = Fluid viscosity, (lb mass)/(ft) (sec) = centipoises ÷ 1488.

†Friction loss is often defined as an energy loss per unit mass of fluid, having the dimensions (ft-lb force)/(lb mass). This definition of friction loss is equivalent to the quotient F/ρ.

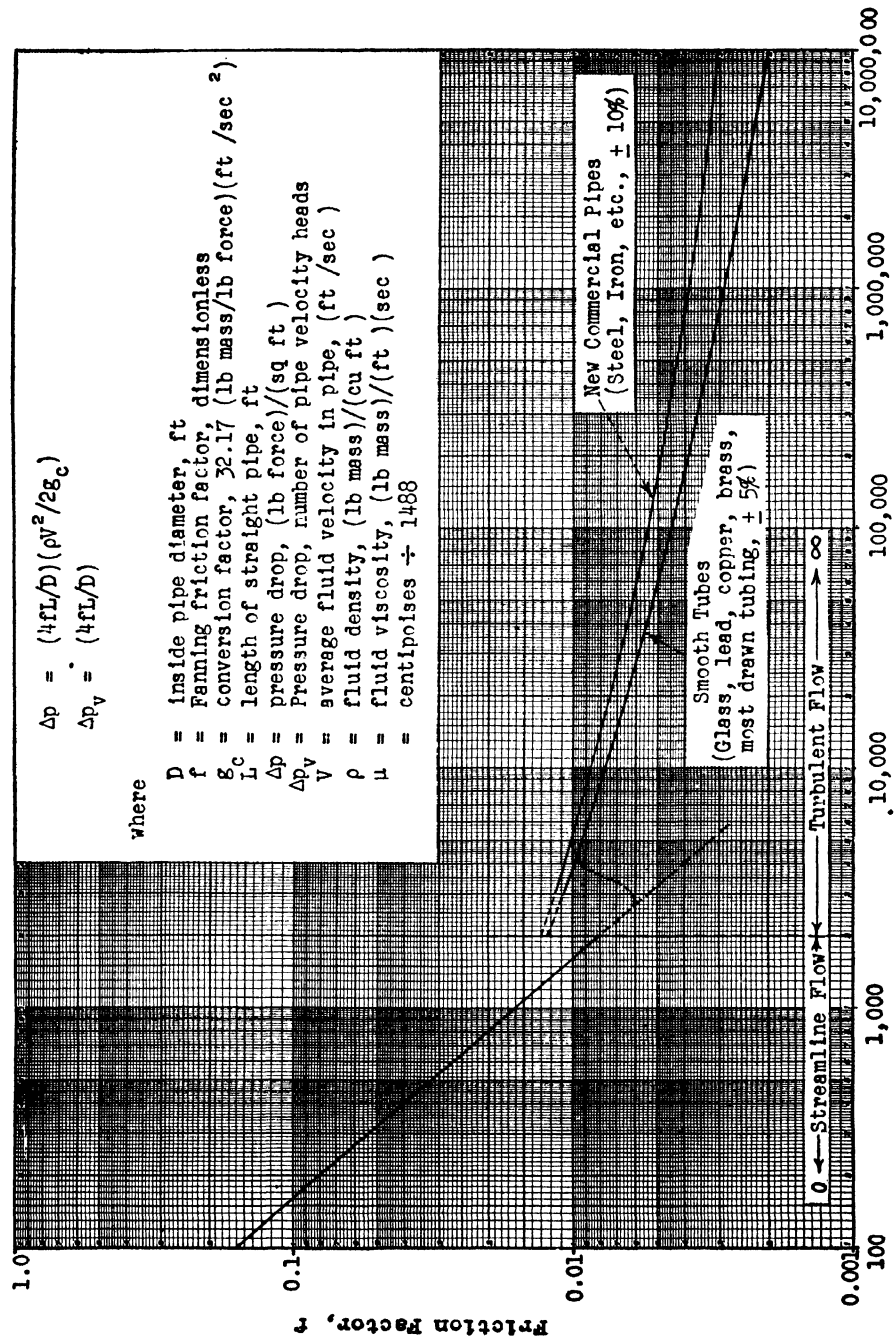


Fig. 4—Friction factor—Reynolds number plot for flow through straight circular smooth and commercial pipe (References 3, 6, and 10)

Table 2—Values of $(L/D)_v$ for New Commercial Pipe

Reynolds Number	Corresponding Value of f	$(L/D)_v$
5,000	0.0101	25
20,000	0.0075	35
50,000	0.0062	40
100,000	0.0054	46
1,000,000	0.0039	64

Equation 10 may be written in terms of velocity head as

$$\Delta p_v = \Delta p/(\rho V^2_{max}/2g_c) \quad \ldots\ldots\ldots\ldots\ldots\ldots [11]$$

where the velocity head is based on the maximum fluid velocity between tubes. The term f_1 is a function of tube arrangement and spacing as well as of the Reynolds number and for more detailed data the reader should refer to References 23-27. Fig. 5 gives a plot of f_1 vs. Re taken from a correlation given by Chilton and Genereaux (see Reference 22). In this plot the friction factor represents average values for the range of spacings commonly encountered in practice. To avoid possible misusage, it should also be pointed out that the line for the streamline flow region (Re less than 25) is shown on this basis merely for simplicity. This line represents the available streamline flow data for two staggered arrangements within ±40 per cent only and a better correlation in terms of hydraulic diameter is available (Reference 22). For Reynolds numbers expressed as $(D_c V_{max} \rho/\mu)$, greater than 100, the term f_1 has an average value of 0.18 and 0.08 for staggered and in-line arrangements, respectively, which is good to better than ±50 per cent for tube spacings commonly encountered in practice. For these average values of f_1, Equation 11 becomes

For staggered tubes:

$$\Delta p_v = 0.72\ N \quad \ldots\ldots\ldots [12]$$

For in-line tubes:

$$\Delta p_v = 0.32\ N \quad \ldots\ldots\ldots [13]$$

which means that each row has a pressure drop of 0.72 velocity head based on the maximum velocity for staggered rows, and 0.32 velocity head for in-line rows.

For a single row of tubes or for a tube bank of either staggered or in-line arrangement with a longitudinal spacing of more than five tube diameters, the flow would correspond to that of a number of rectangular nozzles in parallel. The pressure drop from the front of the tube to the point of minimum flow cross-section would be expected to be 1.0 velocity head. Some pressure recovery would then take place when the fluid expands again behind the tube. The overall pressure drop will then be given by Equation 24, which will be discussed in the section on metering devices. For actual arrangements, however, the longitudinal spacing is usually less than 2.0 tube diameters and the above equations, giving the average pressure drop per row for a tube bank of more than five rows deep, reflect the influence of the rows upon each other. Thus, if the second row is close to the first row, the pressure drop through the second row will be less than for the first row since the fluid still retains some of its high kinetic energy upon entering the second row, so that less pressure drop is required to again accelerate the fluid. Wallis and White (Reference 27) have given quantitative confirmation of the above statements and have shown that the pressure drop across the first row of tubes is the same for in-line or staggered arrangements. For in-line arrangements, close longitudinal spacing will decrease the apparent pressure drop per row, whereas for some staggered arrangements, the apparent pressure drop may increase because of prevention of complete pressure recovery behind the tube.

In practical application to baffled heat exchangers, the actual pressure drops may be as little as 0.1 of the pressure drop calculated from the above equations, because of leakage through the clearance between tubes and baffles (see Reference 21).

For baffled exchangers, the pressure drop across the baffles will depend on the tube configuration and very meager data are available. For most purposes, however, the pressure drop for flow around the baffle may be taken as 2.0 velocity heads based on the free area available for flow around the baffle (Reference 3, page 828).

References

General

1) Dodge, R. A., and Thompson, M. J., "Fluid Mechanics," New

Table 3—Pressure Drop Through Screwed Fittings and Valves (for Turbulent Flow Only)

D = Actual internal diameter of pipe of same nominal size as fitting, ft;
L_e = Equivalent length of straight pipe of same nominal size as fitting, ft;
Δp_v = Pressure drop, equivalent number of velocity heads based on velocity in pipe of same nominal size.

Type of Fitting or Valve		(L_e/D)	Δp_v
45 deg Elbow, standard		15	0.3
45 deg Elbow, long radius		10	0.2
90 deg Elbow, standard		32	0.74
	medium radius	26	0.60
	long sweep	20	0.46
	square	60	1.3
180 deg Bend, close return		75	1.7
	medium radius	50	1.2
Tee, standard, (along run, branch blanked off)		20	0.4
	(used as elbow, entering run)	60	1.3
	(used as elbow, entering branch)	70	1.5
	(branching flow)	..	1.0**
long radius (used as elbow, entering run)		30	0.5
Couplings		2	0.04
Unions		2	0.04
Gate valves,* open		7	0.13
	¾ open	40	0.8
	½ open	200	3.8
	¼ open	800	15.0
Globe valves,* bevel seat, open		350	6.3
	½ open	550	10.0
	composition disk, open	330	6.0
	½ open	500	9.0
	plug disk, open	500	9.0
	¾ open	700	13.0
	½ open	2000	35.0
	¼ open	6000	110.0
Angle valves,* open		170	3.0
Y or blowoff valves,* open		170	3.0
Check valves, swing		110***	2.0***
	disk	500***	10.0***
	ball	3500***	65.0***
Water meters, disk		400	8.0
	piston	600	12.0
	impulse wheel	300	6.0

*Direction of flow of fluid through valves has a negligible effect on pressure drop.
**This value refers to the velocity head in the main stream before branching. Depending on the relative flow split, this value ranges from 0.7 to 1.3 where the main flow enters the run and from 0.9 to 1.5 where the main flow enters the branch. This value gives the pressure differential (not friction loss) between run and branch.
***These values apply only when the check valve is fully open. The wide open condition is generally attained for pipe velocities over 3 ft/sec when handling water.

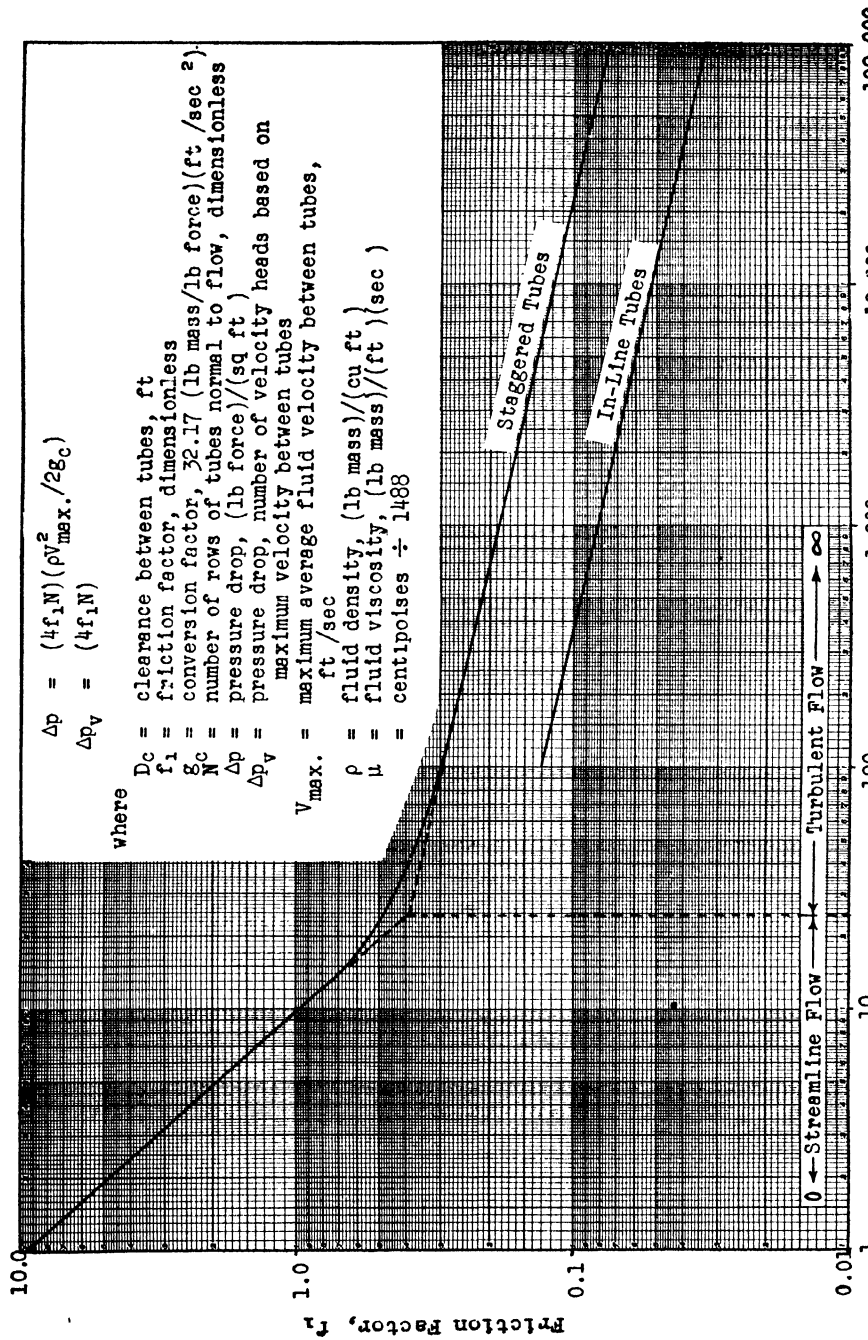


Fig. 5—Friction factor—Reynolds number plot for flow across tube banks. (Average value for tube spacings and arrangements commonly encountered—Reference 22)

York, McGraw-Hill Book Co., 1937.

2) O'Brien, M. P., and Hickox, G. H., "Applied Fluid Mechanics," New York, McGraw-Hill Book Co., 1937.

3) Perry, J. H., "Chemical Engineers' Handbook," 2nd Ed., Section 6, New York, McGraw-Hill Book Co., 1941.

4) Rouse, H., "Fluid Mechanics for Hydraulic Engineers," New York, McGraw-Hill Book Co., 1938.

5) Vennard, J. K., "Elementary Fluid Mechanics," New York, John Wiley & Sons, 1940.

Flow Through Pipes or Conduits

6) Drew, T. B., Koo, E. C., and McAdams, W. H., Trans. Am. Inst. Chem. Engrs., *28* 56-72 (1933); Chem. & Met. Eng., *39* 314 (1932).

7) Genereaux, R. P., Ind. Eng. Chem., *29* 385-8 (1937); Chem. & Met. Eng., *44* 241-8 (1937).

8) Kemler, E., Trans. Am. Soc. Mech. Engrs., *55* 7-32 (1933).

9) Nikuradse, J., Ver. deut. Ing., Forschungsheft No. 356 (1932), Forschungsheft No. 361 (1933); Petroleum Engineer, *11* 164-6 (1940) Mar., 75-82 (1940) May, 124-130 (1940) June, 38-42 (1940) July, 83-87 (1940) Aug.

10) Miller, B., Trans. Am. Inst. Chem. Engrs., *32* 1-26 (1936).

11) O'Brien, M. P., Folsom, R. G., and Jonassen, F., Ind. Eng. Chem., *31* 477-81 (1939).

12) Pigott, R. J. S., Mech. Eng., *55* 497-501, 515 (1933).

Flow Through Fittings and Valves

13) Crane Co., "Flow of Fluids," Technical Paper No. 409, Chicago, May 1942.

14) Freeman, J. J., "Experiments upon the Flow of Water in Pipes and Pipe Fittings," Am. Soc. Mech. Engrs., 1941.

15) Gibson, A. H., "Hydraulics and Its Applications," 3rd Ed., London, Constable and Co., 1925.

16) Giesecke, F. E., and Badgett, W. H., Heating, Piping & Air Conditioning, *3* 430-2 (1931), *4* 53-6, 443-7 (1932).

17) Giesecke, F. E., and Hopper, J. S., Heating, Piping & Air Conditioning, *13* 115-22 (1941).

18) Giesecke, F. E., Reming, C. P., and Knudson, J. W., Jr., Univ. Texas Bull. 2712, March 22, 1927.

19a) Greve, F. W., Purdue Univ. Eng. Exp. Sta. Bull., *27*, Research Series No. 88, May 1943.

19b) Lansford, W. M., Univ. of Illinois Eng. Exp. Sta., *40* Bulletin No. 340, Feb. 2, 1943.

20) Wilson, R. E., McAdams, W. H., and Seltzer, M., Ind. Eng. Chem., *14* 105-119 (1922).

Flow Across Tube Banks

21) Bowman, R. A., "Heat Transfer," pp. 75-81, Am. Soc. Mech. Engrs., 1936.

22) Chilton, T. H., and Genereaux, R. P., Trans. Am. Inst. Chem. Engrs., *29* 161-173 (1933).

23) Grimison, E. D., Trans. Am. Soc. Mech. Engrs., *59* 583-94 (1937).

24) Huge, E. C., Trans. Am. Soc. Mech. Engrs., *59* 573-81 (1937).

25) Jakob, M., Trans. Am. Soc. Mech. Engrs., *60* 381-92 (1938).

26) Pierson, O. L., Trans. Am. Soc. Mech. Engrs., *59* 563-72 (1937).

27) Wallis, R. P., and White, C. M., Engineering *146* 605-7, 665-6, 723-5 (1938); *147* 487-9 (1939); J. & Proc. Instn. Mech. Engrs. (London), *142* 379-87 (1939).

Using the Velocity Head Concept in

PRESSURE DROP CALCULATIONS

By C. E. Lapple*

THE FRICTION loss or pressure drop through a bed of granular solids may be expressed as

$$F = \Delta p = (4f_2 L/D_p)\ (\rho V^2/2g_c) \quad \ldots\ldots\ldots [14]$$

$$\Delta p_v = (4f_2 L/D_p) \quad \ldots\ldots\ldots [15]$$

where f_2 is a form of friction factor which is a function of the Reynolds number, $(D_p V \rho/\mu)$, based on the particle diameter and the superficial fluid velocity based on the gross bed cross-sectional area.

Friction Loss Through Granular Beds

In Fig. 6 is given a plot of f_2 vs. *Re* taken from a correlation reported by Chilton and Colburn (Reference 30). This plot makes no allowance for particle shape or degree of packing, but represents an average value of f_2 for shapes and degrees of packing commonly encountered in practice. Actually the particle shape and degree of packing affect the value of f_2 as well as Reynolds number and for further data along these lines the reader is referred to References 28-32.

For an average value of 15.0 for f_2, which holds to better than $\pm$ 50 per cent for the turbulent flow range $(D_p V \rho/\mu > 80)$ and degree of packing commonly encountered in practice, Equation 15 becomes

$$\Delta p_v = 60\ (L/D_p) \quad \ldots\ldots\ldots [16]$$

which means that for each layer of particles (i.e. $L = D_p$), a pressure drop of 60 superficial velocity heads results. From a velocity head visualization and analysis, it would appear from this value that the maximum velocity head attained by the fluid in passing through a single layer of particles is on the order of 60 times the superficial velocity head. This would imply that the minimum cross-section available for flow between particles is on the order of 0.13 of the overall cross-section of the particle bed. The ratio of minimum flow cross-section to overall bed cross-section can be calculated as 0.09 and 0.21 for triangular and rectangular packing of uniform spheres, respectively. Thus, the pressure drop through each layer of particles may be visualized as on the order of one velocity head based on the minimum area available for flow between particles.

Friction Loss for Abrupt Expansion

The friction loss for an abrupt expansion as derived from a momentum balance is given by

$$F_v = (1 - \alpha)^2 \quad \ldots\ldots\ldots [17]$$

where F_v is based on the velocity head in the smaller (upstream) cross-section and α is the ratio of upstream to downstream cross-section. Thus, for an abrupt expansion into a very large chamber ($\alpha = 0$), the friction loss is one velocity head.

The pressure drop for an abrupt expansion is obtained by adding algebraically the difference between the downstream velocity head and the upstream velocity head to the friction loss. The pressure drop for an infinite expansion is thus zero. For expansion into a finite area, the pressure drop is negative, which means that a pressure recovery is obtained.

Friction Loss for Abrupt Inlet

The friction loss for an abrupt inlet is given by

$$F_v = K_1 (K_2 - \alpha) \quad \ldots\ldots\ldots [18]$$

where F_v is based on the velocity head in the smaller (downstream) cross-section, α is the ratio of downstream to upstream areas, and K_1 and K_2 are constants determined experimentally. The inlet loss is due largely to a contraction of the stream at the inlet with subsequent partial recovery. The values K_1 and K_2 are found experimentally to be

For $\alpha < 0.715$, $K_1 = 0.4$ and $K_2 = 1.25$
For $\alpha > 0.715$, $K_1 = 0.75$ and $K_2 = 1.00$

The friction loss for an abrupt inlet from a relatively large chamber is thus found to be 0.5 velocity head based on the inlet area. The pressure drop is found by algebraically adding the difference between the downstream and upstream velocity heads to the friction loss. For an abrupt inlet from a large chamber, the pressure drop is thus 1.5 inlet velocity heads.

Differential Heads Across Metering Devices

For metering devices in which a differential head is measured, the flow rate is related to the differential head in terms of a discharge coefficient, C, defined in various arbitrary ways. It is also possible

DESIGN OF pipe lines, process equipment, ventilation systems, etc., requires estimation of pressure drops in order to specify the required pump, compressor, fan, or blower capacities. Pressure drop estimates are often necessary, too, in the operation of equipment for purposes of locating possible plugged or corroded lines, checking process performance, or determining bottlenecks for proposed capacity increases. The article of which this is the third and last part (the first was published in the April issue) is intended as a guide to a physical conception or visualization of otherwise seemingly complex fluid flow phenomena. The approximations presented will be found to be entirely adequate for many purposes, and an attempt has been made to point out their limits of accuracy.

*Engineering Dept., Chemical Engineering and Metallurgical Laboratory, Experimental Station, E. I. du Pont de Nemours & Co., Inc.

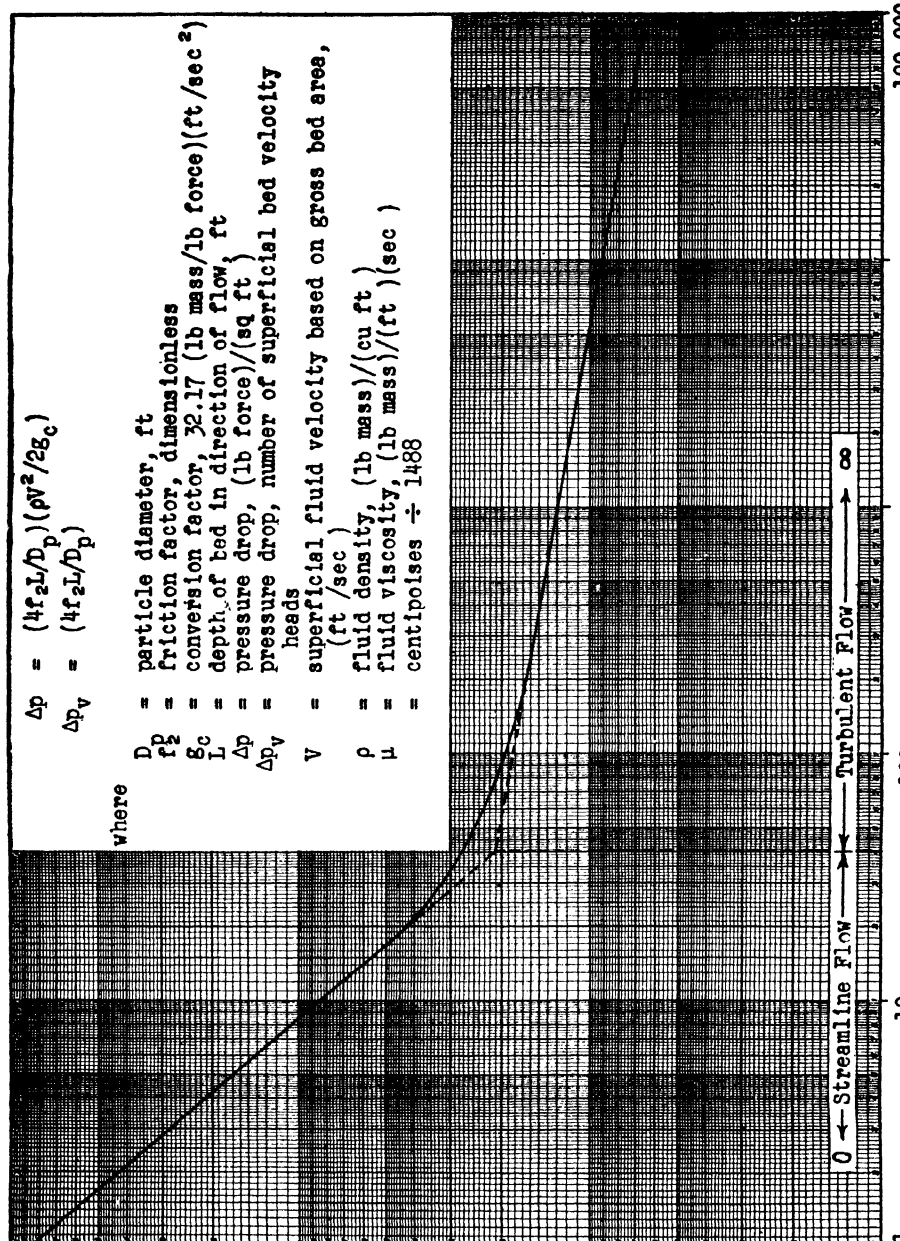


Fig. 6—Friction factor-Reynolds number plot for flow through beds of granular solids. (Average values for particle shapes and degree of packing commonly encountered.) (See Reference 30.)

to express the differential head in terms of number of velocity heads, as will be shown in the following examples for common metering devices.

Pitot Tube

The equation for calculating velocity from a pitot tube reading is commonly given as

$$V = C\sqrt{2g_c\,\Delta p/\rho} \quad \ldots\ldots [19]$$

where C is a coefficient depending on the type of pitot tube used and Δp is the differential reading obtained. This may be rewritten to express Δp as a number of velocity heads

$$\Delta p_v = \Delta p/(\rho V^2/2g_c) = 1/C^2 \quad \ldots. [20]$$

For the standard single-bend pitot tube, the impact tube records the static pressure of the fluid plus the impact or velocity head, while the static holes on the side record substantially the static pressure. The differential head is, therefore, substantially one velocity head, and C is experimentally found to be very close to unity. For a double long-bend pitot tube, the impact tube records the static plus impact pressure of the fluid, while the static tube records the static pressure minus a suction effect dependent on the kinetic energy of the fluid. The differential head is consequently greater than one velocity head by the magnitude of the suction effect. Experimental data indicate C for this type of tube to be 0.855 and hence Δp_v is 1.37, which means that the suction effect is equal to 0.37 velocity head. It should be pointed out that the velocity head in each case refers to that corresponding to the local velocity of the fluid stream at the point where the pitot tube is located.

Nozzle and Venturi Meters

For nozzle and venturi meters, the differential head, Δp, between an upstream pressure tap and the throat of the nozzle or venturi is related to the average fluid velocity at the throat by the expression

$$V = C\sqrt{2g_c(\Delta p/\rho)/(1-\alpha^4)} \quad [21]$$

where α is the ratio of the throat to pipe area and C is a discharge coefficient. Written in terms of velocity head, Equation 21 becomes

$$\Delta p_v = \Delta p/(V^2/2g_c) = (1-\alpha^4)/C^2 \quad \ldots\ldots [22]$$

where Δp_v represents the differential head in terms of velocity head based on the throat area. Expressing Δp_v as the differential head in terms of pipe velocity head, Equation 22 becomes

$$\Delta p_v = (1-\alpha^4)/\alpha^4 C^2 \quad \ldots\ldots [23]$$

In this type of meter, pressure energy is converted into velocity energy in accelerating the fluid from the pipe velocity to the meter throat velocity and the differential head measures essentially the difference in velocity heads at the throat and in the pipe, plus any frictional losses encountered during the acceleration. The coefficient C is found experimentally to be 0.98-0.99 for Reynolds numbers, based on pipe velocity and diameter, greater than 10,000. Thus, Equation 22 indicates that the differential head is substantially one throat velocity head where the throat area is small compared to the pipe area. The differential head is greater than one throat velocity head by only 2 to 4 per cent due to frictional losses. For larger throat areas, the differential head is lower by one pipe or approach velocity head, which is allowed for in Equation 22 by the term $(1-\alpha^2)$, which is commonly known as the velocity of approach correction.

Orifice Meters

For sharp-edged orifice meters Equations 21, 22, and 23 also apply, where V is the velocity based on the orifice area. The coefficient C, however, is found to vary with the ratio of orifice to pipe diameter, but for pipe Reynolds numbers greater than 10,000 and ratios of orifice to pipe diameter of less than 0.8, the value of C is substantially equal to 0.61 where vena contracta taps are employed.

A sharp-edged orifice differs from a nozzle in that the fluid stream contracts to an area less than that of the orifice due to the sharp edge of the orifice. Thus, the differential head from an upstream pressure tap to the vena contracta of the fluid stream must represent the difference in velocity heads at the vena contracta and in the pipe, plus any additional frictional losses. Since, in the usual equations, the velocity is based on the orifice area, the coefficient C must incorporate two factors, an allow-

Nomenclature

C = Discharge coefficient for orifice, nozzle, venturi, or pitot tube, dimensionless;
D = Inside diameter of circular pipe, ft;
D_c = Clearance between tubes in a tube bank, ft;
D_p = Diameter of granular particle, ft;
f_s = Friction factor for flow through beds of granular solids, dimensionless;
F = Friction loss (lb force)/(sq ft)†
F_v = Friction loss, number of velocity heads, dimensionless;
g_c = Conversion factor, 32.17 (lb mass/lb force) (ft/sec²);
K_1, K_2 = Constants, dimensionless;
L = Length of straight horizontal pipe or depth of bed of granular solids in direction of flow, ft;
$(L/D)_v$ = Length of straight pipe expressed as number of pipe diameters, for which pressure drop is one velocity head (i. e., for which $\Delta p_v = 1$), dimensionless;
p_v = Velocity head, (lb force)/(sq ft);
Δp = Pressure drop, (lb force)/(sq ft);
Δp_v = Pressure drop, number of velocity heads, dimensionless;
R_e = Reynolds number, dimensionless = $(DV\rho/\mu)$ for flow through pipes, orifices, nozzles, or venturis; $D_c V_{max.}\rho/\mu)$ for flow across tube banks; $(D_p V\ \rho/\mu)$ for flow through beds of granular solids;
V = Average fluid velocity, (ft/sec);
$V_{max.}$ = Maximum average fluid velocity in flow across tube banks, (ft/sec);
ρ = Fluid density, (lb mass)/(cu ft);
μ = Fluid viscosity, (lb mass)/(ft) (sec) = centipoises ÷ 1488;
α = Ratio of areas, dimensionless—a value less than unity.

†Friction loss is often defined as an energy loss per unit mass of fluid, having the dimensions (ft-lb force)/(lb mass). This definition of friction loss is equivalent to the quotient F/ρ.

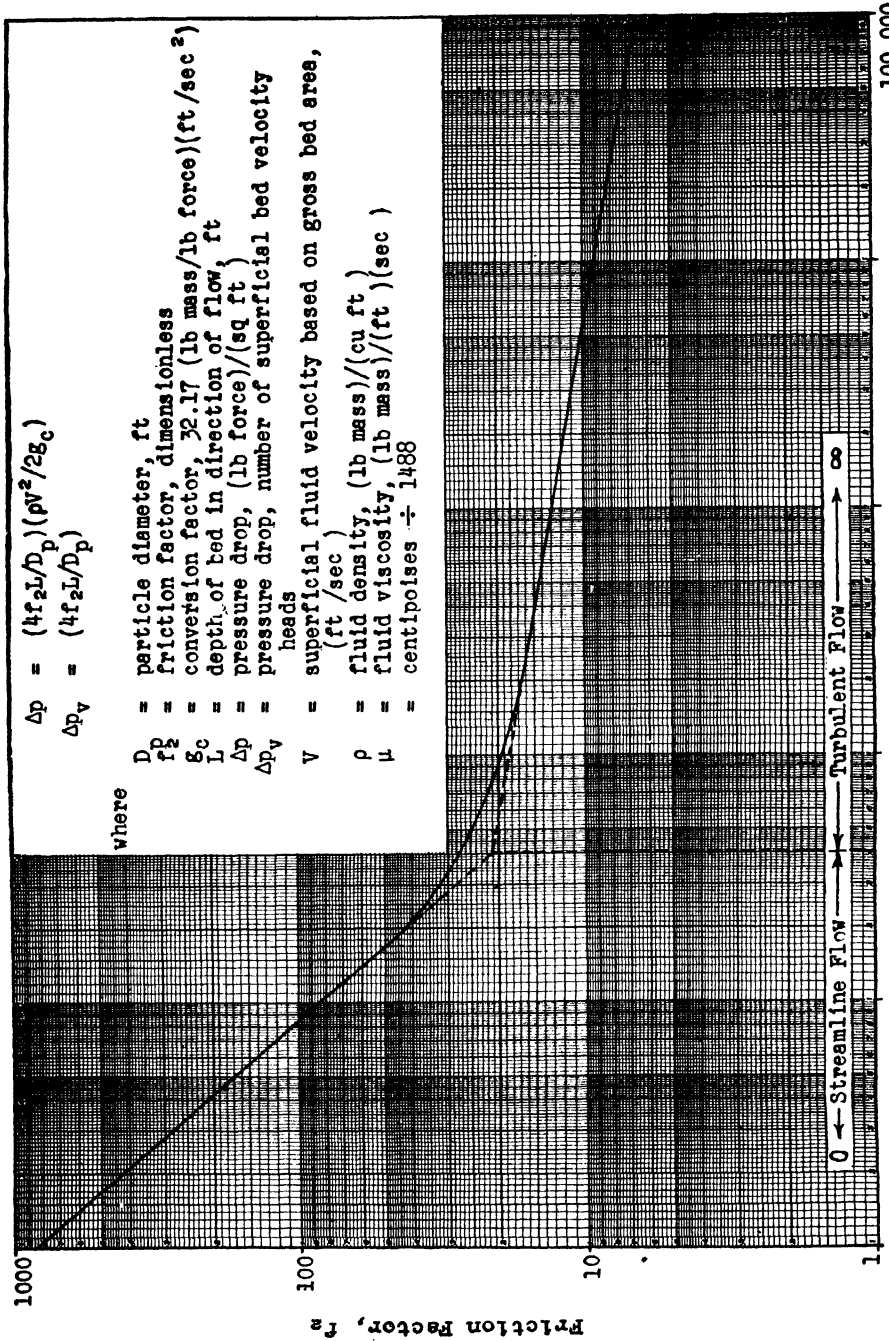


Fig. 6—Friction factor-Reynolds number plot for flow through beds of granular solids. (Average values for particle shapes and degree of packing commonly encountered.) (See Reference 30.)

to express the differential head in terms of number of velocity heads, as will be shown in the following examples for common metering devices.

Pitot Tube

The equation for calculating velocity from a pitot tube reading is commonly given as

$$V = C\sqrt{2g_c\,\Delta p/\rho} \quad \ldots\ldots [19]$$

where C is a coefficient depending on the type of pitot tube used and Δp is the differential reading obtained. This may be rewritten to express Δp as a number of velocity heads

$$\Delta p_v = \Delta p/(\rho V^2/2g_c) = 1/C^2 \quad \ldots. [20]$$

For the standard single-bend pitot tube, the impact tube records the static pressure of the fluid plus the impact or velocity head, while the static holes on the side record substantially the static pressure. The differential head is, therefore, substantially one velocity head, and C is experimentally found to be very close to unity. For a double long-bend pitot tube, the impact tube records the static plus impact pressure of the fluid, while the static tube records the static pressure minus a suction effect dependent on the kinetic energy of the fluid. The differential head is consequently greater than one velocity head by the magnitude of the suction effect. Experimental data indicate C for this type of tube to be 0.855 and hence Δp_v is 1.37, which means that the suction effect is equal to 0.37 velocity head. It should be pointed out that the velocity head in each case refers to that corresponding to the local velocity of the fluid stream at the point where the pitot tube is located.

Nozzle and Venturi Meters

For nozzle and venturi meters, the differential head, Δp, between an upstream pressure tap and the throat of the nozzle or venturi is related to the average fluid velocity at the throat by the expression

$$V = C\sqrt{2g_c(\Delta p/\rho)/(1-a^4)} \quad [21]$$

where a is the ratio of the throat to pipe area and C is a discharge coefficient. Written in terms of velocity head, Equation 21 becomes

$$\Delta p_v = \Delta p/(V^2/2g_c) = (1-a^4)/C^2 \quad \ldots\ldots [22]$$

where Δp_v represents the differential head in terms of velocity head based on the throat area. Expressing Δp_v as the differential head in terms of pipe velocity head, Equation 22 becomes

$$\Delta p_v = (1-a^4)/a^2C^2 \quad \ldots\ldots [23]$$

In this type of meter, pressure energy is converted into velocity energy in accelerating the fluid from the pipe velocity to the meter throat velocity and the differential head measures essentially the difference in velocity heads at the throat and in the pipe, plus any frictional losses encountered during the acceleration. The coefficient C is found experimentally to be 0.98-0.99 for Reynolds numbers, based on pipe velocity and diameter, greater than 10,000. Thus, Equation 22 indicates that the differential head is substantially one throat velocity head where the throat area is small compared to the pipe area. The differential head is greater than one throat velocity head by only 2 to 4 per cent due to frictional losses. For larger throat areas, the differential head is lower by one pipe or approach velocity head, which is allowed for in Equation 22 by the term $(1-a^2)$, which is commonly known as the velocity of approach correction.

Orifice Meters

For sharp-edged orifice meters Equations 21, 22, and 23 also apply, where V is the velocity based on the orifice area. The coefficient C, however, is found to vary with the ratio of orifice to pipe diameter, but for pipe Reynolds numbers greater than 10,000 and ratios of orifice to pipe diameter of less than 0.8, the value of C is substantially equal to 0.61 where vena contracta taps are employed.

A sharp-edged orifice differs from a nozzle in that the fluid stream contracts to an area less than that of the orifice due to the sharp edge of the orifice. Thus, the differential head from an upstream pressure tap to the vena contracta of the fluid stream must represent the difference in velocity heads at the vena contracta and in the pipe, plus any additional frictional losses. Since, in the usual equations, the velocity is based on the orifice area, the coefficient C must incorporate two factors, an allow-

Nomenclature

C = Discharge coefficient for orifice, nozzle, venturi, or pitot tube, dimensionless;
D = Inside diameter of circular pipe, ft;
D_c = Clearance between tubes in a tube bank, ft;
D_p = Diameter of granular particle, ft;
f_s = Friction factor for flow through beds of granular solids, dimensionless;
F = Friction loss (lb force)/(sq ft)†
F_v = Friction loss, number of velocity heads, dimensionless;
g_c = Conversion factor, 32.17 (lb mass/lb force) (ft/sec²);
K_1, K_2 = Constants, dimensionless;
L = Length of straight horizontal pipe or depth of bed of granular solids in direction of flow, ft;
$(L/D)_v$ = Length of straight pipe expressed as number of pipe diameters, for which pressure drop is one velocity head (i. e., for which $\Delta p_v = 1$), dimensionless;
p_v = Velocity head, (lb force)/(sq ft);
Δp = Pressure drop, (lb force)/(sq ft);
Δp_v = Pressure drop, number of velocity heads, dimensionless;
R_e = Reynolds number, dimensionless = $(DV\rho/\mu)$ for flow through pipes, orifices, nozzles, or venturis; $D_cV_{max.}\rho/\mu)$ for flow across tube banks; $(D_pV\rho/\mu)$ for flow through beds of granular solids;
V = Average fluid velocity, (ft/sec);
$V_{max.}$ = Maximum average fluid velocity in flow across tube banks, (ft/sec);
ρ = Fluid density, (lb mass)/(cu ft);
μ = Fluid viscosity, (lb mass)/(ft)(sec) = centipoises ÷ 1488;
a = Ratio of areas, dimensionless—a value less than unity.

†Friction loss is often defined as an energy loss per unit mass of fluid, having the dimensions (ft-lb force)/(lb mass). This definition of friction loss is equivalent to the quotient F/ρ.

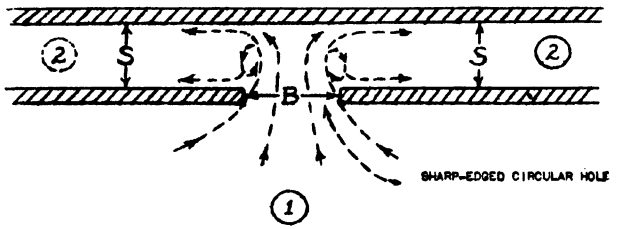


Fig. 7—The text explains flow calculations for such items as this jacket flow distributor.

ance for frictional losses and an allowance for the contraction of the stream. If the equations were based on the velocity or area at the vena contracta, rather than on the orifice area, the coefficient C would be practically the same as for a nozzle, i.e., 0.99, indicating that the frictional pressure loss corresponds to only about 2 per cent of the differential head. The fluid area at the vena contracta, however, is about 62 per cent of the orifice area, so that when the equations are based on orifice area, the effective coefficient, C, must be substantially the product of 0.99 and 0.62. Thus, contrary to a general misconception that an orifice is less efficient than a nozzle because the discharge coefficient is 0.99 for a nozzle and 0.61 for an orifice, an orifice merely behaves like a nozzle with a throat area of 0.62 that of the orifice.

It follows from Equation 22 that for orifice to pipe diameter ratios of less than 0.3, the differential head for vena contracta taps is substantially one velocity head based on the vena contracta area and 2.7 velocity heads based on the orifice area, since the velocity of approach correction is negligible in this case.

Partial recovery of pressure takes place following both an orifice and a nozzle. Such recovery is substantially complete at a distance of four pipe diameters downstream from the orifice or nozzle. The overall pressure drop across an orifice or nozzle for conditions of fully recovered head (which also corresponds to the pressure differential for an orifice or nozzle with pipe taps) can be calculated from a momentum balance, and is very closely approximated by

$$\Delta p_v = \left[\left(\sqrt{\frac{1+a^2C^2-a^2}{a^2C^2}}\right)-1\right]^2 \quad [24]$$

where Δp_v is expressed as number of pipe velocity heads; a is the ratio of nozzle or orifice area to pipe area; and C is the respective discharge coefficient for the nozzle or orifice with vena contracta taps (0.99 for a nozzle, 0.61 for a sharp-edged orifice). In order to obtain a given differential head for a fixed flow rate, a nozzle must have a throat area of 0.62 times that of a sharp-edged orifice, and it can be shown from Equation 24 that the recovered head or overall permanent loss will be the same, in this case, for both the nozzle and orifice.

Estimation of Pressure Drop or Friction Loss

In each of the previous examples, an interpretation in terms of velocity head has been presented to give the reader a semi-quantitative conception of the pressure drop in terms of the physical flow pattern

Cases for which no actual experimental data are available frequently arise in practice, and it is up to the designer to estimate the pressure drop or obtain the required data by laboratory measurements. By visualizing the flow pattern that is apt to occur in such cases, it should be possible for the reader to make a reasonable estimate of the pressure drop for turbulent flow by applying the velocity head concept in a manner similar to the analyses presented in the previous paragraphs. Two further examples will be cited to illustrate the method for making such estimates.

Considering the flow through a sharp welded 90 deg bend, formed by the intersection of two equal cylinders, it is to be expected that the fluid loses its initial kinetic energy by impact at the bend and the kinetic energy required to permit flow out of the bend must be supplied from the pressure energy of the gas. Thus, the pressure drop (or friction loss) would be expected to be 1.0 velocity head. This is in good agreement with actual data. Table 3 (page 265, May HPAC) indicates a loss of 1.3 velocity heads for a square 90 deg screwed fitting. The additional 0.3 velocity head in this case is due largely to the expansion and contraction losses encountered in a screwed fitting.

Fig. 7 is a sketch of an element of a type of flow distributor sometimes encountered in practice for which no data appear to be available. The fluid, after passing through a sharp-edged distributor hole or orifice of diameter B impinges upon a back-up plate (which may actually correspond to a jacket wall) spaced a distance S behind the orifice plate, which deflects the stream laterally as indicated in Fig. 7. The fluid in passing through the sharp-edged hole contracts to a "vena contracta" as in the case of the sharp-edged orifice. The kinetic energy represented by the velocity head at the vena contracta is then substantially lost by impingement on the back-up plate. In order to develop the velocity for lateral movement through the cylindrical area πBS between the plates at the edge of the hole, pressure energy must also be converted into velocity energy. This would correspond to one velocity head based on the area πBS. Since the lateral expansion radially away from the hole is relatively abrupt, this kinetic energy is largely dissipated as heat by turbulence. The overall pressure drop from *1* to *2* may thus be visualized as the sum of the velocity head corresponding to the vena contracta of the stream following the distributor hole and the velocity head corresponding to the area πBS. If the distributor plate containing the hole is relatively thin compared to the hole

diameter (on the order of ½ or less), the contraction will be the same as for a sharp-edged orifice and the area of the fluid stream at the vena contracta will be 0.61 of the hole area, $\pi B^2/4$. Thus, the pressure drop would be expected to be 2.7 velocity heads based on the hole area (since this is the equivalent of 1.0 velocity head based on the vena contracta) plus 1.0 velocity head based on the cylindrical area πBS. Recent unpublished measurements indicated that this prediction checked actual data within ± 10 per cent. These tests were made with air using a 16 ga plate with a sharp-edged orifice of 0.8 in. diameter. The plate spacing, S, was varied from infinity (i.e., no back-up plate employed) to 0.075 in. and the air velocity based on the 0.8 in. diameter hole was varied from 25 to 150 ft/sec corresponding to a Reynolds number range based on the hole area of from 10,000 to 60,000. Two back-up plates, 2⅛ in. and 3¾ in. diameter, were tested, but both gave substantially the same results.

It should be pointed out that the flow pattern and mechanism in these two examples has possibly been oversimplified in order to enable a pressure drop estimate to be made. For example, in the case of the distributor plate, there is probably some recovery of kinetic energy upon impact following passage of the fluid through the hole and some contraction of the fluid must occur as it passes through the area πBS. These two factors, however, tend to counteract each other in so far as overall pressure drop is concerned. Also, if the plate spacing, S, is small compared to the hole diameter, B, the jet contraction following the hole is probably not complete before impingement takes place. In this case, however, the pressure drop across the hole is a relatively small portion of the overall pressure drop. The fact that the simplified flow pattern checked so closely with experiment must be attributed to some extent to a coincidence resulting from a compensation of factors in the actual flow pattern. Thus, in making estimates of this type, due allowances in the form of safety factors should be made. The magnitude of these factors will vary with each case, but some idea of this magnitude can be obtained by considering the possible extreme flow patterns. Usually such estimates of pressure drop can be relied on to better than ± 50 per cent.

Numerical Examples

In order to familiarize the reader further with the application of the velocity head method to actual pressure drop calculations, the following numerical examples are presented.

Example 1: A 2 in. Schedule 40 pipe is handling 50 gal/min of water. What is the pressue drop across 200 ft of this pipe containing 12 standard ells and one fully open globe valve?

Solution:

Pipe diameter = 2.067 in.

Pipe area = (0.785) $(2.067)^2/144$ = 0.0233 sq ft.

Pipe velocity = V = (50)/(7.48) (60) (0.0233) = 4.78 ft/sec.

Velocity head in pipe = $(4.78)^2/(2)(32.17)$ = 0.36 ft of water.

Assume $(L/D)_v = 40$ (actually a calculation of the Reynolds number and corresponding friction factor would show $(L/D)_v = 44$).

Pressure Drop:

Through pipe = (200) (12)/(2.067) (40) = 29.0 pipe velocity heads.

Through ells = (12) (0.74) (from Table 3, page 265, May HPAC) = 8.9 pipe velocity heads.

Through globe valve = (1) (9.0) (from Table 3) = 9.0 pipe velocity heads.

The total pressure drop is thus 46.9 pipe velocity heads, or 46.9 × 0.36 = 16.9 ft of water.

The above calculation does not allow for any inlet or outlet losses from the pipe, which will depend on configuration at the ends of the section considered and will be zero if the section considered is but a portion of a longer, continuous length of piping.

Example 2: A 10.00 in. standard sharp-edged orifice in a 20 in. diameter duct with vena contracta taps indicates a differential reading of 3.5 in. water when handling air at 20 C and atmospheric pressure. What is the air flow rate?

Solution:

$a = (10/20)^2 = 0.25$; assume $C = 0.61$.

Orifice differential = $[1 - (0.25)^2]/(0.61)^2$ = 2.52 velocity heads based on orifice area.

Therefore velocity head based on orifice area = (3.5)/(2.52) = 1.39 in. of water.

From Fig. 1 (page 180, April HPAC), velocity based on orifice area is 78.4 ft/sec.

Orifice area = (0.785) $(10/12)^2$ = 0.545 sq ft.

Therefore air handled = (0.545) (78.4) (60) = 2560 cu ft/min.

Fig. 3 (page 182, April issue)

References

Flow Through Beds of Granular Solids

28) Bakhmeteff, B. A., and Feodoroff, N. V., Trans. Am. Soc. Mech. Engrs., J. Applied Mech. *4*, A97-104 (1937); discussion, *5*, A86-90 (1938).

29) Carman, P. C., Trans. Inst. Chem. Engrs. (London) *15*, 150-66 (1937).

30) Chilton, T. H., and Colburn, A. P., Ind. Eng. Chem., *23*, 913-19 (1931); Trans. Am. Inst. Chem. Engrs., *26*, 178-196 (1931).

31) Hatch, L. P., Trans. Am. Soc. Mech. Engrs., J. Applied Mech., *7*, A109-12 (1940).

32) Meyer, W. G., and Work, L. T., Trans. Am. Inst. Chem. Engrs., *33*, 13-33 (1937).

Nozzles, Orifices, Pitot Tubes, Venturis

33) Am. Soc. Mech. Engrs., Special Committee on Fluid Meters, "Fluid Meters, Description of Meters," Part 2, 1931; "Fluid Meters, Their Selection and Installation," Part 3, 1933; "Fluid Meters, Their Theory and Application," Part 1, 4th Ed., 1937; "Flow Measurement," 1940.

34) Cole, E. S., Trans. Am. Soc. Mech. Engrs., *57*, 281-94 (1935).

35) Goodman, W., Heating, Piping & Air Conditioning, *15*, 413-8, 461-4, 525-8, 596-8, 632-6 (1943), *16*, 8-10, 80-2 (1944).

36) Hubbard, C. W., Trans. Am. Soc. Mech. Engrs., *61*, 477-506 (1939).

37) Pigott, R. J. S., Trans. Am. Soc. Mech. Engrs., *58*, 146-156 (1936).

could also be used in place of the last two steps. Thus, for a 10 in. duct, (ft/sec)/(cu ft/min) = 0.0306. Therefore air rate = (78.4)/(0.0306) = 2560 cu ft/min.

Epilogue

In conclusion, the author must apologize for the numerous cases where scientific accuracy and rigor have been discarded for the sake of simplicity. This paper is intended largely as a guide to a physical conception or visualization of otherwise seemingly complex fluid phenomena, rather than as a survey of available pressure drop data, and this sacrifice was deliberate. For many purposes the approximations presented will be entirely adequate, and an attempt has been made to point out the limits of accuracy in each case. Where more accuracy is required, the reader can supply the necessary refinements by reference to the cited literature. The velocity head method of calculation can still be retained, however, and should serve to guide the designer away from the possible errors that lurk in any calculation in the form of units, decimal points, and general interpretation. For cases where no data are available, the interpretations presented should serve as means of obtaining reasonable estimates in place of a possible temptation to resort to intuitive guessing.

II. Problems

1. Using the velocity head concept, calculate the friction loss, in in. water, through the following for a flow of 150 lb./min. of air at atmospheric pressure and 70°F.:

(a) 1,000 ft. of 12-in. i.d. duct containing 12 standard 90° ells. (Assume ductwork offers the same friction as commercial pipe.)

(b) A 9-in. diameter sharp-edged orifice in a 12-in. diameter duct.

(c) A 20-ft. depth of 1-in. diameter quartz packing in a 4-ft. diameter tower.

2. Calculate the average (square mean root) reading, in in. water, which would be obtained from a pitot tube traverse of the 12-in. diameter duct in Problem 1, the pitot tube being of the double, long-bend type.

3. The front of a house is exposed to a 10 mi./hr. wind. Using the velocity head concept, estimate the air circulation through the house in cu.ft./min., if, in passing through the house, the air must go in series through three archways, each 30 sq.ft. in area, in addition to the front and back doors, each of which is wide open, is 3 ft. wide by 7 ft. high, and is followed by a closed screen door of the same size containing a wire screen composed of sixteen 0.010-in. diameter wires per lineal inch. No other doors or windows are open. Assume the screen occupies 70% of the total door area to allow for the wood framing. Assume also that, in addition to impact pressure of wind, a suction pressure of 0.2 wind velocity heads is created in back of the house.

4. In a system for the recovery of solvents present in relatively dilute concentration in air, 12,000 cu.ft./min. of air at 25°C. and substantially atmospheric pressure are passed successively through the following pieces of equipment.

(1) A 16-ft. diameter vertical entrainment separator packed with 4 ft. of 3/8-in. diameter pebbles, the air passing up through the packing.

(2) Two 40-ft. diameter mist separators operated in parallel, each packed with 2 ft. of 20-mesh (Tyler) coke.

(3) A 24-ft. long by 8-ft. diameter, horizontal carbon adsorber, packed with a 12-in. depth of 10-mesh (Tyler) granulated carbon. The air passes down through the carbon bed which has an average effective width of 7 ft.

(4) A 20.00-in. diameter sharp-edged orifice with vena contracta taps located in a 30-in. o.d. Schedule 30 line.

(5) A total of 210 ft. of straight 30-in. o.d. Schedule-30 pipe containing 6 medium radius 90° ells, 1 gate valve, and 3 standard tees used as ells.

All equipment inlets and exit nozzles are abrupt. The pressure drop due to the supporting grid-work for the packing in all towers can be neglected as well as the loss in the inlet and exit manifolds to the 40-ft. diameter mist separators operated in parallel. No details of bed voidage are available for any of the packings. A centrifugal fan is employed as the motivating force in the exhaust line and discharges directly to the atmosphere.

Using the velocity head concept wherever possible and applicable, calculate

(a) The pressure drop, in inches of water, through each piece of equipment, including exit and entrance losses.

(b) The pressure drop, in inches of water, directly attributable to the piping, fittings, and valves (i.e. not including exit and entrance losses to equipment).

(c) The orifice meter reading, in inches of water.

(d) The total pressure drop, in inches of water, through the system.

(e) The power consumption and annual power cost, assuming a 55% over-all efficiency for the blower, motor and drive, and a power cost of 7 mils/kw.hr. Assume continuous operation (24 hr./day) for 300 days/yr.

5. What is the relationship between the Fanning friction factor and the shear stress at the wall of a pipe, expressed as number of superficial pipe velocity heads?

Chapter 4

FLOW OF COMPRESSIBLE FLUIDS

by

C. E. Lapple*
Engineering Research Laboratory
Engineering Department
E. I. du Pont de Nemours & Co., Inc.
Wilmington, Delaware

TABLE OF CONTENTS

	Page
I. References	52
II. Nomenclature	52
III. Introduction	53
IV. General Principles	53
V. Critical Flow	54
VI. Mach Number	55
VII. Flow Through Convergent Nozzles	55
VIII. Flow Through Convergent-Divergent Nozzles	57
IX. Flow Through Orifices	59
X. Flow Through Pipes	60
XI. Low-Compression Ejectors	63
XII. Numerical Examples	65
A. Pipe Line	65
B. Stack Ejector	66
XIII. Problems	67

LIST OF FIGURES

Figure 1. Area and Velocity Relationships in Design of Convergent-Divergent Nozzles 58
Figure 2. Pressure Drop Through Horizontal Pipes Handling Gases at High Pressure Drop..... 61

LIST OF TABLES

Table I. Flow Properties of Expanding Air and Saturated Steam..... 64

*Present address: Associate Professor, Dept. of Chem. Engineering, Ohio State University, Columbus, Ohio.

I. REFERENCES

1. Bailey, N. P. "The Thermodynamics of Air at High Velocities" - J. Aero Sci, 11, 227-238 (1944); "Abrupt Energy Transformation in Flowing Gases," Trans. Am. Soc. Mech. Engs., 69, 749-763 (1947).
2. Lapple, C. E., "Isothermal and Adiabatic Flow of Compressible Fluids;" Trans. Am. Inst. Chem. Engr., 39, 385-432 (1943).
3. Lapple, C. E. "Velocity Head Concept in Pressure Drop Calculations," Heating, Piping, and Air Conditioning, 17, 179-183, 262-267, 319-324 (1945); "Velocity Head Simplifies Flow Computation," Chem. Eng., 56, 96-104 (1949) May.
4. Liepmann, H. W., and Puckett, A. E., "Introduction to Aero-dynamics of a Compressible Fluid," New York, John Wiley and Sons, 1947.
5. Perry, J. H., "Chemical Engineers' Handbook," 3rd Ed., New York, McGraw-Hill Book Company, 1950.
6. Puckett, A. E., "Supersonic Nozzle Design," J. App. Mech. (Trans. Am. Soc. Mech. Engrs.), 13, A 265 - A 270 (1946) Dec.
7. Shapiro, A. H., and Edelman, G. M., "Method of Characteristics for Two-Dimensional Supersonic Flow - Graphical and Numerical Procedures," J. App. Mech. (Trans. Am. Soc. Mech. Engrs.), 14, A 154 - A 160 (1947) June.
8. Stodola, A., "Steam and Gas Turbines," Vols. I, II, translated by Loewenstein, L. C., New York; McGraw-Hill Book Company, 1927.

II. NOMENCLATURE

Any consistent system of units may be employed; the English system is given by way of example.

- A = cross-sectional area, sq.ft.
- c = reversible (frictionless) velocity of propogation of a pressure wave in the fluid, ft./sec.
- d = "derivative of"
- D = inside diameter of circular pipe, ft.
- e = natural logarithmic base, dimensionless = 2.718 .....
- F = mechanical energy lost by frictional conversion into heat, (ft.-lb.force)/(lb.mass)
- f = Fanning friction factor, dimensionless,
  $= m(dp/dL)/(V^2/2g_cv) = m\ (dp/dL)/(vG^2/2g_c)$
- g_c = conversion factor, 32.17 (lb.mass)(ft.)/(lb.force)(sec.)^2
- G = mass velocity of fluid, (lb.mass)/(sec.)(sq.ft.)
- J = mechanical equivalent of heat, 778 (ft.-lb.force)/(B.t.u.)
- k = ratio of specific heat at constant pressure to specific heat at constant volume, dimensionless.
- L = length of pipe, ft.
- m = hydraulic radius of pipe, ft. = (cross-sectional area of fluid stream/"wetted" perimeter); = (D/4) for circular pipe.
- M = molecular weight of fluid, (lb.mass)/(lb.mole).
- N = resistance factor, dimensionless = (fL/m); = (4fL/D) for circular pipe.
- N_M = Mach number, dimensionless, = (V/c)
- N_{Re} = Reynolds number, dimensionless, = $(4mG/\mu)$; = (DG/μ) for circular pipe
- p = absolute pressure of fluid, lb.force/sq.ft.
- Q = heat added to system from external source, (B.t.u.)/(lb.mass)
- R = gas constant per mole = 1546 (ft.-lb.force)/(lb.mole)(°F.)
- T = absolute temperature of fluid, °F absolute = °Rankine

U = internal (or intrinsic) energy of fluid, (B.t.u.)/(lb.mass).

v = specific volume of fluid, (cu.ft.)/(lb.mass)

V = linear gas velocity, ft./sec.

w = mass flow rate of fluid, (lb.mass)/(sec.)

Z = static head of fluid above any standard datum plane, (ft.-lb.force)/(lb.mass).

μ = viscosity of fluid, (lb.mass)/(ft.)(sec.) = 0.000672 x centipoises.

Subscripts: When subscripts have been referred to above, they are used uniquely and integrally with the specific symbol referred to. The following subscripts are general and may be used with any of the above symbols:

0 = in reservoir ahead of pipe.
1 = in throat of nozzle or nozzle inlet to pipe; in start of mixing section of ejector.
2 = in mouth of nozzle; in pipe at pipe exit; or in pipe at a distance L downstream from throat of nozzle inlet; at end of mixing section of ejector.
3 = in reservoir into which pipe or nozzle discharges.
a = adiabatic flow
c = critical flow condition
i = isothermal flow
m = in mixing section of ejector
n = for nozzle alone (i.e. for L = 0 and N = 0)
p = primary or driving fluid
s = secondary or induced fluid

Where several subscripts are used on a symbol, the individual significance of each subscript is to be added together. The symbol g_c is always used integrally and the subscript, c, in this case adds no additional meaning and should not be confused with the general subscript c. The term g_c has been labelled as such to be consistent with recent trends of nomenclature.

III. INTRODUCTION

Compressibility refers to the condition when the volume or density of a fluid depends on the pressure applied. In flow problems, it is an appreciable factor only when vapors or gases are involved. Liquids can generally be considered incompressible in flow calculations. When the pressure drop in a gas handling system is less than on the order of 20% of the absolute pressure in the system, adequate accuracy is obtained in pressure drop calculations by assuming the fluid incompressible at conditions corresponding to the average pressure in the system. For larger pressure drops, compressibility effects become important. The compressible flow of a fluid is further complicated by the fact that the fluid density is dependent on temperature as well as on pressure. In such a system, temperature may vary as dictated by the thermodynamic conditions in the system.

IV. GENERAL PRINCIPLES

The general principles governing the flow of compressible fluids are discussed in Reference 2. The following is a brief abstract of the essential elements of the development and conclusions.

An energy balance can be written in one of the alternate differential forms:

$$JdQ + dF = JdU + pdv \tag{1}$$

$$JdQ = d(V^2/2g_c) + JdU + dZ + d\,(pv) \tag{2}$$

$$d(V^2/2g_c) + dZ + vdp + dF = 0 \tag{3}$$

The latter is recognized as the usual mechanical energy balance known as Bernoulli's theorem.

The equations may be further simplified by assuming (1) horizontal pipe (i.e. dZ = 0), and (2) the perfect gas laws. For conditions of flow when compressibility is an appreciable factor, variations in Z are generally negligible even if the pipe is not horizontal. The perfect gas laws are sufficiently accurate for most engineering calculations except at relatively high pressures and even then they can be applied by selecting a proper effective gas constant. These simplifying assumptions supply the following additional equations:

$$dZ = 0 \tag{4}$$

$$(k - 1)\, JdU = d(pv) = (R/M)\, dT \tag{5}$$

whereby Equations 1, 2, and 3 reduce to

$$JdQ + dF = [1/(k - 1)]\, [kpdv + vdp] \tag{6}$$

$$JdQ = d(V^2/2g_c) + [k/(k - 1)]\, d(pv) \tag{7}$$

$$d(V^2/2g_c) + vdp + dF = 0 \tag{8}$$

The next conditions imposed on the flow are those determined by thermal considerations. Two standard thermal conditions may be imposed: (1) isothermal, which assumes that enough heat is supplied to maintain constant temperature (i.e., $dT = 0$); (2) adiabatic, which assumes that no heat is transferred between the fluid and the surroundings (i.e. $dQ = 0$). Actually any one of an infinite number of thermal conditions may be encountered. It is shown in Reference 2 that substantially all flows in pipes are adiabatic, even for pipes over 1000 diameters long, unless special arrangements exist for transferring heat. Conditions of isothermal flow, however, offer a convenient basis for comparison since it is a simple case to treat analytically. The thermal conditions imposed will determine the condition of state of the flow.

It is apparent from Equation 5, that the condition of state for isothermal flow is given by

$$d(pv) = 0 \quad \text{or} \tag{9}$$

$$pv = \text{constant} \tag{10}$$

The equation of state for adiabatic flow is obtained from Equation 7

$$d(pv) = -[(k - 1)/k]\, d\,(V^2/2g_c) \text{ or} \tag{11}$$

$$pv\, [1 + (k - 1)\, V^2/2kg_c pv] = \text{constant} \tag{12}$$

By combination with Equation 8, Equation 11 may be written

$$d(pv^k) = (k - 1)\, v^{k-1}\, dF \tag{13}$$

For frictionless flow, $dF = 0$, Equation 13 takes the form of the usual adiabatic equation of state

$$d(pv^k) = 0 \quad \text{or} \tag{14}$$

$$pv^k = \text{constant} \tag{15}$$

It is also apparent from Equation 7 that, for isothermal flow,

$$JdQ = d(V^2/2g_c) \tag{16}$$

In other words, the amount of heat, which must be added to maintain the temperature of the fluid constant, is equivalent to the increase in kinetic energy of the fluid. For adiabatic flow, on the other hand, the decrease in temperature of the fluid is due entirely to the increase in kinetic energy of the fluid.

V. CRITICAL FLOW

The velocity with which a pressure wave is propogated through a fluid is commonly known as the acoustic or sonic velocity and is given by

$$c^2 = k\, g_c\, pv \tag{17}$$

The pressure at which a fluid attains sonic velocity is often called the "critical" pressure and should not be confused with critical pressures associated with phase change relationships.

While the propogation of a pressure wave always takes place under adiabatic conditions, a similar critical reference basis exists for the hypothetical case when isothermal flow is specified. For an isothermal flow, the limiting velocity is given by

$$c^2 = g_c pv \tag{18}$$

VI. MACH NUMBER

Compressibility effects can be characterized by a dimensionless number similar to the Reynolds number. This number is termed the Mach number and is defined as the ratio of the fluid velocity at a given point to the acoustic velocity in the fluid at that point,

$$N_M = V/c \tag{19}$$

Although the subsequent discussions will not deal directly with Mach number, it should be noted that all equations incorporating compressibility effects can be written in terms of Mach number. Such a transformation generally simplifies the form of the equations and is commonly used in the literature on this subject.

The physical significance of the Mach number will become apparent if it is rewritten by substitution from Equations 5 and 17 as

$$N_M^2 = (V^2/2g_c)/(kRT/2M) \tag{20}$$

Since $(V^2/2g_c)$ measures the directed or controlled kinetic energy of the gas and (RT/M) measures the kinetic energy of random motion of the gas molecules (1) it is apparent that the Mach number is a measure of the ratio of directed to random motion of the gas molecules.

VII. FLOW THROUGH CONVERGENT NOZZLES

If a fluid is allowed to expand from an infinite reservoir at pressure p_o through a frictionless convergent nozzle (dF = 0), a direct integration of Equation 8 in conjunction with the respective equation of state yields

For isothermal flow:

$$V_1^2 = 2g_c\, p_o v_o\, \ln\,(p_o/p_1) \tag{21}$$

For adiabatic flow:

$$V_1^2 = \left[2g_c k/(k-1)\right](p_o v_o)\left[1 - (p_1/p_o)^{(k-1)/k}\right] \tag{22}$$

By conversion to mass velocity Equations 21 and 22 become

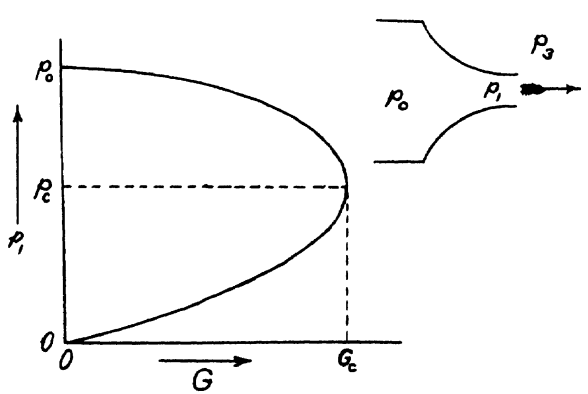
For isothermal flow:

$$G^2 = 2g_c\,(p_o/v_o)\,(p_1/p_o)^2\,\ln\,(p_o/p_1) \tag{23}$$

For adiabatic flow:

$$G^2 = \left[2g_c k/(k-1)\right](p_o/v_o)(p_1/p_o)^{(2/k)}\left[1 - (p_1/p_o)^{(k-1)/k}\right] \tag{24}$$

If G is plotted against p_1 for a given upstream pressure p_o, curves of the following shapes are obtained for either isothermal or adiabatic conditions. Here G is the mass velocity based on the nozzle throat area. These curves would indicate that the mass velocity (or flow rate for a given nozzle) G increases to a maximum as p_1 is decreased and then decreases to 0 as the absolute pressure p_1 is reduced to 0. Actually, however, kinetic considerations indicate that p_1 cannot fall below p_c since it is not possible to transmit pressure from the upstream portion of fluid at a velocity greater than that corresponding to V_c at p_c. Thus G cannot fall below the value G_c corresponding to p_c. The value of G_c and V_c for flow through a frictionless nozzle is given by



For isothermal flow:

$$V_c = \sqrt{g_c p_c v_c} = \sqrt{g_c p_o v_o} = \sqrt{g_c RT_o/M} \tag{25}$$

$$G_c = G_{cni} = \sqrt{g_c p_o/e v_o} = p_o \sqrt{g_c M/eRT_o} \tag{26}$$

For adiabatic flow:

$$V_c = \sqrt{g_c kp_c v_c} = \sqrt{2g_c kp_o v_o/(k+1)} = \sqrt{2g_c kRT_o/M(k+1)} \tag{27}$$

$$G_c = G_{cna} = \left[2/(k+1)\right]^{(k+1)/2(k-1)} \sqrt{g_c kp_o/v_o} \tag{28}$$

Values of p_c are given by

For isothermal flow:

$$p_c = p_o \sqrt{1/e} \tag{29}$$

In adiabatic flow:

$$p_c = p_o [2/(k+1)]^{k/(k-1)} \tag{30}$$

The values G_c and p_c correspond to the maximum flow conditions obtained by differentiating Equations 23 and 24 and equating the derivative to zero.

To clarify the physical significance of the above discussion, consider a convergent nozzle connected to an infinite chamber at pressure p_o and discharging into an infinite chamber at pressure p_3. If p_o remains fixed and p_3 is initially equal to p_o, the initial flow rate as represented by G is zero. As p_2 is reduced, G will gradually increase and p_1, the pressure at the throat of the nozzle, will decrease also and remain equal to p_3. When p_3 reaches p_c, G will reach the value G_c and p_1 will reach p_c. Further reduction in p_3, however, will have no additional effect on either G or p_1, these remaining constant at G_c and p_c no matter how much further p_3 is reduced.

Inspection of the above equations will show that isothermal flow equations are identical with those for adiabatic flow for k = 1.0. In other words the isothermal flow of any fluid may be regarded as equivalent to the adiabatic flow of a hypothetical fluid having a value of k = 1.0. (To make this identity apparent it may be necessary to apply the theory of limits where k = 1.0 results in indeterminate forms in the adiabatic equations). For conditions of (p_3/p_o) close to unity (i.e. low pressure difference across the nozzle), the flow rate and fluid velocity will be substantially identical for either isothermal (Equations 21 and 23) or adiabatic (Equations 22 and 24) flow. For large pressure differentials, however, the flow rate will be greater for adiabatic flow conditions, the difference in rates being the greatest under critical flow conditions. Thus the maximum difference between isothermal and adiabatic flow is obtained by comparing Equations 26 and 28,

$$(G_{cna}/G_{cni}) = [2/(k+1)]^{(k+1)/2(k-1)} \sqrt{ek} \tag{31}$$

Values of (G_{cna}/G_{cni}) for specific values of k are given below:

k	(G_{cna}/G_{cni})
1.0	1.000
1.2	1.069
1.4	1.129
1.6	1.180
1.8	1.229

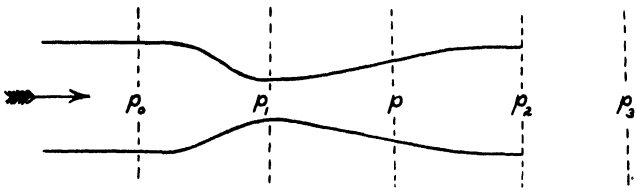
Thus for air (k = 1.4) adiabatic conditions will never result in flow rates more than 13% greater than for isothermal conditions. In practice only adiabatic conditions will ever prevail in flow through nozzles.

The equations for flow through nozzles from an infinite reservoir are shown graphically in Figure 2 by the curves corresponding to N = 0. The use of these curves is discussed in more detail in the Section X on "Flow Through Pipes."

Theoretically the adiabatic expansion of saturated steam thru a nozzle would involve a partial condensation in the throat of the nozzle. Actually, however, the time element is so short that a phase equilibrium cannot be reached and the expansion of saturated steam in a nozzle approximates that of superheated steam. Thus, while the value of k for saturated steam under equilibrium phase conditions

is 1.135, effectively the expansion proceeds as though the value of k were close to 1.3. This applies only to rapid expansion and does not apply to the flow of saturated steam through pipes.

VIII. FLOW THROUGH CONVERGENT-DIVERGENT NOZZLES (DE LAVAL NOZZLE)



Equations of flow for the convergent section of this frictionless nozzle will be exactly the same as for a simple convergent nozzle of the same throat dimensions. For the divergent section the equations of flow are also obtained from Equation 8 (for dF = 0). [Note: in the subsequent discussion on flow through convergent-divergent nozzles only adiabatic flow conditions will be considered.]

$$V^2 = \left[2g_c\, k/(k-1)\right](p_0 v_0)\left[1 - (p/p_0)^{(k-1)/k}\right] \tag{32}$$

$$G^2 = \left[2g_c\, k/(k-1)\right](p_0/v_0)(p/p_0)^{(2/k)}\left[1 - (p/p_0)^{(k-1)/k}\right] \tag{33}$$

where V, G, and p represent corresponding quantities at any cross-section. The values p_0, v_0, and T_0 correspond to those in an infinite reservoir ahead of the nozzle.

If the flow rate is such that p_1 is greater than p_c as given by Equation 30, the nozzle will behave as a simple venturi and p will gradually increase and V decrease as the fluid moves downstream in the divergent section until it is equal to p_3 at the mouth of the nozzle. If p_3 is reduced below the value corresponding to that required for a flow of G_{cna}, as given by Equation 28, through the throat of the nozzle, the pressure p will gradually decrease and V increase as the fluid moves downstream in the divergent section according to Equations 32 and 33, G at any section being directly related to G_{cna} by the ratio of the throat area to that of the cross-section in question. If at the mouth of the nozzle p is equal to p_3, the nozzle is designed properly for realizing the ultimate adiabatic expansion velocity for the specific pressure ratios involved (i.e. p_3/p_0). The flow in such a nozzle will be isentropic. The mouth area, A_2, of a properly designed nozzle for a given pressure ratio, (p_3/p_0), is given in terms of throat area, A_{1c}, by

$$(A_{1c}/A_2)^2 = \left(\frac{2}{k-1}\right)\left(\frac{k+1}{2}\right)^{\left(\frac{k+1}{k-1}\right)}(p_3/p_0)^{(2/k)}\left[1 - (p_3/p_0)^{(k-1)/k}\right] \tag{34}$$

Equation 34 applies only to a nozzle in which critical flow conditions exist in the throat, as implied by the subscript c on A_{1c}. Practically, there is no point in making the throat area less than the mouth area for a nozzle in which critical flow conditions are not attained.

The ratio of the mouth velocity, V_2, to the throat velocity, V_{1c} of such a nozzle is given by combining Equations 27 and 32

$$\left(V_2/V_{1c}\right)^2 = [(k+1)/(k-1)]\left[1 - (p_3/p_0)^{(k-1)/k}\right] \tag{35}$$

Equations 34 and 35 are plotted in Figure 1.

If, for a given value of (p_3/p_0), the actual value of (A_{1c}/A_2) is other than that corresponding to the theoretical value for a properly designed nozzle as given by Equation 34, the flow cannot be isentropic and the expansion will either be incomplete within the nozzle or a compression shock will result depending on whether the actual area ratio, (A_{1c}/A_2), is too large or too small, respectively, for the value of (p_3/p_0). Either of these conditions will result in a loss of available kinetic energy.

The curves shown on page 59 give a plot of the pressure at various points along a given convergent-divergent nozzle for various values of p_3. In curves 1 and 2, p_3 is such that the nozzle behaves as a simple venturi.

In Curve 3, p_1 has just reached its critical value. The mass flow rate of fluid is successively greater for Curves 1, 2, and 3, and the pressure at the mouth of the nozzle is equal to p_3. The linear

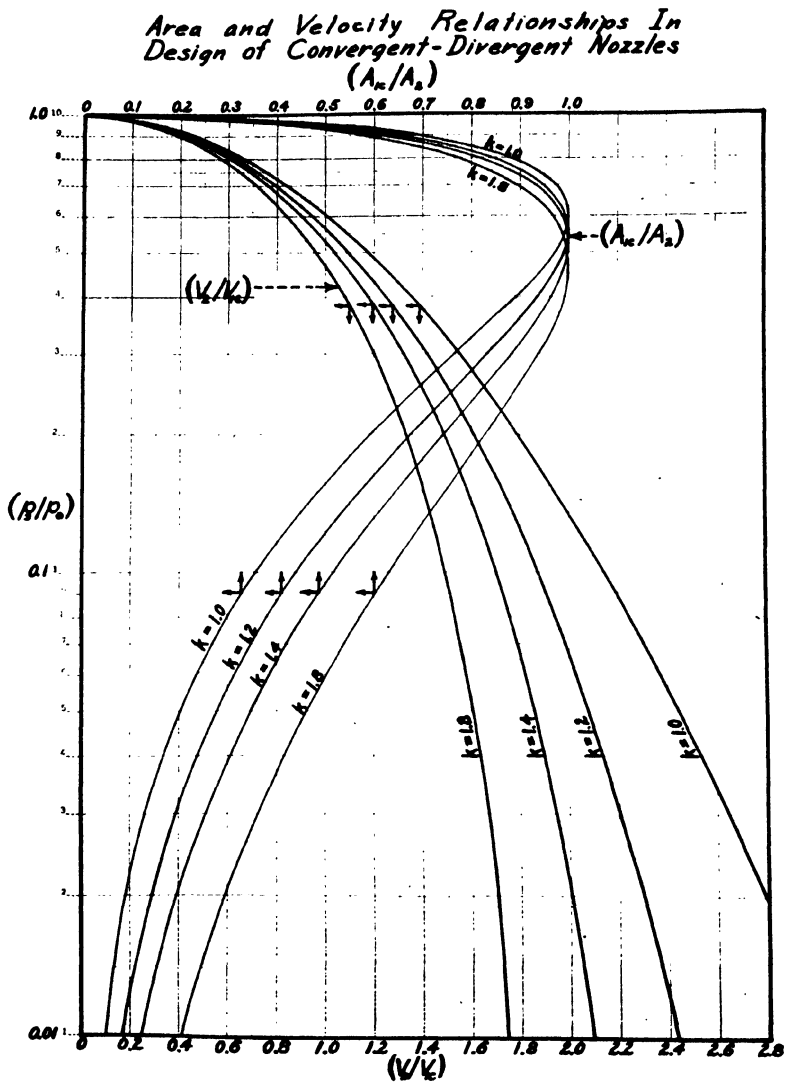
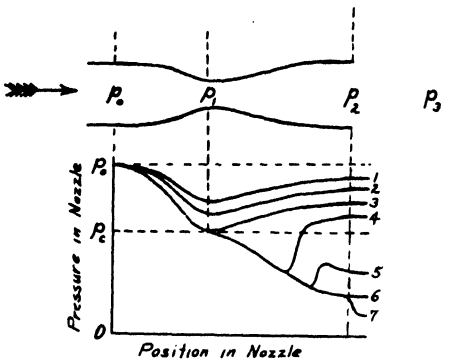


Figure 1. Area and Velocity Relationships in Design of Convergent-Divergent Nozzles

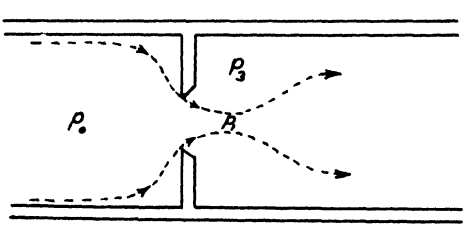


velocity never exceeds the acoustic velocity at any point. For curves 4-7 the mass flow rate remains constant at its value for Curve 3. Curve 6 corresponds to the proper design pressure for this nozzle. The velocity at the throat is equal to the acoustic velocity and becomes increasingly supersonic in the divergent section. The pressure at the mouth of the nozzle, p_2, is just equal to p_3. Curve 7 represents a condition of underexpansion. Velocities in the divergent section become increasingly supersonic. The mouth of the nozzle is too small, however, to realize complete expansion in the nozzle and the pressure at the mouth, p_2, is greater than p_3. Curves 4 and 5 represent conditions of overexpansion. The mouth of the nozzle is too large. Velocities in the divergent section become progressively supersonic and the pressure falls to a point below p_3. A compression shock suddenly ensues with a corresponding loss of available energy as heat. The pressure rises and the velocity drops. The velocity may become subsonic if p_3 is sufficiently large as in Curve 4. Depending on the shape of the nozzle this shock may proceed in a number of steps provided the final velocity in each step is supersonic. In all values of p_3 between Curves 6 and 3, p_2 is equal to p_3.

The increase in velocity as the fluid expands in the divergent section of the nozzle for conditions encountered in Curves 4-7 may seem paradoxical to those accustomed to dealing with incompressible fluids. This condition comes about from the thermodynamic relationships existing at pressures below the critical pressure. In this region the fluid density will decrease more rapidly due to a decrease in pressure than the fluid velocity will increase. Thus such an expansion must be accompanied by a reduction in fluid mass velocity. For a fixed mass flow rate, this means that such an expansion can only take place when accompanied by an increase in the fluid stream cross-section.

The above discussion gives no information as to the proper shape of the divergent section. This is determined by kinetic considerations. For subsonic flow, considerations are identical with those of a venturi requiring a 5° to 7° included angle of divergence. For supersonic flow a 5° to 7° angle is reasonably satisfactory. For very high pressure ratios, however, and high kinetic energy conversion efficiency, special shapes are employed. Methods of design in such cases are beyond the scope of present considerations but can be obtained from References 4, 6, 7, and 8. Allowances for friction also require a somewhat lower $(A_{1\,C}/A_2)$ ratio than calculated theoretically. It should be pointed out, however, that a slight under-expansion is to be preferred to overexpansion since, in the case of underexpansion, additional expansion to convert pressure into kinetic energy can be obtained upon leaving the mouth of the nozzle.

IX. FLOW THROUGH ORIFICES



For the case of incompressible fluids or for relatively small pressure differentials, the equations of flow through orifices, based on the orifice area, are identical with those for nozzles except for a proportionality factor or discharge coefficient. For a sharp edged orifice this coefficient is approximately 0.6, meaning that the flow is 0.6 times that through a frictionless nozzle of the same throat area. This coefficient represents primarily a contraction effect and is essentially a measure of the ratio of the jet area at the vena contracta to the area of the orifice (See also Reference 3, pp. 321-322, for a more detailed discussion). For compressible fluids, the degree of contraction, and hence the discharge coefficient, is a function of the pressure differential across the orifice. For low differentials (i.e. values of (p_3/p_0) close to unity), the discharge coefficient is identical with that for incompressible flow. For higher differentials (i.e. values of (p_3/p_0) appreciably less than unity), the degree of contraction becomes less and the discharge coefficient increases. The pressure, p_3, is taken as that around the vena contracta although for discharge into a relatively large reservoir it is substantially identical with the downstream reservoir pressure. When p_3 is reduced to the critical

pressure, p_c, given by Equation 30, the velocity of the jet at the vena contracta will be essentially equal to the acoustic velocity (Equation 19) and the pressure in the jet, p_1, at the vena contracta will be essentially p_c. Further reductions in p_3 will result in no further change in either the velocity of the jet or the pressure in the jet, but will result in a further decrease in the degree of contraction. For this reason the mass discharge rate, being determined by the product of the velocity and the area at the vena contracta will increase continuously with a decrease in p_3 instead of attaining a limiting value for values of p_3 below p_c as is the case for nozzles. However, the increase in the area of the jet at the vena contracta for pressures of p_3 less than p_c is relatively small. For pressures of p_3 appreciably less than p_c, the mass discharge rate may be regarded as constant and independent of p_3 for all practical purposes. The discharge coefficient for a sharp-edged orifice under such conditions is 0.83, including orifice friction.

The discharge coefficient for sharp-edged orifices is relatively sensitive to the thickness of the orifice plate for incompressible flow since a thick plate will permit partial recovery of kinetic energy as pressure energy. While the discharge coefficient is 0.6 for thin plates (i.e. plates in which the thickness is less than 1/8 the orifice diameter), it may exceed 0.8 for very thick plates. For compressible flow at critical flow (substantially "maximum" discharge rate) conditions, however, the discharge coefficient is substantially independent of plate thickness since any pressure recovery cannot result in any decreased discharge rate.

It should be emphasized that the orifice equations for either compressible or incompressible flow would be identical with those for nozzles without the use of a discharge coefficient if they were based on the vena contracta. They are, however, usually based on the orifice area for convenience since the area of the vena contracta is not known without experiment. It is essentially the variation in this area that represents the variation in the discharge coefficient. Strictly speaking, the above discussion for conditions of compressible flow through orifices is oversimplified since the fluid stream is not confined and hence need not follow a well defined jet through a vena contracta at a specific cross-section. It is, however, a sufficiently accurate description for practical purposes.

X. FLOW THROUGH PIPES

The equations for flow through pipes can be developed in a fashion similar to those for flow through nozzles. For pipes, however, the friction term, dF, in Equation 8 may be a controlling factor. The friction in pipes can be expressed in terms of the usual Fanning friction factor

$$dF = (fV^2/2g_c m)dL \tag{36}$$

Available data indicate that the friction factor, f, is the same function of Reynolds number for compressible flow as for incompressible flow. For a given pipe and flow rate, f depends only on μ which in turn depends only on temperature (the variation with pressure generally being negligible for pressures under 100 atmospheres). Since high Reynolds numbers are involved for flow conditions encountered in cases involving compressibility, the variation of f due to temperature variation along the length of the pipe is small and a constant value of f can be assumed in making integrations. For a constant value of the friction factor, Equation 36 may be written as

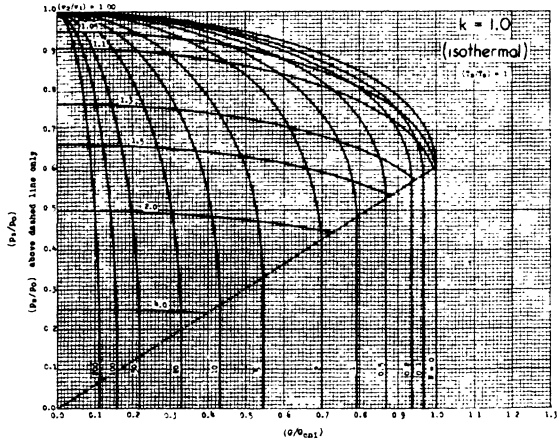
$$dF = (V^2/2g_c)dN \tag{37}$$

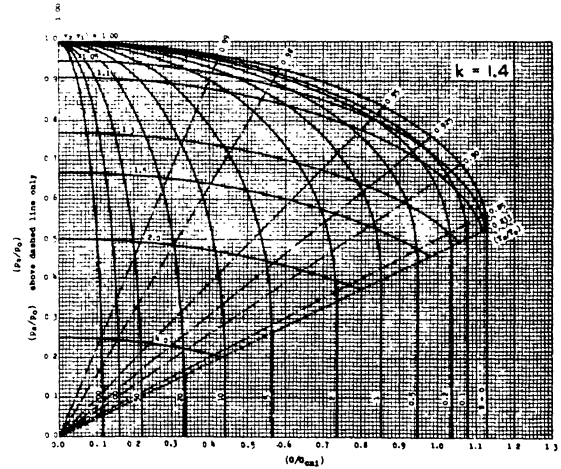
where N represents the group fL/m (or 4fL/D for circular pipe). It should be noted that N is essentially the friction loss expressed as number of velocity heads.

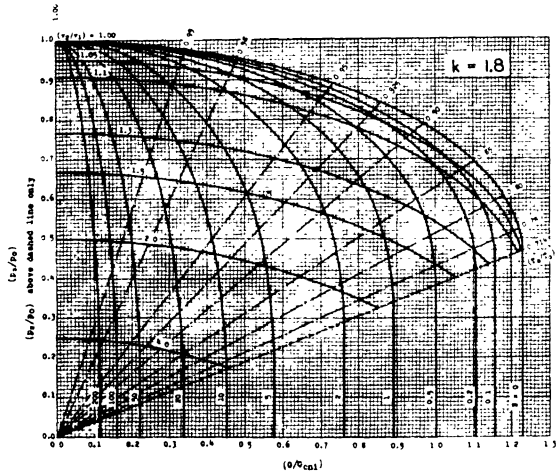
Using this equation for dF in Equation 8 and integrating in conjunction with the respective equations of state will yield the overall equations for pressure drop through a pipe of specified length for either isothermal or adiabatic flow conditions. The complete derivations are given in Reference 2. The final equations, however, are so complex that the relationships between pressure drop and flow rate for a given pipe cannot be expressed explicitly.

For convenience of application, the overall equations for pressure drop in pipes have been expressed graphically in the form shown in Figure 2. These charts have been prepared for values of k of 1.0, 1.4, and 1.8. The chart for a value of k = 1.0 corresponds to the adiabatic flow of a hypothetical gas, (since no known gases have such a low ratio of specific heats) or to the isothermal flow of any gas (since, as for nozzles, the isothermal flow equations become identical with the adiabatic flow equations for a value of k = 1.0). While there is no known gas having a value of k = 1.8 except at very high pressure or low temperature, this chart is included to provide an extreme case so that the performance with all common cases can be obtained by interpolation between these three charts. The following tabulation lists values of k for some common gases:

p. 60, line 18: change "decreased" to "increased".







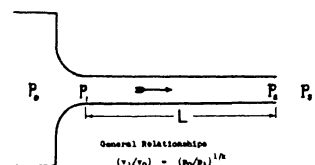
PRESSURE DROP THROUGH HORIZONTAL PIPES HANDLING GASES AT HIGH PRESSURE DROP

c_v = specific heat of gas at constant volume, (B t.u.)/(lb.)(°F.)
c_p = specific heat of gas at constant pressure, (B t.u.)/(lb.)(°F.)
D = pipe diameter, ft.
e = logarithmic base = 2.718
f = Fanning friction factor, dimensionless = function of N_{Re}
g_c = conversion factor, 32.17 (lb.mass)(ft.)/(lb force)(sec.^{2})
G = mass velocity of fluid in pipe, (lb mass)/(sec.)(sq ft.)
G_{cnl} = maximum mass velocity of fluid in frictionless nozzle under conditions of isothermal flow, (lb.mass)/(sec.)(sq ft.)

$$= \sqrt{\frac{g_c p_o}{v_o}} = p_o \sqrt{\frac{2k}{RT_o}}$$

k = ratio of specific heats = (c_p/c_v)
L = length of pipe, ft
m = hydraulic radius of pipe, ft., = (D/4) for circular pipe
M = molecular weight of gas
$N = \left(\frac{D}{m}\right)$, = $\left(\frac{4D}{D}\right)$ for circular pipe
p = gas pressure, (lb.force)/(sq ft.) absolute
R = gas constant per mole, 1545 (ft.)(lb.force)/(lb.mole)(°F.)
N_{Re} = Reynolds number, dimensionless, = $(4mG/\mu)$ = (DG/μ) for circular pipe
T = gas temperature, °F. absolute = ° Rankine
v = specific volume of gas, (cu.ft.)/(lb.mass)
μ = gas viscosity, (lb mass)/(ft.)(sec.)

Subscripts
- o = in reservoir ahead of pipe
- i = in throat of nozzle inlet
- x = in pipe at exit of pipe or at any point, distance L downstream from throat of nozzle inlet
- b = in reservoir into which pipe discharges



General Relationships

$$(v_i/v_o) = (p_o/p_i)^{1/k}$$
$$(T_i/T_o) = (p_i/p_o)^{(k-1)/k}$$
$$(T_x/T_i) = (p_x/p_i)(v_x/v_i)$$
$$pv = RT/M$$

For (p_x/p_o) above dashed line.
$(p_x/p_o) = (p_x/p_o)$

For (p_x/p_o) below dashed line:
$\left(\frac{p_x}{p_o}\right)$ is given by dashed line
$(T_x/T_o) = 2/(k+1)$

The curves for $(v_x/v_i) = 1.00$ and $N = 0$ are identical and may be considered as a plot of (p_x/p_o) vs. (G/G_{cnl}) for the region above the dashed line.

Figure 2

Gas	k
C_2H_6	1.2
CO_2, SO_2, H_2O, H_2S, NH_3, Cl_2, CH_4, C_2H_2, C_2H_4	1.3
Air, H_2, O_2, N_2, CO, NO, HCl	1.4
Monatomic gases	1.67

There are approximate values for 1 atm. and 25 C. A decrease in temperature or an increase in pressure will tend to result in higher values of k. For more detailed data see Ref. 5, p. ~~545~~. 233

In these charts the ratio of downstream to upstream pressure, for straight horizontal pipe having a rounded inlet from a large upstream reservoir, is plotted against the flow rate referred to the flow, G_{cni}. The term, G_{cni}, is the maximum discharge through a frictionless nozzle under isothermal flow conditions and is related to upstream conditions by Equation 26. While this flow cannot be realized physically, it has been employed as a rational, understandable, and convenient reference basis which eliminates specific upstream conditions. Curves of pressure ratio vs. flow ratio are given for pipes of various lengths expressed in terms of N. Also included are curves of (v_2/v_1) and T_2/T_0) which permit complete calculation of fluid conditions in the pipe in cases where such quantities are desired.

In employing the charts, it is necessary to know the friction factor, f, in addition to pipe length in order to be able to calculate N. If the flow rate is unknown (this usually being the desired quantity), a trial and error solution is involved. Fortunately, however, the value of f does not vary over a very wide range and the solution is not too sensitive to the value of f. Consequently an initial assumption of an average value of 0.004 for f will be justifiable in any case. This will yield a value of flow rate, as determined from the proper chart and curve in Figure 2, from which the Reynolds number can be calculated and the corresponding value of f determined. A repeat calculation using this new value of f will give the final answer within a few per cent. It should also be noted that the flow through a frictionless nozzle, as discussed in previous paragraphs, is given by the curve for N = 0.

While the curves of Figure 2 apply to straight horizontal pipes with rounded inlets, they can be used for pipes containing abrupt inlets, bends, and other fittings by adding an appropriate value to the value of N, computed from the length of straight pipe, to obtain an effective value of N for use with Figure 2. An abrupt inlet can be allowed for by adding 0.5 to the value of N computed for the pipe length alone. Fittings and valves may be allowed for by adding the pressure drop, expressed as number of velocity heads, (as given in Table 3 ~~of Ref. 3~~) to the value of N. However, where the fitting contains a contraction to less than the pipe area, as in some valves, special analysis should be made since the contracted section may be a controlling factor in determining the discharge rate, in that sonic velocities may be attained in this section before being attained in any other portion of the pipe. Fortunately such cases are rare and will usually arise only for relatively short lines.

As for nozzles, a limiting or maximum discharge rate is reached when the velocity in the end of the pipe attains that of sound. The point at which this limiting condition is reached is given by the dashed line in Figure 2. For values of p_3 above the dashed line, the pressure, p_2, inside the end of the pipe is equal to p_3. For values of p_3 below the dashed line, the pressure p_2 will correspond to that given by the dashed line and, regardless of how much further p_3 is reduced, p_2 will not change nor will the discharge rate increase.

The temperature, T_2, should not be confused with T_3. The drop in temperature from T_0 to T_2 for adiabatic flow is due entirely to the change in kinetic energy of the gas regardless of the frictional effects that may be present. In adiabatic flow through a pipe into a much larger pipe or reservoir, the value of T_3 will be substantially equal to T_0, except for the Joule-Thompson effect, even though T_2 may be considerably lower. This is due to a conversion of kinetic energy back into heat as the fluid expands from the small to the large pipe.

A comparison of the curves of Figure 2 will show that, for a given pipe line and pressure differential, the gas mass discharge rate under adiabatic conditions will never be more than 20 per cent greater than for isothermal conditions, the difference being the greatest for short pipes. For pipes over about 1000 pipe diameters long, the discharge for adiabatic conditions will be less than 5 per cent greater than for isothermal conditions.

For pipes of N larger than 50 (corresponding to pipes more than about 3000 pipe diameters long), the maximum possible discharge rate is given within 6% or less by the following expression for either adiabatic or isothermal flow conditions:

p. 62, end of first paragraph: change "p. 545" to "p. 233".

p. 62, line 6 of 3rd paragraph: insert comma after "..... Figure 2"

p. 62, line 6 of 4th paragraph: change "of Ref. 3" to "... [illegible]"

$$(G_c/G_{cnl}) = \sqrt{e/N} \tag{38}$$

By substitution from Equation 26, this may be written

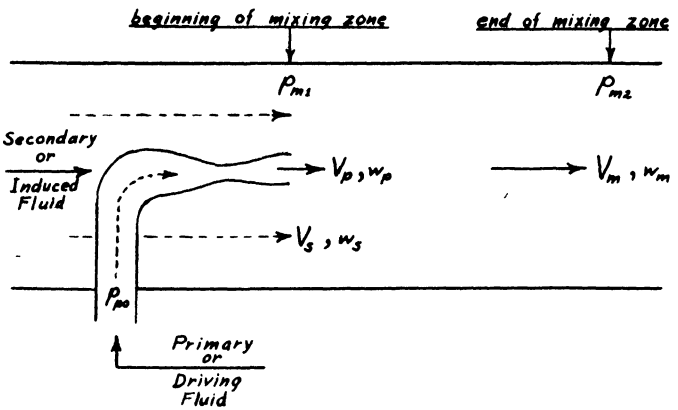
$$G_c = \sqrt{(g_c p_o)/(v_o N)} = p_o \sqrt{(g_c M)/(RT_o N)} \tag{39}$$

For pipes of N larger than 200 these approximations are accurate to better than 2%.

XI. LOW COMPRESSION EJECTORS

Compressed fluids are frequently used as the driving medium for ejectors (or injectors). Performance is readily subject to calculation for low compression ejectors (i.e. those in which the secondary or induced fluid undergoes a small change in pressure as compared to that of the primary or driving fluid).

Considering the conditions in a mixing section of uniform area as shown in the following sketch:



From a momentum balance

$$g_c(p_{m_2} - p_{m_1})A_m = w_p(V_p - V_m) - w_s(V_m - V_s) \tag{40}$$

and from conservation of mass:

$$w_m = w_p + w_s \tag{41}$$

These equations completely define the performance of the ejector. If the primary fluid undergoes a complete isentropic expansion from p_{po} to p_{m_1} the value V_p can be obtained directly from Equation 32. For low compression ejectors using high pressure primary fluids, p_{m_1} will be less than p_{pc} and the mass velocity in the throat of the nozzle is given directly by Equation 28. This determines w_p for a nozzle of given throat area. Assuming a specific secondary flow and a mixing section of given area, the terms w_s, V_s, and V_m can then be calculated from the respective fluid densities. For purposes of density calculation, p_{m_2} will be sensibly equal to p_{m_1} and in most practical problems both pressures will be substantially one atmosphere. The pressure differential, $(p_{m_2} - p_{m_1})$, developed by the ejector for the assumed secondary flow, can then be calculated from Equation 40. Repeat calculations for various secondary flow will yield a complete performance curve.

Actual design applications are usually more complex since it is usually required to design an ejector for a specific performance. Thus ejector details are initially unknown and a direct solution is impossible. The usual design procedure involves a judicious assumption of ejector details and calculation of the performance curve. The primary nozzle size of this ejector is then varied and respective performance curves calculated. From these calculations it is possible to select the ejector proportions which will have the minimum ratio of primary to induced fluid for the specific pressure differential required. The secondary fluid rate corresponding to this design and the desired pressure differential

can then be obtained from the performance curves previously calculated or from interpolation thereon. This will usually be different from the desired secondary fluid rate. The desired ejector dimensions can then be obtained by multiplying all dimensions of the optimum ejector previously calculated by the square root of the ratio of the desired secondary fluid rate to that calculated for the optimum ejector.

The above discussion has been directed at a simple draft tube. The design problem in practice is further complicated by considerations of entrance to and exit from the mixing zone, the desired differential usually being known on the entrance and the discharge side of the ejector rather than within the ejector itself. In many cases it may be desirable to provide a convergent inlet to minimize entrance loss and a divergent section after the straight mixing zone to provide recovery of velocity energy as pressure. This consideration increases the complexity of the trial and error calculation. Entrance pressure differentials can be calculated by usual methods. Conversion of kinetic energy to pressure energy in a divergent section, however, is generally less complete in an ejector than in a venturi meter, due to the turbulence created in the mixing zone. In a venturi about 80% of the theoretical conversion, possible on an area basis, is realized. In an ejector only about 50% can be realized.

In usual applications for handling gases at substantially atmospheric pressure and low compression ratios by means of compressed air or steam, the use of a convergent-divergent ejector will permit on the order of a 40% reduction in the amount of primary fluid required for a given application as compared to the use of a simple tube without the convergent inlet and divergent outlet (often referred to as "draft tube").

In making the calculation previously discussed, for low-compression ejectors, a simplification of Equation 40 can be made which will materially reduce the amount of trial and error required. In such applications, V_m is generally small compared to V_p and not much greater than V_s. The term $w_s(V_m - V_s)$ is generally small compared to the term $w_p(V_p - V_m)$. As first approximations Equation 40 may therefore be written

$$(p_{ms} - p_m) \cong w_p(V_p - V_m)/g_c A_m \cong w_p(V_p - V_s)/g_c A_m \cong w_p V_p/g_c A_m \qquad (42)$$

This equation will serve to indicate the order of magnitude of A_m for a given application or conversely, the order of pressure differential that can be developed in a given mixing area. The actual pressure differential developed will be somewhat less than predicted by this equation for a given mixing zone area, or, for a given pressure differential, a somewhat larger mixing area will be required. In any case, Equation 42 should serve only as a guide and final answers should be obtained from Equation 40. Serious errors can result from failure to do so. In practice optimum designs generally correspond to a value of V_s (or V_m) on the order of 200 ft./sec. Convergent-divergent ejectors will require a somewhat smaller mixing zone area than draft tube types.

Table I. FLOW PROPERTIES OF EXPANDING AIR AND SATURATED STEAM

Upstream Pressure lb./sq.in.ga.	p_o lb./sq.ft.abs.	Dry Air at 70 °F.* v_o (cu.ft./lb.)	Dry Air at 70 °F.* G_{cna} (lb.)/(sec.)(sq.ft.)	Dry Air at 70 °F.* V (ft./sec.)	Saturated Steam* v_o (cu.ft./lb.)	Saturated Steam* G_{cna} (lb.)/(sec.)(sq.ft.)	Saturated Steam* V (ft./sec.)
0	2,117.	13.35	0.0	0.	26.80	0.0	0.
10	3,560.	7.95	81.2†	937.	16.49	55.0†	1359.
20	5,000.	5.66	115.2	1178.	11.94	77.2	1739.
30	6,440.	4.39	148.6	1318.	9.46	98.6	1942.
40	7,890.	3.58	181.8	1412.	7.83	120.0	2122.
60	10,770.	2.624	248.2	1539.	5.84	162.3	2340.
80	13,650.	2.071	314.4	1622.	4.67	204.3	2490.
100	16,530.	1.712	381.1	1682.	3.89	246.4	2600.
125	20,120.	1.405	464.0	1738.	3.23	298.4	2708.
150	23,700.	1.192	547.1	1782.	2.76	350.4	2790.

†These values are really G_{na} and are corrected for the fact that critical flow conditions have not been established in the throat of the nozzle.

*Values for air are based on k = 1.40. For saturated steam the values are based on k = 1.30 since, for adiabatic expansion in a nozzle, the time element is too short to permit any great extent of condensation and saturated steam will behave more like superheated steam. All values of G_{cna} and V are for espansion to 1 atmosphere absolute pressure.

In Table I are given values of V and G_{cna}, as defined by Equations 32 and 28 for compressed air and saturated steam at various pressures expanded to atmospheric pressure. These are theoretical values for complete isentropic expansion and will simplify calculations in applications involving the handling of secondary gases at substantially atmospheric pressure.

Previous considerations have assumed complete isentropic expansion of the primary fluid. To allow for friction, jet contraction, and incomplete expansion in the primary fluid nozzle, the theoretical values must be multiplied by suitable factors to allow for these additional influences. The following coefficients are suggested for various types of nozzles in application to low-compression ejector design:

	Type Nozzle		
Term	Convergent	Convergent-Divergent	Orifice §
G_{cna}	0.98	0.98	0.83 ‡
V	0.95*	0.97†	0.95*

* This will actually be a variable depending on the pressure ratio but should be a good average value for ratios of downstream to upstream nozzle pressure greater than 0.1.

† Assumes correct area relationships for existing pressure ratio as given by Equation 32 or Figure 1.

‡ G_{cna} is based on the orifice area. This coefficient is primarily a contraction effect.

§ Sharp upstream edge.

Previous paragraphs have considered the flow conditions in a convergent-divergent nozzle in detail. It was previously stated that velocities in the throat of a convergent nozzle or in the vena contracta of an orifice cannot exceed the acoustic velocity in the fluid in question. However, where the downstream pressure is below the critical pressure, the fluid is free to expand to supersonic velocities downstream from these positions of minimum stream cross-section even though the mass flow of fluid cannot increase. With a divergent expansion section of suitable design, the velocity at the mouth of the nozzle will be unidirectional along the axis of the nozzle. With a convergent nozzle or orifice, the effluent jet will tend to be so directed by the restraining influence of the more or less stagnant fluid surrounding the fluid jet issuing from the nozzle. Since this stagnant fluid is relatively mobile it does not form a positive means for controlling the expansion and the jet from a convergent nozzle or orifice will flare out more rapidly than in a convergent-divergent nozzle and when fully expanded will have radial velocity components instead of being unidirectional. For application to low-compression ejectors, however, this difference is not very important since radial expansion is immediately accompanied by a corresponding momentum interchange with the surrounding fluid. Thus for such ejectors, a simple convergent nozzle will be practically as efficient as a proper convergent-divergent nozzle as indicated by the slight difference in coefficients on theoretical expansion velocity indicated in the previous tabulation. In fact, a convergent-divergent nozzle with too great an area ratio will be less efficient than a simple convergent nozzle in such application.

XII. NUMERICAL EXAMPLES

A. Pipe Lines:

Problem: A reaction vessel normally operates at 35 lb./sq.in.ga. and 65°C. If the temperature rises to 100°C., a decomposition takes place at almost explosive speed and CO gas is evolved. To relieve the pressure caused by such an explosion, a 6-in. Schedule 80 standard iron pipe, 23 ft. long, containing three standard 45 ells, is provided as a vent. The end of this pipe contains a lead rupture disk scored to break at 100 lb./sq.in.ga. What is the maximum possible rate of formation of carbon monoxide gas (expressed in lb./sec.) so that the pressure in the reaction vessel will never exceed 100 lb./sq.in.ga? 200 lb./sq.in.ga.? Calculate these rates for both isothermal and adiabatic flow conditions. (Assume temperature of gas in chamber at 100°C. and assume CO acts as a perfect gas.)

Solution:

From the conditions of the problem:

Pipe diam. = 5.761 in. i.d. = 0.480 ft.
Pipe area = 0.181 sq.ft.
M = 28 T_o = 672 °R.
k = 1.4 μ_o = 1.45 x 10^{-5} (lb.mass)/ft.)(sec.)
p_o = 16,570 and 31,000 lb.force/sq.ft.
p_s = 2,120 lb.force/sq.ft.

Calculation of N:

Straight pipe:	(4f)(23)(12)/(5.761)	= 192f
45° bends:	(3)(0.3)	= 0.9
Inlet loss:	(assume abrupt)	= 0.5
Total:	N = 192f + 1.4	

Assuming f = 0.0031, N = 2.0
Calculation of G_{cni}:

$$G_{cni} = p_o \sqrt{(32.17)(28)/(2.718)(1546)(672)}$$
$$= 0.01786\, p_o$$

For the assumed value of f, Figure 2 can be used to calculate G at N = 2.0 as indicated by the following tabulation:

Type of Flow	Isothermal		Adiabatic	
k	1.0		1.4	
p_o, lb./sq.in.ga.	100	200	100	200
lb./sq.ft.abs.	16,570	31,000	16,570	31,000
G_{cni}, (lb.)/ (sec.) (sq. ft.)	296	554	296	554
(p_s/p_o)	0.128	0.068	0.128	0.068
(G/G_{cni})(from charts)	0.699	0.699	0.736	0.736
G,(lb.)/(sec.)(sq.ft.)	207	387	218	407
Answer, lb./sec.	37.4	70.0	39.5	73.7

A check of the Reynolds number can now be made which indicates it to be in the range of 6.86 to 13.5 x 10^6 for which f = 0.0032 to 0.0030.

B. Stack Ejector:

Problem: A large reaction tank is vented to the atmosphere through a 24-in. diameter stack, 100 ft. high. In order to avoid a nuisance and hazard around feed holes and other clearances in the tank, it is desired to install a steam nozzle in the base of the stack which will induce a draft of -0.20 in. water in the vessel when handling 5000 cu.ft./min. of atmospheric air. Specify the nozzle size and steam consumption in lb./hr. using 100 lb./sq.in.ga. saturated steam. Assume the nozzle is made by drilling out a pipe cap and assume the air temperature is 25°C. and neglect rise in temperature due to mixing with steam.

Solution: In this case it may be assumed that the steam in the air is negligible in so far as stack friction and momentum change in the air is concerned.

Air rate = 5000 cu.ft./min. = 83.3 cu.ft./sec.
Air velocity in stack = 26.5 ft./sec.
Stack velocity head = 0.156 in. water
N_{Re} = (24)(26.5)(0.0740)(1488)/(0.0183)(12) = 319,000
f = 0.0046
Stack friction = (4)(0.0046)(100)/(2) = 0.92 vel. hds.
Inlet and outlet losses = 1.5 vel. hds.
Total static pressure to be developed by jet
= 0.20 + (1.5 + 0.92)(0.156) = 0.578 in. water
= (0.578)(5.2) = 3.00 lb./sq. ft.

p. 66, line 6: add parenthesis before ft. to read "(lb. mass)/(ft.)(sec.)".

For 100 lb./sq.in.ga. steam, Table I gives the following theoretical values:

V = 2600 ft./sec.
G_{cna} = 246.4 (lb.)/(sec.)(sq.ft.)

Actual values allowing for friction and contraction, are:

V = (2600)(0.95) = 2470 ft./sec.
G_{cna} = (246.4)(0.83) = 205 (lb.)/(sec.)(sq.ft.)

From momentum balance (Equation 42), weight of steam required
= (3.00)(32.17)(3.14)/(2470 - 26.5)
= 0.1240 lb./sec. = 446. lb./hr.

Hole required in pipe cap:

$$= \sqrt{(0.1240)(144)/(205)(0.785)} = 0.333 \text{ in.}$$
$$= 21/64 \text{ in.}$$

An accurate solution will depend on the initial humidity of the air. Assuming initially saturated air, an examination of psychometric charts will indicate that the air temp. after mixing with the steam will be approximately 35°C. and 1/4 of the steam will condense.

Conditions are therefore:

	Entering Mixing Section	Leaving Mixing Section
Temp., °C.	25	35
Air flow, lb./sec.	6.16	6.16
cu.ft./sec.	83.3	86.0
Steam Flow, lb./sec.	0	0.124
Total flow, lb./sec.	6.16	6.28
cu.ft./sec.	83.3	88.1
Velocity, ft./sec.	26.5	28.0
Vel. head, in. water	0.156	0.168

p_{m1} = -0.2 - (1.5)(0.156) = -0.434 in. water ga.

p_{m2} = (0.92)(0.168) = + 0.155 in. water ga.

$(p_{m2} - p_{m1})$ = 0.59 in. water = 3.06 lb./sq.ft.

$w_s (V_m - V_s)$ = (6.16)(28.0 - 26.5) = 9.3

$g_c (p_{m2} - p_{m1}) A_m$ = (32.17)(3.06)(3.14) = 309.

$(V_p - V_m)$ = 2470 - 28.0 = 2442

From Equation 40,

w_p = (309 + 9.3)/(2442) = 0.130 lb./sec.
= 470 lb./hr.

Hole required = $\sqrt{(0.130)(144)/(205)(0.785)}$
= 0.341 in. say 11/32 in.

Thus refined calculation indicates only 5% more steam consumption required than approximate solution.

XIII. PROBLEMS

1. A 1/4-in. Schedule 40 pipe (i.d. = 0.364 in.), 18 ft. long, containing 3 ells and one globe valve, is connected to a compressed gas main at 100 lb./sq.in.ga. Calculate the flow of ammonia in lb./hr. at 70°F. with the globe valve wide open and the pipe discharging into a receiver at atmospheric pressure. The pipe intake is abrupt. Assume the perfect gas laws.

2. A vacuum gage is connected to a distillation column operated at 50 mm. Hg absolute pressure by an 8-ft. length of 1/4-in. Schedule 40 pipe (i.d. = 0.364 in.) containing four 90° standard ells and one

globe valve. Estimate the quantity of air, in cu.ft./min. at atmospheric pressure, that would leak into the column if the gage were accidentally left off with the valve wide open. Assume atmospheric air at 70°F.

3. A 3-in. Schedule 80 explosion-relief vent line from a reactor is 25 ft. long, discharging to the atmosphere, and contains 3 standard 90° ells. In the event of an explosion, the reactor liberates carbon dioxide at 350°F. What is the maximum carbon dioxide evolution rate, in lb./min., if the pressure in the reactor does not exceed 50 lb./sq.in. ga.? What pressure, in lb./sq.in.ga., must the reactor be designed for if the maximum evolution rate were 1000 lb./min.?

4. A 1-in., Schedule 40, steel pipe (i.d. = 1.049 in.), 500 ft. long and containing 15 standard 90° ells and a globe valve, is connected to an 80 lb./sq.in. ga. compressed air main. What is the maximum possible discharge to the atmosphere through this line, expressed in cu.ft./min. of free air? Assume temperature of air in the main is 70°F.

5. What is the maximum suction (or pressure), in in. water, that can be developed with a compressed air nozzle, having a 1/16 in. throat diameter, located in a 1-in. Schedule 40 pipe with an air pressure of 30 lb./sq.in. ga.? With 100 lb./sq.in. ga.? Assume an air temperature of 70°F.

6. Perform the same calculation as in Problem 5, using initially saturated steam in place of compressed air.

7. A large reaction tank is vented to the atmosphere through a 24-in. diameter stack, 100 ft. high. In order to avoid a nuisance and hazard around the feed holes and other clearances in the tank, it is desired to install a steam nozzle in the base of the stack which will induce a draft of 0.20 in. water in the vessel when handling 5000 cu.ft./min. of atmospheric air. Specify the nozzle size and steam consumption in lb./hr. using 100 lb./sq.in. ga. saturated steam. Assume the nozzle is made by simply drilling out a pipe cap. Assume air temperature is 25°C. and neglect rise in air temperature due to mixing with the steam.

8. A compressed air jet is used to draw air from a square ventilation hood, 18 in. on a side, through a vertical 6-in. i.d. round steel duct, 60 ft. high, which discharges through the side of the building through a short, sharp right angle (intersection of two 6-in. diameter cylinders) bend at the top. The compressed air jet points up in the center of the 6-in. duct at a point 6 in. beyond the entrance of the 6 in. duct. This jet consists of a 1-in. pipe cap containing a 5/8-in. diameter hole and is connected to a compressed air main at 10 lb./sq.in. ga. through a pipe of negligible resistance. Calculate the compressed air consumption (in cu.ft./min. at 20°C. and 1 atm.) and the air velocity at the hood intake (in ft./min.) when the duct discharge faces into a 50 mi./hr. wind. What is the hood velocity when the wind has subsided?

9. An organic compound of molecular weight 90 is purified by distillation under vacuum and is recovered in a vertical single-pass condenser in which the vapors are passed down through the tubes. The condenser consists of 225 tubes, 10 B.W.G. gage, 1-in. o.d., each 8 ft. long. The steam jet on the system develops 5 mm. Hg absolute pressure. Estimate the maximum possible capacity of the condenser without exceeding 20 mm. Hg absolute in the top of the column. Assume the pipes connecting the various pieces of equipment are of adequate size so that pressure drop through them is negligible. The organic compound has a boiling point of 107°C. at 20 mm. Hg and the ratio of specific heats is approximately 1.1.

p. 68: delete problem 7 and renumber subsequent problems accordingly.

Chapter 5

EJECTOR DESIGN AND PERFORMANCE

by

George E. Alves
Engineering Research Laboratory
Engineering Department
E. I. du Pont de Nemours & Co., Inc.
Wilmington, Delaware

TABLE OF CONTENTS

	Page
I. References	71
II. Nomenclature	71
III. General	72
IV. Description	72
V. Mixing Processes	73
VI. Low-Compression Ejector Design	73
VII. Nozzle Design	74
VIII. Low-Compression Ejector Performance	75
IX. Low-Compression Ejector Typical Design Values and Performance	75
A. Venturi-Type Ejector	76
1. Fan Operated	76
2. Compressed-Air Operated	76
B. Draft-Tube Ejector	76
1. Fan Operated	76
2. Compressed-Air Operated	76
X. High-Compression Ejector Design and Performance	77
XI. Thermo-Compressors	77
XII. Injectors	77
XIII. Effect of Solids	78
XIV. Performance of Ejectors as a Function of the Molecular Weights of Vapors	78
XV. Problem	78

LIST OF FIGURES

Page

Figure 1. Venturi-Type Ejector 73
Figure 2. Draft-Tube Ejector 73
Figure 3. Performance Curves of Low-Compression Ejectors 75

LIST OF REPRINTS

Reprint 1. McClintock, F. A. and Hood, J. H., J. Ae. Sci., 13, 559-568 (1946) Nov. 80
Reprint 2. Kroll, A. E., Chem. Eng. Progress, 1, 21-24 (1947) Feb. 90

I. REFERENCES

1. Anon., "Design of Injectors for Low-Pressure Air Flow," Heat. and Vent., 44, 82-94 (1947) July.
2. Brada, M., "Fundamental Theory of Thermo-Compressors," Chaleur et Industrie, 7, 673-678 (1926).
3. Croft, T., "Practical Information about Injectors," Power, 55, 460-463 (1922).
4. Elrod, H. G., Jr., "The Theory of Ejectors," J. App. Mech., 12, A170-A174 (1945) Sept. and Discussion, J. App. Mech., 13, A162-A165 (1946) June.
5. Engdahl, R. B., and Holton, W. C., "Overfire Air Jets," Trans. Amer. Soc. Mech. Engrs., 65, 741-754 (1943) Oct.
6. Engdahl, R. B., and Major, W. S., "Application of Overfire Jets to Prevent Smoke from Stationary Plants," Bituminous Coal Research, Inc., Tech. Report No. VII, Revised Aug. 1947.
7. Flügel, G., "Design of Jet Pumps," NACA, TM No. 982, July 1941.
8. Folsom, R. G., "Jet Pumps with Liquid Drive," Paper presented at the regional meeting of Amer. Inst. Chem. Engrs., Sept. 29-Oct. 1, 1947, at Buffalo, N. Y. (Published in Chem. Eng. Progress, 44, 765-770 (1948) Oct.).
9. Gebhardt, G. F., Steam Power Plant Engineering, New York, John Wiley and Sons, Inc., 1925.
10. Gosline, J. E., and O'Brien, M. P., "The Water Jet Pump," Univ. of Calif., Pub. in Eng., 3, 167-190 (1934).
11. Hiscox, G. D., Modern Steam Engineering in Theory and Practice, New York, Norman W. Henley Publishing Co., 1907.
12. Keenan, J. H., and Neumann, E. P., "A Simple Air Ejector," J. App. Mech., 9, A75-A81 (1942) June.
13. Kent, R. T., Mechanical Engineers' Handbook, New York, John Wiley and Sons, Inc., 1923.
14. Kneass, S. L., Practice and Theory of the Injector, New York, John Wiley and Sons, Inc. 1910.
15. Kravath, F. F., "The Venturi Ejector for Handling Air," Heat. and Vent., 37, 17-21, 46-49 (1940).
16. Kroll, A. E., "The Design of Jet Pumps," Chem. Eng. Progress, 1, 21-24 (1947) Feb.
17. McClintock, F. A., and Hood, J. H., "Aircraft Ejector Performance," J. Ae. Sci., 13, 559-568 (1946) Nov.
18. McElroy, G. E., "Design of Injectors for Low-Pressure Air Flow," Bur. of Mines, Tech. Paper 678, 1945.
19. Schutte & Koerting Co., "The Jet and Its Industrial Application," Bulletin J-1.
20. Severns, W. H., and Degler, H. E., Steam, Air, and Gas Power, New York, John Wiley and Sons, Inc., 1939.
21. Weeks, W. S., "The Air Ejector for Auxiliary Ventilation Underground," Eng. and Min. J., 138, 196-199 (1937).
22. Work, L. T., and Haedrich, V. T., "Performance of Ejectors as a Function of the Molecular Weights of Vapors," Ind. Eng. Chem., 31, 464-477 (1939) Apr.
23. Work. L. T., and Miller, A., "Factor C in the Performance of Ejectors as a Function of Molecular Weight of Vapors," Ind. Eng. Chem., 32, 1241-1243 (1940).

II. NOMENCLATURE

Any consistent system of units may be employed; the English system is given by way of example.

A = cross-sectional area, sq.ft.

D = inside diameter, ft.

E = efficiency

g_c = conversion factor, 32.17 (lb.) (ft.)/(lb. force) (sec.)

h = enthalpy, B.t.u./lb.

L_m = length of venturi-throat, ft.

L_n = distance between primary fluid nozzle and entrance to venturi-throat, ft.

p = pressure, lb.force/sq.ft. abs.

q = volumetric rate of flow, cu.ft./sec.

R = weight ratio of secondary fluid to primary fluid, lb./lb.

V = average velocity, ft./sec.

w = weight rate of flow, lb./sec.

α = half-angle of converging section, degrees

β = half-angle of diffuser, degrees

η_D = diffuser efficiency, dimensionless

ρ = density, lb./cu.ft.

When subscripts have been referred to above, they are used uniquely and integrally with the specific symbol referred to. Where several subscripts are used on a symbol, the individual significance of each subscript is to be added together. The term, g_c, has been labelled as such to be consistent with recent trends of nomenclature. The following subscripts are general.

0 = in reservoir; in upstream
1 = at discharge of nozzle; at entrance of venturi-throat
2 = at end of venturi-throat; at entrance to diffuser
3 = at end of diffuser; in downstream
f = feed-water
m = in venturi-throat; in mixing section of draft-tube; mixture
p = primary or driving fluid
s = secondary or induced fluid
x = solids

III. GENERAL

An ejector is a device in which the kinetic energy of one fluid (primary, driving or motive fluid) is used to pump a second fluid (secondary or induced fluid).

Ejectors are used to a large extent in the chemical industry. Some of the many applications are: exhausting fumes, producing vacua, transporting slurries, pneumatic conveyor feeding, and preventing smoke from stationary plants.

Ejectors are given various names depending upon their application. Classifications employed by one large manufacturer (19) are:

Ejector - A general term covering all types of jet pumps which discharge at a pressure intermediate to motive and suction pressures.

Injector - A particular type of jet pump which uses a condensable gas to entrain a liquid and discharge against a pressure higher than either motive or suction pressures. Principally a Boiler Feed-Water Injector.

Syphon - A liquid pump using a condensable vapor, normally steam, as motive fluid.

Eductor - A liquid pump using a liquid as motive fluid.

Exhauster - A gas pump using a liquid or gas as motive fluid.

Jet Blower - A gas jet pumping gases against very low differential pressures.

Jet Compressor - A gas jet pump to boost pressure of gases.

Overfire Jets are Jet Blowers used to supply additional air to furnaces to prevent smoke. A good discussion of the general design and application of overfire jets is given by Engdahl and Major (6).

IV. DESCRIPTION

An ejector may be of either the Venturi Type (Figure 1) or the Draft-Tube Type (Figure 2).

The venturi type is used for both low-compression and high-compression ejectors. It is composed of the following sections: I. - Secondary Fluid Inlet, II. - Contraction, III. - Venturi-Throat, IV. - Diffuser, V. - Discharge, VI. - Primary Fluid Inlet, and VII. - Primary Fluid Nozzle. A low-compression ejector is one where the density change of the secondary fluid is less than 10% of the average density.

The draft-tube type is used only for low-compression ejectors.

In operation, the jet from the nozzle entrains the secondary fluid, and both fluids are mixed with or without a pressure rise. In the case of the venturi type, the mixed streams leave the mixing section at a high velocity and this high velocity is converted to pressure in the diffuser.

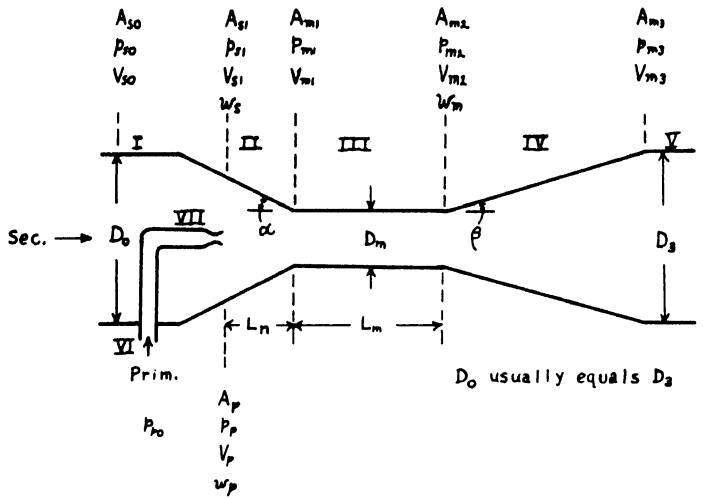


Figure 1. Venturi-Type Ejector

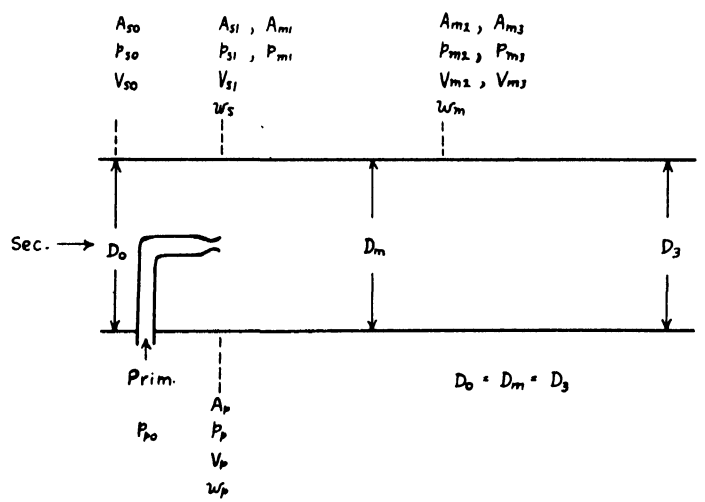


Figure 2. Draft Tube Ejector

V. MIXING PROCESSES

Two commonly used mixing processes are: 1) constant pressure and 2) constant area.

In the constant pressure process, the mixing takes place in the contraction section, II, Figure 1. The distance, L_n, between the nozzle and the venturi throat is approximately equal to the length of the contraction section. The length of the venturi throat, L_m, is zero. The angle, α, of the contraction section is such as to give a constant pressure in the section. The analysis of constant pressure mixing is given by several investigators (2, 7, 12).

In the constant area process, the mixing takes place in the venturi throat, Section III, Figure 1. The length of the venturi throat, L_m, is such as to give complete mixing. The distance, L_n, between the nozzle and the venturi throat is zero; however, in practice this distance is approximately equal to one venturi throat diameter. The mixing process in a draft tube type ejector is of the constant area type. The analysis of constant-area mixing is given in many references (1, 7, 8, 10, 12, 17, 18, 21).

A combination of both mixing processes is also used in commercially manufactured ejectors.

VI. LOW-COMPRESSION EJECTOR DESIGN

The design of high-compression ejectors is somewhat of an art. However, low-compression ejectors may be designed by direct application of the momentum balance equations. The analysis of low-compression ejectors will be presented, together with typical design values. In the case of high-compression ejectors, only typical design values will be presented. The effect of solids upon ejector performance will also be discussed.

A low-compression ejector is one in which the density change of the secondary fluid across the ejector is less than 10% of the average density.

The following analysis has been given by many investigators (1, 7, 8, 10, 12, 17, 18, 21). The analysis will be applied to the venturi-type ejector, Figure 1.

A constant-area mixing process will be used; that is, the mixing will take place in the venturi throat, Section III. Therefore, the distance, L_m, between the nozzle discharge and the venturi throat is zero. It will be assumed that the primary flow and secondary flow consist of the same fluid.

Thus,

$$A_{s1} + A_p = A_{m1} \quad \text{(neglecting the wall thickness of the nozzle)} \tag{1}$$

$$p_{s1} = p_p = p_{m1} \tag{2}$$

$$A_{m1} = A_{m2} \tag{3}$$

$$\rho_s = \rho_p = \rho_m \tag{4}$$

also,

$$w_s + w_p = w_m \tag{5}$$

By applying Bernoulli's equation across Section II, the pressure, p_{s1}, can be determined,

$$\frac{p_{so}}{\rho_s} + \frac{V_{so}^2}{2g_c} = \frac{p_{s1}}{\rho_s} + \frac{V_{s1}^2}{2g_c} \tag{6}$$

bearing in mind that from the continuity equation,

$$A_{so}\ V_{so} = A_{s1}\ V_{s1} \tag{7}$$

The velocity in the venturi throat or mixing section is,

$$V_{m_2} = \frac{w_m}{\rho_m\ A_{m_2}} = \frac{(w_s + w_p)}{\rho_s\ A_{m_2}} \tag{8}$$

The change in pressure across the mixing section, Section III, due to mixing can be determined by a momentum balance (see Chapter 1, "Mass, Energy, and Momentum Balance"),

$$w_p\ V_p + w_s\ V_{s1} - w_m\ V_{m2} = (p_{m2} - p_{s1})\ A_{m2}\ g_c \tag{9}$$

The pressure rise due to the conversion of kinetic energy into pressure in the diffuser, Section IV, can be determined by the application of Bernoulli's equation,

$$\frac{p_{m2}}{\rho_s} + \frac{V_{m2}^2}{2g_c} = \frac{p_{m3}}{\rho_s} + \frac{V_{m3}^2}{2g_c} \tag{10}$$

The total pressure rise across the ejector is the algebraic sum of the pressure changes; that is,

$$(p_{m3} - p_{so}) = (p_{s1} - p_{so}) + (p_{m2} - p_{s1}) + (p_{m3} - p_{m2}) \tag{11}$$
$$\text{Eq. 6} \qquad \text{Eq. 9} \qquad \text{Eq. 10}$$

Equation 10 assumes a diffuser efficiency of 100%. In the general case, Equation 10 may be written as,

$$(p_{m3} - p_{m2}) = \eta_D\ \rho_s\ (V_{m2}^2 - V_{m3}^2)/2g_c \tag{12}$$

η_D is the diffuser efficiency. For a diffuser efficiency of 100%, $\eta_D = 1.0$, Equation 12 reduces to Equation 10. In practice the diffuser efficiency ranges from 50 to 75%.

Several investigators (1, 4, 7, 10, 17, 18) have presented design curves and charts based upon the above equations. These charts and curves give ejector dimensions for maximum efficiency.

The above analysis also applies for a draft tube. In this case the calculations are simplified by the absence of the diffuser; thus, $A_{so} = A_{m1} = A_{m2} = A_{m3}$ and $p_{m2} = p_{m3}$.

VII. NOZZLE DESIGN

For high-pressure primary fluids, compressed air or steam, the nozzle is usually of the converging-diverging (de Laval) type. In Figure 1, the nozzle is Section VII. The design of de Laval nozzles is discussed in many sources, see Chapter 4, "Flow of Compressible Fluids." However, drilled pipe caps will give approximately the same performance (5).

For low-pressure primary fluids, such as air delivered by a fan, a converging nozzle is used.

It has been found that multiple nozzles in parallel ("pepper box") increase the mixing rate; in other words, the length of the mixing section, L_m, required for multiple nozzles is shorter than for a single nozzle (5, 17).

VIII. LOW-COMPRESSION EJECTOR PERFORMANCE

The form of performance curves for low-compression ejectors are sketched in Figure 3. The pressure rise, $(p_{ms} - p_{so})$, across the ejector is usually given in inches of water; and the volumetric rate of flow of secondary fluid, q_s, is usually given in cu.ft./min. These curves give the comparative performance for ejectors in which p_{po}, D_o, D_s, and A_p are the same for both venturi and draft-tube types.

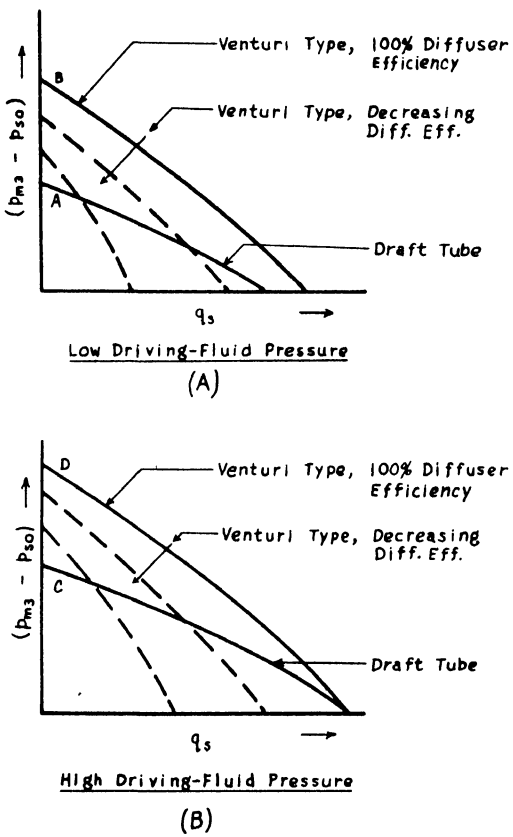


Figure 3. Performance Curves of Low-Compression Ejectors

Figure 3-A is for ejectors whose primary fluid is supplied at low pressure; i.e., a fan. Curve A is for a draft tube. Curve B is for a venturi-type ejector with a diffuser of 100% efficiency. The maximum rate of flow of secondary fluid (at zero pressure rise across the ejector) is higher than for the draft tube because the nozzle discharge pressure, $p_p = p_{s1}$, is appreciable compared to p_{po} (see Equation 6), and, therefore, the jet velocity, V_p, and weight rate of flow of primary fluid, w_p, are greater than the corresponding values for the draft tube. (This assumes that the primary flow can be supplied at a constant pressure, p_{po}). However, in the practical case, the diffuser efficiency is of the order of 50%.

Figure 3-B is for ejectors where the primary fluid is delivered to the nozzle at high pressures. For these cases, critical flow is obtained in the nozzle. Curve C is for a draft tube. Curve D is for a venturi-type ejector with a diffuser of 100% efficiency. It is noted that the maximum capacities of these two ejectors, Curves C and D for zero pressure rise, are almost the same. The reason is that the nozzle discharge pressure, $p_p = p_{s1}$, is very small compared to the nozzle supply pressure, p_{po}. Thus, the high-pressure jet momentum is approximately constant for both ejectors and for all rates of flow of secondary air.

A venturi-type ejector uses from 30 to 40% less weight rate of flow of primary fluid than a draft tube for the same operating conditions.

There are several methods of defining efficiency, each method having merit or utility for specific purposes. One definition is given by the following equation. This equation assumes incompressible flow.

$$E = w_s(p_{ms} - p_{so})/w_p(p_{po} - p_{ms}) \qquad (13)$$

The efficiencies are low, being on the order of 15%.

IX. LOW-COMPRESSION EJECTOR TYPICAL DESIGN VALUES AND PERFORMANCE

It has been determined experimentally that for best performance, the distance, L_n, between the nozzle discharge and the inlet to the venturi throat is not zero as was assumed in the above theory.

Also for best performance, the length of the venturi throat (mixing section), L_m, has to be of sufficient length to insure perfect mixing.

The following values are either based on experimental data or are customarily used. The values are for air as the secondary and primary fluids.

A. Venturi-Type Ejector

1. Fan Operated (Reference 15)

$D_m = D_3/2$

nozzle diameter = 1/6 to 1/3 D_m

L_m = 4 to 10 D_m (optimum = 6 D_m)

L_n = 1/2 to 2 D_m (optimum = D_m)

α = 10° to 30°

β = 2° to 5°

V_p = 100 to 400 ft./sec.

V_{m_2} = 50 to 200 ft./sec.

$(p_{m_3} - p_{s_0})$ = normally not over 6 in. of water

2. Compressed-Air Operated

$D_m = D_3/2$

nozzle is of the de Laval type or the nozzle may be a drilled pipe cap (critical flow)

L_m = 4 to 10 D_m (optimum = 6 D_m)

L_n = 1/2 to 2 D_m (optimum = 1 D_m)

α = 10° to 30°

β = 2° to 5°

V_p = 1100 to 1700 ft./sec.

V_{m_2} = 100 to 400 ft./sec.

$(p_{m_3} - p_{s_0})$ = usually not over 30 in. of water

B. Draft Tube

1. Fan Operated

nozzle diameter = 1/10 to 1/5 D_m

V_p = 100 to 400 ft./sec.

V_{m_2} = 10 to 50 ft./sec.

$(p_{m_3} - p_{s_0})$ = usually not over 3 in. of water

2. Compressed-Air Operated

nozzle is of the critical flow type

V_p = 1100 to 1700 ft./sec.

V_{m_2} = 20 to 100 ft./sec.

$(p_{m_3} - p_{s_0})$ = usually not over 15 in. of water

Several design charts based on experimental data have been published (6, 16, 17). The articles by McClintock and Hood (17) and Kroll (16) are appended to this chapter as Reprints 1 and 2 respectively. The article by Kroll (16) represents a good coverage of the literature and presents design curves for both steam-jet and air-jet air ejectors. Kroll also presents a discussion of the design factors affecting performance. The following corrections and comments should be noted in Kroll's article:

a.) Figure 9 - The nozzle flow chart for steam is in error. The chart for air is correct.

b.) Page 22, center of last column - The following nozzle discharge coefficients are recommended in place of those specified by Kroll:

well-manufactured nozzle, 0.97
drilled pipe cap, 0.83

c.) The data obtained from ejectors without diffusers are correlated with data from ejectors with diffusers.

X. HIGH-COMPRESSION EJECTOR DESIGN AND PERFORMANCE

There are no "convenient" design methods for high-compression ejectors. Manufacturers base their designs on the results of many years experience. The theoretical methods of design involve the use of the adiabatic equations for compression and expansion of the fluids. These methods are tedious to use; however, two papers (2, 7) present the relations in useful forms. The relations given for the design of low-compression ejectors may be used as an approximation by employing the average density for each section. Following are some considerations that may be used as a guide in designing high-compression ejectors for special applications.

The mixing process is generally a combination of constant-pressure and constant-area mixing. Thus the length, L_m, of the venturi throat is a finite value and should be kept to a minimum in order to reduce the frictional losses due to the high throat velocities. The length, L_m, varies from 0 to 1 venturi-throat diameters; that is, $L_m = 0$ to 1 D_m. The distance, L_n, from the inlet to the venturi throat to the nozzle discharge can be adjusted by experimentation to determine the best operating position. The distance, L_n, may vary from 1/2 D_m to a distance equal to the length of the contraction section, depending upon the amount of constant-pressure mixing that can take place in the contraction section.

The angle, α, of the contraction section is approximately 10° for constant-pressure mixing to approximately 30° for constant-area mixing. These values are only approximate.

The angle, β , of the diffuser is approximately 3° and may be increased, after a distance from the discharge of the venturi throat, say 2 to 4 D_m, up to 15° in order that the length of the diffuser may not become excessive. The efficiency of the diffuser can be taken as 50% (a conservative value).

The primary fluid velocity, V_p, is about 1700 ft./sec. for compressed air at about 100 lb.force/sq.in. gage supply pressure and about 2700 ft./sec. for saturated steam at about 125 lb.force/sq.in. gage supply pressure. The velocity in the venturi throat, V_{m_2}, is about 500 to 1000 ft./sec.

The maximum pressure rise across a high-compression ejector depends upon many factors as can be seen from the above. However, in general, the maximum pressure rise for a steam jet-air ejector using 125 lb. force/sq.in. gage steam is approximately 15 lb. force/sq. in.

XI. THERMO-COMPRESSORS

Thermo-compressors are high-compression ejectors used to compress low-pressure steam (slight vacuum to 15 or 20 lb. force/sq. in. gage) through a range of approximately 10 to 15% of the initial pressure of the high-pressure steam (primary fluid). Approximately 1/4 of 2 lb. of low-pressure steam can be compressed with 1 lb. of high-pressure steam, depending upon the pressure-rise required and the initial pressures of the steam.

XII. INJECTORS

The most common application of injectors is to feed water into a boiler using steam at boiler pressure. The high-velocity steam from the nozzle imparts an impulse upon the water and at the same time condenses. The mixing takes place in the converging section (that is, at constant pressure) and the length of the venturi throat is zero. All of the pressure rise is obtained in the duffuser; however, the pressure rise is large due to the high kinetic energy of the water from the venturi throat. Sufficient water must be used in order to completely condense the steam. The relations presented for the design of low-compression ejectors may be used as an approximation by using the average density in each section.

The pumping efficiency for an injector is from 2 to 4%. The heat loss due to radiation and convection is about 2%.

The ratio, R, of the weight of secondary water per unit weight of primary steam is

$$0.98\ (h_p - h_f) = R\ (h_f - h_s) \tag{14}$$

Practical values that can serve as a guide are:

$$R \cong 15\ \frac{\text{lb. water}}{\text{lb. steam}} \text{ for } p_{po} \cong 125 \text{ lb.force/sq.in.gage}$$

$$V_{m\,2} = 100 \text{ to } 150 \text{ ft./sec.}$$

Pressure rise across the injector, $(p_{m3} - p_{so})$, is usually limited to on the order of 50 lb.force/sq.in. greater than the initial steam pressure; that is,

$$(p_{m3} - p_{so}) = (p_{po} + 50) \tag{15}$$

where the pressures are in lb.force/sq.in. absolute.

Much literature (3, 9, 11, 13, 14, 20) has been published on the approximate design and on the description and operation of boiler feed-water injectors. However, the literature, for the most part, dates prior to 1925 and has become difficult to obtain.

XIII. EFFECT OF SOLIDS

Occasionally it is desired to design an ejector to feed and/or to convey solids. Solids suspended in the secondary stream may be taken into account by allowing for the loss in momentum in accelerating the solids to the velocity of the mixture in the venturi throat. The pressure rise obtained by the conversion of the kinetic energy of the solids in the diffuser is computed using the mixture density. Therefore, taking into account the loss in momentum to accelerate the solids, Equation 9 is modified to

$$w_p\ V_p + (w_s + w_x)\ V_{s1} - (w_m + w_x)\ V_{m2} = (p_{m2} - p_{s1})\ A_{m2}\ g_c \tag{16}$$

The above analysis assumes there is no slip between the solids and the gas stream in the venturi throat; however, practice has indicated that there is a slip. The amount of slip is not known quantitatively. Therefore, the above method is conservative from the design standpoint.

Special ejectors are being manufactured commercially with a large throat and provisions for admitting the solids along the center line and for admitting the primary fluid through an annulus formed by the solids inlet tube and wall of the ejector.

XIV. PERFORMANCE OF EJECTORS AS A FUNCTION OF THE MOLECULAR WEIGHTS OF VAPORS

Performance data for ejectors using various vapors for the primary fluid and for the secondary fluid have been empirically correlated as a function of the molecular weight of the vapors by Work, Haedrich, and Miller (22, 23).

XV. PROBLEM

1. Compute and plot the performance characteristics of a draft tube and of a Venturi-type ejector. The dimensions and conditions of operation are:

Dimensions:

a.) Draft tube: duct diameter = 12-in. i.d.
nozzle discharge diameter = 2-in. i.d.

b.) Venturi-type ejector: duct diameter = 12-in. i.d.
Venturi throat diameter = 6-in. i.d.
nozzle discharge diameter = 2-in. i.d.

Operating conditions:

a.) Secondary fluid is air at 70 F. drawn in by the ejector from the atmosphere.

b.) Primary fluid is air at 70 F. delivered by a fan capable of producing a static pressure of 30-in. of water for the rates of primary air required by the ejectors.

The following assumptions are to be made:

a.) Inlet losses = 0

b.) Neglect friction in the ejectors

c.) Diffuser efficiency = 100%

d.) A convergent nozzle is used.

e.) Nozzle wall thickness is negligible.

The performance characteristics required are the pressure, inches of water, developed by the ejector for various secondary air rates of flow, c.f.m. free air (i.e. measured at 70 F. and 1 atm. pressure).

Reprint 1.
Reprinted from Journal of The Aeronautical Sciences Nov. 1946
by Permission from Institute of The Aeronautical Sciences

JOURNAL OF THE AERONAUTICAL SCIENCES

VOLUME 13 NOVEMBER, 1946 NUMBER 11

Aircraft Ejector Performance

FRANK A. McCLINTOCK* AND J. HALL HOOD†
United Aircraft Corporation and Consolidated Vultee Aircraft Corporation

SUMMARY

This paper presents the results of work on the ejector problem carried out by the Research Department, United Aircraft Corporation, over the past few years. Equations are developed which, with the aid of empirical coefficients, enable one to estimate the performance of steady flow ejectors pumping a fluid across a small pressure rise or drop. Experimental data are presented which support the theory and provide information on some variables not covered by the theoretical treatment. An analogy between steady and intermittent flow is presented which makes it possible to estimate the performance of ejectors used in cooling aircraft engines. A method of applying the results to the design of ejectors is suggested.

The principal uses for an ejector in aircraft engine installations appear to be in those cases in which cooling would otherwise have to be obtained by the use of a fan or stalled cowl flaps, or in which the exhaust thrust could not otherwise be used because of flame, noise, or temperature. The results indicate that little gain in thrust can be obtained in an installation in which there is a pressure drop through the ejector so that pumping is not necessary.

INTRODUCTION

AN EJECTOR IS A DEVICE in which the kinetic energy of one fluid is used to pump a second fluid. It consists essentially of a duct through which is discharged a high velocity jet. The secondary fluid is drawn from a region of low pressure, mixes with the high velocity jet in the duct, and is discharged to a region of higher pressure. The ejector may, of course, be operated with no pressure rise or a pressure drop through it. In this case, the ejector may still increase the net thrust of the installation but it will not act as a jet pump.

For airplane installations in which the propeller or flight-induced cooling is inadequate (such as in helicopters or airplanes climbing at slow speeds), some form of pump must be used to maintain the required cooling airflow through the engine. Cowl flaps may be employed as a pumping device. In this case, however, the pressure rise is maintained by stalling the cowl flaps, which results in an increase in form drag. The two alternatives at present are fans and ejectors. Although an ejector is a far less efficient pump than a fan, it need not take power from the engine and it has the advantage that the propulsive efficiency of the exhaust jet may actually be improved by mixing it with the large mass of slow-moving cooling air.

Presented at the National Aircraft Propulsion Meeting, I.A.S., Cleveland March 21, 1946.

* Assistant Project Engineer, Pratt & Whitney Aircraft Division.

† Research Engineer.

THEORETICAL TREATMENT

The object of this analysis is to develop equations for the pressure rise of the secondary stream and for the momentum from the ejector system in terms of the quantity and state of the primary and secondary streams and the dimensions of the ejector. The effects of mixing and velocity distribution are accounted for by empirical coefficients. Incompressible flow is assumed in order to reduce the number of variables required in presenting an overall picture of ejector performance and to give equations that can be solved explicitly for given dimensions. The effects of compressible flow are discussed qualitatively in a later section.

This analysis differs from that of Flugel[1] and Gosline and O'Brien[2] in that the increase in exhaust momentum is calculated and the effect on performance of nonuniform velocity distribution at a section is considered.

When the velocity distribution at any given section of a fluid stream is not uniform, the mean velocities for the continuity equation, the momentum equation, and the energy equation are all different, because one is an arithmetic mean, the second a root mean square, and the third a root mean cube velocity. The empirical coefficients C_M and C_H are used to relate the mean velocities for momentum and velocity head to that for flow,

V. Thus, the equations for flow, momentum, and velocity head at a given section are:

$$\text{Flow} = W = \rho g A V \quad (1)$$

$$\text{Momentum} = F = W(VC_M)/g \quad (2)$$

$$\text{Velocity head} = \rho(VC_H)^2/2 \quad (3)$$

where

W = weight flow
ρ = mass density
g = gravitational constant
V = velocity
A = cross-sectional area
F = momentum at a section

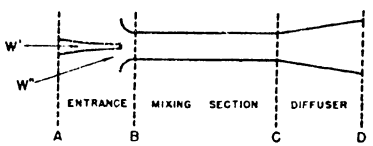


FIG. 1. Schematic diagram of ejector.

Fig. 1 is a schematic diagram of an ejector, indicating the sections considered in this analysis. The following notation is used:

NOTATION

Superscripts:

' refers to primary jet
'' refers to secondary fluid
Terms without superscripts refer to both streams or the mixed stream

Subscripts:

A refers to conditions at zero velocity before the ejector
B refers to conditions before mixing in the throat of the ejector
C refers to conditions at end of mixing section
D refers to conditions at exit of diffuser

The pressure changes in the entrance section and the diffuser sections are found from Bernoulli's equation and the definition of efficiency:

$$P_A'' - P_B = \frac{\rho''(V_B''C_{HB}'')^2}{2\eta_{AB}''} \quad (4)$$

$$P_D - P_C = \eta_{CD}\left[\frac{\rho(V_CC_{HC})^2}{2} - \frac{\rho(V_DC_{HD})^2}{2}\right] \quad (5)$$

where

P = pressure

η_{AB}'' = $\dfrac{\text{ideal pressure drop}}{\text{actual pressure drop}}$ of secondary air in entrance section for a given change in velocity

η_{CD} = $\dfrac{\text{actual pressure rise}}{\text{ideal pressure rise}}$ in the diffuser for a given change in velocity

The pressure rise in the mixing section is found from the momentum equation and the pressure drop due to friction. The friction pressure drop is based arbitrarily on the secondary velocity at section B.

$$P_C - P_B = \frac{1}{A_C}\left(\frac{W'V_B'C_{MB}'}{g} + \frac{W''V_B''C_{MB}''}{g} - \frac{WV_CC_{MC}}{g}\right) - \frac{f\rho''(V_B''C_{HB}'')^2}{2}\frac{L}{D} \quad (6)$$

where the friction factor, f, is defined by the equation

$$\text{Friction pressure drop} = (f\rho V^2/2)(L/D)$$

L = length of mixing section wall
D = diameter of mixing section

In order to reduce the number of variables, the following dimensionless ratios are introduced:

$$\alpha = \frac{\text{Area of diffuser exit}}{\text{Area of mixing section}}$$

$$\lambda = \frac{\text{Area of mixing section}}{\text{Effective area of primary jet}}$$

$$\mu = \frac{\text{Secondary flow}}{\text{Primary flow}}$$

$$\sigma = \frac{\text{Secondary density}}{\text{Primary density}}$$

For incompressible fluids or for the same gas at different temperatures in the primary and secondary streams, the density of the mixed stream is found from the following relation:

$$\rho = \frac{W' + W''}{(W'/\rho') + (W''/\rho'')}; \quad \frac{\rho}{\rho'} = \frac{1+\mu}{1+(\mu/\sigma)} \quad (7)$$

Introducing the dimensionless ratios, and combining Eqs. (1), (4), (5), (6), and (7), the following relationships for the pressure rise from the various sections to the discharge pressure are obtained:

$$\frac{P_D - P_C}{F'/A'} = \frac{\eta_{CD}C_{HC}^2(1+\mu)[1+(\mu/\sigma)]}{2\lambda^2}\left[1 - \left(\frac{C_{HD}}{\alpha C_{HC}}\right)^2\right] \quad (8)$$

From the ejector throat:

$$\frac{P_D - P_B}{F'/A'} = \frac{C_{MB}'}{\lambda} + \frac{\mu^2C_{MB}''}{\sigma\lambda(\lambda-1)} - \frac{\mu^2(C_{HB}'')^2}{2\sigma(\lambda-1)^2}f\frac{L}{D} - \frac{(1+\mu)(1+\mu/\sigma)}{\lambda^2}\left\{C_{MC} - \frac{C_{HC}^2\eta_{CD}}{2}\left[1 - \left(\frac{C_{HD}}{\alpha C_{HC}}\right)^2\right]\right\} \quad (9)$$

From the initial secondary pressure:

$$\frac{P_D - P_A''}{F'/A'} = \frac{C_{MB}'}{\lambda} + \frac{\mu^2C_{MB}''}{\sigma\lambda(\lambda-1)} - \frac{\mu^2(C_{HB}'')^2}{2\sigma(\lambda-1)^2} \times \left(\frac{1}{\eta_{AB}''} + f\frac{L}{D}\right) - \frac{(1+\mu)(1+\mu/\sigma)}{\lambda^2} \times \left\{C_{MC} - \frac{C_{HC}^2\eta_{CD}}{2}\left[1 - \left(\frac{C_{HD}}{\alpha C_{HC}}\right)^2\right]\right\} \quad (10)$$

The momentum of the combined stream at the ejector exit is found from Eq. (2),

$$F = WV_D C_{MD}/g \tag{11}$$

The ratio of this momentum to the momentum of the primary jet is found from Eqs. 1, 2, 7, and 11:

$$F/F' = \frac{(1+\mu)(1+\mu/\sigma)C_{MD}}{\alpha\lambda C_{MB}'} \tag{12}$$

Not all of the coefficients in Eqs. (10) and (12) are worth considering; in fact, a fair correlation between test results and theory can be found by assuming the coefficients η_{AB}'', C_{MB}', C_{MB}'', C_{HB}', and C_{HB}'' equal to unity, neglecting the skin friction, and considering C_{MD} and the group $C_{MC} - \frac{C_{HC}^2\eta_{CD}}{2}\left[1 - \left(\frac{C_{HD}}{\alpha C_{HC}}\right)^2\right]$ (hereafter called K) to be functions of the diffuser area ratio only. Eqs. (10) and (12) then become

$$\frac{P_D - P_A''}{F'/A'} = \frac{1}{\lambda} + \frac{\mu^2}{\sigma\lambda(\lambda-1)} - \frac{(1+\mu)(1+\mu/\sigma)K}{\lambda^2} - \frac{\mu^2}{2\sigma(\lambda-1)^2} \tag{13}$$

$$F/F' = \frac{(1+\mu)(1+\mu/\sigma)C_{MD}}{\alpha\lambda} \tag{14}$$

The experimental flow and thrust coefficients (K) and (C_{MD}) have been calculated from data on compressed air tests of single nozzle ejectors having a cylindrical mixing section five diameters in length and having 8° (included angle) conical diffusers. Fig. 2 gives the average values of these coefficients as a function of the diffuser area ratio, α. Fig. 3 shows a comparison of the theoretical curves based on the coefficients given in Fig. 2, and cross-plots of the actual experimental data. These curves give the pressure rise ratio for the secondary stream and the thrust ratio as a function of the mixing section area ratio, λ, for a constant flow ratio, μ, of 2. Substantially the same degree of correlation was found for other flow ratios. This appears to justify the direct use of the theoretical equations in predicting the performance of this type of ejector. While better values of the empirical thrust and flow coefficients, C_{MD} and K, were observed in some tests, these are probably as good as could be expected in an actual installation, so that their use for preliminary estimates seems justified.

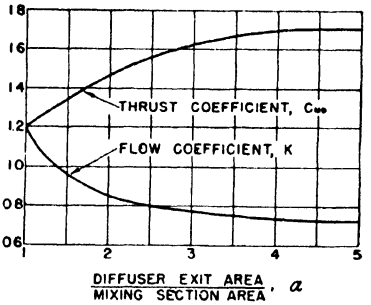


FIG. 2. Empirical thrust and flow coefficients.

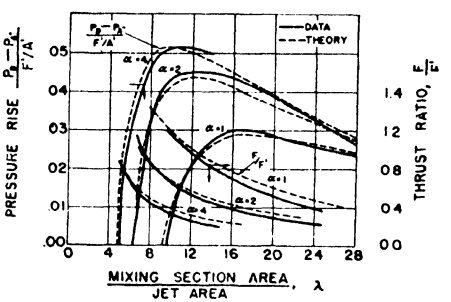


FIG. 3. Comparison of data with theory. Flow ratio, $\mu = 2$; density ratio, $\sigma = 0.92$; α = diffuser area ratio.

EFFECT OF PRIMARY VARIABLES ON EJECTOR PERFORMANCE

For a given primary jet, ejectors can be designed which pump either a little air across a high pressure rise or more air across a small pressure rise with an increase in momentum. The effect of varying the primary jet in a given ejector is more difficult to visualize, because a change in the primary jet affects several of the dimensionless groups of Eqs. (13) and (14) simultaneously. Nor can the effect of changes in the density ratio be seen at a glance; its effect on the flow or thrust must be found by solving the equations for the particular case at hand.

For the purpose of illustrating the design parameters and showing the characteristic performance of steady flow ejectors, a series of curves has been calculated based on the experimental coefficients given in Fig. 2 for a density ratio of 3.5, this being representative of an ejector using steady flow engine exhaust gas as the actuating jet.* Since the flow and the pressure rise are usually specified in ejector design, plots of pressure rise vs. mixing-section area ratio are presented for flow ratios of 2, 6, and 10 as shown in Fig. 4. For a typical engine, a pressure rise of 10 in. of water corresponds to a pressure rise parameter of 0.03. As would be expected, the curves show that in order to get more pressure rise for the same flow and mixing section area, more diffuser must be used. The effectiveness of adding a diffuser falls off as more and more is used. It should also be noted from these curves that for any given flow ratio and diffuser area ratio, there is a mixing section area that gives the greatest possible rise. If the maximum pressure rise is not required, then a range of mixing sections can be used. The use of a

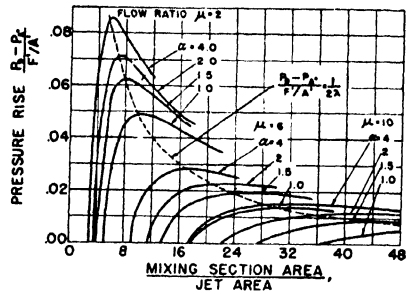


FIG. 4. Theoretical pumping capacity. Density ratio, $\sigma = 3.5$; α = diffuser area ratio.

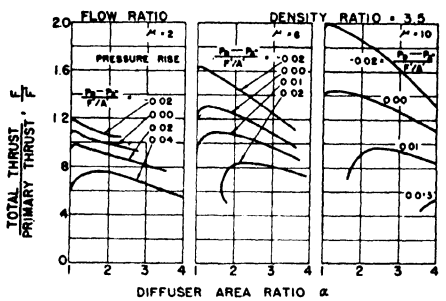


FIG. 5. Theoretical thrust ratio.

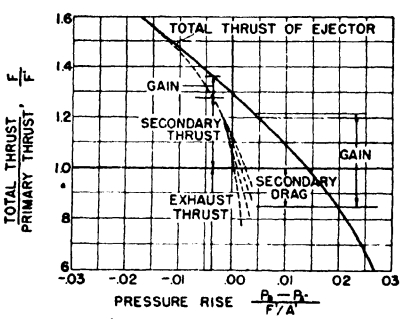


FIG. 6. Theoretical maximum thrust ratio. Flow ratio, $\mu = 6$; density ratio, $\sigma = 3.5$.

smaller mixing section would give more thrust and result in a smaller ejector, but, on the other hand, the mixing section area ratio is less critical if the larger mixing section is used, so that it is easier to meet the design point in that region.

The points of maximum pressure rise for a given flow and diffuser area ratio can be found analytically by differentiating the flow equation, Eq. (13), with respect to the mixing section area ratio, λ, equating to zero, and eliminating the flow coefficient, K, by Eq. (13). The result is:

$$\frac{P_D - P_A''}{F'/A'} = \frac{1}{2\lambda} + \frac{\mu^2}{2\sigma\lambda(\lambda - 1)^2} \qquad (15)$$

The second term is negligible. The simplified equation determines the locus of the points of maximum pressure rise for a given flow and diffuser area ratio, or the points of minimum diffuser area for a given flow and pressure rise, as shown in Fig. 4. The use of this equation will be described in the design section.

For most aircraft installations the momentum of the ejector stream is of interest. Reference to Eq. (14) shows that the smaller the diffuser and mixing section area ratios, the greater the momentum for a given flow. But since these area ratios must be adjusted to maintain the required pressure rise, there is an optimum diffuser area ratio for a given flow and pressure rise. Fig. 5 shows the ratio of total to primary thrust vs. diffuser area ratio at different pressure rises and flow ratios of 2, 6, and 10, respectively. It will be noted from these curves that for a given flow ratio the diffuser area ratio for maximum thrust is greater at the higher pressure rises. The thrust ratio is greatest with high flows and a pressure drop across the ejector. Fig. 6 is a cross-plot of the maximum thrust points for a flow ratio of 6, showing the increase in thrust as the pressure rise decreases and finally becomes a pressure drop. The usefulness of an ejector as a thrust-augmenting device can only be judged by comparing it with other systems. The dotted lines on the right-hand side of Fig. 6 show the drag that might be associated with pumping the cooling air out by means of cowl flaps or the loss in propeller thrust that would result from using a cooling fan. The exhaust thrust less this drag is the net thrust of the alternate system and is less than the total thrust of the ejector, shown by the solid line, so that in this region the ejector will give better performance than other systems. When there is a pressure drop through the ejector, however, the net thrust of the alternate system is that of the exhaust thrust plus the momentum that the cooling air would have if discharged separately. This momentum, neglecting losses, would be:

$$F'' = W'' V_D''/g \qquad (16)$$

The velocity may be found from the available pressure drop of the secondary stream; hence, the momentum is:

$$F'' = (W''/g)\sqrt{2(P_A'' - P_D)/\rho''} \qquad (17)$$

Expressed in terms of the properties of the primary jet, this momentum is:

$$\frac{F''}{F'} = \mu\sqrt{\frac{2}{\sigma}}\sqrt{\frac{(P_A'' - P_D)}{F'/A'}} \qquad (18)$$

Fig. 6 shows that with an increasing pressure drop through the ejector, the sum of the exhaust thrust and this secondary momentum soon equals the ejector thrust.

For a typical engine exhaust and a flow ratio of 6, the ejector yields no gain in thrust when the pressure drop through the ejector is greater than about 5 in of water. This characteristic of ejectors limits their usefulness as thrust augmenters to a small range. They are nonetheless useful in reducing the drag associated with pumping the cooling air, if that is necessary.

Effect of Compressibility

The experimental coefficients in the steady flow theory were derived from compressed air tests in which the primary jet velocity was approximately 700 or 800 ft. per sec. Steady flow tests with superheated steam as the primary fluid were, however, run with primary velocities from 1,200 to 2,800 ft. per sec. The latter tests showed that the design of an ejector is not affected by the primary jet velocity. For supersonic velocities of the primary jet the performance of the ejector was not appreciably affected by removing the divergent section of the nozzle. In designing an ejector, however, the area of the fully expanded stream, rather than the area of the nozzle, must be used. The temperature of the primary jet should also be calculated assuming complete expansion of the jet to the pressure in the ejector throat.

The high-velocity steam tests showed that the performance of an ejector fell off sharply when the flow mean velocity of the mixed streams reached a Mach Number around 0.6. After this velocity was reached, practically no increase in secondary airflow or total ejector thrust could be obtained by further increasing the primary flow and primary velocity. It is, therefore, necessary to check the velocity in the mixing section when designing an ejector for a given condition. If the calculated velocity yields a greater Mach Number than 0.6, the ejector should be redesigned with a larger mixing section area. The theoretical curves presented in this report were based on experimental data in which the Mach Number of the mixed streams was not over 0.3.

The effect of compressibility was also checked analytically by assuming a primary jet Mach Number of unity, zero pressure rise, and a mixing section area ratio of 20. The thrust for a given flow ratio was about 2 per cent less for compressible flow, and the flow ratio for a given diffuser area ratio was about 5 per cent greater for compressible flow. The agreement was even better for ejectors without diffusers, so that the assumption of incompressible flow seems reasonable.

Effect of Altitude

Data obtained from sea-level tests of ejectors cannot be applied in designing an ejector to cool an engine at altitude without considering the effect of the change in densities. A decrease in the density ratio by itself results in a loss in ejector performance. For a given primary flow, however, the jet thrust increases with altitude because of the reduced back pressure on the nozzle. The increase in jet thrust has a greater effect upon the performance than has the change in density ratio. Therefore, if the velocity of the steady flow primary jet is subsonic, the overall performance will improve with an increase in altitude.

If this jet velocity is sonic at any given altitude, a further increase in altitude may be accompanied by a decrease in performance in spite of the increased jet thrust. The reason for this is that the jet expands to a greater area after leaving the nozzle, giving in effect a smaller mixing section area ratio.

The quantitative effect of altitude on the performance of an ejector will depend upon the design conditions and the particular ejector chosen for these conditions. Fig. 7 shows the calculated effect of altitude on the performance of a steady flow ejector designed for an arbitrary set of conditions. The variation in flow and thrust ratio with altitude is calculated for a constant actual pressure rise. The flow and thrust ratio in this case increase with altitude until the jet velocity becomes sonic. The thrust remains constant and the flow decreases with further increase in altitude.

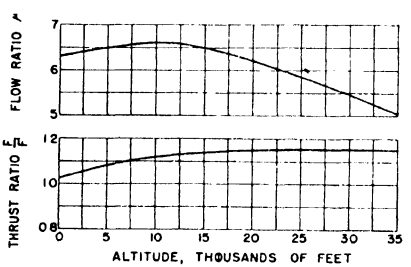


Fig. 7. Calculated effect of altitude. Constant pressure rise.

Divergent Mixing Sections

The ejector with a straight mixing section is not only the easiest to calculate but it also appears to be theoretically the best in the absence of losses. No cases have been observed, either in theory or in experiment, in which a divergent or convergent mixing section led to more thrust or a smaller ejector than a straight mixing section. One exception might be in the case of high Mach Numbers of the secondary stream. In any case, once mixing is complete, the addition of a diffuser section has advantages that have already been discussed.

Intermittent Flow Ejectors

If the exhaust from all cylinders of an engine were collected in a manifold and then discharged through a nozzle, the flow would be steady enough to use the steady flow theory. However, this system would not utilize the impulses of kinetic energy from each cylinder,

so that other arrangements are generally used which involve intermittent flow, and ejectors must be designed to operate with intermittent flow jets.

An analogy can be made between steady flow and intermittent flow by assuming the flow is steady in the latter case and using the primary area that would give the same average primary flow and momentum as the engine exhaust. The effective primary area can then be found from the continuity equation:

$$A' = W'/\rho' g V' \tag{19}$$

and the mean velocity calculated from the primary thrust, which is measured by a balance or a thrust target:

$$F' = W'V'/g \tag{20}$$

Combining these,

$$A' = (W')^2/\rho' g^2 F' \tag{21}$$

The principal objection to making this analogy is that it disregards the effect of the geometrical relationship between the area of the ejector and the primary nozzle. During the period of the cycle when the primary nozzle is actually exhausting the area ratio is smaller than that assumed in using the calculated steady flow primary area. The actual pumping capacity is consequently poorer than predicted by the theory.

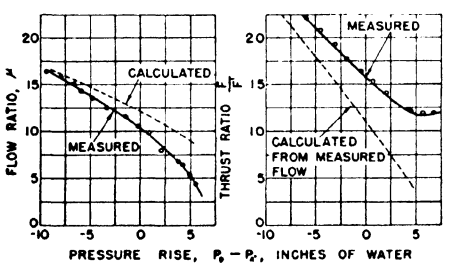


FIG. 8. Comparison of theory with single-cylinder engine ejector data.

SINGLE-CYLINDER EJECTORS

Fig. 8 shows the experimental results of typical single-cyclinder ejector tests compared to the calculated performance using the flow and thrust coefficients, K and C_{MD}, derived from steady flow compressed air tests. The results compare favorably only when there is a fairly high pressure drop through the ejector. The discrepancy is greatest when the ejector is pumping against a pressure rise and the return flow of the secondary fluid is decreasing the quantity of fluid pumped. Also, the nonuniform distribution in time of the velocity of the secondary fluid results in mean thrust per unit flow greater than would be obtained in steady flow of the secondary fluid. This variation between theory and test was consistent for all ejectors without diffusers.

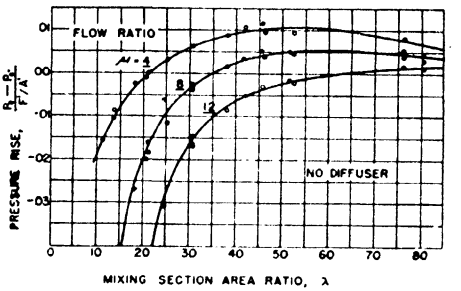


FIG. 9. Correlation of flow data—single-cylinder ejector.

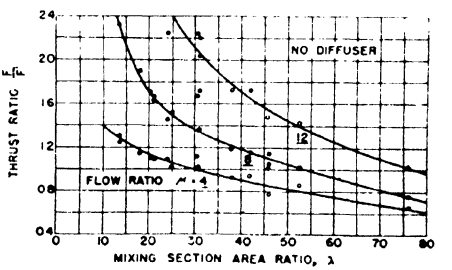


FIG. 10. Correlation of thrust data—single-cylinder ejector.

The variation was more erratic for ejectors with diffusers, but the difference between theory and test in no case appears to be greater for ejectors with diffusers than for ejectors without diffusers. It is evident that the empirical coefficients determined for steady flow ejectors cannot be used to predict the performance of intermittent flow ejectors, so that other means for handling the data must be found.

Figs. 9 and 10 show a correlation of data obtained from tests of ejectors without diffusers actuated by a single cylinder. These plots seem to correlate fairly well data taken over a wide range of engine powers, speeds, fuel-air ratios, and exhaust stack restriction. Fig. 9 gives the pressure rise parameter as a function of the calculated area ratio for various flow ratios. The density ratio is not constant for these tests (varying from 3.5 to 4.5), which accounts for some of the scatter in the data.

Fig. 10 is a plot of the ratio of the total to primary momentum vs. the effective area ratio for various values of the flow ratio. The scatter due to variation in density ratio may be as much as 7 per cent for these data, but there are some isolated points that fall as much as 20 per cent off the average curve. These variations are presumably due to changes in the time distribution of the secondary velocity, which was not accounted for in any way by the analogy.

These plots should not be used in designing ejectors in which "Siamesed stacks" are employed. An ejec-

tor actuated by the exhaust from a number of cylinders having nonoverlapping exhaust periods will pump a considerably greater flow for a given mixing section area ratio than indicated in Fig. 9. The ejector thrust in this case cannot be compared with that given in Fig. 10 because the mixing area required to maintain a given flow is not the same as that for a single-cylinder ejector.

There are insufficient data to plot curves similar to those in Figs. 9 and 10 for ejectors with diffusers. Moreover, these curves do not show the effect of changes in density ratio and cannot, therefore, be used in estimating performance at altitude.

Even if the theory were developed to completely account for all the variables in intermittent flow, it would be of little value at present since the additional data which would be required are not available. It is, therefore, absolutely necessary at present to employ an analogy such as given above in spite of its shortcomings.

Ejectors with Siamesed Stacks

In most engine installations it will be found advantageous to discharge the exhaust from several cylinders into one ejector. The greatest thrust is obtained by having a separate stack for each cylinder, but the piping can be reduced at a small loss in thrust by Siamesing into a single outlet two or three stacks from cylinders whose exhaust periods do not overlap. The outlet area should be the same as that for one individual stack. In this case the primary flow will be more continuous and should approximate more closely that calculated from steady flow theory. However, there are available no experimental data from engine ejectors with Siamesed stacks which are complete enough to check the theory.

Figs. 11 and 12 show a comparison of the theory with results of intermittent flow compressed air tests. Three intermittent flow nozzles were used. The nozzles discharged for one-third of the cycle with a velocity variation representative of that in the exhaust flow from an engine cylinder. In the first case, three separate ejectors were used so that intermittent flow was obtained through each. The pumping performance of these ejectors was markedly lower and the thrust higher than that given by theory. This is in agreement with the comparison made between the theory and the results of single-cylinder engine tests. In the second case, the nozzles were Siamesed into a single nozzle and used in a single ejector having an area equal to the combined area of the three intermittent flow ejectors. The performance in this case was in good agreement with the theoretical calculated performance. The use of three individual stacks instead of the Siamesed stacks in a single ejector gave the same performance in the compressed air tests, but slightly better performance when tried on a six-cylinder Franklin engine.

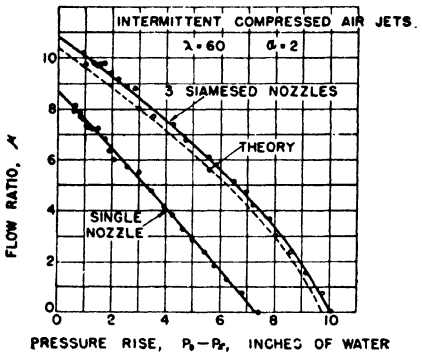


Fig. 11. Effect of Siamesed stacks.

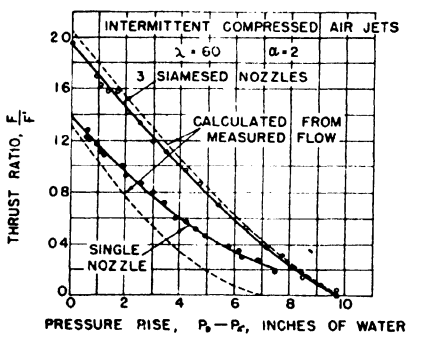


Fig. 12. Effect of Siamesed stacks.

These intermittent flow compressed air tests provide a good enough qualitative check to warrant the use of the theory when Siamesed stacks or a number of individual stacks from nonoverlapping cylinders are used in an ejector so that reasonably continuous flow is maintained. Even if this condition is fulfilled, the results calculated using the empirical thrust and flow coefficients given in Fig. 2 should be considered somewhat optimistic with respect to the flow and conservative with respect to the thrust. Coefficients based on engine tests of the type of ejector being designed should be used whenever the data become available.

Restricted Exhausts

The exhaust momentum in any type of system can be increased by restricting the exit area of the exhaust pipe. The amount of restriction that can be made without a decrease in engine power depends on the type of exhaust system and the exhaust port design of the engine. When individual stacks are used, a loss in engine power will result if the stack area is made less than the area of the exhaust valve passage at the maximum opening of the valve. A restriction in the exhaust

stacks may, however, result in an overall gain in thrust at high speed, if the increase in jet thrust more than offsets the decrease in propeller thrust due to loss of engine power.

Mixing Length

As the mixing length of an ejector is increased from zero, the velocity distribution becomes more uniform and the performance of an ejector improves at first. On further increase, however, wall friction in the mixing duct begins to become important and cuts down the performance. The optimum length results from a compromise between these two factors, and has been found by various investigators to be from 4 to 8 L/D for single-jet ejectors. Fig. 13, from tests on a seven-nozzle ejector, shows the interaction of these two factors and indicates that there is a critical mixing length below which the performance falls off abruptly

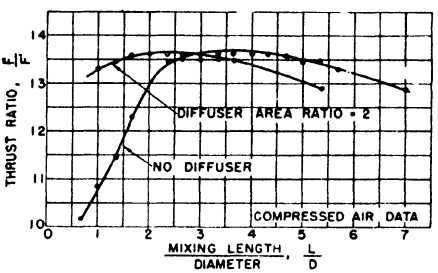


Fig. 13. Effect of mixing length. Seven nozzles. No pressure rise.

For ejectors with several jets, the critical mixing length can be approximated by assuming that the region of mixed stream forms a cone of fixed angle whose apex is at the primary jet. This leads to the rule that the critical mixing section length will vary directly with the mean radial spread of the mixed region to the wall or to another jet, provided that the nozzles are distributed uniformly over the mixing section area. Fig. 14 shows results of compressed air tests which support this rule for various shapes of mixing sections as well as various numbers of nozzles. The diameters of non-circular shapes are taken to be the diameters of circles with equal area. The mean radial spread of the mixed region for multiple-nozzle ejectors is assumed to be the same as that for a circular single-nozzle ejector whose area is equal to that of the whole ejector divided by the number of nozzles. Preliminary tests showed that annular nozzles will also shorten the mixing section if secondary air is allowed to flow through the annulus. All these data were obtained with zero pressure rise across the ejector. It should be emphasized, however, that no advantage will be obtained from distributing the nozzles in the ejector area unless there is essentially a continuous flow from each nozzle. The pressure rise also affects the optimum mixing length. Fig. 15 shows

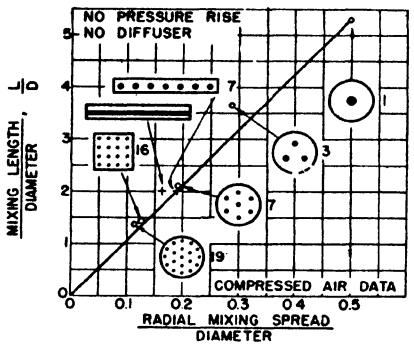


Fig. 14. Critical length of mixing section.

that for the same primary jet, the pressure rise in the mixing section takes place in a much shorter distance when less rise is required, as indicated by the leveling of the curves. Fig. 13 shows that the critical mixing length actually is less with a diffuser, for which less pressure rise occurs in the mixing section even with the same pressure change across the entire ejector.

The performance of an ejector without a diffuser is not appreciably affected by breaking up the primary jet into several scattered jets, provided that the mixing section is above the critical length. The improvement in performance due to the smaller friction loss of the shorter mixing section used is relatively small. However, the improved velocity distribution that results does increase the efficiency of the diffuser, thereby considerably improving the performance of ejectors with diffusers. Fig. 16 shows the comparison between single- and multiple-nozzle ejectors with diffusers of varying area ratio.

Entrance Configuration

Tests have indicated that the entrance radius of the mixing section can be as low as one-sixth of the diameter without affecting the performance. The nozzle should be flush with the entrance or slightly outside the entrance. With steady flow nozzles no appreciable loss

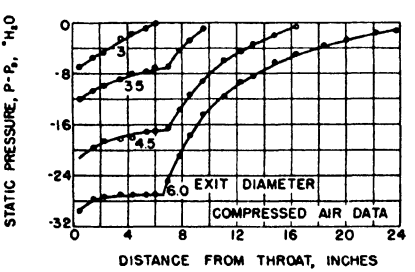


Fig. 15. Static pressure distribution; zero pressure rise; 8° diffuser; seven nozzles in 3-in. mixing section.

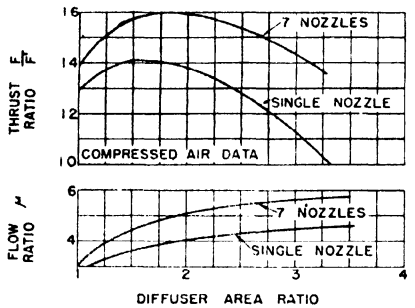


FIG. 16. Effect of multiple nozzles on diffusers.

in performance will be incurred by having the nozzle extend into the duct, other than that which may result from reduction of the effective mixing length. Since the distance from the exhaust stacks to the ejector exit is usually critical in ejector installations, there is no point in withdrawing the nozzles far out of the duct.

In general, the same considerations hold for intermittent flow ejectors as for steady flow ejectors. It is important that the exhaust be correctly distributed in the ejector area. Care should be taken that the stacks exhaust straight in the ducts and do not strike the duct walls. It is extremely important that the stacks do not extend into the duct unless three nonoverlapping cylinder exhausts are Siamesed together for each nozzle. Otherwise, during any given period of the cycle the mixing area is reduced by the blocking effect of the stacks that are not firing.

DIFFUSER ANGLE

The experimental coefficients used in the theoretical calculations were based on ejectors having 8° conical diffusers. The efficiency of such a diffuser is not constant for different diameters and different area ratios. However, in lieu of a more thorough analysis of diffusers and adequate experimental data, it is suggested that 8° conical diffusers be used or, in the case of noncircular cross sections, that diffusers with equivalent cone angle be used (i.e., maintain the same change in area for a given length that a cone with an included angle of 8° would have). Experience has shown this to be a fairly good criterion for designing a diffuser, although it is not fundamentally correct.

For a given overall length somewhat more flow can be obtained at the expense of a loss in thrust by using a greater diffuser angle. This would be practical only in a case where the overall length was limited and it was desired to obtain the maximum flow without regard to the thrust.

It has also been found that the optimum diffuser angle is greater than 8° for extremely small diffuser area ratios. The data are meager, however, and no reliable recommendations can be made for such cases.

DESIGN OF AN INSTALLATION

The foregoing equations and figures should enable the designer to make a rough check on the suitability of an ejector for his particular needs. The final design will, for the time being, have to be verified by flight tests, preferably of several configurations, which seem to be near the optimum.

In any type of installation it is first necessary to find the state of the secondary fluid, the required pressure rise, and the mean state of the primary fluid as described by the intermittent flow analogy (see Eqs. (19), (20), and (21). Strictly speaking, the state of the primary fluid should be obtained at the pressure of the ejector throat, but for most airplane installations the state at atmospheric pressure is close enough. It should be remembered, however, that in the case of a supersonic primary jet, the primary area should be calculated as if the jet had expanded through a converging diverging nozzle, rather than using the throat area as the primary area. The pressure rise of the secondary fluid is usually taken to atmospheric pressure, mainly because of lack of better knowledge of the static pressure at the ejector exit. The calculated thrust will then be roughly correct, even though the calculations may indicate a larger diffuser than will actually be needed. Having determined the states of the primary and secondary fluids, the designer can calculate the required flow ratio, density ratio, and pressure rise coefficient.

Since an adjustable diffuser is mechanically difficult to build, this will be one of the limitations in design. The overall length and the ejector area will be two other limitations imposed by the airplane designer and these must be balanced against the desired performance. If the thrust is not important but the diffuser area ratio is, then the mixing section area for the minimum diffuser can be found from Eq. 15. The required diffuser area ratio can be estimated by solving the flow equation (Eq. 13) for K and finding the area ratio from the empirical plot of flow coefficient, K, vs. diffuser area ratio, Fig. 2. If length is a more critical item than diffuser area ratio, a reduction may sometimes be made by using a slightly smaller mixing section area and a larger diffuser area ratio. The mixing length may be reduced by the use of multiple or annular nozzles.

If thrust is most important, the diffuser area ratio for maximum thrust may be estimated from Fig. 5 and the mixing section area found from Fig. 4 at the given pressure rise coefficient, flow ratio, and diffuser area ratio. If the density ratio differs much from 3.5, or if more precision is desired, the optimum diffuser must be found by assuming several values of mixing section area ratio, solving the flow equation (Eq. 13) for the flow coefficient, K, finding the corresponding diffuser area ratio, α, and then solving the thrust equation (Eq. 14) to find which assumed area ratio gave maximum thrust. For more accurate work, the state of the

primary fluid should be taken at the pressure in the ejector throat rather than at atmospheric pressure.

In the usual airplane installation, however, if an ejector is required at all it should be designed to operate with the maximum allowable diffuser in the most critical cooling condition. Then the diffuser can be closed down at high speeds to prevent overcooling and to increase the thrust. This procedure will seldom result in a diffuser at high speed that is greater than the optimum for thrust.

Outstanding Problems in Ejector Design

There are several uncertainties regarding the performance of ejectors which have not been adequately dealt with. First, there are practically no data on the effect of ejectors on low pressure areas into which they may be discharged, so that for the time being the assumption of atmospheric discharge pressure is used. In the second place, the mixing process has not been considered in detail except by the limited work of Ledgett.[3] Certainly the optimum mixing length varies with Reynold's Number, the steadiness of the flow, the pressure rise on the mixing section, and other quantities. It is still necessary, however, because of lack of better knowledge, to assume that the mixing cone spreads out at a constant angle. A third uncertainty may be observed by studying the plot of flow vs. pressure rise in Fig. 11. Note that the points are actually waving back and forth across the mean line. This waviness is not experimental scatter but was observed to some extent at high and low Mach Numbers, with steady and intermittent flow ejectors, and with both air-air and steam-air ejectors. A fourth problem is that of intermittent flow. Although the data usually correlate, as demonstrated in Figs. 9 and 10, occasionally some peculiar resonance effects will appear, upsetting all estimates of performance.

These problems, along with lack of accurate and complete knowledge of engine exhaust thrust, make it impossible to design ejectors precisely. At the present time, therefore, it seems sufficient to estimate the ejector performance roughly from the foregoing plots and equations, and then to modify the final design after flight-test data are available.

References

[1] Flugel, Gustav, *The Design of Jet Pumps*, N.A.C.A. T.M. No. 982, 1941.

[2] Gosline, James E., and O'Brien, Morrough P., *The Water Jet Pump*, University of California Publications in Engineering, Vol. 3, No. 3, p. 67, 1934.

[3] Ledgett, Lowell A., *The Mixing Fluid Streams*, Preprinted paper, Aero. Hydraulics Meeting, A.S.M.E., Berkeley, Calif., 1934.

Reprint 2.
Reprinted from Chemical Engineering Progress February, 1947
by Permission of Chemical Engineering Progress

THE DESIGN OF JET PUMPS

By A. EDGAR KROLL *

E. I. du Pont de Nemours & Company, Experimental Station, Ammonia Department, Wilmington, Delaware

JET pumps, exhausters, or ejectors, as they are called sometimes, are used widely in the chemical industries, especially steam and compressed-air ejectors which are used for such operations as exhausting fumes; exhausting air from condensers; vacuum evaporation, distillation, and crystallization; refrigeration; filtration; drying; air conditioning, and for pumping large volumes of vapor and gas at low pressures. They are simple in design, have no moving parts, operate with cheap, readily available fluids, and are reliable in service.

In spite of their wide application, readily usable design data are not available in the literature. Consequently, when the engineer is confronted with the problem of designing a jet pump, he uses either a "rule-of-thumb" method or resorts to trial and error. Either method may result in unsatisfactory performance or waste of power, material, and labor. Often the practice in the industrial plant is to use an open steam or air pipe in a duct or stack; or to use commercial exhausters designed for high-vacuum work for moderate vacuums. These practices result in very inefficient operation. Even though well-designed jet pumps may be purchased, it is often necessary for various reasons to use plant-fabricated pumps.

It is the purpose of this paper, then, to provide the engineer with a simple method for the design of single stage steam and air operated jet pumps, having maximum efficiency for handling gases.

General Considerations

When a fluid is discharged from a nozzle or orifice, the stream becomes a jet pump for moving the fluid surrounding it. In some cases at least four processes are involved: (1) acceleration of the particles of the surrounding fluid (induced fluid) by impact of particles from the nozzle fluid (motive fluid); (2) entrainment of the induced fluid by viscous friction at the periphery of the jet; (3) overexpansion of the jet to a pressure below that of the induced fluid with consequent flow of induced fluid toward the axis of the jet; (4) change of state, as in a steam injector, during which a large reduction in volume occurs by condensation, and the energy of latent heat is made available. The theoretical analysis of a jet pump, in which two or more of these processes are involved, becomes very complicated. (*17*) For simplicity, therefore, the correlations given in this paper are based on actual performance data and the theoretical treatments given by Besnjakovic (*2*) Dowson (*3*) Fluegel (*6*) Gosline and O'Brien (*7*) and Kalustian (*8*) are omitted. Where the theoretical figures are shown to be in good agreement with actual performance, e.g., Keenan and Neumann (*9*) for air-jet air pumps, several points were calculated and are included in the correlation.

Taking a steam-jet air pump as an example, the air flow through a given exhauster operating at a fixed steam pressure, P_C, will decrease as the suction increases as shown in Figure 1. There is a maximum suction for no air flow and a maximum air flow for zero suction. If the mass ratio, M_R (the mass of air, M_S, per unit mass of steam, M_J) is plotted instead of air flow, a similar curve will result. Another exhauster with a different diameter ratio, D_R (the ratio of diffuser throat diameter, D_T, to nozzle throat diameter, D_J) will exhibit different characteristics so that for various values of D_R a family of curves as shown in Figure 2 results.

Factors other than D_R also affect the performance. For simplicity, however, let it be assumed that the exhausters are of the same geometrical form shown in Figure 3 and that the curves in Figure 2 represent the performance. Thus, for a given suction pressure, P_S, there is a maximum ratio of induced fluid (air) to motive fluid (steam), M_R, and an optimum D_R corresponding to the envelope of the family of curves. For higher values of the nozzle supply pressure P_O (steam pressure), higher vacuums are possible and the family of curves would be shifted to the left.

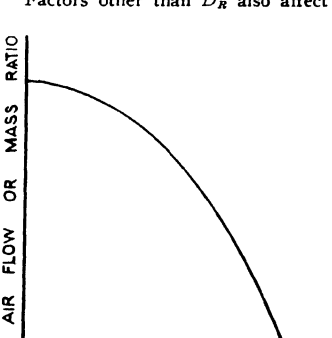


FIG. 1. DECREASE OF AIR FLOW WITH INCREASED SUCTION

The design of a jet pump involves consideration of several independent factors, such as the temperature and pressure of the motive fluid, type of motive fluid (air, steam), type of fluid induced, and pressure and temperature of the induced fluid.

Because of the limited data available the present analysis is limited to exhausting air initially at atmospheric temperature and discharging to atmospheric pressure using compressed air, initially at atmospheric temperature, and steam as the motive fluids. The variables affecting design, then, are the suction pressure, P_S, required, and the nozzle supply pressure, P_O, available.

For discharge pressures, P_D, not greatly different from atmospheric, the performance probably can be safely assumed to depend only on the pressure ratio $P_R = (P_O - P_D)/(P_D - P_S)$ and the data presented may be used accordingly.

After a discussion of the various other factors affecting the performance of jet pumps, correlations of maximum mass ratio and optimum diameter ratio with pressure ratio and their use are given below.

Design Factors Affecting Performance

The important aspects in the design of the various parts of a jet pump as found in the literature are discussed in the following paragraphs.

Diffuser Entrance

The best form for the entrance to the diffuser throat is a well-rounded, bell-mouthed entry.(*5*)(*13*)(*18*) A conical or tapered entry should have an angle, α, larger than 20 degrees so

* Paper written at Lehigh University, Bethlehem, Pennsylvania.

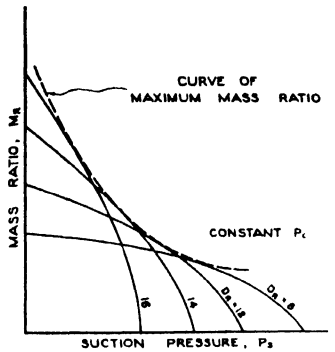


FIG. 2. SUCTION PRESSURE AND MASS RATIO OF INDUCED FLUID TO MOTIVE FLUID

that the nozzle jet, which has a natural angle of about 20 degrees, will not produce objectionable shock and eddy losses at the inlet.(*17*) Experience has indicated that 25 degrees is about the best convergence angle.(*18*)

On the basis of the well-rounded entry such a conical entry reduces the flow 2 per cent while a reducing coupling and sharp entry cause a reduction in flow of 4 per cent and 11 per cent, respectively.(*1*)(*5*)(*16*)

Diffuser Throat

Early work indicated that diffusers with parallel throats produced a higher maximum vacuum than diffusers which had a gradual constriction tapering off to the outlet without having any length parallel.(*13*)(*18*) It was shown that a throat parallel throughout is inferior but surprisingly better than no parallel throat at all.(*13*)

An optimum throat length, T, of seven times the throat diameter was found by two investigators (*4*)(*9*) while another reported 7.5 to be the optimum.(*5*) However, lengths of five to ten times the throat diameter gave within 3 per cent of optimum performance and although the optimum length increased slightly with pressure and throat diameter, the increase was less than 1 diameter even when these factors were doubled.(*9*) Any length between 4 and 14 diameters will give within 4 per cent of optimum performance.(*5*)

The proper throat area is important. A comparatively small change in throat area makes a large difference in the amount of air entrained. If the throat is too small choking will occur and if it is too large a leakage of air back into the system occurs. A method for determining the optimum throat diameter, D_T, is given in this paper.

Distance of Nozzle Outlet to Diffuser Throat

The length, X, was found to affect considerably the performance of an ejector.(*13*)(*18*) The maximum value of this length was found to increase with increased nozzle supply pressure and to decrease with increased vacuum. It is recommended, therefore, that nozzle position be made adjustable so that adjustment for best performance may be made readily in the field. It is important also to have the nozzle centered with the throat tube.

Induced Fluid Entrance

From tests conducted by Mellanby (*13*) it can be concluded that, for all practical purposes, the capacity of a jet for entraining the fluid is independent of the position in which the entrained fluid enters.

Diffuser Outlet, Tail Piece

After the parallel section, a divergent section, R, having an angle, θ, of from 4 degrees to 10 degrees usually is used. Too rapid a divergence immediately after the throat is not desirable. The length may be as little as twice the throat diameter if necessary, although longer length, say from four to eight times the throat diameter, are preferred for pressure recovery.

It was found that a parallel section without the divergent tail piece caused a reduction in the mass ratio of air to steam of about 20 per cent. The length of the parallel section, however, should be 7 to 9 diameters for best performance.

Nozzle

It is known that poorly shaped nozzles cause unnecessary shock losses and useless lateral expansion. However, for the steam-jet pump Engdahl and Holton (*5*) found that nozzles designed by the conventional method for specific pressures performed only slightly better than simple straight-hole nozzles at pressures up to 170 lb./sq.in.gauge. A machined nozzle with a convergent approach and a 10° angle of divergence was only 3 to 6 per cent better above 100 lb./sq.in. than a simple pipe-cap nozzle made by drilling a hole in a standard pipe cap.(*5*) A machined nozzle can be made readily from a standard pipe plug and has the added advantage over the pipe-cap nozzle that corners, which may build up foreign material and clog the throat, are eliminated. In any case it is well to clean the nozzles as frequently as possible for best performance.

It should be mentioned that for maximum jet-pump efficiency the highest available nozzle supply pressure should be used.

To facilitate the determination of nozzle diameter for any desired flow and supply pressure, Figure 9 was drawn. It will be noted that the flow for nozzle discharge coefficients of 0.90 and 0.95 are included. For the purposes of designing a jet pump, a coefficient of 0.95 for a well-designed machined nozzle and a coefficient 0.90 for a straight-hole pipe-cap nozzle may be assumed.

Correlation of Data

Table 1 shows the dimensions of the jet pumps on which the correlation of actual performance data is based. Sources of the data are indicated. Optimum performance figures for the steam-jet air pumps designated as "home made" were obtained on various plant-fabricated exhausters.(*12*)

The actual maximum mass ratio, M_R, is plotted against the pressure ratio, P_R, on logarithmic paper (Figures 4 and 6), which are for steam-jet air pumps and air-jet air pumps, respectively. The ranges of nozzle supply pressures are indicated. All data

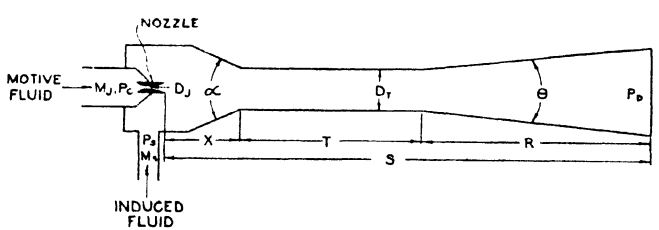


FIG. 8. TYPICAL JET PUMP

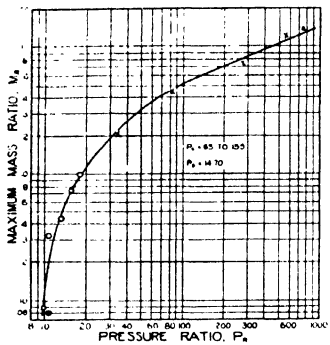


FIG. 4. MAXIMUM MASS RATIOS FOR STEAM-JET AIR PUMPS

△ Du Perow and Bossart. □ Watson. ● Royds and Johnson ($P_D = 13.89$). × Home Made. ○ Commercial

are for discharge pressures, P_D, of 14.70 lb./sq.in. except those of Royds and Johnson, on steam-jet air pumps, which were at 13.89 lb./sq.in. The points labeled commercial were obtained from manufacturers' literature.

The optimum diameter ratio, D_R, is plotted against the pressure ratio in Figure 5, for steam-jet air pumps and in Figures 7 and 8 for air-jet air pumps. Figure 8 shows values of D_R at low values of P_R, which cannot be read from Figure 7. These are based on data of Mellanby.(*12*) Here again, all values are for discharge pressures, P_D, of 14.70 lb./sq.in. The ranges of nozzle supply pressures are the same as shown in Figures 4 and 6 for steam-jets and air-jets, respectively.

Use of these figures in the design of jet pumps is illustrated in the example following.

Example

A steam-jet air exhauster is desired for exhausting 20,000 lb./hr. of air. A vacuum of 15 in. water is required and the maximum steam pressure available is 100 lb./sq.in. gauge. The air is to be discharged to the atmosphere. What diameter nozzle and diffuser throat should be used to obtain the best performance? Assume a nozzle coefficient of 0.95.

$$P_D = 14.70 \text{ lb./sq.in.}$$

$$P_S = 14.70 - (15 \times 0.036)$$

$$= 14.16 \text{ lb./sq.in.}$$

$$P_O = 114.70 \text{ lb./sq.in.}$$

$$P_R = \frac{114.70 - 14.70}{14.70 - 14.16} = \frac{100}{0.54}$$

$$= 185.2$$

The maximum mass ratio for this pressure ratio is found from Figure 4 to be 6.5.

$$M_R = \frac{M_S}{M_J} = 6.5$$

$$M_S = 20{,}000 \text{ lb./hr.}$$

$$M_J = \frac{20{,}000}{6.5} = 3077 \text{ lb./hr.}$$

From Figure 9 for a 0.95 nozzle coefficient at 114.70 lb./sq.in.abs. the nozzle flow for steam is 5950 lb./(hr.)(sq.in.) nozzle throat area.

Then the area of the nozzle throat is $\frac{3077}{5950} = 0.52$ sq. in. and $D_J = 0.81$ in. = nozzle throat diameter.

The optimum diameter ratio for a pressure ratio of 185.2 is found from Figure 5 to be 9.0

$$D_R = \frac{D_T}{D_J} = 9.0$$

$$D_T = (0.81)\,(9.0) = 7.3 \text{ in.}$$

= diffuser throat diameter

The various other dimensions shown in Figure 3 should be made in accordance with the previous discussion under the heading "Design Factors Affecting Performance"

Figures 6, 7, and 8 are used similarly for designing air-jet air pumps.

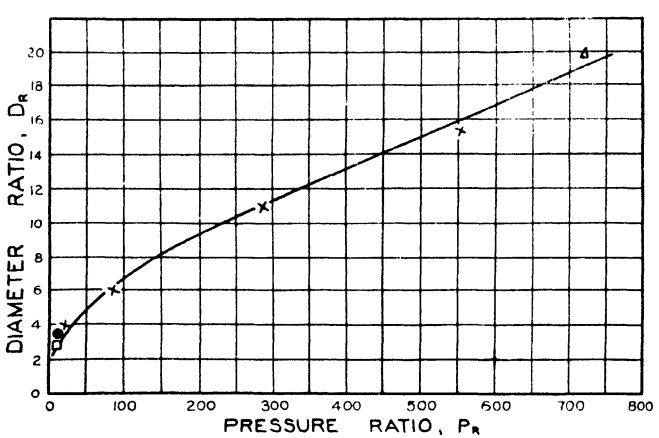


FIG. 5. OPTIMUM DIAMETER RATIOS FOR STEAM-JET AIR PUMPS

△ Du Perow and Bossart. ○ Watson. ● Royds and Johnson ($P_D = 13.89$). × Home Made

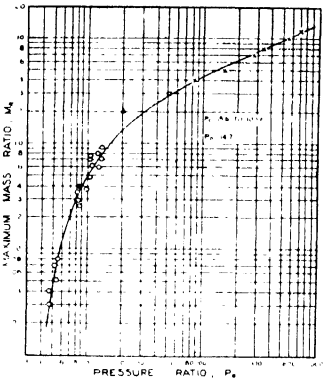


FIG. 6. MAXIMUM MASS RATIOS FOR AIR-JET AIR PUMPS

× Keenan and Neumann. △ Kravath. ○ Mellanby. □ Miller. ● Commercial

Acknowledgment

Thanks are due to J. W. Langhaar for many valuable suggestions, and to M. A. Streicher and E. E. Kroll for help with the drawings.

Nomenclature

D_J = nozzle throat diameter, in.

$D_R = D_T/D_J$ = diameter ratio

D_T = diffuser throat diameter, in.

M_J = weight of motive fluid/unit time

$M_R = M_S/M_J$ = mass ratio of induced fluid to motive fluid

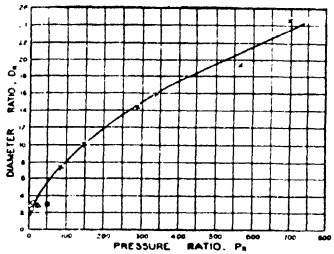


FIG. 7. OPTIMUM DIAMETER RATIOS FOR AIR-JET AIR PUMPS

× Keenan and Neumann. Δ Kravath. ○ Mellanby □ Miller

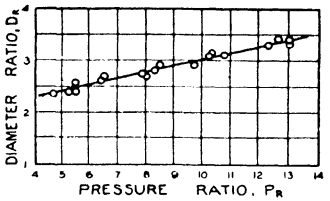


FIG. 8. OPTIMUM DIAMETER RATIOS FOR AIR-JET AIR PUMPS FOR LOW PRESSURE RATIOS BASED ON DATA OF MELLANBY (*13*)

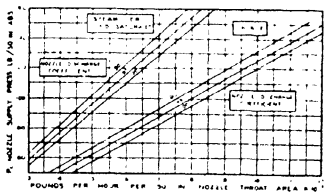


FIG. 9. NOZZLE FLOW CHART FOR AIR AND STEAM

TABLE 1.—DESIGN OF JET PUMPS USED BY THE VARIOUS INVESTIGATORS

Length of Diffuser Throat in. T	Length of Diffuser Outlet or Tail Piece in. R	Length of Pump from Nozzle Outlet to Discharge in. S	Distance of Nozzle Outlet from Diffuser Throat in. X	Convergence Angle of Diffuser Entrance deg. α	Divergence Angle of Diffuser Outlet deg. θ	Reference
Air-Jet Air Pumps						
$7D_T$	0	$7.5D_T$	$0.5D_T$	well rounded	——	Keenan and Neumann (*9*)
$4D_T$	$10D_T$	——	variable	25	12	Mellanby (*13*)
D_T	$12D_T$	$15D_T$	$2D_T$	28	5	Kravath (*10*)
——	——	——	$5D_T$	——	16	Miller (*14*)
Steam-Jet Air Pumps						
——	——	$6D_T$	$1.2D_T$	——	7	DuPerow and Bossart (*4*)
$10D_T$	$15D_T$	——	——	well rounded	——	Royds and Johnson (*15*)
$3D_T$	$4D_T$	$10D_T$	$3D_T$	24	10	Home Made (*12*)
$2D_T$	$6.7D_T$	$12.3D_T$	$3.6D_T$	28	8	Watson (*18*)

M_S = weight of induced fluid/unit time

P_O = nozzle supply pressure, lb./sq.in.abs.

P_D = discharge pressure, lb./sq.in. abs.

$P_R = (P_C - P_D)/(P_D - P_S)$ = pressure ratio

P_S = suction pressure, lb./sq.in. abs.

R = length of diffuser outlet or tail piece, in.

S = length of pump from nozzle outlet to discharge, in.

T = length of diffuser throat, in.

X = distance of nozzle outlet from diffuser throat, in.

α = convergence angle of diffuser entrance, degrees

θ = divergence angle of diffuser outlet, degrees

Literature Cited

1. Bailey, A., and Wood, S. A., Great Britain Aeronaut. Res. Com. R. & M. No. 1545, Feb. (1933).
2. Bosnjakovic, F., *Z. Gesamte-kalte Ind.*, **43**, 229-33 (1936).
3. Dowson, R., *Engineer* (London), **164**, 650-80 (1937).
4. DuPerow and Bossart, Undergraduate Thesis, Case School of Applied Science, Cleveland, Ohio (1927).
5. Engdahl, R. B., and Holton, W. C., *Trans. Am. Soc. Mech. Engrs.*, **65**, 741-54 (1943).
6. Fluegel, G., *Z. Ver. Deut. Ing.*, **83**, 1065-69 (1939). N.A.C.A., *T.M.* No. 982, July (1941).
7. Gosline, J. E., and O'Brien, M. P., *Univ. of Cal. Pub. in Eng.*, **3**, 167-190 (1934).
8. Kalustian, P., *Refrigerating Eng.*, **28**, 188-93 (1934).
9. Keenan, H. P., and Neumann, E. P., *Trans. Am. Soc. Mech. Engrs.*, **64**, A-75 (1942).
10. Kravath, F. F., *Heat. and Vent.*, **37**, 17, June (1940).
11. Kugel, H. K., *Power*, **67**, 638-9 (1928).
12. Langhaar, J. W., Private Communication (1946).
13. Mellanby, A. L., *Trans. Inst. Chem. Engrs.* (London) **6**, 66-84 (1928).
14. Miller, G. P., Master's Thesis, Case School of Applied Science, Cleveland, Ohio (1940).
15. Royds, R., and Johnson, E., *Inst. Mech. Engrs.* (London), **145**, 193-209 (1941).
16. Stern, A. C., *Mech. Eng.*, **54**, 267-8 (1932).
17. Tove, Priester and Wright, *Heat., Piping, and Air Cond.*, **13**, 708-15 (1941).
18. Watson, F. R. B., *Proc. Inst. Mech. Engrs.* (London), **124**, 231-300 (1933). *Engineering* (London), 230-2, 255-7, 262-5 (1933).

p. 2 to Errata to FLUID AND PARTICLE MECHANICS

Chapter 6 - Two-Phase Flow in Pipes

Chapter 6

TWO-PHASE FLOW IN PIPES

by

George E. Alves
Engineering Research Laboratory
Engineering Department
E. I. du Pont de Nemours & Co., Inc.
Wilmington, Delaware

TABLE OF CONTENTS

Page

I. References 97

II. Nomenclature 98

III. Liquid-Gas Flow in Pipes 99

A. Introduction 99

B. Liquid-Gas Flow in Horizontal Pipes 100

1. Constant Liquid and Gas Flow Rates 100

a. Liquid Turbulent—Gas Turbulent 100
b. Liquid Viscous—Gas Turbulent 101
c. Liquid Viscous—Gas Viscous 102
d. Liquid Turbulent—Gas Viscous 103

2. Flashing and "Boiling Liquids" 103

a. Flashing Mixture of Liquid and Vapor 103
b. "Boiling Liquids" 104

3. Flow of a Condensing Vapor in Straight Circular Pipe 104

C. Liquid-Gas Flow in Vertical Pipes 106

1. Introduction 106

2. Liquid-Gas Flow at Various Angles with the Horizontal 106

3. Gas Lifts 106

a. Water-Air Lift 107
b. Other Gas Lifts 109

IV. Solid-Gas Flow in Pipes 109

A. Pneumatic Conveying 109

1. Introduction 109

2. Solids Motion 109

3. Pressure Drop 110

4. Comments on Design Procedures 111

5. Commercial Systems 112

a. Fuller-Kinyon System 112
b. Fuller-Fluxo System 112
c. "Airveyor" 112

V. Liquid-Solid Flow in Pipes 112

VI. Problems 113

LIST OF TABLES

Table I Factors used in Liquid-Gas Flow Pressure Drop Computations (Turbulent—Turbulent) . . . 101
Table II Factors used in Liquid-Gas Flow Pressure Drop Computations (Viscous—Turbulent) 102
Table III Factors used in Liquid-Gas Flow Pressure Drop Computations (Viscous—Viscous) 102
Table IV Comparison of Theory and Experiment for Water-Air Lifts 108

I. REFERENCES

Liquid-Gas Flow in Pipes

1. Babson, E. C., "Range of Application of Gas-Lift Methods", Oil Weekly, 95 (12), 15-20, 22, 35-36 (1939) Nov. 27; 95 (13), 34, 36, 38-40, 42, 43 (1939) Dec. 4; 96 (1), 22, 24, 26, 28, 30, 34-35 (1939) Dec. 11; 96 (3), 20-22, 24, 26, 28 (1939) Dec. 25.
2. Benjamin, M. W., and Miller, J. G., "The Flow of a Flashing Mixture of Water and Steam Through Pipes", Trans. Am. Soc. Mech. Engrs., 64, 657-69 (1942).
3. Bottomley, W. T., "Flow of Boiling Water Through Orifices and Pipes", North East Coast Instn. Engrs. and Shipbuilders, 53, 65-100 (1936).
4. Davidson, W. F., Hardie, P. H., Humphreys, C. G. R., Markson, A. A., Mumford, A. R., and Ravese, T., "Studies of Heat Transmission Through Boiler Tubing at Pressures from 500 to 3300 Pounds", Trans. Am. Soc. Mech. Engrs., 65, 553-591 (1943).
5. Dittus, F. W., and Hildebrand, A., "Method of Determining Pressure Drop for Oil-Vapor Mixtures Flowing Through Furnace Coils", Trans. Am. Soc. Mech. Engrs., 64, 185-92 (1942).
6. Gibson, A. H., Hydraulics and Its Applications, 3rd Ed., New York, Van Nostrand Co., 1925.
7. Gosline, J. E., "Experiments on the Vertical Flow of Gas-Liquid Mixtures in Glass Pipes", Trans. Am. Inst. Min. and Met. Engrs. (Pet. Dev. and Tech.), 118, 56-70 (1936).
8. Hershey, R. L., "The Flow of Gas-Liquid Mixtures in Pipes", D.Sc. Thesis in Chem. Eng., M.I.T., 1935.
9. Lea, F. C., Hydraulics, 5th Ed., New York, Longmans, Green and Co., 1930.
10. Lockhart, R. W., and Martinelli, R. C., "Generalized Correlation of Two-Phase, Two-Component Flow Data", Paper presented at the Am. Inst. Chem. Engrs. regional meeting at Buffalo, N. Y., Sept. 29 - Oct. 1, 1947. (Published in Chem. Eng. Progress, 45, 39-48 (1949) Jan.)
11. Martinelli, R. C., Boelter, L. M. K., Taylor, T. H. M., Thomsen, E. G., and Morrin, E. H., "Pressure Drop for Two-Phase Two Component Flow in a Horizontal Pipe", Trans. Am. Soc. Mech. Engrs., 66, 139-151 (1944).
12. Martinelli, R. C., and Nelson, D. B., "Prediction of Pressure Drop During Forced-Circulation Boiling of Water", Paper No. 47-A-113 presented at the Am. Soc. Mech. Engrs. annual meeting, Atlantic City, N. J., December 1-5, 1947. (Published in Trans. Am. Soc. Mech. Engrs., 70, 695-702 (1948) Aug.).
13. Martinelli, R. C., Putnam, J. A., and Lockhart, R. W., "Two-Phase, Two-Component Flow in the Viscous Region", Trans. Am. Inst. Chem. Engrs., 42, 681-705 (1946).
14. McAdams, W. H., Woods, W. R., and Bryan R. L., "Vaporization Inside Horizontal Tubes", Trans. Am. Soc. Mech. Engrs., 63, 545-552 (1941).
15. McAdams, W. H., Woods, W. K., and Heroman, L. C., "Vaporization Inside Horizontal Tubes - II Benzene-Oil Mixtures", Trans. Am. Soc. Mech. Engrs., 64, 193-200 (1942).
16. Ward, C. N., and Kessler, L. H., "Experimental Study of the Air-Lift Pumps and Application of Results to Design", Univ. of Wisc. Eng. Series 9, Bull. No. 1265 (1924).

Solid-Gas Flow in Pipes

17. Cramp, Wm., "Pneumatic Transport Plants", J. Soc. Chem. Ind., 44, 207T-210T, 211T-213T (1925).
18. Dalla Valle, J. M., "Determining Minimum Air Velocities in Exhaust Systems", Heating, Piping & Air Conditioning, 4, 639-41 (1932) Sept.
19. Gasterstadt, J., "Die Experimentelle Untersuchung des Pneumatischen Fordervorganges", Z. V. D. I., 68, 617-624 (1924).
20. Gasterstadt, J., "Die Experimentelle Untersuchung des Pneumatischen Fordervorganges", Forschungsarb. Gebiete Ingenieurw., 265 (1924).
21. Mann, H. B., "Pneumatic Handling of Dry, Pulverized and Granular Materials", Material Movement, 2, 8-11 (1946) Jan.
22. Wood, S. A., and Bailey, A., "The Horizontal Carriage of Granular Material by an Injector-Driven Air Stream", Proc. Inst. Mech. Engrs. (London), 142, 149-164 (1939).

p. 97 - Reference 14 should read: "...Woods, W. K., ..."

II. NOMENCLATURE

A = cross-sectional area of pipe, sq.ft.

b = a constant

C = constant in Blasius generalized correlation for friction factor

d = particle diameter, inches

D = inside diameter of pipe, ft.

f = Fanning friction factor, dimensionless

f' = friction factor (gas lifts), dimensionless

g_c = conversion factor, 32.17 (lb/lb.force)(ft./sec^2)

g_L = local acceleration due to gravity, 32.17 (ft./sec^2)

G = mass velocity, lb./(sec.)(sq.ft.)

G_c = critical mass velocity, lb./(sec.)(sq.ft.)

h = lift (gas lifts) or height of vertical pipe (pneumatic conveying), ft.

H = enthalpy, B.t.u./lb.

H_g = enthalpy of saturated vapor, B.t.u./lb.

J = conversion factor, 778 (ft.)(lb.force)/B.t.u.

k = a constant

L = length of pipe, ft.

ΔL = incremental length of pipe, ft.

n = a constant

N_{Re} = Reynolds number, dimensionless

p = pressure, lb.force/sq.ft. absolute

Δp = pressure drop or incremental pressure drop for incremental length ΔL, lb.force/sq.ft.

Δp_a = pressure drop for acceleration, lb.force/sq.ft.

Δp_F = pressure drop due to friction (pneumatic conveying), lb.force/sq.ft.

Δp_g = pressure drop due to gas flowing alone at rate w_g of density ρ_g in a pipe of diameter D and length L, lb.force/sq.ft.

$(\Delta p_{K.E.})_f$ = pressure drop to supply inlet kinetic energy to the liquid (gas lifts), lb.force/sq.ft.

Δp_v = pressure drop to support air and solids (pneumatic conveying), lb.force/sq.ft.

$\frac{\Delta p}{\Delta L}$ = pressure drop per unit length, (lb.force/sq.ft.)/ft.

$(\frac{\Delta p}{\Delta L})_{T-P}$ = pressure drop per unit length for two-phase flow of liquid-gas mixtures at constant flow rates in horizontal pipes, (lb.force/sq.ft.)/ft.

q = volumetric rate of flow, cu.ft./sec.

q_m = volumetric rate of flow of mixture (neglecting slip), cu.ft./sec.

q' = gas flow rate relative to the liquid, cu.ft./sec.

Q = quantity of heat transferred, B.t.u./lb.

R = w_x/w_g = loading, lb. solids/lb. air

R_o = gas constant, (ft.) (lb. force)/(lb.) (°R.) = (for air) 53.3 (ft.) (lb. force)/(lb.) (°R.)

R_s = submergence ratio, dimensionless

s = specific gravity, dimensionless

S = slope, dimensionless

Δt = temperature difference between mixture in pipe and heat receiver, °F.

T = absolute temperature, °R.

u_i = heat transfer coefficient based on inside diameter of pipe, B.t.u./(hr.)(sq.ft.)(°F.)

v = specific volume, cu.ft./lb.

$\bar{v}_m$ = average specific volume of mixture, $\frac{\text{cu.ft.}}{\text{lb.}}$

Δv_m = incremental specific volume of mixture for incremental pressure Δp (flashing mixtures), cu.ft./lb.

V = velocity, ft./sec.

V_m = mixture velocity neglecting slip (gas lifts), ft./sec.

$(\bar{V}_m^2)$ = average of the square of the mixture velocity for the flow in a pipe of length L (gas lifts), $(\text{ft./sec.})^2$

w = weight rate of flow, lb./sec.

W = weight, lb.

X = two-phase flow modulus for constant liquid-gas flow rates in horizontal pipes, dimensionless

z = fraction condensed, dimensionless

Z = elevation, ft.

μ = absolute viscosity, lb./(sec.)(ft.)

ρ = density, lb./cu.ft.

ϕ = function of X utilized in computation of two-phase flow pressure drop, dimensionless

ϕ' = ratio of gas volume to liquid volume in pipe at any cross-section (gas lifts), dimensionless

ψ = a function

When subscripts have been referred to above, they are used uniquely and integrally with the specific symbol referred to. Where several subscripts are used on a symbol, the individual significance of each subscript is to be added together. The terms, g_c, g_L, G_c, and R_o, have been so labeled as such to be consistent with recent trends of nomenclature. The following subscripts are general.

o = reference conditions, usually atmospheric
1 = at foot piece of gas lift
2 = at discharge of gas lift
f = liquid
g = gas or vapor
m = mixture
x = solid
tt = flow of both liquid and gas is turbulent
vt = flow of liquid is viscous and that of gas is turbulent
vv = flow of both liquid and gas is viscous

III. LIQUID-GAS FLOW IN PIPES

A. Introduction:

The simultaneous flow of liquids and gases in pipes is complicated by the fact that the action of gravity tends to cause settling and slip of the liquid with the result that the gas flows at a different

velocity in the pipe than does the liquid. The results of this phenomenon are different depending upon the inclination of the pipe with the horizontal.

This subject is therefore treated under separate headings:

B. Liquid - Gas Flow in Horizontal Pipes

1. Constant Liquid and Gas Flow Rates

A wide variety of flow phenomena is possible with simultaneous flow of gases and liquids in horizontal pipes ranging from parallel (two layer) flow at low velocities to dispersed flow at high velocities (gas carried as bubbles in a continuous liquid phase or liquid carried as spray in the gas). It is often desirable to know what type of flow is occurring although this is difficult to predict. Martinelli, et al (11) present photographs and sketches of flow types occurring in a 1-in. glass test pipe, however, only qualitative indications are given of the quantities of flow involved. The pressure drop is greater in liquid-gas flow than that for the single phase flow of either gas or liquid for several reasons. Some of the reasons are the irreversible work done on the liquid by the gas and that the effective cross-sectional area of flow for either fluid is reduced by the flow of the other fluid.

A large amount of experimental work has been published in the literature; however, the only general correlations for pressure drop are those presented by Martinelli, et. al. (10, 11, 13). They present analyses on the four distinct flow mechanisms:

a. Flow of both liquid and gas is turbulent
b. Flow of the liquid is viscous, and the flow of the gas is turbulent
c. Flow of the liquid and gas is viscous
d. Flow of the liquid is turbulent, and the flow of the gas is viscous

The following discussion of the Martinelli correlations is based on material in references (11) and (13). The correlations are for isothermal flow. The analyses assume that the static pressure drop for the liquid phase must equal the static pressure drop for the gas phase for all types of flow, provided that no appreciable static pressure differences exist across any pipe diameter and that the volume occupied by the liquid and by the gas at any instant must equal the total volume of the pipe. Using the above assumptions, the static pressure drop due to the liquid flow and that due to the gas flow is expressed in each case by the Fanning equation using unknown "hydraulic diameters." The hydraulic diameters are then expressed in terms of the actual cross-sectional area of flow and the ratio of the actual cross-sectional area of flow to the area of a circle of diameter equal to the unknown hydraulic diameter. The friction factors are then expressed in the generalized Blasius form (see Equation 5). The unknown hydraulic diameter for the liquid flow is eliminated and finally an expression is obtained for the pressure drop as a function of the single phase pressure drop for gas alone. The function is expressed as ϕ^2 in the analysis in order to reduce the range of the variables when plotting ϕ^2 vs $\sqrt{X}$. Flow in smooth pipes was assumed.

Lockhart and Martinelli (10) in a recent paper presented correlations based on the single phase flow of the liquid instead of the gas as was used in the above method. Martinelli and Nelson (12) apply these correlations in predicting the pressure drop during forced circulation boiling of water. (See also part on Flashing and Boiling Liquids of this section).

The function of the single phase pressure drop for gas alone for the four possible flow mechanisms are given below. In order to establish which flow mechanism a certain set of flow conditions will fall in, the Reynolds Number, $N_{Re} = \frac{4w}{\pi D\mu}$, is computed for each phase using the actual pipe diameter, in other words, a superficial Reynolds Number is computed. For a Reynolds Number less than 2000 for a phase, that phase is taken as being in viscous flow, and if over 2000, it is taken as being in turbulent flow.

a. Liquid Turbulent - Gas Turbulent. For this case, the ratio of the actual cross-sectional area of flow to the area of a circle of diameter equal to the unknown hydraulic diameter for the gas phase was assumed to be unity and the ratio for the liquid phase was determined from experimental data. From the ratio for the liquid phase and the properties of the liquid and gas the following correlations were obtained.

$$\left(\frac{\Delta p}{\Delta L}\right)_{T-P} = \phi_{tt}^2 \left(\frac{\Delta p}{\Delta L}\right)_g$$

p. 100 - line 10 from bottom of page should read:

$$\text{.....} N_{Re} = \frac{4w}{\pi D\mu} \text{.....}$$

p. 100 - line 6 from bottom of page should read:
"....For this case, the ratio of the ...."

where ϕ_{tt} is a function of a dimensionless group,

$$X_{tt} = \left(\frac{\mu_f}{\mu_g}\right)^{0.111} \left(\frac{\rho_g}{\rho_f}\right)^{0.555} \left(\frac{w_f}{w_g}\right) \tag{2}$$

The magnitude of ϕ_{tt} for values of X_{tt} is given in Table I.

TABLE I

ϕ_{tt} vs $\sqrt{X_{tt}}$

$\sqrt{X_{tt}}$	ϕ_{tt}
0	1.00
0.10	1.50
0.20	1.68
0.40	2.13
0.70	3.03
1.00	4.08
2.00	8.30
4.00	19.6
7.00	42.3
10.0	71.0
20.0	222.
40.0	770.
46.2	1000.
for $\sqrt{X_{tt}} > 46$	$\phi_{tt} = \left(\sqrt{X_{tt}}\right)^{1.8}$

b. Liquid Viscous - Gas Turbulent: Using the same procedure as for the preceding case, the correlations are:

$$\left(\frac{\Delta p}{\Delta L}\right)_{T-P} = \phi_{vt}^2 \left(\frac{\Delta p}{\Delta L}\right)_g \tag{3}$$

Where ϕ_{vt} is a function of a dimensionless group, X_{vt}; and,

$$X_{vt} = (N_{Re})_g^{-0.8} \left(\frac{C_f}{C_g} \cdot \frac{\rho_g}{\rho_f} \cdot \frac{\mu_f}{\mu_g} \cdot \frac{w_f}{w_g}\right) \tag{4}$$

The constants C_f and C_g appear in the generalized Blasius expression for the friction factor correlation,

$$f = \frac{C}{(N_{Re})^n} \tag{5}$$

Martinelli, et al., assumed flow in smooth pipes, therefore,

$$C_f = 16 \quad , n_f = 1$$

$$C_g = 0.046 \quad , n_g = 0.2$$

The magnitude of ϕ_{vt} for values of X_{vt} is given in Table II.

p. 101 - line 1 from top of page should read:
"....a dimensionless group, X_{tt}; and, ..."

TABLE II

ϕ_{vt} vs $\sqrt{X_{vt}}$

$\sqrt{X_{vt}}$	ϕ_{vt}
0	1.00
0.07	2.00
0.10	2.14
0.20	2.46
0.40	2.96
0.70	3.42
1.00	3.85
2.00	5.30
4.00	7.87
7.00	11.3
10.0	14.8
20.0	25.4
40.0	46.0
70.0	75.8
100.	105.
200.	203.
400.	400.
1000.	1000.
for $\sqrt{X_{vt}} > 1000$	$\phi_{vt} = \sqrt{X_{vt}}$

c. Liquid Viscous - Gas Viscous: The same procedure was used as in the preceding cases except that both, liquid and gas, ratios of the actual cross-sectional area of flow to the area of a circle of diameter equal to the unknown hydraulic diameter for the gas phase were determined experimentally in capillary tubes.

The following correlations were obtained,

$$\left(\frac{\Delta p}{\Delta L}\right)_{T-P} = \phi^2_{vv}\left(\frac{\Delta p}{\Delta L}\right)_g \tag{6}$$

Where ϕ_{vv} is a function of a dimensionless group, X_{vv}; and,

$$X_{vv} = \frac{\mu_f}{\mu_g} \cdot \frac{\rho_g}{\rho_f} \cdot \frac{w_f}{w_g} \tag{7}$$

The magnitude of ϕ_{vv} for values of X_{vv} is given in Table III.

TABLE III

ϕ_{vv} vs $\sqrt{X_{vv}}$

$\sqrt{X_{vv}}$	ϕ_{vv}
0.2	1.40
0.4	1.69
0.6	1.93
0.8	2.16
1.0	2.44
2.0	3.81
3.0	5.15
4.0	6.40
6.0	8.70 (limit of experimental data)
∞	$\phi_{vv} = \sqrt{X_{vv}}$

d. Liquid Turbulent - Gas Viscous: This type of flow is very unlikely to exist in practice. The solution of this case would follow in detail the solution for the case where the liquid is viscous and the gas is turbulent by interchanging the expressions for the friction factor.

Lockhart and Martinelli (10) present further information for this flow mechanism.

2. Flashing and "Boiling Liquids"

a. Flashing Mixture of Liquid and Vapor: When a saturated liquid flows in a pipe line from a given point at a given pressure to another point at a lower pressure, several processes take place,

(1) As the pressure decreases, the saturation temperature decreases and the enthalpy of the remaining liquid is also reduced.
(2) The heat liberated by the above reductions is used as latent heat in evaporating a portion of the liquid.
(3) The specific volume of the mixture increases.
(4) The available energy is expended as kinetic energy in the mixture and friction.

An expression for the pressure drop can be obtained from substituting the continuity equation,

$$V = Gv \tag{8}$$

into the general energy equation for the flow of fluids, assuming that the mixture behaves as a compressible fluid,

$$vdp + \frac{VdV}{g_c} + \frac{4fV^2}{2g_c D}\,dL = 0 \tag{9}$$

obtaining,

$$v_m dp + \frac{G_m^2}{g}\left[v_m dv_m + \frac{4f}{D}\frac{v_m^2}{2}\,dL\right] = 0 \tag{10}$$

Equation 10 can not be integrated explicitly; however, a numerical integration is possible.

It may be more convenient to rewrite Equation 10,

$$\Delta L = \frac{D}{2f}\left[\frac{g_c}{G_m^2}\frac{\Delta p}{v_m} - \frac{\Delta v_m}{v_m}\right] \tag{11}$$

The expansion can be assumed to be an irreversible adiabatic (constant enthalpy) process. This assumption will give a conservative result.

The coefficient of friction, f, was determined for the flow of a flashing mixture of water and steam, by Bottomley (3) and Benjamin and Miller (2). The average value determined was 0.003.

In an actual numerical integration of Equation 11, increments of pressure are taken and the average specific volume and difference in specific volume of the mixture for this increment are obtained assuming a constant enthalpy process. The enthalpy used is the enthalpy of the saturated liquid at the initial pressure. Then from the value of the coefficient of friction given above and knowing the pipe diameter and the mass velocity, the increment of length for the increment of pressure taken can be computed. The total length of pipe is the sum of the length increments for the pressure increments from the initial pressure to the final pressure. The solving for the length of pipe when the other conditions are known is the simplest computation; in solving for one of the other conditions, i.e., pipe diameter, mass velocity, or pressure drop, the computations involve the above numerical integration plus a "trial and error."

Two points should be considered in the above computation,

(1) The coefficient of friction, f, should perhaps be determined for each specific liquid-vapor mixture as the value of 0.003 was determined for water-steam mixture. However, the value of 0.003 may be used as a guide for the estimation of the pressure drop or other conditions for other liquid-vapor mixtures.

(2) A "critical flow" condition may exist at the discharge. This "critical flow" condition is similar to that for the flow of gases only through pipes. When the discharge pressure is decreased, a pressure is reached at which a further decrease in pressure will have no effect on pressures or flow rate within the pipe. The velocity at the discharge for these conditions is called the "critical velocity." For gases only flowing through pipes, this critical velocity

is equal to the velocity of sound at the discharge pressure and temperature condition; however, for the flow of flashing mixtures, the critical velocity may be much less than the velocity of sound in the vapor phase.

The maximum possible continuous rate of flow of a compressible fluid through a horizontal pipe of constant cross-section occurs when at the discharge end of the pipe all of the energy released by the differential drop in pressure is quantitatively converted into kinetic energy (therefore, frictionless flow),

$$- v\ dp = \frac{V dV}{g_c} \tag{12}$$

Equation 12 is Equation 9 without the friction term. Since,

$$V = Gv \text{ and } dV = G\ dv + v dG$$

Equation 12 can be rewritten, at critical flow conditions, where dG = 0, assuming that the mixture behaves as a compressible fluid,

$$\left(G_{cm}\right)^2 = -g_c\left(\frac{dp}{dv_m}\right) \tag{13}$$

For the reversible adiabatic expansion at the end of the pipe, $\left(\frac{dp}{dv}\right)$ should be taken along a constant entropy path. The value thus obtained will be slightly greater than actually exists but the value can be used as a guide.

In numerically integrating Equation 11 for the length of pipe, as described above, there may be an incremental pressure range for which the incremental length will be zero. This is the condition for "critical flow" and gives the maximum length of pipe and the final discharge pressure. If the incremental length is of a negative value, then the increment of pressure taken has been too large. For cases where this condition exists and the discharge pressure is higher than permissible, a larger pipe diameter should be assumed and the integration repeated until the desired conditions are obtained.

b. "Boiling Liquids:" This is the case where liquids are vaporized at about constant pressure in pipe lines.

Martinelli and Nelson (12) have applied the generalized two-phase flow correlations developed by Lockhart and Martinelli (10) (see also part on "Constant Liquid-Gas Flow") to the prediction of the pressure drop during the forced-circulation boiling of water. The generalized correlations are modified to incorporate the quality of the steam at any point along the pipe. Martinelli and Nelson have compared the method with some data (4) and the method shows promise; however, the method is based on a small amount of data (mainly isothermal data) and further experimental verification is required.

McAdams, et. al,, (14, 15) present pressure drop data on the vaporization of water, benzene, and benzene-oil mixtures inside horizontal pipes.

Dittus and Hildebrand (5) present a method involving the combined use of mathematical equations and graphical solutions for determining the pressure drop for oil-vapor mixtures flowing through furnace coils. It is claimed that calculated results compare very favorably with actual plant conditions.

3. Flow of a Condensing Vapor in Straight Circular Pipe

The study of the flow of condensing vapors in pipes is complicated due to the properties of the mixture constantly changing with changes in pressure, temperature, and fraction condensed. Further, the condensate which forms on the walls requires energy in order to be transformed into spray, and this energy must be obtained from the main vapor stream, resulting in additional pressure drop.

The basic equation for the pressure drop of a condensing vapor in straight circular pipe is, (see Chapter 1, "Mass, Energy, and Momentum Balance in Fluid Mechanics"),

$$-\frac{dp}{dL} = \frac{G_m^2 dv_m}{g_c dL} + \frac{1}{v_m}\frac{dZ}{dL} + \frac{4fG_m^2 v_m}{2g_c D} + \frac{G_m^2 v_m}{g_c}\frac{dz}{dL} \tag{14}$$

Equation 14 can be derived from the consideration of momentum exchange and momentum loss.

Equation 14 can be solved by combination with a heat balance over a differential length of pipe, utilizing the properties of the fluid to express all dependent variables in the resulting equation in terms of pressure and fraction condensed, and finally performing a step-wise integration. The procedure will be outlined in the following paragraphs.

Bernoulli's equation may be written for this case as,

$$- Q = \Delta H + \Delta \left(\frac{V_m^2}{2g_c J} \right) \tag{15}$$

The term $\Delta \left(\frac{V_m^2}{2g_c J} \right)$ is generally small in comparison with Q or ΔH and therefore may be neglected. Therefore, Equation 15 may be written as,

$$- dH/dL = \pi D U_i \Delta t/(3600 w_m) \tag{16}$$

now,

$$H = (1 - z)\, H_g + z\, H_f \tag{17}$$

therefore,

$$dH = (1 - z)\, dH_g - (H_g - H_f) dz + z dH_f \tag{18}$$

The friction factor has been found to be a function of the Reynolds number based on the vapor viscosity and mass velocity,

$$f = C(N_{Re})^{-n} \tag{19}$$

$$N_{Re} = \frac{DG_g}{\mu_g} = \frac{4w_m(1 - z)}{\pi \mu_g D} \tag{20}$$

The vapor properties can now be expressed in terms of pressure; that is,

$$H_g,\ dH_g,\ H_f,\ dH_f,\ v_g,\ dv_g,\ v_m,\ dv_m,\ t,\ \mu_g$$

are written as function of pressure. Note that,

$$v_m \cong (1 - z)\, v_g \tag{21}$$

and

$$dv_m = (1 - z) dv_g - v_g dz \tag{22}$$

By combining Equations 14, 19 and 20, 16 and 18, and the equations for the properties of the vapor as a function of pressure, an expression of the following type is obtained,

$$\frac{dp}{dz} = \psi (p,\ z,\ G_m,\ w_m,\ D,\ U_i,\ \Delta t) \tag{23}$$

The term $\frac{1}{v_m} \frac{dZ}{dL}$ in Equation 14 can be neglected.

Equation 23 can not be formally integrated; however, it can be solved by a step-wise integration procedure. The general method is as follows: Given w_m, D, and U_i, the unknowns are p, z, and Δt. Δt is determined from p and the heat receiver temperature. dp/dz for the inlet conditions and z = 0 can be computed.

Then for z = 0.1, an approximation of the pressure at that point may be obtained from the inlet dp/dz. The Δt at z = 0.1 may be obtained from this approximate pressure, and the value of dp/dz is calculated for z = 0.1. The dp/dz for z = 0 and for z = 0.1 are averaged and a second approximation of p at z = 0.1 obtained. This procedure is repeated until the value of p at z = 0.1 is fixed. The computations are then performed for z = 0.2, 0.3, ------, 0.8. A curve of p vs z is then obtained. The reason why z = 0.8 is the last point considered is that Equation 14 applies only if the condensate is carried by the main gas stream in the form of a spray, and this condition is doubtful for condensate to vapor weight ratios much above 4 to 1. Indications are, however, that the pressure at z = 0.8 is

practically equal to that at z = 1.0. Thus a constant pressure can be assumed in the range z = 0.8 to 1.0. A curve of Δt vs z can now be obtained from the curve of p vs z, and the integrated average Δt may be computed. The pipe length required for total condensation is computed from the total heat transferred per unit time, the integrated average Δt, the heat transfer coefficient, and the heat transfer area per unit length of pipe.

It can be seen that the above procedure would be very tedious and lengthy if either pressure drop or length is given and it is required to determine the flow rate.

C. Liquid-Gas Flow in Vertical Pipes

1. Introduction

When liquid-gas mixtures flow in vertical pipes, there is an increase in liquid concentration or build-up of liquid, due to the density difference, in the case of upward flow, and a decrease in liquid concentration in the case of downward flow.

Little information (13) is available on the downward flow of liquid-gas mixtures. A conservative pressure drop calculation could be made in this case by simply employing the usual friction factor curves and Fanning equation for single fluids and using therein the apparent density of the mixture and the viscosity of the continuous phase. The mixture density would be calculated from the liquid-gas ratio assuming the absence of slip.

Considerable information is available on the upward flow of liquid-gas mixtures. A variety of flow phenomena are possible varying from gas as the disperse phase in a continuous liquid phase, to gas as the continuous phase with liquid carried as spray. One of the intermediate types is where the liquid flows as an annulus and the gas as a central core. This latter type has been found to exist in air lifts having submergences less than 20% for the whole operating range of air rates (7) and probably exists in gas lifts used in the operation of flowing oil wells (1).

2. Liquid - Gas Flow at Various Angles with the Horizontal

Martinelli, et. as. (13) report data obtained with liquid-gas systems in a capillary tube placed at various angles with the horizontal. The gas was air and the liquids were Diesel fuel oil and kerosene; both phases were in the viscous flow. The capillary tube was tested vertically up, vertically down, 30° up, and 30° down with respect to the horizontal.

They neglected the static head, stating that the fraction of the tube volume occupied by the liquid was small, from visual observations. They conclude that, at least for small capillary tubes, the correlations presented for the liquid viscous-gas viscous flow in horizontal tubes is independent of tube angle, unless the omission of the correction for the static head of the liquid in the tube is of considerable importance. The flow in horizontal tubes correlations would not perhaps apply for larger tubes or for other types of flow.

3. Gas Lifts

A gas lift is a vertical pipe (known as the eduction pipe) open at both ends, part of which is submerged below the surface of the liquid to be pumped. Compressed gas is admitted through a foot-piece inside the lower end; a mixture of liquid and gas is thus formed within the pipe. The gas reduces the average density of the mixture in the eduction pipe to a point where the weight of the mixture is less than equivalent to the pressure at the foot-piece. The gas and liquid being supplied at a sufficient rate, the mixture rises upward through the pipe and is discharged at the upper end.

The submergence is the distance from the liquid level to the foot-piece. The lift is the distance from the liquid level to the discharge. The submergence plus the lift is equal to the effective length of pipe flow. The submergence ratio is defined,

$$R = \frac{\text{submergence}}{\text{submergence + lift}} \tag{24}$$

There exists much information on the operation of gas lifts (1, 7, 16) particularly in connection with the operation of flowing oil wells. Considerable operating and experimental data have been reported but little attempt has been made to correlate them. The best analysis of gas lift operation appears to have been made by Hershey (8), who has correlated the data of Ward and Kessler (16) for a water-air lift together with his own data.

a. Water-Air Lift: Hershey analyzed the air lift, taking into account the slip between the water and the air. His analysis is based on the following assumptions:

a) No material transfer between phases
b) Flow is substantially isothermal
c) Weight of gas is negligible with respect to the weight of liquid
d) Liquid is the continuous phase
e) Flow through circular pipes of uniform cross-section

The correlations consist of modifications to the continuity and energy equations. In the continuity equation, Hershey uses a term to account for the slip between the liquid and the gas. This term, designated as ϕ', is the statistical volume ratio of gas to liquid in the pipe. The dependence of the gas-liquid volumetric ratio upon the several variables affecting the flow was analyzed using dimensional analysis. From this analysis and using experimental data, the following correlations for the gas-liquid volumetric ratio were obtained,

$$\phi' = 3.5\left(\frac{q'}{\sqrt{D^5 g_L}}\right)^{0.83} \text{ for } L>15 \text{ ft.} \tag{25a}$$

$$\phi' = 2.4\left(\frac{q'}{\sqrt{D^5 g_L}}\right)^{0.93} \text{ for } L<15 \text{ ft.} \tag{25b}$$

p. 107 - Equation 25b should read: $\phi' = \ldots\ldots$

The continuity equation can then be written as,

$$q_g = q' + \phi' q_f \tag{26}$$

The quantities q' and ϕ' are determined by the simultaneous solution of Equations 26 and 25a or 25b. In the energy equation account must be made for two types of losses,

a) Friction in the pipe. This loss increases with increasing velocity.
b) Relative motion between the gas and the liquid. This loss decreases with increasing velocity.

These combined losses were determined in the form of a correlation with the non-slip velocity from experimental data. The correlation, relating the friction factor to the Reynolds Number, is,

$$f' = \frac{0.048}{(N_{Re})^{0.13}} = \frac{0.048}{\left(\frac{DV_m\rho_f}{\mu_f}\right)^{0.13}} \tag{27}$$

where,

$$V_m = \frac{4(q_g + q_f)}{\pi D^2} \tag{28}$$

The correction for the static head in the eduction pipe is accounted for through the introduction of the gas-liquid volumetric ratio, ϕ'. The energy equation, using the above correlations, can then be written as,

$$-\int_{P_1}^{P_2} \phi' dp = P_2 - P_1 + \rho_f L + \rho_f \frac{\Delta(V_m^2)}{2g_c} + \frac{4f' L\,(\overline{V_m^2})\,\rho_f}{D\,2g_c} \tag{29}$$

In using the energy equation, Equation 29, it may be more convenient to use the differential form,

$$-\frac{dp}{dL}\left(1 + \phi' + \frac{\rho_f V_m}{g_c}\frac{dv_m}{dp}\right) = \rho_f + \frac{2f' V^2 \rho_f}{g_c D} \tag{29a}$$

p. 107 - Equation 29a should read:

$$-\frac{dp}{dL}\left(1 + \phi' + \frac{\rho_f V_m}{g_c}\frac{d V_m}{dp}\right) = \rho_f + \frac{2f' V_m^2 \rho_f}{g_c D}$$

The term $\frac{dV_m}{dp}$ may be computed as follows,

$$q_m = q_g + q_f = q_{go}\frac{p_o}{p} + q_f \tag{30}$$

differentiating Equation 30,

$$\frac{dq_m}{dp} = -\frac{p_o q_{go}}{p^2} = \frac{A dV_m}{dp} \tag{31}$$

therefore,

$$\frac{dV_m}{dp} = -\frac{4\, p_o q_{go}}{\pi D^2 p^2} \tag{31a}$$

From Equation 29a, the pressure gradient can be obtained at the bottom (foot piece) and the discharge of the air lift. If the difference between the two pressure gradients is not too large, the average may be used to compute the pressure drop. If the difference is large, a step-wise calculation up the pipe may be required.

Equations 29 and 29a do not account for the additional pressure drop required to provide the inlet water kinetic energy. This additional pressure drop can be computed as follows,

$$V_f = \frac{q_f}{A\left(\frac{1}{1+\phi'}\right)} \tag{32}$$

$$(\Delta p_{K.E.})_f = \rho_f \frac{V_f^2}{2g_c} \tag{33}$$

The total pressure drop required is the sum of the pressure drop from the energy equation, Equation 29a, and the pressure drop to supply the inlet water kinetic energy, Equation 33. The total pressure drop is equivalent to the submergence.

The above correlations were based on data (16) obtained with a 2-1/2-in. pipe and the middle third of the 60 foot length; additional data (8) obtained with glass tubes ranging in diameter from 0.8 inches to 5.5 inches for no net flow of water in a tube section filled with a mixture of air and water was used to verify the correlation for the gas-liquid volumetric ratio. However, the correlations have been given some additional confirmation by a comparison with other published data. The results are summarized in Table IV.

The isothermal efficiency of an air lift is,

$$\text{Efficiency} = \frac{\text{work done to lift liquid}}{\text{work done by air in isothermal expansion}} = \frac{w_f\, h}{w_g\, RT\, \log_e\left(\frac{p_1}{p_2}\right)} \tag{34}$$

It should be pointed out that the maximum efficiency occurs at an air rate somewhat less than the air rate required for maximum liquid rate. The efficiencies of air lifts are usually low, of the order of 25%.

Table IV

Pipe Diam. in.	total length of eductor pipe ft.	water rate lb./sec.	air rate lb./sec.	Submergence ft. of water exptl.	Submergence ft. of water calc'd.	Source
1.05	26.56	1.0	0.0051	15.0	16.2	Gosline (7)
1.05	26.56	1.52	0.0040	20.0	21.6	Gosline (7)
1.05	26.56	0.51	0.0045	9.6	9.8	Gosline (7)
6.625	261.0	72.0	0.249	156.0	154.3	Lea (9)
7.5	106.5	146.5	0.485	63.0	69.6	Gibson (8)

b. Other Gas Lifts: Hershey attempted to correlate data on oil-air lifts but no correlation similar to the one for water-air lifts was possible. On the whole, the oils showed higher values of ϕ' for the same $\frac{q'}{\sqrt{D^5 g_L}}$. The correlations presented above for water can serve as a rough estimation for other liquids.

Gosline (7) reports the results of his experiments on the flow of air and liquids (water and two oils) in a 26.56 ft. vertical section of 1.05-in. i.d. pyrex pipe. Plots of liquid rate versus gas rate are given for various submergences. The liquid rate and thus the efficiencies were found to decrease appreciably as liquid viscosity increased for a given air rate. Maximum efficiencies were found to exist at about 57% submergence for all the liquids tested. For water, the maximum efficiency was 32% and for one of the oils having a viscosity approximately 105 times that of water, the maximum efficiency was 18-1/2%. Experiments were also carried into the range where the air flowed up the pipe as a central core and the liquid as an annular ring. This type of flow is favored by high air rates and low submergences. Lines are given on the flow charts to indicate the observed division between the unsteady, turbulent type of flow and the annular ring condition.

Babson (1) presents information and data on various types of gas lifts used in oil wells. He states that the flow may be of the annular ring type.

IV. SOLID-GAS FLOW IN PIPES

A. Pneumatic Conveying

1. Introduction: Conveying material pneumatically has been used for many years. The system can be either a pressure system or a suction system. The materials that have been handled include grain, wood shavings, pulverized coal, cement, staple, plastic chips, small metal parts, and money containers in department stores. Pneumatic conveyors are simple, quiet, convenient, and clean; however, pneumatic conveyors have a much lower efficiency than the belt or bucket types.

In a pressure system the material can be fed by a screw conveyor or similar feeder and then forced through the system by compressed air (Fuller-Kinyon system is somewhat of this type), or the material can be fed into a tank and then forced through the system by compressed air (Fuller-Fluxo System is of this type).

In a suction system a fan or blower is installed after the separating system thereby putting the entire system under vacuum. The material, with sufficient air to keep the material in suspension, is then drawn or "sucked" through the system. ("Airveyor" and "Pneu-Vac" are of this type.)

Occasionally it is more convenient to use a combination of a pressure and suction systems. In a combination system the material is drawn in, passes through the fan and then under pressure is forced through the remainder of the system. For cases where the material may damage the fan, an ejector may be used in place of the fan. Also in the use of an ejector the material can be fed at the mixing throat of the ejector.

In the design of pneumatic conveying systems no "straight-forward" "theoretical" method has been developed; the design is based on practical operating experience and empirical correlations of test data. Several articles (17, 19, 20, 22) have been published which present a general treatment of the particle motion and of the pressure drop. The articles by Gasterstadt (19, 20), and Wood and Bailey (22) are good.

2. Solids Motion: The path of the solids in a horizontal pipe is somewhat sinusoidal, the solids striking the bottom of the pipe at intervals and then rising again. The height and length of the rise appears to decrease as the air velocity decreases. The vertical distribution of the solids across the pipe diameter is fairly uniform at low concentrations but becomes more dense at the bottom of the pipe as the loading (ratio of weight rate of solids to weight rate of air) increases and finally, at high loadings a considerable proportion of the solids seems to be sliding along the bottom of the pipe. The difference between the final average velocity of the solids and that of the air stream is almost constant for both horizontal and vertical conveyors. This difference is the "slip" between the solids and the air and increases with increasing velocity of the air stream. This "slip" velocity is of the order of magnitude of the "choking" velocity; that is, the air stream velocity when the velocity of the solids is zero. The "choking" velocity is essentially the minimum transport or conveying velocity. For estimating purposes, the "slip" velocity may be taken as equal to the "choking" velocity. It has been reported (22) that the "choking" velocity is independent of loading for relatively large particles.

The minimum transport velocities of a material can be estimated by testing the solids in horizontal and vertical glass tubes by determining the minimum air velocity to convey the solids in a horizontal tube and the minimum air velocity to just suspend the solids in a vertical tube. The minimum transport velocity of the solids may be several times the free fall velocity.

The minimum velocities to prevent the settling of cinders (sp.gr. = 1.1), carbon (sp.gr. = 1.3), anthracite (sp.gr. = 1.5), and quartz (sp.gr. = 2.7) over a size range of 0.055 to 0.320 inches diameter has been empirically correlated by Dalla Valle (18), based on his tests. Following are the correlations:

$$V_t = k\left(\frac{s}{s+1}\right) d^b \tag{35}$$

where:

	Horizontal pipe	Vertical pipe
k	100	205
b	0.40	0.60

3. Pressure Drop: The total pressure drop in the system can be considered to consist of the sum of the following pressure drops:

a) to accelerate the air to the carrying velocity.
b) to overcome the friction of the air on the pipe walls.
c) to supply the loss of momentum of the air in,
   1) accelerating the solids
   2) keeping the solids in suspension
d) to support the air (vertical pipes)
e) to support the solids (vertical pipes)

From tests on linseed (22), the pressure gradient is steepest near the solids inlet and decreases as the distance traveled increases becoming approximately constant after 30 to 40 pipe diameters. However, in these tests the grain was drawn or "sucked" directly into the conveying pipe and indications are that this distance required to accelerate the solids is much less for an ejector type or venturi type of feeder. Thus it appears the actual distance required depends upon how quickly the momentum transfer between the air stream and solids can take place. Therefore, it seems that the length required to accomplish most of the solids acceleration is constant and independent of loading for materials of uniform size and for any one system.

The pressure drop to accelerate the air can be computed from the energy relation,

$$\Delta p_{ag} = \rho_g \frac{V_g^2}{2g_c} \tag{36}$$

The superficial air velocity, V_g, is used instead of the actual velocity since in practice the actual projected area of the solids across a diameter of the pipe is negligible with respect to the pipe cross-sectional area.

The pressure drop to accelerate the solids can be determined by a momentum balance.

$$\Delta p_{ax} = \frac{w_s}{g_c A} V_x \tag{37}$$

where:

$$V_x \cong V_g - V_t$$

The pressure drops due to overcome the friction of the air on the pipe walls and to supply the loss of momentum of the air in keeping the solids in suspension can be determined conservatively in turbulent flow by the usual friction factor vs Reynolds Number correlation and the Fanning equation by using the viscosity of the air and the density of the mixture. At high solid loadings (>5) the actual pressure drops may be 30 to 40% lower than predicted on this basis. For the usual conveying velocities, the density of the mixture can be computed using the feed loading and not the actual loading existing in the pipe, in other words, neglect the "slip". The Reynolds Number and Fanning equation using the feed loading, $R = w_x/w_g$, to compute the mixture density are as follows:

$$N_{Re} = \frac{D\, G_g}{\mu_g} (1 + R) \tag{38}$$

$$\Delta P_F = \left(\frac{4fL}{D}\right)\left(\frac{G_g^2}{2g_c}\right)(1 + R)\left(\frac{1}{\rho_g} + \frac{R}{\rho_x}\right) \tag{39}$$

Gasterstadt (19) found from tests with wheat in horizontal pipes that the ratio of the pressure drop for the mixture to the pressure drop for air was linear with the loading, that is,

$$\frac{\Delta P_F}{\Delta P_g} = 1 + RS \tag{40}$$

The slope, S, of the line obtained by plotting $\frac{\Delta P_F}{\Delta P_g}$ vs R decreases with increasing air velocity. For loadings up to 14 and for air velocities of approximately 45 to 95 ft./sec., the slope varied from approximately 1/2 to 1/4. It should be emphasized that Equation 40 was tested only with wheat and it is recommended that Equation 39 be used.

The pressure drop to support the air and to support the solids in vertical pipes can be determined from a force balance:

$$\Delta P_v \, A = W_a + W_s \tag{41}$$

or,

$$\Delta P_v = \rho_m h \tag{42}$$

For a conservative approximation, and attempting to account for "slip",

$$\Delta P_v = \rho_g h\left(1 + R\,\frac{V_g}{V_g - V_t}\right) \tag{43}$$

The total pressure drop is then the sum of the above;

horizontal pipes $\Delta P = \Delta P_{ag} + \Delta P_{ax} + \Delta P_F$

vertical pipes $\Delta P = \Delta P_{ag} + \Delta P_{ax} + \Delta P_F + \Delta P_v$

4. Comments on Design Procedures: In an actual design, the quantity of material to be conveyed and the distance are known. One then assumes a loading and conveying velocity, and from these the diameter of the pipe can be computed. Finally, the pressure drop through the system is computed. If the pressure drop is excessive, a smaller loading can be taken and the above procedure is repeated. This is repeated until a reasonable pressure drop is obtained. There is no reliable method to compute the conveying velocities; however, in design a conveying velocity of 70 ft./sec. is usual. Some order of magnitudes of loading, conveying velocities, and pressure drops for various systems are outlined below:

(a) Fan system
pressure drop = 10 to 30 inches of water (50 inches of water is about the maximum)
loading = 0.1 to 2 (possibly 5) lb.solids/lb.air
conveying velocity = 30 to 100 ft./sec., usually 50 to 70 ft./sec.
The fan system is used for distances less than 200 ft.

(b) Vacuum System
pressure drop = 5 to 10 inches of Mercury
loading = 5 to 20 lb.solids/lb.air
conveying velocity = (same as above)

(c) Pressure System
pressure drop = 10 to 50 lb./sq. in. (possibly 100 lb./sq. in.)
loading = 5 to 40 lb.solids/lb.air
conveying velocity = (same as above)

Large radius bends are recommended as the pressure drop will be less than with close bends and also it will be less likely for the solids to collect and choke the bend.

When dry air or a special gas is used for conveying, the air or gas may be recirculated; that is, the air or gas from the discharge is recirculated to the suction.

In conveying fibrous materials, a pressure system may be the best as the cyclone separator, if one is used, will be under a slight pressure and can then discharge the material more quickly. The

discharge opening of a cyclone used with fibrous materials may be large and if a suction system is used much air may be drawn through the cyclone thereby preventing an efficient discharge of the material.

The system is critical to non-uniformity of feeding, and allowance should be made of this.

An ejector may be used to develop the required pressure and also used where solids are to pass through the pressure producing device. However, the power requirements for an ejector are 4 to 10 times that for a fan.

5. Commercial Systems: The following discussion of Fuller Co. systems was obtained from an article by Mann (21), and from Fuller Company catalogues. There are several other manufacturers of pneumatic conveyors, such as Brady Conveyors Corporation, Sprout-Waldron & Company ("Pneu-Vac"), and Dracco Corporation; however, many of these are similar to the Fuller Company Airveyor .

a. Fuller-Kinyon System: This system is a pressure type; that is, the material is forced through by pressure.

The material entering the hopper of the pump is moved through the barrel of the pump by an impeller screw normally driven at 1160 rpm; the impeller screw has flights of decreasing pitch toward the discharge which compacts the material to form a "seal" to prevent the escape of air through the screw. Compressed air is injected into the material just beyond the "seal" through several jets. The material assumes about twice its normal volume and in this state is forced through the pipe line by the expansion of the air and the continual displacement of material into the system. The normal pressure range is between 10 to 30 psig at the pump. Pressure in excess of 35 psig cause excessive wear of the flights of the screw in creating the necessary "seal".

The materials that may be handled must be relatively dry and the finess should be at least 50% through a 200 mesh sieve (0.0029 in.) in order to form a suitable seal. Portland cement, clay, Fullers earth, lime, and starch are examples of materials that can be conveyed by this system.

These systems can have as many as 48 delivery points and be in excess of 3000 ft. in length. One installation elevated cement 300 ft.

b. Fuller-Fluxo System: This system is sometimes called a "blow-tank" system. It consists of a pressure vessel into which the material to be conveyed enters by gravity through a valve. When the tank is almost full, compressed air, approximately 100 psig, is admitted through an aerating ring to cause the material to become fluent. When the material has been thoroughly aerated and the pressure has been built up to overcome the system resistance, additional air is admitted to force the material to the delivery point. The controls are automatic.

These systems are ordinarily recommended where the conveying distance exceeds 3,000 ft. One system for conveying cement is 7,600 ft. long.

c. "Airveyor": This system is of the more conventional type where the materials are carried in suspension in an air stream of high velocity and much greater volume than that used in the above types. In addition to pulverized materials, these conveyors can handle relatively coarse materials such as grains and woodchips. The system can be operated by suction, by pressure, or by a combination of suction and pressure.

V. LIQUID-SOLID FLOW IN PIPES

Suspensions of solids in liquids fall into two general classes (1) Newtonian, and (2) Non-Newtonian. Newtonian suspensions are characterized by a constant viscosity, independent of the rate of shear. In the case of Non-Newtonian suspensions, the viscosity is a variable, being some function of the rate of shear and in some cases a function of the duration or period of shear for viscous flow.

If the suspension is found to be Newtonian in character, the pressure drop can be computed by Poiseuille's equation for viscous flow and the Fanning equation for turbulent flow using the density and viscosity of the mixture.

The procedures for computing the pressure drop for Non-Newtonian suspensions are more involved.

A complete discussion of the flow of suspensions in pipes is given in Chapter 7, "Non-Newtonian Flow".

p. 112 - line 11 from top of page should read:
.....Fuller Company "Airveyor."

VI. PROBLEMS

1. What is the pressure drop for the co-current two-phase flow of air and oil in a horizontal 100-ft. section of 2-in. standard Schedule 40 steel pipe under the following conditions:

air rate = 65.6 c.f.m. free air (i.e. measured at 70° F. and 1 atm. pressure)

oil rate = 10.9 g.p.m.

temperature = 70° F.

average pressure in pipe = 45 p.s.i.g.

specific gravity of the oil at 70° F. = 0.90

viscosity of the oil at 70° F. = 100 cp.

2. From the data on a 7.5-in. i.d. water-air lift presented by Gibson "Hydraulics and Its Applications", see Table I of this chapter under C3a, compute:

a. The submergence required using Hershey's correlation as presented in this chapter.

b. The isothermal efficiency using the experimental determined submergence.

Assume the temperature as being 70° F. and the lift as discharging at atmospheric pressure.

3. Silica dust (100-mesh particle size) is to be conveyed pneumatically through 100 ft. of horizontal 2-in. standard Schedule 40 steel pipe at a rate of 20 lb./min. The conveyor fan is located on the discharge side of a cyclone dust collector. Assuming a required conveying velocity of 50 ft./sec., an air temperature of 70° F., the particle density of silica dust as 130 lb./cu.ft., a friction loss of 6-in. water through the cyclone and line on the discharge side of the cyclone, and a 60% over-all energy conversion efficiency for the fan, motor, and drive, estimate the electrical power consumption in kilowatts.

Chapter 7 - Non-Newtonian Flow

Chapter 7

NON-NEWTONIAN FLOW

by

George E. Alves
Engineering Research Laboratory
Engineering Department
E. I. du Pont de Nemours & Co., Inc.
Wilmington, Delaware

TABLE OF CONTENTS

Page

I. References 117

II. Nomenclature 118

III. General 119

IV. Introduction 119

A. Newtonian 119
B. Non-Newtonian 120

V. Viscous Flow of Non-Newtonian Liquids and Suspensions 120

A. Classification 120

1. Bingham Plastic Type 120
2. Pseudoplastic Type 120
3. Dilatant Type 121
4. Thixotropic Type 121
5. Rheopectic Type 122

B. Flow of a Bingham Plastic Through a Pipe 123
C. Thixotropic Breakdown and its Effect Upon Viscosity 125
D. Measurement of Rheological Properties 126

1. Rotational Viscometers 126

a. Theory 126
b. Commercial Types 129

(1). Mac Michael Viscometer 129
(2). "Green-Weltman" Concentric Cylinder Viscometer 129
(3). Brookfield "Synchro-Lectric" Viscometer 129
(4). Stormer Viscometer 130

c. Miscellaneous Notes on Rotational Viscometers 130

2. Tube Viscometers 130

E. Comparison of Rotational Viscometer Data With Pipe-Line Data 131

VI. Turbulent Flow of Non-Newtonian Liquids and Suspensions 132

VII. Dispersing Agents 132

VIII. Problems 133

LIST OF FIGURES

Figure 1 Shear Diagram of Newtonian Suspension 120
Figure 2 Shear Diagram of Bingham Plastic Suspension 120
Figure 3 Shear Diagram of Pseudoplastic Suspension 121
Figure 4 Shear Diagram of Dilatant Suspension 121
Figure 5 Shear Diagram of Thixotropic Suspension 122
Figure 6 Flow of Bingham Plastic in a Circular Pipe 123
Figure 7 Shear Diagram for Flow of Bingham Plastic in a Circular Pipe 125
Figure 8 Thixotropic Breakdown Curves 125
Figure 9 Shear Diagram of Bingham Plastic from Rotational Viscometer Data 126
Figure 10 Shear Diagram of Bingham Plastic from Pipe-Line Data 130
Figure 11 Shear Diagram of Thixotropic Suspension Showing Effect of Pipe Diameter and Length. . 131
Figure 12 Shear Diagram of Pseudoplastic Suspension on Logarithmic Plot 131
Figure 13 Shear Diagram of Bingham Plastic for Viscous and Turbulent Flows 132

I. REFERENCES

1. Andrade, E. N. daC. and Arnold, J. E., "Viscosity and Plasticity", Paint Tech., 10, 243-247 (1945) Oct.
2. Arnold, K. A., "Flow Properties of Coating Clays at High Rates of Shear", Tech. Assoc. Pulp and Paper Ind. Papers, Series 26, 224-230 (1943)
3. Barr, Guy, A Monograph of Viscometry, Oxford University Press, 1931.
4. Binder, R. C. and Busher, J. E., "A Study of Flow of Plastics Through Pipes", J. Applied Mech., 13, A-101-A105 (1946) June.
5. Bingham, E. C., Fluidity and Plasticity, New York, McGraw-Hill Book Co., 1922.
6. Bingham, E. C., "Some Fundamental Definitions of Rheology", J. Rheology, 1, 507-516 (1930)
7. Caldwell, D. H. and Babbit, H. E., "The Flow of Muds, Sludges, and Suspensions in Circular Pipe", Ind. Eng. Chem., 33, 249-256 (1941).
8. Carr, W., "Experiments on Wetting and Dispersion", Paint Manufacture, 16, 190-192 (1946).
9. Freundlich, H. and Juliusberger, F., "Thixotropy, Influenced by the Orientation of Anisometric Particles in Sols and Suspensions", Trans. Faraday Soc., 31, 920-921 (1935).
10. Green, H., "High-Speed Rotational Viscometer of Wide Range", Ind. Eng. Chem., Anal. Ed., 14, 546-585 (1942).
11. Green, H., "How to Determine the Desirable Rheological Properties of Coatings", Tech. Assoc. Pulp and Paper Ind. Papers, Series 30, 599-603 (1947).
12. Green, H. and Weltmann, R. N., "Analysis of the Thixotropy of Pigment-Vehicle Suspensions", Ind. Eng. Chem., Anal. Ed., 15, 201-206 (1943).
13. Green, H. and Weltmann, R. N., "The Effect of Thixotropy on Plasticity Measurements", J. Applied Physics, 15, 414-420 (1944).
14. Green, H. and Weltmann, R. N., "Equations of Thixotropic Breakdown for the Rotational Viscometer", Ind. Eng. Chem., Anal. Ed., 18, 167-172 (1946).
15. Green, H. and Weltmann, R. N., "Thixotropy", p. 328-347, Vol. VI, Colloid Chemistry, Jerome Alexander (Editor), New York, Reinhold Pub. Corp., 1946.
16. Grunberg, L. and Nissan, A. H., "Viscosity of Ordinary Liquids at High Rates of Shear", Nature, 156, 241 (1945).
17. Hauser, E. A., Colloid Phenomena, New York, McGraw-Hill Book Co., 1939
18. Hauser, E. A. and Lynn, J. E., Experiments in Colloid Chemistry, New York, McGraw-Hill Book Co., 1940
19. Kennedy, H. T., "Chemistry of Drilling Fluids", Oil and Gas J., 45, No. 12, 181-187 (1946).
20. Lindsley, C. H. and Fischer, E. K., "End-Effect in Rotational Viscometers", J. Applied Physics, 18, 988-996 (1947).
21. Mardles, E. W. J., "The Suspensions of Solids in Mixed Liquids", Trans. Faraday Soc., 36, 1189-1198 (1940).
22. Mardles, E. W. J., "Dilatancy and Thixotropy", Nature, 159, 70 (1947).
23. Mooney, M., "Explicit Formulas for Slip and Fluidity", J. Rheology, 2, 210-222 (1931).
24. Perry, J. H., Chemical Engineers' Handbook, 3rd Ed., New York, McGraw-Hill Book Co., 1950
25. Philippoff, W., "Viskositat Der Kolloide", reprinted by J. W. Edwards, Ann Arbor, Mich., 1944.
26. Pryce-Jones, J., "Thixotropy", J. Oil and Colour Chem. Assoc., 17, 305-375 (1934).
27. Rabinowitsch, B., "Über die Viskosität und Elastizität von Solen" Z. Physik, Chem., 145 A, 1-26 (1929).
28. Reiner, Markus, "The Theory of Plastic Flow in the Rotational Viscometer", J. Rheology, 1, 5-10 (1929).
29. Reiner, Markus, Ten Lectures on Theoretical Rheology, Jerusalem, Sheckter and Fainberg, 1943.
30. Reynolds, Osborne, Scientific Papers, Vol II, 203-216, 217-227, Cambridge Univ. Press, 1901.
31. Scott Blair, G. W., An Introduction to Industrial Rheology, Philadelphia, Blakeston's Son and Co., 1938.
32. Scott Blair, G. W., Survey of General and Applied Rheology, New York, Pitman Pub. Corp., 1944.
33. Sheets, H., "Structural Viscosity Studies of Coating Clay Compositions", Tech. Assoc. Pulp and Paper Ind. Papers, Series 25, 528-536 (1942).
34. Voet, Andries, "Dielectrics and Rheology of Non-Aqueous Dispersions", J. Physical and Colloid Chem., 51, 1037-1063 (1947).
35. Weltmann, R. N., "Breakdown of Thixotropic Structure as Function of Time", J. Applied Physics, 14, 343-350 (1943).
36. Weltmann, R. N., "A Flow-Curve Recorder for a Rotational Viscometer", Rev. Scientific Inst., 16, 184-191 (1945).

37. Weltmann, R. N., "Initial Oscillations on a Rotational Viscometer", J. Applied Physics, 18, 933-940 (1947).
38. Weltmann, R. N., "Consistency and Temperature of Oils and Printing Inks at High Shearing Stresses", Ind. Eng. Chem., 40, 272-280 (1948) Feb.
39. Wilhelm, R. H., Wroughton, D. M. and Loeffel, W. F., "Flow of Suspensions Through Pipes", Ind. Eng. Chem., 31, 622-629 (1939).
40. Williamson, R. V., "The Flow of Pseudoplastic Materials", Ind. Eng. Chem., 21, 1108-1111 (1929).
41. Williamson, W. O., "Rheology of Aqueous Felspar-Pastes", Nature, 157, 341 (1946).
42. Winding, C. C., Baumann, G. P., and Kranich, W. L., "Flow Properties of Pseudo-Plastic Fluids- Parts I and II", Chem. Eng. Progress, 43, 527-536, 613-622 (1947).

II. NOMENCLATURE *

B_1 = rotational viscometer instrument constant, 1/cu.cm.*
B_2 = rotational viscometer instrument constant, 1/cu.cm.
D = inside diameter of tube or pipe, ft.*
g_c = conversion factor, $32.17\left(\frac{\text{lb.}}{\text{lb.force}}\right)\cdot\left(\frac{\text{ft.}}{\text{sec.}^2}\right)$
h = inner cylinder (bob) height, cm.
k = Mac Michael viscometer torsional constant, (dyne)(cm.)/radian
k_1 = a proportionality constant
k_2 = a proportionality constant
K = a proportionality constant, lb./(ft.)(sec.)
L = length of tube or pipe, ft.
n = an exponent, a constant
n' = an exponent, a constant
p = pressure, lb.force/sq.ft.
p_1 = upstream pressure, lb.force/sq.ft. abs.
p_2 = downstream pressure, lb.force/sq.ft. abs.
q = rate of flow, cu.ft./sec.
r = a radius, cm.(viscometers), ft.(tubes)
r_i = inner cylinder (bob) radius, cm.
r_o = outer cylinder (cup) radius, cm.
r_w = inside radius of tube, ft.
T = torque, (dyne)(cm.)
T_y = torque intercept, (dyne)(cm.)
V = velocity, ft./sec.
V_r = velocity at radius r, ft./sec.
V_τ = velocity for shear stress τ, ft./sec.
$-(dV_r/dr)$ = rate of shear, 1/sec.
$-(dV_r/dr)_i$ = rate of shear at inner cylinder wall, 1/sec.
$-(dV_r/dr)_w$ = rate of shear at tube wall, 1/sec.

*The c.g.s. system is used with the viscometers and ft.-lb.-sec. units are used in general. However, any consistent set of units can be used.

η = coefficient of rigidity, g./(cm.)(sec.) or lb./(ft.)(sec.)

θ_M = torsion wire deflection, radians

μ = absolute viscosity, lb./(ft.)(sec.)

μ_B = Brookfield instrument calibration viscosity, g./(cm.)(sec.)

μ_e = apparent or effective viscosity, lb./(ft.)(sec.)

μ_i = apparent viscosity at inner cylinder wall, g./(cm.)(sec.)

μ_o = apparent viscosity at outer cylinder wall, g./(cm.)(sec.)

μ_s = apparent viscosity at zero rate of shear, lb./(ft.)(sec.)

μ_∞ = apparent viscosity or limiting viscosity at infinite rate of shear, lb./(ft.)(sec.)

ρ_m = density of the suspension or liquid, lb./cu.ft.

τ = shear stress, dynes/sq.cm. or lb.force/sq.ft.

τ_i = shear stress at inner cylinder wall, dynes/sq.cm.

τ_o = shear stress at outer cylinder wall, dynes/sq.cm.

τ_y = yield stress dynes/sq.cm. or lbs.force/sq.ft.

τ_w = shear stress at tube wall, lb.force/sq.ft.

ϕ = a function

ψ = a function

ω = angular velocity, rad./sec.

ω' = rate of rotation, rev./min.

ω_r = angular velocity at radius r, rad./sec.

III. GENERAL

The study of the mechanics of the flow of liquids and suspensions comes under the science of Rheology. The name Rheology was chosen by Prof. John R. Crawford of Lafayette College, Pa. Rheology (6) is defined as the study of the flow and deformation of matter. The name is a combination of "Rheo" (flow) and "Logos" (theory). The Society of Rheology (affiliated with the American Institute of Physics) was founded in 1929. The following investigators are some of the outstanding of those who have contributed to this modern science.

U.S.A. - E. C. Bingham, R. B. Dow, H. Green, E. A. Hauser, E. O. Kraemer, M. Mooney, Ruth Weltmann, R. V. Williamson
England - E. N. daC. Andrade, G. W. Scott Blair, E. W. J. Mardles, J. Pryce-Jones
Europe - H. Freundlich, W. Ostwald, Markus Reiner

The two books by Scott Blair (31, 32) offer a very good survey of the history and application of Rheology. Reiner (29) presents a highly mathematical study of Rheology.

This chapter represents the results of a fairly complete coverage of the literature and an attempt to present information on the non-Newtonian flow in pipe lines.

IV. INTRODUCTION

Liquids and suspensions of solids in liquids fall into two general classes (a) Newtonian and (b) non-Newtonian.

A. Newtonian: Newtonian liquids or suspensions are characterized by a constant viscosity, independent of the rate of shear; that is,

$$\mu = \frac{g_c \tau}{-(dV_r/dr)} = \text{constant} \qquad (1)$$

The shear diagram of a Newtonian liquid or suspension is given in Figure 1. Figure 1 is a plot of Equation 1. The inverse slope of the straight line is the viscosity, μ. The g_c is a conversion factor to obtain consistent units. A shear diagram is a plot of the rate of shear vs. the shearing stress using arithmetic coordinates.

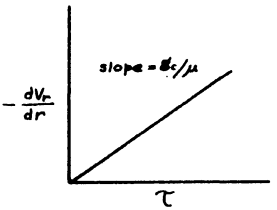


Figure 1. Shear Diagram of Newtonian Suspension

Grunberg and Nissan (16) state that from their theoretical considerations as presented, one may conclude that at high rates of shear the viscosity of Newtonian liquids may be expected to become a function of the rate of shear. Grunberg and Nissan show by computation that the viscosity of n-pentane at 30 C will be dependent upon the rate of shear for rates of shear greater than 5 x 10 (1/sec.), corresponding to shear stresses over 20.9 (lb.force/sq.ft.). Weltmann (38) presents experimental data showing that the viscosities of several oils have a non-Newtonian behavior above a limiting shear stress of approximately 20 (lb.force/sq.ft.).

If the liquid or suspension is found to be Newtonian in character, the pressure drop can be computed by the Poiseuille equation for viscous flow and the Fanning equation for turbulent flow, using the density and viscosity of the liquid or suspension.

V. VISCOUS FLOW OF NON-NEWTONIAN LIQUIDS AND SUSPENSIONS

A. Classification

Non-Newtonian suspensions are classified according to the general type of functional dependence of shear stress on the rate of shear; in other words, according to the general type of shear diagram.

These suspensions fall into five general types: (1) Bingham plastic, (2) Pseudoplastic, (3) Dilatant, (4) Thixotropic, (5) Rheopetic.

Each of the above general types will now be discussed in detail.

1. Bingham Plastic Type: A Bingham plastic gives a shear diagram as shown in Figure 2. The curve consists of a straight line with a positive intercept on the shearing stress axis. This intercept is called the "yield stress", τ_y. The inverse slope of the curve is equal to the "coefficient of rigidity", η. The g_c is a conversion factor to obtain consistent units.

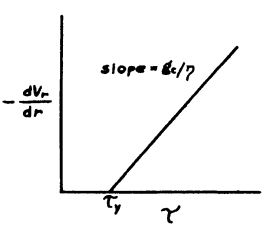


Figure 2. Shear Diagram of Bingham Plastic Suspension

In practice, where the shear diagram is obtained from pipeline data or from some types of rotational viscometers, the lower portion of the curve bends toward the rate of shear axis (see Figure 7). This curvature is due to the transition in flow from "plug" to laminar; that is, the curvature could be entirely caused by an instrumental effect and does not necessarily have to be caused by any change in the structure of the material at low rates of shear or shearing stresses. In other words, Figure 2 is for point values and Figure 7 is the integrated form for the pipe cross-section.

2. Pseudoplastic Type: A pseudoplastic suspension has a shear diagram similar to Figure 3. The curve starts at the origin and generally approaches a straight line at high rates of shear. The apparent viscosity decreases with increasing rate of shear. The inverse slope of the straight line is the apparent viscosity at infinite rate of shear, μ_∞. The inverse slope of the curve for very low rates of shear is constant and called the apparent viscosity at zero rate of shear, μ_S. The g_c is a conversion factor.

One of the explanations (15) for pseudoplasticity is that the applied shear produces a change in the structure of the suspension. The disorganized arrangement of the particles is changed to one of particle alignment with the long axis in the direction of flow. This alignment does not constitute a structural breakdown, as the particles are not joined together; therefore, no buildup is required when the shear is removed; that is, the particles return almost immediately to their original disorganized state.

R. V. Williamson (40) presents a theory of pseudoplastic flow. A review of this theory, together with its application to the viscosities of GR-S latices, is given by Winding, Baumann, and Kranich (42).

p. 120 - line 9 from top of page should read:
"... at 30°C. will ...."

p. 120 - line 10 from top of page should read:
"...than 5 x 10^6 (1/sec.),..."

p. 120 - line 19 from top of page should read:
A. Classification

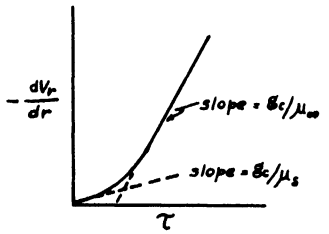


Figure 3. Shear Diagram of Pseudoplastic Suspension

3. Dilatant Type: A dilatant suspension produces a shear diagram as indicated in Figure 4. It may be considered to be the opposite of a pseudoplastic suspension (by comparison of shear diagrams only). The apparent viscosity increases with increasing rate of shear.

Dilatancy was discovered and named by Osborne Reynolds in ca. 1885. Reynolds theory for dilatancy (15, 30) was that a suspension is dilatant when the force of flocculation is quite small or entirely absent, and the amount of the liquid is just sufficient to fill the spaces between the particles when the particles are in the position of minimum or nearly minimum voids. An attempt to force such a material to flow disturbs the position of the particles, resulting in a dilation of the voids; but since there is insufficient liquid present to fill the expanded voids, the material as a whole becomes dry and hard, and develops a very high resistance to flow. When the applied force is removed, the substance returns to its original condition. This is Reynolds' own theory; however, other investigators have accepted it. Reynolds had in mind spherical particles in developing his theory; later, however, other investigators found that some thin, flat particles in suspension were dilatant. (See examples given below).

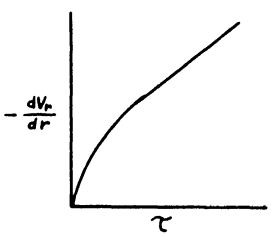


Figure 4. Shear Diagram of Dilatant Suspension

Some examples of dilatant suspensions are: starch and water (fairly high concentration), quick-sand, and beach sand. Feldspar pastes (41) and mica (18) in water were found to be dilatant; thus, giving some evidence that dilatancy does not depend upon spherical particles as has been frequently assumed. Some clay suspensions(2) show weakly dilatant behavior at low rates of shear and thixotropic behavior at high rates of shear.

It should be pointed out that a shear diagram for the laminar - turbulent flow of suspensions is of the same general shape as a shear diagram for a dilatant suspension and care must be exercised in deciding whether or not a suspension is dilatant or is flowing under turbulent conditions.

4. Thixotropic Type: A Thixotropic suspension possesses a structure, the breakdown of which is a function of time as well as of the rate of shear. The structure can rebuild itself, if not prevented from doing so by externally applied forces.

The definition of thixotropy, as given by Freundlich ca. 1934, is the isothermal gel-sol-gel transformation upon agitation and subsequent rest. This phenomenon was called "Thixotropy" by Peterfi and Freundlich around 1927. The name was derived from two Greek words meaning "to change by touching"

Weltmann (35) states that a material is thixotropic if any one of the following phenomena are observed:

(a) The breakdown of the structure is continuously increased as a function of the increased rate of shear:
(b) The structure is rebuilt upon rest after a previous exposure to violent motion.
(c) The breakdown increases continuously with the time during which the material is rapidly agitated.

There are many explanations and theories for thixotropy. Thixotropy is especially associated with asymmetric particles; that is, needles, rods, or plates (22). When agitated, these suspensions tend to become oriented in the flow stream with a resultant lowering of the apparent viscosity. It seems to be fairly well established that thixotropy can not exist without flocculation; but the converse of this is not necessarily true(15). Two of the theories proposed to explain thixotropy are briefly outlined as follows (see Hauser (17, 18) and Carr(8) for other theories and details).

(a) balanced-force theory

This is a recent theory and the most plausible. It assumes that the dispersed particles arrange themselves in such a way that the forces of attraction and repulsion acting between them are balanced.

(b) wetting theory

This theory takes into account the degree of wetting the particles.

However, it appears that each theory may have its merits for a particular suspension; and perhaps, for certain suspensions, combinations of the theories must be considered.

Pryce-Jones (26, 31) has introduced a classification which he calls "false-body". A "false-body" suspension behaves somewhat like a thixotropic one, except that a "false-body" suspension can regain its original viscosity (structure build-up) more rapidly than a thixotropic one after the shearing stress has been removed. "False-body" suspensions also differ from truly thixotropic suspensions by their high concentration and by the fact that some dispersion medium is squeezed to the surface due to the sedimentation of the dispersed particles and close packing. Some investigators (1, 32) consider the distinction between "false-body" and thixotropy as arbitrary, the two types of behavior probably being the extremes of the same general phenomenon. Commercial paints exhibit "false-body".

Voet (34) subdivides thixotropy into two types:

(a) "False-Body"

Caused by the time effect of particle agglomeration, orientation, or both.

(b) "Ferric-oxide"

Caused by minima of the potential energy function of the particles at a distance. Both time and magnitude effects may be quite large.

Voet states that from his investigations it is apparent that all plastic systems show a time effect, irrespective of whether or not plasticity originates from particle agglomeration or orientation or from both. Consequently, all plastic systems appear to be thixotropic.

One can see from the above that thixotropy has not as yet been completely defined and that no explanation of this phenomenon has been fully accepted.

Some examples of "thixotropic" materials are: ferric oxide and vanadium pentoxide sols, blood, milk, mayonnaise, greases, drilling muds, paints, inks, gypsum in water. Quartz, felspar, and glass show thixotropy in benzene but not in water (21). Voet.(34) states that quartz powder in carbon tetrachloride behaves more or less as a liquid when violently agitated, but does not flow immediately afterwards while at rest; Voet considers this system as thixotropic but some investigators differ. Mardle (21) states that thixotropy occurs especially in organic liquids of low polar character.

The brushing qualities of paints on a vertical wall are a function of thixotropy (26). The paint must have a sufficiently high viscosity to enable the paint to stay on a plane surface until dry and yet the paint must not have a too high a viscosity or the brush marks will not even out. Brushing lowers the viscosity due to thixotropy and the paint, after the brushing has stopped, sets before gravity causes any appreciable flow.

The shear diagram for a thixotropic type suspension is shown in Figure 5.

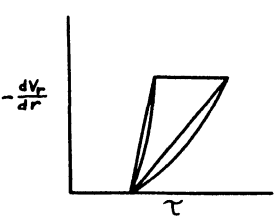


Figure 5. Shear Diagram Thixotropic Suspension

5. Rheopectic Type: By rhythmically shaking or tapping certain thixotropic suspensions, the suspensions will "set" or build-up (increase in apparent viscosity) very rapidly. This phenomenon was called "rheopexy" by Freundlich and Juliusberger (9). The name appears to be derived from Rheo (to flow) and a Greek word meaning, "solidified", "curdled".

A rheopectic material may be considered to be the opposite of a thixotropic material; that is, its apparent viscosity increases with time at any constant rate of shear.

This phenomenon has been observed with only a few thixotropic systems. No fully satisfactory reason has been given to explain rheopexy.

Some examples of rheopectic suspensions are: vanadium pentoxide and bentonite sols, gypsum in water.

Hauser and Lynn (18) give instructions for the preparation of several thixotropic, dilatant, and rheopectic sols. Note that a "sol" is a colloidal dispersion; the particle size being of the order of 0.5 to 0.001 microns.

p. 122 - line 16 from bottom of page should read:
5. Rheopectic Type: .....

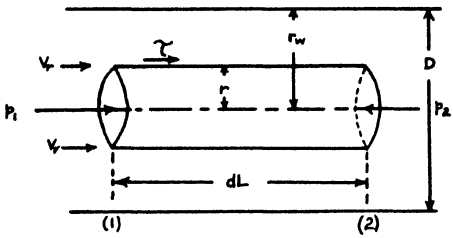


Figure 6. Flow of Bingham Plastic in a Circular Pipe

B. Flow of a Bingham Plastic through a Pipe.

The mathematical analysis of the laminar flow of a Bingham plastic in a circular pipe was first presented by Bingham (5). Caldwell and Babbitt (7) present Bingham's analysis. The analysis of Schofield (31) will be presented herewith. Schofield's analysis is of general form and reduces to Bingham's as a special case.

The following assumptions are made:

(a) each particle travels in a straight line, at a constant velocity, parallel to the axis of the tube.
(b) there is no slip at the wall.
(c) the velocity gradient at any point is a function only of the shearing stress at that point.

Referring to Figure 6, a force balance is made between sections (1) and (2),

$$(p_1 - p_2)(\pi r^2) = \pi r^2 dp = 2\pi r \tau dL \tag{2}$$

Therefore,

$$\tau = \frac{r}{2}\frac{dp}{dL} \tag{3}$$

$$\tau_w = \frac{r_w}{2}\frac{dp}{dL} = \frac{D}{4}\frac{dp}{dL} \tag{4}$$

From equations 3 and 4,

$$d\tau = \frac{1}{2}\left(\frac{dp}{dL}\right) dr$$

$$= \frac{2\tau_w}{D}\, dr \tag{5}$$

By definition,

$$\frac{dV_r}{dr} = -\left(\frac{g_c}{K}\right)\phi(\tau) \tag{6}$$

or

$$dV_r = -\left(\frac{g_c}{K}\right)\phi(\tau)\, dr \tag{6a}$$

From Equations 5 and 6a, eliminating dr,

$$dV_r = -\left|\frac{g_c D}{2K\tau_w}\right| \phi(\tau)\, d\tau \tag{7}$$

Integrating between the limits $V_r = V_\tau$ at $\tau = \tau$ and $V_r = 0$ at $\tau = \tau_w$,

$$V_\tau = \frac{g_c D}{2K\tau_w}\int_\tau^{\tau_w} \phi(\tau)\, d\tau \tag{8}$$

But,

$$dq = 2\pi r V_\tau\, dr \tag{9}$$

By substituting for V_τ from Equation 8, and for r from Equations 3, 4, and 5 and integrating between the limits q = q at $r = \frac{D}{2}$ and q = 0 at r = 0,

$$q = \frac{\pi g_c D^3}{4K\tau_w^3}\int_0^{\tau_w} \tau \int_\tau^{\tau_w} \phi(\tau)\, d\tau d\tau \tag{10}$$

and since by definition,

$$V = \frac{q}{\left(\frac{\pi D^2}{4}\right)} \tag{11}$$

Therefore,

$$\frac{V}{D} = \frac{g_c}{K\tau_w^3}\int_0^{\tau_w}\int_{\tau}^{\tau_w} \phi(\tau)\, d\tau d\tau \tag{12}$$

Equation 12 is for the general case and indicates that a plot of V/D vs τ_w should give a unique curve for a given suspension provided the three assumptions specified above are satisfied.

For a Bingham plastic, by definition, see Figure 2,

$$\phi(\tau) = \tau - \tau_y \qquad \text{for } \tau \geq \tau_y \tag{13}$$

$$\phi(\tau) = 0 \qquad \text{for } \tau < \tau_y \tag{13a}$$

$$K = \eta$$

When such a material is forced through a pipe, a central cylinder of diameter, D (τ_y/τ_w), within which the stress is less than τ_y, moves as a solid plug and only material outside this cylinder slips. Thus, in applying the definitions of $\phi(\tau)$ and η in this case, Equation 12 must be integrated in two parts. That is, the part due to the flow of the solid plug, "plug flow",

$$\int_0^{\tau_y} \tau \left[\int_0^{\tau_y} (0) d\tau + \int_{\tau_y}^{\tau_w} (\tau - \tau_y) d\tau \right] d\tau$$

and the part due to the flow of the material between the plug and the wall,

$$\int_{\tau_y}^{\tau_w} \tau \int_{\tau}^{\tau_w} (\tau - \tau_y) d\tau d\tau$$

The final equation to be integrated is,

$$\frac{V}{D} = \frac{g_c}{\eta \tau_w^3}\left[\int_0^{\tau_y} \int_y^{\tau_w} (\tau - \tau_y)\, d\tau d\tau + \int_{\tau_y}^{\tau_w} \tau \int_{\tau_y}^{\tau_w} (\tau - \tau_y)\, d\tau d\tau \right] \tag{14}$$

(Note: the equation, pg. 39, Scott Blair (31) has an incorrect lower limit on the fourth integral sign.)

The integration of Equation 14, yields,

$$\frac{V}{D} = \frac{g_c \tau_w}{8\eta}\left[1 - \frac{4}{3}\frac{\tau_y}{\tau_w} + \frac{1}{3}\left(\frac{\tau_y}{\tau_w}\right)^4 \right] \tag{15}$$

Since $(\tau_y/\tau_w)^4$ is relatively small except at large values of (τ_y/τ_w), (i.e., at small shear stresses or pressure drops), a good approximation of Equation 15 is,

$$\frac{8V}{g_c D} = \frac{1}{\eta}\left[\tau_w - \frac{4}{3}\tau_y \right] \tag{16}$$

The error in omitting the last term in Equation 15 is less than 2% when (τ_y/τ_w) is less than 0.4.

The plot of Equation 15, that is, $\frac{8V}{g_c D}$ vs τ_w is given in Figure 7. The solid curve corresponds to Equation 14 and the asymptote (dotted straight line) corresponds to Equation 16. This curve is unique for a given Bingham-type suspension.

The apparent viscosity, μ_e, can be found as follows:

Defining the apparent viscosity from Poiseuille's equation,

$$\frac{dp}{dL} = \frac{32\mu_e V}{g_c D^2} \tag{17}$$

p. 124 - Equation 14 should read:

$$\cdots\left[\int_0^{\tau_y} \tau \int_{\tau_y}^{\tau_w} \cdots + \int_{\tau_y}^{\tau_w} \tau \int_{\tau}^{\tau_w} \cdots \right]$$

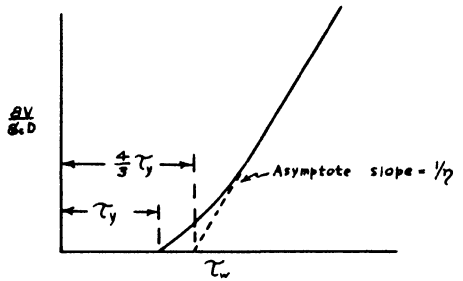


Figure 7. Shear Diagram for Flow of Bingham Plastic in a Circular Pipe

and by combining Equations 4, 16, and 17, the apparent viscosity is,

$$\mu_e = \frac{g_c \tau_y D}{6V} + \eta \qquad (18)$$

μ_e in the general case is the inverse slope of a line joining the origin and a point on the curve (Figure 7) corresponding to the τ_w in question. For the straight line portion of the curve, μ_e is given by Equation 18.

Additional discussion of the above equations will be presented in later sections.

C. Thixotropic Breakdown and its Effect Upon Viscosity

The following discussion was obtained from the papers by Green and Weltmann (12, 13, 14, 15).

In order to measure thixotropy or some characteristic of it, the material must be studied both before and after a thixotropic change in consistency has been made. The difference in consistency before and after a thixotropic change is a function of the thixotropy. If there is no difference, then there is no thixotropy, even though the material is plastic. As was mentioned previously, if an increasing rate of shear is imposed upon a thixotropic suspension, the suspension will have an increasing "thixotropic breakdown". Now if the material is then subjected to a decreasing rate of shear, no further change in the thixotropic structure will take place during the period of decreasing shear. This is the foundation for the use of the "double-consistency" curve.

A double-consistency curve, Figure 8a, is composed of "up-and-down" curves plotted on the same figure. These curves are obtained with a rotational viscometer (this will be discussed in a later topic). The loop ABCDA is called the "hysteresis loop". The curvature of the up-curve, ABC, is the result of breaking down of the structure continuously; and the linearity of the down-curve CDA indicates a temporarily stable structure. The area within the loop is an indication of the amount of thixotropy — a large loop indicating considerable thixotropy, and no loop indicating no thixotropy.

The slope of the down-curve depends upon the amount of breakdown that has taken place. The breakdown can take place by rate of shear and various down curves can be obtained depending upon from what rate of shear the down curve commenced, see Figure 8b. Breakdown can also take place with time at a constant rate of shear and another series of down curves can be obtained, see Figure 8c. With increasing time point C will move along the line BD (constant rate of shear) towards point D. After a sufficient time at a constant rate of shear, the breakdown will reach an equilibrium and no further breakdown can take place, point D in Figure 8c.

A study of the down curve for a Bingham type plastic can be made by the use of the Reiner and Riwlin equation (27). This will be discussed in more detail in a later topic.

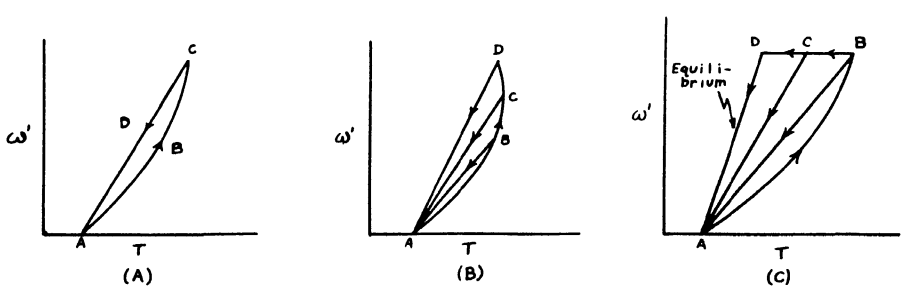


Figure 8. Thixotropic Breakdown Curves

p. 125 - Equation 18 should read:

$$\mu_e = \frac{g_c \tau_y D}{6V} + \eta$$

D. Measurement of Rheological Properties

It was indicated that the yield value, viscosity, thixotropic properties, and other desired rheological properties could be obtained from the shear diagram of the material. As the shear diagram is a plot of the rate of shear vs the shear stress, it is then only necessary to measure the rate of shear and shear stress in a suitable instrument.

The question now is what is a suitable instrument? The main requirements (from a rheological standpoint) for a suitable instrument are:

(1) the flow pattern existing must be streamline, in order to lend itself to mathematical treatment.

(2) the rate of shear must be applied in such a manner as to be able to vary it rapidly and also to be able to study the effect of time upon the shear stress at a constant rate of shear.

(3) must be able to adjust the control the temperature.

There are many various types of viscometers on the market; however, only two types fully satisfy the above requirements; they are,

(1) rotating concentric cylinders.

(2) oscillating disks

There are others that satisfy some of the requirements and can be used; only one type will be mentioned:

(1) tubes-capillary and pipes

The present discussion will be limited to rotational viscometers and tubes. Other types are discussed in many sources (example, Barr (3)), a fairly good article is the one by Green (11).

1. Rotational Viscometers

a. Theory: Rotational viscometers are composed of two concentric cylinders—outer (called the " cup"), and inner (called the "bob" or "spindle"). There are two types—one, the bob rotates and the cup remains stationary; e.g. Brookfield and Stormer; and the other, the cup rotates and the bob is stationary; e.g. Mac Michael and "Green-Weltmann".

In each case, the material under test is between the two cylinders. The torque on the bob is measured for various rates of rotation of the rotating cylinder and from these measurements a shear diagram can be obtained. It should be pointed out that rotational viscometers are suitable to evaluate flow properties of suspensions which do not settle rapidly, as the particles also tend to be thrown from the rotating cylinder due to centrifugal force.

The general equations will now be presented; followed by the specific equations for the "makes" mentioned above.

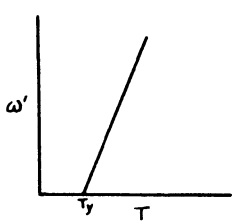


Figure 9. Shear Diagram of Bingham Plastic from Rotational Viscometer Data

The shape of the shear diagram for a Bingham type plastic obtained by plotting the rate of rotation vs. torque is shown in Figure 9. The straight portion of the curve (in the case of a thixotropic material, the down-curve) can be analyzed by the use of the Reiner-Riwlin equation (10, 28):

$$\omega = \left(\frac{T}{4\pi h\eta}\right)\left(\frac{1}{r_i^2} - \frac{1}{r_o^2}\right) - \frac{\tau_y}{\eta} \ln \frac{r_o}{r_i} \tag{19}$$

$$\eta = \frac{9.55(T - T_y)B_1}{\omega'} \tag{20}$$

$$B_1 = \left(\frac{1}{r_i^2} - \frac{1}{r_o^2}\right)/(4\pi h) \tag{21}$$

$$\tau_y = \tau_y B_2 \tag{22}$$

$$B_2 = \left(\frac{1}{r_i^2} - \frac{1}{r_o^2}\right)/(4\pi h \ln \frac{r_o}{r_i}) \tag{23}$$

where:

p. 126 - Equation 26 should read:

$$B_2 = \left(\frac{1}{r_i^2} - \frac{1}{r_o^2}\right) \Big/ \left(4\pi h \ln \frac{r_o}{r_i}\right)$$

B_1 = instrument constant, 1/cu.cm.

B_2 = instrument constant, 1/cu.cm.

h = inner cylinder (bob) height, cm.

r_i = inner cylinder radius, cm.

r_o = outer cylinder (cup) radius, cm.

T = torque, (dyne)(cm.)

T_y = torque intercept of straight line, (dyne)(cm.)

η = coefficient of rigidity, g./(cm.)(sec.)

τ_y = yield stress, dynes/sq.cm.

ω = angular velocity, rad./sec.

ω' = rate of rotation, rev./min.

The c.g.s. system of units is used as instruments are dimensioned in convenient values of centimeters and viscosity is usually given in poises. The values of τ_y and η can be converted to English units and employed with Equations 15, 16, 17, and 18. However, any consistent set of units can be used. Some convenient conversion factors are:

1 dyne = 1 (g.) (cm.)/sec.^{2}

1 g./(cm.) (sec.) = 1 poise

1 poise = 0.0672 lb./(ft.)(sec.)

1 dyne/sq.cm. = 0.00209 (lb.force)/sq.ft.

Occasionally it is desired to determine the rate of shear and shear stress at the inner cylinder wall. Under the discussion on pipe-line viscometers a method will be given to compare pipe-line results with rotational viscometer results on the basis of the rate of shear and shear stress at the wall. The derivation of the general equations for determining the rate of shear and shear stress is presented herewith.

By definition,

$$\tau = -\mu \left(\frac{dV_r}{dr} \right) \tag{24}$$

where,

$$\mu = \psi(\tau) \tag{25}$$

now,

$$\frac{dV_r}{dr} = r\frac{d\omega}{dr} \tag{26}$$

By substituting Equations 25 and 26 into Equation 24 and integrating, by noting that,

$$\tau = \frac{T}{2\pi h r^2} \tag{27}$$

where, T = constant

results in,

$$2\omega = \int_{\tau_o}^{\tau_i} \frac{d\tau}{\psi(\tau)} \tag{28}$$

and,

$$2\frac{\delta\omega}{\delta T} = \frac{\delta}{\delta T}\int_{\tau_o}^{\tau_i} \frac{d\tau}{\psi(\tau)} \tag{29}$$

$$= \int_{\tau_o}^{\tau_i} \frac{\partial}{\partial T}\left[\frac{1}{\psi(\tau)}\right] d\tau - \frac{1}{\psi(\tau_o)}\frac{\partial \tau_o}{\partial T} + \frac{1}{\psi(\tau_i)}\frac{\partial \tau_i}{\partial T} \tag{29a}$$

p.127 - Equation 29 should read:

$$2\frac{\partial \omega}{\partial T} = \frac{\partial}{\partial T}\int_{\tau_o}^{\tau_i} \frac{d\tau}{\tau(\tau)}$$

$$2\frac{\partial \omega}{\partial T} = -\frac{1}{\psi(\tau_o)}\frac{1}{2\pi h r_o^2} + \frac{1}{\psi(\tau_i)}\frac{1}{2\pi h r_i^2} \tag{30}$$

or by substituting Equation 25 into Equation 30,

$$2\frac{\partial \omega}{\partial T} = \frac{1}{2\pi h r_i^2}\left[\frac{1}{\mu_i} - \left(\frac{r_i}{r_o}\right)^2 \frac{1}{\mu_o}\right] \tag{30a}$$

and by substitution of Equation 27 into Equation 30a,

$$2\left(\frac{d\omega}{d\tau_i}\right) = \frac{1}{\mu_i}\left[1 - \left(\frac{r_i}{r_o}\right)^2 \frac{\mu_i}{\mu_o}\right] \tag{31}$$

Equation 31 is the general relation for rotational viscometers consisting of concentric cylinders.

Assuming that, (see reference 25),

$$\mu = k_1 \tau^{-n'} \tag{32}$$

and from Equation 27,

$$\frac{\mu_i}{\mu_o} = \left(\frac{\tau_o}{\tau_i}\right)^{n'} = \left(\frac{r_i}{r_o}\right)^{2n'} \tag{33}$$

now,

$$\mu = \frac{\tau}{2\omega}\left[1 - \left(\frac{r_i}{r_o}\right)^2\right] \tag{34}$$

from Equation 32 and 34,

$$\tau = k_2 \omega^{1/1 + n'} \tag{35}$$

let,

$$n = 1 + n' \tag{36}$$

from Equations 31, 33, and 36,

$$2\left(\frac{d\omega}{d\tau_i}\right) = \frac{1}{\mu_i}\left[1 - \left(\frac{r_i}{r_o}\right)^{2n}\right] \tag{37}$$

or,

$$\mu_i = \frac{1}{2}\left(\frac{d\tau_i}{d\omega}\right)\left[1 - \left(\frac{r_i}{r_o}\right)^{2n}\right] \quad \text{(c.g.s. units)} \tag{37a}$$

and from Equations 35 and 36,

$$n = \frac{d(\log \omega)}{d(\log \tau)} \tag{38}$$

n is the slope of the straight portion of the curve of the plot of log ω vs. log τ.

In addition to the symbols defined following Equation 23, there are (using c.g.s. units):

k_1 = a proportionality constant

k_2 = a proportionality constant

n = exponent, a constant

n' = exponent, a constant

r = a radius, cm.

V_r = velocity at radius r, cm./sec.

(dV_r/dr) = rate of shear, 1/sec.

μ = apparent viscosity, g./(cm.)(sec.)

μ_1 = apparent viscosity at the inner cylinder wall, g./(cm.)(sec.)

μ_o = apparent viscosity at the outer cylinder wall, g./(cm.)(sec.)

τ = shear stress, dynes/sq.cm.

τ_1 = shear stress at the inner cylinder wall, dynes/sq.cm.

τ_o = shear stress at the outer cylinder wall, dynes/sq.cm.

ψ = a function.

The rate of shear at the inner cylinder wall can be then computed as follows,

$$-\left(\frac{dV_r}{dr}\right)_1 = \frac{\tau_1}{\mu_1} \quad \text{(c.g.s. units)} \tag{39}$$

Notes: a) Equations 32, 35, and 38 apply in many cases.

b) In determining μ_1 from Equation 37a, the term $(d\tau_1/d\omega)$ can be determined by measuring the slope of the curve of τ_1 vs ω at values of τ_1.

b. Commercial Types

(1) Mac Michael (sold by Eimer and Amend): The cup rotates and the bob is stationary. The torque on the bob (inner cylinder) is measured by determining the amount of twist on a torsion wire attached to the bob. The amount of twist is measured in degrees MacMichael where one degree MacMichael = 1/300 of a circle. The cup can be rotated at various speeds. This voscometer is one of the best to study non-Newtonian liquids and suspensions.

The shear stress at the inner cylinder wall is computed as follows:

$$\tau_1 = \frac{T}{2\pi h r_1^2} \tag{40}$$

$$T = k\,\theta_m \tag{41}$$

where:

θ_m = torsion wire deflection, radians

k = torsional constant, (dyne)(cm.)/radian

Equations 19 to 39, inclusive, apply.

(2) "Green-Weltmann" Concentric Cylinder Viscometer (sold by Precision Scientific Co.): This viscometer was developed by Green and Weltmann (10) of the Interchemical Corporation, New York City. It is similar to the MacMichael, except that the torque is measured by the twist of a helical spring instead of a wire. A recorder has been developed (36) that enables the instrument to automatically record the deflection for various speeds and thus the consistency curves can be obtained rapidly.

(3) Brookfield "Synchro-Lectric" (sold by Brookfield Engineering Laboratories): For this instrument, the torque on the rotating spindle is measured by a calibrated spring. The scale is graduated from 0 to 100 and a calibration is given for each spindle. The calibration is given directly in poises; however, this is the viscosity of a Newtonian material that would give the same scale reading. Only four different rates of shear can be obtained.

This instrument, though not as flexible as the MacMichael, provides a quick means of determining the presence and extent of the various rheological properties.

In the actual use of this instrument, the "cup" consists merely of a large beaker. Thus, $\frac{r_1}{r_o} \cong 0$.

The rate of shear, shear stress, and viscosity, all at the inner cylinder (spindle) wall, are the only values that can be directly computed. Substituting Equation 26 into Equation 24 and integrating,

$$T = 4\mu_B \pi h r_1^2 \omega \tag{42}$$

where: μ_B = instrument calibration viscosity (Newtonian viscosity for the reading), g./(cm.)(sec.)

From Equation 27,

p. 129 - line 16 from top of page should read:
"...This viscometer is ..."

$$\tau_1 = \frac{T}{2\pi h r_1^2} \tag{43}$$

and from Equation 37a for $\frac{r_1}{r_0} \cong 0$,

$$\mu_1 = \frac{1}{2}\left(\frac{d\tau_1}{d\omega}\right) \tag{44}$$

The rate of shear at the inner cylinder (spindle) wall is obtained from Equation 39.

(4) Stormer (sold by Arthur H. Thomas Co.): In this viscometer the inner cylinder rotates and the cup is stationary. The inner cylinder is rotated by a falling weight; thus for each rotational speed the weights must be changed. The rotational speed is determined by measuring the time required for a definite number of revolutions. The weight and radius of the pulley gives the torque.

The obtaining of rheological properties with this instrument is very time consuming and tedious. This instrument is not suitable for the study of Thixotropy.

c. Miscellaneous Notes on Rotational Viscometers

a) The end-effect (effect of the bottom of the inner cylinder) in rotational viscometers is discussed by Lindsley and Fischer (20). They found that virtually the same traction is exerted at the bottom of a open and closed bob. The effect of the bottom of the bob is greater than the top. The end effect decreases with viscosity and increases with clearance. Trapping air beneath the bob is not effective in reducing the end effect.

b) Weltmann (37) discusses the effects of the initial oscillation of the bob (where the bob is stationary and the cup rotates) upon the reheological measurements. One of the general recommendations is that the system should be slightly over damped.

c) Weltmann (38) presents data on the temperature increase at the bob wall for various bob materials and rates of shear in a rotational viscometer.

2. Tubes

Tubes such as capillaries and pipes can be used as viscometers. Several investigators (4, 7, 42) have used tubes to study the rheological properties of materials.

The equipment consists of a length of tubing with either a blow-case or a pump to force the material through the tube. The pressure drop across the tube is measured for various rates of flow. Several tube sizes are used in order to determine the scale-up factor if any and also to determine if thixotropy exists.

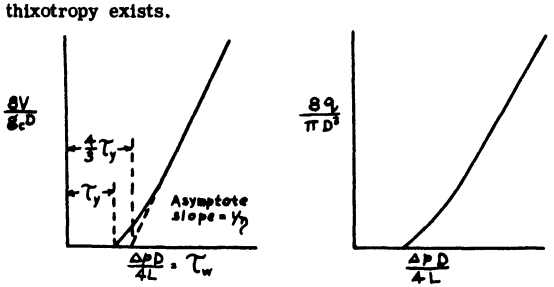


Figure 10. Shear Diagram of Bingham Plastic from Pipe-line Data

It should be pointed out that if a material is thixotropic, it is preferable to use a blow-case since a pump (gear or centrifugal) will break the material down before the material flows through the pipe.

Figures 10a and 10b show the two methods of plotting the shear diagram. Figure 11 shows the effect of increasing the tube diameter and of increasing the tube length for a thixotropic material.

The shear diagram as plotted in Figure 10a is really a plot of Equation 15, From Figure 10a the value of η and τ_y can be obtained and used in Equation 18 for the apparent viscosity. A single curve is obtained for all tube sizes except if the material is thixotropic. If the material is thixotropic, i.e. a shear diagram similar to Figure 11, the value of η will be different for each tube size and a scale-up factor must be used in designing a plant size pipe-line.

Rabinowitsch (27) developed an expression for the rate of shear at the pipe wall regardless of the form of the flow curve. Mooney (23) later showed how the expression could be applied to pipe-line data. The expression is,

$$-\left(\frac{dV_r}{dr}\right)_w = 3\left(\frac{8q}{\pi D^3}\right) + \left(\frac{\Delta pD}{4L}\right)\frac{d\left(\frac{8q}{\pi D^3}\right)}{d\left(\frac{\Delta pD}{4L}\right)} \tag{45}$$

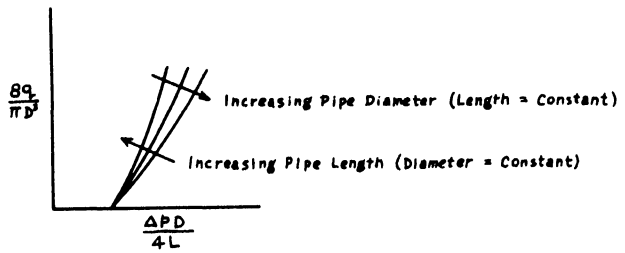


Figure 11. Shear Diagram of Thixotropic Suspension Showing Effect of Pipe Diameter and Length

As can be seen, the rate of shear at the pipe wall, $-\left(\frac{dV_r}{dr}\right)_w$, can be obtained by using Figure 10b with Equation 45. The slope of the curve, Figure 10b, at any point is $d\left(\frac{8q}{\pi D^3}\right)/d\left(\frac{\Delta pD}{4L}\right)$

In the next topic use will be made of Equation 45 in comparing rotational viscometer data with pipe-line data.

E. Comparison of Rotational Viscometer Data with Pipe-Line Data.

Rotational viscometer data can be compared with pipe-line data by plotting $-(dV_r/dr)_i$ and $-(dV_r/dr)_w$ vs. τ_i and τ_w on logarithmic paper. Note that $\tau_w = (\Delta pD)/4L$ and that $-(dV_r/dr)_i$ is determined from Equation 39 for rotational viscometers and $-(dV_r/dr)_w$ is determined from Equation 45 for pipe-line data. The units of both τ_i and τ_w are (lb.force/sq.ft.).

Figure 12 shows the type of plot (25) that results from the above correlation for a pseudoplastic suspension. The correlation is very good if the material is not thixotropic. The lower portion of the curve approaches an asymptote since the apparent viscosity at zero rate of shear, μ_s, is constant. Flow in large pipes fall in this region. The central portion ("curved") of the curve is the region where rotational viscometer and small pipe-line data fall. The upper portion of the curve approaches an asymptote since the apparent viscosity at very high rates of shear, μ_∞, is constant. Data from very small pipes and from capillary tubes fall in this region. The lower portion of the curve does not exist for Bingham type plastic suspensions.

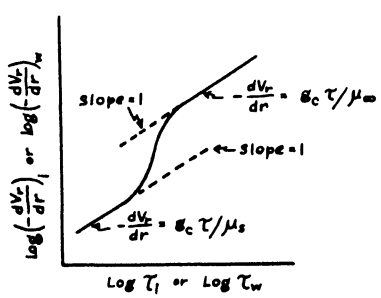


Figure 12. Shear Diagram of Pseudoplastic Suspension on Logarithmic Plot

This means that if the rate of shear at the inner cylinder wall of a rotational viscometer is the same as the rate of shear at the pipe wall for a pipe-line, the shear stress is the same in both. Therefore, this affords a convenient method of designing large pipe-lines for the flow of non-Newtonian fluids that are not thixotropic. Brookfield, MacMichael, or similar rotational viscometer data can be obtained of the suspension in question and the rate of shear, $-(dV_r/dr)_i$ vs. the shear stress, τ_i, can be plotted on arithmetic coordinates. The equation of this curve can be obtained, that is,

$$-\left(\frac{dV_r}{dr}\right)_i = \psi\left(\tau_i\right) \tag{46}$$

Generally an equation of the parabolic type will fit the curve. Equation 46 can then be substituted into Equation 45; obtaining,

$$\psi\left(\frac{\Delta pD}{4L}\right) = 3\left(\frac{8q}{\pi D^3}\right) + \left(\frac{\Delta pD}{4L}\right)\frac{d\left(\frac{8q}{\pi D^3}\right)}{d\left(\frac{\Delta pD}{4L}\right)} \tag{47}$$

Equation 47 can then be integrated.

The apparent viscosity can be computed from Equation 17,

$$\mu_e = \frac{\tau_w g_c D}{8V} = \tau_w \left(\frac{g_c}{4}\right)\left(\frac{\pi D^3}{8q}\right) \qquad (48)$$

$$\text{where, } \tau_w = \frac{\Delta p D}{4L}$$

and therefore, from the integrated form of Equation 47 and with Equation 48, the apparent viscosity can be determined. Equation 48 is essentially another form of Poiseuille's equation.

It should be pointed out that the above discussion and correlations apply only to viscous flow. The flow is considered turbulent if the Reynolds Number is 2100 or greater. In large pipe-lines the rate of shear or shear stress does not have to be very large to have turbulent flow. The Reynolds Number is computed as follows,

$$N_{Re} = \frac{VD\rho_m}{\mu_e} \qquad (49)$$

VI. TURBULENT FLOW OF NON-NEWTONIAN LIQUIDS AND SUSPENSIONS.

The shear diagram for the turbulent flow of a Bingham type plastic is shown in Figure 13. The lower part of the curve ("dotted") is for viscous flow and is the same as in Figure 10b. The upper part of the curve ("solid") is for turbulent flow and it is noted that this portion of the curve branches off somewhat sharply from the remainder of the curve. The branch-off point occurs at lower values of the rate of shear as the diameter of the pipe increases. It is somewhat difficult to distinguish turbulent flow from dilatancy as can be seen by comparing Figure 13 with Figure 4.

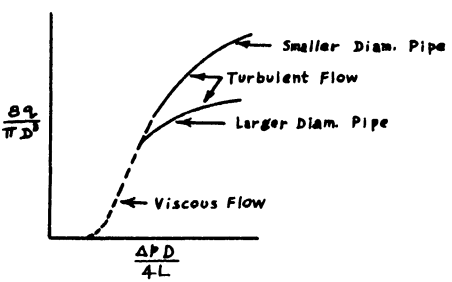


Figure 13. Shear Diagram of Bingham Plastic for Viscous and Turbulent Flows

From tests on various suspensions, it has been shown that the apparent viscosity of the suspension in turbulent flow, determined from the friction factor-Reynolds Number curve, see Fig. 6 p. 811 Perry (24), is constant for all rates of shear.

Caldwell and Babbitt (7) report that from their tests of clay and sewage suspensions acting as Bingham plastics the usual friction factor plots can be used provided the viscosity of the fluid medium and the density of the slurry is used. The pressure drop was found to be independent of yield stress and coefficient of rigidity. Wilhelm, et al (39) found that for the cement rock suspensions tested, apparent viscosities higher than that of the dispersion medium must be used. Binder and Busher (4) present data on grain suspensions, the apparent viscosities were greater than that of the dispersion medium. The difference in all of these tests is probably due to concentration or particle size, or both. In some unpublished work on lime and titanium dioxide slurries, it was found that the apparent viscosities for turbulent flow are constant for all rates of shear and are from a few times to several times as great as the viscosity of the dispersion medium.

Winding, et al (42) present a very interesting discussion of the tests and results of the viscosities of GR-S latices. In turbulent flow they obtained a very good correlation by using the limiting viscosity at infinite shear, μ_∞, in the computation of the Reynolds Number.

If tests can not be made of the suspension in question in turbulent flow, it is recommended that for Bingham type plastics the coefficient of rigidity, η, and for pseudoplastics the limiting viscosity at infinite rate of shear, μ_∞, be used for the apparent viscosity. The coefficient of rigidity or the limiting viscosity at infinite rate of shear can be determined by the methods discussed in the previous sections. The friction factor vs Reynolds Number plot can be used; where the coefficient of rigidity or the limiting of viscosity at infinite rate of shear and density of the suspension are used in the Reynolds Number. The pressure drops computed in this manner will probably be within ±50%.

VII. DISPERSING AGENTS

Only a brief discussion of dispersing agents will be presented.

p. 132 - line 20 from top of page should read:
"...see Fig. 23 p. 382 Perry (24), ..."

Dispersing agents have various effects upon a suspension. Sheets (33) found that with coating-clay suspensions, sodium pyrophosphate will decrease the viscosity then increase the viscosity as the concentration of the sodium pyrophosphate is increased. When the concentration of the agent is a little less than that required to give minimum viscosity the suspension is thixotropic. Sodium silicate has the same effect upon the viscosity of these clay suspensions and in concentrations greater than that for minimum viscosity, it enhances the dilatant tendencies of the suspension. Kennedy (19) presents curves showing the effect of various dispersing agents on bentonite clay drilling muds. The dispersing agents reported upon are: sodium pyrophosphate, sodium chloride, sodium hydroxide, sodium oleate, calcium chloride, gum ghatti, and tannates. With sodium oleate, the viscosity increased with increasing concentration of agent. With sodium chloride and calcium chloride, the viscosity increased and then decreased with increasing concentration of agent. With gum ghatti and tannates, the viscosity decreased and then increased with increasing concentration of agent. With sodium pyrophosphate, the viscosity decreased with increasing concentrations of agent. The maximum concentration of agent studied was about 1% by weight of total solids.

VIII. PROBLEMS

1. The following experimental data were obtained with a slurry of density = 72.5 lb./cu.ft. flowing through a 10-ft. horizontal section of 0.255-in. i.d. stainless steel pipe,

Rate of Flow $q \times 10^5$ cu.ft./sec.	Pressure Drop Δp lb.force/sq.in.
0	3.9
18.7	5.2
37.4	6.11
93.5	7.15
224	9.75
374	12.75
430	14.3
486	18.2
655	33.5
935	59.2

From the above data determine:

a. The coefficient of rigidity

b. The equation for the apparent viscosity as a function of the velocity and of the diameter of the pipe (for viscous flow).

c. The shear stress at the wall as a function of the rate of shear at the wall (for viscous flow). Plot the results on logarithmic paper.

2. From the data and results of Problem 1, compute the pressure drop for the flow of the same slurry as in Problem 1 at a rate of 2 g.p.m. through 20-ft. of horizontal 0.500-in. i.d. stainless steel pipe.

Chapter 8

FLUID METERING

by

Donald F. Boucher
Engineering Research Laboratory
Engineering Department
E. I. du Pont de Nemours & Co., Inc.
Wilmington, Delaware

TABLE OF CONTENTS

	Page
I. References	138
II. Nomenclature	139
III. Introduction	140
IV. Head Meters	141
A. General Principles	141
B. Venturi Meter	141
1. Structural Details	141
2. Flow Equations	142
3. Flow of Gases	142
4. Flow of Liquids	143
5. Accuracy	143
6. Permanent Pressure Drop	143
C. Flow Nozzles	143
1. Structural Details	143
2. Flow Equations	144
3. Accuracy	144
4. Permanent Pressure Drop	144
5. Critical Flow Nozzle	144
D. Orifice Meters	145
1. Structural Details	145
a. Corner Taps	145
b. Radius Taps	145
c. Pipe Taps	145
d. Flange Taps	145
e. Vena Contracta Taps	145
2. Flow Equations	145

3. Concentric Circular Orifices 146
4. Orifice Nomograph 146
5. Segmental Orifice 148
6. Annular Orifices 148
7. Permanent Pressure Drop 148

V. Pitot Tube 149
A. Principle of Operation 149
B. Structural Details 149
C. Flow Equations 149
D. Traversing for Mean Velocity 149
E. Direction Indicators 150

VI. Rotameters 150
A. Principle of Operation. 150
B. Flow Measurement Theory 150
C. Structural Details 151
D. Permanent Pressure Drop 152
E. References 152

VII. Pulsating Flow 152

VIII. Vane Anemometer 153

IX. Hot-Wire Anemometers 156

X. Weirs 156
A. General Principles 156
B. Rectangular Sharp-Crested Weir. 157
C. Triangular-Notch Weir 158
D. Cipolletti Weir 158
E. Other Types of Weirs. 158

XI. Problems 158

LIST OF FIGURES

Figure 1. Venturi Meter 142
Figure 2. Flow Nozzle 144
Figure 3. Flow Nozzle Contour. Low β Series 144
Figure 4. Flow Nozzle Contour. High β Series 144
Figure 5. Orifice Meter 145
Figure 6. Orifice Discharge Coefficient 146
Figure 7. Orifice Nomograph 147
Figure 8. Annular Orifice 148
Figure 9. Pitot Tube 149
Figure 10. Typical Rotameter Float Shapes 152
Figure 11. Pulsating Flow—Metering Error Chart—Simplex Double-Acting Compressor 154
Figure 12. Pulsating Flow—Metering Error Chart—Duplex Double-Acting Compressor. 155
Figure 13. Pulsating Flow—Metering Error Chart—Triplex Double-Acting Compressor 155

Figure 14. Rectangular Sharp-Edged Weir 157
Figure 15. Triangular-Notch Weir 158
Figure 16. Cipolletti-Notch Weir 158
Figure 17. Problem 2 159

LIST OF TABLES

Table I Classification of Fluid Meters 140
Table II Size of Pressure Tap Holes 142
Table III Location of Vena Contracta Downstream Tap—Concentric Circular Orifice 146
Table IV Discharge Coefficients for Segmental Orifices—Flange Taps 148

I. REFERENCES

A. General References

1. Am. Soc. Mech. Engrs. Research Publication, "Fluid Meters - Description of Meters," Part 2, 1931.
2. Am. Soc. Mech. Engrs. Research Publication, "Fluid Meters - Their Selection and Installation," Part 3, 1933
3. Am. Soc. Mech. Engrs. Research Publication, "Fluid Meters - Their Theory and Application," Part 1, 4th Ed., 1937
4. Am. Soc. Mech. Engrs. Power Test Codes, Part 5 - "Measurement of Quantity of Materials," Chapt. 4 - "Flow Measurement by Means of Standardized Nozzles and Orifice Plates," 1940.
5. Eason, A. B., "Flow and Measurement of Air and Gases," 2nd Ed., London, Chas. Griffin & Co., 1930.
6. Gibson, A. H., "Hydraulics and Its Applications," 3rd Ed., London, Constable & Co., 1925.
7. King, H. W., "Handbook of Hydraulics," 2nd Ed., New York, McGraw-Hill Book Co., 1929.
8. Ower, E., "Measurement of Air Flow," 2nd Ed., London, Chapman & Hall, 1933.
9. Pannell, J. R., "The Measurement of Fluid Velocity and Pressure," 1st Ed., London, Ed. Arnold & Co., 1924.
10. Perry, J. H., "Chemical Engineers' Handbook," 3rd Ed., New York, McGraw-Hill Book Co., 1950.
11. Rhodes, T. J., "Industrial Instruments for Measurement and Control," 1st Ed., New York, McGraw-Hill Book Co., 1941.
12. Schoder, E. W., and Dawson, F. M., "Hydraulics," 2nd Ed., New York, McGraw-Hill Book Co., 1934.

B. Specific References

13. Bean, H. S., Beitler, S. R., and Sprenkle, R. E., "Discharge Coefficients of Long-Radius Flow Nozzles when Used with Pipe-Wall Pressure Taps," Trans. Am. Soc. Mech. Engrs., 63, 439-46 (1941) July.
14. Bean, H. S., Buckingham, E., and Murphy, P. S., "Discharge Coefficients of Square-Edged Orifices for Measuring the Flow of Air," Bur. Stand. J. Res., 2, 561-658 (1929).
15. Eckert, B., "Experiences with Flow-Direction Instruments," N.A.C.A. Tech. Memo. No. 969, 1941; taken from Jahrbuch 1938 der Deutschen Luftfahrtforschung, pp. II 381-6.
16. Fischer, K., "The Rotameter and Petroleum Refinery Flow Rate Measurement," Pet. Refiner, 26, 30-6 (1947) Jan.
17. Hamilton, W. S., "A Direction-Indicating Velocity Tube," Civil Eng., 16, 265-7 (1946).
18. Herning, F., and Schmid, C., "Durchflussmessung bei pulsierender Strömung," Zeit. Ver. deut. Ing., 82, 1107-14 (1938).
19. Hodgson, J. L., "The Laws of Similarity for Orifice and Nozzle Flows," Trans. Am. Soc. Mech. Engrs., 51, 303-32 (1929).
20. Howell, A. R., "Note on R.A.E. Annular Airflow Orifice," Great Britian, Aero. Res. Comm. Reports and Memoranda No. 1934 (1939) Nov.
21. King, L. V., "On the Convection of Heat from Small Cylinders in a Stream of Fluid: Determination of the Convection Constants of Small Platinum Wires with Applications to Hot-Wire Anemometry," Trans. Roy. Soc. (London), A214, 373-432 (1914).
22. Lindahl, E. J., "Pulsation and Its Effect on Flow-meters," Trans. Am. Soc. Mech. Engrs., 68, 883-94 (1946) Nov.
23. Lohmann, H., "Segmental Orifices for the Measurement of Fluids in Closed Pipes," Archiv. fur Technische Messen, 90, T155-6 (1938) Dec.
24. Pardoe, W. S., "The Effect of Installation on the Coefficients of Venturi Meters," Trans. Amer. Soc. Mech. Engrs., 65, 337-49 (1943) May.
25. Piret, E. L., James, W., and Stacey, M., "Heat Transmission from Fine Wires to Water," Ind. Eng. Chem., 39, 1098-1103 (1947).
26. Rayleigh, "Aerial Plane Waves of Finite Amplitude," Proc. Roy. Soc. (London), A84, 247-84 (1911).
27. Schoenborn, E. M., and Colburn, A. P., "The Flow Mechanism and Performance of the Rotameter," Trans. Amer. Inst. Chem. Engrs., 35, 359-89 (1939).
28. Schmid, C., "Messfehler bei der Durchflussmessung pulsierender Gasströme," Zeit. Ver. deut. Ing., 84, 596-8 (1940).

29. Sprenkle, R. E., "Piping Arrangements for Acceptable Flowmeter Accuracy," Trans. Amer. Soc. Mech. Engrs., 67, 345-60 (1945) July.
30. Weske, J. R., "Methods of Measurement of High Air Velocities by the Hot-Wire Method," N.A.C.A. Tech. Note No. 880, Feb. 1943.
31. Weske, J. R., "Measurement of the Arithmetic Mean Velocity of a Pulsating Flow of High Velocity by the Hot-Wire Method," N.A.C.A. Tech. Note No. 990, April 1946.
32. Weske, J. R., "A Hot-Wire Circuit with Very Small Time Lag," N.A.C.A. Tech. Note No. 881, Feb. 1943.

II. NOMENCLATURE

Any consistent system of units may be employed. The English system is given by way of example.

A = cross-sectional area, sq.ft.

A_f = projected cross-section of rotameter float perpendicular to flow, sq.ft.

c_v = specific heat at constant volume, B.t.u./(lb.)(°F.)

c_p = specific heat at constant pressure, B.t.u./(lb.)(°F.)

C = discharge coefficient, dimensionless

d = differential operator

D = inside diameter, ft.

D_d = diameter of disk-shaped core in annular orifice, ft.

D_e = equivalent diameter, ft.

g_c = conversion factor, 32.17 (ft.)(lb.)/(lb.force)(sec.)^2

g_L = local acceleration due to gravity, ft./(sec.)^2

h = height of liquid level above crest of weir, ft. of fluid

k = ratio of specific heats, c_p/c_v, dimensionless

L = weir length, ft.

n = pulsation frequency, 1/sec.

N_{Re} = Reynolds number, dimensionless

p = pressure, lb.force/sq.ft. abs.

p_i = pitot tube impact pressure, lb. force/sq.ft. abs.

p_s = pressure in surge chamber, lb. force/sq.ft. abs.

q = volume flow rate, cu.ft./sec., based on the pressure in the surge chamber

Q = volume of surge chamber and connecting pipe in pulsating flow installation, cu.ft.

t = time, sec.

T = absolute temperature, °R. = °F. + 460

U = dimensionless grouping

v = specific volume, cu.ft./lb.

v_f = volume of rotameter float, cu.ft.

V = linear velocity, ft./sec.

w = weight rate of flow, lb./sec.

Y_o = expansion factor, dimensionless

Z = elevation, ft.

α = fractional open area (ratio of aperture cross-sectional area to pipe cross-sectional area), dimensionless

β = diameter ratio, dimensionless

γ = a coefficient, dimensionless

Δp_s = permanent pressure drop between metering element and the surge chamber, lb.force/sq.ft.

ρ = fluid density, lb./cu.ft.

ρ_f = rotameter float density, lb./cu.ft.

μ = fluid viscosity, lb./(sec.)(sq.ft.) = centipoises/1488

Subscripts

Where subscripts have been used above, they are unique and integral with the specific symbol. The following subscripts are general and may be used with any symbol.

0 = corresponding to point 0
1 = corresponding to point 1
3 = corresponding to point 3
4 = corresponding to point 4
a = refers to aperture
av = average
A = pertaining to fluid A
B = pertaining to fluid B
c = corresponding to critical flow conditions
max. = maximum

III. INTRODUCTION

Flowmeters can be divided into two functional groups. One of these measures primarily quantity of flow while the other measures primarily rate of flow. All fluid meters are made up of two distinct parts: a primary actuating element, and a secondary indicating or recording element. The former is in direct contact with the fluid and is acted on by the fluid, while the latter translates the action of the primary element into volumes, weights, or rates of flow. For example, an orifice meter will have an orifice plate and adjacent piping, flanges, and pressure taps for the primary element, while the secondary element will be a differential pressure gage possibly together with some mechanism for translating the pressure difference into rate of flow and indicating or recording the result.

The primary elements depend for their operation upon a few relatively simple principles. The design, conditions for installation, accuracy, and other characteristics of the primary element are usually altogether independent of the secondary element so that the two can be treated separately. The treatment from here on will be confined almost exclusively to the primary elements of fluid meters.

The following table gives a classification of metering equipment, and was taken in part from the A.S.M.E. Research Report on Fluid Meters (3), p. 8.

TABLE I

CLASSIFICATION OF FLUID METERS

Division	Class		Type
1. Quantity Meters	Weighing		Weighers Tilting Traps
	Volumetric		(Tank
		Liquids	(Reciprocating Piston (Nutating Disk (Lobed Impeller- Rotary
		Gases	(Bellows (Wet Gas Meter

(Continued on Next Page.)

TABLE I - CONTINUED

CLASSIFICATION OF FLUID METERS

Division	Class	Type
2. Rate Meters	Head	Venturi Flow Nozzle Orifice Plate Concentric Eccentric Segmental Venturi Segment
	Kinetic	Pitot Tube Elbow (Centrifugal)
	Area	Gate Orifice and Plug Cylinder and Plunger Rotameter
	Head-Area	Weirs Flumes
	Force	Hydrometric Pendulum Vane
	Velocity Open Channel	(Propeller (Cup
	Closed Channel	(Turbine (Propeller (Helical
	Thermal	Electric Hot-Wire Anemometer
	Special	Mixtures Salt Velocity Electromagnetic

The flow meters which are discussed in detail in the following sections are mainly those whose performance can be predicted on the basis of established basic principles of fluid mechanics.

IV. HEAD METERS

A. General Principles

If a constriction is placed in a channel carrying a steady stream of fluid, there will be an increase in the velocity and hence an increase in kinetic energy at the constriction. From an energy balance, it follows that there must be a corresponding reduction in pressure at the constriction. The discharge rate can be calculated knowing this pressure reduction, the area of the constriction, and the coefficient of discharge. Meters which operate on this principle are generally known as head meters.

B. Venturi Meter

1. Structural Details

The constriction in a venturi meter consists of a short length of straight tubing connected at either end to the pipe line by conical sections (see Figure 1). The inlet cone generally has an included angle of 25 to 30°, while the discharge cone included angle is generally between 5 and 7°. The throat section is about one-half throat diameter in length. The pressure differential is taken between a point located one-half to one pipe diameter upstream from the inlet cone and the mid-point of the venturi throat. Either a single pressure tap at each location or a piezometer ring may be used. The pressure tap holes should be large enough to avoid plugging and small enough to avoid flow disturbances. Table II will serve as a guide for the upper limit.

TABLE II

SIZE OF PRESSURE TAP HOLES

Pipe I.D., in.	Max. Hole Diameter, in.
2	1/4
3	3/8
over 4	1/2

The straight and conical sections should be joined by smooth curved surfaces. Small venturis (2-in. pipe or smaller) are commonly made of brass or bronze and machine finished on the inside. Large venturis are usually of cast iron, the throat sometimes being lined with brass or bronze. Fabricated sheet metal venturis are satisfactory but should be carefully made to avoid obstructions and sharp corners.

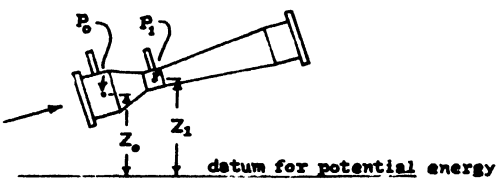


Figure 1. Venturi Meter

2. Flow Equations

The equation for the flow through a venturi meter can be derived from an energy balance between points 0 and 1.

$$\int_o^1 v\,dp + (Z_1 - Z_o)\, g_L/g_c + (V_1^2 - V_o^2)/2g_c = 0 \quad (1)$$

3. Flow of Gases

Adiabatic, frictionless flow of a perfect gas can be assumed, whence:

$$p\,v^k = \text{constant} \quad (2)$$

$$v = p_o^{1/k} v_o / p^{1/k} \quad (3)$$

Neglecting $(Z_1 - Z_o)$ and combining Equations 1 and 3 gives

$$\sqrt{V_1^2 - V_o^2} = \sqrt{\frac{2g_c\,k}{k-1}\, p_o\, v_o \left[1 - \left(\frac{p_1}{p_o}\right)^{(k-1)/k}\right]} \quad (4)$$

From the equation of continuity

$$\rho_o\, V_o\, A_o = \rho_1\, V_1\, A_a \quad (5)$$

$$V_o^2 = \left(\frac{\rho_1\, V_1\, A_a}{\rho_o\, A_o}\right)^2 = V_1^2 \left(\frac{A_a}{A_o}\right)^2 \left(\frac{p_1}{p_o}\right)^{2/k} \quad (6)$$

Combining Equations 4 and 6 gives

$$V_1 = \sqrt{\frac{\frac{2\,g_c\,k}{k-1}\, p_o\, v_o \left[1 - \left(\frac{p_1}{p_o}\right)^{(k-1)/k}\right]}{1 - \left(\frac{A_a}{A_o}\right)^2 \left(\frac{p_1}{p_o}\right)^{2/k}}} \quad (7)$$

The weight rate of flow is given by

$$w = \rho_1\, V_1\, A_a = \rho_o\, V_1\, A_a \left(\frac{p_1}{p_o}\right)^{1/k} \quad (8)$$

Combining Equations 7 and 8 and incorporating a discharge coefficient, C, gives

$$w = CA_a \sqrt{\frac{\frac{2\,g_c k}{k-1}\frac{p_o}{v_o}\left[\left(\frac{p_1}{p_o}\right)^{2/k} - \left(\frac{p_1}{p_o}\right)^{(k+1)/k}\right]}{1 - (\alpha^2)\left(\frac{p_1}{p_o}\right)^{2/k}}} \tag{9}$$

The practical equation for the weight rate of flow through a venturi meter adopted by the A.S.M.E. Special Research Committee on fluid meters is as follows:

$$w = C\,Y_o\,A_a \sqrt{\frac{2\,g_c\,(p_o - p_1)\,\rho_o}{1 - \alpha^2}} \tag{10}$$

The adiabatic expansion factor for a venturi can be obtained from a comparison of Equations 9 and 10.

$$Y_o = \sqrt{\left(\frac{p_1}{p_o}\right)^{2/k}\left(\frac{k}{k-1}\right)\left(\frac{1 - (p_1/p_o)^{(k-1)/k}}{1 - (p_1/p_o)}\right)\left(\frac{1 - \alpha^2}{1 - \alpha^2(p_1/p_o)^{2/k}}\right)} \tag{11}$$

This factor makes allowance for the fact that the density of the gas changes as it passes through the venturi meter due to the change in pressure and temperature. Values of Y_o can be conveniently obtained from the chart given by Perry (10) on p. 403.

The value of the discharge coefficient, C, for a venturi meter depends upon the Reynolds number and to a minor extent upon the size of the venturi, being higher the larger the venturi. A value of 0.98 is a good average for a well made venturi tube for Reynolds numbers (based on the throat velocity and diameter) greater than 10,000. For additional details see Reference (3), Chapter C-2, p. 99.

It can be shown that if ρ_1 is employed in place of ρ_o in Equation 10, then Y_o can be taken as unity for the flow of a gas with an error no greater than 2% for all values of (p_1/p_o) between 1.0 and the critical pressure ratio for both venturi meters and flow nozzles. The throat pressure p_1 cannot fall below the critical pressure p_c because of the sonic velocity limitation (see the notes on "Flow of Compressible Fluids"). Consequently Equations 9 and 10 apply only for values of p_1 greater than p_c.

4. Flow of Liquids

The rate of flow of a liquid through a venturi meter can be calculated from Equation 10 taking Y_o as unity. In the case of an inclined or vertical venturi meter handling a liquid, the proper equation is

$$w = CA_a \sqrt{\frac{[2\,g_c\,(p_o - p_1) + 2\,g_L\,\rho\,(Z_o - Z_1)]\,\rho}{1 - \alpha_2\,\alpha^2}} \tag{12}$$

5. Accuracy p. 143 - Equation 12 : the denominator should be $1 - \alpha^2$

A standard commercial venturi should be accurate to within 1 or 2%. Care must be exercised to avoid abnormal velocity distributions and swirling or helical flow in the upstream channel. Straightening vanes can be used to eliminate swirl, and an abnormal velocity distribution can be ironed out by inserting a sufficient length of straight pipe between the meter and the fitting or obstruction causing the disturbance. A large amount of data were presented by Pardoe (24) showing the effect of installation on the coefficients for venturi meters. For an interpretation of some of these data, see an article by Sprenkle (29) on piping arrangements for acceptable flowmeter accuracy.

6. Permanent Pressure Drop

A well-made venturi meter will have a permanent pressure loss in the range of 10 to 20% of the differential pressure.

C. Flow Nozzles

1. Structural Details

A simple form of flow nozzle is illustrated in Figure 2. It consists of a short cylinder with one end flared out in the form of a flange to fit between a pair of pipe flanges. The contour of the curved entrance section is preferably elliptical. The proportions for the ellipse, as shown in Figures 3 and 4, were those adopted by an A.S.M.E. subcommittee on flow nozzle research (see Reference 13). Conical entrance sections have also been employed with a total included angle of 25 to 30°. Larger angles than

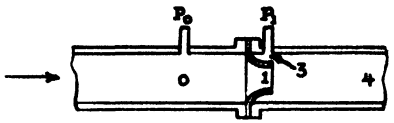


Figure 2. Flow Nozzle

this can be used but calibration is required. The upstream pressure tap is located about one pipe diameter ahead of the entrance section while the downstream tap may be located in the straight portion of the nozzle throat, as shown in Figure 3, or in the pipe wall behind the nozzle discharge point, as shown in Figure 4. The pressure at points 1 and 3 (see Figure 2) will be practically identical for sub-critical flow.

FLOW NOZZLE CONTOURS

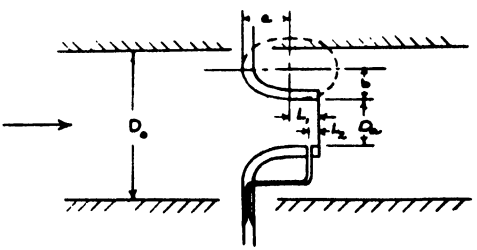


Figure 3. Low β Series $\beta < 0.5$

$a = D_a \quad b = 0.67D_a \quad L_1 = 0.6D_a$

$L_2 = 0.15D_a$

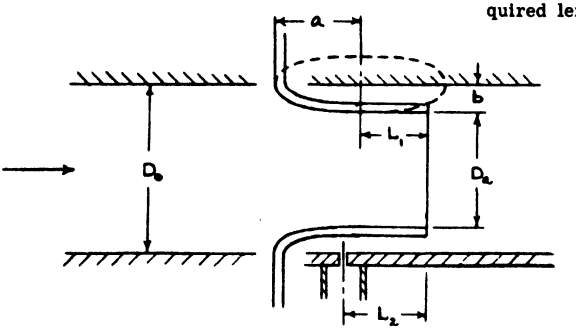


Figure 4. High β Series $\beta > 0.5$

$a = 0.5\ D. \quad b = 0.5\ (D. - D_a) \quad L_1 = 0.6\ D_a$

$L_2 = 1.5$ in. if possible

2. Flow Equations

The rate of discharge through a flow nozzle for sub-critical flow can be determined from the pressure differential and fluid density using the equations given for venturi meters, Equation 10 for gases and Equation 12 for liquids. The adiabatic expansion factor, Y_0, is the same for both venturi meters and flow nozzles. The discharge coefficient, C, is about 0.98 for a well-made flow nozzle. See Bean, Beitler, and Sprenkle (13) for additional information on flow nozzle coefficients.

3. Accuracy

A well-made flow nozzle should be accurate to within 1 or 2%. As in the case of venturi meters, care must be exercised to avoid abnormal velocity distributions and swirl in the upstream channel. Considerable information is given by Sprenkle (29) on the minimum lengths of straight pipe required before and after a flow nozzle with various types and combinations of fittings and valves. The required length on the upstream side increases rapidly with diameter ratio for values of diameter ratio above 0.5.

4. Permanent Pressure Drop

The permanent pressure drop across the flow nozzle expressed as a fraction of the differential pressure is approximated by Equation 13

$$(p_0 - p_4)/(p_0 - p_1) = (1 - \alpha)/(1 + \alpha) \quad (13)$$

Equation 13 was derived from momentum balance theory assuming constant fluid density.

5. Critical Flow Nozzle

For a given set of upstream conditions, the discharge of a gas from a nozzle will increase with a decrease in the absolute pressure ratio, p_1/p_0, until the linear velocity in the throat reaches that of sound in the gas at the conditions existing at that point. The value of p_1/p_0 for which the acoustic velocity is just attained is called the critical pressure ratio. The pressure in the throat, p_1, does not fall below p_c even if a much lower pressure exists at points 3 and 4. The critical pressure ratio is given by

$$\frac{k+1}{\left(\frac{p_1}{p_0}\right)_c^{2/k}} - \frac{2}{\left(\frac{p_1}{p_0}\right)_c^{(k+1)/k}} - \frac{k-1}{(A_0/A_a)^2} = 0 \quad (14)$$

For large values of A_o/A_1, this reduces to

$$(p_1/p_o)_c = \left[2/(k+1)\right]^{k/(k-1)} \tag{15}$$

For k = 1.30, $(p_1/p_o)_c$ = 0.545
k = 1.40, $(p_1/p_o)_c$ = 0.528

Under critical flow conditions, only p_o and T_o need be known to determine the flow rate, which is then given by the following equation—

$$w = CA_a\sqrt{(g_c k)(p_o/v_o)\left(\frac{2}{k+1}\right)^{\left(\frac{k+1}{k-1}\right)}} \tag{16}$$

$$w = CA_a K_n\sqrt{p_o/v_o} \tag{17}$$

For k = 1.30, K_n = 3.78
k = 1.40, K_n = 3.89

A value of 0.98 can be used for the discharge coefficient.

D. Orifice Meters

1. Structural Details

The term orifice usually refers to a square-edged or sharp-edged opening in a thin plate. The opening may be circular, annular, or segmental, although for metering purposes the concentric circular orifice is the most common. The orifice plate is generally mounted between a pair of pipe flanges.

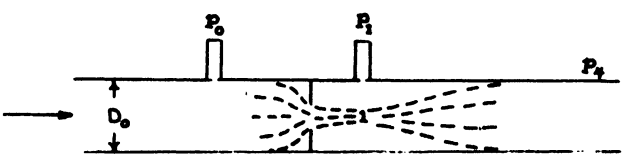


Figure 5. Orifice Meter

The orifice differential is customarily measured between one of the following pressure-tap pairs. Except in the case of flange taps, all measurements of distance from the orifice are made from the upstream surface of the plate.

a. Corner taps. Static holes drilled one in the upstream flange and one in downstream flange with the openings as close as possible to the orifice plate.

b. Radius taps. Static holes located one pipe diameter upstream and one-half pipe diameter downstream from the plate.

c. Pipe taps. Static holes 2-1/2 pipe diameters upstream and 4-1/2 to 8 pipe diameters downstream.

d. Flange taps. Static holes located 1 in. upstream and 1 in. downstream from the orifice plate.

e. Vena contracta taps. The upstream static tap is located one-half to two pipe diameters from the orifice, and the downstream tap is located at the point of minimum pressure. The latter is a function of the diameter ratio, β, as indicated in Table III, page 146.

2. Flow Equations

The rate of discharge through an orifice is given by Equation 10 for liquids or gases and by Equation 12 for liquids.

The expansion factor, Y_o, for orifices is approximated by Equation 18

$$Y_o = 1 - \left[(p_o - p_1)/(p_o k)\right](0.41 + 0.35\,\alpha^2) \tag{18}$$

It may also be conveniently obtained from a plot of Y_o vs. $(p_o - p_1)/(p_o k)$, for various values of β, given by Perry (10), p. 403. While Equation 18 applies strictly only to concentric circular orifices, it may be used for other openings in the absence of specific data.

TABLE III
LOCATION OF VENA CONTRACTA DOWNSTREAM TAP
CONCENTRIC CIRCULAR ORIFICE

Diameter ratio β	Location, pipe diameters downstream		
		Extreme Range*	
	Recommended	Minimum	Maximum
0.2	0.86	0.37	1.30
0.4	0.74	0.47	0.98
0.6	0.55	0.42	0.69
0.8	0.32	0.23	0.41

p. 146 - Footnote on Table III missing - Should
*For ±0.5% accuracy in discharge coeff

3. Concentric Circular Orifices

The coefficient of discharge (C) for orifices is a function of Reynolds number as shown qualitatively in Figure 6. Calibration is required if an orifice is to be used in the transition region. At Reynolds numbers (based on the orifice diameter and velocity) greater than 10,000 the coefficients are substantially constant. For concentric circular orifices the value will fall between 0.60 and 0.62 for vena contracta or radius taps for β up to 0.8, and for flange taps for β up to 0.5. The coefficients will be the same, within ± 2%, for square-edged orifices if the plate thickness at the throat is less than (1/30) D_o, (1/8) D_a, or (1/8) (D_o - D_a), whichever is smallest. If the plate thickness is greater than these limits, the situation can be remedied by beveling the downstream side, using a 90° or greater included angle on the bevel. Otherwise the orifice should be calibrated. One of the best sources of information on concentric circular orifice coefficients is the A.S.M.E. Research Report on Fluid Meters (3), Chapt. C-4. Tables and plots are given of orifice coefficient vs. diameter ratio for a range of Reynolds numbers and pipe sizes for flange taps, vena contracta taps, and pipe taps.

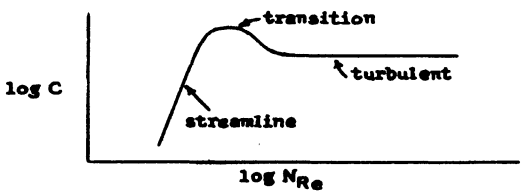


Figure 6. Orifice Discharge Coefficient

A sharp-edged orifice should be accurate to within 1 or 2%. Care must be exercised to avoid abnormal velocity distributions or swirl in the upstream channel. A table is given by Perry (10), p. 407, listing minimum lengths of straight pipe required before and after an orifice plate for various types and combinations of fittings and valves. The required length on the upstream side increases rapidly with increasing diameter ratio for values of diameter ratio above 0.5.

Bean, Buckingham, and Murphy (14) showed that if ρ_{av} were employed in place of ρ_o in Equation 10, then Y_o could be taken as unity for the flow of a gas through a concentric circular orifice with an error no greater than 2% for all values of (p_1/p_o) between 1.0 and the critical pressure ratio. Critical flow through a sharp-edged orifice is discussed in the notes on "Flow of Compressible Fluids."

4. Orifice Nomograph

Equation 10 has been put into the form of a nomograph, by C. E. Lapple, which is presented in Figure 7. A constant coefficient of 0.61 (vena contracta taps at $N_{Re} > 10{,}000$) was used in the construction of the chart. It is recommended for design calculations (selection of orifice diameter) and for a rough check on orifice flow calculations. It is not recommended for use in orifice calibrations or in accurate calculation of flow rates. Equation 10 should be used for the two latter purposes.

The following examples are given to illustrate the use of the chart:

a. Given: Air with a density of 0.075 lb./cu.ft. is flowing through a 2.82-in. orifice in a 4-in. i.d. pipe. The orifice differential is 10 in. of water. What is the flow rate?

Solution: Calculate β = (2.82/4.0) = 0.70. Join β = 0.70 with D_a = 2.82 in., cutting R_2 at 7.77. Join R_2 = 7.77 with (p_o - p_1) = 10 in. water, cutting R_1 at 8.84. Join R_1 = 8.84 with ρ = 0.075 cutting w/Y_o at 0.50. Then for Y_o = 1.0, the flow rate equals 0.50 lb./sec.

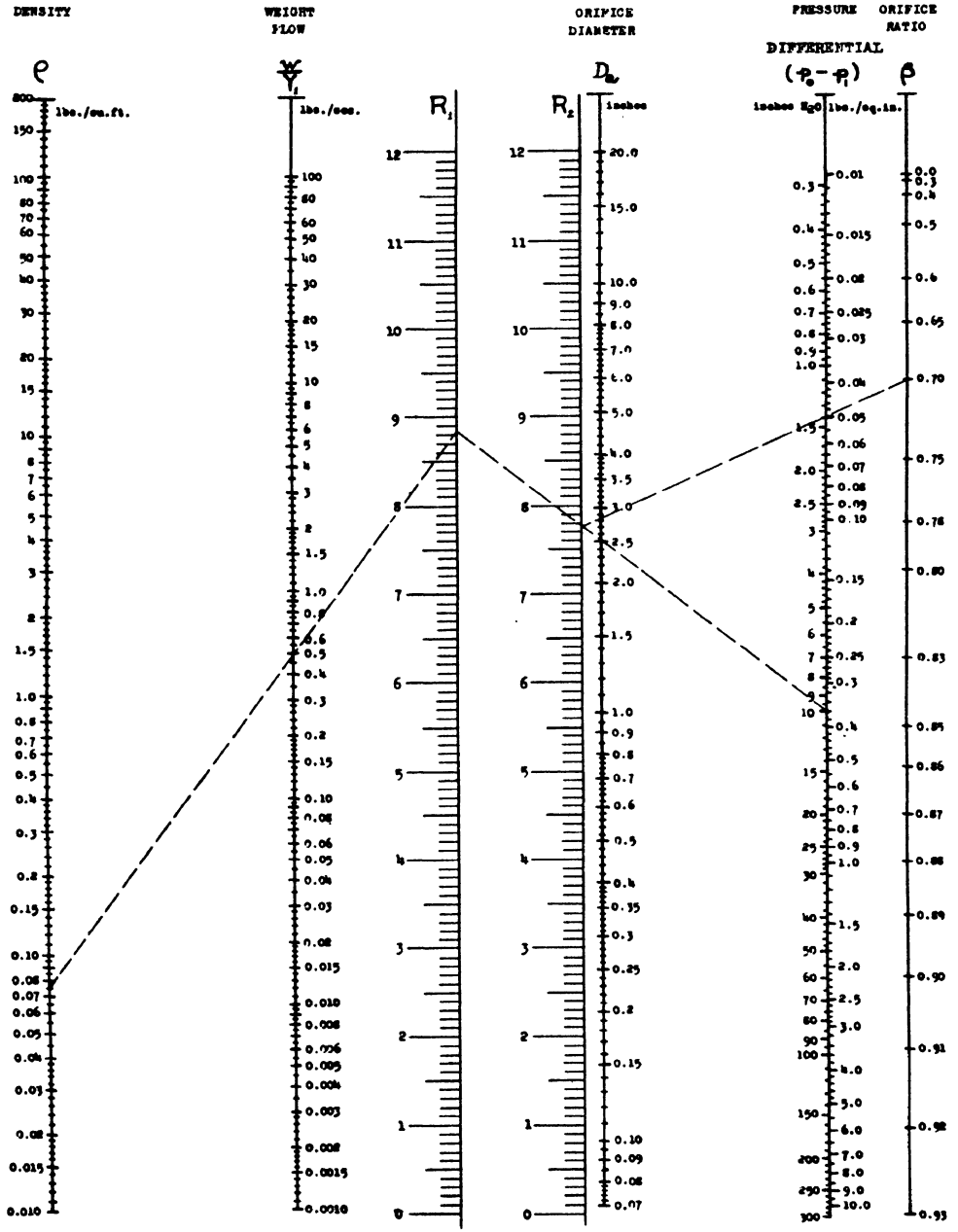


Figure 7. Orifice Nomograph
(Vena Contracta Taps)
$N_{Re} > 10{,}000$

b. Given: Air with a density of 0.075 lb./cu.ft. is flowing at the rate of 0.50 lb./sec. in a 4-in. i.d. pipe. What sized orifice should be used to give an orifice differential of 10 in. water?

Solution: Y_o may be taken as unity. Connect ρ = 0.075 with (w/Y_o) = 0.50, cutting R_1 at 8.84. Join R_1 and $(p_o - p_1)$ = 10 in. water cutting R_2 at 7.77. Join R_2 = 7.77 and β = 0 and from the intersection with D_a obtain 3.0 in. as a first approximation. Calculate β = (3.0/4.0) = 0.75. Join R_2 = 7.77 and β = 0.75 and obtain D_a = 2.75 in. Calculate β = (2.75/4.0) = 0.70. Join R_2 = 7.77 and β = 0.70 and obtain D_a = 2.82 in. as the final orifice size.

5. Segmental Orifices

Segmental or half-moon orifices are frequently used where there is a possibility of entrained liquid or solids which would build up or accumulate behind a concentric circular orifice. This is avoided if the segmental opening is placed on the bottom side. In the case of liquid flow with entrained gas, the opening should be on the top side.

Coefficients of discharge for use with Equations 10 and 12 have been determined experimentally by Lohmann (23) and by Hodgson (19) for sharp-edged segmental orifices with flange taps. Their results are in good agreement, and interpolated values are given in Table IV. It is strongly recommended, however, that a calibration be made on any segmental orifice with an α greater than 0.5.

TABLE IV

DISCHARGE COEFFICIENTS FOR SEGMENTAL ORIFICES—FLANGE TAPS

α	C	Limiting* N_{Re}
0.2	0.61	25,000
0.4	0.60	70,000
0.6	0.575	160,000
0.7	0.54	200,000
0.8	0.48	250,000
0.9	0.395	300,000

*These values of Reynolds number (based on pipe diameter and velocity) were given by Lohmann as the lower limit for a constant coefficient. Below this the coefficients tend to increase rapidly.

In the absence of specific information, the same precautions should be taken with segmental orifices as with concentric circular orifices in the matter of location with respect to valves, fittings, etc.

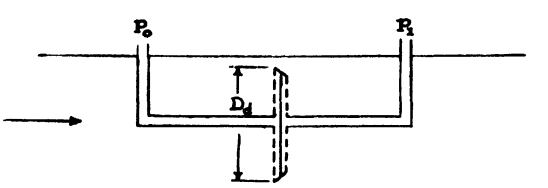


Figure 8. Annular Orifice

6. Annular Orifices

The performance of the annular orifice assembly pictured in Figure 8 is given by Howell in a Ministry of Aircraft Production Report (20). An average discharge coefficient of 0.645 was obtained for a sharp-edged orifice for ratios of D_d/D_o in the range of 0.7 to 0.9. This type of orifice is reported to be relatively insensitive to entrance conditions (upstream flow disturbances), and is therefore particularly useful where space limitations preclude the use of other types of head meters.

7. Permanent Pressure Drop

The ratio of permanent pressure drop to orifice differential can be obtained for incompressible flow from a chart given by Perry (10), p. 404. This curve which applies to a concentric circular orifice with vena contracta taps can be approximated by Equation 19

$$(p_o - p_4)/p_o - p_1) = 1 - \alpha \qquad (19)$$

V. PITOT TUBE

A. Principle of Operation

The velocity of a fluid at any point in a stream can be calculated if the kinetic energy or velocity head at that point is known. This cannot be measured directly, but can be obtained by difference from impact and static pressure readings, the impact pressure being the sum of the velocity pressure and the static pressure.

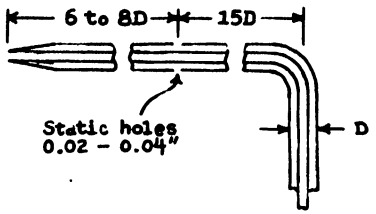


Figure 9. Pitot Tube

B. Structural Details

A simple impact tube (i.e., an open-ended tube facing upstream) may be used to register the impact pressure with pipe sidewall pressure taps for the static pressure. If the two legs of an ordinary differential manometer are connected one to the impact tube and one to the static taps, the manometer will automatically record the velocity pressure.

A more common design incorporates both impact and static openings in a single assembly, as shown in Figure 9. The inner passage constitutes the impact tube while the static holes connect to the annular passage. If the static holes are properly located with respect to the tip and the tube is properly aligned with the stream, the static reading given by this type will be very close to actual, although wall taps will give still greater accuracy. A hemispherical tip may also be used.

A modified pitot tube, known as a pitometer, has one opening facing upstream and another facing downstream. A drawing of this type is shown in the A.S.M.E. Research Report on Fluid Meters (3), p. 41. The differential recorded by this instrument is 35 to 40% greater than the standard instrument, the reason being that the static tube faces downstream and records the "trailing pressure" which is lower than that of the surrounding fluid. This increased differential aids with the measurement of very low velocities. Also the short tip length makes it possible to insert it into relatively small openings in pipes or ducts.

C. Flow Equations

The velocity of liquids or of gases (up to 200 ft./sec.) is given by the following equation

$$V_o = C\sqrt{2\, g_c\, (p_i - p_o)/\rho_o} \tag{20}$$

where $(p_i - p_o)$ is the velocity pressure indicated by the differential manometer reading.

With gases at velocities over 200 ft./sec., the effect of gas compressibility must be taken into account. The velocity in this case is given by Equation 21, which is the theoretical relation for a perfect gas.

$$V_o = C\sqrt{\left(\frac{2\, g_c\, k}{k-1}\right)\frac{p_o}{\rho_o}\left[\left(\frac{p_i}{p_o}\right)^{\frac{k-1}{k}} - 1\right]} \tag{21}$$

For gas velocities near that of sound, see Rayleigh (26).

A well-made pitot tube of the design shown in Figure 9 will have a coefficient, C, in the range of 0.98 to 1.00, while the pitometer will have a coefficient on the order of 0.85.

D. Traversing for Mean Velocity

The pitot tube measures only the local velocity, which means that a traverse has to be made if the flow rate or average velocity in a duct is to be determined by this means. If the duct cross-section is rectangular in shape, then it can be divided up into a number of small rectangles or squares and the velocity measured at the center of each one of these. An average of these velocities gives the mean velocity for the duct. In circular ducts, the cross-section is divided into a central circular area and several annular areas, all of which are equal in cross-section. The most common circular traverse is known as the 10-point traverse. Readings are taken across a diameter at the following distances from the wall: 0.026D, .082D, 0.146D, 0.226D, 0.342D, 0.658D, 0.774D, 0.854D, 0.918D, and 0.974D. An

average of the velocities at these points will give a mean velocity which is theoretically only 0.3% high for a normal velocity distribution. The often-used practice of measuring the velocity at the centerline and applying a correction factor to give the average velocity is generally unreliable. The ratio $V_{av.}/V_{max.}$ has been found to be 0.81 for Reynolds numbers greater than 50,000 under ideal conditions. However, in actual practice ratios as high as 0.91 have been found. A good place for a traverse is at a contraction, if not too abrupt, since the velocity distribution will generally be quite uniform. Such would be the case, for example, in the throat of a venturi meter or flow nozzle.

E. Direction Indicators

Various designs of multi-impact-tube direction meters have been devised to indicate stream direction. One such design is shown by Perry (10), p. 400. Four prongs are inclined at 45° with the instrument axis which is parallel to the direction of the stream. If one pair of probes is located in the horizontal plane, the second pair will be in the vertical plane. In addition, the axes of any two tubes in a given pair are perpendicular. Each pair is connected to a differential manometer and when the instrument is perfectly aligned with the fluid stream, the two manometers will read zero.

A number of other designs are described by Eckert (15) in a German reference, now available as an N.A.C.A. translation. In addition, Hamilton (17) has described a new direction-indicating pitot tube.

VI. ROTAMETERS

A. Principle of Operation

The rotameter is the most widely used form of area meter. With an area meter, the pressure differential across the metering element remains substantially constant, the free area for flow changing with the flow rate and thereby indicating the magnitude of the flow rate. The rotameter is essentially a vertical tapered glass tube inserted into a pipe line by means of special end connections and containing a float which moves up and down as the flow increases or decreases. Graduations are etched onto the side of the tube to indicate the rate of flow.

B. Flow Measurement Theory

Under equilibrium conditions in a rotameter tube, the weight of the float is counter-balanced by an upward-acting force which is the sum of the impact on the float due to the approach velocity and the product of the pressure difference across the float and the projected area of the float. This pressure difference is taken from a point upstream of the float to a point just behind the float, which corresponds to the tap locations for orifice meters with vena contracta taps. Assuming a cylindrical float of volume v_f and projected area A_f, the above can be stated mathematically as follows:

$$v_f \rho_f g_L/g_c = (p_o - p_1 + \rho V_o^2/2 g_c) A_f \tag{22}$$

$$p_o - p_1 = \rho (Z_1 - Z_o) g_L/g_c + \rho V_1^2/2 g_c - \rho V_o^2/2 g_c \tag{23}$$

$$Z_1 - Z_o = v_f/A_f \tag{24}$$

$$q = V_1 A_a \cdot \tag{25}$$

Combining Equations 22 - 25, solving for q, and inserting a coefficient C to allow for contraction in the annulus and frictional effects, gives

$$q = C A_a \sqrt{\frac{2 g_L v_f (\rho_f - \rho)}{\rho A_f}} \tag{26}$$

Since $w = q\rho$

$$w = C A_a \sqrt{\frac{2 g_L v_f (\rho_f - \rho)\rho}{A_f}} \tag{27}$$

The coefficient, C, has been found to be a function of the Reynolds number ($D_e V_1 \rho/\mu$), where the equivalent diameter is taken as the local tube diameter minus the float diameter.

By proper design, the free area for flow can be made almost a linear function of float position, in which case a flow rate scale etched onto the tube will be almost uniform throughout its length. This permits measurement over a large range of flow rates (as much as ten-fold) with a single tube-float combination.

The ratio of flow rates for two different fluids at the same rotameter reading is given by Equations 28 and 29 as follows

$$\frac{q_A}{q_B} = \frac{C_A}{C_B}\sqrt{\frac{(\rho_f - \rho_A)}{(\rho_f - \rho_B)}\frac{\rho_B}{\rho_A}} \tag{28}$$

$$\frac{w_A}{w_B} = \frac{C_A}{C_B}\sqrt{\frac{(\rho_f - \rho_A)}{(\rho_f - \rho_B)}\frac{\rho_A}{\rho_B}} \tag{29}$$

It is possible to introduce self-compensation, with respect to weight rate of flow, for fluid density changes through the use of a float with a density twice that of the fluid being metered. Referring to Equation 27, it can readily be seen that a 10% increase in ρ will produce a decrease of only 0.5% in the weight rate of flow, provided ρ is initially one-half of ρ_f.

It is not convenient to use a plot of C vs. N_{Re} in the determination of flow rate for a given scale reading since V_1 or q appears in both terms. However, in this case it is convenient to use a plot of C vs. N_{Re}/C since V_1 has been eliminated from the latter term, as shown by Equation 30a.

$$N_{Re}/C = \frac{D_e V_1 \rho}{\mu}\quad\frac{1}{V_1}\sqrt{\frac{2 g_L v_f (\rho_f - \rho)}{\rho A_f}} \tag{30}$$

$$N_{Re}/C = \frac{D_e}{\mu}\sqrt{\frac{2 g_L v_f (\rho_f - \rho)\rho}{A_f}} \tag{30a}$$

The calculation of flow rate for a given fluid and a particular scale reading can be made with greater reliability by conversion from a known calibration-fluid flow rate than by straight prediction from the C vs. N_{Re}/C curve. The latter requires very accurate values of the annular cross-sectional area for each reading, whereas it is possible to convert from one fluid to another without this requirement. The following procedure is suggested:

1) A curve of C vs. N_{Re}/C must be available for the rotameter in question, or must be prepared from calibration data on a fluid of known properties and from the dimensions of the float and tube.

2) Values of N_{Re}/C are calculated for both of the fluids for the reading in question.

3) Relative values of C_A and C_B are found from the plot of N_{Re}/C vs. C.

4) The desired rate of flow, q_B, is then calculated using Equation 28 where q_A is the known flow rate for the calibration fluid.

C. Structural Details

A wide variety of float shapes are commonly employed, the simplest being in the shape of a sphere. The ball type is used mainly in very small rotameters. The plumb-bob shape, shown in Figure 10, sketch (a), was one of the earliest ones to be used. The coefficient for this type is relatively constant for Reynolds numbers above 5,000 but diminishes rapidly below that. The float shown in sketch (b) was designed to eliminate the effect of viscosity as much as possible. The coefficient is relatively constant down to a Reynolds number of about 100. The float shown in sketch (c) has a constant coefficient down to a Reynolds number of about 50. Types (b) and (c) are used with guide wires to keep them centered. Types (d) and (e) were designed for use with bead-guide tubes. These tubes have three or more vertical ribs formed integrally with the inner bore of the tube. The ribs serve to keep the float centered, thereby eliminating the need for a guide wire. This type can be used with opaque liquids since the ribs are almost in contact with the float rims.

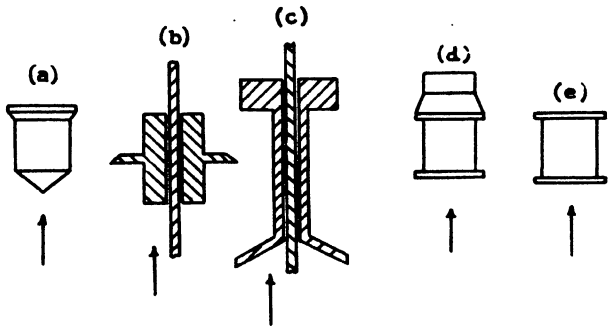


Figure 10. Typical Rotameter Float Shapes

For high pressure applications, a tapered metal tube may be used with a sight chamber equipped with high pressure sight glasses located above or below the tube. Attached to the float is a small rod which extends into the sight chamber where its movement can be observed through the sight glasses. This type has also been used with opaque liquids, the sight chamber being filled with a compressed gas if located above the tube, or with a sealing liquid if located below the tube.

Unlike most head meters, the rotameter appears to be relatively insensitive to flow disturbances, and thus no particular care has to be taken in their installation relative to valves and fittings. While they should be installed as near vertical as possible, an inclination of 10°, which is readily detected by eye, will produce an error of less than 1%. Rotameters are generally supplied with a calibration curve, and although the tubes and floats are precision made, discrepancies on the order of 5% can occur. For precise measurements, calibration after purchase is generally advisable.

D. Permanent Pressure Drop

The pressure drop across a rotameter is the sum of the friction loss in the end connections, the friction loss across the float, and the static head between the inlet and outlet connections. It is generally more convenient to obtain this by test rather than by calculation. The friction loss across the float is less than the float pressure differential resulting from the kinetic energy increase, because of the pressure recovery which takes place above the float when the annular jet re-expands to fill the tube. This recovery was found by Schoenborn and Colburn (27) to be about one-half of that given by a standard circular orifice at comparable area ratios. The float friction loss thus actually decreases as the meter reading increases. At low readings the friction loss in the end connections is negligible compared with the float friction loss, however, at high readings, it may be equal to or greater than the float friction loss.

E. References

For additional information on rotameters, see Rhodes (11), pp. 301-9, Schoenborn and Colburn (27), and Fischer (16).

VII. PULSATING FLOW

It is sometimes necessary to measure the flow of a fluid at a point where the flow is pulsating although this should be avoided where possible. Under such conditions the use of a quantity meter is to be preferred to a rate meter. When a rate meter has to be used, steps should be taken to eliminate or reduce the pulsations at the meter location or to reduce the effect of the pulsations on the indicating or recording mechanism. Pulsations are most likely to be encountered in discharge lines from reciprocating pumps or compressors and in steam lines supplying steam to reciprocating machinery. The frequency of pulsation is frequently too great for the indicating mechanism to follow, in which case some average position is assumed. At lower frequencies, the indicating mechanism will oscillate and an average reading has to be selected by eye.

A special rotameter design is available, for use with pulsating flow, in which the float is connected to a plunger located in a dash pot. This prevents the float from oscillating rapidly. The float roughly assumes a position midway between the extremes. This midpoint roughly corresponds to the average flow rate since the float position is practically a linear function of the flow rate. No information is available on the reliability of this method.

Head meters such as the orifice, venturi, or flow nozzle are particularly susceptible to errors due to pulsating flow. The pressure differential across a head meter is proportional to the square of the flow rate. Therefore, if the indicator assumes an average position, its reading will correspond to the square root of the mean differential pressure. This is always higher than the required reading, which

is the mean square root of the differential pressures. Expressed mathematically, the meter registers

$$\sqrt{\frac{1}{t}\int_0^t h\,dt}$$

whereas it should register

p. 153 - line 4 should be $\frac{1}{t}\int_0^t$

$$\frac{1}{t}\int_0^t \sqrt{h\,dt}$$

Pressure waves which travel at sonic velocity constitute another source of error when head meters are employed with pulsating flow. The error in this case may be either positive or negative. According to the American Meter Company (Bulletin E-2), this error can be reduced or eliminated by making the manometer leads equal in length and identical in composition and size.

The general practice of throttling manometer lines until a constant reading is obtained is considered to be poor practice and may lead to large errors. In the case of gas flow the effect of velocity variation can be eliminated or reduced by inserting a surge chamber and a constriction in the line between the metering element and the source of pulsation. The surge chamber is generally installed as close as possible to the pulsation source with the constriction located between the surge chamber and the metering element. This arrangement can be used for either a suction or discharge line. Schmid (28) and Herning and Schmid (18) have presented charts from which the surge chamber volume and constriction pressure drop can be calculated for various operating conditions. These have been reproduced in Figures 11, 12, and 13. In each case, per cent metering error is plotted against the dimensionless ratio $Qn\ \Delta p_s/q\ p_s$. The term Q is the volume of the surge chamber plus the volume of the lines between the metering element and the source of pulsation, while Δp_s is the pressure drop between the surge chamber and the metering element including the permanent pressure drop across the metering element. These charts indicate that the metering error diminishes with an increase in the ratio of chamber volume to volume discharged per pulsation and with an increase in the ratio of pressure drop to absolute pressure. The numbers on the curves represent the intake or discharge time expressed as a percentage of the time per stroke. The charts in Figure 11 are for a simplex double-acting compressor; Figure 12 is for duplex double-acting compressor; and Figure 13 is for triplex double-acting compressor. For design work, a value of $Qn\ \Delta p_s/q\ p_s$ is obtained from the appropriate chart and the permissible metering error. The product $Q\ \Delta p_s$ is then obtained from this dimensionless grouping. For a small system, values of Q and Δp_s can then be artibrarily selected, while for a large system a economic balance should be used.

A surge chamber filled with compressed air is frequently used on the discharge side of reciprocating pumps handling liquids. The chamber in this case is connected to the discharge line by means of a tee or branch connection.

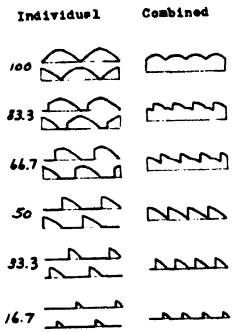
Lindahl (22) describes a mechanical pulsameter which can be used to test a metering installation in place. The pulsameter is connected to the pressure leads from the metering element and records the maximum differential pressure across the meter. A chart is given which shows the permissible maximum differential as a function of the meter reading for an accuracy of 1%. For meter readings above 30 in. of water, the claimed permissible maximum differential is about 4/3 of the meter reading.

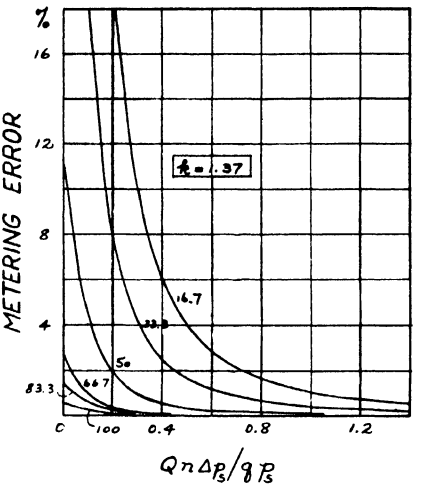
VIII. VANE ANEMOMETER

A vane anemometer is in effect a windmill consisting of a number of light blades mounted on radial arms attached to a common spindle which rotates in two jeweled bearings. The blades are inclined at an angle to the axis of the spindle so that when the latter is placed parallel to the gas stream, the forces on the blades cause the spindle to rotate at a rate depending mainly on the gas velocity. The spindle is attached to a revolution counter, the gearing and blade angle being such that the dial reads directly the feet of gas which passes the instrument during the test period. The gas velocity is determined by using a stop-watch to find the time interval required to pass a given number of feet of gas.

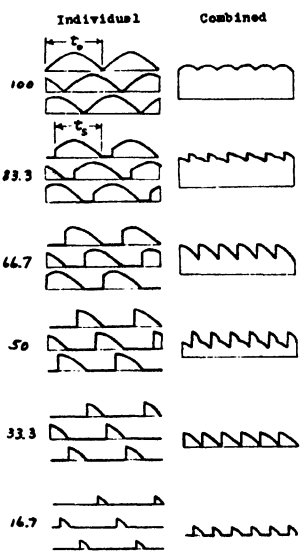
The instrument has a useful velocity range of about 2 ft./sec. up to 40 ft./sec. Below about 2 ft./sec. the accuracy becomes very poor due to the increasing effect of frictional resistance. Velocities over about 40 ft./sec. impose an excessive strain on the standard instrument. When measurements are made, care must be exercised to hold the instrument well away from the body or from any object not

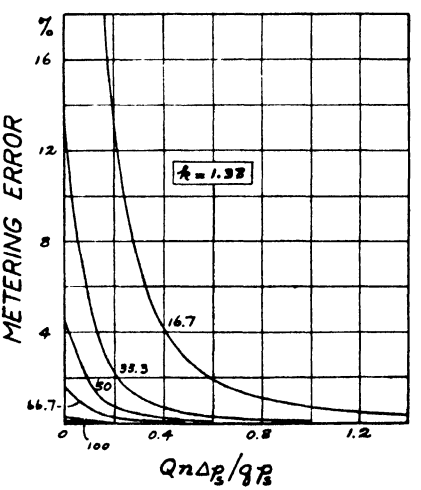
CHARTS TAKEN FROM SCHMID (28)





DUPLEX DOUBLE-ACTING COMPRESSOR



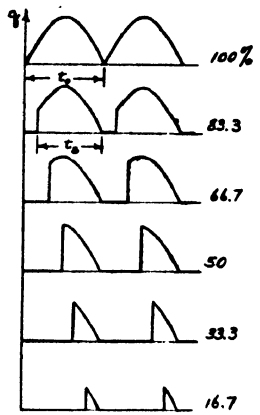


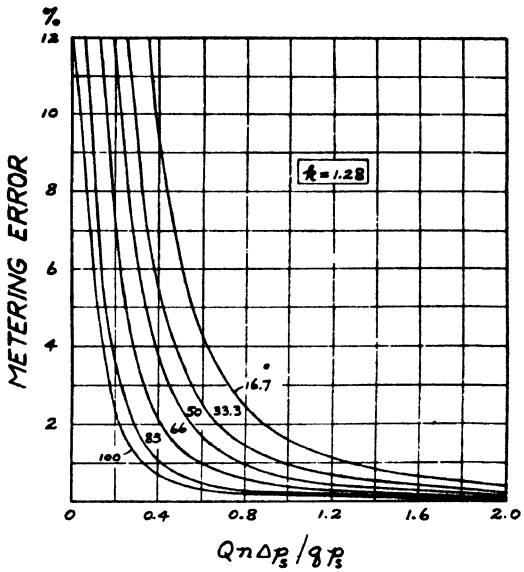
TRIPLEX DOUBLE-ACTING COMPRESSOR

THE NUMBERS ON THE CURVES REFER TO THE PISTON DISCHARGE TIME EXPRESSED AS A PERCENTAGE OF THE TIME PER STROKE - t_s/t_o

Figure 11. Pulsating Flow Charts

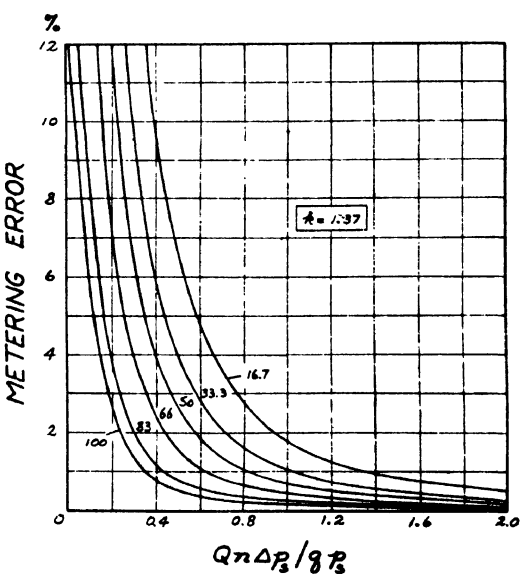
p. 154 - the two figures shown on this page should be labeled Figures 12 and 13.





SIMPLEX
DOUBLE ACTING
COMPRESSOR

THE NUMBERS ON THE CURVES REFER TO THE PISTON DISCHARGE TIME EXPRESSED AS A PERCENTAGE OF THE TIME PER STROKE - t_d/t_o



CHARTS TAKEN FROM HERNING AND SCHMID (16)

Figures 12 and 13. Pulsating Flow Charts

p. 155 - the figure shown on this page should be labeled Figure 11.

normally present in the gas stream. Because the instrument is normally 3 to 4 in. in diameter, it cannot be used in small ducts. It is possible to field calibrate the instrument by holding it at arms length and walking over a measured distance using a stop-watch for timing.

The velocity reading given by the instrument is inversely proportional to the square root of the gas density. If the calibration was carried out in a gas of density ρ_m and the density of the gas stream being metered is ρ_n, the true gas velocity, V_{tn}, can be found as follows: On the calibration curve, find V_{tm} corresponding to V_{Rm} where $V_{Rm} = V_{Rn}\sqrt{\rho_n/\rho_m}$. Then obtain V_{tn} from $V_{tn} = V_{tm}\sqrt{\rho_m/\rho_n}$, where

V_{tn} = true gas velocity at gas density ρ_n.

V_{tm} = true gas velocity at calibration density ρ_m.

V_{Rn} = instrument reading at gas density ρ_n.

V_{Rm} = instrument reading at gas density ρ_m.

For additional information, see Ower (8), Chapt. VII.

Vane anemometers of the type described above can be obtained from Julien P. Friez & Sons, Inc., of Baltimore, Maryland, and from Taylor Instrument Co., of Rochester, New York.

A special swinging vane type of velometer called the Alnor velometer is produced by Illinois Testing Laboratories, Inc., of Chicago, Illinois. It is especially adapted to ventilation work and to the measurement of low velocities—down to 50 ft./min. The accuracy is not too good below 50 ft./min., however.

IX. HOT-WIRE ANEMOMETERS

The hot-wire anemometer consists essentially of a fine, electrically heated wire exposed to the gas stream in which the velocity is being measured. The orientation is generally such that the gas flow is perpendicular to the axis of the wire. The velocity of the gas determines the cooling effect upon the wire, which in turn affects the electrical resistance. A suitable electrical circuit is provided to measure this resistance. The instrument finds its greatest use in the measurement of gases at very low velocities and in turbulence measurements. For additional general information on hot-wire anemometers see Pannell (9), Chapt. III, Ower (8), Chapt. X, King (21), and Eason (5), Chapt. X.

The use of the hot-wire anemometer for high air velocities is discussed by Weske (30). Also see Weske (31), (32) for the use of the instrument on fluctuating velocities. A hot-wire anemometer for use with liquids is described by Piret, James, and Stacey (25).

Until recently the hot-wire anemometer has been used exclusively as a laboratory instrument because of its delicate construction. The laboratory instruments are usually custom built for specific applications. A more rugged instrument is now produced for industrial application by the Hastings Instrument Co. of Hampton, Virginia. It has a velocity range of 0 - 6000 ft./min.

X. WEIRS

A. General Principles

Liquid flow in an open channel is frequently metered by means of a weir, which consists of a dam over which, or through a notch in which, the liquid flows. A weir for metering generally has a flat upstream face perpendicular to the bed and sides of the channel. The level to which liquid must ascend to initiate flow corresponds to the part of the weir known as the crest. The head (h_o) on a weir is the height above crest level of the surface of the liquid upstream from the weir. The head must be measured sufficiently far upstream to avoid the drop in level occasioned by the overfall. The depression in surface level begins at about a distance equal to 2 h_o upstream from the weir. Surface level measurements should be made a distance of 4 h_o or more upstream. For precise measurements, a stilling box fitted with a hook gage or float gage may be attached to the channel.

The sheet of discharging liquid is called the nappe. With sharp-edged weirs the nappe contracts as it leaves the edges of the opening and a free discharge occurs. Rounding the upstream edge will reduce the contraction and increase of the flow rate for a given head. A clinging nappe may result if the head is very small, if the weir is rounded and wide, or if air is prevented from flowing in beneath the nappe, and the result is an increase in the discharge rate.

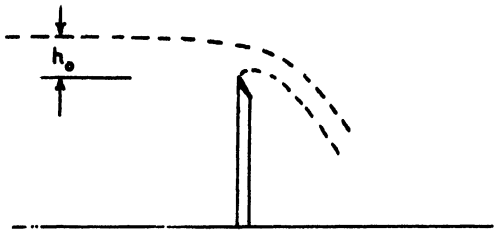


Figure 14. Rectangular Sharp-edged Weir

B. Rectangular Sharp-Crested Weir

With a rectangular weir, the crest is horizontal and may extend part way or all the way across the channel. The expression for flow over a weir can be derived if the flow is regarded as the summation of the elemental flows through a series of horizontal slits one above the other, each discharging in accordance with the orifice equation, as follows——

From an energy balance

$$h\, g_L/g_c + V_o^2/2\, g_c = V_1^2/2\, g_c \tag{31}$$

$$V_1 = \sqrt{2\, g_L\, (h + V_o^2/2\, g_L)} \tag{32}$$

$$q = \int_o^{h_o} V_1\, L\, dh = L \int_o^{h_o} \left(\sqrt{2\, g_L (h + V_o^2/2 g_L)} \right) dh \tag{33}$$

$$q = \frac{2}{3} L \sqrt{2\, g_L} \left[(h + V_o^2/2\, g_L)^{3/2} \right]_o^{h_o} \tag{34}$$

Incorporating a coefficient, C, to allow for contraction at the crest and friction and a coefficient, γ to allow for the fact that $V_o^2/2\, g_L$ does not exactly allow for the integrated average kinetic energy contribution to the head causing flow over the weir, gives

$$q = \frac{2}{3} CL \sqrt{2\, g_L} \left[(h_o + \gamma V_o^2/2\, g_L)^{3/2} - (\gamma V_o^2/2\, g_L)^{3/2} \right] \tag{35}$$

Experiment indicates C = 0.62 for a sharp-crested rectangular weir. Although γ ranges from 1.0 to 2.0 depending upon the distribution of velocities in the approach channel, an average value of 1.5 may be used. Where the velocity of approach correction is small, Equation 35 becomes

$$q = 3.33\, L\, h_o^{3/2} \tag{36}$$

This form is commonly called the Francis formula.

For a rectangular notch, cut in thin plate, or with the edges, as well as the bottom square-edged, the effective length is reduced by 0.2 h_o due to end contraction. Thus,

$$q = 3.33\, (L - 0.2\, h_o)\, h_o^{3/2} \tag{37}$$

This is the modified Francis formula for a rectangular sharp-edged weir with two end contractions.

The coefficients reported for weirs are based on the flow of water but should be good for other liquids provided the viscosity is not so high that frictional effects become appreciable. In the case of high viscosity liquids, calibration is required.

The Francis formula agrees with experiment within 3% or less if (a) L is greater than 2 h_o, (b) velocity of approach is 2 ft./sec. or less, (c) height of crest above bottom of channel is at least 3 h_o, and (d) h_o is not less than 0.3 ft.

Narrow rectangular notches ($h_o > L$) have been found to give about 93% of the discharge given by the Francis formula. Thus,

$$q = 3.10\, L\, h_o^{3/2} \tag{38}$$

Note that no end corrections are applied even though this applies only for sharp-edged or thin square-edged weirs. For notches with L between h_o and 2 h_o, the coefficient increases and merges into values given by the Francis formula for two end corrections. See Schoder and Dawson (12), p. 175.

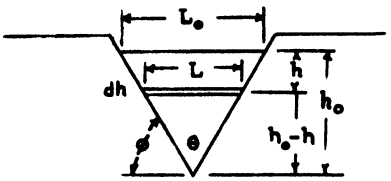


Figure 15. Triangular-notch Weir

C. Triangular-Notch Weirs

A triangular-notch weir is frequently used because a single notch can accomodate a wide range of flow rates, although this in turn reduces the accuracy. The theory given for the rectangular weir is modified only by expressing the lengths of the horizontal elemental slits in terms of h.

$$\phi = 90° - \theta/2 \tag{39}$$

$$\tan \phi = (h_o - h)/(L/2) \tag{40}$$

$$L = 2\,(h_o - h)/\tan \phi \tag{41}$$

Neglecting the velocity of approach

$$dq = (2\, g_L\, h)^{1/2}\, L\, dh \tag{42}$$

$$dq = 2\,(2\, g_L\, h)^{1/2}(h_o - h)\, dh/\tan \phi \tag{43}$$

$$q = 2\sqrt{2\, g_L}\int_0^{h_o} (h_o h^{1/2} - h^{3/2})\, dh\,/\tan \phi \tag{44}$$

$$q = 8\sqrt{2\, g_L}\, h_o^{5/2}/15\, \tan \phi \tag{45}$$

Here, too, a coefficient C has to be incorporated to allow for contraction. For square-edged notches, it has a value of about 0.58.

For $\theta = 90°$ and $C = 0.58$

$$q = 2.48\, h_o^{5/2} \tag{46}$$

For $\theta = 60°$ and $C = 0.58$

$$q = 1.43\, h_o^{5/2} \tag{47}$$

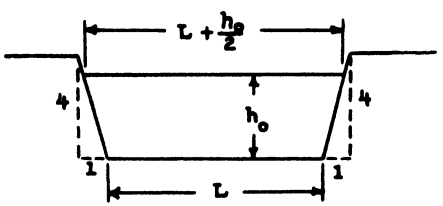


Figure 16. Cipolletti-notch Weir

D. Cipolletti Weir

The Cipolletti weir is widely used in western United States for measuring irrigation water. The ends are flared as shown in Figure 16. The discharge is increased by the flared ends just as much as vertical ends would decrease the discharge. Thus, the discharge is given by the standard Francis formula, Equation 36. Note that the L term in this case is the length of the crest, and not the width of the notch at the water level.

E. Other Types of Weirs

Broad-crested weirs, inclined weirs, submerged weirs, and other miscellaneous types are not discussed here because of their limited application in metering. Experimental data and literature abstracts for circular, parabolic, and triangular weirs are given by Greve, F. W., Purdue Univ. Eng. Exp. Sta. Research Bull. No. 40 (1932). For additional general information see standard texts on hydraulics such as those by Schoder and Dawson (12), King (7), or Gibson (6).

XI. PROBLEMS

Problem 1—A rotameter with a plumb-bob type float is being used to meter the flow of an oil having a density of 58 lb./cu.ft. and a viscosity of 75 centipoises. A millimeter scale is etched on the tube. The tube has an internal diameter of 2.99 in. at a reading of 0 mm. and 3.54 in. at a reading of 354 mm. The float has a diameter of 2.95 in. at the top, weighs 6.44 lb., and has a sp.gr. of 7.92. The following calibration curve had previously been obtained with water and other fluids.

N_{Re}	C
50	0.32
100	0.44
300	0.64
1000	0.81
3000	0.95
6000	1.00
20,000	1.03
40,000	1.08

What is the flow rate for the oil corresponding to a reading of 100 mm. if the same reading gave 33 gal./min. of water at 70° F.?

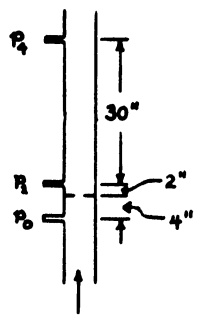


Figure 17. Problem 2

Problem 2—A sharp-edged concentric circular orifice with radius taps is to be mounted in a vertical run of 4-in. Schedule 40 pipe. Water at 70° F. is flowing upward at the rate of 150 gal./min. What size orifice is required to give a pressure differential ($p_o - p_1$) of 4.5 lb./sq.in.? Assume C = 0.61. Also compute the pressure at p_4 if p_o is 30 lb./sq.in. gage.

Problem 3—A pitot tube of the type shown in Figure 9 of the notes is inserted in an air stream and a differential reading of 36 in. of water is obtained. What is the local air velocity if the pressure of the flowing stream is 1 atm. and the temperature is 70°F.? Assume a coefficient of 0.99 for the pitot tube.

Problem 4—Prepare a plot of orifice permanent pressure drop, expressed as a fraction of the orifice differential pressure, versus the diameter ratio β. Assume vena contracta taps and use the approximate relation given by equation 19. Compare with the results obtained in Problem 2 of Chapter 1.

Chapter 9

PIPE LINE DESIGN

by

H. L. Bunker
Design Division
Engineering Department
E. I. du Pont de Nemours & Co., Inc.
Wilmington, Delaware

TABLE OF CONTENTS

		Page
I.	References	163
II.	Nomenclature	163
III.	Purpose and Importance	163
IV.	Definition	163
V.	Types of Piping	163
	A. Water Lines	163
	B. Steam Piping	165
	C. Compressed Air Piping	165
	D. Gas Lines	165
	E. Sanitary Plumbing Lines	165
	F. Drain Piping	165
	G. Sewer Piping	165
	H. Process Piping	165
	I. Instrument Piping	166
	J. Manufacture	166
VI.	Metallurgy	166
VII.	Cost	167
VIII.	Pipe, Valve and Fitting Dimensions	167
	A. Dimensions	167
	B. Manufacturing Tolerances	168
	C. Flanges	169
	D. Bolts, Nuts and Gaskets	169
	E. Valves	169

IX. Design 169
A. General Arrangement 169
B. Route 170
C. Size 170
D. Valves and Fittings 171
E. Insulation 171
F. Supports and Anchors 171
G. Valves 171
H. Fire and Safety 171
I. Specifications 171
X. Fabrication and Erection 172
XI. Cleaning and Sterilization 172
XII. Testing 173
XIII. Sample Problem 173
XIV. Problems 173

LIST OF FIGURES

Figure 1. Cast Iron and Steel Joints 164
Figure 2. Sketch for Sample Problem 174

APPENDIX

Appendix A. Fluid Friction in Conduits 177

I. REFERENCES

1. Walker, J. H. and Crocker, S., "Piping Handbook," McGraw-Hill Book Company, 1939.
2. Plum, S., "Plumbing Practice and Design," Vol. I & II, John Wiley & Sons, Inc., 1943.
3. "Tubefitters Manual," Handbook #111 of the Parker Appliance Company, undated.
4. Sarchet, B. R. and Colburn, A.P., Ind. Eng. Chem., 32, 1249-52 (1940).

II. NOMENCLATURE

C = allowance for threading, mechanical strength and corrosion. Proper values of C also appear in ASA publications or Piping Handbooks).
D = outside diameter of the pipe, inches
P = maximum internal service pressure, lb./sq.in.
S = allowable bursting stress in the pipe material, lb./sq.in. (The S value varies by material, grade of material and temperature and the allowable S values may be found in ASA publications or Piping Handbooks).
t_{min} = minimum pipe wall thickness allowable on inspection, inches

III. PURPOSE AND IMPORTANCE

The purpose of pipe line design is to transfer fluids between two points. However, to accomplish adequate design it is necessary to study, evaluate and select the proper alternates that are offered in cost, materials of construction, size, supports, insulation and painting. The task of the designer is not an easy one. In addition to the many details he must keep in mind at all times, he is also faced with the problem of weighing initial cost against future returns. To insure overall plant efficiency at all times the piping must be given the same serious consideration as prime movers, condensers, and mechanical equipment of all types.

The importance of pipe line design can be stressed by realizing that about 30% of the investment in most chemical plants is for piping. We must also consider that approximately 20% of the design cost in the preparation of construction drawings for a new plant cover pipe line design. In addition to the cost factor, we have the very important factors of reliability of service, safety and fire protection and process quality considerations as well as a design which can be inexpensively maintained.

Reliability of service is usually considered as the ability to maintain essential steam, water and raw material services to a process as their failure immediately shuts down profit producing manufacturing facilities. Frequently these service pipes are not given the consideration their importance justifies.

IV. DEFINITION

Industrial piping might be subdivided into several major classifications for purposes of definition:

A. Outside overhead main lines
B. Outside underground main lines
C. Outside overhead lateral or distribution lines
D. Outside underground lateral or distribution lines
E. Process headers within buildings or tank farms
F. Lateral distribution of process lines within buildings or tank farms
G. Service headers in process or manufacturing buildings or tank farms
H. Control and panel piping used with instrumentation
I. Sewers, plumbing and drain lines

V. TYPES OF PIPING

Piping may be classified by services which in this section are defined as piping to transport water, steam, compressed air, gas, sewage, drains, sanitary plumbing, process and instrument lines.

A. Water Lines are designed normally in either cast iron, steel or concrete construction. Cast iron and concrete are generally used underground. Concrete is usually less expensive in the larger sizes. The common types of joints used in underground piping are shown on Figure 1 and vary from straight bell and spigot construction to standard bolted flanged connections. A combination of these types of construction is frequently used and is referred to as a mechanical packed joint pipe, which is a bell and spigot end construction using a bolted on gland to maintain pressure on the packing. This style has the advantage of having flexibility in the joints after they have been made up and the advantage of preassembly above ground which may result in the lowest installed cost. There is no single

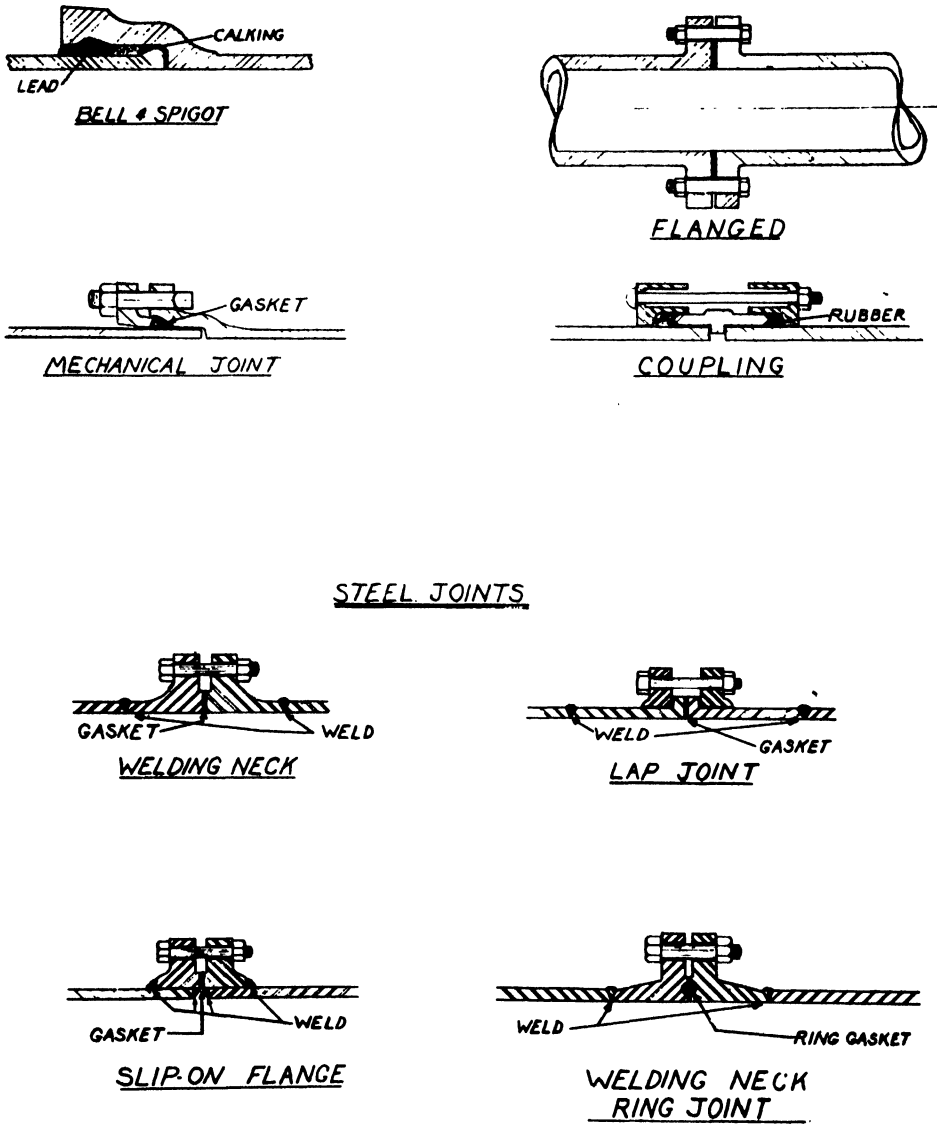


Figure 1. Cast Iron Joints

style of joint which is uniformly less expensive than others since depth of excavation, ground conditions, labor cost and many other factors vary from site to site and hence economic analyses should be made based on the facts applicable to the specific job being designed.

Flanged cast iron pipe is generally used above ground for large headers or where the cast iron material itself is desired for process reasons. In past years cast iron pipe was frequently used for water headers within buildings but the economic trend is to welded steel lines wherever possible.

Above ground water can be easily transported in ordinary steel lines providing precautions are taken against freezing. Practically the only problem in water piping other than that of mechanical considerations is water hammer, which is usually caused by the rapid retardation of water flow due to a rapidly closed valve. This problem is frequently complex and reference (1) will supply information and in turn furnishes additional references for those who care to pursue this subject in detail.

B. Steam Piping, in addition to water piping, is probably found in essentially all manufacturing plants today. It is so common that a designer is apt to forget that proper steam line design is just as important as water, process or vacuum lines. Industrial steam pressures rarely exceed 550 pounds per square inch, 725°F. in the manufacturing areas. The bulk of the steam piping is undoubtedly in the neighborhood of 150 pounds per square inch with little or no superheat. A good rule of thumb to keep in mind is that steam pipe expansion will be 1 inch per 100 lineal feet of pipe per 100°F. increments above atmospheric temperature. The biggest problem in steam line design is the provision for expansion, as expansion joints, or their equivalent, must be incorporated in all long runs of piping and space provided for them.

C. Compressed Air Piping is fairly simple to handle providing the moisture in the air does not become a problem in the winter time. Dryers of the silica gel type are generally used to remove water vapor where necessary. Air lines connected to pulsating equipment must, of course, be well supported and anchored.

D. Gas Lines are also fairly simple to handle providing the gas does not contain tars or other substances that will deposit in the line. If so, steaming-out connections or their equivalent, as well as drain legs, etc., must be provided.

E. Sanitary Plumbing Lines are a distinct type of piping which is common to both industrial, office and stores, and residential construction. Local city or state codes must first be consulted to determine the requirements set forth by law as it is generally necessary to secure approval of drawing by these authorities prior to the start of construction. Sanitary plumbing piping may be roughly divided into two sections -- that piping supplying hot or cold water to the fixtures and that piping which drains the effluent from the fixtures. The former grouping is usually of copper or steel pipe whereas the latter within buildings is primarily of cast iron construction with the occasional use of lead. Additional information on the design of such systems may be found in reference (2).

F. Drain Piping usually refers in industrial practice to that piping system which handles floor drains, rain water conductor run-offs, and handles discharge of cooling water effluent from process equipment. Occasionally process effluents proper are discharged into floor and rain water drains but in many localities the code requires process effluents to be treated, neutralized or otherwise made unobjectionable and then discharged into the sanitary sewer system.

G. Sewer Piping is of the two types referred to above; namely, sanitary combined with process and strictly drainage sewers. It is general practice to use cast iron bell and spigot pipe inside buildings and to a point 5 or 10 feet outside the building wall at which point terra cotta pipe is used. The reason for using cast iron pipe inside buildings is to take advantage of the greater strength of cast iron, the longer lengths for ease of supporting, the ability to make joints tighter in cast iron. Underfloor runs are of cast iron for strength considerations. Drains from laboratory sinks or other drains handling acid water are frequently specified as Duriron to take advantage of its greater corrosion resistance to acids. Again, however, the acid water is handled in terra cotta drains outside the buildings.

Terra cotta or vitrified tile is customarily laid using a Portland cement joint. However, in acid service it is customary to use an acid resisting cement joint such as Vitrabond.

In soft marshy ground where settlement may be expected it is necessary to support terra cotta pipe as it is easily broken. This is frequently done by pouring a concrete footing in the bottom of the trench and laying the pipe in this so-called cradle. By taking these precautions the alignment of the sections of the pipe will be maintained and the risk of joint leakage or breakage of the pipe is reduced.

H. Process Piping really covers the water front. One would hesitate to guess the number of different liquids, gases, slurries, etc., that are handled in pipe and included in this category. It is, therefore, impossible to lay down any suggested procedure that will adequately serve the field. Subsequently the various elements of design will be discussed and these must be selected and tailored to suit the particular problem in this category.

Pressure piping is also a major category in the consideration of types of piping. Pressure varies from low vacuum to hundreds of atmospheres and in the future possibly to thousands of atmospheres. Vacuum lines are quite common and require essentially only proper consideration of joints, whereas

high pressure piping involves strength of materials and special joints to a large extent.

I. Instrument Piping is a major factor in a modern chemical plant. Instruments are very widely used today and will be probably even more so in the future as developments make it possible for them to handle more and more operations that still require human control. Instruments are usually related to each other or to actuating pick-up devices by air piping or "electrical piping". The former is generally handled in copper tubing using compression fittings. These fittings are described in reference (3). Copper tubing or plastic tubing which is coming into more general use are relatively delicate materials when compared to their surrounding water, steam or process piping. Hence it is necessary that they be supported carefully and protected against accidental impacts by operating or maintenance personnel since it is very easy to pinch off or flatten out an instrument line which would make it, of course, inoperable. These lines occasionally must be sloped and are frequently, particularly in the vicinity of panel boards, fairly numerous. Where a number of instrument lines follow the same path, it is sometimes desirable to band them together for rigidity and strength. They are frequently supported by means of inverted angle irons or channels.

J. Manufacture: Pipe is made by a number of different methods as well as from a variety of materials. Iron, Duriron, and concrete pipe are cast, steel pipe may be seamless, welded, rivetted or forged whereas copper, brass and some steel may be drawn.

Lap and butt welded pipes are made from long strips of steel plate or "skelp" as it is commonly referred to. The strips are heated to welding temperature and then pulled through a ring die wherein the pipe is formed and welded simultaneously. The welding pressure is supplied by the equivalent of an anvil inside the ring die. Seamless pipe is made by piercing solid round billets. In rivetted pipe construction the steel plate is spirally wrapped and hence the rivet joint is a spiral one to insure maximum strength and to hold the pipe round.

Drawn pipe is usually made by piercing a solid round billet and the resulting hollow cylinder is drawn or pulled through a series of progressively smaller dies until the desired outside diameter is obtained. Variations in the original wall thickness of the cylinder determine the wall thickness in the final tubing but outside diameter is held constant within commercial tolerances.

Electric resistance or fusion welded pipe is widely manufactured at the present time in both carbon and stainless steel.

Flanges and other fittings are also made by many methods. Forgings are commonly used for carbon steel flanges while welding fittings may be made by reforming short lengths of seamless pipe on a suitable mandrel.

Special pipe materials such as glass, plastic organic materials or vitrified products all have special manufacturing techniques peculiar to their physical properties.

Pipe is frequently coated inside or out, and sometimes both, to obtain additional properties not inherent in the pipe material. Galvanizing, silver lining, stainless or copper cladding, rubber lining or electroplating are examples of coatings. Bitumastic products are frequently used to protect steel pipe from corrosion, particularly in underground installations.

VI. METALLURGY

It has been pointed out previously that pipe line materials include non-metallic, non-ferrous as well as ferrous products. The importance of metallurgy is, of course, primarily one of corrosion resistance and quality of product. This problem is extremely complicated and by the same token extremely important. Many common fluids have been handled a sufficient length of time that the proper materials of construction of pipe lines for them are well known. The characteristics of new materials to be handled in pipe lines must be evaluated in research laboratories to determine the most economical materials of construction. In many cases, the economical material of construction cannot be used because of quality considerations. Many, many products cannot tolerate the trace of some materials which are common to pipe line construction and hence less desirable materials are required. When specifying and purchasing materials for pipe lines it is imperative that trade terminology be used. Throughout industry, for example, A.S.T.M. specifications are well known. Some companies have their own stainless steel specifications. In many cases of special materials the manufacturer's standard manufacturing specifications are used.

The metallurgy and strengths of metals or non-metals underlie all piping codes. These codes specify the temperature and/or pressure limitations for most common piping materials. The American Standards Association referred to hereinafter as ASA, has correlated and established many standards in cooperation with industry and other testing and engineering organizations. These standards recognize different classes of materials with their inherent variations in physical properties and base their requirements accordingly.

Data on codes and specifications are covered by publications of the ASA, American Society for Testing Materials, American Water Works Association, etc. Abstracts of these are readily available in reference (1).

VII. COST

Materials of construction are obviously one of the main cost factors that must be considered by the designers even where quality may be a factor. The use of expensive materials can be kept to a minimum by their efficient use and by that is meant the proper arrangement of equipment within a building to keep pipe line runs as short as possible and with the fewest number of fittings, welds, valves and joints.

VIII. PIPE, VALVE & FITTING DIMENSIONS

A. Dimensions: Since 1939 the A.S.A. Standard which designates pipe wall thickness by schedule numbers has been in effect. In this standard the former terminology of "standard", "extra strong" and "double extra strong" was discarded. "Extra strong" and "double extra strong" were also known as "extra heavy" and "double extra heavy". The schedule numbers as set up by the A.S.A. are an approximation of the value of the expression--schedule number is equal to $1000 \frac{P}{S}$.

The schedule numbers, therefore, represent a rational relationship between wall thickness and pipe diameter. However, in order not to depart too far from the then existing commercial terminology and specifications, some of the schedule number thicknesses were made to agree as closely as possible with these existing commercial sizes. As a result the former designation of "standard pipe thickness" now becomes Schedule 40 in sizes 10" and smaller, "extra strong pipe thickness" becomes Schedule 80 in sizes 8" and smaller. Dimensions and weights for "standard weight" and "extra strong" have been retained in pipe sizes 1/8" thru 3/4" but the terminology was changed to Schedule 40 and Schedule 80. In addition Schedule #10, 20, 30, 60, 100, 120, 140 and 160 have also been listed in some sizes to permit economic wall thicknesses in the larger sizes of pipe.

The dimensions of pipes, valves and fittings is of extreme importance to the designer as he must allow sufficient space for headers, take-offs, valves, special connections, etc., in the area of his equipment. American industry has come a long way toward the standardization of dimensions but there are still one or two glaring exceptions. For example, until recently, there was no industry or association standard for face to face dimensions of stainless steel valves. Most manufacturers were consistent above 2". The stainless steel valve standard for 150 pound valves is known as SP-42 of the Manufacturers Standardization Society of the Valve and Fitting Industry, 420 Lexington Avenue, New York 17, New York. The American Standards Association has correlated and established most of the standard dimensions in use by industry today where piping, fittings or valves are involved. This standardization also affects the equipment manufacturers since in most cases equipment includes companion flanges for the process or service piping. The A.S.A. codes also supply pressure temperature ratings for ferrous pipe materials normally encountered.

In calculating the thickness of pipe wall required for any specific pressure, temperature and corrosive condition, the following formula has been standardized by the A.S.A. and appears in reference (1):

$$t_{min} = \frac{PD}{2S} + C$$

In many cases the value to be used for P is a higher figure than the maximum internal service pressure actually occurring in the pipe, for example, plants may standardize on design conditions of 600 pounds per sq.in., 750°F total temperature for high pressure steam lines where the actual pipe lines pressure may be in the vicinity 525 pounds per square inch, 700°F total temperature. This is done for standardization purposes. In many cases the existing pressure in the line might be quite a bit lower than is planned for the future in which case the larger future pressure is used in the design calculations so that an expensive replacement job is not involved since in most cases the slightly heavier wall thickness indicated for future requirements would increase the original cost by only a few percent. Many large companies today are standardizing on 1, 1-1/2, 2, 3, 4, 6, 8, and 12" pipe mainly to cut down on maintenance stores of pipe, valves and fittings.

Process piping and equipment frequently utilizes what is known as tubing. The diameters and wall thicknesses of tubing may be entirely different for corresponding nominal sizes of pipe. Tubing is normally used in condensers and other heat exchanger equipment and some times for stainless steel lines. The heavier wall construction of the steel standards is normally not required in many processes.

Tubing of thin wall construction has several advantages. Thin walls are imperative where "rolled-in" joints are used as in tubing of condensers since heavy walls cannot be easily expanded into the tube sheet. Thin wall tubing is also used for economy of materials where pressure is not a factor of importance. There are disadvantages, however, particularly with valves in the lines. Valve flanges and openings are all designed for steel pipe sizes. When used with tubing undesirable pockets or lips occur which are subject to severe erosion and corrosion and also prevent cleaning of lines. In some processes pockets of fluids cannot be tolerated due in some cases to settling out of solids or possibly polymerization or other reasons.

To overcome this matching disadvantage the A.S.A. is currently considering the adoption of Schedule 5 pipe which is a thin wall pipe with iron pipe size outside diameter. Many pipe manufacturers have been supplying thin wall pipe to iron pipe size outside diameter dimensions for several years when customers have specifically ordered it.

B. Manufacturing Tolerances: Typical tolerances for seamless steel mechanical tubing are approximately as follows:

Tolerances are applicable only to two dimensions (length excepted) thus if the outside diameter and wall thickness are specified the theoretical inside diameter may not conform to published tolerances. If the outside diameter and inside diameter are specified, the wall thickness may not conform to published tolerances except that the average wall thickness will not vary more than indicated under the permissible variations in wall thickness.

The following table lists a few examples of tolerances:

Size O.D., Inches	Permissible Variations					
	O.D., Inches		I.D., Inches		Wall Thickness %	
	Over	Under	Over	Under	Over	Under
1/2 to 1-1/2 excl.	0.005	0	0	0.005	10	10
3-1/2 to 5-1/2 ex.	0.015	0	0.005	0.015	10	10
5-1/2 to 8 excl. when wall is from 5% to 7.5% of O.D.	0.020	0.020	0.025	0.025	10	10

Food industries use special "sanitary" type fittings for ease in frequent dismantling and cleaning.

The manufacturing tolerances that apply to standard dimensions of carbon steel pipe are illustrative of the type of information that is required as basic data for a pipe designer. Commercial tolerances specify that the minimum wall thickness at any point shall not be any more than 12.5% under the nominal wall thickness. The nominal wall thickness is that thickness given in the A.S.A. standards. For pipe 2" and over in nominal diameter the outside diameter shall not vary more than 1% over or under the standards specified. ASTM designation A-106 is widely used carbon steel pipe of either lap welded or seamless steel manufacture. In addition to the above tolerances the actual weight shall not vary by more than 3.5% under and 6.5% over nominal weight of Schedules Nos. 10 to 120.

Glass tubing has become fairly common in industry today as its mechanical properties and provisions for assembling have been greatly improved. Any person contemplating an installation of glass piping are advised to secure first-hand detailed information direct from the manufacturer, although the following data are typical of the tolerances involved:

Size OD mm	Total Variation OD + or - mm	Absolute Wall Thickness mm	Approx. lbs/ft.
3	.55	.6	.0068
12	.62	1.0	.052
25	1.05	1.5	.166
51	1.60	2.0	.46

Many other diameters are, of course, available but the standard length is 4 feet according to manufacturers information.

C. Flanges: It is common practice in industry today in carbon steel piping to use screwed connections up to and including 1-1/2" and sometimes up to 2-1/2" and normally using flanged connections from either 2" or 3" up. The types of flanges available are fairly numerous but their designs are not competitive, by that it is meant that design of flanged connections vary with increasing fluid pressures. The A.S.A. have standardized dimensions on flanges for nominal ratings of 150, 300, 400, 600, 900, 1500, and 2500 pounds per square inch. The nominal service pressure rating so designated means the allowable working pressure at 750°F at the pressure rating indicated with the exception of the 150 pound rating which is at 500°F. The allowable working pressure increases with a reduction in temperature and vice versa. The A.S.A. bulletins and up-to-date handbooks list these service pressure rating tables for commercially available materials. Figure 1 indicates typical flange facings which are commercially available. The most commonly used flanged connection is the raised face type using either a welding neck flange or a lap joint flange. The lap joint flange is advantageous for two main reasons --one, there is no difficulty in alignment of bolt holes when installing piping as the flanges are free to rotate and hence can be easily matched; two, when using expensive materials the backing flange is made of ordinary carbon steel which results in appreciable dollar savings.

D. Bolts, Nuts and Gaskets: In addition to specifying the pipe, fitting and flange materials required it is also necessary to specify the bolts and nuts and gasket material to be used in all joints. Consult reference (1) for information on steel bolts and nuts for various pressure and temperature services. The choice of gaskets is wide and in general is determined by the material being handled in the pipe line and cannot be generalized.

E. Valves: All piping systems include valves. Valves are of every conceivable type and design and are made from hundreds of different materials. The most common types of valves are gate, globe, angle, check and plug cock. Most other valves are variations in design to these basic types due to special materials of construction which are not suitable for standard manufacturing thickness and other specialities to achieve certain valve actions which are of a specialized nature and not commonly required.

A gate valve is simply a stop or shut off valve and consists of a single or double disc lowered into the fluid stream by means of a threaded stem in the bonnet of the valve. Gate valves should be used only as shut off valves and should never be used in throttling service. A globe valve is primarily a conical or spherical plug lowered into a horizontal round opening within a valve to achieve a grinding action of the plug on the seat and hence secure a tight shutoff, whereas the gate valve has a sliding action of the disc on the seat. Globe valves are used principally as regulating valves. Angle valves are a fundamental adaptation of the globe valve but the fluid makes a 90° change of direction in the valve whereas it has a reasonably straight-thru flow in a globe valve. Check valves consist of a valve body usually with a hinged disc in the valve so that the flow can readily pass thru in one direction but cannot reverse its flow. These valves are used primarily on pump discharges to prevent back flow thru the pump. Back flow thru a pump under certain hydraulic conditions might cause the pump to run faster than the speed for which it was designed and actually explode. The normal use, however, is to prevent back flow of material for process reasons rather than for physical protection of the pump.

Plug cocks are another type valve in very common usage. These valves consist of a body with a tapered cylinder which rotates inside the body. This cylinder has normally a straight-thru hole in line with the inlet and outlet of the valve so that when open the fluid has a straight-thru opening. It is closed by rotating the cylinder 90° which forms a solid stop for the fluid. The plug cocks have the major advantage of having absolutely no internal pockets or space in which the fluid flowing can settle out or cake inside the valve. Therefore, it is widely used in slurry lines and other uses where fluid pockets cannot be permitted in the pipe line. Other types of valves less commonly used are pinch type, needle, gage glass and "Y" valves. All valves incorporate variable mechanical features such as packless types, outside screw and yoke versus inside screw rising stem, flanged, screwed, hub ends, socket welding ends, fusion welded ends, bolted bonnets, union bonnets and other variation to achieve specific features necessary to meet certain operating conditions. Naturally, with all the variations possible opinion and human judgment enter very strongly into the actual selection of the details of any valve. Manufacturers valve catalogs are excellent reference material on this subject for those interested in a more detailed analysis of valve specification and uses.

IX. DESIGN

A. General Arrangement: The many physical parts that comprise piping system have been previously discussed. In the actual design of a piping system these elements plus many others must be considered. Before starting an actual piping layout on the drawings considerable study must be given to the chemical and physical arrangement of the respective pieces of equipment which the piping system

is to tie together and their relative location to each other in both a horizontal and vertical plane. Additional consideration must be given to the allocation of space for operating aisles, instrument control boards or central control rooms, electrical control rooms, on-the-job laboratory facilities for frequent checking of chemical reactions, ready access to stairwells in case of fire, etc. The accessibility of equipment for maintenance must also be carefully considered as good design must not so surround the particular piece of equipment with piping so that a large amount must be dismantled before a high maintenance piece of equipment can be removed.

The basic principles of piping layout should be simplicity of design, safety considerations for operation, operating accessibility, ease of maintenance, and due consideration of special factors applicable to specialized processes or materials of construction. Process piping should be given priority for location in any manufacturing building to permit short runs and hence lowest material and construction cost, to maintain adequate head room over passageways and to provide convenient and accessible locations in the lines for operating valves and instruments.

B. Route: Once the general arrangement of equipment has been established the designer roughly determines the number and size of lines to be run in any particular portion of the building and plans the space in which these lines will be run to provide the design elements previously described. Some piping systems within a building where the piping is complex are set up on a so-called lane system which allocates certain definite locations for piping, for example, all north-south lines may be specified to run between a certain pair of columns and within a space of 2 feet immediately below the ceiling of one or more floors. The east-west lines are so allocated between another pair of columns at 90° to the first pair. The vertical lines would probably be allocated to one or more wall areas and kept within 1 or 2 feet of the wall itself. Such a system may at times involve slightly longer runs of piping, but good design, low construction cost and low maintenance cost are achieved as a result of careful planning. Where only a moderate amount of piping is involved, this relatively extreme degree of planning is not necessary but consideration must still be given to good design practice.

Outside the building for lines running to an adjacent building, tank farm, or to car loading or unloading locations similar problems exist. The route of the outside line must therefore be considered with relationship to existing plant practices as relating to space allocations or head room clearances, future utilization of the plant property, etc. Outside lines vary greatly in height. Obviously the cheapest installation is to run the lines on blocks of concrete or similar material a few inches above the ground. However, this prevents the crossing of the lines by pedestrians, cars, trucks, or railroads. Common practice is to elevate the lines so that they have an 8 foot clearance in areas where personnel walk, 12 foot clearance thru manufacturing areas to allow for maintenance handling of normal size equipment under the lines, 15 foot clearance over roads for general plant traffic, and as much as 22 foot over railroads to clear a man standing on top of a box car.

In planning outside lines consideration must also be given to the number of lines involved. A single pole line will normally support 5 or 6 medium size lines. If the number of lines is in the neighborhood of 15-20 a double pole support would normally be required and if even more lines are involved an actual bridge structure is the most economical support. Double pole supports or bridge supports usually require at least a 10 foot wide strip of land which is not usable for any other purpose as it is normally unsafe for people to walk or work under lines containing chemical fluids as a leak might be extremely hazardous.

C. Size: The selection of the proper size pipe to be used is also one in which a number of factors must be considered. Some of these factors are:

1. Economic diameter based entirely on cost of material, power, installation costs and return on investment.
2. Sizing pipe to maintain higher than normal velocity to prevent slurries from settling out in the pipe line.
3. Larger lines than otherwise required on pump suctions to alleviate the possibility of flashing or cavitation.
4. Larger than normal lines to realize low velocities in downcomers from condensers, etc., to permit bubbles of occluded vapors to work back up the pipe.
5. Extremely high velocities to increase pressure drop so as to dissipate excess pressure or to let down from a high pressure to a low pressure.
6. Larger diameter than ordinary required so that the pipe can span longer distances to minimize the cost of supporting the pipe.

Appendix A of this Section is a reprint of a paper "Fluid Friction in Conduits" by R. P. Genereaux*

* Published in Chemical and Metallurgical Engineering, Vol. 44 241-48, May 1937 and copyrighted by the McGraw-Hill Publishing Company, New York, New York. Reproduced herein with their permission.

in which is included derivation of Equation 19 to permit the selection of pipe diameter on an economical basis so that the total annual cost of owning and operating the fluid handling system will be a minimum. Figure 4 shows the equation converted to a convenient chart. It has been common practice in the past to pick a certain design velocity and to install a pipe of such size as to give this velocity. However, when turbulent versus viscous flow is considered it can be readily demonstrated that there is no one economic velocity. Mr. Genereaux' paper considers the initial cost, depreciation, and maintenance cost of pumping or blowing but does not consider allowances for a return on the investment nor includes a provision for Federal income taxes. These last two items are substantial today and should be considered in any economic calculations. The basis of the formula is the relation of investment costs, maintenance, etc., to the diameter of the pipe. For additional information consult a paper by Sarchet and Colburn, reference (4). Mr. Genereaux primarily covered turbulent flow, whereas Sarchet and Colburn have covered viscous flow.

The proper spacing of outside line supports requires some analysis but in general it is not economical to run a single pipe line less than 3 inches in diameter on poles spaced 20 feet apart. On this basis a 4 inch pipe would span 25 feet and a 6 inch, 30 feet.

D. Valves and Fittings: The designer must choose, with the basic data at hand for his specific job, the type flanged joints, valves and fittings and their materials of construction that are to be used.

E. Insulation: In these notes it is not the intention to discuss types of insulation but merely indicate that many lines must be insulated and hence the thickness of the insulation where required must be considered in laying out pipe lines for accessibility, ease of maintenance, clearances, and supports.

F. Supports and Anchors: The designer all too often passes the buck on the pipe supports and leaves this complete item to the construction engineer, who is responsible for the installation of the equipment and the piping. In many cases this method is entirely satisfactory as the lines do not have appreciable expansion nor other characteristics which set them apart. Steam lines or hot process lines must be designed to either have inherent flexibility or to actually incorporate expansion loops or joints in their runs. Lines subject to appreciable expansion must also be adequately anchored at certain intervals so that the expansion joints function properly. Inherent flexibility can be designed in the piping systems by the inclusion of right angle bends in at least two directions. A wrought material ell with a straight run on either side has a certain amount of flexibility for springing which can readily be calculated and in most cases is adequate to take care of the expected expansion. Extreme care must be taken that the stresses set up in a pipe system due to expansion are not transmitted to the nozzles on the pieces of equipment being connected by the piping. The magnitude of these stresses or forces is sufficient in many cases to distort or actually break these nozzles. In the case of pumps the force may be sufficient to cause the rotating shaft to bind or cause the packing to wear out very rapidly and cause excessive maintenance. It is suggested that those interested in studying this phase of pipe design in detail consult reference (1) for preliminary information and additional references on this highly technical but important phase of work.

G. Valves: The selection of valves in general can be made from information previously described in these notes. The choice of gaskets between flanges in addition to valve bonnet flanges and valve packing are dependent mainly upon the corrosive or other properties of the fluid being handled.

H. Fire and Safety: Fire and safety precautions must be designed into any good piping system. Acid lines are notoriously hazardous and unusual precautions must be taken for the more corrosive ones. These precautions usually take the form of installing the line in such a location that a leak is less apt to strike a worker. Flanged joints, valve packings, etc., which are common sources of leaks are shielded so that when a leak occurs it will not spray out over a large area but will be confined to a small space. The degree of fire protection is dependent upon the inflammability of the fluid but the usual precautions usually consist of design that will insure a tight system and depending on maintenance to detect any probable leaks due to corrosive attack of the pipe walls. This is normally accomplished by routine inspection of the line so that the line may be replaced before a failure actually takes place.

I. Specifications: A very fundamental part of the design of a piping system is the writing of specifications wherein are set down the requirements which the designer has incorporated on his drawings. These specifications are a written description of the properties of pipe, fittings, valves, insulation, supports, flanges, gaskets, etc., of his system. They are necessary so that the people responsible for the procurement of these materials secure the correct items and for the guidance of the construction forces so that they will not install other than specified materials in any one line. These specifications must incorporate and recognize commercial standards both physical and metallurgical wherever possible. Naturally, an economical piping system should not contain any special materials or items if possible.

However, corrosive or quality considerations frequently require special materials in which case standard dimensions should be adhered to. In any type of business specialities are extremely expensive as compared to the standard products.

X. FABRICATION AND ERECTION

When the designer has completed his piping drawings, incorporating all the features described in Paragraph IX, he has completed what are known as "Piping Arrangement Drawings", which are two dimensional plans and elevations showing the location of the piping within a building and its relation to the equipment and building proper. It is generally customary to dimension the location of these lines for all pipe 2" and larger.

The next step in the development of an economical piping system is the preparation of detail piping drawings, which can be made on two different bases--one, detail drawings prepared from the piping arrangement drawings; second, detail drawings made in the field by field measurements taken from one piece of equipment to the other by a field selected route but guided by the route shown on the piping arrangement drawing. Industrial practice varies widely. Many companies prefer to make piping details in the field so that exact dimensions are obtainable whereas some companies have always prepared details before actual dimensions were available with allowances for field fit. It is impossible for any construction crew to erect a building and install major equipment to exact dimensions. In normal practice variations of not more than 1/4" are considered excellent. This is not intended as a reflection on construction personnel but merely reflects the accumulated tolerances of the concrete foundations, steel work, concrete floor, variations in vendors equipment from their drawings and many other factors. The attitude of union officials in the crafts involved have discouraged the use of regular pipe fitters for dimensional take-off work in the field. It is therefore becoming more desirable to prepare pipe details in the design sections rather than in the field.

Pipe detail drawings may be of two general types--(1) two dimensional type drawings, (2) isometric drawings. These drawings are, of course, prepared for prefabrication or shop fabrication of piping in order to achieve the lowest installed cost. The tendency or trend is now to the use of isometric drawings for shop fabrication as well as field erection of piping. These are always made from the theoretical viewpoint of the observer looking down on the piece of pipe. When a particular piece of pipe has been suitably marked with identifying symbols, it can be easily erected in the field using the main piping arrangement drawing as a guide to the basic arrangement. The size of any piece of fabricated piping is dependent only on the limitations set by railroad car shipping facilities or erection clearances.

High temperature lines as previously mentioned must include provisions in their design for expansion and anchoring. It is necessary to supply the construction personnel with the necessary information so that they can properly install these lines. For example, it is possible by cold springing a high temperature line during erection to reduce the maximum stress in its fully expanded position by approximately one-half. By cold springing is meant installing the line, naturally at atmospheric temperature, in a stretched condition by deliberately pre-stressing the pipe in an opposite direction in which the expansion stress will take and hence the resultant stress under the fully expanded conditions is approximately one-half the normal amount.

XI. CLEANING AND STERILIZATION

It is customary that all fabricated piping either shop or field be adequately pickled and cleaned before installation. The same applies for all fittings. Valves should be carefully examined and cleaned. After erection the completed line should again be cleaned. Normally this is done by flushing carefully or blowing out with steam and where necessary followed by air to leave the line in an absolutely dry condition where water is undesirable in the fluid being transported in the line. The purpose of the pickling and cleaning is first to loosen and remove mill scale from the inside of the steel pipe to prevent the same scale from contaminating the process fluid or lodging in valves or small openings in the pipe after operation has been started, and, second, to insure that foreign matter that might get into the pipe during erection is removed prior to use of the pipe.

It is customary and frequently mandatory to sterilize drinking water lines before they are put into service. The requirements vary from state to state. In general, sterilization consists of filling the lines with water containing from 50 to 200 parts per million of chlorine and leaving the chlorinated water in the line from 24 to 48 hours. A small flow should be maintained during this period to insure uniform sterilization of the entire line. Chlorine gas is normally less expensive for large systems whereas calcium or sodium hypochlorite is more economical as a source of chlorine for sterilization of small systems.

Precautions should be taken when the line is laid to keep it clean and free from contaminants and

nuisances and to use pre-sterilized packing. Some packings are almost impossible to sterilize after installation.

After sterilization the line is thoroughly flushed and then may be put into service. Drinking water lines should never be cross-connected at any point with non-chlorinated water, otherwise the drinking water may become contaminated.

XII. TESTING

It is customary to subject all fabricated piping to a hydrostatic test before erection to determine if there are any defects in the materials or workmanship. The A.S.A. Code for Pressure Piping describes the technique to be followed. Some companies adopt the practice of testing process piping to double the system design pressure after fabrication and to 1-1/2 times the system design pressure after erection. The test after erection normally cannot be as high as the original test pressure without damage to the gaskets or bolting of the flanges. Service piping is tested after erection in accordance with the A.S.A. Code for Pressure Piping. It is customary to conduct all these tests with water although occasional exceptions are made whereby the lines are tested with gas or air. Air or gas testing may be hazardous and should not be specified unless absolutely necessary and proper precautions are made in the event of a failure. Underground lines are customarily hydrostatically tested before back filling the excavation so that if leaks occur they are easily located and the expense of re-excavation obviated.

XIII. SAMPLE PROBLEM

A sample problem, Figure 2, has been drawn up to attempt to illustrate some of the design elements which have been included in these notes and to show in a simplified manner the application of these elements.

It is assumed that a batch tank is located on the second floor of a new building. The process material is to drain by gravity from the batch tank to a pump located on the ground floor from which it is pumped through a filter, also on the ground floor, to a group of four tanks located approximately 80 feet from the building. The process liquid has a freezing point of 20°C, a viscosity of 5 centipoises, a temperature of 30°C and a specific gravity of 1.0. The pumping rate is 10 gallons per minute, the pressure drop through the filter is 10 pounds per square inch, steel construction is adequate and the plant location is New England.

The piping shown on Figure 2 is designed in this fashion to minimize length of runs, maintain headroom, keep working space clear, slope lines for drainage and follow lane allocation. Valves are all accessible for easy operation.

At the flow rate specified which is equivalent to 5000 pounds per hour, Mr. Genereaux' Figure 4 indicates an economic inside diameter of approximately 1.3 inches. The nearest larger commercial pipe size is 1-1/4 inches which has an inside diameter of 1.380 inch in Schedule 40 pipe. If this plant, for standardization purposes to achieve lower maintenance costs, does not use 1-1/4 inch pipe then 1-1/2 inch should be specified by designer.

The increased cost of 1-1/2 inch over 1-1/4 inch might possibly be in the ratio of 84 to 72 but under certain circumstances, as mentioned above, can be economically justified.

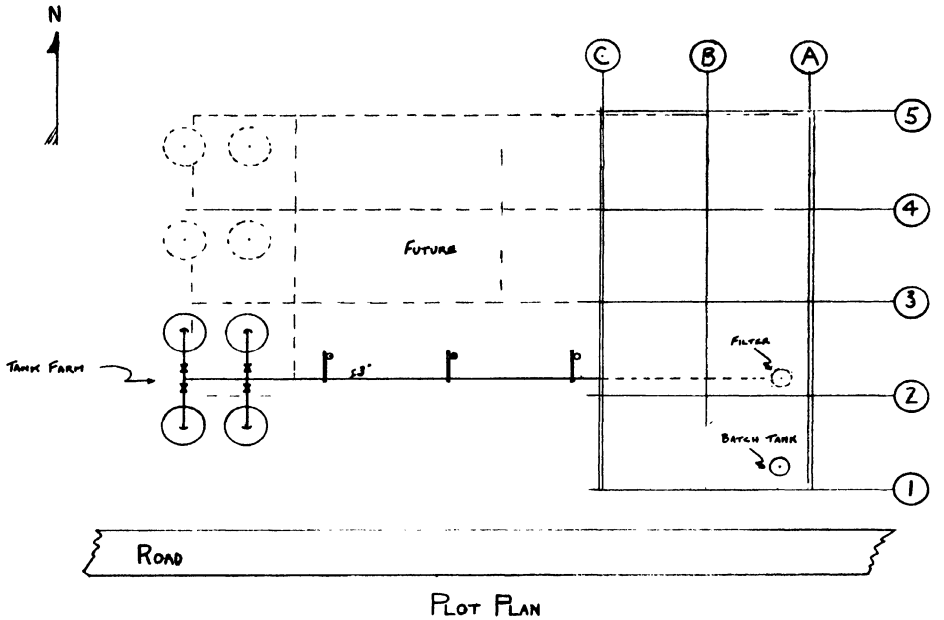
Outside the building, 3 inch size should be specified to achieve economical outside line construction cost. The location is obviously through a future manufacturing area so that 12 foot clearance to the bottom of the pipe would be specified.

As previously pointed out the 1-1/2 inch portion of the line would have screwed connections, valves and fittings and the connections at the tank farm should also be 1-1/2 inch. The intermediate section will be 3 inch using 3 by 1-1/2 inch welding reducers for the transition.

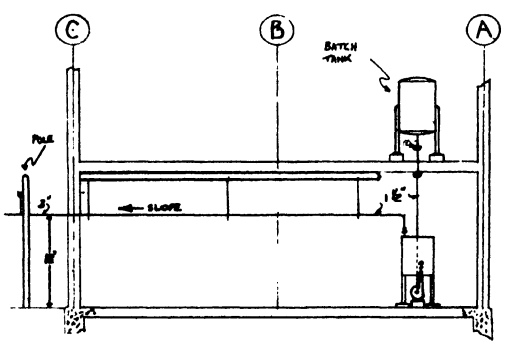
The selection of the valves indicated is based on the use of a shutoff valve at the tank while a batch is being prepared, a shutoff valve on the pump suction in case pump or filter need cleaning during cycle of operation, a check valve on pump suction to prevent back flow temporarily and a gate valve for permanent shutoff, and distribution valves at tank farm. Valves would be specified as 150 pound per square inch A.S.A. rating steel valves.

XIV. PROBLEMS

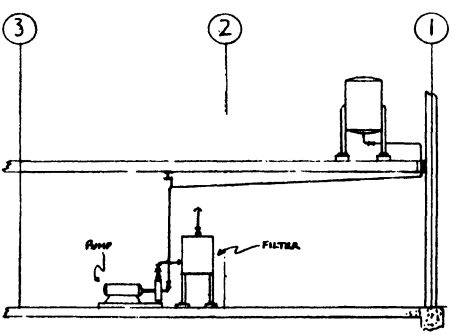
1. What is the economical inside pipe diameter for a liquid having a specific gravity of 1.0 flowing at a rate of 10 gpm?
2. What standard pipe size would be specified for flow conditions in problem 1?
3. What are the advantages of lap joint flanges?



PLOT PLAN



SOUTH ELEVATION



WEST ELEVATION

Figure 2.

4. What size pipe and what height would be used to carry a flow of 10,000 pounds per hour over a railroad track?

5. Assume a pipe line from a ground floor storage tank to a transfer pump to a weigh tank on the fourth floor. Specify line sizes for a flow of 15,000 pounds per hour of clear liquid and describe type of valves to be used at pertinent points?

6. What is the major design problem difference between a water line and a steam line?

7. Prepare a brief specification for a drinking water system with a flow capacity of 5 gallons per minute.

8. Describe "schedule" system of identifying wall thickness of steel pipe.

APPENDIX A

Fluid Friction in Conduits

By RAYMOND P. GENEREAUX

DESIGN ENGINEER, ENGINEERING DEPT.
E. I. DU PONT DE NEMOURS & CO.,
WILMINGTON, DEL.

AMONG THE UNIT OPERATIONS of chemical engineering, probably the most consistently present, and therefore generally most important is the flow of fluids. The economics of the flow of fluids is of great and frequent application to industrial processes.

The selection of the diameter of pipe for greater economy under given flow conditions is often made by considering arbitrarily a narrow range of velocity as the optimum. This "velocity method" is generally and approximately correct for such commonly encountered fluids as water, air, and steam. The application of this "velocity method" to other fluids may cause erroneous results and so cannot be recommended for general or promiscuous use.

The purpose of this article is to simplify certain problems of fluid flow by offering rational formulas based on fundamental principles. In addition, a rational method for determining the economic size of pipe for given conditions will be described.

In the majority of cases encountered in plant design, the requirements of accuracy are governed by certain conditions, some of which are enumerated below. Commercial pipe and tubing are fabricated in certain standard inside diameters. It will be demonstrated later that it is economical to select an actual pipe size larger than the accurately calculated size, rather than one smaller. It is rare in plant operation that flow conditions are known with great accuracy. Consideration of these conditions leads to a conclusion that in most plant design problems, *there is more to be gained by being on the economical and "safe side" than to strive for great accuracy.*

Attaining desired results in engineering design is based upon intelligent use of the available information. In the field of fluid flow we have at our disposal the results of many theoretical and experimental investigations which, when properly applied, enable us to solve most of our problems with a minimum of error. Flow phenomena may be completely expressed in mathematical form when the data fully substantiate the theory, all the variables concerned having been considered. When the theory does not fully substantiate the data, rational methods of correlating the data are used to obtain the most adequate equations pending complete reconciliation with theory.

That portion of the subject of fluid flow which deals with steady (constant weight rate) flow in conduits is the most common in chemical engineering design. It is more fully understood when approached from the fundamental viewpoint which considers all the variables; the resulting methods are applicable to all fluids.

Reynolds Number and Friction Factor

The greatest impetus was given to this subject by Osborne Reynolds in 1883. His investigations of flow in cylindrical conduits demonstrated two types of flow, commonly designated as viscous (or laminar or streamline) and turbulent, separated by a "critical region." By means of dimensional analysis he derived a law of similarity which expresses the fact that flows in geometrically similar vessels are mechanically similar when they have the same value of $DV\rho/\mu$, a dimensionless relationship, now called the Reynolds number. By plotting a sufficiently wide range of pressure drop data on logarithmic coordinates with Reynolds number, Re, as the abscissa and the friction factor, f, as the ordinate, the types of flow mentioned above are indicated graphically, as in Fig. 1. The friction factor is also a dimensionless group in the form

$$f = 2gD\Delta P/4\,L\rho\,V^2 \qquad (1)$$

For Reynolds numbers below about 2,000, the data fall on a straight line with a slope of minus one. This is the viscous region. The relationships involved were determined independently by Hagen and Poiseuille in 1839 and 1840, respectively. (This relationship is variously called Hagen's law, Poiseuille's law, and more correctly the Hagen-Poiseuille law.) It is independent of pipe wall roughness but holds for circular pipe only. It can be stated as

$$\Delta P = 32\,\mu LV/gD^2 \qquad (2)$$

and can be obtained from Fig. 1 by substituting for f in Equation (1) its value

$$f = 16\,Re^{-1} = 16\,\mu/DV\rho \qquad (3)$$

which states mathematically the viscous line, A, of Fig. 1. The substitution results in

$$2gD\Delta P/4L\rho\,V^2 = 16\,\mu/DV\rho$$

and by simplifying and solving for ΔP, Equation (2) is obtained. This equation can also be derived from Newton's differential expression for viscosity".

By referring again to Fig. 1, it can be seen that the values of f increase as the Reynolds number increases from about 2,000 to about 4,000. This Reynolds number range is known as the "critical region" or "transition region". No attempt is made to formulate any relationship for this region because it is normally narrow in extent, its values depend upon pipe entrance conditions, and vibration of the pipe tends to accelerate the transition from viscous flow. Under the usual plant conditions it is safe to assume it part of the turbulent region. The term "critical velocity" is generally understood to mean that average linear velocity above which a given fluid at a given temperature and pressure, flowing in a given apparatus, will move in turbulent flow.[1]

As the Reynolds number increases above the critical region the flow becomes turbulent and the values of f decrease, but at a more gradual rate than in the viscous region. The resistance to flow becomes dependent also upon the pipe wall roughness. A considerable quantity of pressure drop data on flow in the turbulent region has been published and when plotted on the friction factor versus Reynolds number basis, present what at first glance appears to be a maze of points. When segregated according to a measure of pipe wall roughness, some semblance of order emerges.

The values of f for data on the so-called "smooth pipe," (made of materials such as glass, lead, copper, brass, i.e., most drawn tubing) fall in a narrow band that is within ±5 per cent of curve B in Fig. 1, which can be expressed by the formula

$$f = 0.00140 + 0.125\,Re^{-0.32} \qquad (4)$$

which was obtained by Drew, Koo, and McAdams[3] from their plot of 1,328 points over the extremely wide Reynolds number range of 3,000 to 3,000,000.

The data on clean "commercial pipe" (iron and steel) lie above those for smooth pipe and form a band that is within ±10 per cent of curve C, Fig. 1, which Drew, Koo, and McAdams expressed by the formula

$$f = 0.00307 + 0.1886\,Re^{-0.32} \qquad (5)$$

Essentially the same data on commercial pipe were analyzed by Pigott[2] and Kemler[4]. They segregated the friction factor *vs.* Reynolds number data into several pipe diameter groups and plotted them separately. After weighting the points on the separate plots and selecting mean curves for each, they assembled them on one sheet and found they had a family of curves in general similar to curves B and C, Fig. 1. The top curve was for the smallest diameters, the others ranging down toward the largest diameters. Their analysis indicated that small pipes are relatively more rough than large pipes. The data used, however, are from many investigators during a long period of time, and the pipes being compared inherently differed in roughness regardless of diameter because they were fabricated under a variety of conditions. Their analysis does not adhere strictly to the requirements of geometric similarity but it does serve as an indication of variation of roughness with pipe diameter. There are reliable data

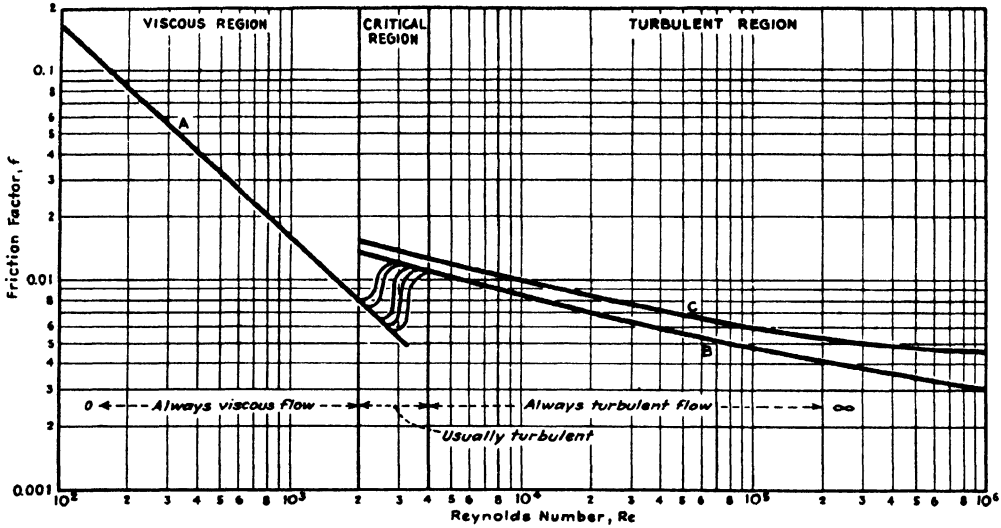


Fig. 1—Friction factor curves for viscous and turbulent regions; Curve (*B*) is average for "smooth pipe," Curve (*C*) averages data for "commercial pipe"

which do not fit into their family of curves.

There are also data on old, tuberculated, corroded, or eroded pipe, and on artificially roughened pipe. The friction factor curves obtained from these data lie in general above those for "commercial pipe".

The problem which now arises is: What friction factor data are we to use in our calculations of pressure drop, pipe diameter, flow rate, etc.? Obviously, we should be guided by the problem, the kind of pipe, the accuracy required, and the time available for obtaining the desired results. The most accurate method is to use data obtained on the kind of pipe and the diameters to be used. Such data are rarely available; pipe manufacturers have an excellent opportunity to assist in this by collaborating on a program of properly directed research. Our present alternative is to select the data which most nearly approach the conditions involved.

Let us advance first to the methods of calculation with which these friction factors are used and then discuss their selection. Consistent units will be used, e.g., all terms will have the units of feet, pounds, seconds. Later the equations will be stated in units more commonly in use by American engineers.

The fundamental equation for pressure drop due to friction is that derived[3] from Bernoulli's Theorem. The following form is generally called the Fanning Equation:

$$\Delta P = \frac{4fL\rho V^2}{2gD} \qquad (6)$$

When this equation is solved for f, the friction factor, we obtain:

$$f = \frac{2gD\,\Delta P}{4L\rho V^2} \qquad (1)$$

which is identical with Equation (1), which was the form used to determine f from actual data, and then plotted against the Reynolds number. To determine the friction loss in any pipe, the Reynolds number is calculated according to the equation:

$$Re = \frac{DV\rho}{\mu} = \frac{DG}{\mu} \qquad (7)$$

and the value of f corresponding to it is selected from the friction factor plot and substituted in Equation (6). This method permits the selection of whatever friction factor curve best fits the kind and roughness of pipe, regardless of the flow region involved.

Since kind and roughness of pipe are not involved in the viscous region, i.e., a single friction factor curve suffices, that curve can be expressed mathematically as

$$f = 16\,\mu/DV\rho \qquad (3)$$

and substituted in Equation (6) to obtain

$$\Delta P = \frac{32\,\mu LV}{gD^2} \qquad (2)$$

as stated above. This equation can then be transposed into any desired form, e.g., to solve for velocity:

$$V = \frac{gD^2\,\Delta P}{32\,\mu L} \qquad (8)$$

In the turbulent region, however, the conditions are not so simple. Many friction factor curves exist, due to roughness. As stated above, we can use Equation (6) and the most adequate friction factor curve. But when calculating pipe diameter, with known values of rate of flow, fluid density and viscosity, and pipe length, the Reynolds number cannot be calculated, and hence the friction factor cannot be determined. If the friction factor chart is to be used in these cases, the problem must be solved by trial and error, i.e., solving several times by assuming values of diameter until the correct answer is obtained. This same condition exists when solving for rate of flow. When strict accuracy is required, this is the most adequate method. However, in view of the conclusion drawn in the introduction that "There is more to be gained by being on the economical and 'safe side' than to strive for great accuracy," and because most of the pipe selected for plant installation falls in the "commercial pipe" class, use of friction factors on the "safe side" of the band of commercial pipe data will give adequate accuracy for the usual design problem.

In Fig. 2, the shaded area indicates the band of data on commercial pipe as plotted by Drew, Koo, and McAdams[4] and many more points[5] extending the Reynolds number range up to about 20,000,000. The points are for pipe

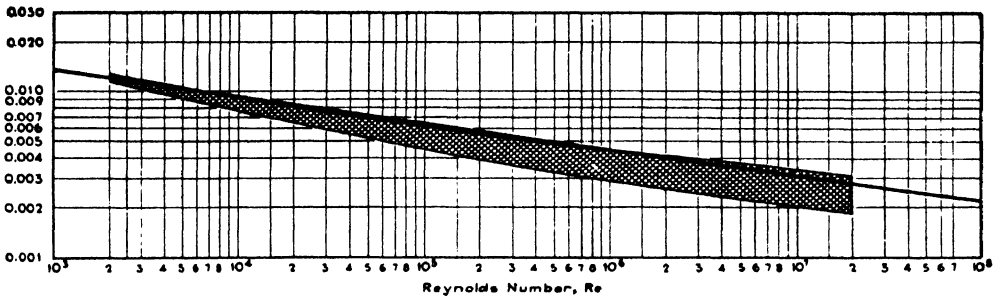


Fig. 2—Straight-line friction factor plot which gives "safe-side" results with commercial pipe, superposed on a data band bounded by Curves (*B*) and (*C*) of Fig. 1

diameters ranging up to 14 ft. in diameter. It is possible to express the mean curve, or the upper border curve, by an equation for f in terms of Re similar to Equation (5), i.e., in a mathematical expression of additive terms. Substitution of this expression in the Fanning Equation (6) would result in a cumbersome equation.

However, a simpler method is to express the data by an equation of a straight line in the same mathematical form as Equation (3). Substitution of this expression in the Fanning Equation would result in a single equation for all fluids in turbulent flow in commercial pipe. Error enters in fitting such a straight line to the shaded area, but in view of the simplicity of the resulting equation, and the retention of economic conditions in being on the "safe side", the following line was selected:

$$f = 0.04\,Re^{-0.16} = 0.04\,(\mu/D\,V\rho)^{0.16} \qquad (9)$$

and its position relative to the shaded area is shown on Fig. 2. (For the actual fitting of this line to the data, see Genereaux[8].) Substitution of this equation for the friction factor line in the Fanning Equation gives

$$\Delta P = 0.00249 L\,\mu^{0.16}\,\rho^{0.84}\,V^{1.84}/D^{1.16} \qquad (10)$$

which can be rearranged to solve for any of the variables involved.

Summary of Equations

Equation (2) is for the *viscous region*. It is stated in consistent units, any set such as ft., lb., sec. (or cm., gm., sec.) can be used. In certain commonly used (but not consistent) units, the equation is

$$\Delta p = 0.034 LZm/\rho\,D_i^4 = \text{lb. per sq. in.} \qquad (11)$$

It is exact for all circular pipe irrespective of wall roughness. It can be seen by inspection that the pressure drop varies directly with the viscosity, pipe length, and weight rate of flow, and inversely as the fourth power of the diameter. It can be used safely up to a Reynolds number of 2,000—in the units stated in Equation (7).

Equation (10) is for the *turbulent region* and is also stated in consistent units. In certain common units, the equation is

$$\Delta p = \frac{0.1325\,L\,Z^{0.16}\,m^{1.84}}{\rho\,D_i^{4.84}} = \text{lb. per sq. in.} \qquad (12)$$

It is intended for use in plant design problems when extreme accuracy is not required. The results obtained by its use are on the "safe side" of what might occur in commercial pipe over the entire turbulent region for which data are at present available, i.e., up to $Re = 20{,}000{,}000$. It is valid for all Newtonian fluids in steady flow (constant weight rate). Newtonian fluids are those whose values of shearing stress are directly proportional to the rate of shear. They include all the gases and most of the common liquids. Examples of "liquids" which are non-Newtonian are suspensions and plastic liquids, see Perry[1], page 1271.

Special Cases

In non-isothermal flow of liquids there is a temperature gradient between the tube wall and the main stream of the liquid. It is necessary to use some average temperature in evaluating the viscosity. Sieder and Tate[10] correlated pressure drop data taken under conditions of heating and cooling. The terms used were: μ_a = the viscosity at the main stream temperature, and μ_w = the viscosity at the tube wall temperature. With Reynolds number calculated as DG/μ_a, they suggested the following factors:

Viscous region: Multiply f by 1.1 $(\mu_a/\mu_w)^{0.25}$

Turbulent region: Multiply f by 1.02 $(\mu_a/\mu_w)^{0.16}$

For isothermal flow of gases, the arithmetic mean density is used when the pressure drop does not exceed 10% of the final pressure; see Perry,[1] page 721. When the pressure drop is large and one of the end pressures is unknown, the following equation may be used:

$$p_1^2 - p_2^2 = \frac{518\,T\,L\,f\,m^2}{(m.w.)\,D_i^5} \qquad (13)$$

For non-isothermal flow of gases when the pressure drop or temperature change is large, a kinetic energy correction may be made by adding algebraically Δp_k, Equation (14), to the pressure drop calculated by Equation (12) in which average values of density and viscosity were used.

$$\Delta p_k = \frac{0.0042\,G^2\,T_{av}}{(m.w.)\,p_{av}} \times \left(\frac{T_2 - T_1}{T_{av}} + \frac{p_1 - p_2}{p_{av}}\right) = \text{lb. per sq. in.} \qquad (14)$$

If Equation (12) were used in problems on "smooth pipe", the calculated pressure drop would be too high. (The error would range from zero at $Re = 3{,}000$ to 50 per cent at $Re = 3{,}000{,}000$.) If it were used in problems on very rough pipe, the resulting pressure drop would probably be too low (pipe may become tuberculated and the actual diameter decreased, or it may become corroded and the actual diameter be increased).

Nomographic Chart for Flow

Equation (12) can be adapted readily to a nomographic chart which affords rapid calculations, and by including density and viscosity data, it can be made independent for solving the majority of problems. The effect of altering the value of any variable can be determined quickly. It also makes unnecessary the solution of fractional exponents which to many engineers are time consuming. Fig. 3 is based on Equation (12). The same type of chart has been published previously.[3,12,6] It has been revised to conform with new friction factor data,[9] and additional points for fluids have been added by the use of a more convenient grid method.

The chart consists essentially of scales for actual inside pipe diameter, D_i; weight rate of flow, m; pressure drop per ft. of pipe length, $\Delta p/L$; and a kinematic viscosity, $Z^{0.16}/\rho$. A scale of mass velocity, M, has been added to permit its determination and provide for using it with D_i or m when m or D_i, respectively, is unknown.

PIPE FLOW CHART

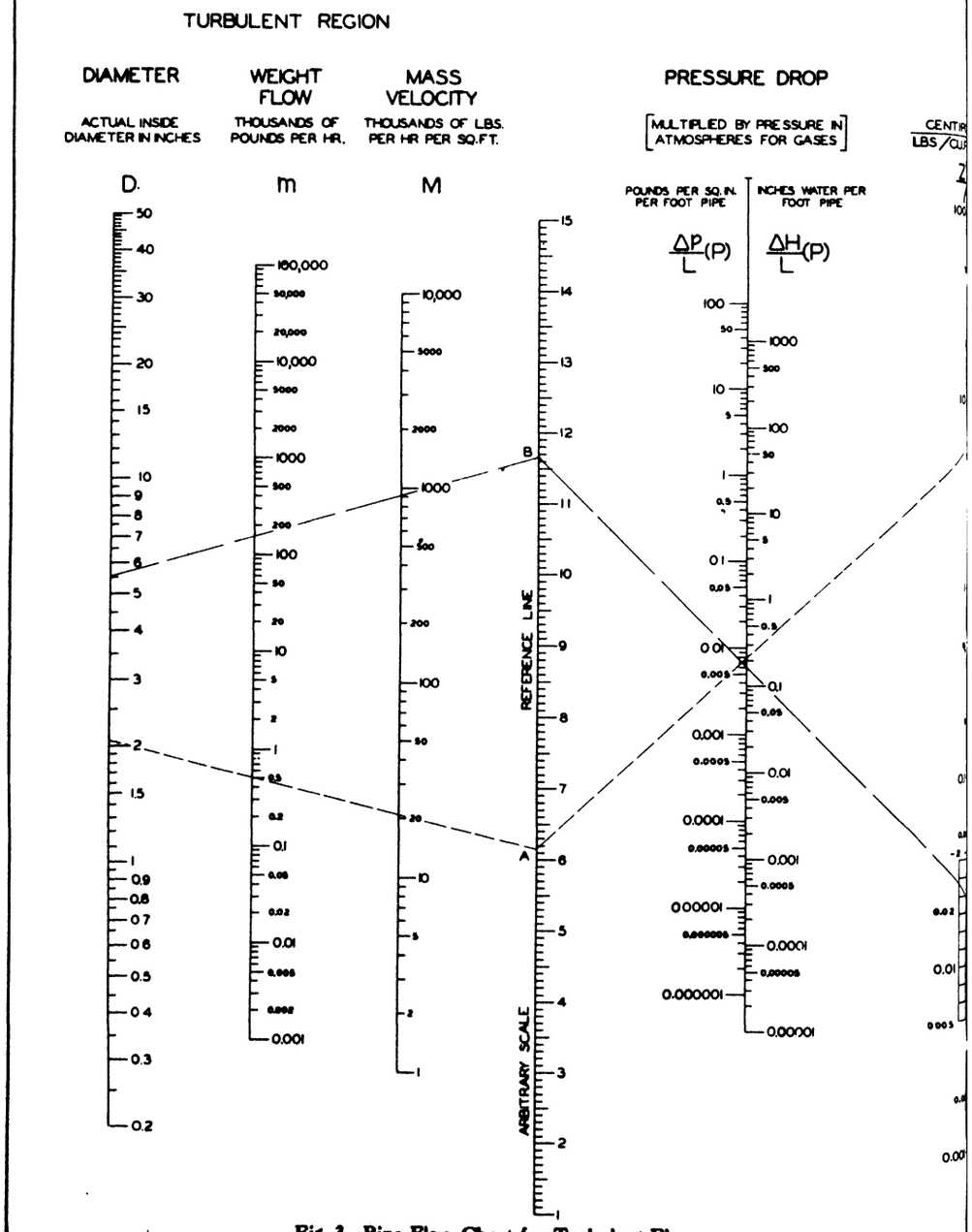
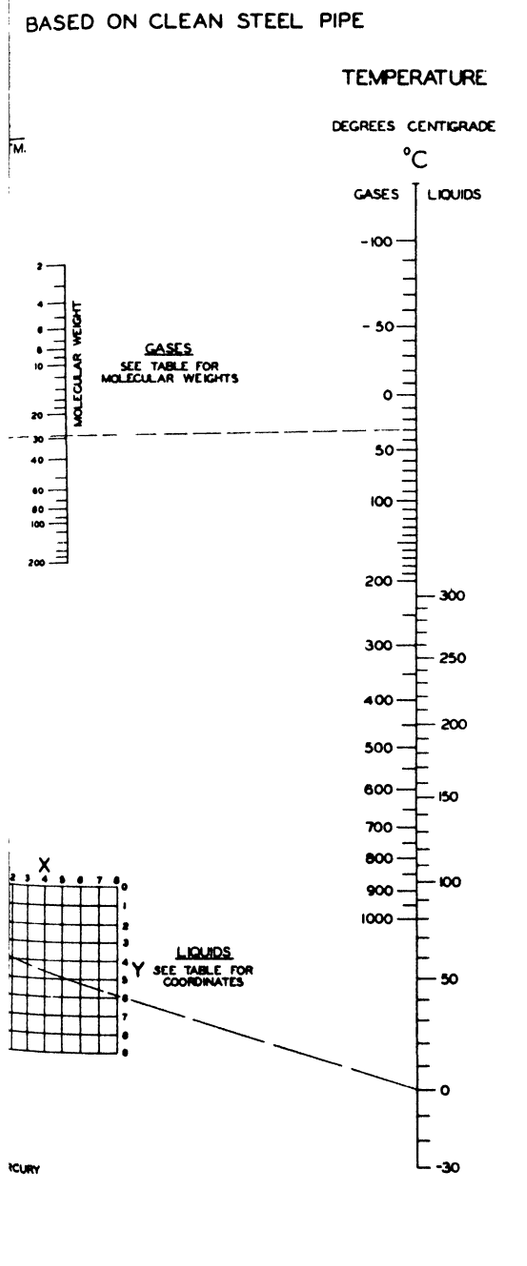


Fig. 3—Pipe Flow Chart for Turbulent Flow



MOLECULAR WEIGHTS OF GASES

Acetylene	26.0	*Freon 11B*	170.9
Air	29.0	Helium	4.0
Ammonia	17.0	Hexane	86.1
Argon	39.9	Hydrogen	2.0
Bromine Vapor	159.8	Hydrogen Bromide	80.9
Butane	58.1	Hydrogen Chloride	36.5
Butylene	56.1	Hydrogen Cyanide	27.0
Carbon Dioxide	44.0	Hydrogen Fluoride	20.0
Carbon Monoxide	28.0	Hydrogen Sulfide	34.1
Chlorine	70.9	Methane	16.0
Cyanogen	52.0	Methyl Chloride	50.5
Ethane	30.1	Nitric Oxide	30.0
Ethylene	28.0	Nitrogen	28.0
Fluorine	38.0	Oxygen	32.0
Freon 11	137.4	Pentane	72.1
Freon 12	120.9	Propane	44.1
Freon 21	102.9	Propylene	42.1
Freon 22	86.5	Sulfur Dioxide	64.1
Freon 113	187.4	Water	18.0

COORDINATES FOR LIQUIDS (AND AQUEOUS SOLUTIONS)

	X	Y		X	Y
Acetaldehyde	-0.3	3.7	*Freon 113*	0.9	6.2
Acetic Acid, 100%	1.0	4.0	*Freon 114*	-0.4	6.2
Acetic Acid, 77%	2.6	3.8	Glycerol, 100%	6.9	1.8
Acetic Anhydride	0.7	4.5	Glycerol, 50%	3.0	3.7
Acetone, 100%	0.9	3.8	Hydrochloric Acid, 31.5%	1.1	4.2
Acetone, 35%	2.7	3.7	Linseed Oil, Raw	3.4	1.8
Ammonia, Anhydrous	0.9	3.6	Mercury	See Chart	
Ammonia, 26%	1.9	3.6	Methanol, 100%	0.8	3.3
Aniline	2.5	3.4	Methanol, 40%	2.8	3.6
Benzene	0.6	3.6	Methyl Acetate	0.0	3.2
Butanol	2.6	2.6	Methyl Chloride	-0.2	4.3
Calcium Chloride			Nitric Acid, 95%	0.8	5.4
Brine, 25%	2.6	4.2	Nitric Acid, 60%	1.5	4.8
Carbon Disulfide	0.0	5.6	Nitrobenzene	1.7	4.4
Carbon Tetrachloride	0.7	6.0	Octane	0.4	2.7
Chloroform	0.0	6.0	Phenol	2.6	3.4
Chlorosulfonic Acid	1.5	5.8	Propionic Acid	0.6	3.8
Cyclohexanol	5.3	2.2	Sodium Chloride		
Diphenyl	0.0	3.5	Brine, 25%	2.1	4.4
Ether	-0.3	3.2	Sodium Hydroxide, 50%	5.3	3.7
Ethyl Acetate	0.2	3.9	Sulfur Dioxide	-0.2	6.1
Ethyl Alcohol, 95%	1.9	3.0	Sulfuric Acid, 110%	3.7	4.7
Ethyl Alcohol, 65%	3.3	3.4	Sulfuric Acid, 98%	3.2	4.8
Ethyl Chloride	0.2	6.3	Sulfuric Acid, 78%	3.8	4.8
Ethylene Glycol	3.5	2.9	Tetrachloroethylene	0.3	6.2
Formic Acid	1.5	4.5	Toluene	0.4	3.6
Freon 11	0.0	6.2	Trichloroethylene	0.1	5.9
Freon 12	-1.2	5.9	Turpentine	1.1	3.1
Freon 21	-0.4	5.9	Vinyl Acetate	0.4	4.2
Freon 22	-1.7	5.5	Water	2.0	4.2

DIRECTIONS FOR USING CHART

This chart is based on the Fanning Equation: $\Delta p = 4 f L \rho v^2/2gD$, and the following friction factor vs. Reynolds number relationship: $f = 0.0\dot{4}\,(D\rho/\mu)^{-0.16}$ which represents a safe straight line for commercial steel pipe in the turbulent region. The units in these equations are consistent; for example, in the ft., lb., sec. system: Δp = pressure drop, lb./sq.ft., L = length, ft.; ρ = density, lb./cu.ft.; v = velocity, ft./sec., D = diameter, ft.; μ = viscosity, lb./(ft.)(sec.). In these units, the critical Reynolds number is about 2100.

In the units used on the chart, the equation with the friction factor line substituted is $\Delta p = 0.1325\ f\rho^{0.16}v^{1.84}/D_i^{1.84}$, and the critical Reynolds number in these units is about $w/D_i = 0.33$.

For viscous flow, i.e., Reynolds numbers below the critical, the Hagen-Poiseuille equation should be used. In the units used on the chart, the equation is $\Delta p = 0.03\dot{4}\ L\mu w/\rho D_i^4$.

Gas Example: Air at a pressure of 120 lb. gage and a temperature of 30° C. is flowing at the rate of 500 lb./hr. through a 2-in. standard steel pipe. What is the pressure drop per foot of pipe? The actual inside diameter is 2.067 in. The pressure of the air is (120 + 14.7)/14.7 = 9.16 atm. absolute. Connect D_i = 2.067 with w = 0.5 and extend the line to intersect the reference line at A = 6.15. Connect 30° C. on the gas temperature scale with molecular weight = 29 and intersect the $\rho^{0.16}/\rho$ line at 7.1. Join this last intersection with point A, intersecting the $\Delta p(P)/L$ line at 0.008. The pressure drop is then 0.008/9.16 = 0.0008 lb./sq.in. per foot of pipe.

Liquid Example: A 20% calcium chloride brine is to be pumped through a line at 250 gal./min. at a temperature of 0° C. If the allowable pressure drop is 0.006 lb./sq.in. per foot of pipe, what size of pipe is required? Connect 0° C. on the liquid temperature scale with the intersection of grid values X = 2.6 and Y = 4.2 shown in the table of "Coordinates for Liquids". Extend the line to $\rho^{0.16}/\rho = 0.017\dot{9}$ and connect that point to $\Delta p/L = 0.006$ and extend to the reference line at point B = 11.65. Connect point B through w = 147 (since at density of 73.3 lb./cu.ft., 250 gal./min. = 147,000 lb./hr.) to intersect at D_i = 5.5 in., indicating a 6-in. pipe.

E. I. du Pont de Nemours & Co., Inc.
Engineering Dept., Technical Division
Wilmington, Delaware. RPG 11/15/38

Temperature and molecular weight scales are given in the form of a line-coordinate chart by which values of $Z^{0.16}/\rho$ at atmospheric pressure are determined directly. While it is true that the viscosities of gas mixtures are not exactly proportional to the molecular weight, the error is small when the 0.16 power of the viscosity is used.

For liquids, a separate temperature scale and a table of certain liquids with coordinate points for locating their positions on the grid are given. The grid system is used because the points for the data would be compacted into too small a space for clarity. The coordinates for locating points for liquids not listed in the table may be located as follows. Values of $Z^{0.16}/\rho$ for two temperatures are calculated and the corresponding values connected by straight lines. The intersection locates the point. For example, in locating the point for 95 per cent ethyl alcohol:

Temperature Deg. C.	0	70
Viscosity, centipoises, Z	1.798	0.504
$Z^{0.16}$	1.099	0.896
Density, lb./cu.ft., ρ	51.2	47.8
$Z^{0.16}/\rho$	0.0215	0.0188

By connecting 0 deg. C. with 0.0215 and 70 deg. C. with 0.0188, the grid coordinates $X = 1.9$ and $Y = 3.1$ are obtained.

Choosing Pipe Diameter for Economy

It has previously been mentioned that the selection of pipe should be made on an economical basis so that the total annual cost of owning and operating the fluid handling system will be a minimum.

The method to be used in arriving at the most economical pipe size will be clear from a consideration of the factors entering into this total cost. The initial cost of the pipe and fittings is directly proportional to the diameter, as are the other factors of pipe operating cost, depreciation and maintenance, which are a constant percentage of initial pipeline cost. The cost of pressure drop (cost of pumping or blowing), however, is inversely proportional to the diameter, so that a balance can be struck at a diameter which will give the minimum sum for these two costs.

The cost of pipe can be expressed approximately in terms of that of 1-in. pipe, multiplied by the actual diameter raised to a power, or XD_i^n. For steel pipe, the slope of the cost curve is essentially $n=1.5$, and the equation, therefore, $XD_i^{1.5}$. The total annual cost of pipe may be expressed as follows:

$$C_p = (a+b)\,(F+1)\,XD_i^n \qquad (15)$$

where cost is the total of depreciation and maintenance on a pipe line costing initially XD_i^n for the pipe, plus $F \times D_i^n$ for fittings, valves, erection, etc.

The second item in total annual cost, the cost of pressure drop, is taken as zero when it is not charged to operation, as in drawing water from a main. When pumping of liquids or compressing of gases is required, that cost must be included. In the case of liquids, the volume of flow multiplied by the pressure drop expresses exactly the work done, but for gases, this is not exact. Assuming it to be true introduces a percentage error equal to about half the percentage pressure drop, an error which is unimportant for small pressure drops. Hence this approximation will be made. (This method cannot, of course, apply to steam, since the value of the pressure lost in a steam line depends on the temperature and pressure level.)

Cost of Pressure Drop

Assuming, then, that the cost of pressure drop is proportional to the product of flow volume and pressure drop, the hourly energy consumption is $1{,}000(m/\rho)(144\Delta p)$ ft. lb. or $1{,}000m(144\Delta p)/(2{,}654{,}200E\rho)$ kw.-hr. In dollars per year this cost becomes $0.0542m\Delta pYK/(E\rho)$, or substituting for Δp its value from Equation (12), the annual dollar cost of pressure drop per foot of pipe becomes:

$$C_{p.d.} = \frac{0.0072\,m^{2.84}Z^{0.16}\,YK}{D_i^{4.84}\rho^2 E} \qquad (16)$$

The total annual dollar cost of pipe plus pressure drop is $C = C_p + C_{p.d.}$, which expression is differentiated with respect to the diameter and the differential set equal to zero to determine minimum cost. The resulting equation is:

$$D_i^{4.84+n} = \frac{0.0348\,m^{2.84}Z^{0.16}\,YK}{n(a+b)\,(F+1)\,XE\rho^2} \qquad (17)$$

which is a general expression for any kind of pipe. Substituting for n its value of 1.5 for steel pipe and solving for D_i the equation becomes:

$$D_i = \frac{m^{0.448}Z^{0.032}}{\rho^{0.215}} \times \left[\frac{0.0232\,YK}{(a+b)\,(F+1)\,XE}\right]^{0.188} \qquad (18)$$

In order to simplify still farther, the "fixed cost" expression within the brackets was evaluated for extreme and normal values, and an average figure of 2.2 taken. Since $Z^{0.032}$ is nearly unity for most viscosity values, another simplification is to neglect it, giving as the final simplified expression:

$$D_i = 2.2\,m^{0.448}/\rho^{0.215} \qquad (19)$$

Although for most accurate results it may be desirable to use Equation (17), Equation (19) is adequate for ordinary plant conditions, for fluids having viscosities lying between 0.02 and 30 centipoises.

The alignment chart, Fig. 4, has been constructed for its ready solution. In using the chart, select the next standard size of pipe above the actual diameter determined. To do so is to be on the "safe side" and will prove most economical.

The following example illustrates the relation between pipe diameter and total annual cost of pipe and pressure drop. The costs of pipe and of pressure drop for conveying water at 20 deg. C. at the rate of 75,000 lb. per hr. (150 gal. per min.) for 1,000 ft. were calculated for actual pipe sizes of 1 to 8 in. The results are given graphically in Fig. 5, and indicate a 4-in. pipe as the most economical. It is also indicated that the total annual cost of 6-in. pipe is practically identical with that for 3-in. pipe. Note that Fig. 4 gives exactly the same result, namely a 4-in. pipe, taking ρ at 62.5 lb. per cu.ft.

TABLE I—NOMENCLATURE

A_1 = area, upstream	Δp_c = pressure drop due to contraction
A_2 = area, downstream	Δp_e = pressure drop due to expansion
a = amortization (fractional, *i.e.* 0.10 for 10 per cent)	Δp_k = pressure drop due to high pressure or temperature change
b = maintenance, fractional	p_1 = inlet pressure, lb./sq. in.
C = cost expression	p_2 = outlet pressure, lb./sq. in.
C_p = annual cost of pipe, dollars	p_{av} = arithmetic mean pressure, lb./sq. in.
$C_{p.d.}$ = annual cost of pressure drop, dollars	Q = thousands of cu.ft./hr.
D = diameter, feet	Re = Reynolds number, dimensionless
D_i = diameter, inches	r = hydraulic radius, feet
E = overall efficiency, pump and motor, fractional	r_i = hydraulic radius, inches
F = factor for fittings and erection	T = absolute temperature, °K.
f = friction factor, dimensionless	T_1 = absolute temperature, °K, at inlet
G = mass velocity, lb./(sec.) (sq. ft.) = $V\rho$	T_2 = absolute temperature, °K, at outlet
g = acceleration due to gravity, ft./sec.^{2}	T_{at} = absolute temperature, °K, arithmetic mean
K = factor in contraction loss	V = velocity, ft./sec. (i.e., average over the cross-section)
K = cost of electrical energy, dollars per kw.hr.	X, Y = coordinates for grid, Fig. 3
L = length, feet	X = cost of 1 in. pipe per ft. length, dollars
L_e = length, feet, equivalent to fittings, etc.	Y = hours of operation per year
M = mass velocity, thousands of lb./(hr.) (sq. ft.)	Z = viscosity, centipoises
m = weight rate of flow, thousands of lb./hr.	μ = viscosity, lb./ft.sec. = $Z/1{,}488$
$m.w.$ = molecular weight.	μ_a = viscosity, lb./ft.sec., at the main body temperature
n = slope of pipe cost curve	μ_w = viscosity, lb./ft.sec., at the tube wall temperature
P = pressure, absolute, in atmospheres	ρ = density, lb./cu.ft.
ΔP = pressure drop, lb./sq. ft.	
Δp = pressure drop, lb./sq. in.	

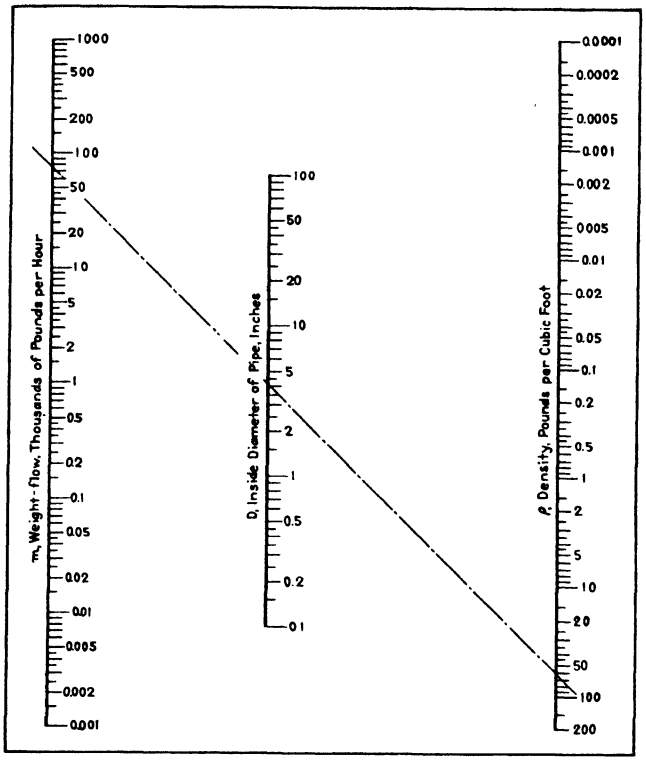


Fig. 4—Economical pipe diameter chart, based on simplified Equation (19) in text; connect weight flow and fluid density to obtain economical inside diameter of pipe

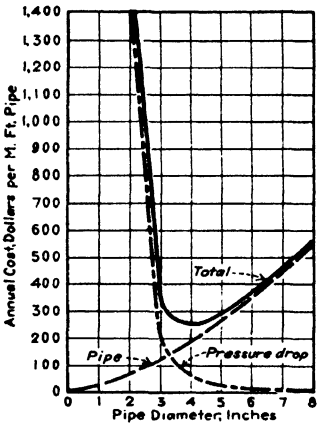


Fig. 5—Example illustrating interrelations of cost of pipe, cost of pumping and total cost in the case where water at 20 deg. C. is being pumped at the rate of 75,000 lb. per hour

Miscellaneous Pipe-Line Losses

Expansion and Contraction Losses—When the cross-sectional area is *suddenly enlarged* the velocity head decreases, and if there were no friction losses the static head would increase a corresponding amount. However, a part of the head is lost due to friction. When the cross-sectional area is *suddenly reduced* there is a similar loss of pressure. These losses may be calculated by means of the equations shown in Table II in which Δp_e = expansion loss, lb. per sq.in. and Δp_c = contraction loss, in lb. per sq. in.

Pipe Fittings and Valves—In calculating fluid flow problems on piping systems in which elbows, bends, tees, valves, etc., occur, it is convenient to add to the pipe length, L, the equivalent length of pipe, L_e, which would give the same pressure drop. The values given in the second part of Table II are in terms of the number of diameters of pipe length. For example, if a 90 deg. elbow in a 3-in. line is equivalent to 40 diameters, then the equivalent length of straight 3-in. pipe is 40(3/12) = 10 ft.

Table II — Miscellaneous Losses in Pipe Lines

Equations for Expansion and Contraction Losses

$$\Delta p_e = \frac{\rho (V_1 - V_2)^2}{2g \times 144} = \frac{0.279\, m^2}{\rho}\left(\frac{1}{D_1^2} - \frac{1}{D_2^2}\right)^2 \qquad (20)$$

$$\Delta p_c = \frac{K \rho V_2^2}{2g \times 144} = \frac{0.279\, m^2}{\rho}\left(\frac{1}{D_2^2}\right)^2 K \qquad (21)$$

$$K = 0.4\left(1.25 - \frac{A_2}{A_1}\right) = 0.4\left(1.25 - \frac{D_2^2}{D_1^2}\right) \text{ when } \frac{A_2}{A_1} < 0.715$$

$$K = 0.75\left(1 - \frac{A_2}{A_1}\right) = 0.75\left(1 - \frac{D_2^2}{D_1^2}\right) \text{ when } \frac{A_2}{A_1} > 0.715$$

Losses in Fittings and Valves

(Turbulent Flow Only)

	Pipe diameters
90 deg. elbows, ¾–2½ in.	30
3–6 in.	40
7–10 in.	50
45 deg. elbows, 1–3 in.	15
4–10 in.	20
90 deg. long radius elbows	15–20
Tee used as elbow	60

	Pipe diameters
Tee when fluid enters branch	90
Square elbow (intersection of two cylinders)	50
Return bend, made of two elbows, use twice the value for one 90 deg. elbow.	
Gate valves, open	10
Globe valves, open	100–300

For further descriptions, see [12] and [2].

Flow in Uniform Non-Circular Conduits

The friction factor has been found to be a function of the Reynolds number for flow in pipes and ducts of all cross-sectional shapes so far examined. The form of Reynolds number used is

$$Re = 4r\,V\rho/\mu = 4rG/\mu \qquad (22)$$

The hydraulic radius r = area of stream cross-section divided by wetted perimeter. For a circle, $r = D/4$ or $D = 4r$. Substitution of D for $4r$ in Equation (22) results in the Reynolds number for circular pipe as given previously in Equation (7):

$$Re = D\,V\rho/\mu = DG/\mu \qquad (7)$$

The velocity V in Equation (22) is that calculated from the actual area of the duct, for example,

$$V\rho = G \qquad (23)$$

where G is the mass velocity, lb. per sec. per sq.ft., or the weight rate of flow divided by the actual area of the duct.

The friction factor for non-circular ducts is the same as that for circular pipe, Equation (1), with $4r$ substituted for D:

$$f = 2gr\,\Delta P/L\rho V^2 = 2gr\rho\,\Delta P/LG^2 \qquad (24)$$

The general form of the Fanning Equation is obtained by transposing Equation (24) or by substituting $4r$ for D in Equation (6):

$$\Delta P = fL\rho\,V^2/2gr = fLG^2/2g\rho r \qquad (25)$$

By referring to Fig. 6, it can be seen from the positions of the viscous region lines for rectangular ducts of various aspect ratios (length/breadth) that each duct shape has a different line. The ones illustrated are taken from Davies & White[3] who also give values for ellipses and the equilateral triangle. They stated, after analyzing the available data, that the friction factor in the turbulent region is independent of the form of the cross-section, for all practical purposes. The curves B and C from Fig. 1 are therefore shown on Fig. 6 for turbulent flow. From this, it can be assumed that the straight line selected for circular pipe, Equation (9), is equally applicable to non-circular conduits. In terms of the hydraulic radius, it is stated as:

$$f = 0.032\,(\mu/r\,V\rho)^{0.16} = 0.032\,(\mu/rG)^{0.16} \qquad (26)$$

and when substituted in Equation (25):

$$\Delta P = 0.000498\,L\,\mu^{0.16}\rho^{0.84}\,V^{1.84}/r^{1.16} \qquad (27)$$

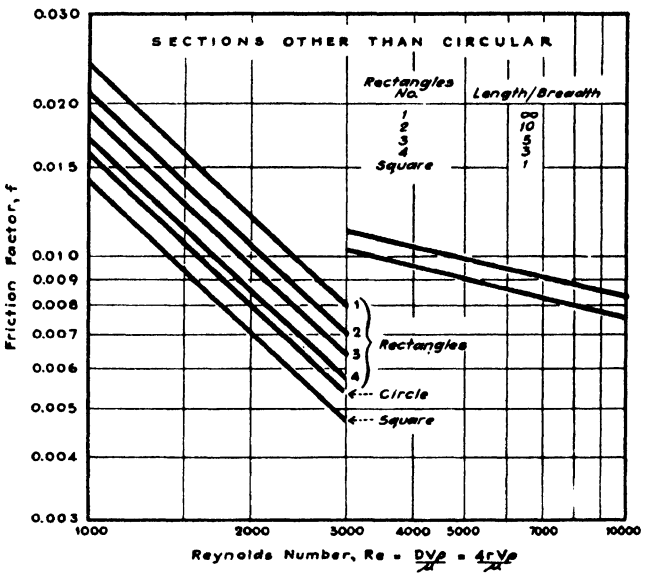


Fig. 6—Friction factor plots for non-circular ducts

Equations (22) to (27) are in consistent units. Equation (27) expressed in more commonly used units is:

$$\Delta p = 0.000019\,LZ^{0.16}\rho^{0.84}\,V^{1.84}/r^{1.16} \qquad (28)$$

Values of the hydraulic radius r for various cross-sections are given in Table III. Others may be found in Perry[10].

Table III—Hydraulic Radius for Various Sections

Pipes and Ducts Running Full	Hydraulic Radius
Circle, diam. = D	$D/4$
Annulus, inner diam. = d, outer diam. = D	$(D-d)/4$
Square, side = D	$D/4$
Rectangle, sides a, b	$ab/2\,(a+b)$

REFERENCES

(1) Chilton, Colburn, Genereaux, & Vernon. Trans. Am. Soc. Mech. Engrs. PME 55–2, 7–14 (1933).
(2) Crane Co., Technical Paper No. 405 (1935).
(3) Davies & White. *Engineering*, 78, 69 et seq. (1929).
(4) Drew & Genereaux. Trans. Am. Inst. Chem. Engrs. 32, 17–19 (1936).
(5) Drew, Koo, & McAdams. Trans Am. Inst. Chem. Engrs. 28, 56–72 (1932).
(6) Genereaux. *Ind. Eng. Chem.* 29, 385–8 (1937).
(7) Kemler. Trans. Am. Soc. Mech. Engrs. HYD 55, 7–32 (1933).
(8) Perry, Chemical Engineers' Handbook, McGraw-Hill Book Co., New York, 1934. p. 720.
(9) Perry, *ibid.*, p. 721.
(10) Perry, *ibid.*, p. 722.
(11) Perry, *ibid.*, p. 727.
(12) Perry, *ibid.*, p. 730.
(13) Perry, *ibid.*, p. 735.
(14) Perry, *ibid.*, p. 1271.
(15) Pigott, *Mech. Eng.* 55, 497–501 (1933)
(16) Sieder & Tate. *Ind. Eng. Chem.* 28, 1429–35 (1936).
(17) Tietjens, Applied Hydro- and Aero-Mechanics, McGraw-Hill Book Co., New York, 1934. p. 19.

Chapter 10

PUMPS

by

M. S. Maleson

Maleson Company
Philadelphia, Pa.

TABLE OF CONTENTS

		Page
I.	References	188
II.	Nomenclature	188
Part No. 1	—Pumps For General Service	188
III.	General Classification of Pumps	188
IV.	Centrifugal Pumps	190
	A. Side Suction Centrifugal Pumps	190
	1. Types of Impellers	192
	B. Double Suction, Single Stage Centrifugal Pumps	192
	C. Multi-Stage Centrifugal Pumps	193
	D. Centrifugal Pump Casings, Volute and Diffuser Type	194
	E. Materials Handling Centrifugal Pumps	196
	F. Steam Turbine Driven Centrifugal Pumps	196
	G. Friction in Pipe Lines	196
	Centrifugal Pump Problems	196
V.	Deep Well Pumps	198
VI.	Temperature Versus Suction Lift	199
VII.	Pump Losses Handling Viscous Liquids	199
VIII.	Net Positive Suction Head	199
	A. Correction for High Temperatures	200
IX.	Turbine Pumps	200
X.	Mixed Flow Pumps	202
XI.	Specific Speed	202

XII. Rotary Pumps 203
A. Slip 205
B. Volumetric Efficiency 206
C. Cavitation 206
XIII. Reciprocating Pumps 206
Part No. 2—Pumps For Chemical and Process Industries 209
I. Centrifugal Pumps, Gravity Feed 210
II. Self Priming Centrifugal Pumps 212
III. Corrosion 215
IV. Controlled Volume Pumps 216
V. Engineering Calculations for Centrifugal Pumps 220
Engineering Calculation Problems 222

LIST OF FIGURES

Figure 1. Types of Centrifugal Pumps 189
Figure 2. Diagrams of Operation of Centrifugal Pumps 190
Figure 3. External View of Centrifugal Pumps 191
Figure 4. Internal View of Centrifugal Pumps 191
Figure 5. Performance Curve of Centrifugal Pump 192
Figure 6. Cross-Section of Double Suction, Single Stage Centrifugal Pump 192
Figure 7. Cross-Section of Two-Stage Pump 193
Figure 8. Performance Curve of Multi-Stage Centrifugal Pump 194
Figure 9. Materials Handling Pumps 195
Figure 10. Steam Turbine Driven Single Stage Centrifugal Pump 196
Figure 11. Friction in Pipe Lines 197
Figure 12. Deep Well Turbine Pumps, Oil Lubricated and Water Lubricated 198
Figure 13. Temperature Versus Suction Lift Curve 199
Figure 14. Reduction in Viscosity Curves 200
Figure 15. Turbine Type Pump 201
Figure 16. Turbine Pump Performance Curve 202
Figure 17. Mixed Flow Pump Curve 202
Figure 18. Rotary Pumps 204
Figure 19. Curve of Screw Type Pump 204
Figure 20. Reciprocating Pumps 207
Figure 21. Power Driven Reciprocating Pump for High Pressure 208
Figure 22. Diagrams of Pulsating Flow from Reciprocating Pumps 209
Figure 23. Exploded View of Chemical Centrifugal Pump 210
Figure 24. Cross-Section of Chemical Centrifugal Pump 210
Figure 25. Casing of Chemical Centrifugal Pump 211
Figure 26. Curve of Chemical Pump 211
Figure 27. Curve of Low Capacity High Head Pump 212
Figure 28. Cross-Section of Low Capacity High Head Pump 212
Figure 29. Section of Self Priming Centrifugal Pump 213
Figure 30. Illustration of Self Priming Action 213
Figure 31. Tank Car Unloading 213
Figure 32. Vertical Self Priming Centrifugal Packingless Pump 214
Figure 33. Corrosion 215
Figure 34. Controlled Volume Chemical Pump 217

Figure 35. Micro Adjustment With Cover Plate Liquid End Design Controlled Volume Chemical Pump 217
Figure 36. Controlled Volume Chemical Pump with Master Speedranger 217
Figure 37. Controlled Volume Chemical Pump with Timer (System A) and Controlled Volume Chemical Pump with Thymotrol (System B) 218
Figure 38. Sine Curve of Controlled Volume Pumps 218
Figure 39. Gang Type Pump 219
Figure 40. Automatic pH Control with Constant Main Line Rate of Flow 219
Figure 41. Automatic pH Control with Varying Main Line Rate of Flow 220
Figure 42. Application of Titrimetric System to Caustic Concentration Control 220
Figure 43. Titrimetric System 221

I. REFERENCES

1. "Pumps" by F. A. Kristal and F. A. Annett, McGraw-Hill Book Company, Page 119, Figure 116 and Page 128, Figure 179.
2. "Standards of Hydraulic Institute", Rotary Pump Section C, Page 1.
3. "Mechanics of Corrosion" by H. E. LaBour.
4. "Instrumentation By and With Controlled Volume Pumps", Paper 48-43 by Robert T. Sheen.
5. "Controlled Volume Chemical Pumps - Design and Operation", Paper 57 by Robert T. Sheen.
6. LaBour Company, Inc.
7. Aurora Pump Company
8. Leyman Manufacturing Company
9. Morris Machine Works
10. J. S. Coffin, Jr. Company
11. Sier Bath Gear and Pump Company
12. Aldrich Pump Company
13. Milton Roy Company

II. NOMENCLATURE

A = area, square feet.

D = rotor diameter, feet

E = pump efficiency

f = frequency in cycles per second

g = acceleration due to gravity, (ft.)/(sec.)(sec.)

GPM = gallons per minute

h = head, ft. of fluid flowing

HP = horsepower

NPSH = net positive suction head

n_m = impeller speed, rev./min.

n_{sm} = specific speed

N = number of poles in motor

n = rotor speed, rev./min.

PSI = pounds per square inch

q = flow rate, cubic ft./sec.

q_{gm} = pumping rate, gal./min.

RPM = revolutions per minute

v = velocity, ft./sec.

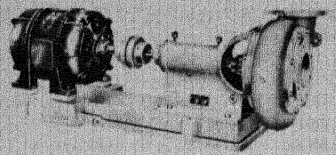
PART NO. 1

PUMPS FOR GENERAL SERVICE

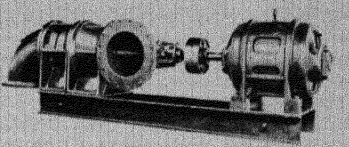
Pumping is a vast subject. To attempt to cover it completely in the time and space available here is not practical. All we can hope to do in the first half of this text is to examine the principal types of pumps and in the second half to concentrate on the pumps for the chemical and process industries.

III. GENERAL CLASSIFICATION OF PUMPS

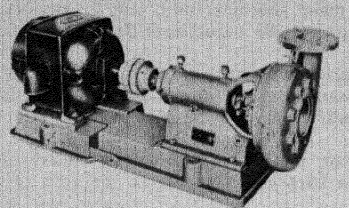
To begin with, pumps may be classified generally in two groups. First, there are positive displacement pumps including the reciprocating or piston type pumps, rotary pumps and the diaphragm type pumps. The second general classification is the centrifugal type pump.



Type KGG Aurora Horizontal Non-Clog Pumps. Sizes up to 10"



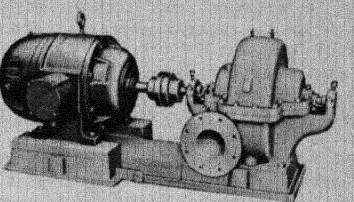
Type SRH Aurora Mixed Flow Large Capacity Horizontal Pump



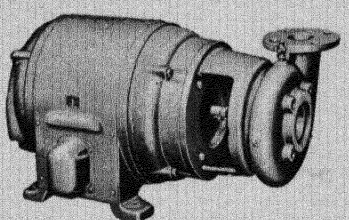
Type GGU Aurora Side Suction. Semi-open or Enclosed Impeller.



Type SRV Vertical Caisson Pumps up to 12,000 G.P.M.



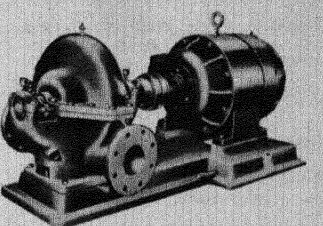
Type AD Aurora Two Stage Horizontally Split Case Centrifugal



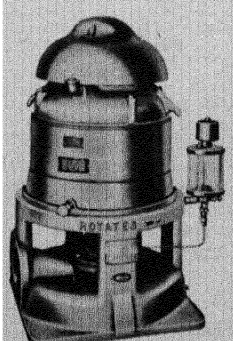
Type GMC Aurora Close-Coupled Centrifugal



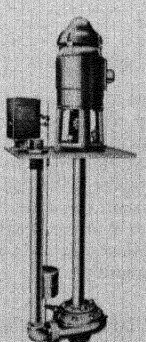
Type DSM Cellar Drainers. ¾ H.P. 2800 G.P.H.



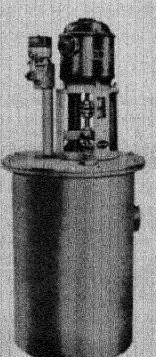
Type OD Aurora Double Suction Horizontally Split Case Centrifugal



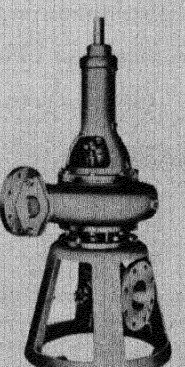
Aurora Deep Well Turbine Pumps Sizes 4" to 24"



Vertical Sump Pumps. Heavy or Light Duty



Aurora Vertical Condensation Return Units



Type KU Vertical Non-Clog Pumps

Figure 1. Types of Centrifugal Pumps

The various types of positive displacement pumps may vary considerably in design and construction but all use the same operating principle and all have the same basic characteristics. The liquid always flows or is drawn into the pump and in a calm condition is moved through the pump and discharged by mechanical displacement action. This flow may be reciprocating, for example, as a result of a moving piston or it may consist of turning vanes which push the liquid ahead of these vanes slowly.

The centrifugal pump runs comparatively fast. Energy from the driver is transferred to an impeller turning in the liquid. This impeller transfers energy and motion to the liquid and the kinetic energy thus given to the liquid is changed to pressure within the pump. The liquid is expelled as a result of pressure difference and not because of displacement.

Between the two fundamental types of pumps, the centrifugal and the positive displacement, we have several that are a mixture of both. For example, there is the turbine type of pump sometime referred to as the peripheral type. This particular pump has a drooping pump characteristic, that is, the head falls off as the capacity increases. However, unlike centrifugal pumps the horsepower falls off as the capacity increases.

Also somewhere between the centrifugal and the positive displacement pump we have the mixed flow pump. This has an impeller which develops velocity and at the same time lifts with a positive displacement action. A further variation is the propeller type of pump which can best be described by the action of the marine type propeller.

In a centrifugal pump the capacity varies directly as the speed; the head varies as the square of the speed; the head varies as the square of the diameter; and the horsepower varies as the cube of the speed.

The first statement arises from the equation: $q = AV$

The second is derived from: $h = V^2/2g$.

Where q = flow rate, cu. ft./sec.
A = area, sq. ft.
V = velocity, ft./sec.
h = head, ft. of fluid flowing
g = acceleration due to gravity, (ft.)/(sec.)(sec.)

Inasmuch as: $V = \pi Dn$

Where D = rotor diameter, ft.
n = rotor speed, rev./sec.

The velocity varies directly as both the diameter and the speed, so that the head (h) varies directly as the square of the diameter for a given speed (n).

Horsepower is proportional to the product of flow rate and head. Since q is proportional to V and h is proportional to V^2, the horsepower is proportional to V^3.

IV. CENTRIFUGAL PUMPS

Figure 1 illustrates several of the types of centrifugal pumps. Here we have the side suction centrifugal pump, side suction non-clog pump, close coupled pump, deep well vertical sump pump, double suction single stage and double suction two stage pumps and also the non-clog vertical pump. In addition, there is included the mixed flow pump in both horizontal and vertical designs.

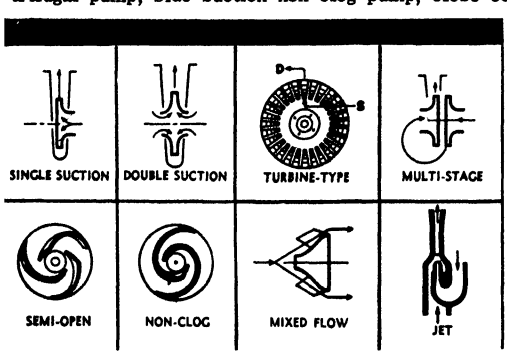


Figure 2. Diagrams of Operation of Centrifugal Pumps

Figure 2 shows diagrams of operation of some of the various types of pumps. The illustrations are self-explanatory.

A. SIDE SUCTION CENTRIFUGAL PUMPS

Figure 3 shows the external view and Figure 4 shows the details of a side suction centrifugal pump. The liquid enters through the suction opening at the eye of the impeller and is given velocity by the spinning impeller. The liquid is expelled out of the discharge opening at the top. Note that after the

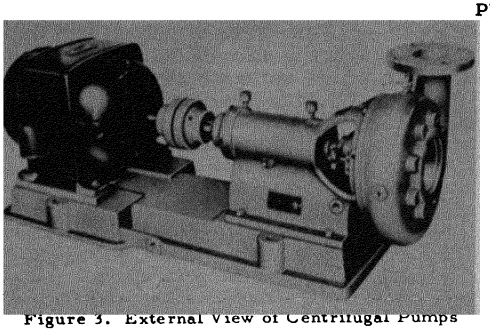
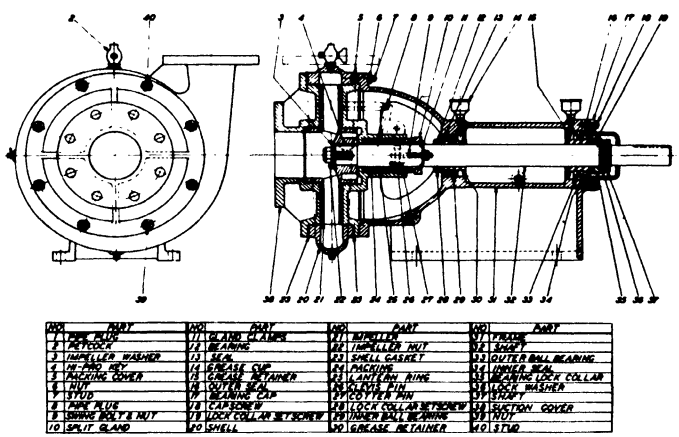


Figure 3. External View of Centrifugal Pumps

liquid enters the eye of the impeller it travels between the blades and is thrown off the impeller blades all around the circle. The liquid is added at all points but is expelled at only one point. In order to compensate for this it is customary to increase the area as the outlet is approached. By doing this we slow down the tangential velocity at a more gradual rate and thereby attain more efficient conversion of the velocity head into pressure head. It is customary to give the case a snail-like shape which is called a volute. This continuously expands in a definite ratio. In general, the impeller blades that curve backward give better results.

You will note that this pump has no internal bearings. The bearings are both external in the bearing bracket and the impeller in overhung. The arrangement you see with the side suction and the top discharge is the most common. However, it is possible to turn the casing through 360° and the number of positions depend on the number of supporting bolts. If there are eight supporting bolts between the pump back and the bearing bracket, there will be eight positions for the discharge opening. This particular pump design shows no wearing rings. It is quite common to put wearing rings either on the casing or the impeller or on both. These wearing rings break down the pressure which tends to flow from the discharge side of the suction, The normal running clearance at this point is 0.010 inches.



NO.	PART	NO.	PART	NO.	PART	NO.	PART
1	PIPE PLUG	11	GLAND CLAMPS	21	IMPELLER	31	FRAME
2	FOOTPIECE	12	BEARING	22	IMPELLER NUT	32	SHAFT
3	IMPELLER WASHER	13	SEAL	23	SHELL GASKET	33	OUTER BALL BEARING
4	IMPELLER KEY	14	GREASE CUP	24	PACKING	34	INNER SEAL
5	PACKING COVER	15	GREASE RETAINER	25	LANTERN RING	35	BEARING LOCK COLLAR
6	UNIT	16	OUTER SEAL	26	CLOSE FIT	36	SEAL WASHER
7	STUD	17	BEARING CAP	27	FOOTPIECE THIN	37	SHAFT
8	PIPE PLUG	18	CAPSCREW	28	LOCK COLLAR SETSCREW	38	SUCTION COVER
9	SPRING BOLT & NUT	19	LOCK COLLAR SETSCREW	29	INNER BALL BEARING	39	NUT
10	SPLIT GLAND	20	SHELL	30	GREASE RETAINER	40	STUD

Figure 4. Internal View of Centrifugal Pumps

On a side suction pump there is always a thrust towards the suction side of the impeller. This thrust is due to the fact that the liquid from the discharge cuts in back of the impeller. With the added area on the back face as compared to the cutout face due to the eye of the impeller, there is a thrust towards the suction. In this type of pump axial thrust is handled by an oversize ball bearing either next to or farthest from the pump.

The side suction pump is usually made with one impeller, although sometimes two, three or even four impellers are used. Multi-staging in side suction centrifugal pumps is common in hot oil work where high pressures are required.

Figure 5 shows a typical performance curve for the side suction centrifugal pump with enclosed impeller. With the largest impeller for this pump at 1750 RPM we can reach heads in the neighborhood of 75 ft. and capacities generally in the neighborhood of 240 GPM. As the impeller diameters are reduced, so are the capacities and heads, and the curves follow parallel lines. Please note the constant efficiency curves and the constant horsepower curves. When we know the head and the capacity we can pick the size impeller required and read the efficiency and also the horsepower.

In the close coupled design of side suction centrifugal pumps the impeller is hung on the end of the extended motor shaft, thus eliminating the use of separate bearings for the pumps. This design has the advantage of price and also of small space requirement. Due to the fact that they are usually difficult to repack and also because the motor is so dangerously close to the pump, we normally recommend this arrangement only for water or similar pumping applications. Mounting connections can be made on this design for horizontal, vertical and even ceiling.

p. 191, 2nd paragraph: Change to "from the discharge side to the suction," (instead of "of the suction"). Place a period after suction, and add "The normal running clearance at this point is 0.010 to 0.020 inches".

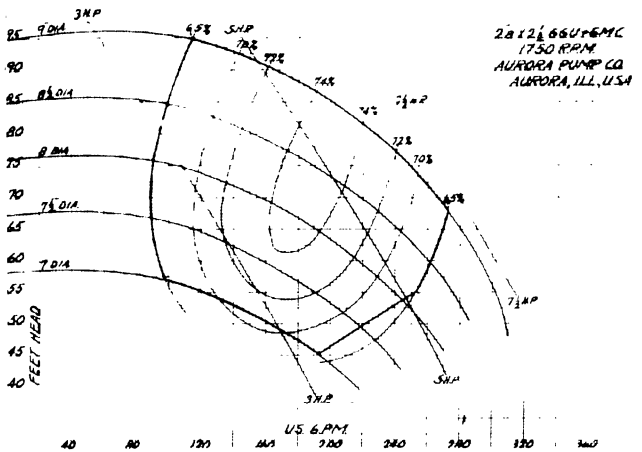


Figure 5. Performance Curve of Centrifugal Pump

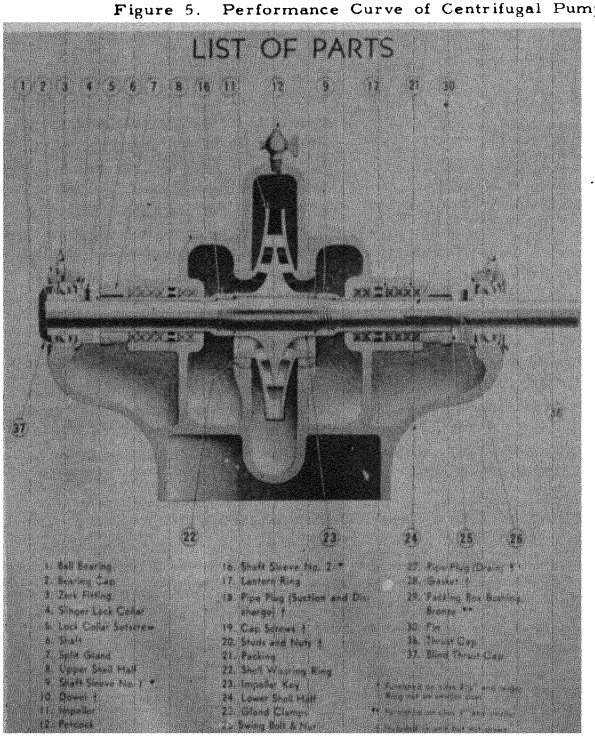


Figure 6. Cross-Section of Double Suction, Single Stage Centrifugal Pump

1. TYPES OF IMPELLERS

There are various types of impellers which can go into the side suction pump. First, we have the fully open impeller. (Refer to fig. 25.) This type is used extensively in chemical work. The side clearances are large, not under 1/32 inch and the top clearances are anywhere from 1/4 inch to 1 inch depending on the head conditions.

Next there is the semi-open impeller. (Refer to fig. 2.) This has a shroud on one side of the impeller vanes. An impeller like this is often desirable for handling solutions containing solids. The third type of impeller is the enclosed type. (Refer to fig. 6 and 7.) It has a shroud on the back side, the same as the semi-closed, but in addition has a web on the inlet side except for the eye opening. By enclosing the impeller it is possible to get higher efficiency than with either of the two other types. For clean and non-corrosive solutions the enclosed impeller is recommended.

The next impeller is the non-clog type. This is used in specially designed pumps for handling solids. For example, we talk about a pump that would handle 3 inch balls, another that would handle 4 inch balls and so on. These are made both in the enclosed and semi-enclosed type. The semi-enclosed is often recommended for fibrous or highly viscous applications.

B. DOUBLE SUCTION, SINGLE STAGE CENTIRFUGAL PUMPS

Figure 6 is a cross-section of the double suction, single stage centrifugal pump. In this the liquid enters the suction opening and then divides two ways to either side of the casing. This liquid then enters each eye of the impeller and develops kinetic energy as it passes from the eye of the impeller to the volute. The volute casing gradually expands and converts the major portion of this velocity head into pressure head and the liquid then leaves through the discharge opening.

The impeller on this type of pump is always enclosed. By placing the bearings at either end of the pump we get a simple beam effect as compared to the cantilever design which is used on the side suction pump. On the double suction pump the axial thrust is always balanced. With this design pump it is possible to remove the top casing and get at the pump without disturbing the pipe

p. 192 - Heading B: "Centrifugal" - not "Centirfugal".

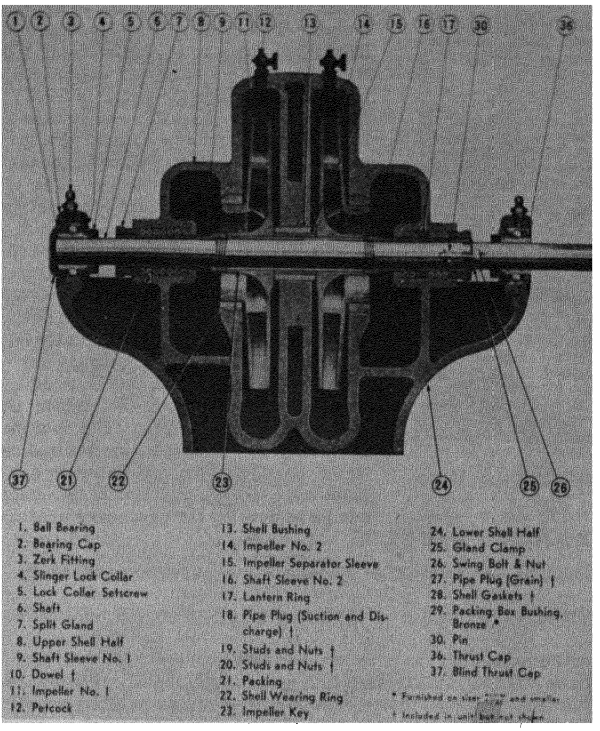


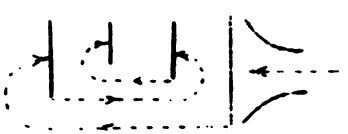
Figure 7. Cross-Section of Two-Stage Pump

connections. Generally this is not true on the side suction pump. Many engineers prefer this type of pump over the side suction pump due to the more rugged construction. However, there are just as many engineers, maybe more, who prefer the side suction pump wherever possible because of price advantage, which may be as much as one-half that of the double suction pump. Second, there is only one stuffing box to maintain on the side suction pump. The efficiency of both are comparable.

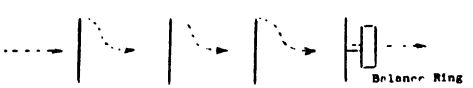
It may be of interest to know that side suction pumps are normally built for not over 2000 GPM which corresponds to approximately an 8 inch pump. One of the principal reasons is that as the suction opening gets larger it is also necessary to increase the size of the impeller so to avoid bypassing over the impeller from the suction side. If the impeller gets too large, the heads developed are too great and it is an expensive item to use slow speed motors. With a double suction pump we separate the flow in two and enter on each side of the impeller. This enables us to use smaller wheels, if they are indicated, without going into excessive pressures.

C. MULTI-STAGE CENTRIFUGAL PUMPS

Figure 7 shows the cross-section of a two stage pump. In multi-stage pumps we combine several single stage pumps so that the discharge of one impeller is delivered to the suction of the next impeller. From the suction the liquid enters the eye of the impeller and is discharged into the volute. From there it enters a cross-over not shown in the casing. The liquid passes into the eye of the second impeller and is discharged into its volute and finally into the discharge opening. By placing the impellers back to back the thrust is cancelled. Sometimes impellers are places like this:



Often we have an arrangement like this:



Sometimes we have double suction multi-stage pumps instead of a series of side suction stages on the same shaft. This requires a heavier shaft construction due to the increased distance between main bearings.

Figure 8 illustrates a typical performance curve on a two stage centrifugal pump running at 1750 RPM. You will note the heads run up to 460 ft. and the capacities up to 500 GPM.

Multi-stage pumps have been built with as many as 317 impellers for heads up to 8000 ft. Installations like these are found in the oil fields. Pumps with 54 stages have been installed on many occasions and 34 stages are not too uncommon. However, with multi-stage pumps you will go normally to 16 stages maximum for use in boiler feed pumps and refineries for charging pumps. Both of these are for high pressures, over 1000 PSI.

In general, the single stage centrifugal pumps, both the side suction and also the double suction, produce heads up to about 400 ft. maximum at 3600 RPM and, of course, one-fourth of that at half this speed. When we operate by motor drive 3600 RPM is the maximum speed for 60 cycle current. The motor speed is represented by the formula: $N = \frac{2f60}{rpm}$.

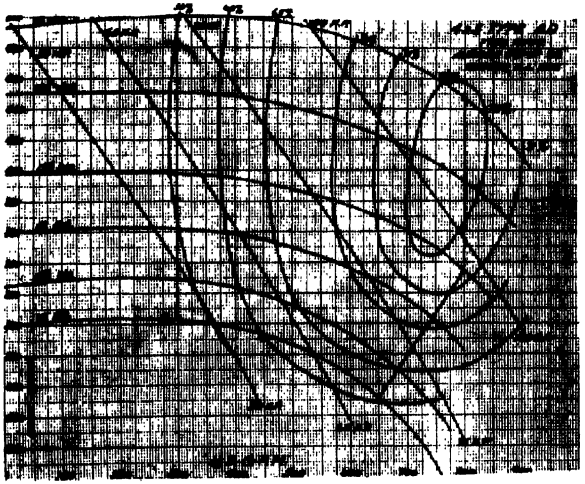


Figure 8. Performance Curve of Multi-Stage Centrifugal Pump

From this it is apparent that for a 2 pole motor and 60 cycle current the speed is 3600 RPM, for 4 poles, the speed is 1800 RPM; for 6 poles the speed is 1200 RPM and for 8 poles the speed is 900 RPM. Since the motor cannot have less than 2 poles the maximum speed of the pump when direct driven by a 60 cycle motor cannot be over 3600 RPM.

When higher heads are required we use multi-stage pumps. The pressure produced by all the stages are added together to determine the pressure at the discharge of the pump.

Multi-stage pumps have been developed in many forms in order to eliminate hydraulic thrust, to maintain low pressure on the packing and between stages and to gain other advantages. Outside of the very high pressures encountered in power plants, refineries and deep wells, most pumping requirements can be taken care of by application of two stage pumps to develop the necessary pressures

D. CENTRIFUGAL PUMP CASINGS, VOLUTE AND DIFFUSER TYPE

Centrifugal pumps can have two types of casings, the volute type which is almost universal and the diffuser type.

The volute type which we have been describing up to now has an expanding casing, changing velocity head into pressure head.

The diffuser type pump, however, has a set of expanding vanes around and close to the impeller circumference. These expanding vanes immediately convert the velocity head into pressure as it leaves the impeller. If you will picture the steam turbine in reverse, that is, with its expanding nozzles and rotor, you will easily recognize the diffuser type pump.

Claims have been made that the diffuser type of pump has a somewhat higher efficiency than the volute type, but volute pumps can be designed with an efficiency comparable to the diffuser type. The diffuser pump has the disadvantage that when the diameter of the impeller is once established, the head cannot be reduced by turning down the impeller.

High efficiency, however, is not the only advantage claimed for the diffuser type pump. In the volute type pump, the impeller discharges into a gradually expanding volute. Experiments have shown that pressure distribution along the volute is not equal. Particularly at reduced capacities, it is possible to get heavy radial thrust on the impeller that tends to deflect the shaft. These loads are of a pulsating nature and have caused shaft failures due to fatigue. In the diffuser type, the impeller discharges in a uniform ring of nozzles, and the radial loading on the impeller is balanced.

Centrifugal pumps are built in so many designs and for so many purposes that it would be impossible to include them all here.

To give an example, hot oil pumps and boiler feed pumps are often made in the barrel type design. Many stages of impellers are lined up on the shaft and held in a casing which is bolted lightly together. This pump casing is then enclosed in a heavy steel shell. The discharge pressure, which may be 1000 PSI or more, with temperatures up to 850° F., is applied against the underside of the barrel so that only light bolts or no bolts at all are needed for the actual pump shell itself. Incidentally, the staging of these impellers is such that you may have the first impeller a double suction and wide impeller so as to help handle the gases that may come to it. The discharge then goes from this all the way to the other end of the shaft for the second stage. The next group of stages may be in series after the second stage. The discharge leaves from say the fourth stage back to next to the first stage impeller. The series begins over again before it leaves the discharge flange of the pump.

To give you an idea what can be done with centrifugal pumps, the Grand Coulee project in the state of Washington uses 12 pumps, each 700,000 GPM capacity and each connected to a 65,000 HP motor.

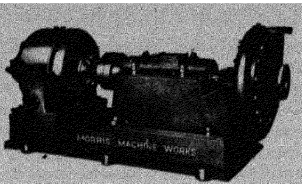


Fig. 742 Standard side-suction pump direct connected to electric motor. Also furnished for belt drive. Described in Bulletin 165.

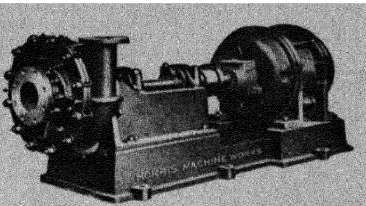


Fig. 605 Motor-driven slurry and sludge pump for handling fine, sharp abrasives. Described in Bulletin 173.

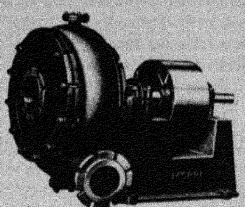


Fig. 953 Type K sand pump arranged for bel drive. An extremely simple design with only 3 wearing parts. Described in Bulleltin 174.

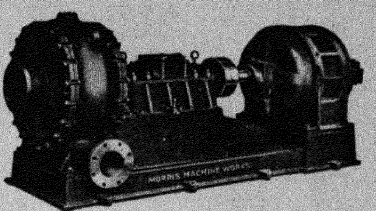


Fig. 915 Type F heavy-duty material-handling pump direct connected to electric motor. Described in Bulletin 158.

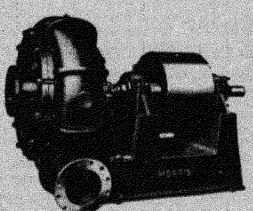


Fig. 1120 Type KM heavy duty sand pump arranged for belt drive. A sturdy, simple design for handling coarse abrasives.

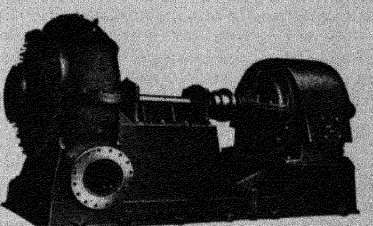


Fig. 678 Type H heavy-duty lined material-handling pump direct-connected to electric motor. Described in Bulletin 143.

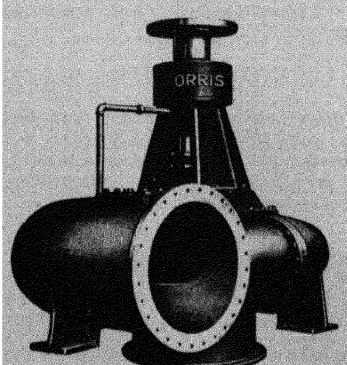


Fig. 771 Large side-suction vertical pump for dry-dock pumping service.

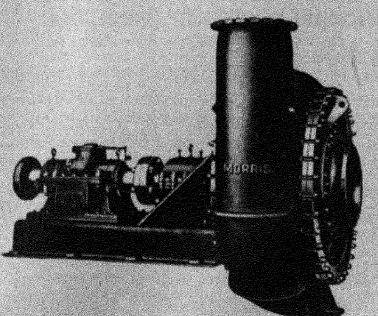


Fig. 1081 Large dredging pump arranged for direct connection to Diesel engine.

Figure 9. Materials Handling Pumps

p. 195 - Figure 9, subfigure 953: "Bel" should read "belt".

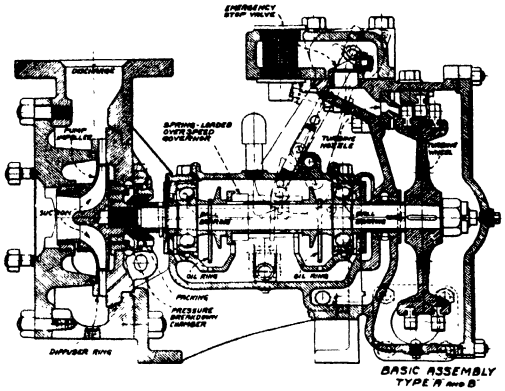


Figure 10. Steam Turbine Driven Single Stage Centrifugal Pump

E. MATERIALS HANDLING CENTRIFUGAL PUMPS

Figure 9 covers a group of materials handling pumps of the side suction type for conveying sand, gravel and sometimes even chunks as big as 2 inches. Notice the heavy design. Inside the casing are placed abrasion-resisting liners. These liners may be made of Flint metal. This is a white alloy cast iron of the Ni-Hard type which has a hardness of 600 - 700 Brinnell. Flint metal has an average service life of three to four times that of unalloyed iron. These liners are too hard to machine and must be ground. When wear occurs, the liners are replaced. On sand these pumps handle normally up to about 10% by weight. Velocities in the pump and in the pipe lines are kept high in order to keep the material in suspension and thus prevent settling out. These velocities are usually in the neighborhood of 12 ft. per second.

F. STEAM TURBINE DRIVEN CENTRIFUGAL PUMPS

Figure 1 illustrates a steam turbine driven single stage pump which is used for high pressure boiler feed service. Since the head and consequently the pressure developed by a centrifugal pump varies as the square of the speed, we can, if we run the speed up high enough, develop unusually high pressures. For example, for a speed of 7000 RPM, we can with one impeller of average size develop pressures up to 700 PSI with capacities up to approximately 300 GPM.

You will notice this is driven by a steam turbine with speeds up to 7000 RPM. In the case of a motor, the highest speed we can get with 60 cycle current is 3600 RPM. This steam turbine driven pump has been used on ships for boiler feed service. It has the advantage of compactness and light weight without sacrificing sturdiness. Incidentally, notice the diffuser rings used in this pump.

G. FRICTION IN PIPE LINES

The reason we put Figure 11 in at this point is to briefly introduce the subject of friction in pipe lines. This is so important in connection with pumping equipment. The particular table shown is the Hazen and Williams Friction Table with friction losses for 15 year old pipe. The coefficient on which this is based is one. For clean pipe just as it comes from the steel mill, the coefficient is 1.4 with corresponding 40% less friction. For normal water pumping operation we use the table which is shown. For chemical work, this is not reliable enough. For figuring flow losses in pipe lines when handling chemical solutions, let us suggest the curves developed by Raymond P. Genereaux of E. I. duPont de Nemours & Company, Inc. These are sounder and safer for figuring friction. Mr. Genereaux uses an average coefficient of 1.2.

CENTRIFUGAL PUMP PROBLEMS

Problem 1

Determine the total dynamic head required for selecting a horizontal centrifugal pump to handle 1500 GPM of water, temperature 60 F., taking suction from a standpipe, water level 50 ft. above centerline of pump suction, suction pipe 10 inches. One 10 inch gate valve, discharge to open tank, water level 120 ft. above centerline of pump discharge. Discharge pipe is 8 inches with 3 size 8 inches gate valves and 250 ft. of pipe (total length including 50 ft. rise) plus 2 side outlet tees and 6 short radius ells.

Problem 2

Determine the total dynamic head required for selecting a horizontal centrifugal pump to handle 750 GPM of gasoline, specific gravity 0.75. Vertical suction lift is 8 ft. size of pipe is 3 inches plus 1 foot valve and strainer, plus 50 ft. of linear pipe in suction. Discharge through 200 ft. of 2 inch pipe plus 8 short radius ells, 4 side outlet tees. Discharge to open tank 45 ft. elevation to top of tank. With a 70% pump efficiency, what is the brake horsepower required.

Problem 3

Determine the total dynamic head required for selecting a horizontal centrifugal pump to handle 100 GPM of water, temperature 80°C. Suction conditions 5 ft. positive through 30 ft. suction pipe 3 inches. One 3

196 - Problem 2, 2nd line: insert comma after "8 ft."

196 - Problem 3 should read: "Suction conditions 5 ft. positive through 30 ft. of 3" suction pipe including one 3" gate valve, discharge through 75 ft."... etc.

Friction Head Loss of Water in Pipes

Friction head in feet per hundred feet of pipe. Velocity in feet per second. Capacity in U. S. gallons.

¾-INCH PIPE			1-INCH PIPE			1¼INCH PIPE			1½-INCH PIPE			2-INCH PIPE			2½-INCH PIPE			3-INCH PIPE		
Cap. in GPM	Vel. in FPS	Frict. Head Loss in Ft. Per 100 Ft.	Cap. in GPM	Vel. in FPS	Frict. Head Loss in Ft. Per 100 Ft.	Cap. in GPM	Vel. in FPS	Frict. Head Loss in Ft. Per 100 Ft.	Cap. in GPM	Vel. in FPS	Frict. Head. Loss in Ft. Per 100 Ft.	Cap. in GPM	Vel. in FPS	Frict. Head Loss in Ft. Per 100 Ft.	Cap. in GPM	Vel. in FPS	Frict. Head Loss in Ft. Per 100 Ft.	Cap. in FPS	Vel. in FPS	Frict. Head Loss in Ft. Per 100 Ft.
2	1.20	2	4	1.49	2.1	5	1.07	.84	5	.79	.4	10	1.02	.5	15	.98	.36	30	1.36	.54
3	1.80	4	6	2.23	4.6	10	2.14	3.1	10	1.57	1.5	15	1.65	1.1	20	1.31	.61	40	1.82	.91
4	2.41	7	8	2.98	7.8	15	3.21	6.5	15	2.35	3.1	20	2.04	1.8	30	1.96	1.29	60	2.72	1.92
5	3.01	11	10	3.72	11.7	20	4.29	11.1	20	3.15	5.2	25	2.55	2.7	40	2.61	2.2	80	3.63	3.28
6	3.61	15	15	5.57	25.	25	5.36	16.6	25	3.93	7.8	30	3.06	3.8	50	3.27	3.3	100	4.54	4.96
8	4.81	25	20	9.44	42.	30	6.43	23.5	30	4.72	11.0	35	3.57	5.1	60	3.92	4.6	120	5.45	7.0
10	6.02	38	25	9.30	64.	35	7.51	31.2	35	5.51	14.7	40	4.08	6.6	70	4.58	6.2	140	6.35	9.2
12	7.22	53	30	11.15	89.	40	8.58	40.	40	6.30	18.8	50	5.11	9.9	80	5.23	7.9	160	7.26	11.8
15	9.02	80	35	13.02	119.	50	10.72	60.	50	7.87	28.4	60	6.13	13.9	90	5.88	9.8	180	8.17	14.8
20	12.03	136	40	14.88	152.	60	12.87	85.	60	9.44	39.6	70	7.15	18.4	120	7.84	16.8	200	9.08	17.8
						70	15.01	113.	70	11.02	53.0	80	8.17	23.7	140	9.15	22.3	220	9.99	21.3
									80	12.54	68.0	90	9.19	29.4	160	10.46	29.0	240	10.89	25.1
												100	10.21	35.8	180	11.76	35.7	260	11.80	29.1
												120	12.25	50.	200	13.07	43.1	280	12.71	33.4
												140	14.30	67.	220	14.38	52.0	300	13.62	38.0
															240	15.70	61.0	320	14.52	42.8
																		340	15.43	47.9

4-INCH PIPE			5-INCH PIPE			6-INCH PIPE			8-INCH PIPE			10-INCH PIPE			12-INCH PIPE			14-INCH PIPE		
60	1.53	.47	100	1.63	.41	100	1.12	.17	200	1.27	.20	300	1.23	.1	1000	2.84	.40	1000	2.10	.19
70	1.79	.63	120	1.96	.58	150	1.70	.31	250	1.59	.23	400	1.64	.19	1200	3.41	.60	1100	2.31	.23
80	2.04	.80	140	2.29	.76	200	2.27	.59	300	1.91	.34	500	2.05	.27	1400	3.97	.78	1200	2.52	.26
100	2.55	1.22	160	2.61	0.11	250	2.84	.90	400	2.55	.56	600	2.46	.4	1600	4.54	1.03	1500	3.15	.39
120	3.06	1.7	180	2.94	1.22	300	3.41	1.4	500	3.19	.82	800	3.28	.7	1800	5.11	1.23	2000	4.20	.66
140	3.57	2.3	200	3.27	1.48	350	3.97	1.7	600	3.83	1.2	1000	4.10	1.	2000	5.68	1.60	2500	5.25	1.01
160	4.08	2.9	220	3.59	1.77	400	4.54	2.3	700	4.43	1.5	1200	4.92	1.5	2200	6.23	1.80	3000	6.30	1.47
180	4.60	3.61	240	3.92	2.08	450	5.51	2.8	800	5.12	2.1	1400	5.64	1.8	2400	6.72	2.	3500	7.35	1.81
200	5.11	4.4	260	4.25	2.41	500	5.57	3.16	900	5.72	2.5	1600	6.56	2.4	2600	7.38	2.5	4000	8.40	2.47
220	5.62	5.2	280	4.58	2.77	600	6.8	5.0	1000	6.38	2.8	1800	7.38	2.9	2800	7.95	2.7	4200	8.82	2.80
240	6.13	6.2	300	4.90	3.14	700	7.92	6.1	1200	7.66	4.2	2000	8.20	3.8	3000	8.52	3.3	4500	9.45	3.22
260	6.64	7.2	350	5.72	4.19	800	9.08	8.1	1300	8.30	4.7	2200	9.02	4.2	3200	9.08	3.7	5000	10.50	3.92
280	7.15	8.2	400	6.54	5.4	900	10.2	10.9	1400	8.94	5.5	2400	9.74	5.1	3400	9.65	4.1	5500	11.55	4.65
300	7.66	9.3	450	7.35	6.7	1000	11.2	12.9	1500	9.57	6.5	2600	10.66	6.0	3600	10.25	4.5	6000	12.60	5.59
320	8.17	10.5	500	8.17	8.10	1100	12.3	14.6	1600	10.20	7.6	2800	11.48	6.5	3800	10.70	4.9	6500	13.65	6.45
340	8.68	11.7	550	8.99	9.6	1200	13.6	18.1	1800	11.50	9.0	3000	12.30	7.9	4000	11.36	5.6	7000	14.70	7.15
360	9.19	13.1	600	9.80	11 3	1300	14.7	20.2	2000	12.76	11.5	3200	13.12	8.6	4400	12.50	6.7			
400	10.21	16.0	700	11.44	15.1	1400	15.8	22.5	2200	13.95	13.0	3400	13.94	9.7	4800	13.64	7.6			
450	11.49	19.8	800	13.07	19 4	1500	17.0	25.9	2400	15.31	15.1	3500	14.10	10.08	5200	14.77	8.8			
500	12.77	24.0	900	14.71	24 0										5600	15.91	9.9			
550	14.04	28.7	1000	16.34	29 2										6000	17.04	12.0			
600	15.32	33.7	1100	17.97	34 9															
700	17.87	44.9	1200	19.61	40 9															
800	20.42	57.0																		
900	22.98	71.0																		

16-INCH PIPE			20-INCH PIPE			24-INCH PIPE			30-INCH PIPE			36-INCH PIPE			42-INCH PIPE			48-INCH PIPE		
1800	2.88	.30	3500	3.58	.34	5000	3.55	.27	8000	3.61	.238	13000	4.10	.21	20000	4.52	.25	30000	5.34	.27
2000	3.19	.39	4000	4.09	.47	6000	4.25	.38	9000	4.03	.278	14000	4.42	.24	22000	5.08	.28	32000	5.69	.29
2400	3.73	.51	4500	4.60	.58	7000	4.95	.50	10000	4.53	.36	15000	4 73	.30	24000	5.54	.32	34000	6.05	.34
2800	4.47	.68	5000	5.12	.67	8000	5.68	.69	11000	4.96	.40	16000	5.20	.35	26000	6.01	.39	36000	6.40	.38
3200	5.11	.87	5500	5.57	.81	9000	6.39	.83	12000	5.00	.47	17000	5.36	.37	28000	6.47	.43	38000	6.75	.41
3600	5.75	1.13	6000	6.14	.93	10000	7.20	1.10	13000	5.91	.54	18000	5.60	.41	30000	6.93	.52	40000	7.10	.46
4000	6.38	1.40	6500	6.65	1.11	11000	7.81	1.19	14000	6.36	.62	19000	5.94	.46	32000	7.39	.56	42000	7.45	.51
4400	7.02	1.68	7000	7.16	1.28	12000	8.51	1.34	15000	6.82	.71	20000	6.30	.54	34000	7.86	.64	44000	7.80	.54
4800	7.57	1.99	7500	7.68	1.46	13000	9.22	1.62	16000	7.28	.83	21000	6.62	.58	36000	8.32	.69	46000	8.18	.59
5200	8.30	2.17	8000	8.19	1.69	14000	9.95	1.81	17000	7.72	.91	22000	6.95	.62	38000	8.79	.78	48000	8.52	.64
5600	8.93	2.42	8500	8.70	1.87	15000	10.64	2.17	18000	8.20	1.01	23000	7.22	.65	40000	9.25	.89	50000	8.90	.68
6000	9.57	2.90	9000	9.20	2.01	16000	11.38	2.47	19000	8.64	1.14	24000	7.56	.71	42000	9.70	.97	52000	9.25	.71
6500	10.37	3.25	9500	9.72	2.30	17000	12.00	2.62	20000	9.09	1.19	25000	7.88	.76	44000	10.30	1.03	54000	9.60	.80
7000	11.17	3.68	10000	10.20	2.52	18000	12.80	2.99	21000	9.55	1.30	26000	8.18	.82	46000	10.65	1.14	56000	9.95	.84
7500	11.96	4.21	10500	10.75	2.61	19000	13.50	3.37	22000	10.00	1.47	27000	8.32	.92	48000	11.11	1.22	58000	10.30	.89
8000	12.76	4.80	11000	11.25	2.95	20000	14.20	3.51	23000	10.48	1.58	28000	8.82	.98	50000	11.52	1.38	60000	10.65	.95
8500	13.55	5.52	11500	11.76	3.12				24000	10.96	1.75	29000	9.45	1.12	52000	12.05	1.39	62000	11.0	1.02
9000	14.35	5.80	12000	12.26	3.38				25000	11.40	1.83	30000	9.09	1.26	54000	12.49	1.50	64000	11.4	1.07
9500	15.16	6.21	12500	12.80	3.68				26000	11.81	1.97	31000	10.72	1.38	56000	12.95	1.59	66000	11.75	1.13
10000	15.95	6.80	13000	13.30	4.05				27000	12.30	2.21	32000	10.09	1.42	58000	13.4	1.62	68000	12.1	1.21
10500	16.75	7.80	14000	14.29	4.49				28000	12.75	2.38	33000	11.35	1.64				70000	12.45	1.27
												34000	11.94	1.66						
												35000	12.60	1.91						
												42000	13.25	1.99						

Based on Hazen-Williams formula with C—100.

FRICTION OF WATER IN 90- ELBOWS

Size Elbow, inches	¾	1	1¼	1½	2	2½	3	4	5	6	8	10	12	14	16	20	24	30	36	42	48
Friction Equivalent Feet Straight Pipe	6	7	8	8	8	11	15	16	18	18	24	30	40	55	56	70	80	100	120	140	160

Figure 11. Friction in Pipe Lines

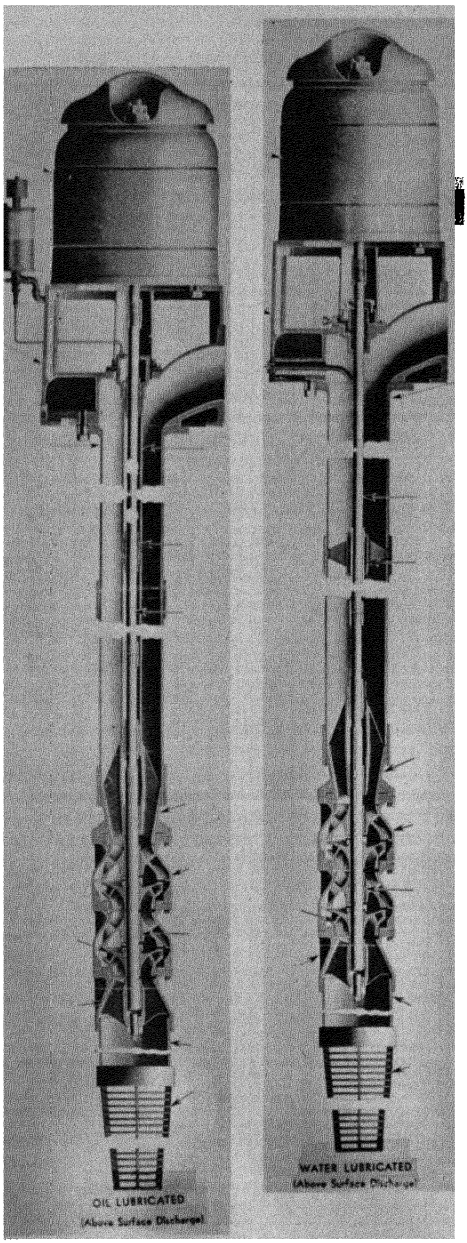


Figure 12. Deep Well Turbine Pumps, Oil Lubricated and Water Lubricated

inch gate valve, discharge through 75 ft. 3 inch pipe, one gate valve, no fittings, vertical elevation 25 ft. discharging to a pressure tank under 25 PSI.

Problem 4

Determine the total dynamic head required for selecting a horizontal centrifugal pump to handle 200 GPM of water, temperature 275°F. Pump taking suction through 4 inch pipe from a pressure vessel under 45 PSI, elevation of water on suction side above centerline is 45 feet. Vertical discharge 120 ft. plus 200 ft. 4 inch pipe, one swing check valve, 4 globe valves, 4 short radius ells plus 3 long radius ells, plus automatic control valve with 10 PSI drop, discharge to open tank.

Problem 5

Given a horizontal centrifugal pump rated 75% efficiency, 500 GPM, 80 ft. ahead, what would be the efficiency head, capacity and horsepower required when handling liquid of 550 SSU viscosity.

V. DEEP WELL PUMPS

Deep well pumps are one phase of the pump field which we want to mention briefly. Figure 12 shows the deep well turbine pump, both oil lubricated and water lubricated. Turbine pumps have come into wide use for deep wells. These have been built for heads up to 1000 ft. and capacities up to 8000 GPM in pumping wells large enough to take a pump 24 inches in diameter. This pump represents an application of vertical centrifugal pumps for deep well service.

The cross section of a deep well pump shows two principal parts; the head with a vertical driving motor, the discharge column and also a support for the vertical line shaft bearings plus the pumping unit. The pumping unit is that part installed under the pump head below the surface of the ground. It comprises a pump column, shafting and pump stages. The pump stage shown consists of bowls and impellers. The number of units comprising a deep well pump depends upon the head to be pumped against. For high heads, twenty or more stages are used.

Deep well pumps are made with enclosed and semi-enclosed impellers. If the water is clean, enclosed impellers can be used, and if there is abrasive matter like sand to be handled, then semi-open wheels are provided.

Normally deep well pumps are offered in the water lubricated design or in the oil lubricated design. If it is a water lubricated design, either bronze or cutless bearings are usually used. If oil lubricated, an oiler is placed in the approximate vicinity of the motor above the ground with copper pipes extending to the bearing below In general the water lubricated design is recommended for short settings and the oil lubricated design for deep settings. The reason for this is apparent when we consider the lubrication of the bearings. With oil lubricated bearings the oil can be made to run before the pump is started to make sure the bearings are not run dry. For deep settings with the water at a low level it is evident this is necessary. For short settings with the water

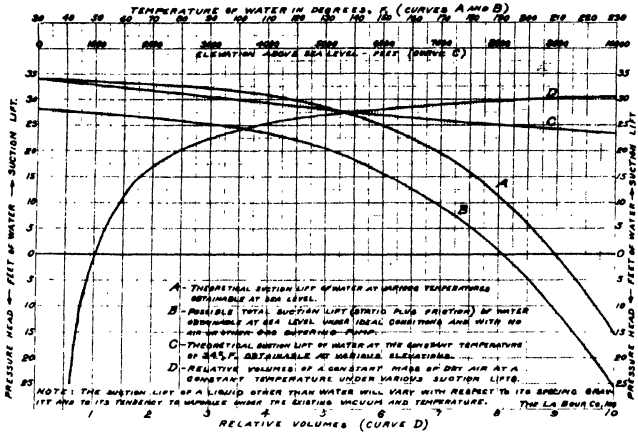


Figure 13. Temperature Vs. Suction Lift Curve

level fairly close to the pump discharge, the water quickly lubricates the bearings so that the oil service is not necessary. In the water lubricated type of deep well pump the shaft revolves in the water. In the oil lubricated type the shaft is surrounded by a protecting tube and the shaft runs dry in bronze lubricated bearings. These bearings are threaded on the outside and form the coupling for the protecting tube. This tube protects the shaft from rust and corrosion and avoids hydraulic losses caused by the shaft rotating in the water.

On a number of deep well pumps that have been developed in recent years, arrangements have been made to put the motor at the bottom with the bowls above. This eliminates the need for a long shaft such as we have when the motor is placed above the ground.

VI. TEMPERATURE VERSUS SUCTION LIFT

Figure 13 is a curve of temperature versus suction lift. "A" is the theoretical curve and "B" is the design curve. "B" is the curve that we normally use. You will note that at 192°F. on the centrifugal pump the liquid should have at least zero suction in order to get any pumping. At 150°F. we can lift water 15 ft. on the suction side, while at 210°F. we must have a positive head of at least 12 ft. on the suction. Pumping capacity is sacrificed for any reduction in positive head for temperature above 192°F. at sea level. The exact reduction in capacity can be obtained from curves which are available.

VII. PUMP LOSSES HANDLING VISCOUS LIQUIDS

Figure 14 comprises a set of curves which can be used in connection with changes in viscosity to determine the corresponding changes in capacity, head, efficiency and horsepower. For example, at 50 SSU the efficiency of the pump is 80%. Let us assume the viscosity changes to 1000 SSU, the efficiency then drops to 45%. At the same time the capacity drops from 80 to 57% and the head falls off from 80% to 61%. Normally we can use the centrifugal pump curves for viscosities up to about 300 to 400 SSU. This is similar to light engine oil. Centrifugal pump curves are based on water and you will have to make the corresponding reductions from these curves. Centrifugal pumps have been tested and information is available on handling liquids with viscosities up to 3500 SSU. The reduction in capacity, head and horsepower as compared to the same pump handling water is available in data and curves furnished by some of the pump manufacturers. Normally for a minimum 10 inch impeller, centrifugal pump manufacturers hesitate to offer these pumps for handling viscosities higher than 1500 SSU.

Centrifugal pumps can be listed in various groups depending upon the field of application. To illustrate, there are boiler feed pumps, chemical pumps, sanitary pumps, materials handling pumps, condensate pumps, Underwriters' Approved fire pumps, refinery hot oil pumps, high pressure hydraulic pumps, mine pumps, sewage pumps and paper stock pumps.

Obviously in a text of this scope it is out of the question to discuss the pumps under each of these headings. All obey the same basic centrifugal pump laws which we have covered.

VIII. NET POSITIVE SUCTION HEAD

If the absolute pressure in the suction line or pump chamber falls below the vapor pressure corresponding to the temperature of the liquid being pumped, vaporization will occur. When this situation prevails, cavitation and loss of capacity ensues. The term "Net Positive Suction Head" (NPSH), as recently defined by the Hydraulic Institute, is the total suction head in feet of liquid absolute determined at the suction nozzle and referred to datum less the vapor pressure of the liquid in feet absolute. When suction conditions require the pumping of volatile liquid without sufficient NPSH, best results may be obtained with short suction lines and high liquid velocities. This is due to the time element involved in vaporization of the liquid.

p. 199 - VII - 1st paragraph, last line should read:
"Normally, centrifugal pump manufacturers hesitate to offer these pumps for handling viscosities higher than 1500 SSU with impellers smaller than 10 inch diameter"

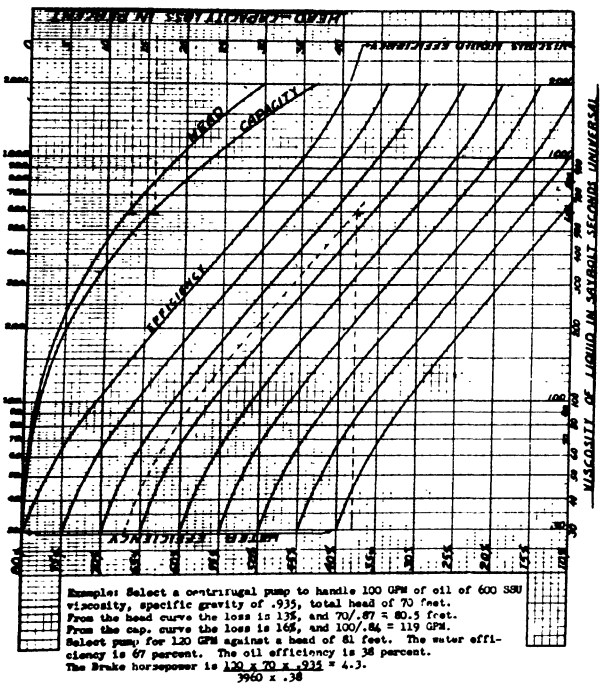


Figure 14. Reduction in Viscosity Curves

An example of NPSH is as follows: Pump handling water at 300°F., 100 PSI, velocity at suction nozzle is 8 ft. per second, what is the NPSH. Density of water at 300°F. equals 57.23 lbs. per cubic foot. Vapor pressure equals 67.00 PSI. Vapor pressure equals $67 \times \frac{144}{57.3} = 168$ PSI. Velocity head equals $\frac{V^2}{2g} = \frac{8^2}{32.2} = 1.98$ ft. Total suction head equals (100 x 14.7) x $\frac{144}{57.33}$ plus 1.98 = 287 ft. abs. NPSH = 287 less 168 = 119 ft.
Applications requiring these calculations occur in boiler feed pumps.

A. Correction for High Temperatures

Assume temperature of water at 60°F. From steam tables, vapor pressure of 0.256 PSI. Maximum suction lift at sea level equals 14.7 minus 0.256 equals 14.444. 14.444 x 2.31 equals 33.3 ft. If suction lift is 15 ft. the NPSH equals 33.3 minus 15.0 equals 18.3 ft. (NPSH). If temperature of water is 190 F. and positive head is 3 ft., vapor pressure for 190° water is 9.34 PSI. 14.7 plus $\frac{3}{2.31}$ x 0.964 = 15.95 PSI absolute. 15.95 corresponds to 3 ft. positive head. This is then used in connection with available curves to determine the specific speed to use. Corrections must be made for variation above or below sea level.

IX. TURBINE PUMPS

Figure 15 shows the turbine type pump, sometimes called a regenerative or peripheral pump. This is closest to the centrifugal pump but has some features of a positive displacement pump. It operates pretty much as a centrifugal pump but is so designed that it can develop several times the pressure obtained from a greater impeller diameter and operating at the same speed.

Maximum pressure produced by a turbine pump bears no relation to impeller diameter and its speed. It involves capacity and the design of the impeller and the fluid channel in which the blades of the impeller run.

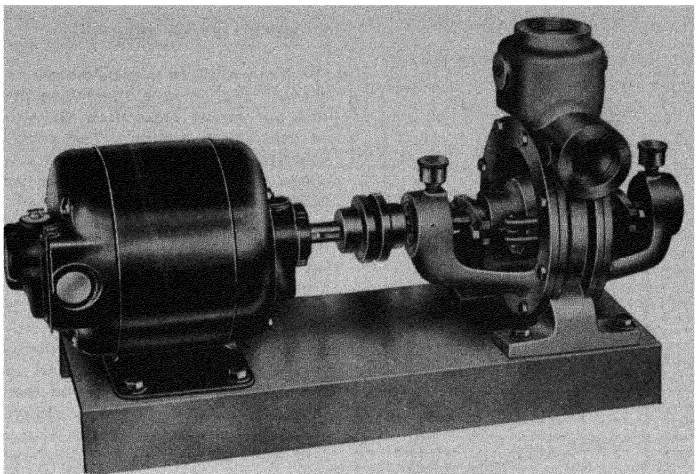
Power required to drive a centrifugal pump decreases as the operating head increases, whereas power input to a turbine pump increases with the operating head even though the discharge decreases rapidly. In this respect the turbine pump resembles a positive displacement pump.

In a centrifugal pump the liquid enters at the eye of the impeller and flows in between the vanes. By the action of the centrifugal force the liquid is thrown outward into the volute channel. In the turbine type pump the liquid enters at the tip of the impeller, flows along the channel and discharges on the outside of the casing.

In a centrifugal pump the liquid passes between the impeller vanes only once and has energy supplied to it while moving the short distance from the eye of the impeller to the tip of the impeller. In the turbine pump the liquid is re-circulated between the vanes. Energy is supplied to the liquid as a result of a number of impulses that are given to it by the impeller vanes by travelling the distance from the suction to the discharge nozzle.

These impulses are comparable to the multi-staging of centrifugal pumps. In multi-stage centrifugal pumps, the energy supplied to the liquid is an addition of the kinetic energy received from a number of impellers in series. In the same way energy supplied to the liquid in a turbine pump is the addition to that received from a number of impeller blades. The number of impulses given to the liquid by the blades of the

p. 200 - next to last paragraph, last line: "..impulses that are given to it by the impeller vanes while travelling" (instead of "by travelling").



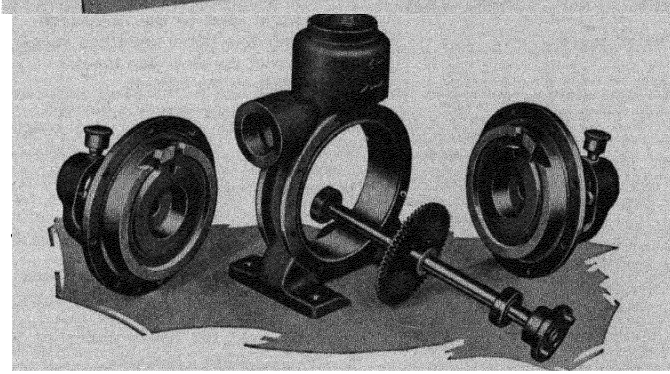


Figure 15. Turbine Type Pumps

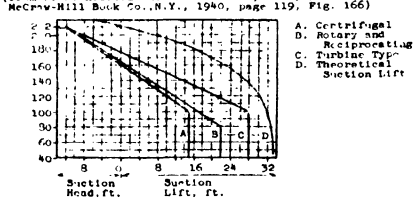
impeller depends upon the discharge pressure and speed of rotation. The pressure developed in the channel of a turbine pump is variable. It is minimum at the suction opening and gradually increases to a maximum at the discharge port.

Figure 16 is a typical curve from a turbine type pump. Note the capacity head curve has a drooping characteristic somewhat similar to centrifugal pumps. On the other hand, the power requirement for turbine pumps increases as the discharge head increases reaching a maximum at the shutoff pressure. The centrifugal pump, on the other hand, has the lowest power requirement at shutoff pressure.

Primarily, the turbine pump has a small capacity and high head design. For capacities up to 50 GPM, it is more efficient than a centrifugal pump, and for capacities up to 100 GPM, it has comparable efficiency.

For high suction lifts, the turbine pump is ideal as it has the highest practical lift characteristic of any of the liquid handling pumps. This is shown in the accompanying chart. This characteristic makes it a desirable unit for handling hot and volatile liquids. Turbine type pumps are not suited, however, for handling highly viscous liquids or abrasives in suspension.

Suction Lift for Different Types of Pumps
(from F. A. Kristal and F. A. Annett, "Pumps," McGraw-Hill Book Co., N.Y., 1940, page 119, Fig. 166)



Turbine type pumps operate with more success at speeds not over 1750 RPM. With a single stage and the safe speed of 1750 RPM we can easily get heads up to 250 ft. or 300 ft. If heads higher than this are required, we put two stages in series exactly as in the centrifugal pump. The total head is the sum of the heads developed by each impeller. Turbine pumps have been built with as many as five impellers in one casing for heads up to approximately 1100 ft. for water service.

In certain cases the tandem setup has been used. With these two two-stage turbine pumps mounted on the same base with only one motor at the end, the discharge from the second stage of the first pump is piped to the first stage of the second pump. This is equivalent to four stages.

An application of the turbine type pump is for water systems. This is extensively used in farms and homes for taking water from a shallow well and putting it into a tank with air pressure on the top.

Another application of the turbine pump is for use on condensate water systems, in connection with a float valve and a receiver. This pump can handle rather hot water, for example, 200 F., with very little positive suction head, not over 2 ft.

p. 201 - next to last paragraph, 2nd line: "With these, two two-stage.." etc.

p. 201 - next to last paragraph, 6th line: "This is used extensively.." (instead of "This is extensively used").

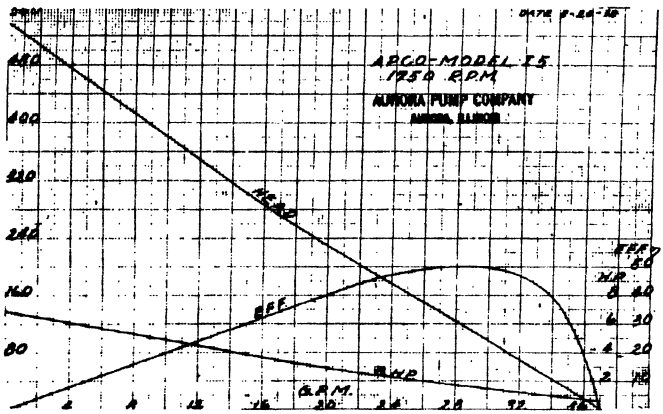


Figure 16. Turbine Pump Performance Curve

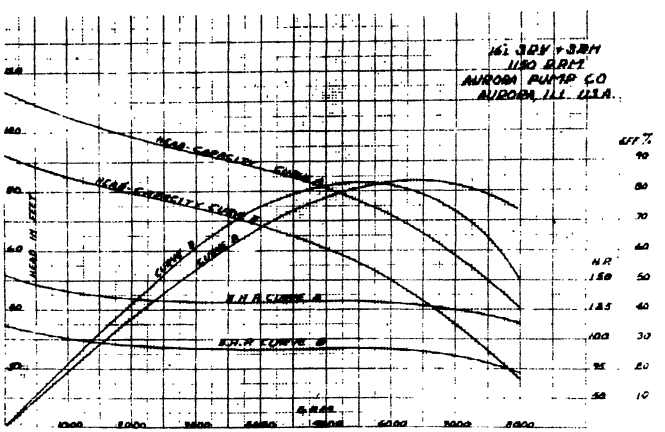


Figure 17. Mixed Flow Pump Curve

X. MIXED FLOW PUMPS

Figure 17 is a mixed flow curve. Please note the heads drop with increasing capacities, the same as centrifugal pumps. The power, however, generally rises with reduced capacity the same as in turbine type pumps. We mentioned before that the mixed flow pump is half-way between the centrifugal and the positive displacement pump. The impeller is of the open type with a large clearance between it and the casing. This type of impeller develops its head partly by centrifugal force and partly by the lifting action of the vanes on the liquid. This type of pump always has a single inlet impeller with the flow entering axially and discharging in both axial and radial direction. Right next to the discharge of the impeller there are fixed vanes which direct the flow into the discharge side of the casing.

Propeller pumps are similar in action to the propeller of a boat enclosed in a tube, as mentioned above. The liquid is drawn into the pump, flows axially, and is pushed out without changing its direction of flow. These pumps have very little suction or lift power, but they do have push power that can be applied to large volumes of liquid. Propeller pumps are normally used for heads under 40 ft. and for large volumes.

XI. SPECIFIC SPEED

Suction lift in a centrifugal pump is important as it affects the operating characteristics. Suction lifts which are too high cause cavitation, reduction in capacity and efficiency. For centrifugal pumps the suction lift bears a relation to the impeller speed, head and capacity. This brings up the subject of specific speed.

The specific speed of an impeller is the RPM at which a geometrically similar impeller would run if it were of such size as to discharge 1 GPM against 1 ft. head and is defined by:

$$n_{sm} = n_m \, q_{gm}^{1/2} / h^{3/4}.$$

Where n_m = impeller speed, rev./min.
n_{sm} = specific speed
q_{gm} = pumping rate, gal/min.
h = head developed, ft. of fluid flowing.

The specific speed of an impeller is an index to its type. It is used when designing impellers to meet different conditions of head, capacity, speed and suction lift.

p. 202 - 2nd paragraph, line 3: Eliminate "as mentioned above".

p. 202 - 2nd paragraph, line 4: "The liquid enters the pump" (instead of "The liquid is drawn into the pump").

Impellers for high heads usually have low specific speeds and impellers for low heads usually have high specific speeds.

	Type of Pump			
	Centrifugal "A"	Centrifugal "B"	Mixed Flow "C"	Propeller "D"
Specific speed, (n_{sm})	1,250* 2,400	2,200* 2,400	6,200 2,400	13,500 2,400
Flow, gal./min.	70	48	33	20
Head, ft.	870	1,160	1,750	2,600
Speed, rev./min.	19	12	10	7
Runner diam., in.				
Ratio of eye to runner diameter	0.5	0.7	0.9	1.0

*Based on single suction

From "Pumps" by F. A. Kristal and F. A. Annett, McGraw-Hill Book Co., 1940, p. 128, Fig. 179.

As shown in the above table, a pump of low specific speed has a narrow impeller and radial vanes and the eye of the impeller is small compared to its diameter. This is particularly true of the centrifugal type impeller "A" which has a specific speed of 1250. It has an outside diameter of 19 inches and a suction eye diameter of 9.5 inches or one-half of the impeller diameter. Impeller "B" has a specific speed of 2200 and is good for a capacity of 2400 GPM against a 48 ft. head when operating at 1160 RPM. The diameter of the impeller is only 12 inches but its eye has a diameter of 8.5 inches and even though it operates at nearly 50% higher speed than type "A" it develops 30% less head.

The mixed flow impeller "C" has a specific speed of 6200 and delivers 2400 GPM against 33 ft. head when operating at 1750 RPM. This impeller, although it operates at twice the speed of type "A", develops less than one-half the head. It has an outside diameter of 10 inches and an eye diameter of 9 inches. Propeller or axial flow impeller "D" has a specific speed of 13,500 or more than ten times that of impeller "A" but develops only about 30% of the head, namely 20 ft. with a discharge of 2400 GPM. When operating at 2600 RPM this impeller, which is 7 inches in diameter, has an eye of equal diameter.

It can be seen that with an increase in specific speed the impeller diameter becomes wider and the ratio of eye to impeller diameter increases until this ratio reaches one for the propeller pump. This pump has an extremely high specific speed, low head, high capacity, and high operating speed. With an increase in specific speed, the pump operating speed increases and its physical dimensions become smaller.

Knowing the specific speed permits us to determine the allowable suction lift or minimum net positive suction head for acceptable operating condition. It is well worth knowing that a slow speed impeller and therefore a low specific speed operates with a longer suction lift. Curves are available for determining the speed for the optimum conditions.

XII. ROTARY PUMPS

Figure 18 illustrates types of rotary pumps. Actually there are many types of rotary pumps manufactured in this country. A rotary pump may be defined as a machine which accomplishes the transfer of liquid by mechanical means through the action of rotating pistons, gears, cams, screws, or vanes in a fixed casing. The liquid is directly displaced without application of centrifugal force. The picture will serve to explain several of the principal varieties.

In the upper right hand corner, we have a spur gear which has an outside turning medium that causes the top gear to revolve. This gear meshes with and turns the bottom gear. The liquid enters the suction from the left. It is caught in the tooth and carried through the casing to the discharge. The same thing happens on the other gear. The liquid is prevented from flowing from the discharge back to the suction by means of meshing teeth. The actual width of contact in the spur gear is 0.02 inches. When this clearance is gone, so is the pump.

The pump at the lower right is known as the gear-and-crescent type. In this we have a spur gear off center which is driven by some outside driving medium. This spur gear meshes with an internal

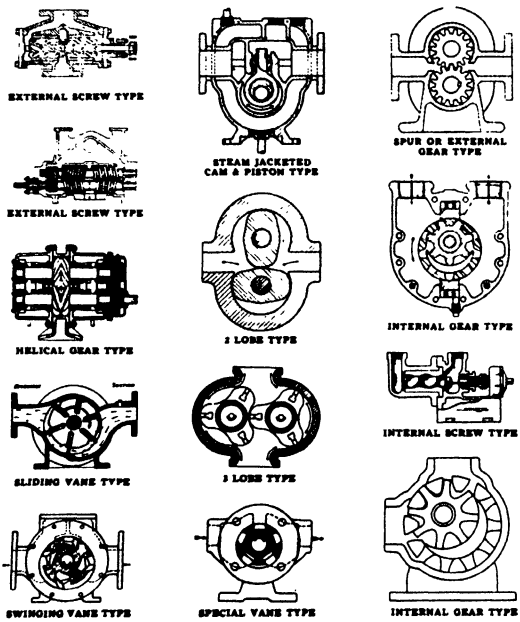


Figure 18. Rotary Pumps (Reprinted from the Std. of Hydraulic Institute, Rotary Pump Section, Copyright 1947, by Hydraulic Institute, New York 6, N.Y.)

gear. The volume of liquid trapped in the spur gear tooth is carried around the inside of the crescent to the discharge. Either a spur gear or a gear-and-crescent type pump can operate in either direction.

Under the gear type pump is shown another variation of the gear-and-crescent type with an internal relief valve. At the upper center is a steam jacketed cam and piston type. As the piston revolves around in the casing, it pushes the liquid ahead of it. The pump shown under this is a two lobe type. The liquid in this enters on the left, is trapped between the lobe and the casing and is pushed to the discharge. Each lobe has the same pumping action. Under the two lobe type is a three lobe type, just a variation. Under that is a special vane type. This also has a positive displacement action.

In the screw type pump the liquid enters at the opening shown at the top, divides and flows to each end of the pump. Here this liquid is trapped in the screws and flows to the center from each side and then out of the common discharge. The unit shown has internal timing gears lubricated by the material handled and the pumping screws are kept apart from each other and also from the outside casing. There is no contact. In this particular design only one stuffing box is used. If the material does not have lubricating properties then the timing gears are placed external to the pumping screws and emersed in an oil bath. All bearings would then be external and the pump would have four stuffing boxes. For handling heavy thick paste a hopper would be placed above the screws so as to permit easy entrance. Except for the screw type pumps shown in the upper lefthand corner and for the sliding vane type pump, all of the other pumps are low pressure types with maximum pressures up to approximately 200 PSI. The screw type pump is used up to 1000 PSI if the liquid handled is viscous enough. In the screw type pumps the stuffing boxes are under suction whereas in all of the other pumps illustrated the stuffing boxes are under pressure. The amount of this pressure is somewhere between the suction and discharge pressure.

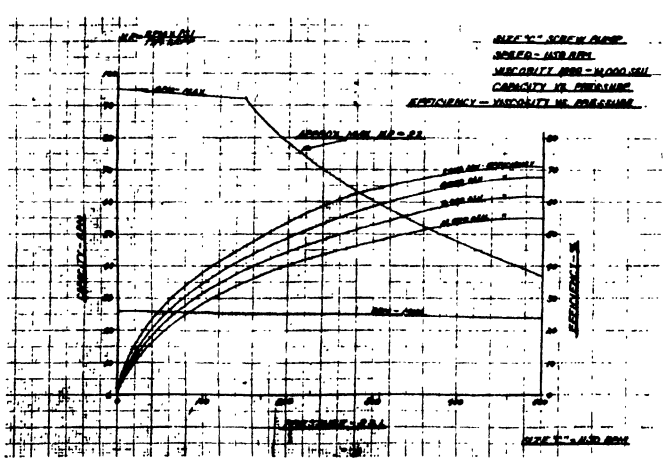


Figure 19. Curve of Screw Type Pump

Figure 19 shows a curve of a screw type pump. You will note that the capacity falls off slightly with increase in pressure up to 170 PSI. The reason the curve drops rapidly at that point is due to structural limitations in the pump. The shaft can carry only a certain amount of horsepower. In this case, the line represents a constant horsepower of about 22. Also note that for a high viscosity

p. 204 - 2nd paragraph, line 12: change "emersed" to "immersed".

the efficiency drops. This is due to the power wasted to overcome shear in the pump.

In the sliding vane type, centrifugal force holds the vanes against the side of the casing and the vanes push the liquid from the suction to the discharge. These pumps are made for pressures up to 5000 PSI on high pressure service.

The pump at the lower left is the swinging-bucket type. Centrifugal force holds the buckets against the side of the casing and the buckets push the liquid from the suction to the discharge. This pump is suitable for 150 PSI.

The last type pump is the internal screw type. This uses a single helix in the rotor which is surrounded by a double helix in the casing. This surrounding double helix is normally made of rubber. A pump of this type has been successful for handling fibrous materials up to medium pressures of 100 - 150 PSI.

Positive displacement pumps have favorable vacuum characteristics and are self priming. With these pumps it is possible to handle liquids containing entrained gases or vapors without loss of prime. A loss of volumetric efficiency will result when pumping entrained vapor or gases. To vary the pump capacity it is necessary to vary the pump speed. The horsepower required by a rotary pump is expressed by the equation

$$HP = \frac{gpm \times psi}{1714\ E}$$

Where: HP is the brake horsepower required. gpm is gallons per minute
psi - pounds per square inch E - pump efficiency.

Pressure developed by rotary pumps is independent of speed and is determined by the total dynamic head. Positive displacement pumps cannot be operated against closed discharge lines without damage to the pump or prime mover. When such operation is required, it will be necessary to provide a bypass relief valve in the pump or in the discharge line.

Power requirements for a positive displacement pump will vary directly with the head, provided the speed is constant. The brake horsepower required is determined by the capacity, dynamic head and efficiency.

The efficiency of the rotary pump is somewhat dependent on the clearances of the rotating members. Actual clearance is determined by the size of the pump, viscosity of the fluid and temperature of the liquid. With thin liquids rather close clearances are desirable so as to reduce the slip to a minimum. Highly viscous and tacky liquids require relieved clearances for maximum efficiency.

Rotary pumps have been developed to cover pressures up to 10,000 PSI and capacities up to several thousand gallons per minute. Rotary pumps may be used when high vacuums are required. The outstanding field of application for the rotary pump is the pumping of highly viscous liquids. Liquids with viscosities in excess of 90,000 poises have been pumped with rotary pumps. The absence of valves in the rotary pump greatly facilitates pumping very viscous fluids.

Rotary pumps find application when positive displacement characteristics are required. Applications requiring suction lift, pumping of liquids with entrained vapor, small capacities at medium or high pressure are all within the rotary pump field of application.

Successful operation of any pump is dependent on proper proportioning of the suction line. When suction lines are too long, or not of sufficient size, cavitation will occur. The effect of cavitation will be a loss of capacity and noisy operation.

When proportioning the suction line, it is necessary to consider the following factors:

Vertical distance from the source of supply.
Entrance losses.
Velocity losses.
Friction losses.
Absolute pressure required to prevent vaporization of the liquid in the suction line of the pump.

The effect of viscosity on suction line size, length, and capacity is very important. Viscosity is that property of a liquid which resists any force tending to produce flow. Consequently greater frictional losses will be encountered with increased viscosity. High frictional losses in the suction line will occasion a reduction in capacity and in the velocity of the liquid in the suction line. The reduction in suction line capacity occasioned by increased viscosity will require a reduction in pump speed so that the pump displacement does not exceed the line capacity.

A. Slip

Slip in rotary pumps is the liquid lost by leakage through the pump clearances. Increased clearance will result in greater slip. The size and shape of the rotor determines the slip. Rotors with long sealing surfaces have less slip. On most pumps the shortest sealing surface will be found at the sides of the rotor and it is at this point that the majority of slip occurs.

Theoretically, slip will vary as the square root of the pressure differential for a condition of turbulent flow and directly for a condition of laminar flow through the pump clearances. Most rotary pump applications are for laminar flow.

Viscosity is a factor in determining slip. Theoretically the slip will vary inversely with the viscosity. The effect of slip may be disregarded with very viscous liquids as the quantity become negligible.

Slip is independent of pump speed. This factor must be taken into consideration when operating at low speeds with thin liquids. For example, the quantity of slip at 400 RPM pump speed will be the same as the quantity at 100 RPM provided the pressure is constant.

B. Volumetric Efficiency

The volumetric efficiency of a rotary pump is the ratio of the actual capacity to the theoretical displacement of the pump. With thin liquids this is greatest at maximum pump speed since the slip is constant per unit of time. With highly viscous liquids, the effect of slip may be disregarded in figuring the volumetric efficiency.

The presence of entrained gas or air in the liquid being pumped will reduce the volumetric efficiency with suction lift conditions. Air leaks in the suction line or through the stuffing box will also reduce the volumetric efficiency.

Volatile liquids require an excess of NPSH to prevent loss of volumetric efficiency. Viscous liquids require pump speed and displacement to be synchronized with suction line capacity so as to preclude cavitation and loss of volumetric efficiency.

C. Cavitation

Cavitation in a pump is an undesirable vacuous space in the part of the pump rotor normally occupied by the liquid. Vaporization of liquid in the suction line of the pump or in the pump chamber is a common cause of cavitation. Vapor bubbles will be carried along with the liquid until a region of high pressure is encountered, at which time the bubbles will collapse with shock. The magnitude of the shock is dependent on the pressure, amount of slip and nature of the pump. To prevent vaporization, increase the NPSH.

When pumping highly viscous liquids, the speed of the pump must be adjusted to the viscosity of the liquid. Viscosity is a friction effect and reduces the capacity and velocity of the flow through the suction line. Cavitation will occur if the velocity of the rotor does not allow sufficient time to fill the liquid cavity of the rotor. It is interesting to note that there is a definite relation between suction line velocity and rotor velocity.

Cavitation in pumps handling highly viscous liquids will usually be accompanied by greater shock and noise than occurs with cavitation in pumps handling thin liquids. This is because less slip is encountered on highly viscous liquid and slip accomplishes the partial collapse of the vacuous space before the region of high pressure is reached.

Excessive cavitation is the most commonly encountered of all pump difficulties. It occurs with all types of pumps; rotary, reciprocating or centrifugal. When encountered, excessive pump speed or adverse suction conditions will be found responsible. Reducing the pump speed or remedying the suction condition will usually eliminate the difficutly.

Losses in timing gears and bearings may possibly amount to 10% of the power consumption. Stuffing boxes are large consumers of power.

Viscosity has a marked effect on pump efficiency. A reduction in efficiency is encountered with increased viscosity. This is due to the energy required in effecting viscous sheer in the pump clearances. Viscous liquids often possess adhesive properties which will occasion a further reduction in pump efficiency. This is due to the additional power required to start a pump handling a tacky liquid. After the pump has been started, the power requirements may diminish with a tacky liquid. With viscous tacky liquids, improved efficiency will be obtained with relieved clearances.

Rotary pump efficiency seldom exceeds 75%. With very viscous liquids, pump efficiency may be as low as 15 - 20%.

XIII. RECIPROCATING PUMPS

Figure 20 illustrates some of the types of reciprocating or piston type pumps. In the upper left is shown the duplex piston packed valve plate type, double acting. The linkage from one side operates the valve for the other to cause the steam end of the cylinder to move back and forth. Under this is the duplex side pot type, normally for higher pressures. The valves are put in the side pots as shown.

Under this is a single cylinder, outside packed type pump. In the single cylinder pump, as the plunger or piston moves forward, the valve linkage moves a stop on the valve rod and lets steam into the cylinder to reverse the flow. Incidentally, we have both plunger and packed type of piston. In the

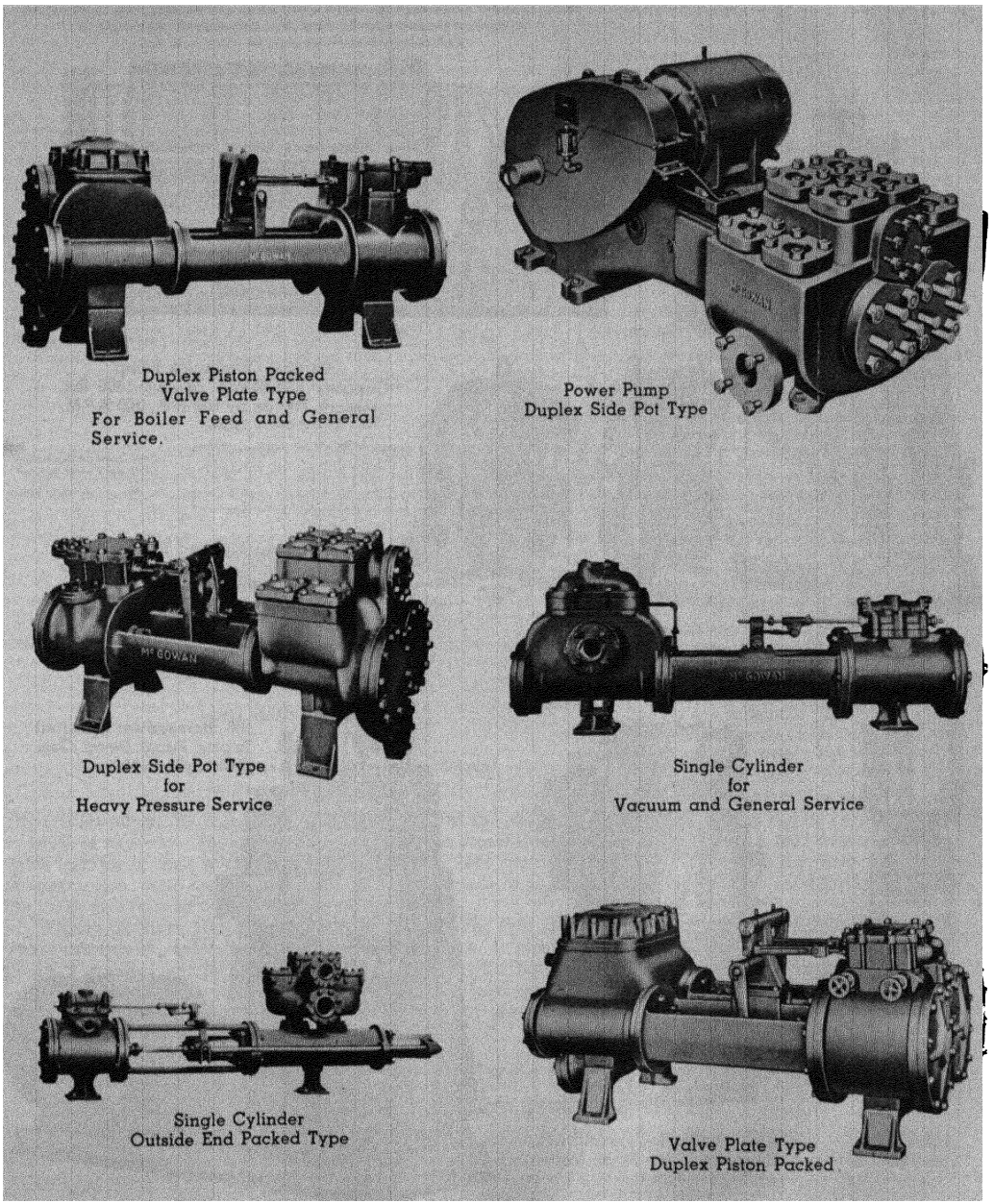


Figure 20. Reciprocating Pumps

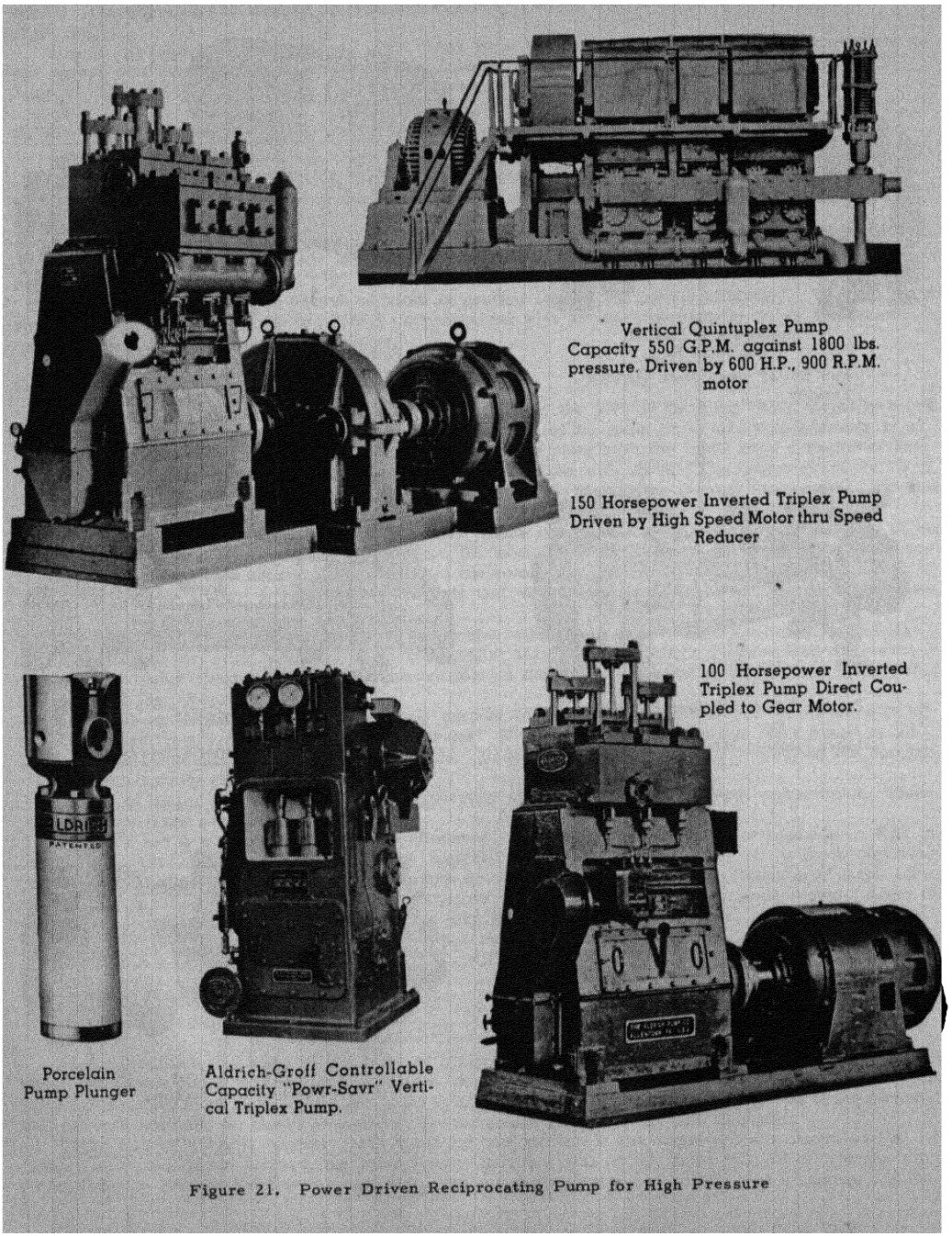


Figure 21. Power Driven Reciprocating Pump for High Pressure

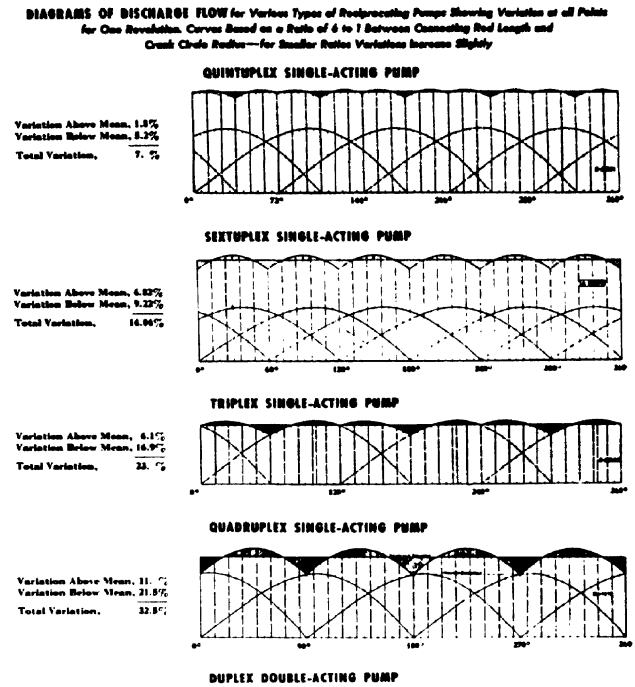


Figure 22. Diagrams of Pulsating Flow from Reciprocating Pumps

piston type the snap rings on the piston operate inside the cylinder. In the plunger type the plunger enters the chamber and moves the liquid directly by displacement of the plunger into the liquid.

In the upper right hand corner, we have a motor driven duplex side pot type pump. In this the motor drives a chain and a set of gears and finally the plungers. Under the motor drive job is another single cylinder type and under that is another duplex valve plate type.

Figure 21 illustrates a power driven reciprocating pump for high pressures. In the upper left we have a triplex pump driven by a motor through a reduction gear. In the upper right is a quintuplex pump with five plungers, single acting. Note that the capacity is 500 GPM against 1200 PSI and is driven by a 600 HP, 900 RPM motor. In the lower right is another triplex pump of the vertical type. With this design it is possible to put the motor and crankshaft on the ground. These types of pumps have been built for triplex, quintuplex, septuplex and nonaplex. These are 3, 5, 8 and 9 cylinders respectively. Cylinders are added to get capacity. In the oil fields of Texas, with multi-cylinder pumps, for example, specifications often call for pipe line pumps to handle 1000 GPM against 1000 PSI. A pump to do this would be a nonaplex pump with a 600 HP motor.

The pump shown in the lower center is an Aldrich-Groff controllable capacity triplex pump. By means of a stroke adjustment and shoe, the stroke of this pump can be varied from zero to 100% of capacity. The stroke adjustment can be controlled by an oil cylinder with a four way open center valve such as is used on the Servo motor control. This can be further operated from a regulator or other instrumentation. With the use of controlled volume pumps it is possible to eliminate the need for an accumulator, such as are used on hydraulic systems.

Figure 22 illustrates the diagrams of the pulsating flow from the various types of reciprocating pumps. These are triplex, quintuplex, septuplex and nonaplex. In pipe line pumping it would be in order to install a group of nonaflex pumps to carry the main portion of the load and take the swings on the variable stroke unit.

Triplex pumps are always power driven. In a triplex pump due to the fact that the plungers are placed 120° the maximum pressure is the pressure from any one cylinder. There is no help as far as pressure is concerned from any other one.

PART NO. 2

PUMPS FOR CHEMICAL AND PROCESS INDUSTRIES

The design of centrifugal pumps for handling the corrosive liquids has advanced rapidly in the last 25 years. Previous to that various types of pumping equipment were used ranging from the reciprocating or piston type pump to the standard centrifugal pumps normally for use on water. The blow-case using compressed air was a common form of transferring corrosive liquids.

With the introduction of the nickel chromium alloys the advancement in design and use of centrifugal pumps for the chemical and process industries was rapid. At first we were limited to several of the high priced chromium nickel alloys. We, of course, had the common metals, like lead, aluminum, bronze and

p. 209 - 3rd paragraph: "eliminate the need for accumulators" (instead of "for an accumulator").

p. 209 - 3rd paragraph; 2nd line: "By means of a stroke adjustment, the stroke..." (omit "and shoe").

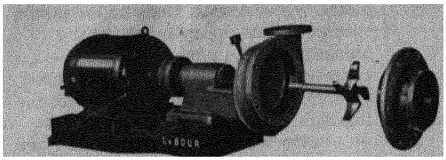


Figure 23. Exploded View of Chemical Centrifugal Pump

cast iron. But the real strides were made in the development of centrifugal pumps for handling corrosive liquids when the production of corrosion resistant alloys increased. The introduction of self priming centrifugal pumps in 1923 also materially increased the use of chemical pumps.

I. CENTRIFUGAL PUMPS—GRAVITY FEED

Figure 23 is an exploded picture of a chemical centrifugal pump. Note its unusual construction as

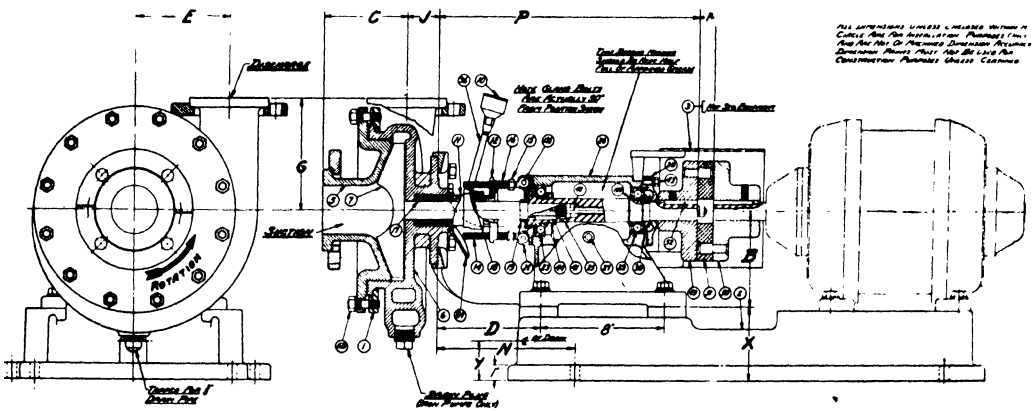


Figure 24. Cross-Section of Chemical Centrifugal Pump

compared with a standard pump. The base plate is short so that drippage from the stuffing box is outside of the base plate and this leakage can be kept in a suitable receptacle for disposal. In the chemical centrifugal pump, the best procedure is to use a coupling type of pump like this. The reason is we want to keep the motor as far as possible from the pump to protect the motor.

Figure 24 shows a cross-section of this pump. Note how the gasket is put off to one side so as not to be subjected to the direct pressure of the liquid in the casing. Also examine the method of fastening the casing with stud bolts through the clamping flanges. In a chemical pump we never put the bolts in a position where they will be in direct contact with the liquid handled.

The stuffing box in this type is unusual. It is what we term a floating stuffing box. First, there is the conventional five or six rings of packing; then a grease packed space fed by a grease cup; then we have two outside rings that are compressed by the gland follower. This assembly is floating and hung on the end of the bearing bracket. In a chemical pump it is important that the shaft run within close limits. When the pump leaves the factory, the whip is usually not over plus or minus a thousandth of an inch at the stuffing box. Bearings should be rugged for long life. Eventually the bearings will wear and the impeller shaft will force the packing to become egg shaped.

The second stuffing box or the floating gland type follows every small movement of the shaft attempting to prevent leakage that tends to get by a conventional stuffing box. Note that the gland is on only spring tight. In a water pump you want some leakage to lubricate the packing. In a chemical pump we want to avoid any leakage. It is necessary that the packing be lubricated and for this reason we furnish a grease cup. A packing of this size with approximately eight rings acts as a brakeshoe and generates heat which burns the packing to a hard abrasive mass. The shaft grooves at the packing gland. Further tightening of the stuffing box produces more pressure and wear and we are working against ourselves.

For chemical work the fully open impeller is recommended. This type of impeller is shown in Figure 23. With a 1/32" clearance on each side and large end clearances the pump is better to handle the corrosive liquids and in many cases slurries. When these clearances open up to 3/32 inches, factory tests show that the actual loss in pumping capacity is only 7%. The size of solids this type of impeller can handle varies from 1/4 inch to 1 inch depending on the clearance. If the solids get between the blades, there is plenty of room to pass.

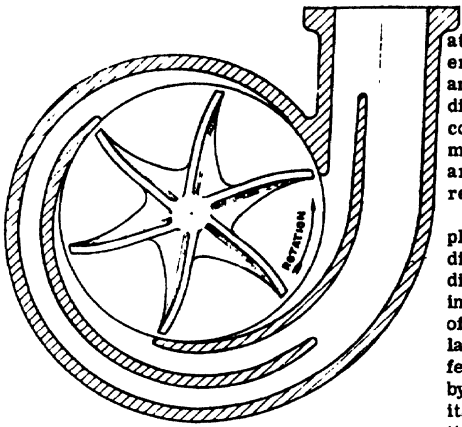


Figure 25. Casing of Chemical Centrifugal Pump

Figure 25 shows a section of the casing of the pump at which you have just looked. This pump is really several pumps in one casing arranged so that the liquid takes an extremely short path of travel from the suction to the discharge. Full pressure is developed in less than the complete rotation of the impeller. It was found that the maximum velocity is generated about one-third of the way around and from then on dragging the liquid through the remainder produces friction and eddy currents.

After the work has been done by the impeller, the simplest thing to do is to pipe it away. These three openings discharge the liquid 120° apart then empty into the same discharge opening. Efficiencies are exceptionally high and in some cases run over 80%. A favorable characteristic of this pump is that it will not air bind but will handle large quantities of air if both the air and the liquid are fed to the pump. Actually this pump handles 20% of air by volume. The average centrifugal pump loses a lot of its capacity with 1% and 2% and with 3% the pump is entirely finished and airbound. The reason this particular pump handles 20% of air volume is because of the unbalanced throat condition that acts similar to the self priming centrifugal pump which will be discussed shortly. Due to the air handling capacity of this chemical pump, it is used on volatile liquids. Taking from the bottom of vacuum evaporators, this pump is ideal. It is used as a standard by such companies as Swenson Evaporator Company, Goslin-Birmingham and Burt.

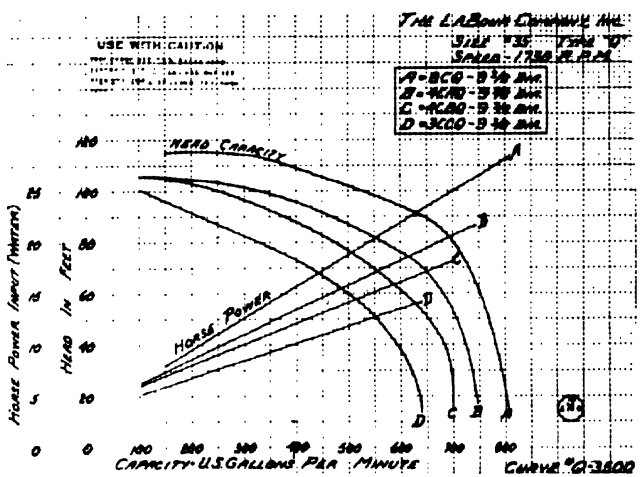


Figure 26. Curve of Chemical Pump

Further this makes a good pump for handling abrasive slurries and viscous liquids, since the liquid is in and out of the pump quickly without the necessity of having to travel entirely around the casing. Obviously one-third of the wear occurs because of that much less travel in the casing.

Figure 26 is a curve of the chemical pump which you just saw. The pump characteristics show a flat curve for capacity and a sharp break at the end. These are made in capacities up to about 1200 GPM and heads up to 150 ft. Efficiencies run in the neighborhood of 75% maximum with a fully open impeller. Obviously a sharp breaking curve is an indication of more capacity than the pump suction is able to handle and the beginning of cavitation.

Figure 27 is a curve of the low capacity, high head pump. You will note that with a 7 inch wheel, although this pump runs at 3450 RPM, you can get heads close to 250 ft. while the capacities are normally 150 GPM maximum.

Figure 28 is a section of this type of pump. This has a single throat rather than the three throat design previously discussed.

p. 211 - 2nd paragraph, line 12, should read: "The reason this particular pump handles 20% of air by volume.." (instead of "20% of air volume..")

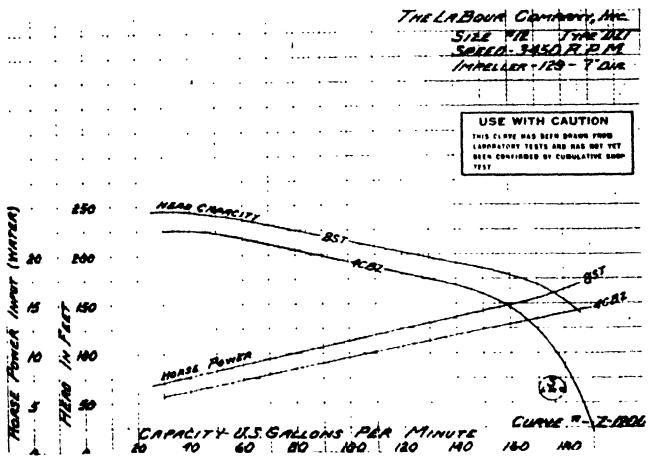


Figure 27. Curve of Low Capacity High Head Pump

II. SELF PRIMING CENTRIFUGAL PUMPS

Figure 29 shows a section of the self priming centrifugal pump. The impellers, shafts, and bearings are constructed the same as on the two pumps previously described. In the second chamber you will note a strainer. This is merely a cup type strainer to keep out tramp material. It has nothing to do with the operation of this pump.

Figure 30 will serve to illustrate just how this pump is self priming. When you first install the unit, several gallons of liquid are put into the pump through the suction trap. On top of the suction trap is a flanged cover which can be quickly removed. Closing this cover and pressing the starter, the impeller revolves at standard motor speeds of 1150 RPM, 1450 RPM or 1750 RPM.

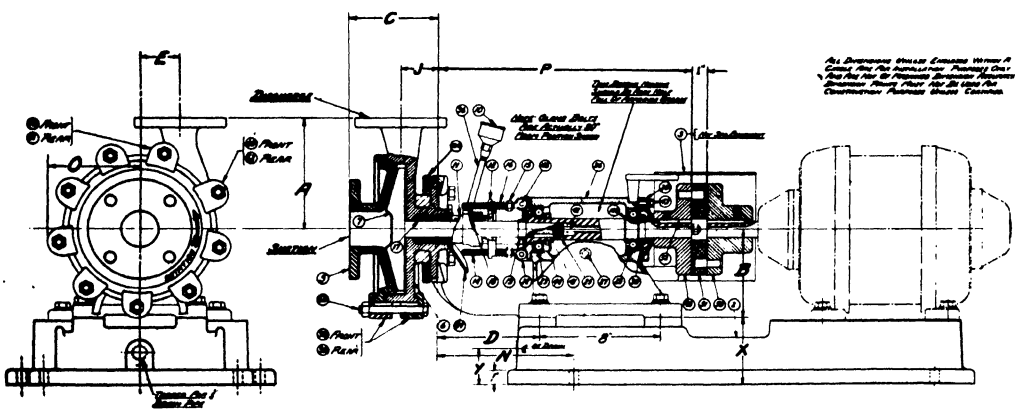


Figure 28. Cross-Section of Low Capacity High Head Pump

The impeller spins counter-clockwise looking at it from the suction end. This impeller throws the liquid that you first put into the pump up through the first opening into the air separator. It returns through the other opening to the pump casing to be used over again to pump air that has come in from the suction line. The liquid passes out the first discharge throat and returns to pick up more air. When all the air is exhausted from the suction line, pressure is established in the pump and not before. The pressure on the tips of the blades and, therefore, on both throats is the same. We now have a side suction centrifugal pump until the pump gets more air when it goes through its priming cycle again. The rate of air handled is such that the liquid rises about 1 ft./sec. on the suction side with a 10 ft. suction lift.

Figure 31 shows a typical and common application of the self priming centrifugal pump. Here we are unloading tank cars by placing the pump below the source of supply. To start up, the pump develops a vacuum and lifts the liquid over the top and into the pump. Once the prime is established, the pump

p. 212 - 1st paragraph, 6th line, should read: "suction chamber", instead of "second chamber".

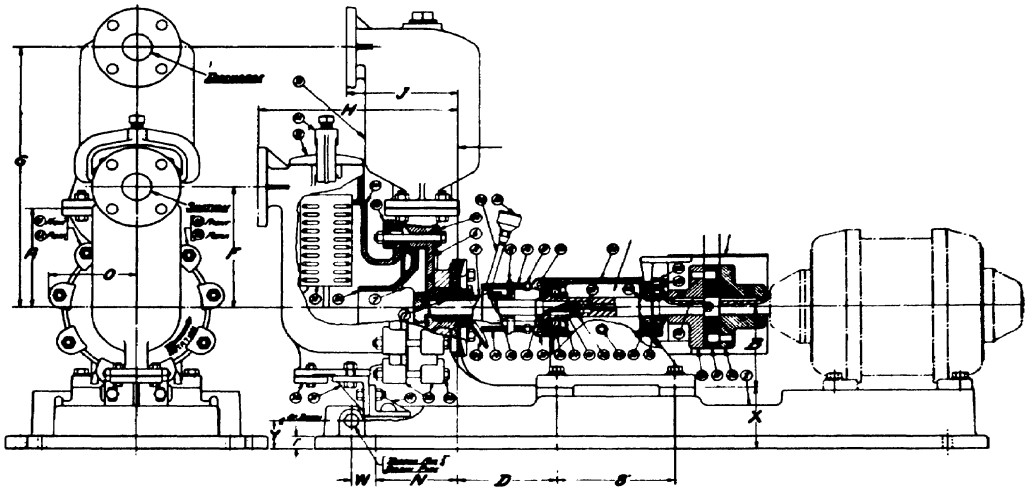


Figure 29. Section of Self Priming Centrifugal Pump

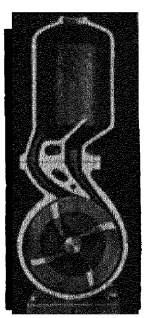


Figure 30. Self Priming Action

acts as a flooded suction pump. The liquid from the tank car syphons into the pump suction.

Figure 32 shows the external view and the cross-section of a vertical type self priming centrifugal packingless pump. This is made in the coupling type as shown and also in the close coupled type for handling water or non-corrosive solutions, while the coupling type is for acid and other mean corrosive services.

The liquid enters on the suction side through a strainer and drops into the inside chamber and on to the impeller. The impeller spins clockwise looking down on it from the motor end. This liquid is thrown out of the discharge openings, one of which is shown on the right of the impeller, into the outside chamber and then out through the discharge on the left side. There are no clearances less than 1/32 inch inside the pump casing. Self priming is accomplished the same way we mentioned before the horizontal self priming centrifugal pump. The outside chamber corresponds to the air separator and the chamber inside corresponds to the suction trap. Only one discharge port to the separator is shown but actually there is a return there, the same as is used for the horizontal self priming centrifugal pump.

Now in regard to the elimination of stuffing boxes and calling this a packingless pump, we explain as follows. There is a spinning shaft with the impeller. Around it is a stationary sleeve. Between the impeller shaft and the stationary sleeve there is a full 1/8 inch opening. Atmosphere can get in around this opening at a point below the bottom pump bearing which is higher than the bottom of the suction opening. Liquid enters the suction line, drops into the inside chamber, and then passes through an annular opening on the outside of the sleeve. The liquid can enter the sealing chamber on top of the horizontal section of the separator sleeve. Inside the top chamber of the seal

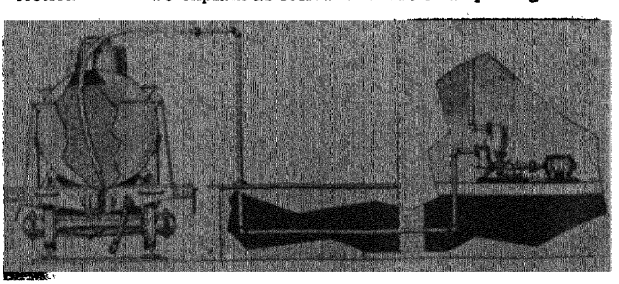


Figure 31. Tank Car Unloading

p. 213 - 2nd paragraph, 6th line, should read: "Self priming is accomplished in the same manner which we mentioned before for self priming centrifugal pumps' (instead of "self priming is accomplished the same way we mentioned before...")

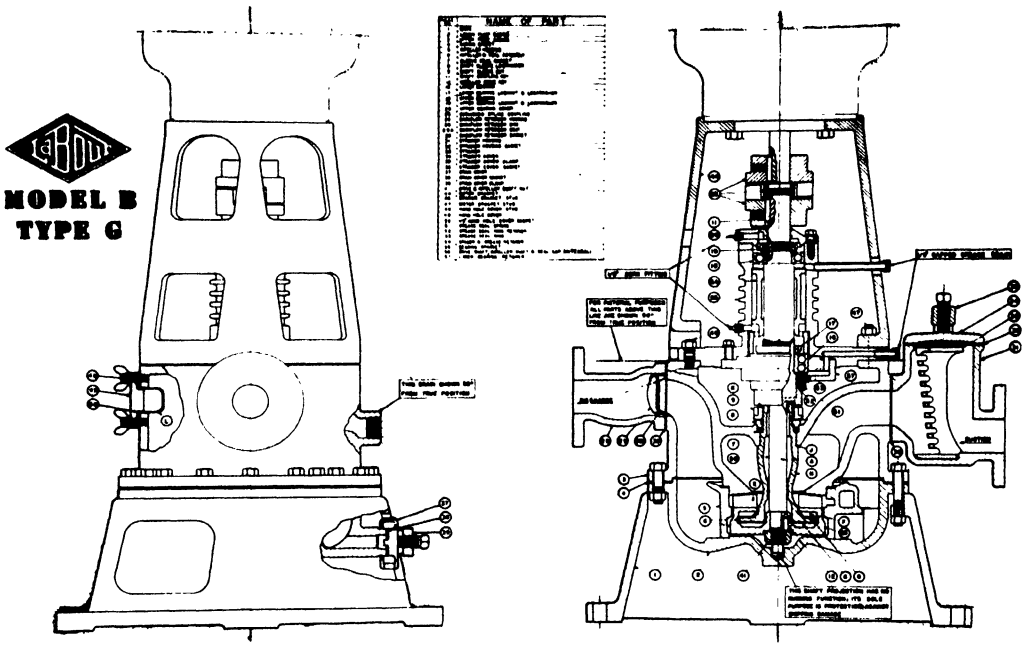


Figure 32. Vertical Self Priming Centrifugal Packingless Pump

there are vanes that spin with the seal and pump the liquid around the 1/32 inch opening into the bottom chamber of the seal. Attached to the bottom part of the bottom chamber are also vanes which pump the liquid back. In other words, we get a bucking action from the two sets of vanes. There is a pressure developed equivalent to 30 PSI when using water. That is the design pressure. The suction line pressure, which is negative, plus the pressure developed by the vanes in the lower part of the seal is equal to the pressure developed by the upper part of the seal plus atmospheric pressure which comes down along the 1/8 inch opening around the shaft.

When you first start the pump, the liquid is drawn down along the shaft and held in the seal by equalization of the pressure. When the pump stops, the force of the seal is lost and the liquid around the shaft travels up but does not overflow as the top of the shaft sleeve is above the bottom of the suction opening of pump.

Now in the discharge opening there is a valve with an orifice hole in it. When the liquid is pumped, this valve rises open. However, when the flow stops, this valve shuts. The liquid from the discharge returns slowly through the orifice opening back to the pump casing. The excess liquid drops out of the pump suction to the tank from which it is taken. The flow back to the pump is slow enough so that the liquid is not forced out of the opening at the top of the shaft sleeve. This pump is made in the hard metals only, like cast iron, R55, Elcomet, 304 and 316 stainless steel.

The application of self priming pumps in the chemical and process plants is quite broad. For example, these are used for sumps, taking clean water or corrosive chemical, as the case may be, from suction lifts of 20 ft. maximum on a water basis. Due to the fact that they handle reasonably large amounts of solids, the pumps can be expected to stay on the job a long time.

For vacuum evaporator service, self priming centrifugal pumps have been used for years. They can be used interchangeably with the gravity feed type pump with the three throats. Self priming pumps are used for tank car unloading. They also make an excellent application for decanting.

One type of application is mine water gathering. When there is water, it takes it and, if not, it pumps air. Many installations are in service for transferring chemicals by placing the pump on top.

p. 214 - 2nd paragraph, 4th line: "taking" instead of "taken".

III. CORROSION

In order for us to identify defective castings and the cause of the trouble, let us look at Figure #33. "A" illustrates an advanced case of general corrosion accelerated by erosion. Attention is called to the fact that all parts of the interior of this pump casing show severe action even to the central portion next to the shaft opening. However, the action is increasingly severe at the outer periphery of the casing bore as here the velocity of the liquid is the greatest and hence the combined effects of corrosion and erosion have increased the damage.

"B" shows a case of erosion without corrosion. Notice here that the action is almost completely confined to the periphery of the casing bore and to such other parts of the casing as were subject to the action of high velocity liquids.

"C" shows corrosion due to gas concentration. This is often confused with corrosion due to defective castings. Gas concentration corrosion may always be identified by the spongy porous appearance of the affected area.

"D" illustrates a casing partly cut away at the throats. Two points of corrosion, indicated as "A" and "B" show the beginnings of gas concentration corrosion. This pump had been handling a corrosive liquid but with such a restricted flow to the suction that there was present an insufficient amount of liquid to fill the discharge throat, yet a large amount of gas was present. This caused a vacuum pocket at point "A" on the low velocity side of the discharge throat. Note the characteristic spongy, ragged appearance of the corroded area.

"E" shows a less advanced case of gas concentration corrosion. The area most deeply affected is at "A". This is the location of the zone adjacent to the main discharge throat. Here is found the combination of gas concentration together with high velocity liquid. Hence maximum corrosion. Notice that even at the start this corroded area has the characteristic spongy appearance shown by all cases of gas concentration corrosion.

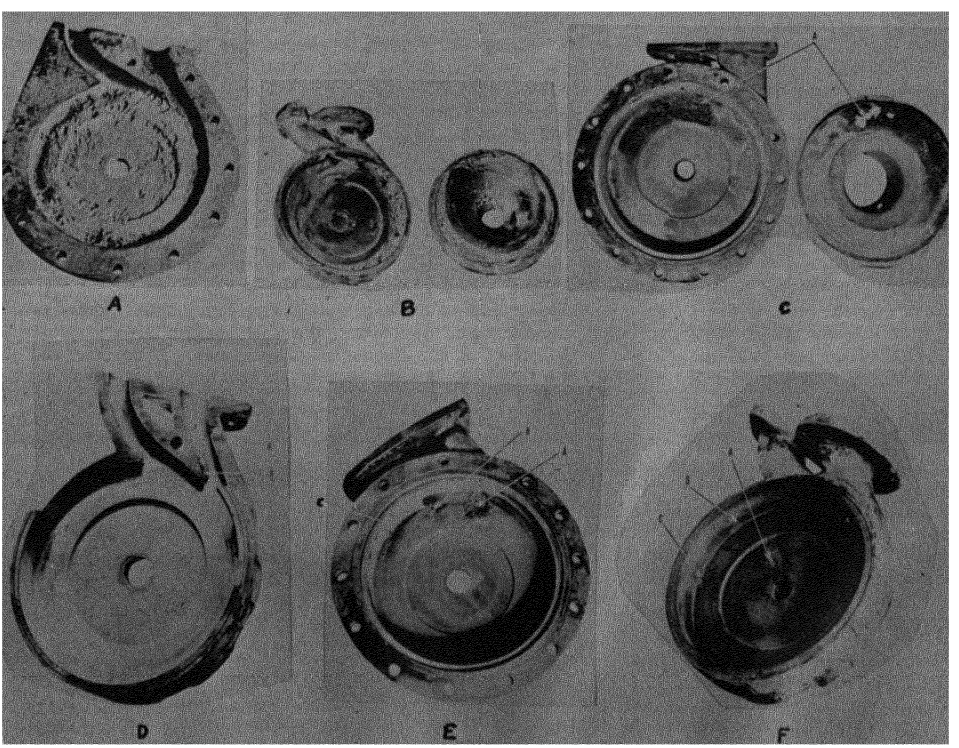


Figure 33. Corrosion

"F" shows defective casting. Generally speaking the casting is most apt to show defects at certain specific points. Usually the bad spots will occur very locally and without any regard to or in connection with any other type of corrosion.

In advancing the knowledge of pumps for the chemical and process industries the nickel chromium alloys have contributed most heavily. Any attempt to discuss these alloys would only be of a general nature since variations in analysis and manufacturing methods influence the resistance to corrosion. Other factors such as the density of the castings, impurities and distribution of these impurities have a bearing on the results.

Practically all chemicals with the exception of the chlorine group can be handled in pumps with available materials of construction. For handling nitric acid the chromium iron alloys, such as 18 chromium and 8 nickel are accepted for the entire range of strength, provided the acid is cold. These alloys may be 18-8S or 18-8 SMO. Also for handling nitric acid, R-55 is acceptable. This is a nickel base alloy. The use of R-55 here applies only if the nitric acid is cold. For elevated temperatures 18-8S, while not fully resistant, is more suitable than the others.

For handling sulphuric acid the rate of corrosion will vary with the strength and temperature of the acid. Weak sulphuric acid solutions at normal temperature are handled in lead or in some of the chromium nickel alloys. Lead is soft and should not be used if abrasive material is present as the lead cuts out easily. The most corrosive range encountered in handling sulphuric acid lies approximately between 40° and 50° Baume. Lead and the nickel base alloy R-55 are serviceable in this range. The iron base chromium alloys like Elcomet, Durimet and Worthite should not be used in this range.

Between 15 and 60° Baume intergranular corrosion of the alloys is quite apt to occur even though tests indicate satisfactory corrosion rates. Many lead pumps are in service handling 60° Baume sulphuric acid and lead has been used successfully up to 66° Baume. On sulphuric acid of 60° Baume strength lead should be chosen with caution. Cast iron pumps for handling 60° Baume sulphuric are commonly used and from there on up to and including 66° Baume sulphuric acid. However, indifferent results are obtained in these ranges. Either iron base or nickel base chromium alloys of proper composition are suitable for this range.

Cast iron is used in the ranges from 66° Baume up to 100% sulphuric acid provided the acid is cold. At elevated temperatures it is necessary to go to nickel base alloys. For handling oleum we can use either iron base or nickel base alloys.

For the chlorine group, as yet no alloys are regarded as satisfactory. Success is reported in certain cases but just as many are the record of failures. In pumping hydrochloric acid the local conditions have much to do with the results. The presence of air with the acid enormously increases the rate of corrosion.

As yet no practical method has been devised for anticipating the results of corrosion on an alloy under every condition. This brings on the necessity for more alloys and the list is already great. It is all confusing to the pump user.

Chemical pumps, of course, are made in materials other than the metals and in many cases have been successful. These may be rubber, neoprene, plastic, carbon and glass.

As a general rule, every pump application should be studied individually for possible effect of corrosion and erosion due to abrasive solids, temperature, viscosities, possible hazards from explosive and toxic standpoints, possible changes due to the effect of non-Newtonian suspensions. Under the last should be considered; Bingham Plastic, pseudoplastic, dilatant, thixotropic and rheopectic. Also check into NPSH, maximum suction lift, operation near shut off or wide open condition, each of which should be avoided.

In general avoid dissimilar metals from parts in contact with the liquid. This is to avoid electrolytic action. When two metals are known to operate satisfactorily together then the two different metals are acceptable in the pump.

Whether or not to use packed stuffing boxes or mechanical seals will depend on the particular application. No firm statement can be made to cover all cases or even a partial number. The use of mechanical seals in pumps has made startingly rapid strides but must not be accepted as a substitute for stuffing boxes except where definitely proved of value. In general and from the information available at this moment, mechanical seals would be acceptable for handling clean non-corrosive solutions. Beyond this each and every case must be examined in order to justify the use of mechanical seals.

IV. CONTROLLED VOLUME PUMPS

Controlled volume pumps are positive displacement units that deliver a definite quantity of liquid in controlled volume that remains constant regardless of the discharge pressure. Capacities are designed as low as a few cubic cm./hr. to approximately 50 GPM and for pressures up to 20,000 PSI. In some cases these pumps are offered for 50,000 PSI.

p. 216 - line 58: "In some cases these pumps are offered for pressures as high as 50,000 PSI". (instead of "In some cases, these pumps are offered for 50,000 PSI")

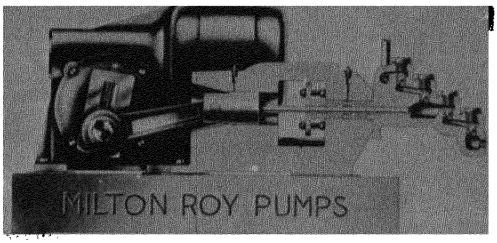


Figure 34. Controlled Volume Chemical Pump

A typical design of a controlled volume chemical pump is shown in Figure 34. A double check valve is employed on both the suction and discharge of the displacement chamber. In the event one ball is half off the seat by any particle in suspension in the liquid being pumped, the chances are that the second ball will hold, assuring positive check valve action.

According to law of probability, there are several times the probability of positive check valve action with the double check than can be obtained with a single check valve. This is important to assure positive metering action. This liquid end is further designed to automatically discharge any air or gas that may enter with the liquid in a single stroke of the pump. Note the continuous upward flow throughout. Any pockets in the displacement chamber in which air could be trapped would impair the efficiency of the pump by permitting alternate compression and expansion of the gas bubble with reciprocation of the plunger and consequent loss in volumetric efficiency of displacement.

A modification of the basic step valve design is what is termed the cover plate valve, a modification specifically designed for handling slurries and more difficult materials to pump. In this liquid end, the ball rises out of the stream of flow on a gate in the castings, the flow going underneath the balls into the displacement chamber on the suction stroke. There is tangential action on the balls by means of this flow, causing ball rotation and aiding to give a self cleaning action. Lime has been handled in this design in concentrations as high as 40%. Diatomaceous earth, activated carbon, and slurries have been handled successfully in this design.

Capacity of a controlled volume pump is a function of three variables: the area of the plunger; the stroke length; and the speed. Figure 35 illustrates adjustment of stroke to obtain variation in the capacity of a given pump by alternating the position of the trunion in the slot of the drive wheel while the pump is operating by screw method of adjustment. Micro adjustment of stroke while the pump is running permits precise adjustment of stroke length by means of a hand wheel operating over a chain through a gear train in the rocker box. This is a fixed throw from the low speed shaft of a motor gear driver to this rocker box and a variable throw to the cross head by means of the positioning of the connecting rod adjusted by the lead screw. A vernier dial in the top of this rocker box indicates stroke length to within 1/750 of full stroke. A change in capacity, therefore, down to 0.13% may be indicated by means of this adjustment.

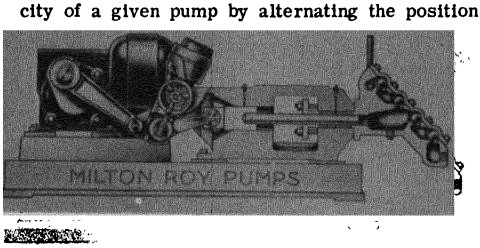


Figure 35. Micro Adjustment with Cover Plate Liquid End Design Controlled Volume Chemical Pump

Figure 36 is an illustration of a pump arranged for change in speed while the pump is in operation through a mechanical adjustment in the gear box. This employs a Master Speedranger and is available to give variation in speed and, therefore, variation in capacity over various ranges as high as a 15 to 1 range in certain sizes.

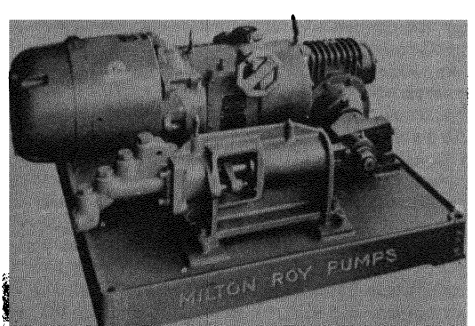
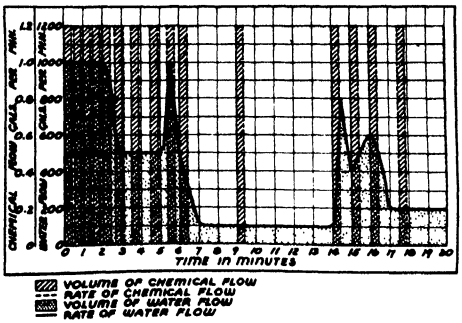


Figure 36. Controlled Volume Chemical Pump with Master Speedranger

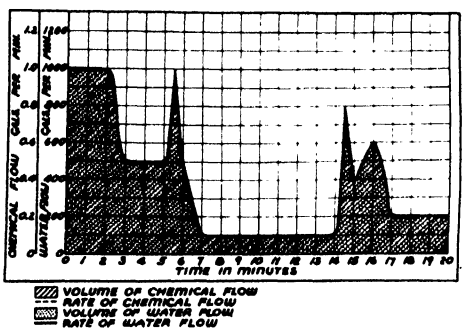
These pumps are made in the following materials of construction:

Cast iron	Hastelloy B
Cast steel	Hastelloy C
Acid resisting bronze	Monel
Methyl methacrylate	316 SMO stainless steel
18-8 stainless steel	Nickel
Milroy stainless	

Figure 37 (System A) illustrates a controlled volume pump used in connection with a General Electric Thymotrol. As the capacity of a controlled volume pump is directly proportional to the speed of operation, because of metered displacement, a positive



System A



System B

Figure 37. Controlled Volume Chemical Pump with Timer (System A) and Controlled Volume Chemical Pump with Thymotrol (System B)

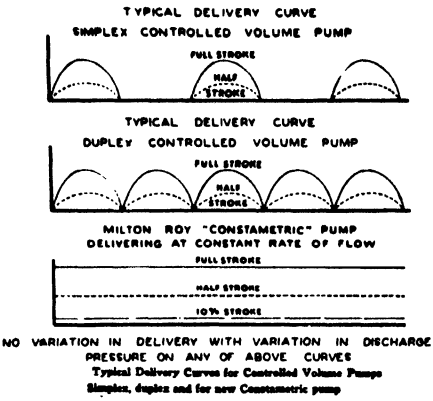


Figure 38. Sine Curve of Controlled Volume Pumps

control of speed results in a positive and direct control of the exact volume delivered by the pump. Positive speed regulation can be effected by an electronic system employing Thymotrol, as developed by the General Electric Company. Alternating current is the source of power and full wave rectification by the Thymotrol converts to direct current for motor operation. The speed may be regulated within the normal range of 5 to 100% accurately controlled and directly proportional to the setting of a potentiometer, located in the Thymotrol circuit. The speed will not vary more than plus or minus 1% with voltage variation of plus or minus 5%. The drive provides constant torque over the entire specified speed range. At a given potentiometer setting, speed is automatically held constant irrespective of change in load. For an automatic control system a 10,000 ohm potentiometer to regulate the motor speed may be mounted in a meter or a controller and the speed thereby set by the meter or controller. This electronic control is available for motors from small fractional horsepower sizes up to practically any large integral horsepower and has been furnished on controlled volume pumps on several installations on sizes up to 5 HP.

In the past, previous to the introduction of the Thymotrol, the arrangement which had been used for controlling the volume in connection with the flow in the main line was made by means of an electrical timer. An electrical contact to the timer operates the motor for a definite duration of time, for example for every 500 gallons flow. The timer holds the controlled volume pump in operation for a given period of time.

Figure 37 (System B) shows the action you get with a timer and controlled volume pump. On the other hand, with the Thymotrol the feed of chemical is in exact proportion to the changes of flow in the line. It is instantaneous, as compared with the timer which gives a history of flow.

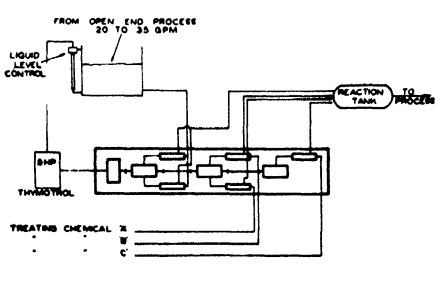


Figure 38 shows the sine curve you can expect from the flow of a simplex controlled volume pump and a duplex controlled volume pump. The flow is pulsating. A new type of pump has been brought out in a controlled volume duplex type whereby the rate of the discharge is always at constant volume. Such a pump is useful for many chemical processes where constant discharge and controlled volume are required. This is done by having the one plunger slow up at 30% before the end of its stroke, while the second plunger starts to take up at that exact point.

Liquid level control has been successfully employed to regulate the speed of a controlled volume pump. Figure 39 is a typical application. A food product was received from an open end process at

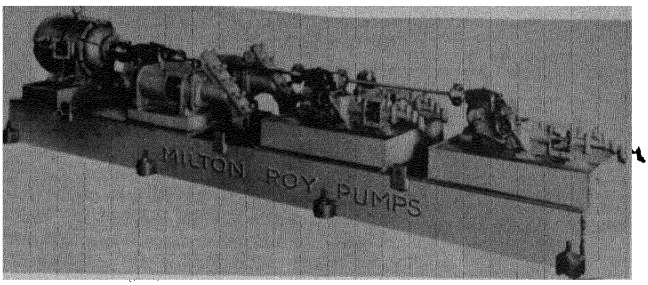


Figure 39. Gang Type Pump

the rate of 20 to 35 GPM. It was desired to add three treating chemicals to this food product at a rate exactly proportional to the rate at which the material was received and then pump the material together with the three treating chemicals under pressure to a reaction vessel. The problem was solved by receiving the food product in a small surge tank and putting liquid level control on this surge tank. The first two chambers of a controlled volume duplex pump handled the liquid from the surge tank handling the liquid from the process. The speed of the drive on this unit was regulated through Thymotrol from the liquid level so that should the liquid level start to rise the entire pump speeds up or if the level starts to fall, the pump unit slows down. From the same high speed shaft, drives are taken through speed reducers to the three chemical pumps so that these three pumps speed up or slow down also in exact proportion to the speed of the main pump handling the liquid from process. Proportionality of feed is assured, and it is possible to change the ratio of any of the three treating chemicals while the entire system is in operation. Also shown is the same gang type pump in an external view.

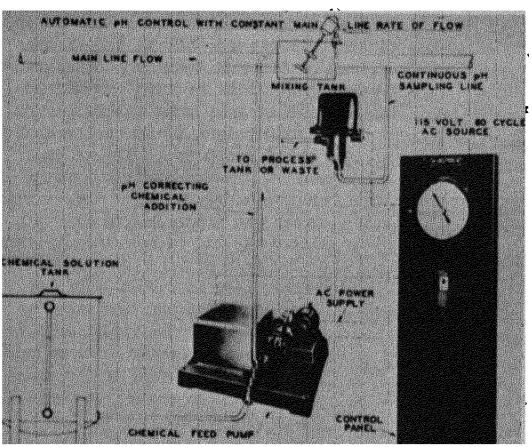


Figure 40. Automatic pH Control with Constant Main Line Rate of Flow

Figure 40 illustrates the arrangement of a pH control. It shows another method of controlling the volume through automatic regulation of the length of the stroke instead of speed control. On this control a small reversible motor is used to increase or decrease the length of the stroke on the micro indicating stroke adjustment. On the other end of the control motor is mounted a speed reducer and a potentiometer that is balanced with a potentiometer in the controller circuit. The pH controller calomel cell takes a continuous supply from the main line flow and sends the indication to the control board. This in turn sends the a.c. impulse to the torque type motor on the stroke adjustment which speeds up or slows down in order to keep the potentiometer circuit in balance.

In the system shown before, it is quite necessary to allow for lag and rate of reaction. If a flow controller must follow a large change in rate of flow, considerable hunting would result. It is then advisable to compensate for rate of flow on the pH control system by adjusting for each of the two controlled variables on a single pump as shown in Figure 41. This is done by varying the speed of the pump through a Thymotrol to regulate the speed of the pump drive directly proportional to rate of flow and using the second variable, pH value, to automatically set the length of the stroke of the plunger on the pump. On such a design the pH may be controlled without hunting and with a higher degree of uniformity than possible with single pH control alone.

In a number of processes, it is desirable to control the strength of a caustic bath or the strength of an acid bath within limits where there is relatively little change in conductivity, and relatively little change in pH value. In other words, the change in pH value between the desired control limits is on the flat part of the curve (Figure 42) and would not be detectable or controllable to measure this direct. In such cases it is possible to use a controlled volume pump to automatically titrate a sample continuously from the liquid bath handling a sample of the liquid from the bath on one side of the pump and metering to that sample in direct ratio and exact proportion a fixed quantity of titrating medium.

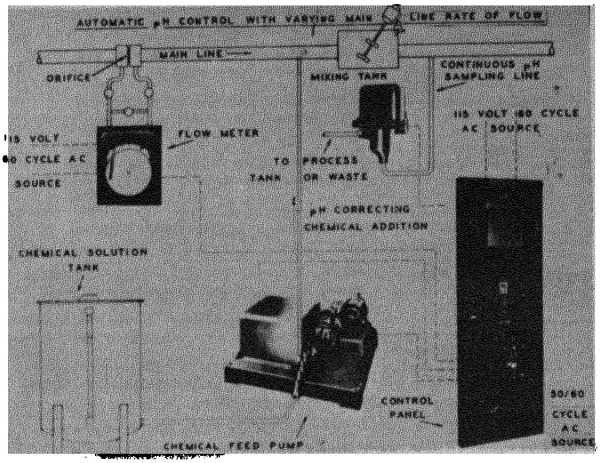


Figure 41. Automatic pH Control with Varying Maining Line Rate of Flow

For example, (Figure 43) if control were desired on a caustic bath, phosphoric acid would be used for the titration, the second side of the duplex pump handling a standard solution of phosphoric acid to the sample of caustic delivered by the second side of the titration unit. The mixture of the two reagents would then give a resulting pH value on the steep portion of the curve that would directly indicate the strength of the caustic bath. A pH meter measuring this pH value would automatically set the feed of caustic to the caustic bath to maintain the desired standard strength of caustic required in the bath, increasing the feed of caustic to the bath in the event that the titration indicated a falling pH value below the control point or decreasing the feed of caustic soda in the event that the titration indicated a bath of higher concentration than that required. The same type of system can be used to maintain the strength of acid baths within certain control points, using one controlled volume pump as a titration unit and the second controlled pump automatically regulated by the pH meter and controller to maintain a feed of acid to hold the strength of the bath at the required control point. This is a relatively new application and one that must be studied in each individual case to determine the proper control point to be used according to the slope of the titration curve, desired buffer action, etc.

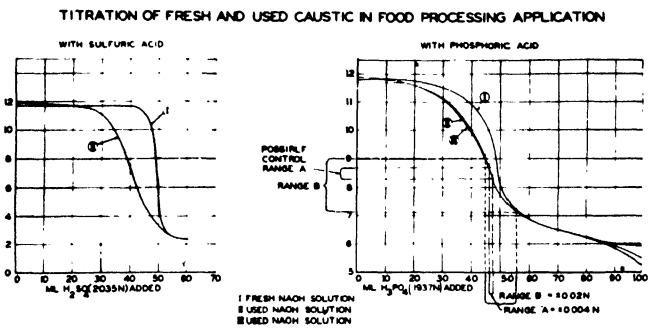


Figure 42. Application of Titrimetric System Caustic Concentration Control

V. ENGINEERING CALCULATIONS FOR CENTRIFUGAL PUMPS

Now the total dynamic head against which a pump works is equal to the suction head, discharge head and friction head. In this particular case, taking from a tank and discharging to a high elevation, we assume that the tank is empty and the pump should be designed for the worst condition. In this case the total dynamic head is equal to the static discharge head plus the friction. We are not including the pipe velocity head. This is usually small, normally 0.4 ft. or less. Incidentally, for chemical work it is customary to limit the pipe line velocities to 4 ft./sec. on the suction side and 5 ft./sec. on the discharge side.

Specific gravity effects horsepower and the pressure gauge readings but not the static discharge head, expressed in feet of fluid flowing.

The head of fluid flowing produced by the centrifugal pump depends upon the tip speed of the wheel regardless of whether we are pumping mercury or gasoline. The pressure at the discharge of the pump will vary directly as the specific gravity varies. If we consider the pressure at the bottom of a column of liquid, the pressure there will vary directly as the specific gravity of the liquid varies. Since we have both variables cancelling each other out as far as effectiveness is concerned in terms of feet of fluid head, we can disregard the effect of the specific gravity on the discharge when considering the static head. Actually you cannot do this in the case of friction because here you do not get the effect of the static head.

On the suction side of the pump, the pump itself does not do the lifting. All it does is to cancel out a portion of the atmospheric pressure balance. Regardless of the liquid, the pump can never cancel

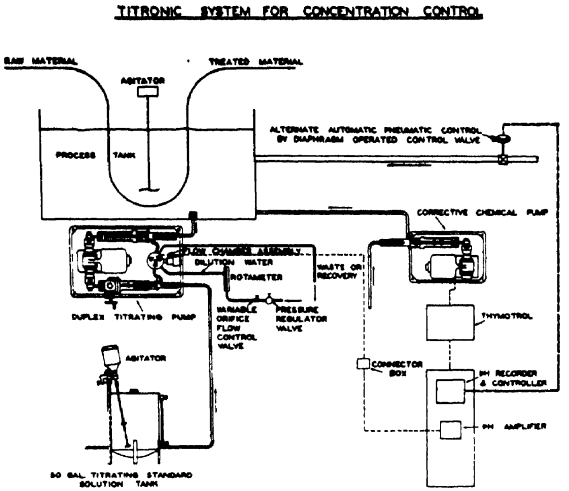


Figure 43. Titrimetric System

out more than the complete atmospheric pressure. Consequently as far as the pump is concerned, you disregard specific gravity but as far as the effect on the ability of atmospheric pressure to lift the liquid is concerned, you must consider specific gravity as here again you have the weight at the bottom of the column of liquid just as you had it on the discharge side but you do not have any increase in pressure due to the pump and consequently you do not have any increased ability to lift this liquid. Since we are considering this from a pumping standpoint, we must consider that the ability of the pump to lift liquid on the suction side varies inversely as the specific gravity although actually the pump itself does not do the work.

As long as you convert this to terms representing the ability of the pump to perform, regardless of what the force is that permits this performance, you are justified in adding together both the suction and the discharge sides.

For a suction lift of 10 ft. of material, specific gravity 1.5, and a static discharge head of 100 ft., we multiply the 10 ft. suction lift by the specific gravity 1.5 which gives us 15 ft. water equivalent. This is then added to the 100 ft. making the total head 115 ft. We then proceed to use our performance curves which the manufacturers draw on a water basis. The maximum suction lift guaranteed on the self priming centrifugal pumps is 20 ft.

Another application you run into is pumping from a vacuum filter with, for example, 29 inches of mercury vacuum. The pump manufacturers guarantee a maximum suction at the pump of 20 inches of mercury. You determine the positive head which should be carried to the suction side of the pump as follows: 29 minus 20 equals 9 inches of mercury. This must be multiplied by a factor of 1.3 bringing the total head of 11.2 ft. This then represents the positive head of liquid we must have on the suction side of the pump when pulling from 29 inches of mercury. The above is based on the material with a specific gravity of 1.00. If the specific gravity is 1.4 then we would have multiplied by 1.3 and divided by 1.4. The reason we use the figure of 1.3 instead of 1.13 (which is actually correct and comes from 1 inch mercury equals 1.13 ft. H_2O) is due to the fact that liquids in motion act differently than liquids at rest.

As far as capacity is concerned on these vacuum filter jobs, we multiply the required capacity by a factor of 1.2 to 1.4. This is due to the fact that there is a certain amount of gas present and also because of the internal slippage of the pump at these high vacuums. This slippage at 22 inches mercury vacuum can amount to 35%.

Incidentally, the pump with three throats, which we mentioned earlier, is recommended for this type of work because of its 20% air handling capacity. This prevents gas binding, pumps the gas that comes in and is easier for starting up this system.

Another application is on pressure filter service. In this a centrifugal pump is ideal because it has a large capacity at the start and a high shut off pressure. When the filter cloths are clean, the flow can be large and when the cake builds up, more pressure is required. With a definite end pressure on centrifugal pumps, we cannot built up an excessive head that might break the cloths.

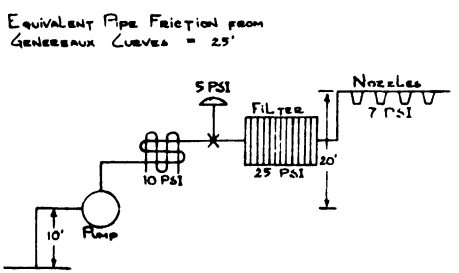
To obtain the head, in feet of fluid flowing, required for a pressure filter job, we multiply the pressure in PSI by 2.3 and divide by the specific gravity.

In tank car unloading, the pump is figured for the worst condition; that is, when the suction line is just about empty. In that case we handle it just like a gravity feed type pump. When the pump is first started up, it is not pumping anything out of the discharge so that the pump is merely used to establish a prime.

A rather complete and representative chemical pump problem is illustrated. The pump is to take liquid with a 10 ft. suction lift and 20 ft. static discharge head through a heat exchanger and a pressure filter and discharge into nozzles at the end of the line. The specific gravity of the liquid is 1.5 with

viscosity similar to that of water, temperature 100 °F. The vapor pressure is low and can be neglected.

The 10 ft. suction lift must be multiplied by 1.5 which becomes 15 ft. water equivalent. 10 PSI through the heat exchanger plus 25 PSI through the filter plus 7 PSI through the nozzles equals 42 PSI. This must be multiplied by 2.3 and divided by the specific gravity of 1.5 which gives us an equivalent head of 64.5 ft. The total dynamic head against which the pump would operate would be:



Suction - (water equivalent)	--- 15 ft.
Static discharge head (do not multiply by spec. grav.)	--- 20 ft.
Pressure drop, heat exchanger, filter and nozzles	--- 64.5 ft.
Friction drop through piping	--- 25 ft.
Total head	--- 124.5 ft.

Let us remind you in closing that finding the ideal pump for each and every application is often a problem as pump applications overlap and in many cases the solution depends upon the ideas of the engineer or engineers involved.

Problem 1

Determine the total dynamic head for selecting a pump to handle 100 GPM when taking liquid from a vacuum evaporator with 29 inches of mercury, flooded suction on pump, static discharge head 30 ft. through 150 ft. of 2 1/2 inch standard weight pipe with 6 short radius elbows and 2 gate valves. The specific gravity of the liquid handled is 1.5, viscosity 20 cps. State the minimum positive suction head which should be maintained on the pump.

Problem 2

Determine the total dynamic head for selecting a pump to handle 100 GPM of 60° Baume sulphuric acid, temperature atmospheric, suction lift 8 ft. through 20 ft. lineal feet of pipe with 2 short radius elbows and 1 gate valve. Static discharge head 40 ft. to open tank with head exchanger in discharge line, pressure drop 5 lbs. discharge out end of line through nozzles, pressure drop 15 lbs. Assume pump efficiency of 70%. What is the brake horsepower required.

Chapter 11

VENTILATION

by

M. G. Kershaw
Design Division
Engineering Department
E. I. du Pont de Nemours & Co., Inc.
Wilmington, Delaware

TABLE OF CONTENTS

		Page
I.	References	225
II.	Introduction	225
III.	General Principles	225
IV.	Duct Work Design	225
V.	Procedure for Duct System Design	231
VI.	Duct Construction	234
VII.	Heating Coils	235
VIII.	Re-Heaters	239
IX.	Air Cleaning Devices	240
	A. Air Filters	242
X.	Fans	242
XI.	Supply Air Inlet	246
	A. Wall Grille	246
	B. Ceiling Diffusers	249
XII.	Ventilation Required	249
XIII.	Roof Ventilators	252
XIV.	Hoods or Enclosures	259
XV.	Duct Construction for Exhaust and Conveying Systems	262

LIST OF FIGURES

Figures 1, 2, 3, 4, 5, 11, 12, 13 reprinted by permission from Reference 1.

Figures 6, 7, 8, 9, 10 reprinted by permission from Reference 2.

Figures 14, 15 reprinted by permission from Reference 4.

The following companies have kindly permitted reproduction from their catalogs:

Aerofin Corporation — Tables 2-8
American Air Filter Co. — Fig. 20
Anemostat Corporation of America — Figs. 17, 18
Buffalo Forge Co. — Fig. 15a
H. H. Robertson Co. — Fig. 19
B. F. Sturtevant Co. — Fig. 19a
Tuttle and Bailey, Inc. — Fig. 16

I. REFERENCES*

1. American Society Heat. & Vent. Engrs., Heating, Ventilating, and Air Conditioning Guide, 1947.
2. Buffalo Forge Co., Fan Engineering, 1938.
3. Bussy, Frank L., "Loss of Pressure due to Elbows in the Transmission of Air through Pipes or Duct," Trans. A.S.H. & V.E., 1913.
4. Hagen, Harold, F., "Discussion of Fan Types," Director of Research, Sturtevant Div. of Westinghouse Electric also Professor of the Practice of Mech. Engr., Harvard University, Graduate School of Engineering.
5. Hemeon, W.C.L., "Air Dilution in Industrial Ventilation," Industrial Hygiene Foundation, Mellon Institute, Pittsburgh, Pa., Heating and Ventilation, Nov., Dec. 1943; Feb., March 1941.

5a. Heath, W. R. and Criqui, A. E., "The Axial Flow Fan and Its Place in Ventilation," paper presented at 50th Annual Meeting, New York, Jan. 1944.

6. Madison, R. D. and Parker, J. R., "Pressure Losses in Rectangular Elbows," A.S.M.E. Trans. - AER 58-2, April 1936.
7. Moody, L. F., "Friction Factors for Pipe Flow," A.S.M.E. Trans., Vol. 66, p. 671, 1944.
8. Nelson, D. W. and Smedberg, G. E., "Performance of Side Outlets on Horizontal Ducts," A.S.H. V.E. Research Report No. 1226 - A.S.H.V.E. Trans., Vol. 49, p. 58, 1943.
9. Nelson, D. W., Kraus, D. H., and Tuthill, A. F., "The Performance of Stack Heads," A.S.H.V.E. Research Report No. 1155, A.S.H.V.E. Trans., Vol. 46, p. 205, 1940.
10. Robertson, H. H. Company - A.I.A. File No. 12-K, p. 17.
11. Sturtevant, B. F., Div. Westinghouse Electric Co., Cat. 500.
12. U. S. Dept. of Labor, "The National Silicosis Conference Report," Bulletin No. 13, Feb. 3, 1937.

II. INTRODUCTION

Previous chapters have covered "Mass, Energy, Momentum," "Velocity Head Concept in Pressure Drop Calculation," and "Flow of Compressible Fluids." Flow of air in ventilating systems is subject to the fundamentals covered in those lectures. We are, therefore, in this chapter placing the emphasis on teaching you the general principles and methods rather than details, giving you a feel for the field and developing a sense of values.

III. GENERAL PRINCIPLES

The general object in ventilation is to provide an atmosphere inside an occupied area that is healthful and pleasant to those within the zone. The general principles involve calculating the required amount of air that must be handled and the necessary duct work, fans, heaters, filter drives, and motors required.

IV. DUCT WORK DESIGN

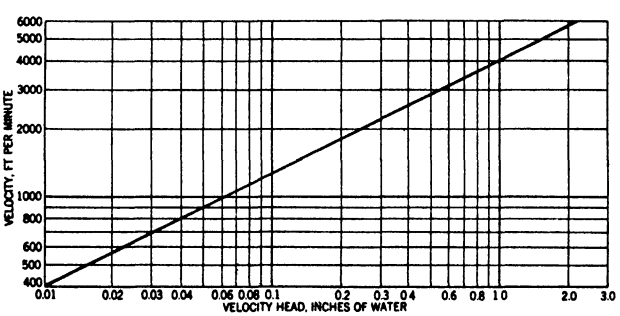


Figure 1. Relation between Velocity and Velocity Head for Standard Air

Pressure drop in duct work is due to velocity (dynamic) losses and static pressure (friction) losses. Dynamic losses are those due to change in the direction or change in the velocity of air flow. The losses due to flow turbulence are the result of resistance of the side walls and internal friction between air molecules. Dynamic losses occur principally at entrance to the piping, in the elbows, and wherever a change in velocity occurs. The entrance loss is the difference between the actual pressure required to produce flow and the pressure corresponding to the flow produced; it may vary from 0.03 to 0.90 times the velocity head.

The relation of air velocity and

*Information shown refers to typical manufacturers' rating tables which were convenient to locate. There are other companies who manufacture similar equipment and who would be pleased to furnish catalog information.

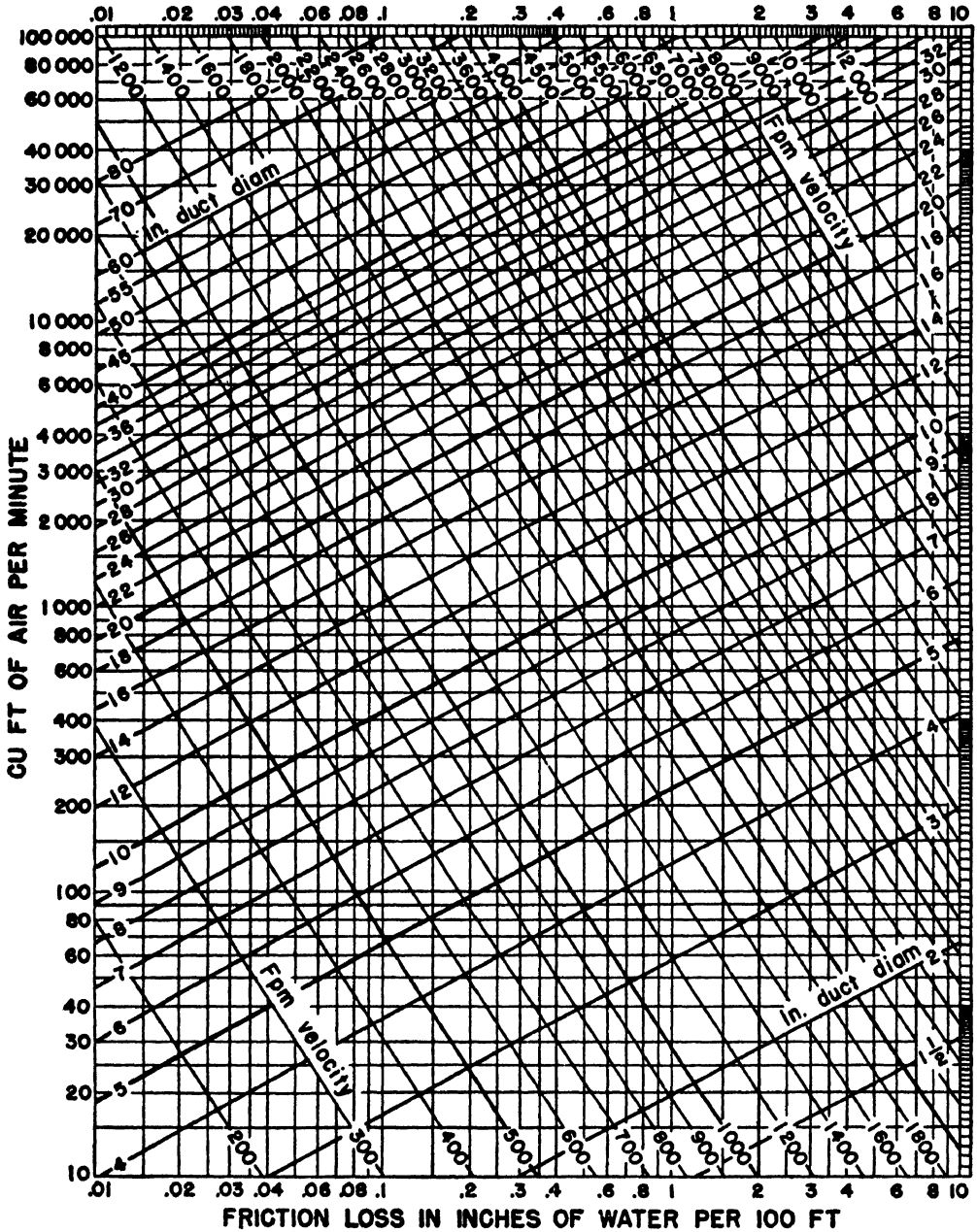


Figure 2. Friction of Air in Straight Ducts

velocity head is shown diagrammatically in Figure 1 (1) for dry air at 69.41°F. and 29.921 in. Hg barometer.

Friction loss in straight duct is most readily calculated by means of air friction chart Figure 2 (1), which was developed by research at the A.S.H.V.E. Research Laboratory. This chart is constructed from the basic flow equation:

$$h_F = f \frac{L}{D} \frac{V^2}{2g} \quad (1)$$

where

h_F = head loss due to friction, in ft. of fluid flowing
L = length of conduit, ft.
D = inside diameter of conduit, ft.
V = fluid velocity, ft./sec.
g = acceleration due to gravity, 32.17 (ft.)/(sec.) (sec.)
f = a non-dimensional friction coefficient, which for ventilation work depends upon Reynolds number and the relative roughness of the conduit. Appropriate values of f were taken from the work of Moody (7).

The air friction chart is based on standard air at 29.921 in. of mercury barometer and 69.41°F., flowing through average, clean, round, galvanized metal duct and having approximately 40 joints per 100 ft. Do not extrapolate to obtain values below the chart because critical (transition from turbulent to laminar) flow would occur in this region and values so obtained would be unreliable. For the average application, it should prove sufficiently accurate, without corrections, for any air temperature from 50°F. to 90°F., for any relative humidity, and for any normal variation in barometric pressure. The friction values obtained from chart should be corrected, for widely varying air pressures or temperatures, or for unusual duct conditions.

For duct of other than standard sheet metal construction, correction factors may be obtained from Figure 3 (1).

Example 1 - Desired to circulate 10,000 cu.ft./min. of air through 75 ft. of 24-in. diameter galvanized duct. Find 10,000 cu.ft./min. on the left- hand scale of Figure 2 and move horizontally right to the diagonal line marked 24 in. The other intersecting diagonal shows that velocity in the pipe is 3,200 ft./min. Directly below the intersection it is found that the friction per 100 ft. is 0.50 in.; then for 75 ft. the friction will be 0.75 x 0.50 = 0.38 in. In a like manner any two variables may be determined by intersection of the lines representing the other two variables.

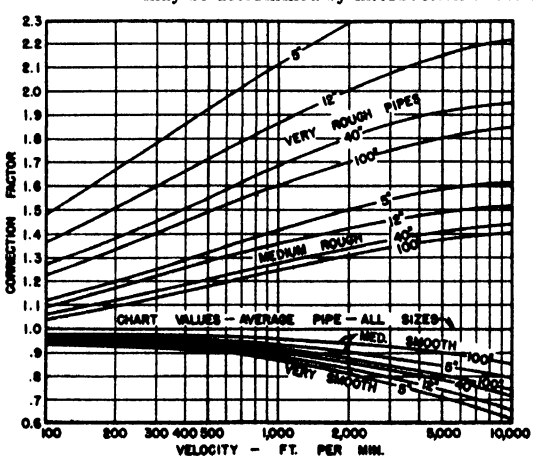


Figure 3. Correction Factors for Pipe Roughness

To correct for pipe roughness multiply friction loss obtained from Figure 2 by correction factor obtained from Figure 3.

Example 2 - If the duct in Example 1 is very rough, instead of galvanized with 40 joints/100 ft., find the total friction. On Figure 3 find (by interpolation between 12-in. and 40-in. pipe) the intersection of the 24 in. very rough line and the 3,200 ft./min. velocity ordinate, and at the left margin read a correction factor of 2. The friction loss in the rough duct is therefore 2 x 0.38 = 0.76 in.

An air handling system is usually sized first for round duct and if rectangular ducts are desired, then sizes are selected to provide air-carrying capacities equivalent to those of the round duct originally selected. Figure 4 (1) gives directly the rectangular duct sizes equivalent to each size of circular duct in friction and capacity. The values in this chart were obtained from the equation:

$$D_e = 1.265 \sqrt[5]{\frac{(ab)^3}{a+b}} \quad (2)$$

where

a = one side of rectangular duct, ft. or in.
b = other side of rectangular duct, ft. or in.

Table 5—Circular Equivalents of Rectangular Ducts for Equal Friction and Capacity

Side Rectangular Duct	4.0	4.5	5.0	5.5	6.0	6.5	7.0	7.5	8.0	8.5	9.0	9.5	10.0	10.5	11.0	11.5	12.0	12.5	13.0	13.5	14.0	14.5	15.0	15.5	16
3.0	3.8	4.0	4.2	4.4	4.6	4.8	4.9	5.1	5.2	5.4	5.5	5.6	5.7	5.9	6.0	6.1	6.2	6.3	6.4	6.5	6.6	6.7	6.8	6.9	7.0
3.5	4.1	4.3	4.5	4.6	4.8	5.0	5.2	5.3	5.5	5.7	5.8	6.0	6.1	6.3	6.4	6.5	6.7	6.8	6.9	7.0	7.2	7.3	7.4	7.5	7.6
4.0	4.4	4.6	4.8	4.9	5.1	5.3	5.5	5.7	5.9	6.1	6.3	6.4	6.6	6.8	6.9	7.1	7.2	7.3	7.5	7.6	7.7	7.8	7.9	8.1	8.2	8.3
4.5	4.6	4.9	5.1	5.2	5.4	5.6	5.9	6.1	6.3	6.5	6.7	6.9	7.0	7.2	7.4	7.5	7.7	7.8	8.0	8.1	8.2	8.4	8.5	8.6	8.7	8.9
5.0	4.9	5.2	5.5	5.7	6.0	6.2	6.4	6.7	6.9	7.1	7.3	7.4	7.6	7.8	8.0	8.1	8.3	8.4	8.6	8.7	8.9	9.0	9.1	9.3	9.4
5.5	5.1	5.4	5.7	6.0	6.3	6.5	6.8	7.0	7.2	7.4	7.6	7.8	8.0	8.2	8.4	8.6	8.7	8.8	9.0	9.2	9.4	9.5	9.6	9.8	9.8

Side Rectangular Duct	6	7	8	9	10	11	12	13	14	15	16	17	18	19	20	22	24	26	28	30	32	34	36	38	40	42	44	46	48	50	52	56	60	64	68	72	76	80	84	88	Side Rectangular Duct
6	6.6																																								6
7	7.1	7.7																																							7
8	7.5	8.2	8.8																																						8
9	8.0	8.6	9.3	9.9																																					9
10	8.4	9.1	9.8	10.4	10.9																																				10
11	8.8	9.5	10.2	10.8	11.4	12.0																																			11
12	9.1	9.9	10.7	11.3	11.9	12.5	13.1																																		12
13	9.5	10.3	11.1	11.8	12.4	13.0	13.6	14.2																																	13
14	9.8	10.7	11.5	12.2	12.9	13.5	14.2	14.7	15.3																																14
15	10.1	11.0	11.8	12.6	13.3	14.0	14.6	15.3	15.8	16.4																															15
16	10.4	11.4	12.2	13.0	13.7	14.4	15.1	15.7	16.3	16.9	17.5																														16
17	10.7	11.7	12.5	13.4	14.1	14.9	15.5	16.1	16.8	17.4	18.0	18.6																													17
18	11.0	11.9	12.9	13.7	14.5	15.3	16.0	16.6	17.3	17.9	18.5	19.1	19.7																												18
19	11.2	12.2	13.2	14.1	14.9	15.6	16.4	17.1	17.8	18.4	19.0	19.6	20.2	20.8																											19
20	11.5	12.5	13.5	14.4	15.2	15.9	16.8	17.5	18.2	18.8	19.5	20.1	20.7	21.3	21.9																										20
22	12.0	13.1	14.1	15.0	15.9	16.7	17.6	18.3	19.1	19.7	20.4	21.0	21.7	22.3	22.9	24.1																									22
24	12.4	13.6	14.6	15.6	16.6	17.5	18.3	19.1	19.8	20.6	21.3	21.9	22.6	23.2	23.9	25.1	26.2																								24
26	12.8	14.1	15.2	16.2	17.2	18.1	19.0	19.8	20.6	21.4	22.1	22.8	23.5	24.1	24.8	26.1	27.2	28.4																							26
28	13.2	14.5	15.6	16.7	17.7	18.7	19.6	20.5	21.3	22.1	22.9	23.6	24.4	25.0	25.7	27.1	28.2	29.5	30.6																						28
30	13.6	14.9	16.1	17.2	18.3	19.3	20.2	21.1	22.0	22.9	23.7	24.4	25.2	25.9	26.7	28.0	29.3	30.5	31.6	32.8																					30
32	14.0	15.3	16.5	17.7	18.8	19.8	20.8	21.8	22.7	23.6	24.4	25.2	26.0	26.7	27.5	28.9	30.1	31.4	32.6	33.8	35.0																				32
34	14.4	15.7	17.0	18.2	19.3	20.4	21.4	22.4	23.3	24.2	25.1	25.9	26.7	27.5	28.3	29.7	31.0	32.3	33.6	34.8	36.0	37.2																			34
36	14.7	16.1	17.4	18.6	19.8	20.9	21.9	23.0	23.9	24.8	25.8	26.6	27.4	28.3	29.0	30.5	32.0	33.0	34.6	35.8	37.0	38.2	39.4																		36
38	15.0	16.4	17.8	19.0	20.3	21.4	22.5	23.5	24.5	25.4	26.4	27.3	28.1	29.0	29.8	31.4	32.8	34.2	35.5	36.7	38.0	39.2	40.4	41.6																	38
40	15.3	16.8	18.2	19.4	20.7	21.9	23.0	24.0	25.1	26.0	27.0	27.9	28.8	29.7	30.5	32.1	33.6	35.1	36.4	37.6	39.0	40.2	41.4	42.6	43.8																40
42	15.6	17.1	18.5	19.8	21.1	22.3	23.4	24.5	25.6	26.6	27.6	28.5	29.4	30.4	31.2	32.8	34.4	35.9	37.3	38.6	39.9	41.1	42.4	43.6	44.8	45.9															42
44	15.9	17.5	18.9	20.2	21.5	22.7	23.9	25.0	26.1	27.2	28.2	29.1	30.0	31.0	31.9	33.5	35.2	36.7	38.1	39.5	40.8	42.0	43.2	44.4	45.6	46.9	48.1														44
46	16.2	17.8	19.2	20.6	21.9	23.2	24.3	25.5	26.7	27.7	28.7	29.7	30.6	31.6	32.5	34.2	35.9	37.4	38.9	40.3	41.7	43.0	44.3	45.6	46.8	47.9	49.1	50.3													46
48	16.5	18.1	19.6	20.9	22.3	23.6	24.8	26.0	27.2	28.2	29.2	30.2	31.2	32.2	33.1	34.9	36.6	38.2	39.7	41.2	42.6	43.9	45.2	46.5	47.8	48.9	50.2	51.3	52.6												48
50	16.8	18.4	19.9	21.3	22.7	24.0	25.2	26.4	27.6	28.7	29.8	30.8	31.8	32.8	33.7	35.5	37.3	38.9	40.4	42.0	43.5	44.8	46.1	47.4	48.6	49.8	51.2	52.3	53.6	54.7											50
52	17.0	18.7	20.2	21.6	23.1	24.4	25.6	26.8	28.1	29.2	30.3	31.4	32.4	33.4	34.3	36.2	38.0	39.6	41.2	42.8	44.3	45.7	47.1	48.3	49.7	50.8	52.2	53.3	54.6	55.8	56.9										52
54	17.3	19.0	20.5	22.0	23.4	24.8	26.1	27.3	28.5	29.7	30.8	31.9	32.9	33.9	34.9	36.8	38.7	40.3	42.0	43.6	45.0	46.5	48.0	49.2	50.6	51.8	53.2	54.3	55.6	56.8	57.9										54
56	17.6	19.3	20.9	22.4	23.8	25.2	26.5	27.7	28.9	30.1	31.2	32.4	33.4	34.5	35.5	37.4	39.3	41.0	42.7	44.3	45.8	47.3	48.8	50.1	51.5	52.7	54.1	55.3	56.5	57.8	58.9	61.3									56
58	17.8	19.5	21.3	22.7	24.2	25.5	26.9	28.2	29.3	30.5	31.7	32.9	33.9	35.0	36.0	38.0	39.8	41.7	43.4	45.0	46.6	48.1	49.6	51.0	52.4	53.7	55.0	56.2	57.5	58.8	60.0	62.3									58
60	18.1	19.8	21.6	23.0	24.5	25.8	27.3	28.7	29.8	31.0	32.2	33.4	34.5	35.5	36.5	38.6	40.4	42.3	44.0	45.8	47.3	48.9	50.4	51.8	53.3	54.6	55.9	57.1	58.5	59.8	61.0	63.3	65.7								60
62	18.3	20.1	21.7	23.3	24.8	26.2	27.6	29.0	30.2	31.4	32.6	33.8	35.0	36.0	37.1	39.2	41.0	42.9	44.7	46.5	48.0	49.7	51.2	52.6	54.2	55.5	56.8	58.0	59.4	60.7	62.0	64.3	66.7								62
64	18.6	20.3	22.0	23.6	25.2	26.5	27.9	29.3	30.6	31.8	33.1	34.2	35.5	36.5	37.6	39.7	41.6	43.5	45.4	47.2	48.7	50.4	52.0	53.4	55.0	56.4	57.7	59.0	60.3	61.6	62.9	65.3	67.7	70.0							64
66	18.8	20.6	22.3	23.9	25.5	26.9	28.3	29.7	31.0	32.2	33.5	34.7	35.9	37.0	38.1	40.2	42.2	44.1	46.0	47.8	49.5	51.1	52.8	54.2	55.8	57.2	58.6	59.9	61.2	62.5	63.9	66.3	68.7	71.1							66
68	19.0	20.8	22.5	24.2	25.8	27.3	28.7	30.1	31.4	32.6	33.9	35.1	36.3	37.5	38.6	40.7	42.8	44.7	46.6	48.4	50.2	51.8	53.5	55.0	56.6	58.0	59.5	60.8	62.1	63.4	64.8	67.3	69.7	72.1	74.4						68
70	19.2	21.1	22.8	24.5	26.1	27.6	29.1	30.4	31.8	33.1	34.3	35.6	36.8	37.9	39.1	41.3	43.3	45.3	47.2	49.0	50.9	52.5	54.2	55.8	57.3	58.8	60.3	61.7	63.0	64.3	65.7	68.3	70.7	73.1	75.4						70
72															39.6	41.8	43.8	45.9	47.8	49.7	51.5	53.2	54.9	56.5	58.0	59.6	61.1	62.6	63.9	65.2	66.6	69.2	71.7	74.1	76.4	78.8					72
74															40.0	42.3	44.4	46.4	48.4	50.3	52.1	53.9	55.6	57.2	58.8	60.4	61.9	63.3	64.8	66.1	67.5	70.1	72.7	75.2	77.6	79.9					74
76															40.5	42.8	44.9	47.0	49.0	50.8	52.7	54.6	56.3	57.9	59.5	61.2	62.7	64.1	65.6	67.0	68.4	71.0	73.6	76.1	78.6	80.9	83.2				76
78															40.9	43.3	45.5	47.5	49.5	51.5	53.3	55.2	57.0	58.6	60.3	62.0	63.4	64.9	66.4	67.9	69.3	71.8	74.5	77.1	79.6	81.8	84.2				78
80															41.3	43.8	46.0	48.0	50.1	52.0	53.9	55.8	57.6	59.3	61.0	62.7	64.1	65.7	67.2	68.7	70.1	72.7	75.4	78.1	80.6	82.8	85.2	87.5			80
82															41.8	44.2	46.4	48.6	50.6	52.6	54.5	56.4	58.2	60.0	61.7	63.4	64.9	66.5	68.0	69.5	71.0	73.6	76.3	79.0	81.5	83.8	86.2	88.6			82
84															42.2	44.6	46.9	49.1	51.1	53.2	55.1	57.0	58.9	60.7	62.4	64.1	65.7	67.3	68.8	70.3	71.8	74.5	77.2	79.9	82.4	84.8	87.2	89.6	91.9		84
86															42.6	45.0	47.4	49.6	51.6	53.7	55.7	57.6	59.5	61.3	63.0	64.8	66.4	68.0	69.5	71.1	72.6	75.4	78.1	80.8	83.3	85.8	88.2	90.6	92.9		86
88															43.0	45.4	47.8	50.1	52.2	54.3	56.3	58.2	60.1	62.0	63.7	65.4	67.0	68.7	70.3	71.8	73.4	76.3	79.0	81.6	84.2	86.8	89.2	91.6	93.9	96.3	88
90															43.4	45.9	48.3	50.6	52.8	54.8	56.9	58.8	60.7	62.6	64.4	66.0	67.8	69.4	71.1	72.6	74.2	77.1	79.9	82.5	85.1	87.8	90.2	92.6	94.9	97.3	90
92															43.8	46.3	48.7	51.1	53.4	55.4	57.4	59.4	61.3	63.2	65.0	66.8	68.5	70.1	71.8	73.3	74.9	77.8	80.8	83.4	86.0	88.7	91.2	93.6	95.9	98.3	92
94															44.2	46.7	49.1	51.6	53.9	55.9	57.9	60.0	61.9	63.8	65.6	67.5	69.2	70.8	72.5	74.1	75.6	78.6	81.7	84.3	86.9	89.6	92.1	94.6	96.9	99.3	94
96															44.6	47.2	49.5	52.0	54.4	56.3	58.4	60.5	62.4	64.4	66.2	68.2	69.8	71.5	73.2	74.8	76.3	79.4	82.6	85.2	87.8	90.5	93.0	95.6	97.9	100.3	96

Heating, Piping & Air Conditioning, December 1947
A.S.H.V.E. Research

Figure 4. Circular Equivalents of Rectangular Duct for Equal Friction and Capacity.

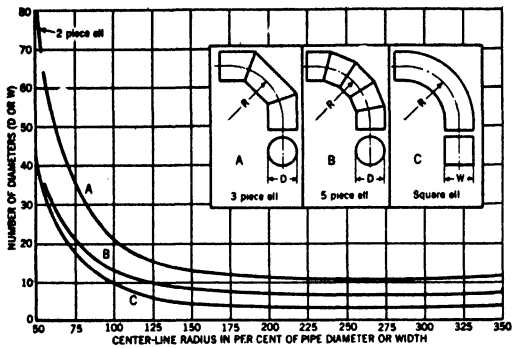


Figure 5. Loss of Pressure in Elbows

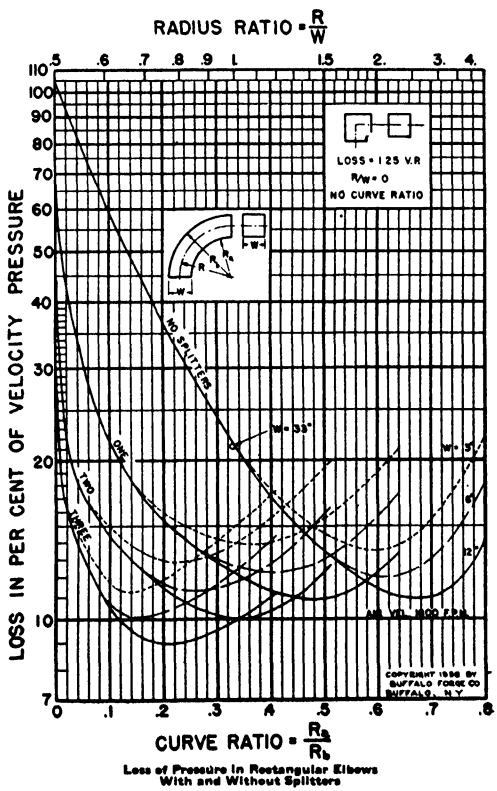


Figure 6.

D_e = equivalent diameter of round pipe for equal friction per foot of length to carry the same capacity, ft. or in.

A comprehensive study of equivalent duct size is being made by the A.S.H.V.E. Research Laboratory. The first issue of the results to date is shown in Figure 4.

The pressure loss in an elbow is of a comlicated nature varying with size, shape, velocity, and even the conditions of the ducts leading to and from the elbow. In most cases, it will not be possible to take all of these factors into consideration nor will it be necessary. In systems involving large air flow and consequently large horsepower, it will be good economy to give the matter of elbow losses careful consideration.

As indicated in Figure 5, long-radius elbows will offer much less resistance to the flow of air than short-radius elbows. Experience has shown that good results may be expected when the radius to the center of the elbow is 1.5 times the pipe diameter or duct width parallel to the radius. Examination of the curve will indicate that little advantage is to be gained by selecting elbows having a centerline radius of more than two diameters. Elbows having a radius of more than three diameters show a slightly increased resistance due to the increased length of pipe but, when used, they reduce the over-all resistance of the system and therefore should not be avoided.

When conveying materials, long-sweep radius elbows are used to minimize the chance of eddies in elbows effecting the travel of the material.

Tests (2) (3) to determine effect of curve ratio (CR) upon elbows of round cross-section were made by Busey in the laboratory of the Buffalo Forge Company. Similar tests on rectangular cross-section were made by Madison and Parker in the same laboratory. These results are shown on Figure 6 and Figure 7 and are based upon the fact that the elbow is in a run of duct and followed by at least three or four diameters of straight duct. The values given are for the complete loss of the elbow, including surface friction, but do not include the friction loss of any of the straight duct preceding or following the elbow. It may be observed that the pressure loss increases as the inside radius becomes less and is a maximum when both the outside and inside radii are square corners. As the rate of curvature becomes less, that is, CR becomes larger, the value of the elbow loss diminishes until at about 0.6 to 0.7 CR a minimum value is reached. If, however, the friction of the extra length of straight duct is added to an elbow of this curvature to make the equivalent of an elbow of even greater curvature, the total loss would undoubtedly be less in the latter case. The reasons that elbows of very large curve ratio are not regularly used is because the cost of construction is out of proportion to the saving effected. Generally, then, a low-loss elbow is considered to be one of 0.5 curve ratio (1-1/2 RR) and this has become an accepted standard for most engineering work.

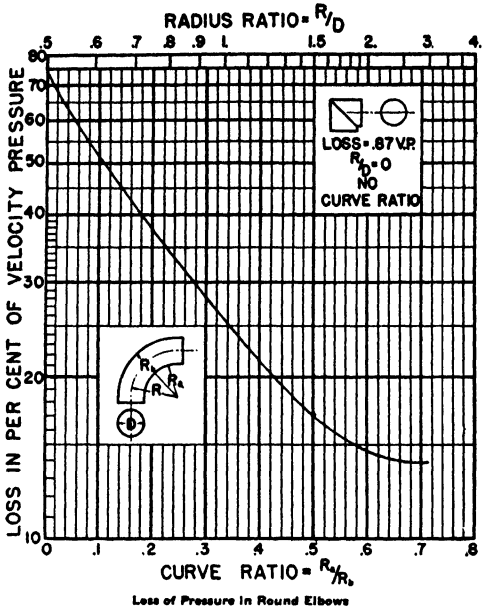


Figure 7.

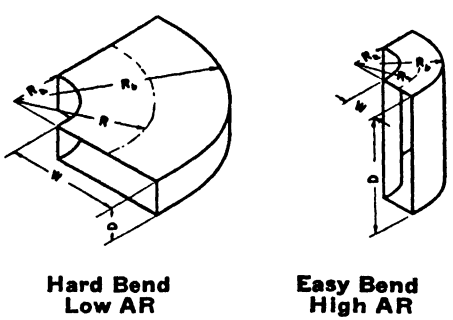


Figure 8.

In rectangular ducts the effect of shape has considerable bearing upon pressure loss. The term aspect ratio (AR) is used to represent shape in relation to the bend. Aspect ratio is the depth of elbow along the axis of bend divided by the width in the plane of the bend. In the accompanying cut, (Fig. 8), the aspect ratio is D/W and consequently large aspect ratios characterize "easy bend" and small aspect ratios, "hard bends." Aspect ratio cannot be expressed as a factor independent of radius ratio but may be closely approximated by two curves shown on Figure 9. These curves give the loss in per cent of the unity aspect ratio losses found on Figure 6.

Example 3 - Find the loss in a 6 - x 24-in. elbow (axis parallel to the 24-in. side) and an inside radius of 3 in. The curve ratio = 3/9 = 0.333. Loss for elbow of square section may be read 21% velocity pressure, from the upper curve on Figure 6. The aspect ratio is 24/6 = 4. The aspect ratio factor may be read 0.88 from upper curve on Figure 9. The loss for this particular elbow then is 0.88 x 21 = 18.5% velocity pressure.

If the velocity pressure is 1/4 in. (corresponding to 2,000 ft./min. standard air) the loss is 0.185 x 0.25 = 0.046 in. of water pressure.

Splitters are curved vanes placed in an elbow concentric with the inside and outside radii and extend the full 90° angle from face to face. They divide the flow into parallel channels, each having a larger curve ratio and a larger aspect ratio than that of the original elbow. The change in aspect ratio has much less effect upon elbow loss than a change in curve ratio. Consequently, the ideal location for splitters is such as to divide the elbow into components, each with the same curve ratio. This not only tends to produce an elbow of minimum loss, but greatly simplifies the pressure loss calculation.

Where splitters are used in elbows with high or low aspect ratios the influence of the new aspect ratio due to splitters should be considered, and an average aspect value may be used for this purpose (2). A very material benefit may be obtained with the use of two or three splitters in elbows of low curve ratio. Little or nothing can be gained installing splitters in elbows of large curve ratio.

Example 4 - Consider an elbow of square cross-section with inside radius of 2 in. and outside radius of 20 in. The curve ratio is 2/20 = 0.1. Select a value of 0.1 at base of Figure 6 and move vertically to the line of no splitters and then to the left scale. Such an elbow would have a loss of 59% velocity pressure. If two splitters were used, move down the same vertical line to the curve of two splitters and read 14% velocity pressure from the left scale. If three splitters were used, the loss would be 10.5% velocity pressure. After deciding on number of splitters to use turn to Figure 10. Our elbow has an inside radius of 2 in. and outside radius of 20 in. If two splitters are to be used, lay a straight edge across the chart intersecting 2 in. on left hand scale and 20 in. on right hand scale. Read the radius of the smaller splitter as 4.3 in. and the larger splitter as 9.25 in. from the corresponding intermediate scales.

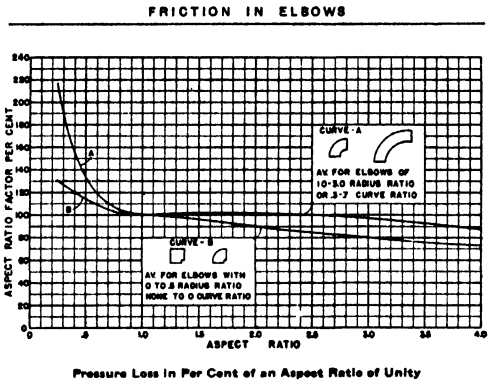


Figure 9.

V. PROCEDURE FOR DUCT SYSTEM DESIGN (1)

Design of a complete system includes air inlet, heaters, filters, fans, ducts, etc. While sizing the various parts, thought must be given to the pressure loss that part will contribute to the system. The entrance loss through the outside air intake louvres will vary with the design of the weather-proof louvre having an average loss of 1-1/2 velocity heads at a velocity of 1,000 ft./min. The louvre should have 75% free area with connecting duct having 15 tapered sides. Wherever air passes through a plenum space having a negligible velocity, allowance must be made for the loss in velocity head. This loss in velocity head may be taken as the difference in velocity heads in the plenum and the duct. Where ducts are very smooth with long transformation fittings, a regain in static pressure is sometimes allowed, but ordinary construction does not warrant a consideration of this factor and it is customary to neglect it. When it is allowed, the regain is estimated at one-half the difference between the velocity pressure at the fan outlet and the velocity pressure in the last run of pipe.

The pressure loss that occurs in heater coils, filters, and washers must be included in the sum of the other losses. Pressure losses thru this apparatus is obtained from manufacturers' data.

The air velocities ordinarily used are given in the following tabulation and the sheet metal specifications given later are for these velocities. Where higher velocities are used, the ducts should be cross-braced to prevent breathing, buckling, or vibration, and should be constructed of heavier gage metal. At the higher capacities, it is particularly important to design the ducts for minimum resistance.

For industrial buildings, air noise is seldom given much consideration because of other machinery noises within the building. Main velocities of 2,800 or 3,000 ft./min. or higher are often used.

For high-velocity diffusing outlet, the duct velocity should not be less than the throat velocity of the diffusers, as dynamic losses occur wherever velocities are stepped up or down. Present-day trend is toward much higher grille and branch duct velocities, but great care must be exercised as noise and/or drafts may result.

There is a trend toward fatigue reduction studies in industry. If these studies point to the advisability of acoustic application on machinery, then air noises in duct work will be subject to the same considerations as when they are installed in so-called quiet operations.

The following velocities are given as a guide: (1)

TABLE I

	Recommended Velocity ft./min.			Maximum Velocity, ft./min.		
Designation	Residences	Schools, Theaters, Public Buildings	Industrial Buildings	Residences	Schools, Theaters, Public Buildings	Industrial Buildings
Outside Air Intakes*	700	800	1000	800	900	1200
Filters*	250	300	350	300	350	350
Heating Coils*	450	500	600	500	600	700
Air Washers	500	500	500	500	500	500
Suction Connections	700	800	1000	900	1000	1400
Fan Outlet	1000-1600	1300-2000	1600-2400	1700	1500-2200	1700-2800
Main Duct	700-900	1000-1300	1200-1800	800-1000	1100-1400	1300-2000
Branch Duct	600	600-900	800-1000	700	800-1000	1000-1200
Branch Risers	500	600-700	800	650	800-900	1000

*These velocities are for total face area, not the net free area.

From Heating Ventilating Air Conditioning Guide, 1947. Used by permission.

Velocity method of designing a duct system involves the arbitrary selection of velocities for various sections of the duct system with highest velocities at the fan and progressively lower velocities toward

FAN ENGINEERING—BUFFALO FORGE COMPANY

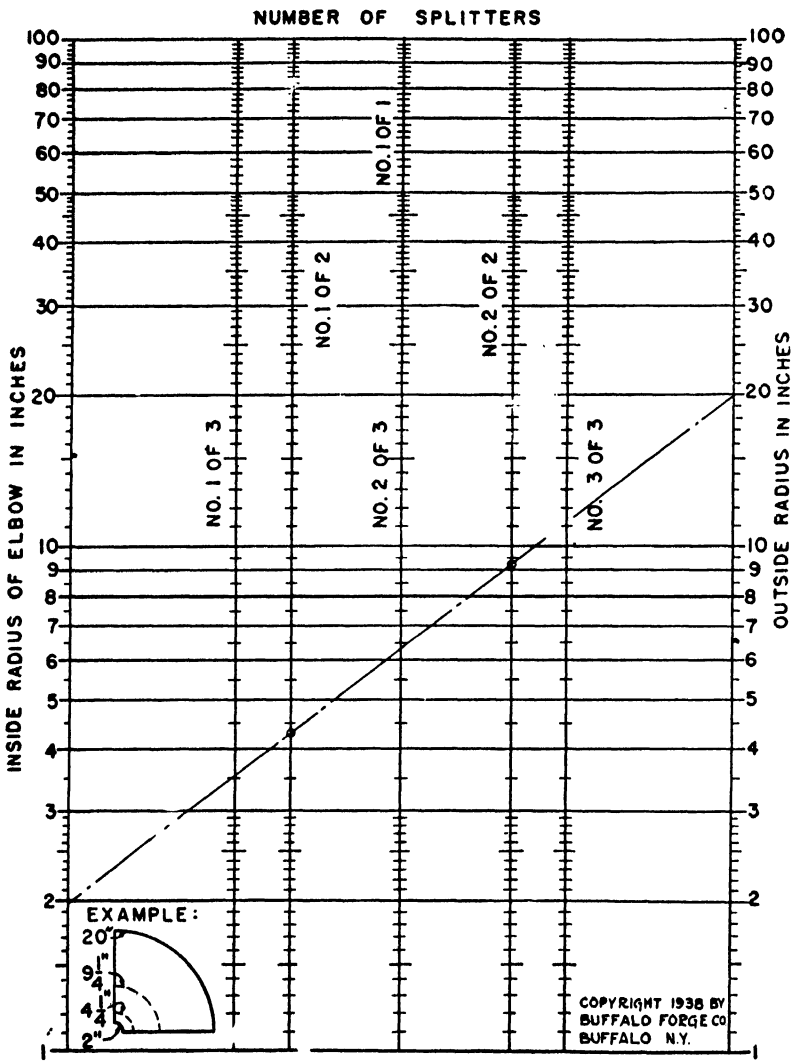


Chart for Determining the Location of Elbow Splitters

The chart shown above is based on the above relationship and facilitates the location of splitters in an elbow. The example illustrated by the chart shows an elbow with inside radius of 2″ and an outside radius of 20″. If two splitters are to be used lay a straight edge across the chart intersecting 2″ and 20″ on the outside scales.

Figure 10.

the duct openings to the room. The static pressure loss for each section must be calculated separately and the total loss found by adding the individual losses of the various sections of the run having the highest resistance. In this type of system sometimes the shorter run may have the higher resistance pressure because of more elbows, transformations, booster heater, etc. This method requires more judgment and experience in choosing the proper velocities to approach equal friction for all lengths of runs.

The equal friction method of design is based on selecting a main duct velocity consistent with good practice from standpoint of noise for the particular type of building.

All main ducts and branch ducts are sized for equal friction per unit length by the use of Figure 2 and Figure 3. Where package-type supply units are used, check what external resistance they will develop and still deliver its capacity rating. It will be necessary to divide the available resistance by the total equivalent length of the longest or most complicated run of duct to determine the resistance per 100 ft. and then to size all ducts at this resistance value. This will automatically determine the duct velocities and give the desired total duct resistance. Regulating dampers are recommended in each branch, even though each branch duct is so sized that it has a resistance equal to the resistance of the main system at the point of juncture.

Example 5 - Figure 11 shows typical layout of an air distribution system which is applicable for ventilation of hotel dining rooms and offices. The volume of air in cu.ft./min. for the room has been specified as 22935 cu.ft./min. The dining room is 135 ft. x 85 ft. x 15 ft.

The free area of the outdoor air inlet is based on a velocity of 1,000 ft./min. or 22935 + 1000 = 22.94 sq.ft. The duct velocity selected from Table I is 1250 ft./min., which gives a main duct area of 22935 + 1250 = 18.354 sq.ft. Assume 60 x 44 in. duct and from Figure 4 we find this size duct is approximately equivalent to 56 in. diameter. Figure 2 shows for a volume of 22935 cu.ft./min. through a 56-in. diameter duct gives a resistance of 0.033 in./100 ft. The amount of air to be handled by each section of duct is shown on Figure 9 and by locating each of these values on the 0.033-in. friction line the round pipe sizes are obtained and then referring to Figure 4, the equivalent rectangular sizes are selected as shown in the following table:

Volume of Air cu.ft./min.	Diameter of Pipe in.	Equivalent Size of Rectangular Duct, in.
22,935	56	60 x 44
12,510	45	58 x 30
10,425	42	50 x 30
8,340	39	42 x 30
6,255	35	42 x 24
4,170	29.5	30 x 24
2,085	23	30 x 15

The pressure at the outlet nearest the fan will be greater than at the outlets further along the run so that the former will tend to deliver more than the calculated amount of air. To remedy this condition, volume regulating dampers should be located at the base of each riser, or in each branch duct, and adjusted for proper distribution. At points where branches leave the main, it may be advisable, depending upon the nature of the installation, to install adjustable splitters where the main duct divides into the 58 x 30 in. and 58 x 30 in. branches.

Resistance Losses for This System:

(1) Outdoor air intake, 1000 ft./min. velocity (1.5 heads x 0.0625)	0.094 in.
(2) Filters (from manufacturer's tables)	0.250
(3) Tempering coil loss (from manufacturer's tables)	0.074
(4) Air Washer loss (from manufacturer's tables)	0.250
(5) Reheat coil loss (from manufacturer's tables)	0.083
(6) Duct resistance	

The longest run is 150 ft.

2 elbows 58 x 30 in. (150% ratio) - $\frac{2 \times 13 \times 58}{12}$ = 126 ft.

2 elbows 30 x 15 in. (150% ratio) -

$$\frac{2 \times 13 \times 30}{12} = 65 \text{ ft.}$$

3 elbows 15 x 30 in. (75% ratio) -

$$\frac{3 \times 35 \times 15}{12} = 131 \text{ ft.}$$

Total equivalent run 472 ft.

472 ft. at 0.33/100 ft.	0.156 in.
(7) Allowance for damper adjustment 25% of 0.156	0.039
(8) Supply grille resistance (from manufacturer's table)	0.036
Total static pressure loss of system	0.982 in.

Example 6 - If the rooms and offices in the above example are to be served from a manufactured package-type unit with a capacity of 22935 cu.ft./min. against an external resistance of 0.35 in., the known resistance is calculated as:

(1) Outdoor air inlet	0.094 in.
(2) Supply grilles resistance (from manufacturer's tables)	0.036
Total known resistance	0.130 in.

Subtracting this from the total available resistance 0.35 - 0.13 in. = 0.220 in. If 25% is allowed for damper adjustment, the total allowable duct friction equals (0.220)/(1.25) = 0.176 in.

Known length of run	150 ft.
Four 150% ratio elbows, 4 x 13 x 35 ft.	182 ft.
Three 75% ratio elbows, 3 x 35 x 1.5 ft.	158 ft.
Total estimated length	490 ft.

The duct friction per 100 ft. is then (0.176)/(4.90) = 0.036 in. and the mains and branches are sized from the 0.036-in. friction line in Figure 2. If it is desired to size each branch for equal resistance, the total resistance back to the point of juncture is calculated and the branch is then sized in a manner similar to that outlined in Example 4.

VI. DUCT CONSTRUCTION

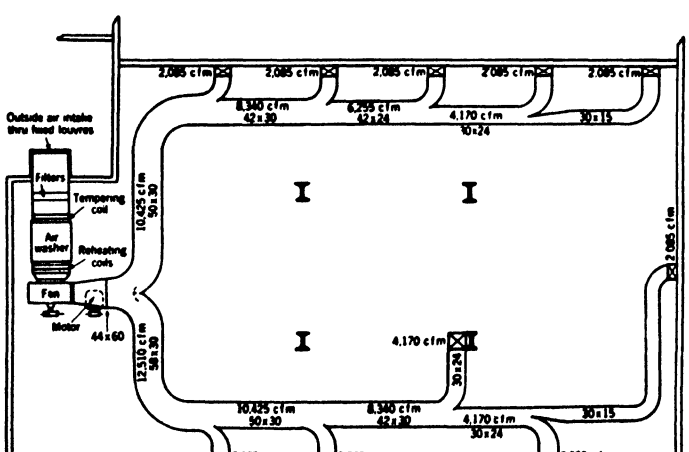


Figure 11. Typical Layout of Air Distribution System

Longitudinal seams of both round and rectangular duct should be grooved type. Elbows and transformation sections as well as larger size rectangular ducts are generally formed with Pittsburgh corner seams because this seam is easier to lock in place than the double seam, but complicated fittings such as double compounded elbows are usually constructed with double-seam corners.

The construction of the various seams and joints are shown on Figure 12. The end slip may be used wherever "S" slips are recommended. Where drive slips are used, the end slip may be applied on the narrow side of the duct and the drive slips on only the maximum side. Ducts 25 to 30 in. in size should be reinforced between joints. Ducts 31 in. and up should be reinforced at the joint and between the joint.

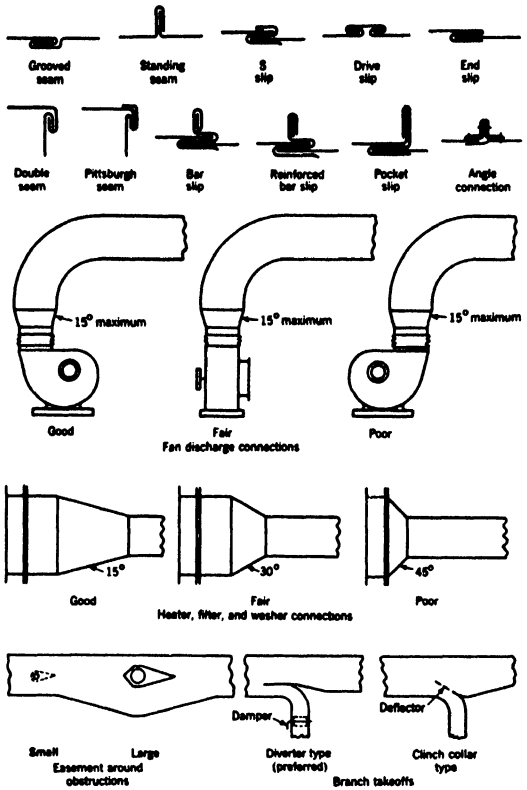


Figure 12. Sheet Metal Duct and Arrangement Details

It is good to cross-break or kink all flat surfaces to prevent vibration or buckling due to the air flow and accompanying variations in internal pressure.

Heavy canvas connections (asbestos cloth if there is fire hazard) are recommended on both the inlet and outlet of all fans. The new rubber impregnated glass fibre cloths may also be used for this service.

Recommended sheet metal gages for rectangular duct construction are shown in Figure 13. Duct work used in exhaust and conveying work will be discussed later.

VII. HEATING COILS

In making selection of fin coil type heating coils, we will use the same capacity of 22,935 cu.ft./min. and assume we are required to heat this amount of air from 0°F. to 96°F. and we also have sufficient steam available, at 12 lb./sq.in.ga. pressure. We will further assume that the steam control valve will take a 5 lb./sq.in. pressure drop and the piping will take a 2 lb./sq.in. pressure drop. This leaves us 5 lb./sq.in. pressure for operating the heater coils.

It simplifies controlling the temperature of air leaving the heating coils if we divide the total temperature rise between several separate heating coils through which the air passes in series. The steam flow to each bank of heating coils is controlled in step action by the same thermostat or individually by separate thermostats.

On this type of heating surface, usually the manufacturers rate the capacity on a velocity based on using the total net face area, instead of using free area.

For public buildings or factory work, the preferable velocities are from 500 to 800 ft./min. through net face area; however, desired temperature rise or limited allowable static pressure may dictate using other velocities.

The first bank of heaters that the air passes through is usually called the pre-heaters and the second bank is then referred to as re-heaters.

On pre-heaters it is generally necessary to throttle the steam flow as the outdoor temperature rises above the minimum because the heat load then becomes less.

Pre-heaters are sometimes selected and installed so that their heating capacity is only sufficient to raise the entering air temperature from 35°F. to 70°F. The steam is turned on full when the outdoor temperature drops to 35°F. and the steam is kept on full until the outdoor air again rises above 35°F. at which time the steam is turned off. This means that at 0°F. outdoor temperature the air leaves the coil at 35°F. The re-heat coil must be selected so it will raise the air temperature from 35°F. to the required final temperature. If the minimum outdoor temperature is below 0°F. and it is still desired to have the temperature of the air leaving the pre-heater above freezing, then more heating capacity must be included in the pre-heat coil. If the larger capacity pre-heat coil is turned on full at 35°F., then the large capacity will be sufficient to heat the air passing through the coil above 70°F. and the result will be overheating of the ventilated area.

It would then be necessary to throttle the steam supply to the pre-heat coils. When the steam is throttled to this type coil, there is a chance of freezing the coil when the outdoor temperature is around 25 to 28°F. If temperature controls start hunting or swinging when outdoor temperatures are in that range the result will undoubtedly be a freeze in the coil.

RECOMMENDED SHEET METAL GAGES FOR RECTANGULAR DUCT CONSTRUCTION[a]

U. S. STD. GAGE	MAXIMUM SIDE, INCHES	TYPE OF TRANSVERSE JOINT CONNECTIONS[b]	BRACING
26	Up to 12	S, Drive, Pocket or Bar Slips, on 7 ft 10 in. centers	None
24	13 to 24	S, Drive, Pocket or Bar Slips, on 7 ft 10 in. centers	None
	25 to 30	S, Drive, 1 in. Pocket or 1 in. Bar Slips, on 7 ft 10 in. centers[c]	1 x 1 x ⅛ in. angles 4 ft from joint
22	31 to 40	Drive, 1 in. Pocket or 1 in. Bar Slips, on 7 ft 10 in. centers[c]	1 x 1 x ⅛ in. angles 4 ft from joint
	41 to 60	1½ in. Angle Connections, or 1½ in. Pocket or 1½ in. Bar Slips with 1⅜ in. x ⅛ in. bar reinforcing on 7 ft 10 in. centers[c]	1½ x 1½ x ⅛ in. angles 4 ft from joint
20	61 to 90	1½ in. Angle Connections, or 1½ in. Pocket or 1½ in. Bar Slips 3 ft 9 in. maximum centers with 1⅜ x ⅛ in. bar reinforcing	1½ x 1½ x ⅛ in. diagonal angles, or 1½ x 1½ x ⅛ in. angles 2 ft from joint
18	91 and up	2 in. Angle Connections or 1½ in. Pocket or 1½ in. Bar Slips 3 ft 9 in. maximum centers with 1⅜ x ⅛ in. bar reinforcing[d]	1½ x 1½ x ⅛ in. diagonal angles, or 1½ x 1½ x ⅛ in. angles 2 ft from joint

[a]For normal pressures and velocities (see Table 4) utilized in typical ventilating and air conditioning systems. Where special rigidity or stiffness is required, ducts should be constructed of metal two gages heavier. All uninsulated ducts 18 in. and larger should be cross-broken. Cross-breaking may be omitted on uninsulated ducts if two gages of heavier metal are used.

[b]Other joint connections of equivalent mechanical strength and air tightness may be used.

[c]Duct sections of 3 ft 9 in. may be used with bracing angles omitted, instead of 7 ft 10 in. lengths with joints indicated.

[d]Ducts 91 in. and larger require special field study for hanging and supporting methods.

Figure 13

To eliminate or minimize this possibility, a non-freeze type coil has been developed and is now on the market. The steam flow to this coil may be throttled, but as long as the condensate and air are removed and sufficient steam flows around the condensate outlet, freezing up of coil will not take place. We will, therefore, consider the non-freeze type coil for our pre-heat coil.

Example 7 - Heat 22,935 cu.ft./min. from 0° to 96° F., using steam at 5 lb./sq.in.ga. pressure. Turn to Table 2 and we see a tabulation of final temperatures and condensation rates for various face velocities, at various entering air temperature, for various numbers of tubes deep when the heater coils are supplied with sufficient steam at a pressure of 5 lb./sq.in. ga.

Assuming that the pre-heat will take care of raising the air half the total rise, we see that air entering at 0° F., one tube deep with a face velocity of 500 ft./min. the final temperature will be 52.4° F. and the condensate will equal 29.4 (lb.)/(hr.)(sq.ft.).

We divide the total cu.ft./min. of 22,935 by the face velocity of 500 ft./min. and find we need 46 sq.ft. of net face area.

Now we look on Table 3 for selecting the size of pre-heater we need. Usually the shape of the heaters are picked to match up with filters, air washers, etc. The longer the tube length normally means the cheaper the first cost of the heaters. For an efficient air flow at low static pressure loss, a shape of heater approaching a square lends itself to more gradual transformations in direction of air flow. The fewer number of heater sections required in a bank results in lower installation cost because there are fewer connections, fittings, valves, etc., required.

Now from Table 3 we could select two sections of 24 tube face with nominal tube length of 8 ft., 6 in., which would have 23.90 sq.ft. of face area each or a total of 47.8 sq.ft. If

TABLE 2

AEROFIN — TYPE F NON-FREEZE COIL

FINAL TEMPERATURES AND CONDENSATIONS

5 lbs. Steam — 227° Temperature — TYPE F NON-FREEZE **71&72**

Temp. Air Ent. °F	Rows Tubes Deep	Velocity of Air Through NET FACE AREA†—in feet per minute—Measured at 70° F. and 29.92" Barometer											
		300 FACE VEL		400 FACE VEL		500 FACE VEL		600 FACE VEL		700 FACE VEL		800 FACE VEL	
		F. T.°	Cond.‡	F. T.°	Cond.‡	F. T.°	Cond.‡	F. T.°	Cond.‡	F. T.°	Cond.‡	F. T.°	Cond.‡
0°	1	63.5	21.0	56.7	25.5	52.4	29.4	49.7	33.5	47.8	37.2	45.0	40.5
	2	108.9	36.8	100.6	45.4	93.2	52.6	88.1	59.7	84.4	66.6	80.6	72.7
	3	141.6	48.0	132.8	60.0	124.9	70.6	118.9	80.6	113.9	89.6	108.1	97.8
	4	165.2	56.0	156.9	71.0	148.0	84.0	142.6	96.5	136.9	108.0	130.7	118.0
	5	182.5	61.8	174.4	79.0	167.2	94.4	160.7	108.8	155.3	122.8	149.5	135.0
	6	195.2	66.0	187.9	85.0	181.1	102.4	175.2	118.6	170.1	134.5	164.4	148.5
20°	1	77.0	19.2	71.7	23.3	67.8	26.8	65.3	30.6	63.1	34.0	61.1	37.0
	2	119.4	26.8	111.9	33.5	105.0	40.0	101.3	46.5	97.0	60.8	93.6	66.2
	3	147.7	31.2	141.3	39.0	133.4	46.0	128.5	53.5	123.0	81.6	118.8	88.2
	4	166.8	36.0	163.0	44.8	155.6	76.6	150.0	88.0	144.7	98.5	139.0	107.4
	5	186.2	56.3	179.0	72.0	171.8	85.8	166.8	99.5	161.2	111.7	156.2	123.0
	6	197.6	60.0	191.5	77.6	184.5	91.0	179.9	108.0	175.0	122.1	170.0	135.4
30°	1	84.5	18.1	79.2	22.1	75.5	25.6	73.1	29.0	71.0	32.2	69.1	35.3
	2	126.6	31.9	117.4	38.4	111.0	45.7	106.5	51.8	103.3	58.0	100.0	63.1
	3	152.9	41.6	145.3	52.3	138.4	[illegible]	133.2	70.0	128.6	77.8	123.9	84.7
	4	173.6	48.1	166.2	61.6	159.3	[illegible]	153.6	81.7	148.2	93.8	143.5	102.5
	5	188.5	53.0	181.4	68.6	173.2	82.0	169.5	94.6	164.0	106.5	159.8	117.0
	6	199.4	57.3	193.1	74.0	187.3	[illegible]	183.0	103.0	177.6	116.6	172.7	128.8
40°	1	91.5	17.4	86.7	21.0	83.2	[illegible]	81.0	27.6	79.0	30.5	77.1	33.3
	2	129.7	30.2	122.0	37.4	116.8	[illegible]	111.6	48.4	109.6	55.0	106.5	60.0
	3	150.7	39.6	144.6	49.4	142.0	[illegible]	137.9	66.0	133.7	74.0	129.1	80.3
	4	170.1	46.0	169.3	58.5	162.4	[illegible]	157.3	79.4	152.8	89.0	147.7	97.2
	5	190.4	51.0	183.7	65.0	177.8	[illegible]	172.5	89.8	168.0	101.0	163.1	111.0
	6	200.9	54.4	194.8	70.0	189.3	[illegible]	184.4	97.8	180.1	110.6	175.5	113.3
50°	1	98.8	16.4	94.3	20.0	90.9	23.0	88.5	26.1	86.9	29.0	85.1	31.6
	2	135.0	28.7	128.5	35.4	122.8	41.0	118.8	46.5	115.9	52.0	113.0	56.8
	3	160.0	37.0	154.0	47.0	147.5	55.0	143.0	63.0	138.0	69.4	133.9	75.6
	4	179.0	43.6	172.0	55.0	166.0	65.3	161.2	76.0	156.5	84.0	152.2	92.3
	5	192.3	48.0	186.2	61.6	180.0	73.3	175.7	85.2	171.0	95.3	166.7	105.4
	6	202.0	51.3	196.7	66.3	190.8	79.4	187.0	92.8	182.5	104.5	178.3	116.0
60°	1	106.0	15.5	101.7	18.6	98.6	21.6	96.6	24.7	94.8	27.3	93.2	30.0
	2	140.1	27.0	134.1	33.5	128.9	38.6	126.9	43.8	121.1	48.2	119.5	53.6
	3	164.3	35.2	158.2	44.3	151.9	52.0	147.5	59.3	143.7	66.0	139.8	72.0
	4	181.6	41.0	175.4	52.1	169.5	61.8	164.8	71.0	160.7	79.4	156.2	87.0
	5	194.4	45.1	188.4	58.0	182.0	69.4	178.3	80.0	174.3	90.3	170.0	99.2
	6	203.8	48.6	198.3	62.6	193.3	75.2	189.0	87.3	185.2	99.0	181.0	109.2
70°	1	113.3	14.6	109.2	17.5	106.3	20.3	104.4	23.2	102.7	25.6	101.1	27.9
	2	145.4	25.4	139.6	31.1	134.5	36.4	131.0	41.1	128.4	46.0	125.9	50.4
	3	168.0	33.0	161.9	41.4	156.4	48.8	152.3	55.8	148.6	62.0	144.8	67.5
	4	184.3	38.7	178.5	49.0	173.0	58.0	168.5	66.5	164.7	74.6	160.4	81.6
	5	196.3	42.6	190.7	54.6	185.7	65.3	181.2	75.3	177.5	83.0	173.4	93.4
	6	205.1	45.6	200.0	58.8	195.3	70.8	191.3	82.1	187.2	92.6	183.8	102.9

†F. T.—Final Temperature of Air
†Net Face Area is Area occupied by finned tubes only

‡Cond.—Condensation in Pounds per Hour per Square Foot of Face Area.

For other Temperature Base conditions see Chart, page 16.

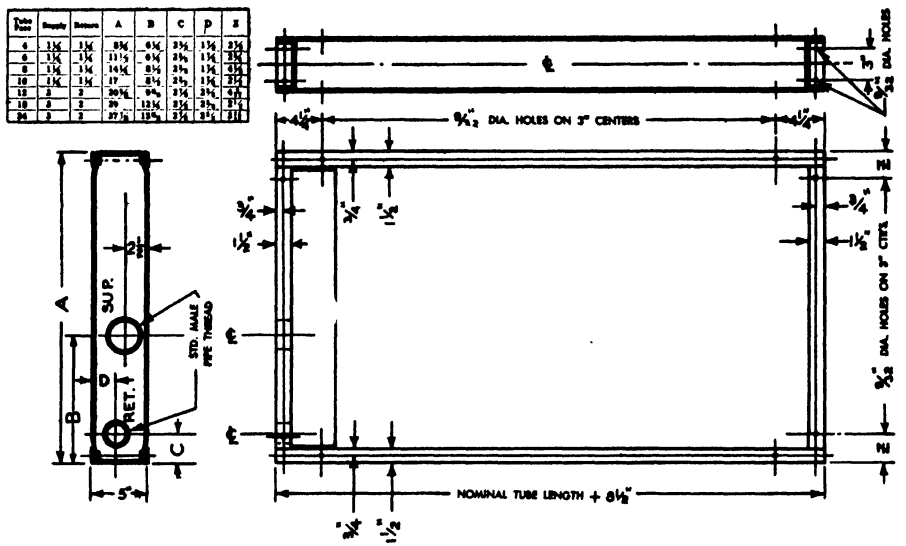
In all Fin-tube Aerofin designations (such as Fin-tube Aerofin-71 or Fin-tube Aerofin-72) the numerals following the name indicate the type of tubing (first numeral) and the number of rows of tubes deep (in description of old Sect'l. Heaters). Thus Fin-tube Aerofin-71 designates tubing with 16 in. fins, pitched 3 per in., and 4 Unit Rows of tubes deep, while Fin-tube Aerofin-72 designates tubing with 16 in. fins, pitched 3 per in., and 6 Unit Rows of tubes deep.

these sections were installed with tubes vertical, the over-all dimensions would be 6 ft., 2-14/16 in. wide by 9 ft., 2-1/2 in. high by 5 in. in direction of air flow. The over-all height of the installed heater bank would be 18 in. to 2 ft. higher than the first heater coil height to allow for piping connections. As an alternate choice, we could pick 18 tube face coils, and we would need three sections with 7 ft., 6 in. nominal tube length. This heater bank would measure 7 ft., 3 in. wide by 8 ft., 2-1/2 in. high (space below for piping) by 5 in. in direction of air flow. Each section would have 15.57 sq.ft. face area or a total of 46.71 sq.ft. face area.

Another alternate would be four sections wide of 18 tube face by nominal tube length of 5 ft., 6 in. each having 11.40 sq.ft. for face area or a total of 45.6 sq.ft., which is just 1/2 sq.ft. less than the total we figured. This difference is so small that the shortage in rise in pre-heat can be provided or made up for in the selection of the re-heater.

The dimensions of this last selection would be 9 ft., 8 in. wide by 6 ft., 2-1/2 in. high (plus 2 ft. for piping would make over-all installed height of 8 ft., 2-1/2 in.) by 5 in. in direction of air flow.

TABLE 3



FACE AREA TABLE (Square Feet)

Overall Casing Width	Tube Face	NOMINAL TUBE LENGTH																							
		1'0"	1'3"	1'6"	1'9"	2'0"	2'3"	2'6"	2'9"	3'0"	3'3"	3'6"	4'0"	4'6"	5'0"	5'6"	6'0"	6'6"	7'0"	7'6"	8'0"	8'6"	9'0"	9'6"	10'0"
8¾"	4	.48	.60	.72	.84	.96	—	—	—	—	—	—	—	—	—	—	—	—	—	—	—	—	—	—	—
11½"	6	.71	.89	1.06	1.24	1.41	1.57	1.77	1.95	2.12	2.3	—	—	—	—	—	—	—	—	—	—	—	—	—	—
14¼"	8	—	1.17	1.40	1.64	1.87	2.11	2.34	2.57	2.81	3.04	—	—	—	—	—	—	—	—	—	—	—	—	—	—
17 "	10	—	1.46	1.75	2.04	2.33	2.62	2.91	3.20	3.49	3.78	4.07	—	—	—	—	—	—	—	—	—	—	—	—	—
20⅝"	12	—	—	—	—	2.74	—	3.43	—	4.14	—	4.82	5.54	6.24	6.91	7.64	8.34	9.04	9.74	10.42	11.11	11.81	12.51	13.21	13.90
29 "	18	—	—	—	—	4.09	—	5.14	—	6.18	—	7.22	8.27	9.31	10.36	11.40	12.45	13.56	14.53	15.57	16.62	17.65	18.71	19.73	20.80
37⅛"	24	—	—	—	—	5.54	—	6.95	—	8.37	—	9.78	11.20	12.60	14.00	15.42	16.84	18.26	19.66	21.04	22.50	23.90	25.30	26.70	28.20

All dimensions approximate. Certified dimension prints upon request.

Sq. Ft. of Heating Surface equals Face Area x S

Type Ser. No.	31	71	72	81	82
S	9.3	13.4	26.8	16.6	33.2

Comparison of above selections based on tubes set vertical:

Number Sections Required	Tube Face	Nominal Tube Length	Face Area, sq.ft. Per Section	Face Area, sq.ft. Total	Sq.Ft. Face Area Required	Width	Height	Depth
2	24	8' 6"	23.90	47.8	46	6' 3"	9' 2-1/2"	5"
3	18	7' 6"	15.57	46.71	46	7' 3"	8' 2-1/2"	5"
4	18	5' 6"	11.40	45.6	46	9' 8"	6' 2-1/2	5"

One tube in direction of air flow per section as made by this manufacturer is known as a No. 71. The specification for the first heater bank selection made would read 2 sections of No. 71 Type F non-freeze 24 T.F. - 8' 6" T.L. Since we have selected non-freeze heating surface, we can throttle the steam flow to the coils and thus control the final leaving temperature of the air as long as the outdoor air temperature is a couple of degrees below desired temperature going to the ventilated area. Usually the temperature of the air rises one to two degrees passing through the fan which accounts for the couple of degrees just mentioned.

Below is a table showing the final temperatures and condensation rates that would result at various entering air temperatures if full steam flow was allowed to enter heater coils.

No. 71 Type F - Non-Freeze; 500 ft./min. face velocity; 5 lb./sq.in. ga. steam		
Entering Temp., °F.	Final Temp., °F.	Condensation lb./sq.ft.
0	52.4	29.4
+ 20	67.8	26.8
+ 30	75.5	25.6
+ 40	83.2	24.2
+ 50	90.9	23.0
+ 60	98.6	21.6

Now we refer to Table 4 and under Friction of Air - Type F Non-Freeze 70 Series and we find that for one row deep with a velocity of 500 ft./min. the static pressure loss will be 0.074 in. water.

For figuring the steam condensation required to heat the air passing through the pre-heat coil we may use the following:

$$\text{Condensate, lb./hr.} = \frac{\text{cu.ft./min.} \times T_2 - T_1 \times 1.08}{\text{Latent Heat of Steam}} \qquad (3)$$

where

T_2 = final air temperature, °F.

T_1 = initial air temperature, °F.

cu.ft./min. = volume at 70°F. and 29.92 in. Bar.

$$1.08 = \frac{60 \times \text{Sp.H} \quad .24}{\text{cu.ft./lb.air} \quad (13.3)}$$

$$\text{lb./hr.} = \frac{22{,}935 \times 52.4\text{-}0 \times 1.08}{960.4} = 1{,}350 \text{ lb./hr.}$$

Alternate Method

Condensate lb./hr. = condensate (per sq.ft. of face area from temperature tables x face area = 29.4 x 11.4 x 4 = 1345 lb./hr.

Per Table No. 2

Note: Strainer must be installed in steam line, ahead of this type coil, to prevent scale and other foreign particles from entering and clogging the coil.

VIII. RE-HEATERS

Normally when selecting re-heat coils, it is not necessary to invest in the more expensive non-freeze type heater coils. Instead, the regular type of fin tube coils are used.

Where this type of coil is installed ahead of the fan, the steam flow to the coil may be throttled with reasonable assurance that after the air passes through the fan, stratification will not occur at fan discharge.

Example 8 - Heat 22,935 cu.ft./min. from 52.4 F. to 96 F. using steam at 5 lb./sq.in. ga. pressure.

Referring to Table 5 we find that the nearest entering temperature shown to 52.4 is 50 F. As it generally makes the best layout to have pre-heater and re-heater the same shape, we will use the same 500-ft./min. velocity for the re-heaters as we did for the pre-heaters.

Looking under the 500-ft./min. velocity column, we see that one row of tube only heats to 90.9 F., which is 5.1 F. short of our required final temperature. If we picked two rows of tube deep the final temperature would be 122.8 F. or 26.8 F. above what we require. So, we see that No. 71 section is under our requirement and a No. 72 is over our requirement. Rather than install so much over capacity, which may give us a swinging on our controls, let us see if we can find a coil that will more nearly meet our requirement.

Referring to Table 6, we again find that the nearest entering temperature listed to 52.4 F is 50 F. Following across toward the right-hand side from 50 entering temperature, we find under 500-ft./min. velocity that one row of tube will give a final temperature of 98.4 F. and a condensation rate of 27.3 (lb.)/(hr.)(sq.ft.) of face area. As this final temperature is only 2.4 degrees higher than we require, it is the one we will choose. This is correct and has ample capacity providing the minimum temperature we selected was based

TABLE 4

AEROFIN — TYPE F NON-FREEZE COIL

FRICTION OF AIR

In inches of Water for 70° F. Air and 29.92" Barometer*

TYPE F NON-FREEZE 30 SERIES

Rows of Fin. Tubing Deep	Velocity of Air Through NET FACE AREA† in feet per minute					
	300	400	500	600	700	800
1	.020	.037	.061	.090	.127	.170
2	.038	.068	.106	.154	.210	.276

TYPE F NON-FREEZE 70 SERIES

Rows of Fin. Tubing Deep	Velocity of Air Through NET FACE AREA† in feet per minute					
	300	400	500	600	700	800
1	.030	.050	.074	.103	.136	.174
2	.066	.098	.138	.184	.221	.285
3	.088	.101	.158	.225	.306	.396
4	.072	.127	.200	.286	.391	.507
5	.087	.153	.241	.347	.476	.618
6	.101	.178	.282	.408	.561	.729
7	.115	.204	.325	.466	.646	.840
8	.130	.230	.367	.530	.731	.951
9	.144	.255	.409	.594	.816	1.062
10	.158	.281	.450	.652	.901	1.172

TYPE F NON-FREEZE 80 SERIES

Rows of Fin. Tubing Deep	Velocity of Air Through NET FACE AREA† in feet per minute					
	300	400	500	600	700	800
1	.032	.055	.083	.117	.157	.200
2	.053	.093	.145	.205	.275	.353
3	.078	.135	.207	.293	.393	.506
4	.101	.175	.269	.381	.511	.659
5	.126	.215	.331	.469	.629	.812
6	.147	.255	.393	.557	.747	.965
7	.170	.295	.455	.645	.865	1.118
8	.193	.335	.517	.733	.983	1.271
9	.216	.375	.579	.821	1.101	1.424
10	.239	.415	.641	.909	1.219	1.577

*For average air temperatures other than 70°, refer to Air Friction Correction Table, page 18.
†Net Face Area means only that area facing the tubes and does not include headers or casing

NET WEIGHT (Lbs.)

NOMINAL TUBE LENGTH

Nominal Height	Tube Rows	Type No.	12"	18"	24"	30"	36"	42"	48"	54"	60"	66"	72"	78"	84"	90"	96"	102"	108"
9¼"	4	72	7	9	11	13	15	17	19	21	23	25	27	29	31	33	35	37	39
		82	7	9	11	13	15	17	19	21	23	25	27	29	31	33	35	37	39
		81	8	10	12	14	16	18	20	22	24	26	28	30	32	34	36	38	40
11¼"	6	72	9	12	15	18	21	24	27	30	33	36	39	42	45	48	51	54	57
		82	9	12	15	18	21	24	27	30	33	36	39	42	45	48	51	54	57
		81	10	13	16	19	22	25	28	31	34	37	40	43	46	49	52	55	58
13¼"	8	72	11	15	19	23	27	31	35	39	43	47	51	55	59	63	67	71	75
		82	11	15	19	23	27	31	35	39	43	47	51	55	59	63	67	71	75
		81	12	16	20	24	28	32	36	40	44	48	52	56	60	64	68	72	76
15¼"	10	72	13	18	23	28	33	38	43	48	53	58	63	68	73	78	83	88	93
		82	13	18	23	28	33	38	43	48	53	58	63	68	73	78	83	88	93
		81	14	19	24	29	34	39	44	49	54	59	64	69	74	79	84	89	94
17¼"	12	72	15	21	27	33	39	45	51	57	63	69	75	81	87	93	99	105	111
		82	15	21	27	33	39	45	51	57	63	69	75	81	87	93	99	105	111
		81	16	22	28	34	40	46	52	58	64	70	76	82	88	94	100	106	112
19¼"	14	72	17	24	31	38	45	52	59	66	73	80	87	94	101	108	115	122	129
		82	17	24	31	38	45	52	59	66	73	80	87	94	101	108	115	122	129
		81	18	25	32	39	46	53	60	67	74	81	88	95	102	109	116	123	130
21¼"	16	72	19	27	35	43	51	59	67	75	83	91	99	107	115	123	131	139	147
		82	19	27	35	43	51	59	67	75	83	91	99	107	115	123	131	139	147
		81	20	28	36	44	52	60	68	76	84	92	100	108	116	124	132	140	148

on a thorough study of weather data for the part of the country where the system will be installed. If system must take up unusual low temperatures that may only occur once in a while and dips in ventilated area cannot be tolerated, then more spare capacity in the way of possible higher final temperature or lower entering temperature must be selected. In the case of corrosive atmosphere, a factor of safety is sometimes introduced to overcome the decrease in heater efficiency as the bond between the tubes and fins decreases. This condition may also be met by building the coils of suitable material to withstand the corrosive action.

Now, by referring to Table 7, we find that we can pick re-heaters with the same number of sections and dimensions to match the pre-heaters.

Referring to Table 8, we find that one section deep of No. 81 Flexitube heater when passing air through it at a 500-ft./min. velocity will have a static pressure loss of 0.083 in. H_2O.

Installations where a small stratification of air temperatures cannot be tolerated then non-freeze or non-stratifying type coil must be used as pre-heater and re-heaters.

Where re-heaters are on discharge side of fan or where re-heaters are in branches of the main to act as booster coils to take care of unequal heat loss loads, then these re-heaters should also be non-freeze or non-stratifying type.

Heater coils ratings are not given for all steam pressures and desired temperature conditions, but manufacturers' catalogs generally contain tables of constants for obtaining temperature rise at various steam pressures and entering air temperatures not shown in tables. Most catalogs on coils also give correction tables for determining air friction for average air temperatures other than 70 F.

Example 8A - Friction through coils was given at 70 F. as 0.286 in. of water. Actually the air entered at 0 F. and left at 187 F. or the average temperature through the coil was 93-1/2 F. The factor in this case was 1.044. Therefore, multiplying the 70 F. friction of 0.286 x 1.044 we find that the air friction at 93-1/2 F. is 0.298 in. Normally this difference will not affect over-all result, but the fact must be known because in some systems it may be the difference between success and failure of performance.

IX. AIR CLEANING DEVICES

An air cleaner (1) is a device for removing solid matter from a stream of air. This solid matter includes fibrous material such as lint and hair as well as dust, fumes, smoke, cinders, etc. The character of these airborne solids varies with the locality and with such factors as wind direction and velocity, industrial activity, etc.

These air cleaning devices are generally referred to as air filters. The air filters classified as viscous impingement types are widely used in general ventilating systems.

For industrial applications and in locations where the larger part of the atmospheric impurities are of fine particle size, such as smoke and fumes, more effective dry filters and electric precipitators are proving economical. By use of combinations of filters, advantage may be taken of specific characteristics of the various types of filters. In at least one industrial application, the air is passed through a series of filters, consisting of a bank of viscous impingement filters following by an electric precipitator, which in turn is followed by a dry-type filter using wool felt as a filter medium and, for absorbing certain gases, an activated carbon filter. Installations of this type which have been in operation for several years have proved to be economical on the basis of a reduction in cost of maintenance of the electrical equipment housed in the ventilated space.

There is at the present time no recognized standard test guide or method of measuring the cleaning efficiency of an air filter and expressing the efficiency in terms of the economic value which would result from

TABLE 5

Final Temperatures and Condensations 5 lbs. Steam—227° Temperature — FLEXITUBE and BOOSTER — 71 & 72

Temp. of Air	Rows Deep	Velocity of Air Through NET FACE AREA† — in feet per minute — Measured at 70° F. and 29.92" Barometer									
		500 FACE VEL.		600 FACE VEL.		700 FACE VEL.		800 FACE VEL.		900 FACE VEL.	
		F. T.*	Cond.‡	F. T.*	Cond.‡	F. T.*	Cond.‡	F. T.*	Cond.‡	F. T.*	Cond.‡
0°	1	62.5	21.0	56.7	25.3	53.4	29.4	49.7	34.5	47.3	37.2
	2	108.5	36.8	100.6	46.4	93.2	53.6	86.3	59.7	84.5	66.0
	3	141.8	48.0	132.8	60.0	124.0	70.6	118.9	80.6	112.6	89.6
	4	166.2	56.0	156.0	71.0	146.9	84.0	142.4	96.5	136.9	108.0
	5	183.5	61.8	174.4	79.0	167.2	94.4	160.7	108.8	156.3	122.8
	6	195.2	66.0	187.9	85.0	181.1	103.4	175.2	118.6	170.1	134.5
30°	1	77.0	19.2	71.7	23.2	67.8	26.8	65.2	30.6	63.1	34.0
	2	119.4	34.6	111.9	43.5	106.0	49.0	101.2	54.5	97.0	60.8
	3	147.7	43.5	141.3	55.0	135.4	64.0	128.5	72.5	123.0	81.8
	4	169.2	50.6	161.0	64.2	152.6	76.6	146.0	88.0	140.5	98.5
	5	186.2	56.3	179.0	72.0	171.8	85.8	166.0	99.5	161.3	111.7
	6	197.8	60.0	191.5	77.8	184.8	93.0	179.9	108.0	175.0	122.3
50°	1	84.5	18.3	79.2	22.1	73.5	25.6	72.1	29.0	71.0	32.3
	2	124.6	31.9	117.4	39.4	111.0	45.7	106.5	51.8	102.3	58.0
	3	152.9	41.6	145.3	53.3	138.5	61.3	133.2	70.0	128.6	77.8
	4	173.4	48.5	166.2	61.6	158.7	72.0	153.8	82.7	148.8	93.5
	5	188.5	53.6	181.4	68.6	175.2	82.0	169.3	94.6	164.8	106.3
	6	199.4	57.3	193.1	74.0	187.3	89.0	182.0	103.0	177.0	116.6
40°	1	91.5	17.4	86.7	21.0	83.2	24.2	81.0	27.6	79.0	30.5
	2	129.7	30.2	122.9	37.4	116.8	43.4	111.9	49.4	108.0	55.0
	3	156.7	39.6	149.4	49.4	142.0	58.0	137.0	66.0	132.7	74.0
	4	176.1	46.0	169.0	58.5	162.5	68.5	157.3	78.4	152.3	88.5
	5	190.4	51.0	183.7	65.0	177.8	77.8	172.3	89.4	168.0	101.0
	6	200.9	54.4	194.8	70.0	189.3	84.4	184.4	97.8	180.1	110.6
50°	1	98.8	16.4	94.3	20.0	90.9	23.0	88.8	26.1	86.9	29.0
	2	135.0	28.7	128.5	35.4	122.8	41.0	118.4	46.5	115.9	52.0
	3	160.0	37.0	154.0	47.0	147.5	55.0	143.0	63.0	138.0	69.4
	4	179.0	43.5	172.7	55.0	166.4	65.0	161.5	74.0	156.5	84.0
	5	192.5	48.0	186.5	61.8	180.0	73.5	175.7	85.2	171.0	95.5
	6	202.0	51.3	196.7	66.3	190.8	79.4	187.0	92.8	183.3	104.5
60°	1	106.0	15.5	101.7	18.8	98.6	21.6	96.6	24.7	94.8	27.3
	2	140.1	27.0	134.1	33.5	128.6	38.6	124.9	43.9	121.1	48.3
	3	164.1	35.2	158.2	44.3	151.9	52.0	147.5	59.3	143.7	66.0
	4	181.6	41.5	175.8	52.3	169.5	61.8	164.9	70.0	160.7	79.4
	5	194.4	45.8	188.4	58.0	182.0	69.4	178.2	80.0	174.3	90.2
	6	203.6	48.6	198.3	62.6	192.3	75.2	189.0	87.3	185.3	99.0
70°	1	113.3	14.6	109.2	17.5	106.3	20.5	104.6	23.2	102.7	25.6
	2	145.4	25.4	139.5	31.5	134.5	36.4	131.1	41.3	128.4	46.0
	3	168.0	33.0	161.9	41.4	156.4	48.8	152.3	55.8	148.6	62.0
	4	184.3	38.7	178.5	48.7	173.0	58.0	168.5	66.5	164.7	74.6
	5	196.3	42.6	190.7	54.0	185.7	64.5	181.3	75.3	177.5	85.0
	6	205.1	45.0	200.0	58.0	195.3	70.0	191.3	82.1	187.2	92.0

*F. T. = Final Temperature of Air
†Net Face Area is Area accepted by Sound tubes only
‡Cond.—Condensations in Pounds per Hour per Square Foot of Face Area.

For other Temperature Rise conditions see Chart, page 25

In all *Flexitube Aerofin* Designations (such as *Flexitube Aerofin*-31 or *Flexitube*-72) the numerals following the name indicate the type of tubing (first numeral) and the number of tubes deep (in direction of airflow), (second numeral). Thus *Flexitube Aerofin*-31 designates tubing with ½" fins pitched 3 per inch, and a unit 1-row of tubes deep, while *Flexitube Aerofin*-72 designates tubing with ½" fins, pitched 7 per inch, and a unit 2-rows of tubes deep.

TABLE 6

Final Temperatures and Condensations 5 lbs. Steam—227° Temperature — FLEXITUBE and BOOSTER — 81 & 82

Temp. of Air	Rows Deep	Velocity of Air Through NET FACE AREA† — in feet per minute — Measured at 70° F. and 29.92" Barometer									
		500 FACE VEL.		600 FACE VEL.		700 FACE VEL.		800 FACE VEL.		900 FACE VEL.	
		F. T.*	Cond.‡	F. T.*	Cond.‡	F. T.*	Cond.‡	F. T.*	Cond.‡	F. T.*	Cond.‡
0°	1	76.0	25.6	68.0	30.6	63.0	35.0	57.3	38.9	54.0	42.5
	2	132.0	42.2	114.2	51.8	104.5	60.4	101.2	68.5	96.3	76.0
	3	158.3	53.5	146.1	67.0	134.0	79.0	123.2	90.3	118.1	101.1
	4	180.1	62.5	167.4	77.6	157.2	92.1	147.2	104.4	141.8	116.0
	5	196.1	69.3	185.0	85.0	180.7	102.0	174.0	118.4	170.3	134.6
	6	207.2	70.3	199.5	90.3	193.2	109.0	188.2	127.4	183.8	145.5
30°	1	89.4	23.4	82.0	28.0	76.3	31.8	72.5	35.4	69.2	38.8
	2	154.0	38.5	134.4	47.2	117.8	55.2	113.5	63.5	108.0	69.4
	3	184.6	48.8	154.0	60.5	147.4	72.0	142.0	82.5	137.4	92.8
	4	196.2	55.8	176.2	70.6	167.6	84.0	161.7	97.2	156.2	109.3
	5	199.4	60.8	191.6	77.6	184.0	93.0	179.7	108.0	174.8	124.5
	6	208.0	63.7	201.7	81.2	196.5	99.8	192.2	116.6	187.7	132.5
40°	1	96.0	22.2	89.0	26.2	83.8	30.2	79.8	33.7	76.9	37.0
	2	158.5	36.6	139.5	45.4	123.0	52.6	117.8	59.2	112.6	66.0
	3	187.5	46.5	158.3	58.0	151.0	68.2	145.4	78.2	141.0	87.6
	4	199.2	53.2	179.8	67.4	171.3	79.8	165.2	92.2	161.7	104.0
	5	200.3	57.9	193.0	73.8	186.5	88.5	181.8	102.8	177.4	116.0
	6	209.2	60.7	203.2	78.3	197.7	94.8	193.4	110.5	189.4	126.0
50°	1	102.6	21.0	94.0	25.2	91.1	28.8	87.4	32.0	84.5	35.0
	2	163.0	34.8	142.5	43.6	128.3	49.0	122.4	56.4	119.1	62.8
	3	170.9	44.2	161.7	55.0	154.8	64.8	149.6	74.1	145.0	83.0
	4	201.7	50.6	184.7	70.2	176.2	84.0	169.3	97.5	165.1	109.5
	5	201.7	54.6	194.7	70.2	188.7	84.0	184.1	97.5	179.8	114.4
	6	210.3	57.0	204.4	74.3	199.3	90.0	195.1	105.0	191.2	119.4
60°	1	109.3	20.0	103.0	23.8	98.4	27.3	94.9	30.3	93.2	33.3
	2	167.5	33.0	146.3	40.4	132.0	47.1	126.1	53.5	122.7	59.4
	3	171.3	41.7	165.1	52.0	158.6	61.1	154.2	70.4	149.0	78.2
	4	191.8	47.5	188.8	60.8	181.5	74.0	174.5	84.0	170.5	95.0
	5	203.2	52.0	198.8	69.4	190.8	79.5	185.5	92.5	182.0	104.2
	6	210.8	54.5	205.6	70.4	201.0	85.2	197.0	99.5	193.3	113.2
70°	1	116.0	18.9	110.1	22.4	105.6	25.6	102.3	28.5	99.8	31.2
	2	152.0	31.1	146.4	38.1	138.9	44.3	133.0	50.1	130.3	56.1
	3	177.1	39.5	168.0	49.2	162.5	57.8	158.0	66.2	153.6	73.8
	4	194.2	45.2	188.2	57.2	180.0	69.7	176.0	79.4	172.2	89.6
	5	204.5	48.8	198.2	62.5	192.0	75.2	188.0	87.0	184.6	98.0
	6	212.1	51.3	206.9	66.4	202.4	80.4	198.3	93.8	195.0	106.8
80°	1	122.6	17.7	117.1	21.1	112.0	24.0	109.8	26.8	107.4	29.4
	2	160.5	29.2	154.5	35.8	146.2	41.8	140.0	47.3	137.0	52.8
	3	180.0	37.0	172.5	46.4	166.4	54.5	162.2	62.5	158.0	69.3
	4	198.0	42.5	192.5	53.8	185.0	65.5	178.7	74.6	176.0	84.0
	5	205.8	46.0	200.0	58.8	195.0	70.8	191.2	82.0	187.4	91.5
	6	212.9	48.4	208.0	62.5	204.0	75.5	200.3	88.5	197.0	100.2

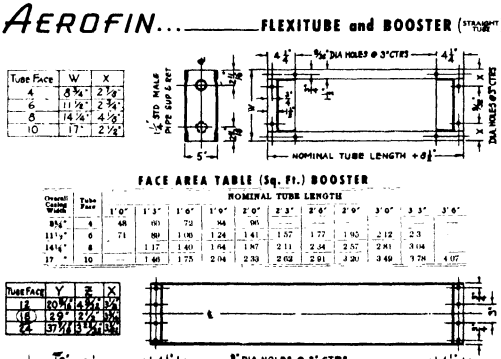
*F. T. = Final Temperature of Air
†Net Face Area is Area accepted by Sound tubes only
‡Cond.—Condensations in Pounds per Hour per Square Foot of Face Area.

For other Temperature Rise conditions see Chart, page 26.

In all *Flexitube Aerofin* Designations (such as *Flexitube Aerofin*-31 or *Flexitube*-72) the numerals following the name indicate the type of tubing (first numeral) and the number of tubes deep (in direction of airflow), (second numeral). Thus *Flexitube Aerofin*-31 designates tubing with ½" fins pitched 3 per inch, and a unit 1-row of tubes deep, while *Flexitube Aerofin*-72 designates tubing with ½" fins, pitched 7 per inch, and a unit 2-rows of tubes deep.

TABLE 7

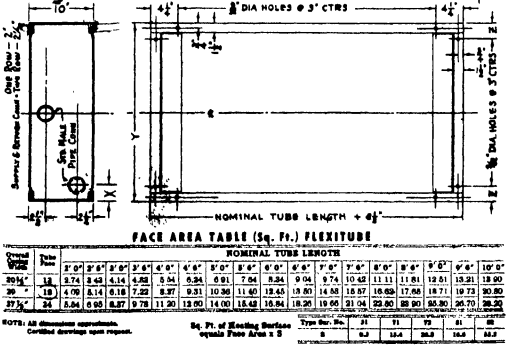
AEROFIN... — FLEXITUBE and BOOSTER (STRAIGHT TUBE)



Tube Face	W	X
4	6¾"	2⅛"
6	11½"	2⅛"
8	14¼"	4⅛"
10	17"	2⅛"

FACE AREA TABLE (Sq. Ft.) BOOSTER

Overall Casing Width	Tube Face	NOMINAL TUBE LENGTH 1'-0"	1'-3"	1'-6"	1'-9"	2'-0"	2'-3"	2'-6"	2'-9"	3'-0"	3'-3"	3'-6"
8¾"	4	.48	.60	.72	.84	.96						
11½"	6	.71	.89	1.06	1.24	1.41	1.57	1.77	1.95	2.12	2.3	
14¼"	8		1.17	1.40	1.64	1.87	2.11	2.34	2.57	2.81	3.04	
17"	10		1.46	1.75	2.04	2.33	2.62	2.91	3.20	3.49	3.78	4.07



FACE AREA TABLE (Sq. Ft.) FLEXITUBE

Overall Casing Width	Tube Face	NOMINAL TUBE LENGTH 2'-0"	2'-6"	3'-0"	3'-6"	4'-0"	4'-6"	5'-0"	5'-6"	6'-0"	6'-6"	7'-0"	7'-6"	8'-0"	8'-6"	9'-0"	9'-6"	10'-0"
20⅝"	12	2.74	3.43	4.14	4.82	5.54	6.24	6.91	7.64	8.34	9.04	9.74	10.42	11.11	11.81	12.51	13.21	13.90
29 "	16	4.09	5.14	6.18	7.22	8.27	9.31	10.36	11.40	12.45	13.50	14.55	15.57	16.62	17.66	18.71	19.73	20.80
37⅛"	24	5.84	7.35	8.87	9.78	11.20	12.60	14.00	15.42	16.84	18.26	19.66	21.04	22.50	23.90	25.30	26.70	28.20

NOTE: All dimensions approximate. Certified drawings upon request.

Sq. Ft. of Heating Surface equals Face Area × S	Type Fin: Per Inch	31	51	72	81	82
	S	5.3	10.4	20.8	10.5	21.0

TABLE 8

AEROFIN... — FLEXITUBE and BOOSTER (STRAIGHT TUBE)

• AIR VELOCITY AND FRICTION

By using the total net *face* area of *Aerofin*, instead of using free area, as with cast iron, engineering calculations are based on approximately half the old familiar velocities, because the net *face* area of *Aerofin* (only that area facing tubes, not including headers or casing) is approximately twice the free area, and thus the actual velocity thru *Aerofin* is the same as that thru equivalent cast iron

Therefore a face velocity of 600 ft per minute thru *Aerofin* corresponds to a free area velocity of approximately 1200 ft per minute thru cast iron

The friction thru *Aerofin* is about the same as that thru equivalent cast iron surface

For Public Building or Factory work the preferable velocities are from 500 to 800 ft per minute thru Net Face Area

• EXAMPLE — Showing use of Tabular Data

To heat 12,450 cu ft of air per minute, from 0° F to either 85 1° F or 112° F *using Steam Pressure* of 5 lbs

Assume a Face Velocity of 500 ft per minute (equivalent to 1000 ft per minute free area velocity)

Then, from *Flexitube Aerofin*-41 Table for 5 lbs Steam, page 14, it is shown that one Unit 3 deep will give a Temperature Rise from 0° F to 36° F, and that the Friction will be 0 061 in of water (Table, page 11) This is the outside Tempering Coil handling the Air below Freezing Temperature, and should be controlled from the Fresh Air Intake with a positive acting Thermostat or else Hand Controlled

The Net Face Area required will be 12,450 divided by 500, or 24 9 sq ft

From the *Flexitube* Table, page 13, it is shown that two Units wide of *Flexitube Aerofin*-31, having tubes 6 ft long, 18 tube face, will give 24 9 sq ft, net Face Area. (These may be set "two Units high," one above the other, tubes horizontal, or "two Units wide," one beside the other, tubes vertical)

The over-all dimensions of the battery to be 4 ft 10 in wide by 6 ft. 8½ in high, if set "two Units wide," tubes vertical, or 6 ft 8½ in wide by 4 ft 10 in high, if set "two Units high," tubes horizontal In either case the depth of the heater is 10 in (standard depth of casing, in direction of air flow), and the weight is 258 lbs

For a Re-heating Coil, selection can be made of *Flexitube Aerofin*-81 of the same size, two Units wide or high. This Re-heater will heat the air (at 500 ft face velocity and 5 lbs Steam Pressure) from 36° F. to 88 1° F. with a Friction of 0 083 in of water (See page 14 for Temperature Rise and page 11 for Friction.) The weight of these two Units will be 302 lbs.

As an alternate, one can select *Flexitube Aerofin*-72 (two Units wide or high of the same size).

This Re-heater will heat this air volume (at 500 ft face-velocity and 5 lbs. Steam Pressure) from 36° F to 114 4° F with a Friction of 118 in. of water (See page 14 for Temperature Rise and page 11 for Friction.) The weight of these two Units will be 408 lbs

It will be noted that if the combination of *Flexitube Aerofin*-41 and *Flexitube Aerofin*-81 is used under the above conditions, the Temperature Rise will be from 0° F to 88 1° F and the combined Friction will be 0 144 in. of water, and the combined Weight of two *Flexitube Aerofin*-31 Units and two *Flexitube Aerofin*-81 Units will be 560 lbs

If the combination of *Flexitube Aerofin*-31 and *Flexitube Aerofin*-72 is used the Temperature Rise will be from 0° F to 114 4° F and the combined Friction 0 177 in and the combined Weight of two Units of *Flexitube Aerofin*-31 and two Units of *Flexitube Aerofin*-72 will be 696 lbs

If higher air temperatures are desired, use additional sections of either *Flexitube Aerofin*-71 or 72 or *Flexitube Aerofin*-81 or 82 as best suits the requirements

• FRICTION OF AIR — In Inches of Water For 70° Air and 29.92" Barometer

Rows of Tubes in Direction of Flow	Velocity of Air Through NET FACE AREA† in feet per minute					
	500	600	700	800	900	1000
AEROFIN FLEXITUBE—31						
1	.030	.037	.061	.090	.127	.170
2	.038	.066	.106	.154	.216	.276
AEROFIN FLEXITUBE—71 & 72						
1	.030	.050	.074	.103	.136	.174
2	.044	.076	.116	.166	.221	.283
3	.058	.101	.158	.228	.306	.389
4	.073	.127	.200	.289	.391	.507
5	.087	.153	.241	.347	.469	.618
6	.101	.178	.283	.408	.561	.739
7	.115	.204	.325	.469	.646	.860
8	.130	.230	.367	.530	.731	.951
9	.144	.255	.409	.591	.816	1.062
10	.158	.281	.450	.652	.901	1.173
AEROFIN FLEXITUBE—81 & 82						
1	.033	.055	.083	.117	.157	.200
2	.055	.095	.145	.208	.278	.353
3	.078	.135	.207	.299	.398	.506
4	.101	.178	.269	.391	.511	.659
5	.124	.215	.331	.480	.629	.812
6	.147	.253	.393	.537	.747	.965
7	.170	.295	.455	.644	.866	1.118
8	.193	.335	.517	.723	.983	1.271
9	.216	.375	.579	.821	1.101	1.424
10	.239	.415	.641	.909	1.219	1.577

†For gravity air temperatures other than 70°, refer to Air Friction Correction Table, page 31.
Net Face Area means only that area facing the tubes and does not include headers or casing.

the use of the filter. Air filters are usually selected on the basis of experience or judgment guided by the results of various test procedures. The two test procedures generally used are: (a) the weight method, and (b) blackness test.

Air filters are available in the form of units. A single unit may have the required capacity or a number of units can be assembled in a bank to make up the total capacity.

Pressure drop through filters based on average resistance during use will vary from 0.03 to 0.4 in. water, depending on type and general capacity rating of filter.

A. Air Filters

Considering the wide diversification of materials and particle sizes to be removed and the varying requirements which have to be met in the field, it is obvious that many kinds of air cleaning devices used cannot be shown satisfactorily in a simple outline. Classification on three different bases are enumerated herewith:

1. Principle of air cleaning
   a. Viscous-impingement filters
   b. Dry filters
   c. Washers
   d. Centrifugal devices
   e. Electrical precipitators
2. Methods of servicing
   a. Automatic
   b. Non-automatic
      (1) Throw-away (replaceable elements)
      (2) Manually cleaned in place (including one type of electrostatic)
      (3) Removable for cleaning
3. Classification according to application
   a. General air conditioning
      (1) Central cleaning system
      (2) Unit ventilator
      (3) Window installation
      (4) Warm air furnace

X. FANS

Fans used in the ventilating field are centrifugal as one type and propeller or axial flow as the second type. Centrifugal fan characteristics depend, for the most part, on the type of blading used in their wheels.

The first fans were equipped with paddle-type blades. This type wheel is now referred to as a radial blade. Then came the fans with blades that were forwardly curved. Further development lead to the backwardly curved blades and still other developments lead to a double curved blade which scoops the air in on the lead edge and backwardly curved on the leaving edge, allowing the air to slide off the blade.

There are fan wheels manufactured with modifications of the above general blade forms.

When we speak of fan characteristics (4), we refer to modifications in: (1) cu.ft. of air/min. handled by the fan; (2) static pressure developed; and (3) horsepower consumed. All three at a constant speed.

The radial blade type fan has a raising pressure increase with a decreasing cu.ft./min. capacity and a decrease in horsepower required to drive the fan and will operate in parallel.

The forwardly curved blade fan has a dip in its pressure curve and a rapid rise ini its horsepower curve. It is quite apt to require more horsepower than anticipated if static pressure of system is less than calculated. Its pressure curve is such that it is a poor type fan for parallel operation.

The backwardly curved blade fan has a rising pressure characteristic like the radial blade. The horsepower increases less than other types and develops a convex horsepower curve that limits the maximum power consumed.

The various fan manufacturers make many claims as to the efficiency of their equipment and the outstanding advantages of using their particular piece of apparatus. In general, the static efficiency of forwardly curved blade type fan will be between 60 to 70%, that of the radial blade type fan will be between 60 to 73%, and that of the backwardly or double curved blade type will be between 72 and 80%. The propeller, or axial type fans, which include the disc wheel, have been developed to a much higher degree of efficiency performance just prior and during World War II.

The old-time typical disc-type fan has a horsepower volume characteristic opposite that of a forwardly curved fan. The disc fan has a constantly rising static pressure and horsepower curve with a decreasing cubic feet of air handling capacity.

In designing the axial flow fan (5a), the manufacturers have taken advantage of widespread research of aeronautical sciences in aeroplane propellers. Airfoil sections are used in the blade construction and as the center section of the wheel does little work, it is eliminated and replaced by a large tub.

It is not unusual to find present wheel designs have hubs of 50%, 60%, and some as high as 70% wheel diameter.

The combination of twisted blade and large hub thus gives substantially constant flow over all the working face of the wheel, which is essential if high efficiencies are to be attained when working with high pressure differences. Best efficiencies demand streamlining of all parts and careful manufacture with close tolerance.

For fans drawing air from a room with no duct work on the inlet, belled entrance pieces are usually indicated. For directly connected units, the normal large hub permits locating the motor close to the wheel without obstruction. The location of the motor directly in the air stream will be objectionable in many cases.

Use of elbows either on the fan inlet or outlet may have serious effect on the fan efficiency.

Axial flow fan characteristics have semblance to the pressure characteristic of the backwardly curved blade fan, but they are subject to their own variations. These fans are offered in three arrangements. One is a high-speed flat pitch that has the long desired perfect pressure characteristic that starts from wide open and continually rises to blocked tight. This is the type required by the Navy for forced draft. They operate in parallel. Horsepower is three or four times as great at blocked tight condition.

The steeper pitch axial flow fan does not have this increasing horsepower at blocked tight. This type blade can be so designed that the horsepower is substantially constant throughout the entire range, but when so designed, develops a dip in the pressure characteristic similar to that of the forwardly curved blade centrifugal fan. This type fan is not as undesirable from this standpoint as the centrifugal because peak efficiency does occur out in a range where the pressure curve is entirely stable. Navy uses this type fan for hull ventilation.

The third type axial flow has stationary vanes ahead of the impeller so designed to spin the air against the rotation of the impeller. This type fan has rising pressure characteristic in the region of best efficiency. It handles very large volume at low efficiency with the horsepower curve that builds upward like the forwardly curved blade centrifugal.

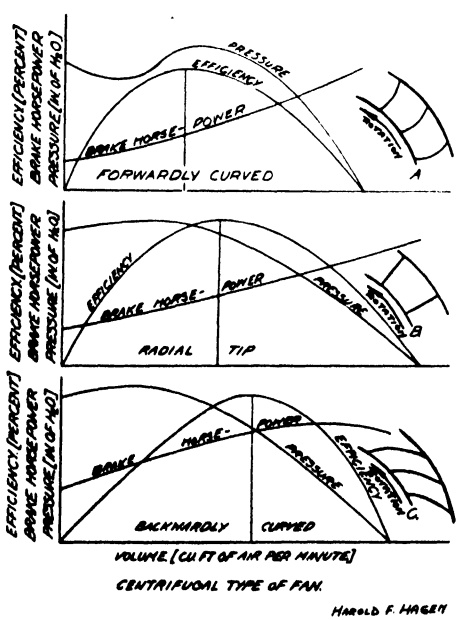


Figure 14. Centrifugal Type of Fan

Most manufacturers test and rate their centrifugal and axial fans in accordance with standard code for testing, prepared jointly by the Engineering Committee of the National Association of Fan Manufacturers and the Fan Test Code Committee of the American Society of Heating and Ventilating Engineers. The fans are tested in straight duct of uniform cross-sections. Symmetrical throttling devices are used to make eight or more determinations, covering a range of performance from approximately free delivery to no delivery (blocked tight) with approximately equal increments of capacity. Each determination is to be two or more traverses.

After the performance has been calculated for each determination, the results, as corrected to standard air conditions and constant speed, are plotted using volume as abscissa and pressure, horsepower as ordinates. Curves are then drawn through these points, giving pressure and horsepower, and from these data the efficiency is calculated and also plotted as one of the ordinates.

Figure 14 shows characteristic curves: (a) for forwardly curved; (b) radial tip; (c) backwardly curved bladed centrifugal type of fans.

Figure 15 shows characteristic for: (a) flat pitch; (b) steep pitch; and (c) vanes ahead for axial flow type fans.

Now let us consider where and when to use the different types of fan. The radial blade fan is well adapted to conditions where solid matter must go through

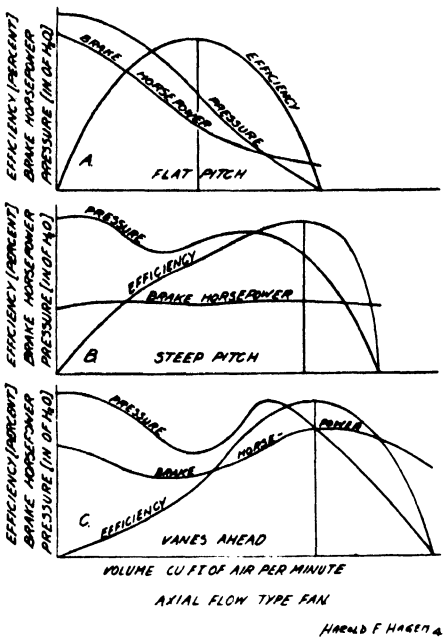


Figure 15. Axial Flow Type Fan

the fan as well as air. This type blade has another use and there is no evident way to displace it from that use, which is high pressure duty. The backwardly curved bladed fans would have higher efficiency in some cases for high pressure work, but as their tip speed for a given duty is high and their construction calls for high stresses, we have to compromise and use the stronger radial blade. Most of the centrifugal compressors offered by the various manufacturers are of the radial blade type. Most of those cases where manufacturers have earnestly tried to develop backwardly curved blade centrifugal compressors have been costly and unsatisfactory.

Forwardly curved blade fans are now used mostly in smaller capacity range, and when they are operated in the neighborhood of 1 in. water, they may be a little quieter from a noise standpoint. The backwardly curved blade fan with its steep pressure characteristic makes it admirably suited to the accuracy of operation required in ventilation, and its non-overload feature limits the size motor that need be installed.

Axial fan in a system requiring little or no static pressure will perform better than a centrifugal fan; however, a common propeller or disc fan would perform almost equally as well, but the lower cost of the propeller fan would more than offset any loss in efficiency.

Maximum pressures for which axial flow fan may be designed are above the ventilating system requirement. To develop the higher static pressures, multi-rotor units are used. Space saving is the biggest advantage of the axial fan. Not necessarily will the axial fan be cheaper, but the over-all installed cost, including duct work, supports, building, etc. To date, the ideal application for axial flow fans is on ships where their small size, light weight, high efficiency, and relatively quiet operation are so advantageous. Relatively quiet operation is mentioned becuase the noise level considered quiet aboard ship may not be considered quiet in a building ashore.

When a comparison is to be made in order to select a fan to operate under very exacting conditions, then the latest performance information should be obtained direct from the fan manufacturer. The manufacturers of centrifugal and axial fans are continuously carrying on research and may have developed a different fan with characteristics that would better fit your problem.

For ordinary application of fans, use only those which are fully rated in standard capacities tables published by the manufacturer.

Example 8B - Now to select fan to go with ventilation system given previously.

As an example, we turn to Figure 15A. To arrive at this chart we know from our calculations and design information that we will have a capacity of 23,405 cu.ft./min. and want to pick a fan with an outlet velocity of approximately 1400 ft./min. After referring to manufacturer's catalog, we come upon rating like Figure 15A. Here we see that a No. 9 Type LL (load limit) centrifugal fan will handle a capacity of 23,405 cu.ft./min. at 1400 outlet velocity. Following this line to the right, we find that this fan will handle this capacity under 1 in. water S.P. (static pressure) and will be operated at 356 rev./min. and under these conditions will require 5.28 brake horsepower. As this is a limit load or non-overloading type fan, the chart will also specify the maximum horsepower required for a given speed. Referring to the extreme right-hand columns, we find that our speed falls between shown speeds of 340 rev./min. with 5.01 hp. maximum and 360 rev./min. with 5.95 hp. maximum. By varying the horsepower as the cube of speed, we find at our speed of 356 rev./min. the fan will not take more than a maximum of 5.56 brake horsepower. The horsepower of the motor installed to operate this fan will depend on practice used in picking motors and penalty paid for electrical power factor variation.

In a plant where they must keep power factor high and where they have an operating personnel of high intelligence, a 5-hp. motor could be used which would be operating with a constant overload of 11%. In most cases, you will find that a 7-1/2-hp. motor would be installed.

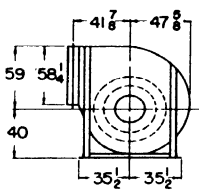
Buffalo Limit-Load Conoidal Fan

REG. U.S. PAT. OFF.

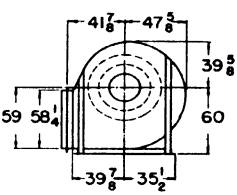
SIZE 9 — **SINGLE WIDTH TYPE "LL"** — **SIZE 9**

Wheel Diameter 54 In. Over-all Wheel Width 25 In. Outlet Area 16.72 Sq. Ft.

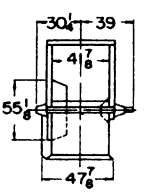
Outlet Velocity Feet Per Minute	Capacity Cubic Feet of Air Per Min.	¼" S. P.		⅜" S. P.		½" S. P.		⅝" S. P.		¾" S. P.		⅞" S. P.		1" S. P.		1¼" S. P.		Limit Load	
		RPM	HP	RPM	HP	RPM	HP	RPM	HP	RPM	HP	RPM	HP	RPM	HP	RPM	HP	RPM	HP
800	13374	188	.801	212	1.11	234	1.44	254	1.77	273	2.14	292	2.51	309	2.91	341	3.72	180	.742
900	15046	199	.963	222	1.30	243	1.65	262	2.02	280	2.40	298	2.80	315	3.21	346	4.09	200	1.02
1000	16718	210	1.16	232	1.52	252	1.89	271	2.29	288	2.70	305	3.12	321	3.54	352	4.47	220	1.36
1100	18390	222	1.39	243	1.76	262	2.18	281	2.59	298	3.03	312	3.48	328	3.92	358	4.88	240	1.76
1200	20061	236	1.65	255	2.05	274	2.48	290	2.93	307	3.38	322	3.86	337	4.35	365	5.34	260	2.24
1300	21733	249	1.96	267	2.36	284	2.82	301	3.30	316	3.78	332	4.28	346	4.79	373	5.86	280	2.81
1400	23405	264	2.33	279	2.74	296	3.21	312	3.71	328	4.22	342	4.75	356	5.28	382	6.40	300	3.44
1500	25077	278	2.72	292	3.16	308	3.66	323	4.17	338	4.70	352	5.26	365	5.82	392	6.97	320	4.18
1600	26748	292	3.17	306	3.65	321	4.14	335	4.68	349	5.23	362	5.81	376	6.41	401	7.61	340	5.01
1700	28420	307	3.69	321	4.17	334	4.69	349	5.24	361	5.80	374	6.40	387	7.02	411	8.30	360	5.95
1800	30092	322	4.26	334	4.78	347	5.30	360	5.87	372	6.45	385	7.06	398	7.71	421	9.03	380	7.00
1900	31764	338	4.88	349	5.42	362	6.00	372	6.55	385	7.14	398	7.80	409	8.46	433	9.84	400	8.16
2000	33435	352	5.58	364	6.15	375	6.77	387	7.29	398	7.92	409	8.59	421	9.26	444	10.68	420	9.44
2200	36778	383	7.14	394	7.78	405	8.42	415	9.10	425	9.70	435	10.40	445	11.10	467	12.53	440	10.87
2400	40121	415	8.85	424	9.63	434	10.41	443	11.10	452	11.82	462	12.53	472	13.20	491	14.72	460	12.40
2600	43465	446	11.08	455	12.00	464	12.74	473	13.50	481	14.20	490	15.0	499	15.8	515	17.3	480	14.1
2800	46809	478	13.73	486	14.44	495	15.5	502	16.1	511	17.0	519	17.8	526	18.6	543	20.2	500	15.9
3000	50153	510	16.6	518	17.17	525	18.5	533	19.2	541	20.2	549	21.0	555	21.8	571	23.5	520	18.0



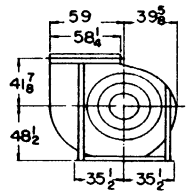
TOP HORIZONTAL



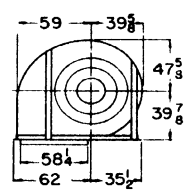
BOTTOM HORIZONTAL



SINGLE WIDTH



UP DISCHARGE



DOWN DISCHARGE

Outlet Velocity Feet Per Minute	Capacity Cubic Feet of Air Per Min.	1½" S. P.		1¾" S. P.		2" S. P.		2¼" S. P.		2½" S. P.		3" S. P.		4" S. P.		5" S. P.		Limit Load	
		RPM	HP	RPM	HP	RPM	HP	RPM	HP	RPM	HP	RPM	HP	RPM	HP	RPM	HP	RPM	HP
1300	21733	398	6.94	422	8.08	446	9.26	469	10.50	491	11.77	530	14.38	605	19.9	670	25.9	540	20.2
1400	23405	407	7.55	431	8.72	452	9.92	475	11.20	496	12.6	536	15.3	609	21.0	674	27.1	560	22.4
1500	25077	416	8.18	438	9.44	460	10.7	481	12.00	502	13.3	541	16.2	614	21.8	678	28.4	580	24.9
1600	26748	425	8.86	447	10.2	468	11.5	489	12.80	508	14.2	546	17.1	618	23.3	683	29.8	600	27.5
1700	28420	435	9.59	456	10.9	477	12.3	496	13.70	516	15.1	552	18.2	625	24.4	686	31.2	620	30.5
1800	30092	445	10.4	466	11.8	486	13.2	505	14.70	525	16.2	561	19.2	630	25.6	692	32.8	640	33.4
1900	31763	455	11.25	475	12.68	495	14.1	515	15.7	533	17.2	569	20.4	635	27.0	697	34.2	660	36.7
2000	33435	465	12.12	485	13.63	504	15.15	525	16.7	542	18.3	576	21.6	641	28.4	704	35.8	680	40.2
2200	36778	486	14.1	506	15.60	525	17.4	542	19.0	561	20.7	595	24.2	658	31.4	716	39.0	700	43.8
2400	40121	510	16.4	528	18.1	547	19.8	565	21.7	580	23.4	615	27.0	674	34.9	730	42.8	720	47.7
2600	43465	534	19.0	551	20.7	568	22.6	585	24.6	602	26.4	633	30.3	692	38.3	747	46.9	740	51.7
2800	46809	559	22.0	575	23.8	592	25.8	608	27.8	624	29.7	655	33.8	710	42.2	765	50.9	760	56.0
3000	50152	585	25.3	601	27.3	616	29.2	631	31.2	646	33.4	676	37.6	730	46.5	784	55.9	780	60.5
3200	53152	612	29.2	626	31.2	641	33.2	655	35.2	670	37.5	697	41.7	750	51.2	801	60.9	800	65.4
3400	56839	641	33.4	655	35.6	667	37.5	681	39.6	695	41.8	723	46.5	774	56.2	822	66.3	820	70.4
3600	60183	670	38.3	683	40.4	695	42.5	706	44.6	720	47.0	745	51.5	795	61.6	844	72.2	840	75.5
3800	63526	699	43.4	710	45.7	724	47.9	735	50.1	746	52.5	770	57.4	819	67.6	865	78.5	860	81.1
4000	66870	729	49.3	740	51.5	750	54.0	764	56.1	774	58.5	796	63.4	843	74.1	888	85.3	880	87.0

NOTE: Capacities and static pressures at 70° F. and 29.92" barometer.
Actual fan horsepowers are shown in table. Add for loss thru drive when selecting motor.

BUFFALO FORGE CO.

Figure 15A.

In an existing system if more capacity is required, the following are the fan laws applying:

a. Speed varies directly as capacity.
b. Static pressure varies as the square of the speed.
c. Horsepower varies as the cube of the speed.

Take an existing system with a capacity of 23,405 cu.ft./min. It is required to increase the capacity to 32,800 cu.ft./min.

Example 8C - To vary the capacity with constant size fan, the conditions are that fan size, duct system, and air density remain constant and the capacity is increased from 23,405 to 32,800 cu.ft./min.

$$\text{Speed} = 356 \times \frac{32,800}{23,405} = 500 \text{ rev./min.}$$

$$\text{Static Pressure} = 1 \times \left(\frac{500}{356}\right)^2 = 1.98 \text{ in. water S.P.}$$

$$\text{Horsepower} = 5.28 \times \left(\frac{500}{356}\right)^3 = 14.6 \text{ hp.}$$

This example is given to emphasize how much the operating horsepower increases when it becomes necessary to handle more air with the original system.

XI. SUPPLY AIR INLET

When air is supplied into a space, the distribution of this air must be given careful study. A large amount of air entering at one spot or at too high a velocity may cause air movements which will be objectionable. The air movement may also defeat the successful operation of an exhaust system by actually blowing the contaminate away from the exhaust outlet and into the operating zone.

A. Wall Grille (13)

Duct approaches to outlets must be designed so that the air is delivered to the outlets or grilles in such a pattern that the performance of the grille is not affected adversely.

Experiments (9) with various elbow outlets on a 14-in. x 6-in. vertical stack with air velocities of 200 to 1400 ft./min. indicated that enlargement of the outlet area, whether used in connection with square or rounded elbows, would not reduce either the angle of discharge (which was 20° to 30° above the horizontal) or the outlet velocity. The effect of the enlargement of the outlet was mainly to increase the reverse flow area in the lower part of the outlet, but in each case enlargement of the outlet reduced the static pressure in the duct below the elbow.

Splitters in the elbows had the effect of dividing the air stream into a number of streams or eliminated the reverse flow area and made the outlet velocity quite uniform.

Turning vanes having 2-in. inner and 1-in. outer radii, located in the center of the elbow, were found most effective in improving performance in regard to angle of discharge, outlet velocity, and elimination of reverse flow area.

Pressure loss through stack heads may be reduced by use of splitters or turning vanes or by increasing the inner radius of an elbow.

Pressure loss through stack heads may be reduced by use of splitters or turning vanes or by increasing the inner radius of an elbow. Considering the sum of the velocity and static pressure as a measure of the energy required to change the direction of the air stream and to deliver the air into the atmosphere and considering the energy required for a plain fitting as 100%, it was found that turning vanes dropped the energy requirement of the square-type stack heads to 45%. Splitters reduced the energy requirement to 90% in long-radius elbows and to 74% in short-radius turns. In expanding heads, splitters reduced the energy requirement to 58%.

Side outlets in air ducts have a normal forward drift to the air flow in the same general direction as in the horizontal duct. In many cases, it is, therefore, necessary to use directive devices within the duct at each outlet in order to obtain a uniform velocity of delivered air and to obtain a direction of flow perpendicular to the face of the outlet.

In tests (8) conducted with 3-in. x 10-in., 4-in. x 9-in., and 6-in. x 6-in. outlets in a 6-in. x 20-in. horizontal duct at duct velocities of 200 to 1400 ft./min. (in the 6-in. x 20-in. section), it was found that multiple curved deflectors produced the best flow characteristics. Vertical guide strips in the collar ahead of the outlet were not so effective as curved deflectors but second best. The tests also showed the beneficial effect of equipping outlets with collar extensions. A length of 13-in. was superior to a 1-in. length.

Controlling the cubic feet per minute air flow through an outlet by means of either multiple or single-blade dampers may cause considerable deflection of the air stream.

Dampers of special construction may be used to maintain a constant direction of blow, approximate distance of blow, and constant outlet velocity regardless of the damper's position.

Where the temperature of the air being delivered through the outlet grille is below the temperature of the room, the entering air will tend to spill downward if its velocity through the outlet is allowed to decrease as the volume of air handled through the grille is reduced.

Maintaining the general pattern of air distribution requires that approximately a constant distance of throw be realized even when a reduced capacity is temporarily being handled.

Today manufactured grilles are available to meet almost any requirement. Some manufacturers have testing laboratories of their own, in which they develop performance data for their products. Catalogs are issued by these concerns in which they publish tables, from which you may select the type, size, and number of grilles to meet your requirement.

Problems of air distribution that cannot be easily solved by the information in the manufacturers' tables should be considered special. This applies to where there are beams, columns, and other obstructions to air flow or where the air flow pattern such as to distances and coverage is not covered in the published data.

In these special cases, consultation with the engineers from the grille manufacturer will minimize many of the headaches that will otherwise occur.

There will be some cases that will arise where the manufactured grilles will not solve the problem. In these cases, it will be necessary to develop a special outlet to fit the exact condition. It may be necessary to install a test installation and modify the design ideas until the problem is solved.

As the manufacturers develop new ideas and improved performance of outlets, there will be fewer air flow problems that cannot be solved by using a commercial type grille.

Location of outlet grilles in walls are sometimes dictated by physical construction of the building. A great deal of emphasis is sometimes placed on the architectural treatment where the location is dependent on concealing by furring, etc.

The bottom of the grille should be at least 8 ft. above the floor. If the grille is too close to the floor, it is difficult to prevent draft on people's heads. If the grille is too close to the ceiling, induction of room air may cause dirt streaking on the ceiling; also changing of upward projectory is limited.

Size of grille for a required capacity depends on throw which directly establishes the velocity, in ft./min. through the grille, and in some tables this also establishes the aspect ratio of the grille.

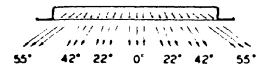
The measurement of noise is an extremely difficult study which involves the consideration of many factors. Furthermore, it is made even more difficult by the lack of standardization of ratings of the sound level of various types of rooms.

Basically the sound caused by an air outlet in operation is directly proportional to the velocity of the air passing through it. Therefore, by selecting outlets of the proper sizes the air velocity can readily be controlled within safe sound limits.

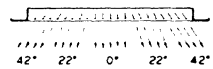
The following table gives recommended outlet velocities for various applications:

Application	Recommended Velometer Velocities, ft./min.
Broadcasting studios	500
Residences	500 to 750
Apartments	500 to 750
Churches	500 to 750
Hotel bedrooms	500 to 750
Legitimate theaters	500 to 1,000
Private offices, acoustically treated	500 to 1,000
Motion picture theaters	1,000 to 1,250
Private offices, not treated	1,000 to 1,250
General offices	1,250 to 1,500
Stores, upper floors	1,500
Stores, main floors	1,500
Industrial buildings	1,500 to 2,000

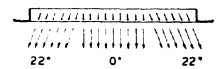
Example No. 9 - To illustrate selection of this type grille, we will use air quantity in previous problem of 2,085 cu.ft./min. In order to get good distribution, we will supply this amount of air through two grilles, thus each will have a capacity of 1,043 cu.ft./min.



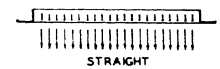
DEFLECTION SETTING "G"



DEFLECTION SETTING "E"



DEFLECTION SETTING "C"



DEFLECTION SETTING "A"

CHART NO. 3

C.F.M.	THROW GIVEN IN FEET																							
	8	10	12	14	16	18	20	22	24	26	28	30	32	34	36	38	40	42	44	46	48	50
800						36 G 7 .042 450 12	30 G 7 .027 603 10	36 G 7 .030 628 8	30 G 7 .043 828 8	24 G 7 .068 1040 8	20 G 7 .098 1264 8	24 G 7 .124 1410 6	[illegible]	24 G 8 .124 1410 6	24 E 8 .108 1315 6	[illegible]	24 E 9 .108 1315 6	20 E 9 .187 1890 6	24 E 10 .162 1610 5		24 E 10 .162 1610 5	24 E 11 .162 1610 5
825						36 G 7 .013 463 12	36 G 7 .020 560 10	36 G 7 .031 710 8	30 G 7 .046 854 8	24 G 7 .072 1070 8	30 G 7 .084 1160 6	20 G 7 .104 1290 8	[illegible]	24 G 8 .132 1455 6	24 G 8 .132 1455 6	24 E 9 .115 1367 6	[illegible]	24 E 11 .116 1557 6	24 E 11 .116 1557 6	24 E 12 .115 1557 6	24 C 13 .099 1222 6	
850										30 G 7 .048 879 8	24 G 7 .076 1100 8	20 G 7 .111 1330 8	[illegible]	24 G 8 .140 1495 6	24 G 9 .140 1495 6	24 E 9 .122 1398 6	24 E 9 .122 1398 6	[illegible]	24 E 11 .122 1398 6	24 E 12 .122 1398 6	24 C 13 .099 1259 6	
875										30 G 7 .051 905 8	24 G 7 .081 1135 8	30 G 7 .095 1230 6	20 G 7 .117 1370 8	[illegible]	24 G 8 .148 1540 6	24 G 7 .148 1540 6	24 E 10 .123 1439 6	[illegible]	24 E 10 .123 1439 6	24 E 10 .123 1439 6	24 E 10 .123 1439 6	24 C 13 .105 1296 6
900										30 G 7 .054 930 8	24 G 7 .086 1168 8	30 G 7 .100 1265 6	20 G 7 .124 1410 8	[illegible]	24 G 8 .157 1685 6	24 G 9 .157 1685 6	24 E 9 .137 1480 6	24 E 9 .137 1480 6	[illegible]	24 E 10 .137 1480 6	24 E 10 .137 1480 6	24 C 10 .137 1480 6
925										24 G 7 .057 955 10	30 G 7 .057 965 8	24 G 7 .090 1195 8	30 G 7 .106 1300 6	24 G 8 .166 1630 6	[illegible]	24 G 8 .166 1630 6	24 E 8 .166 1630 6	24 E 9 .144 1520 6	24 E 9 .144 1520 6	[illegible]	24 G 10 .144 1520 6	24 G 10 .144 1520 6
950										36 G 8 .042 816 8	30 G 8 .060 982 8	24 G 8 .095 1290 8	30 G 8 .111 1336 6	[illegible]	20 G 8 .138 1486 8	20 G 8 .138 1486 8	20 E 10 .120 1386 8	20 E 10 .120 1386 8	[illegible]	[illegible]	24 G 10 .162 1563 6	24 G 10 .162 1663 6
975										36 G 8 .044 837 8	24 G 8 .063 1005 10	30 G 8 .064 1010 8	24 G 8 .100 1265 8	20 G 8 .146 1526 8	[illegible]	20 G 9 .146 1526 8	20 G 9 .126 1420 8	20 E 9 .126 1420 8	[illegible]	20 E 10 .126 1420 8	20 G 10 .126 1420 8	20 G 10 .126 1420 8
1000										24 G 8 .045 848 12	24 G 8 .067 1030 10	30 G 8 .067 1085 8	24 G 8 .105 1296 8	30 G 8 .124 1406 6	[illegible]	20 G 9 .153 1665 8	20 G 9 .153 1665 8	20 E 10 .132 1458 8	[illegible]	[illegible]	20 E 11 .132 1458 8	20 G 11 .132 1468 8
1025						[illegible]	36 G 8 .021 575 12	[illegible]	30 G 8 .044 837 10	36 G 8 .045 880 8	[illegible]	30 G 8 .070 1060 8	30 G 8 .190 1445 6	20 G 8 .161 1606 8	[illegible]	20 G 8 .161 1606 8	20 E 11 .139 1494 8	20 E 11 .139 1494 8	[illegible]	[illegible]	20 E 11 .139 1494 8	20 G 11 .139 1494 8
1050						36 G 8 .022 590 12	30 G 8 .031 708 12	36 G 8 .038 712 10	36 G 8 .031 904 8	[illegible]	24 G 8 .074 1085 10	30 G 8 .074 1086 8	24 G 8 .116 1362 8	[illegible]	[illegible]	30 G 9 .137 1480 6	30 G 9 .137 1480 6	30 E 10 .119 1382 6	[illegible]	30 E 11 .119 1382 6	[illegible]	20 G 11 .146 1681 8
1075							36 G 8 .023 604 12	36 G 8 .033 730 10	24 G 8 .038 912 12	24 G 8 .038 1110 10	30 G 8 .077 1112 8	24 G 8 .122 1385 8	[illegible]			30 G 9 .144 1416 6	30 G 9 .144 1515 6	30 G 10 .144 1416 6	30 E 10 .124 1416 6	[illegible]	20 G 11 .163 1567 8	
1100								36 G 8 .024 618 12	36 G 8 .036 767 10	30 G 8 .060 898 10	36 G 8 .036 946 8	[illegible]	30 G 8 .081 1136 8	24 G 8 .120 1430 8	[illegible]	30 G 8 .180 1480 6	30 G 9 .130 1448 6	30 E 9 .130 1448 6	30 E 10 .130 1448 6	[illegible]	[illegible]	30 G 11 .130 1448 6

EXAMPLE

GRILLE WIDTH IN INCHES — 36

DEFLECTION SETTING — G

DROP OF AIR IN FEET WITH 15° TEMPERATURE DIFFERENTIAL — 9

TOTAL PRESSURE IN INCHES OF WATER REQUIRED BEHIND GRILLE — .036

VELOMETER VELOCITY IN FEET PER MINUTE — 758

GRILLE HEIGHT IN INCHES — 12

Figure 16.

Now we refer to Figure 16 and we note that across the top of sheet there are four arrangements of deflection setting. The exact number of deflectors vary with different width grilles, but the general idea of setting is indicated, thus setting "A" gives the farthest blow and setting "E" gives the shortest blow. It is well to pick the throw of a grille so that "A" setting overblows and "G" setting under blows, thus adjustment in field gives necessary flexibility.

We now run down the left-hand column under cu.ft./min. and find 1,050 cu.ft./min. Since the blow is 42 ft., 6 in., we move to the right along this line and try under the vertical 40-ft. throw line. The grille width of 30 in. is given in upper left-hand corner of this square. Deflection is shown in upper right corner as "G." A velometer velocity of 1,480 ft./min. is shown in lower left-hand corner. Grille height of 6 in. is shown in lower right-hand corner. A static pressure of 0.137 in. of water will be required behind grille as shown at right-hand side at center. At left-hand center, it states that in a throw of 40 ft. the air stream will drop 9 ft.

Inspecting to the left horizontally along the same capacity line of 1,050 cu.ft./min., we see that a 30-in. x 6-in. grille is also recommended down to a 36-ft. blow. Inspecting to the right horizontally along same capacity line, we see that a 30-in. x 6-in. grille is recommended for a throw of 46 ft. with a deflection setting "E."

In ordering grilles to contain all of the flexibility that may be required, the grille would consist of vertical deflectors, backed up with horizontal deflectors, backed up by multi-shutter damper.

B. Ceiling Diffusers

Many installations today are being made introducing the air through the ceiling. A circular diffuser is installed, the upper part of which is flush with the under side of the ceiling. The diffuser consists of several cones which usually extend down below the ceiling.

They are selected by dividing the ceiling area of the room, as nearly as possible, into squares the sides of which do not exceed four times the ceiling height. A diffuser is located in the center of each square. If, due to obstructions, constructional peculiarities, etc., the diffuser cannot be placed in the center of the square, the distance to one side within the maximum radius of diffusion should not be more than 1-1/2 times the length of the other side, which must be within the minimum radius of diffusion.

If the room cannot be divided into squares, rectangles may be used. The long side of the rectangle should not be greater than 1-1/2 times the length of the short side. Divide the total cu.ft./min. by the number of squares or rectangles, determined for the room, which gives the cu.ft./min. each diffuser will be required to handle

Example No. 10 - In a room 135 ft. by 85 ft. by 15 ft. ceiling, we find that it can easily be divided into six areas 45 ft. by 42 ft. 6 in. Total air to be handled into room being 18,765 cu.ft./min. we divide by six and find 2,085 cu.ft./min. must be handled per diffuser.

We will assume that the diffuser can be mounted flush under the 15-ft. ceiling and there is space above the ceiling for supply duct work. Now we refer to Figure 17 and see that graph line D shows that, for auditoriums with 15-ft. ceiling, a neck velocity of 1,400 ft./min. may be used.

On Figure 18 capacity table under neck velocity of 1,400 ft./min. shows a size 45 with a neck diameter of 18 in. will handle 2,474 cu.ft./min. This is slightly over our required capacity, but the next smaller size is under required capacity.

Under Radius of Diffusion Table on bottom of Figure 18, we see that size 45 diffuser will cover 15 - 31 ft. on each side. This coverage meets our needs.

On Figure 18 under Resistance Pressure Chart, we find a size 45 diffuser with 1,400-ft./min. neck velocity requires a static pressure in the supply duct of 0.278 in. water.

Equalizing deflectors and dampers should be installed with each diffuser.

XII. VENTILATION REQUIRED

The most prevalent expression used when people speak of "ventilation" is the "air change". If ventilation is specified as minute air change, we may solve for cu.ft./min. as follows:

$$\text{Minute Air Change} = \frac{\text{Cu.Ft. Volume of Room}}{\text{Cu.Ft./Min. of Air through Room}} \tag{4}$$

$$\text{cu.ft./min.} = \frac{\text{Cu.Ft. Volume of Room}}{\text{Minute Air Change}} \tag{4a}$$

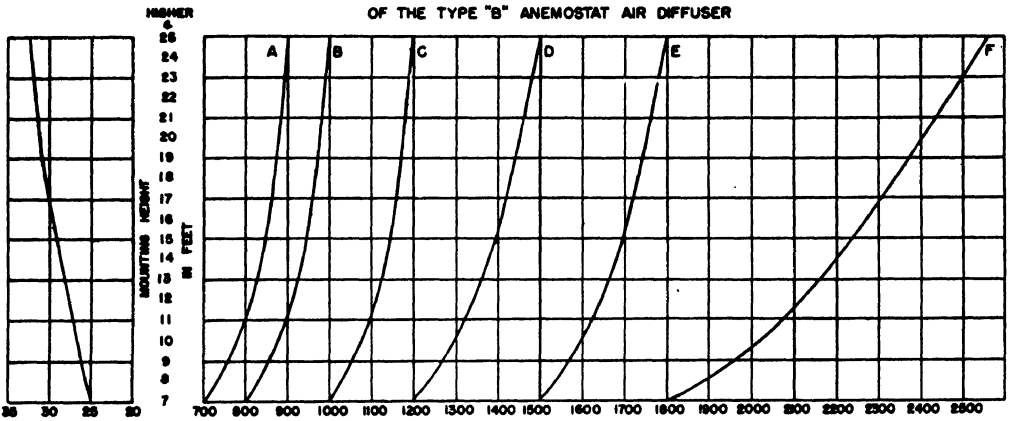
If ventilation is specified as number of air changes per hr., we may solve for cu. ft./min. as follows:

ANEMOSTAT CORPORATION OF AMERICA

SELECTION DATA—CONTINUED—

CHART NO. 1

FOR THE SELECTING OF NECK VELOCITIES AND COOLING TEMPERATURE DIFFERENTIALS OF THE TYPE "B" ANEMOSTAT AIR DIFFUSER



RECOMMENDED MAXIMUM COOLING TEMPERATURE DIFFERENTIAL FOR THE VARIOUS MOUNTING HEIGHTS.

THE RECOMMENDED MAXIMUM HEATING TEMPERATURE DIFFERENTIAL IS SIXTY DEGREES F. FOR ANY CEILING HEIGHTS.

GRAPH LINE

"A" Film, Television & Sound Recording Studios, and Broadcasting Control Rooms.
"B" Private Offices, Hotel Bedrooms, Sick Rooms, Broadcasting Studios and Residences.
"C" Libraries, under Balconies of Theatres and Auditoriums, Concert Halls, Classrooms, Museums, and Hospital Operating Rooms.
"D" General Offices, Restaurants, Theatres & Auditorium Ceilings, Lecture Halls, Stores, Large Hotel Dining Rooms, and Dance Halls.
"E" Department Stores, Hotel Lobbies, Industrial Exhibit Rooms and Restaurant Kitchens.
"F" Factories, Store Rooms, Engine Rooms, Greenhouses, and spaces where Duct Noise is of no importance.

RESISTANCE PRESSURE CHART TYPE "B" ANEMOSTAT AIR DIFFUSER

Size No.	Neck Dia. In.	NECK VELOCITY IN FEET PER MINUTE																	Neck Dia. In.
		700	800	900	1000	1100	1200	1300	1400	1500	1600	1700	1800	1900	2000	2200	2500	3000	
		STATIC PRESSURE IN INCHES OF WATER																	
10	4	.020	.026	.035	.043	.050	.060	.072	.083	.093	.105	.116	.130	.142	.155	.191	.246	.395	4
12.5	5	.025	.033	.040	.050	.060	.070	.083	.095	.107	.120	.134	.147	.162	.178	.227	.290	.450	5
15	6	.037	.050	.063	.080	.100	.120	.140	.167	.193	.220	.245	.270	.296	.320	.372	.450	.580	6
20	8	.045	.060	.075	.094	.115	.136	.160	.186	.215	.243	.270	.300	.330	.358	.415	.500	.640	8
25	10	.057	.070	.090	.110	.130	.150	.175	.202	.232	.260	.290	.320	.350	.380	.449	.553	.670	10
30	12	.064	.080	.100	.120	.140	.160	.188	.218	.248	.280	.310	.340	.370	.400	.472	.580	.710	12
35	14	.070	.088	.107	.127	.150	.173	.200	.230	.260	.294	.325	.356	.388	.420	.482	.575	.730	14
40	16	.074	.092	.110	.133	.155	.182	.215	.245	.277	.310	.340	.370	.400	.430	.492	.585	.740	16
45	18	.090	.110	.135	.160	.186	.216	.247	.278	.307	.337	.366	.396	.428	.458	.515	.600	.760	18
50	20	.085	.106	.128	.150	.180	.206	.237	.268	.297	.327	.356	.386	.416	.445	.505	.595	.740	20
55	22	.078	.097	.120	.140	.166	.194	.244	.254	.284	.314	.343	.356	.405	.435	.495	.585	.730	22
60	24	.072	.090	.110	.130	.155	.180	.210	.240	.268	.298	.326	.356	.384	.412	.471	.560	.700	24
65	26	.060	.076	.096	.116	.138	.160	.185	.215	.245	.273	.300	.330	.360	.390	.448	.533	.680	26
75	30	.047	.060	.075	.090	.110	.130	.150	.172	.200	.228	.258	.286	.315	.345	407	.490	.640	30
95	38	.040	.053	.067	.083	.100	.120	.140	.165	.190	.220	.248	.276	305	334	.391	.476	.620	38

"NO AIR CONDITIONING SYSTEM IS BETTER THAN ITS AIR DISTRIBUTION"

Figure 17.

ANEMOSTAT CORPORATION OF AMERICA

SELECTION DATA—CONTINUED—

CAPACITY TABLE TYPE B ANEMOSTAT AIR DIFFUSER

Size No.	Neck Dia. in	Neck Area Sq. In.	Neck Area Sq. Ft.	NECK VELOCITY IN FEET PER MINUTE															
				700	800	900	1000	1100	1200	1300	1400	1500	1600	1700	1800	1900	2000	2200	2500	3000
				CAPACITY IN CUBIC FEET PER MINUTE																
10	4	12.56	.087	61.1	69.8	78.5	87.3	96.0	105	113	122	131	140	148	157	166	175	192	218	262
12.5	5	19.63	.136	95.4	109	123	136	150	164	177	191	205	218	232	245	259	273	300	341	409
15	6	28.27	.196	137	157	177	196	216	236	255	275	295	314	334	353	373	393	432	491	589
20	8	50.26	.349	244	279	314	349	384	419	454	489	524	558	593	628	663	698	768	873	1047
25	10	78.54	.545	382	436	491	545	600	655	709	764	818	873	927	982	1036	1091	1200	1364	1636
30	12	113.10	.785	550	628	707	785	864	942	1021	1100	1178	1257	1335	1414	1492	1571	1728	1964	2356
35	14	153.94	1.069	748	855	962	1069	1176	1283	1390	1497	1604	1710	1817	1924	2031	2138	2352	2673	3207
40	16	201.06	1.396	977	1117	1257	1396	1536	1676	1815	1955	2094	2234	2374	2513	2653	2793	3072	3491	4189
45	18	254.47	1.767	1237	1414	1590	1767	1944	2121	2297	2474	2651	2828	3004	3181	3358	3534	3888	4418	5302
50	20	314.16	2.181	1527	1745	1963	2182	2400	2618	2836	3054	3272	3491	3709	3927	4145	4363	4800	5454	6545
55	22	380.13	2.639	1848	2112	2376	2640	2904	3168	3432	3696	3960	4224	4488	4752	5016	5280	5808	6600	7919
60	24	452.39	3.141	2199	2513	2827	3142	3456	3770	4084	4398	4712	5027	5341	5655	5969	6283	6912	7854	9425
65	26	530.93	3.687	2581	2950	3318	3687	4056	4424	4793	5162	5531	5899	6268	6637	7005	7374	8111	9218	11061
75	30	706.86	4.908	3436	3927	4418	4909	5400	5891	6381	6872	7363	7854	8345	8836	9327	9818	10799	12272	14726
95	38	1134.10	7.875	5513	6301	7088	7876	8663	9451	10238	11026	11814	12601	13389	14176	14964	15751	17327	19689	23627

HOW TO USE THE CAPACITY TABLE

1. Determine the Air Volume to be distributed by the Anemostat Air Diffuser.
2. Determine the Neck Velocity of the Anemostat Air Diffuser. (See Chart No. 1.)
3. Select in the first horizontal line of figures, the determined Neck Velocity.
4. Follow the column down to the figure nearest to the required Air Volume. By interpolation the exact Volume and Velocity required may be determined.
5. Follow the line with the determined Volume towards the left to find the Neck Diameter and the Anemostat Air Diffuser Size Number.
6. Check this selection with the Radius of Diffusion Table below to insure correct coverage.

RADIUS OF DIFFUSION TABLE
Type "B" Anemostat

Size No.	Neck Dia.	NECK VELOCITIES IN FEET PER MINUTE																
		700	800	900	1000	1100	1200	1300	1400	1500	1600	1700	1800	1900	2000	2200	2500	3000
10	4"	3-5	3-5	3-6	3-6	3-6	3-7	3-7	3-7	3-7	3-8	4-8	4-8	4-8	4-9	4-9	5-10	5-11
12.5	5"	3-6	3-7	3-7	3-7	4-8	4-8	4-9	4-9	4-9	4-10	5-10	5-10	5-11	5-11	5-11	6-12	7-14
15	6"	4-8	4-8	4-9	4-9	4-9	4-10	5-10	5-11	5-11	5-11	6-12	6-12	6-12	6-13	7-13	7-15	8-17
20	8"	5-10	5-11	5-11	6-12	6-12	6-13	6-13	7-14	7-15	7-15	8-16	8-16	8-17	8-17	9-18	10-20	11-23
25	10"	6-13	6-13	7-14	7-15	7-16	8-16	8-17	8-17	9-18	9-19	9-20	10-20	10-21	10-22	11-23	12-25	14-28
30	12"	8-15	8-16	8-17	9-18	9-19	9-19	10-20	10-21	11-22	11-23	11-23	12-24	12-25	13-26	13-27	15-30	17-34
35	14"	9-18	9-19	9-20	10-21	10-22	11-23	12-24	12-24	12-25	13-26	13-27	14-28	14-29	15-30	16-32	17-35	20-39
40	16"	10-21	10-22	11-23	11-24	12-25	13-26	13-27	14-28	14-29	15-30	15-31	16-32	16-33	17-34	18-36	20-40	22-45
45	18"	11-23	12-24	12-25	13-27	13-28	14-29	15-30	15-31	16-33	17-34	17-35	18-36	18-37	19-39	20-41	22-45	25-50
50	20"	12-26	13-27	14-28	14-30	15-31	16-32	16-33	17-35	18-36	18-37	19-39	20-40	20-42	21-43	22-46	25-50	28-56
55	22"	14-28	14-30	15-31	16-33	17-34	17-35	18-37	19-39	20-40	20-41	21-43	22-44	23-46	23-47	25-50	27-54	31-62
60	24"	15-31	16-32	17-34	17-35	18-37	19-39	20-40	21-42	21-43	22-45	23-47	24-48	25-50	25-51	27-54	30-60	33-67
65	26"	16-33	17-35	18-37	19-38	20-40	21-42	21-44	22-45	23-47	24-49	25-50	26-52	27-54	28-55	29-59	32-64	36-73
75	30"	19-38	20-40	21-42	22-44	23-46	24-48	25-50	26-52	27-54	28-56	29-58	30-60	31-62	32-64	34-68	37-74	42-84
95	38"	24-48	25-51	26-53	27-56	29-58	30-61	31-63	33-66	34-69	35-71	36-74	38-76	39-79	40-81	43-86	47-94	53-106

HOW TO USE THE RADIUS OF DIFFUSION TABLE

In the first column of the table select the figure corresponding to the Anemostat Air Diffuser Size Number and follow horizontally to the right of this column below the selected Neck Velocity. The two figures at this point are the minimum and maximum radii of diffusion of this selected Anemostat Air Diffuser. Should the required radius of diffusion be below the minimum or above the maximum as shown on this Table, contact our nearest Sales Office.

"NO AIR CONDITIONING SYSTEM IS BETTER THAN ITS AIR DISTRIBUTION"

Figure 18.

$$\text{Number of Air Changes per Hour} = \frac{\text{Cu.Ft./Hr. of Air through Room}}{\text{Cu.Ft. Volume of Room}} \quad (5)$$

Also

$$\text{cu.ft./min.} = \frac{\text{Cu.Ft. Volume of Room x Air Changes per Hr.}}{60} \quad (6)$$

Ventilation requirements (10) for various types of buildings specified on above basis.

Type of Bldg.	Remarks	Air Changes per Hr.
Horse barns	4,296 cu.ft./hr./horse	--
Cow barns	3,542 cu.ft./hr./cow	--
Attic roof space	80 cu.ft./hr./sq.ft. roof area	--
Boiler house	Base on radiation of boilers - or minimum 60 air changes/hr. in space above boilers	--
Cleaning and pressing sugar mills - main building	--	10 - 15
Forge shops	--	18 - 20
Gymnasium	--	35
Heat treating room	--	12
Kitchen	Hood ranges	20
Laundry	--	20 - 30
Offices	Quiet fans (bases summer)	12 - 18
Toilet rooms	--	10 - 15
Warehouses	--	2 - 4

Note: Where two air changes are indicated, such as 20 - 30, the lowest figure should be used for moderate conditions, and the highest figure for extreme conditions.

XIII. ROOF VENTILATORS

The air (10) change method has been effective where heat and ordinary odors are concerned. In these cases, large amounts of air are handled at relatively no pressure. In most cases the air is vented from the area through ventilators located on the roof. In some cases, the air flow is entirely dependent on temperature difference between indoors and out-of-doors, wind velocity pass the ventilator, and stack effect (vertical difference between air inlet to area and base of ventilator).

Example 11 - Laundry 100 ft. x 40 ft. x 12 ft. according to list 20 - 30 changes per hr. should be figured. As this laundry is supposed to have moderate heat load, we use 20 changes per hr.; therefore

$$\frac{(100 \times 40 \times 12)}{60} = 16{,}000 \text{ cu.ft./min.}$$

The building being 100 ft. long with five 20-ft. bays, we will decide on using five ventilators, thus requiring each vent to handle 3,200 cu.ft./min. In the location where this laundry will be erected, we find has a minimum wind velocity of 6 mi./hr. during most of the warm season.

Referring to Figure 19, we see that with a 6-mi./hr. wind and a 10°F. temperature difference and 10-ft. height of ventilator above air intake (this is not exact because air will be allowed to enter through open windows in the outside walls), a 48-in. diameter ventilator will be required per bay.

As an alternate to five round ventilators, a continuous roof ventilator might be installed on peak of roof.

Another alternate would be to use ventilators with fans and motor in them. For instance, if noise did not matter a 20-in. ventilator with a 18-in. diameter fan on a 1/4-hp., 1,750-rev./min. motor could handle 3,200 cu.ft./min.

VENTILATORS

Wind Velocity, M.P.H.	Temp. Diff., °F.	Height Above Intake, Feet	SIZE OF VENTILATOR (Dia. of Stack in Inches)													
			12	14	16	18	20	24	30	36	42	48	54	60	66	72	84	96
6	0	10	144	208	284	387	470	580	905	1306	1787	2323	2937	3630	4356	5227	7056	9199
		20	144	208	284	387	470	580	905	1306	1787	2323	2937	3630	4356	5227	7056	9919
		30	144	208	284	387	470	580	905	1306	1787	2323	2937	3630	4356	5227	7056	9199
		40	144	208	284	387	470	580	905	1306	1787	2323	2937	3630	4356	5227	7056	9199
		50	144	208	284	387	470	580	905	1306	1787	2323	2937	3630	4356	5227	7056	9199
		100	144	208	284	387	470	580	905	1306	1787	2323	2937	3630	4356	5227	7056	9199
	5	10	204	293	397	462	666	822	1282	1850	2516	3291	4163	5140	6168	7402	10092	13168
		20	259	389	446	518	745	980	1434	2069	2814	3680	4655	5750	6900	8280	11178	14576
		30	248	357	483	563	810	998	1557	2246	3049	3996	5054	6240	7488	8971	12110	15835
		40	264	380	514	597	859	1061	1655	2387	3246	4246	5655	6633	7959	9552	12895	16790
		50	278	400	542	630	907	1117	1743	2514	3419	4471	5871	6988	8385	10063	13585	17745
		100	331	476	645	749	1078	1328	2070	2988	3604	5304	6709	8300	9960	11952	16135	21063
	10	10	229	329	446	518	745	920	1434	2069	2814	3680	4655	5750	6900	8280	11178	14578
		20	264	380	514	598	859	1061	1655	2387	3246	4246	5371	6633	7959	9552	12895	16840
		30	292	421	569	660	950	1171	1827	2635	3564	4685	5926	7320	8784	10541	14230	18680
		40	314	453	612	711	1023	1368	1968	2840	3868	5051	6389	7890	9468	11368	15338	20007
		50	332	476	649	755	1087	1340	2191	3016	4002	5364	6785	8380	10056	12067	16300	12648
		100	412	595	803	933	1343	1655	2579	3724	5065	6623	8378	10350	12420	14904	20120	26291
	20	10	264	380	514	598	859	1061	1655	2387	3246	4246	5371	6633	7959	9552	12895	16840
		20	314	455	612	711	1023	1262	1968	2840	3864	5051	6389	7890	9468	11368	15338	20007
		30	352	506	686	795	1144	1412	2205	3178	4322	5653	7151	8831	10597	12717	17167	22520
		40	384	552	748	869	1251	1542	2405	3468	4716	6171	7806	9635	11572	13874	18729	24431
		50	413	595	803	933	1343	1653	2580	3724	5065	6623	8378	10350	12420	14904	20120	26420
		100	585	756	1023	1185	1706	2102	3283	4736	6441	8418	10648	13150	15780	18936	25563	33379
	30	10	292	421	569	660	950	1171	1826	2635	3564	4685	5926	7320	8784	10541	14230	18599
		20	352	506	686	795	1144	1412	2205	3178	4322	5653	7151	8831	10597	12717	17167	22420
		30	399	574	778	903	1300	1601	2497	3606	4904	6411	8109	10031	12037	14445	19500	25486
		40	439	632	856	991	1427	1760	2745	3956	5380	7038	8903	10992	13190	15828	21367	27899
		50	473	681	922	1069	1539	1898	2957	4268	5804	7586	9596	11860	14232	17078	23055	30111
		100	670	878	1189	1379	1985	2448	3815	5506	7488	9783	12375	15280	18336	22003	29074	38008
8	0	10	193	278	379	435	626	775	1207	1742	2470	3098	3970	4840	5808	6969	9398	12012
		20	193	278	379	435	626	775	1207	1942	2470	3098	3970	4840	5808	6969	9398	12012
		30	193	278	379	435	626	775	1207	1742	2470	3098	3970	4840	5808	6969	9398	12012
		40	193	278	379	435	626	775	1207	1742	2470	3098	3970	4840	5808	6969	9398	12012
		50	193	278	379	435	626	775	1207	1742	2470	3098	3970	4840	5808	6969	9398	12012
		100	193	278	379	435	626	775	1207	1742	2470	3098	3940	4840	5808	6969	9398	12012
	5	10	253	364	473	571	822	1017	1584	2286	2809	4066	5136	6350	7620	9144	12344	15983
		20	278	400	542	626	901	1115	1736	2505	3407	4455	5645	6960	8335	10022	13529	17641
		30	297	427	579	671	966	1193	1859	2682	3648	4771	6042	7450	8940	10728	14482	18901
		40	313	451	610	706	1016	1256	1957	2823	3839	5021	6356	7843	9411	11294	15246	19906
		50	327	470	637	738	1062	1312	2045	2950	4012	5246	6638	8198	9837	11805	15938	20811
		100	380	547	741	857	1234	1523	2372	3424	4657	6079	7685	9510	11412	13694	18486	24130
	10	10	278	400	542	626	901	1115	1736	2505	3407	4455	5645	6960	8335	10022	13529	17645
		20	313	451	610	706	1016	1256	1957	2823	3839	5021	6356	7843	9411	11294	15246	19904
		30	341	491	664	768	1105	1366	2129	3071	3877	5460	6907	8530	10236	12283	16582	21666
		40	363	522	707	819	1179	1457	2270	3276	4455	5826	7367	9100	10920	13104	17690	23073
		50	382	547	744	863	1252	1535	2393	3452	4675	6139	7760	9590	11408	13810	18643	24330
		100	461	663	898	1041	1499	1850	2881	4160	5658	7398	9341	11560	13872	16646	22472	29357
	20	10	313	451	610	706	1016	1256	1957	2823	3839	5021	6356	7843	9411	11294	15246	19906
		20	363	522	707	819	1179	1457	2270	3276	4455	5826	7367	9100	10920	13104	17690	23073
		30	401	577	781	903	1300	1607	2507	3614	4915	6428	8123	10041	12049	14459	19519	25486
		40	433	623	844	977	1406	1737	2707	3904	5309	6946	8764	10845	13014	15617	21092	27547
		50	462	665	898	1041	1499	1848	2882	4160	5658	7398	9341	11560	13872	16646	22472	29357
		100	573	825	1117	1293	1861	2297	3585	5172	7034	9193	11595	14360	17232	20678	27825	37752
	30	10	341	491	664	768	1105	1366	2128	3071	3877	5460	6907	8530	10236	12283	16582	21666
		20	401	577	781	903	1300	1607	2507	3614	4915	6428	8123	10041	12049	14459	19519	25486
		30	448	645	873	1011	1455	1796	2799	4042	5497	7186	9030	11220	13464	16157	21811	28503
		40	488	702	951	1099	1582	1953	3043	4392	5973	7813	9883	12202	14640	17571	23720	30966
		50	522	751	1018	1177	1694	2093	3259	4704	6398	8361	10578	13070	15684	18821	25408	33178
		100	659	948	1285	1487	2141	2643	4117	5942	8081	10558	13355	16490	19788	23746	32057	41866
10	0	10	241	348	474	545	784	968	1510	2178	2963	3870	4895	6045	7254	8705	11751	15078
		20	241	348	474	545	784	968	1510	2178	2963	3870	4895	6045	7254	8705	11751	15078
		30	241	348	474	545	784	968	1510	2178	2963	3870	4895	6045	7254	8705	11751	15078
		40	241	348	474	545	784	968	1510	2178	2963	3870	4895	6045	7254	8705	11751	15078
		50	241	348	474	545	784	968	1510	2178	2963	3870	4895	6045	7254	8705	11751	15078
		100	241	348	474	545	784	968	1510	2178	2963	3870	4895	6045	7254	8705	11751	15078
	5	10	301	433	586	681	980	1210	1887	2722	3720	4838	6120	7555	9066	10879	14686	19149
		20	326	469	635	736	1059	1308	2039	2941	3999	5227	6612	8165	9798	11758	15873	20709
		30	345	496	672	781	1124	1386	2162	3118	4240	5343	6758	8635	10386	12463	16825	21967
		40	361	519	703	816	1175	1449	2260	3259	4432	5793	7328	9048	10857	13029	17589	22973
		50	375	540	731	848	1211	1505	2348	3386	4605	6018	7712	9403	11283	13540	18279	23874
		100	428	616	834	967	1398	1716	2675	3860	5250	6851	8666	10715	12858	15430	20830	27347
	10	10	326	469	635	736	1059	1308	2039	2941	3999	5227	6612	8165	9798	11758	15873	20711
		20	361	519	703	816	1175	1449	2260	3259	4432	5793	7328	9048	10857	13029	17589	23375
		30	389	560	768	878	1248	1539	2432	3507	4770	6232	7883	9735	11682	14018	18924	24733
		40	411	591	801	929	1337	1650	2573	3712	5040	6598	8346	10305	12366	14839	20032	26140
		50	430	610	838	973	1401	1728	2696	3883	5281	6911	8742	10795	12954	15545	20985	27397
		100	499	718	973	1151	1657	2043	3184	4596	6251	8170	10335	12705	15246	18295	24697	32223
	20	10	361	519	703	816	1175	1449	2260	3257	4432	5793	7328	9048	10857	13029	17589	22973
		20	411	591	801	929	1337	1650	2573	3712	5040	6598	8346	10305	12366	14839	20032	26140
		30	449	646	875	1013	1458	1800	2810	4050	5508	7200	9108	11246	13495	16194	21851	28503
		40	481	692	937	1087	1565	1930	3010	4340	5902	7718	9763	12050	14460	17352	23425	30564
		50	510	718	973	1151	1657	2041	3185	4596	6251	8170	10335	12765	15246	18295	24697	32223
		100	672	967	1312	1403	2020	2490	3888	5608	7627	9965	12605	15565	18678	22414	30258	39512
	30	10	389	560	768	878	1242	1559	2431	3507	4770	6232	7885	9735	11682	14018	18924	24732
		20	449	646	875	1013	1458	1800	2810	4050	5508	7200	9108	11246	13495	16194	21851	28560
		30	546	786	964	1131	1614	1949	3102	4478	6090	7956	10064	12425	14910	17992	24289	31730
		40	586	843	1042	1209	1740	2148	3346	4828	6565	8585	10860	13407	16088	19306	26063	34032
		50	620	892	1109	1287	1853	2286	3562	5140	6990	9133	11553	14275	17130	20556	27760	36043
		100	706	1016	1376	1397	2299	2836	4420	6378	8674	11331	14333	17695	21234	25481	34399	44691

These capacity figures have been derived from tests under actual service conditions.

H. H. ROBERTSON COMPANY, PITTSBURGH, PA.

Figure 19.

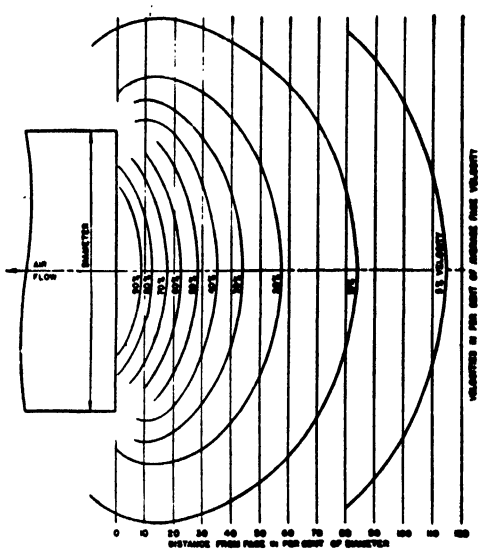


Figure 19A. Velocities at the Open End of a Round Pipe Orifice

Using "air change" specification may be very misleading as to actual capacity required. For a given amount of leakage a certain amount of air is required to dilute the mixture to or below a maximum allowable concentration either from an explosive or toxic standpoint. If the process is located in a 12-ft. high building, a certain air change will result. If the process is located in a 24-ft. high building and the same amount of dilution air used, the resultant air change would be one-half that which occurs in the 12-ft. high building. If the air change method was used, it would dictate twice the cu.ft./min. of air being handled.

Example 12

3,200 cu.ft./min. air to be handled through room. 20 ft. wide x 40 ft. long = 800 sq.ft. floor area.

(a) - Room with 12-ft. ceiling height would have 9,600 cu.ft./volume

$$\frac{9{,}600 \text{ cu.ft.}}{3{,}200 \text{ cu.ft./min.}} = 3\text{-min. air change}$$

or

$$\frac{3{,}200 \times 60}{9{,}600 \text{ cu.ft.}} = 20 \text{ air changes/hr.}$$

cu.ft./min. of air handled per sq.ft. of floor area

$$\frac{3{,}200}{800} = 4 \text{ cu.ft./min./sq.ft.}$$

(b) - Room with 24-ft. ceiling height would have 19,200 cu.ft. volume

$$\frac{19{,}200 \text{ cu.ft.}}{3{,}200 \text{ cu.ft./min.}} = 6\text{-min. air change}$$

$$\frac{3{,}200 \times 60}{19{,}200} = 10 \text{ air changes/hr.}$$

We still handle 4 cu.ft./min./sq.ft.

Now, if a 3-min. air change had been specified instead of the cu.ft./min. of air, we would have for the 12-ft. ceiling height

$$\frac{9{,}600 \text{ cu.ft. volume}}{3\text{-min. air change}} = 3{,}200 \text{ cu.ft./min. required}$$

We still handle 4 cu.ft./min./sq.ft.

For the 24-ft. ceiling height, we would have

$$\frac{19{,}200 \text{ cu.ft. volume}}{3\text{-min. air change}} = 6{,}400 \text{ cu.ft./min. required}$$

Cu.ft./min./sq.ft. floor area would be eight and yet we have the same amount of fume released in either room.

Now, if the air flow pattern was arranged so the supply air entered at the ceiling and moved down evenly distributed and was exhausted at the floor line, the lower 12-ft. height would receive

$$\frac{9{,}600 \text{ cu.ft.}}{6{,}400 \text{ cu.ft./min.}} = 1.5\text{-min. air change}$$

or

$$\frac{6{,}400 \times 60}{9{,}600} = 40 \text{ air changes/hr.}$$

Another example which indicates the fallacy of air change method is to take a particular case of a laboratory which has 533 sq.ft. of floor area and 11 ft. 0 in. ceiling giving a volumetric content of 5,863 cu.ft. Based on one laboratory hood being installed with 12.5 sq.ft. open face area and a 75-ft./min. velocity there would be a total exhaust from the laboratory of 935 cu.ft./min. through the hood with a resultant air change of once every 6.28 min. If there were two hoods in this size laboratory, both operating at one time, then a total of 1,870 cu.ft./min. would be exhausted, which would give a resultant change of air of once every 3.14 min.

The actual ventilation requirement of a building deserves more attention and a more logical solution than just the general air change method. However, we do not believe we will ever get away entirely from mentioning "air change" as it is a convenient method of comparison.

The requirements of ventilation in a building are due to heat build-up, fume conditions, or dust nuisance. Heat build-up is due to transmission of heat through building construction from sun effect and/or high outside temperature, sometimes added to by heat given off by people and by apparatus inside the building.

Fume conditions originate from leakage out of apparatus or handling of materials and may present toxic or explosion possibilities.

Dust conditions are due to leakage from apparatus or open crushing or handling of materials and present possibilities of dermatitis, respiratory disorders, and explosions. There are many state laws which specify allowable fume and dust concentrations. The "underwriters" are quite active in recommending safe limit under which explosive mixtures should be kept.

The quantity of air handled in a ventilation system should be calculated from facts and exact data. In some cases, life is at stake and facts must replace guesses.

How do we decide on the amount of ventilation air required and what type system should be installed.

The problems which are quickest to calculate are generally the ones where heat gain through building construction and heat liberated by apparatus and people within the space are to be considered. After deciding the maximum temperature rise that will be tolerated above entering air temperature, a simple mathematical equation gives the cubic feet of air per minute that must be handled through the space to control the over-all temperature rise.

In most cases, if ample means are provided for the hot air to escape through the roof, and for the cooler air to enter through the openings near the floor line, this type of problem is rather easy to solve as indicated in Example 11.

In some cases where motors must be kept cool, or where local high heats are released, the mechanical type of systems are installed. Where a combination of small amounts of fume and dust and large amounts of heat are present, then dilution by handling large amount of air through a building gives good results. In all cases where there is apt to be heavy concentration of objectionable fumes or dust liberated at certain points, then, by all means, these offenders should be caught at their source and removed in such a manner as to prevent them for escaping into the operating zone. This is usually most effectively accomplished by means of hoods and mechanical exhaust systems. The exhaust hoods should be so located that the fumes or dust are pulled away from the operators. In some cases, a blast of supply air passing the operators has been successful in banking the fume or dust away from the operator and actually deflected the fume into the exhaust hood.

The complete hooding and direct exhaust of contaminants is the safe way. The general natural flow of the fume or dust should be determined. Light gas or hot air rises while heavy gas or cold air falls. Simply keep them moving in their natural direction and your problem is greatly simplified. When contaminants are sufficiently diluted, the mixture with air will normally follow the air currents in the space. To try to change their natural course requires more ventilating power and in some cases has meant defeat.

We will first take up a ventilating problem involving sun effect on a building plus people and apparatus heat pick-up inside.

Example 13 - We have a small shop 80 ft. x 50 ft. x 10 ft. ceiling with (1) sun load equals 125,800 B.t.u./hr., (2) light equal to 16,000 watts, (3) motor load equal to 7-1/2 hp., (4) 85 people working in shop at rate equal to that of moderately active office worker (metabolic rate, 500 B.t.u./hr.) giving off a sensible heat gain of 225 B.t.u./hr.

Solution:

	B.t.u./hr.
Sun load on building	125,800
Light - 16,000 watts x 3.4	54,400
Motor 7-1/2 hp. x 2.545	19,080
Sensible heat 225 x 85 people	19,120
Total	218,400

$$\frac{\text{B.t.u./hr. x 55.6}}{60 \times T_R} = \text{cu.ft./min.}$$

55.6 = 1 B.t.u. will rise 55.6 cu.ft. 1°F.

60 = min./hr.

T_R = temperature rise required to pick up heat, °F.

$$\frac{218{,}400 \text{ B.t.u./hr. x } 55.6}{60 \times 10^{\circ} \text{ rise above outside}} = 20{,}200 \text{ cu.ft./min.}$$

20,200 cu.ft./min. air required to be moved through shop in such a way as to pick up heat and remove it from building.

Cubic contents of building - 80 x 50 x 10 = 40,000 cu.ft.

$$\frac{40{,}000 \text{ cu.ft. contents}}{20{,}200 \text{ cu.ft./min.}} = 1.98\text{-min. air change}$$

$$\frac{20{,}200 \text{ cu.ft./min. x } 60}{40{,}000} = 30.2 \text{ air changes/hr.}$$

Comparison by air change method:

$$\frac{40{,}000 \text{ cu.ft. contents}}{5\text{-min. air change}} = 8{,}000 \text{ cu.ft./min.}$$

which would mean

$$\frac{218{,}400 \text{ B.t.u./hr. x } 55.6}{60 \times 8{,}000 \text{ cu.ft./min.}} = 25.3^{\circ}\text{F. temp. rise}$$

The above illustrates that by air change method if the outdoor temperature was 80°F., the resulting indoor temperature would be 105.3°F. as compared to a resulting indoor temperature of 90°F. if figured correctly by the heat pick-up calculation.

Another method of estimating ventilating air requirements is based on cubic feet of air supplied or exhausted per square foot of floor area for a desirable degree of occupancy.

	Cu.Ft./Min. per Sq.Ft. of Floor Area
Human occupancy; space more than 800 cu.ft./person	0.5
Human occupancy; space less than 150 cu.ft./person	2.5
Public building corridors	0.5
Gymnasiums	1.5
Class rooms	2.0
Auditoriums	2.0
Bath and toilets	2 - 3.0
Large dining rooms	1.5
Average kitchens	4.0
Small, congested kitchens	10.0
General industrial buildings having no localized sources of toxic or explosive vapors	1.0
Enclosures or booths for arc welding	50.0
Rooms for abrasive blasting or metal spraying	100.0
Workrooms containing heated surfaces	2.0

The above is based on not less than 15 sq.ft. of floor area per person.

State and city codes should be consulted to make certain that minimum outdoor air requirements are provided.

Where toxic solvent vapors are released within an area, the first line of attack should be to install a hood and remove the vapors before the vapors escape into the operator's working zone. If this is not feasible, then the vapors should be diluted to maximum allowable concentration as quickly as possible.

Various medical authorities and state codes establish the maximum allowable concentration (M.A.C.).

Knowing the amount of toxic solvent released over a given time, the amount of diluting air required can be calculated.

Calculate volume of solvent as follows (5):

$$\text{cu.ft./min. (vapor)} = \frac{\text{lb. liquid solvent}}{\text{min.}} \times \frac{400}{\text{molecular wt.}} \tag{7}$$

The figure 400 is the pound-molecular weight in "round numbers" at room temperature.

Cubic feet of air required for maximum allowable concentration may be solved as follows:

$$\text{cu.ft./min. (air required)} = \frac{\text{cu.ft./min. vapor} \times 10^6}{\text{N.A.C.}} \tag{8}$$

Combining the two, we have:

$$\text{cu.ft./min. (air required)} = \frac{\text{lb. liquid solvent}}{\text{min.}} \times \frac{400}{\text{M.W.}} \times \frac{10^6}{\text{M.A.C.}} \tag{9}$$

Example 14 - Room 20 ft. wide x 45 ft. long x 12 ft. ceiling in which 5 lb. of ethyl acetate is released per hour.

Substituting values in above formula we have:

$$\text{cu.ft./min. required } \frac{5}{60} \times \frac{400}{88} \times \frac{10^6}{75} = 5{,}060 \text{ cu.ft./min.} \tag{10}$$

$$20 \times 45 \times 12 = 10{,}800 \text{ cu.ft.}$$

$$\frac{10{,}800 \text{ cu.ft.}}{5{,}060 \text{ cu.ft./min.}} = 2.13 \text{ min. A.C.}$$

Where flammable solvents are released within an area, explosive mixtures of vapor air may result. This mixture must be diluted below explosive range as soon as possible in order to insure safe operating conditions within the room.

Approximate limits of explosive range have been determined for many of the gases and vapors used in industry. This information is published from time to time by recognized sources. The lower limit per cent by volume, together with closed-cup flash point in F., are usually included in these tabulations.

In order to take care of possible variation and to insure a factor of safety, the quantity of air is sometimes (check with codes and other authorities) calculated to maintain an air vapor mixture equal to 1/3 of the lower explosive limit (1/3 L.E.L.). Where the L.E.L. of vapor is, say, 1-1/2%, this means the air vapor mixture after dilution would consist by volume of 1/2% vapor and 99-1/2% air.

Example 15 - Room 20 ft. wide x 45 ft. long x 12 ft. ceiling in which 5 gal. of solvent thinned paint is sprayed per hour.

How much air is required to dilute the vapor air mixture to 1/3 of lower explosive limit (L.E.L.).

The actual information on the formula of the paint sprayed must be obtained from the manufacturer. In this case, we will assume that the paint used weighed 8.1 lb./gal. of which 70% was solvent and 30% pigment, etc.

$$8.1 \text{ lb./gal.} \times 70\% \times 5 = 28.3 \text{ lb. of solvent/hr.}$$

The solvent in this case was a mixture of solvents with an average molecular weight of 60 and the L.E.L. is 1-1/2% by volume. Then we solve

$$\frac{\text{Wt.cu.ft. sol. at } 70°\text{F.}}{} = \frac{\text{av.mol.wt.sol.}}{\text{av. mol. of air}} \frac{60 \times 0.075 \text{ wt.air cu.ft. at } 70°\text{F.}}{29}$$

$$\text{Wt. of cu.ft. sol. at } 70°\text{F.} = 0.155 \text{ lb.}$$

$$28.3 \text{ lb.} \div 0.155 = 183 \text{ cu.ft. of solvent/hr.}$$

$$\frac{183 \text{ cu.ft. solvent}}{1/3 \text{ L.E.L.} = .33 \times 1.5\% = 1/2\% = 0.005} = 36{,}600 \text{ cu.ft. air vapor mixture}$$

$$\frac{36{,}600 \text{ cu.ft./hr.}}{60 \text{ min.}} = 610 \text{ cu.ft./min.}$$

$$20 \times 45 \times 12 = 10{,}800 \text{ cu.ft.}$$

$$\frac{10{,}800 \text{ cu.ft.}}{610 \text{ cu.ft./min.}} = 17.7 \text{ min. A.C.}$$

On this type of work, codes and other references give minimum air changes of 2 or 3 min. in order to insure good air movement through the room in order to prevent dead pockets.

Based on these recommendations we would have:

$$\frac{10{,}800 \text{ cu.ft.}}{3 \text{ min. A.C.}} = 3{,}600 \text{ cu.ft./min. required}$$

Where codes apply, use the air changes specified, but always check by dilution method and use the larger of the two quantities indicated.

Air volume required for dilution to M.A.C. is far greater than that required to dilute the same solvent below the L.E.L.

A list of some of the solvents follows:

Chemical Name	Cu.Ft.of Vapor per Pint of Liquid at 70 F.	Satisfactory Concentration for Human Exposure, 8 hr./day (p.p.m.)*	Explosive Range, % by volume	Closed-Cup Flash Point, °F.
Acetone	5.5	500	2.1-13.0	0
Amyl acetate	2.7	100	1.1	77
Carbon tetrachloride	4.2	25	--	--
Diethyl ether	3.9	500	1.7-48.0	-20
Ethyl acetate	4.1	75	2.2-11.5	24
Gasoline or napthta	3.0 approx.	500	1.3-6.5	-50
Toluene	3.8	200	1.3-7.0	40
Turpentine	2.6	100	0.8	95
Xylene	3.3	100	1.0-6.0	63

*Check requirements of state and local codes.

Special care must be exercised in both the above cases of toxic and explosive vapors that the process is closely studied to obtain a complete history of the cycle. In many cases, operating groups specify a quantity of material being handled in a given over-all time. This statement may be taken or assumed that the release of vapor is at a constant rate over the period stated.

Upon close study, it may develop that in a 1-hr. cycle, 20 min. is used in set-up time, 5 min. is used to remove finished object. Thus 25 min. of the 60 min. no vapor is released. In the remaining 35 min., it is possible that all of the vapor is released in 20 min. of this time.

Therefore, if the statement was made that 1 gal. of solvent was evaporated in 1 hr., and it was assumed that this accrued at a constant rate, then 1/60 would be released per minute.

If, actually, the release was completed in 20 min. of the hour, the system installed on the first assumption would have only 1/3 the required capacity.

The above is emphasized because failure of some systems to accurately take care of a requirement was the direct result of misunderstanding in statement of quantities used or lack of sufficient knowledge of the operation.

XIV. HOODS OR ENCLOSURES

We emphasized above that the first line of attack should be the entire enclosure or partial hooding of the area so as to prevent escape of contaminant into the operating area.

The efficient exhaust pattern of air into a hood opening has a very narrow zone of influence. Therefore, the exhaust must be placed close to the source of the material to be controlled. This fact dictates total enclosure wherever possible.

With unobstructed flow of air into a hood, the air velocity at any point along the axis of the hood may be determined by the formula:

$$V = \frac{0.1Q}{b^2 + 0.1A}$$

where

V = velocity, ft./min.
A = area of hood, sq.ft.
b = distance along axis, ft.
Q = volume of air handled, cu.ft./min.

Example 16 - Given 8-in. diameter pipe with 4,000 ft./min. velocity entering. What will be the velocity of air 6 in. in front of pipe?

Capacity of 8-in. pipe = 0.3491 sq.ft. x 4,000 ft./min. = 1,396 cu.ft./min.

substituting in formula:

$$\frac{0.1 \times 1396 \text{ cu.ft./min.}}{(0.5)^2 + (0.1 \times 0.3491)} = 488 \text{ ft./min.}$$

$$\frac{488}{4000} = 12.2\% \text{ of velocity at pipe face.}$$

See Figure 19 for general pattern of air velocities in front of exhaust pipe. After studying information on Figure 19 you will see why we emphasize the total enclosure or at least hood enclosure over the source of contaminant.

When flanges are installed around hood or pipe opening, the sneaking around of air into the hood is reduced, thus increasing the air flow in front of the hood. The height of the flanges should be approximately 1/3 the depth of the hood.

With the flanges, the air volume for a given velocity in the effective zone will be approximately 75% of the air volume required by an unflanged hood. (11)

Canopy or overhead type of hoods are most generally used over tanks, kettles, forges, and furnaces where smoke and vapors usually rise. The hood should extend beyond the tank 6 in. on all sides for an elevation of 2 ft. For each additional foot in elevation, the sides should be extended 6 in. more in each direction.

The bottoms of these hoods are usually equipped with a 6-in. apron and the bottom of the apron is installed as low as possible. It is preferable to extend the two sides and back aprons down to top of tank. This arrangement reduces the quantity of air required and minimizes the escape of fume due to cross-draft around the hood.

When the canopy-type hood is installed and there is a tendency for the fume to roll out under the hood, an inside baffle is sometimes installed. This baffle is so installed that a 3/4-in. to 1-in. slot is left between the baffle and the outer sides of the hood. There is also an opening provided in the center of the baffle under the exhaust pipe from the main hood.

The exhaust pipe from this type hood is generally 10 to 15% the area of the hood. This exhaust pipe area should be checked so that the leaving velocity through it is between 1,500 and 2,500 ft./min.

Where materials must be handled by overhead track systems and basket of part or heavy pieces are lowered vertically down into tank, then overhead- or canopy-type hoods cannot be used.

Cross-flow of air is then used. This flow is created by installing a horizontal slot and plenum along the back of the tank exhausting air across the open surface.

The slot height varies with the quantity of air handled; 2,000 ft./min. velocity in a 1-in. slot should take care of a tank not more than 18-in wide. If tank is wider than 18-in., slot should be installed on both sides of tank.

On tanks over 18-in., another method sometimes used is to maintain the 2,000 ft./min. velocity and increase the height of slot 1/4 in. for each additional 12-in. of width.

On long slots, the plenum duct must be designed to insure equal distribution of suction along each foot of length. The bottom of the slot should be at least 6-in. above the top of the tank to minimize entrainment of liquid from the tank.

The following gives a general pattern of velocities to consider maintaining across the open face of a hood depending on condition of release. The right-hand column gives some ideas as to the type process (1).

Condition of Generation of Contaminant	Min. Air Velocity ft./min.	Process
Released without noticeable movement	50 - 100	Evaporation of vapors, exhaust from pickling, washing, degreasing, plating, welding etc.
Released with low velocity	100 - 200	Paint spraying in booth; inspection, sorting, weighing, packaging, low-speed conveyor transfer point, rotating mixtures, barrel filling
Active generation	200 - 500	Foundry shakeout, high-speed conveyor transfer points, crushers, screens
Released with great force	500 - 2000 and higher	Grinding, tumbling mills, abrasive cleaning

For wood working, grinding, and buffing, and other processes, there are state codes that specify the size duct and cu.ft./min. to be handled for each size wheel.

After having decided on minimum face opening for the hood which will effectively control the contaminant and having established the necessary velocity of air flow, we arrive at the cu.ft./min. of air required for the different hoods.

Knowing the quantity of air required, the size of the duct may be computed from the following

$$A = \frac{Q}{V}$$

where

A = cross-section area of duct, sq.ft.

Q = air quantity to be handled by the duct, cu.ft./min.

V = velocity of air, ft./min.

For duct systems wherein no dust or solid material is conveyed, velocities from 1,200 to 2,000 ft./min. are desirable.

Where solid material is being conveyed the following gives approximate velocities to use (1).

Material Conveyed	Design Velocity, ft./min.
Vapors, gases, fumes, very fine dust	2,000
Fine dry dust	3,000
Average industrial dust	3,500
Coarse particles	3,500 - 4,500
Large particles, heavy loads, moist materials	4,500 and over

Higher velocities are sometimes required than the above when air is used for conveying material from one point to another.

GENERAL AIR ENGINEERING DATA

TABLE 1
Area of Circles

Dia.	Sq. Ft.
1½	.0123
2	.0218
2½	.0341
3	.0491
3½	.0668
4	.0873
4½	.1104
5	.1364
5½	.1650
6	.1964
6½	.2304
7	.2673
7½	.3068
8	.3491
8½	.3942
9	.4418
9½	.4923
10	.5454
11	.6600
12	.7854
13	.9218
14	1.069
15	1.227
16	1.396
17	1.576
18	1.767
19	1.969
20	2.182
21	2.405
22	2.640
23	2.885
24	3.142
25	3.409
26	3.687
27	3.976
28	4.276
29	4.587
30	4.909
32	5.585
33	5.940
34	6.305
36	7.069
38	7.876
40	8.727
42	9.621
45	11.045
48	12.566

TABLE 2
Velocity Pressure

WG	FPM
.10	1266
.15	1550
.20	1791
.25	2003
.30	2193
.35	2373
.40	2533
.45	2688
.50	2832
.55	2973
.60	3102
.65	3230
.70	3351
.75	3468
.80	3582
.85	3692
.90	3800
.95	3905
1.00	4005
1.10	4208
1.20	4390
1.30	4566
1.40	4735
1.50	4905
1.60	5065
1.70	5225
1.80	5380
1.90	5522
2.00	5684
2.20	5940
2.40	6210
2.60	6460
2.80	6700
3.00	6937
3.20	7170
3.40	7390
3.60	7600
3.80	7810
4.00	8010
4.20	8210
4.40	8400
4.60	8490
4.80	8590
4.80	8770
5.00	8950

TABLE 3
Temperature—Density

Temp. °F	Density Factor	Wt. Per Cu. Ft.
0	1.152	.0864
70	1.000	.0749
100	.946	.0709
150	.869	.0651
200	.803	.0602
250	.747	.0560
300	.697	.0522
350	.654	.0490
400	.616	.0462
450	.582	.0436
500	.552	.0414
550	.525	.0393
600	.500	.0375
650	.477	.0358
700	.457	.0342
750	.438	.0328
800	.421	.0315
850	.404	.0303
900	.390	.0292
950	.376	.0282
1000	.363	.0272

TABLE 4
Altitude—Density

Elev. In Ft.	Density Factor	Wt. Per Cu. Ft.
0	1.000	.0749
500	.981	.0735
1000	.962	.0721
1500	.944	.0707
2000	.926	.0694
2500	.909	.0681
3000	.891	.0668
3500	.874	.0655
4000	.858	.0643
4500	.842	.0631
5000	.826	.0619
5500	.810	.0607
6000	.795	.0596
6500	.780	.0585
7000	.766	.0574
7500	.751	.0563
8000	.737	.0552
8500	.723	.0542
9000	.710	.0532
9500	.697	.0522
10000	.685	.0514

TABLE 5—AIR VOLUME IN CFM HANDLED THROUGH BRANCH PIPES

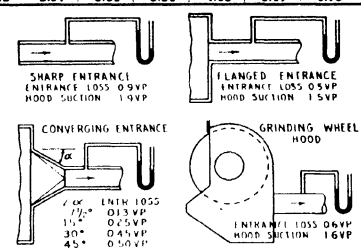
Diameter of Pipe	Velocity in Pipe in FPM								
	2000	2500	3000	3500	4000	4500	5000	5500	6000
1½"	25	31	37	43	49	55	62	68	74
2"	44	54	65	76	87	98	109	120	131
2½"	68	85	103	120	137	154	171	188	205
3"	98	123	147	172	197	221	246	270	295
3½"	134	167	200	234	267	300	334	367	400
4"	175	218	262	306	350	393	437	480	524
4½"	221	276	331	387	442	497	552	608	663
5"	273	341	409	478	546	614	682	750	818
5½"	330	413	495	578	660	742	825	908	990
6"	393	491	589	688	786	884	982	1080	1178
7"	534	668	802	936	1070	1204	1338	1472	1605
8"	699	874	1048	1220	1396	1571	1745	1920	2095
9"	882	1105	1325	1546	1766	1988	2210	2430	2650
10"	1092	1364	1637	1910	2182	2456	2730	3000	3278

TABLE 6—SUCTION IN INCH W.G. FOR VARIOUS ENTRANCE LOSSES
(Suction Equals 1 VP + Entrance Loss)

Entr. Loss in VP									
0.2	0.30	0.47	0.67	0.92	1.20	1.52	1.87	2.27	2.70
0.4	0.35	0.55	0.78	1.08	1.40	1.77	2.18	2.64	3.15
0.6	0.40	0.62	0.89	1.22	1.60	2.02	2.50	3.02	3.60
0.8	0.45	0.70	1.01	1.39	1.80	2.28	2.81	3.40	4.05
1.0	0.50	0.78	1.12	1.54	2.00	2.53	3.12	3.78	4.50
2.0	0.75	1.17	1.68	2.31	3.00	3.80	4.68	5.67	6.75

TABLE 7—Equivalent Resistance of Elbows and Branch Entries (in Feet of Straight Pipe)

Dia. of Pipe	90° Elbow Inside Radius 1 D	1½ D	2 D	Angle of Entry 30°	45°
3"	5	4	3	2	3
4"	7	5	4	3	5
5"	9	6	5	4	6
6"	11	7	6	5	7
7"	13	9	7	6	9
8"	14	10	8	7	11
10"	20	13	11	9	14
12"	25	17	14	11	17
14"	30	21	17	13	21
16"	36	24	20	16	25
18"	41	28	23	18	28
20"	46	32	26	20	32
24"	57	38	32		
30"	75	51	42		
36"	87	60	49		
For 60° Ell ... X .75					
For 45° Ell ... X .50					



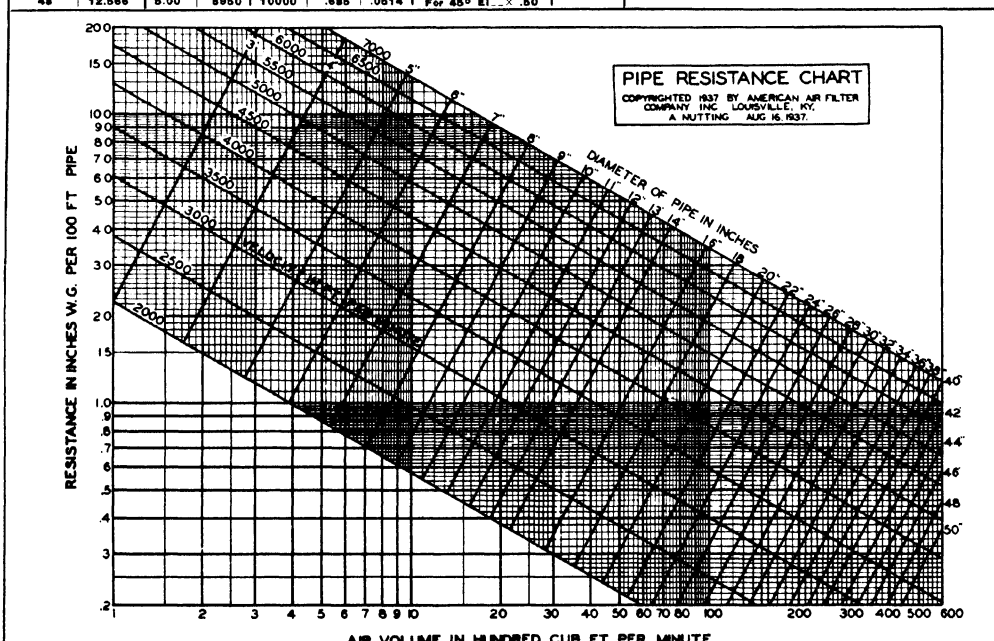


Figure 20.

The main duct may be sized from Figure 2 by totalling air quantities from the hoods and picking size of main at various points based on the cu.ft./min. of air being handled at that point.

Where material is contained in the air flow, the area of the main duct at any point will be equal to the sum of areas of all the branch ducts up to that point. Some state codes allow the area of the main to be equal to the sum of the areas of all branch pipes plus 20%. This large area main gives better distribution of pressure drop in the main. The velocity in the branch pipes must be high enough so that the reduced velocity that occurs in the main is still sufficient to convey the material.

Knowing the cu.ft./min. and duct size, the pressure drop may be calculated from Figure 2.

Elbows whose centerline radii vary from 100 to 300% of pipe diameter, the loss may be estimated from the following: (1)

Elbow Centerline Radius in % of Pipe Diameter or Depth	Approximate Loss in % of Velocity Head
50	75
100	26
150	17
200 - 300	14

It is sometimes convenient to express the resistance of an elbow in terms of an equivalent length of duct of the same diameter. Thus with a centerline radius equal to the pipe diameter, the resistance is equivalent to a section of straight pipe approximately 10 diameters long, while with a centerline radius 1-1/2 times the diameter, the resistance is apparently the same as that of seven diameters of straight pipe.

Miscellaneous pressure drops are shown on Figure 20 and Figure 21.

Exhausting air through a hood is associated with an entrance loss. This loss is usually figured in per cent of velocity head and varies from 0.03 to 0.90 velocity head - open ended pipe entrance - no flange. Suction, in inches of water measured in pipe connections adjacent to hood, will indicate one velocity head equal to velocity of air in pipe plus fraction of velocity head loss.

Some state codes specify suction in in. of water that must be maintained in take-off connection.

Knowing the suction at this, the volume of air handled from the hood is shown in the following:

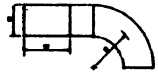
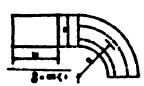
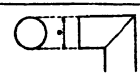
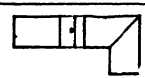
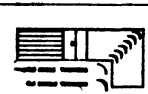
Cubic Foot of Air at 0.075 Density Handled per Minute through Average Collecting Hoods - Based on Entry Coefficient of 0.71 with 10% Added for Leakage (11)

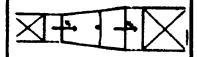
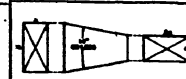
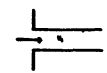
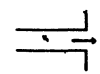
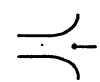
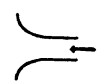
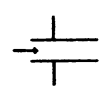
Diameter of Connection Pipe, in.	Maintained Suction - in. water gauge						
	1"	1-1/2"	2"	2-1/2"	3"	4"	5"
	3130 ft./min.	3830 ft./min.	4430 ft./min.	4950 ft./min.	5420 ft./min.	6260 ft./min.	7000 ft./min.
1-1/2	38	47	54	61	67	76	86
2	68	84	97	108	118	136	153
2-1/2	107	131	151	168	185	214	238
3	153	188	217	243	266	306	343
3-1/2	209	256	296	330	362	418	466
4	273	334	386	431	473	546	609
4-1/2	345	423	488	546	598	690	775
5	427	523	605	676	741	854	955
6	614	751	867	970	1062	1228	1373
7	835	1023	1181	1322	1448	1670	1870
8	1092	1337	1546	1727	1892	2184	2440
9	1381	1694	1953	2184	2387	2762	3091
10	1705	2090	2409	1695	2559	3410	3806

Pressure drop through collecting equipment or discharge stacks should be added to duct losses to arrive at total amount of static pressure that fan must develop.

XV. DUCT CONSTRUCTION FOR EXHAUST AND CONVEYING SYSTEMS

The interior of all ducts (1) should be smooth and free from obstructions at joints, and soldered or welded air-tight. Other sealing mediums are permissible where soldering is impracticable.

Element	Illustrations	Conditions	Value of n
Round Radius Elbow		$\frac{R}{D}$ = .5	.73*
		.75	.38
		1.0	.26
		1.5	.17
		2.0	.15
Rectangular Radius Elbow		$\frac{W}{D}$ $\frac{R}{D}$	†
		0.5 { .5	1.3
		0.5 { .75	.47
		0.5 { 1.0	.28
		0.5 { 1.5	.18
		1 to 3 { .5	.95
		1 to 3 { .75	.33
		1 to 3 { 1.0	.20
		1 to 3 { 1.5	.13
Rectangular Radius Elbow		No. of vanes $\frac{R}{D}$	†
		1 { .5	.70
		1 { .75	.16
		1 { 1.0	.13
		1 { 1.5	.12
		2 { .5	.45
		2 { .75	.12
		2 { 1.0	.10
		2 { 1.5	.15
Round Section Mitre Elbow		.....	.87*
Rectangular Section Mitre Elbow		.....	1.25†
Rectangular Section Square Elbow		(a) with single thickness turning vanes	.35‡.
		(b) with double thickness turning vanes	.10†
Radius Tee		Consider equal to an elbow. Base loss on entering velocity.	
Rectangular Tee			

Element	Illustrations	Conditions	Value of n
45° Elbow		Either rectangular or round; vaned or unvaned.	½ of value for similar 90° elbow
Expansion		a = 5°	.17
		a = 10°	.28
		a = 20°	.45
		a = 30°	.59
		a = 45°	.73
		Loss referred to $(h_{v_1} - h_{v_2})$	
Contraction		a = 30°	.02
		a = 45°	.04
		a = 60°	.07
		(Loss referred to V_2)	
Transformer		.....	.15
Abrupt Entrance		.....	.50
Abrupt Exit		.....	1.0
Bell-Mouth Entrance		.....	.03
Bell-Mouth Exit		.....	1.0
Re-Entrant Entrance		.....	.85

* Frank L. Busey, *Trans. A.S.H.V.E.*, 1913.
† Madison and Parker, *Trans. A.S.M.E.*, Vol. 58, April, 1936.
‡ A. L. Brown—Power Plant Eng. 6/15/32.

Figure 21.

Ducts should be constructed of galvanized sheet metal except when the presence of corrosive fumes or gases, temperatures above 400 F., or other factors would make galvanized matter impractical.

For the usual exhaust system, use the following gauges of metal:

Diameter of Round Pipe or Greatest Dimension of Rectangular Pipe, in.	Thickness of Duct Material U.S. Gage Number	
	For Highly Abrasive Material	For Other Matter
Up to 8 inclusive	20	22
Over 8 to 18 inclusive	18	20
Over 18 to 30 inclusive	16	18
Over 30	14	16

Elbows and angles should be a minimum of two gages heavier than straight lengths of equal diameter. Hoods should be a minimum of two gages heavier than straight sections of a connecting branch.

Longitudinal joints of ducts should be lapped and riveted or spot-welded on 3-in. centers maximum. Girth joints or ducts should be made with lap in direction of air flow, with 1-in. lap for duct diameters through 19 in. and 1-1/4-in. lap for diameters over 19 in. Elbows and angles should have an inside or throat radius of two pipe diameters whenever possible. Large radii are recommended for heavy concentrations of highly abrasive dusts. Elbows 6 in. or less in diameter should be constructed of at least five sections and, if over 6 in. in diameter, of seven sections, with angles pieced proportionally. Hoods should be free of sharp edges or burrs and reinforced to provide necessary stiffness. Transitions in mains and sub-mains should be tapered with a taper 5 in. long for each 1-in. change in diameter whenever possible. All branches should enter the main at the large end of the transition at an angle not to exceed 45 or preferably 30 . Branches should be connected only to the top or sides of mains, with no two branches entering diametrically opposite to each other. Dead-end caps should be provided within 6 in. from last branch of all mains and sub-mains. Cleanouts should be provided every 10 ft. and near each elbow, angle, or duct junction in horizontal sections. Ducts should be supported sufficiently to place no load on connected equipment and to carry weight of a system plugged with material. The maximum distance between supports should be 12 ft. for 8-in. or smaller ducts and 20 ft. for larger ducts. Six inches minimum clearance should be provided between ducts and the ceiling, wall, or floor. Blast gates for adjustment of the system should be placed near the connection of a branch to the main and means of locking gates after the adjustments have been made should be included. Rectangular ducts should be used only when clearances prevent the use of round construction. Rectangular ducts should be as nearly square as possible. The weight of metal and the lap, and other construction details, should be the equal of round duct construction having a diameter equal to the longest side. All pipes passing through roofs should be equipped with collars so arranged as to prevent water from leaking into the building.

The main trunks and branch pipes should be as short and straight as possible.

Either a large cleanout door should be placed in the main suction pipe near the fan inlet, or a detachable section of pipe, held in place by lug bands, may be provided.

No fixed screens should be placed in pipes, although the use of a trap at junction of the hood and branch pipe is permissible, provided it is not allowed to fill up completely. The passing of pipes through fire-walls should be avoided whenever possible, and floor sweep connections should be so arranged that foreign material cannot be easily introduced into them.

Contaminants in exhaust air in many cases cannot just be blown through the roof or the outside wall and be forgotten. The relation between air supply intake and exhaust air discharge must be so located that the discharge does not contaminate the supply air.

The discharged air also must have contaminants removed or so diluted that they are below the allowed M.A.C. In some cases, the contaminants have a salvage value so that elaborate arrangements can be justified for their collection.

The best type of collector must be selected to meet the requirements of the particular material.

In cases where the contaminants are only a nuisance and not a hazard, the main requirement is to discharge them so they do not resettle in occupied areas.

Tall stacks are usually considered for this purpose.

After the exhaust air is discharged from the top of the stack, the mixture will be further diluted with outside air as it drifts toward the ground. In the absence of downdrafts, the mixture may reach the ground at a distance from the stack, equal to 6 to 20 times the stack height. An average figure of 10 times the height of the stack often is used.

Stack location and weather greatly influence dissipation of the contaminants, as well as height of stack.

State health organizations are becoming active on air pollution problems which usually assume legal aspects; therefore, specialists in this type of work should be consulted before releasing designs.

After the most complete calculations have been made to obtain the total amount of static pressure the fan must handle, some systems fail to handle the required amount of air because no provision has been made to allow air to enter the room to replace the air being exhausted. This shows up in the winter time when windows and doors are usually kept closed because of drafts.

With starved rooms, the amount of air exhausted may be reduced to such a degree that the contaminant excapes out into the operating area. Also when a room is put under a suction sometimes it is difficult to open or close doors. Also the room is drafty due to air being pulled into the room through cracks or other openings.

The above information was to acquaint you with the feel of applying your fluid flow studies to ventilating problems. As you have seen, ventilation deals mostly with the handling of air. The handling of water, steam, and condensation is involved in a much less degree and was not touched upon because of the limited time and because the theory was given in previous lectures.

If you become thoroughly familiar with the above, you will have the foundation on which to base calculations for figuring a ventilation system. Actual experience is required to lay out a successful operating system. Ventilation has come a long way from being a rule-of-thumb proposition; it has become an art and is fast becoming a science, but at the present time, it is not an exact science, as there is much that must be determined by research.

*

Chapter 12

PARTICLE TECHNOLOGY

by

C. E. Lapple*
Engineering Research Laboratory,
Engineering Department
E. I. du Pont de Nemours & Co., Inc.
Wilmington, Delaware

TABLE OF CONTENTS

	Page
I. References	268
II. Properties of Particle Dispersoids	268
A. Particle Size	268
B. Particle Shape	269
C. Particle Surface	269
D. Uniformity or Size Distribution	269
E. Physical, Chemical, and Physiological Properties	269
III. Methods of Particle Size Representation	270
A. Frequency Distribution	270
B. Cumulative Distribution	270
C. Analytical Relationships	270
D. Log-Probability Plot	271
IV. Sampling of Dispersoids	271
A. Atmospheric Pollution Measurements	271
B. Process Gas Sampling	272
V. Particle Size Analysis	272
VI. Problems	275

LIST OF FIGURES

Figure 1. Typical Frequency Particle Size Distribution Plots 270
Figure 2. Typical Cumulative Particle Size Distribution Plot 271
Figure 3. Log-Probability Graph Paper (Codex Book Co. No. 3228) 271

LIST OF TABLES

Table I. Tyler and U. S. Standard Screen Scales 268
Table II. Outline of Methods for Particle Size Analysis 272

*Present address: Associate Professor, Dept. of Chem. Engineering, Ohio State University, Columbus, Ohio.

I. REFERENCES

1. British Standards Institution, "The Method of Testing Dust Extration Plant and the Emission of Solids from Chimneys of Electric Power Stations" London, April, 1940.
2. Dalla Valle, J. M., "Micromeritics," 2nd Ed., New York, Pitman Publishing Corp., 1948.
3. Drinker, P. and Hatch, T., "Industrial Dust," New York, McGraw-Hill Book Co., 1936.
4. Gibbs, W. E., "Clouds and Smokes," Philadelphia, P. Blakiston's Son and Co., 1924.
5. Hatch, T., J. Franklin Inst., 215, 27-37 (1933).
6. Hatch T. and Choate, S. P., J. Franklin Inst., 207, 369-87 (1929).
7. Heywood, H., Proc. Inst. Mech. Engrs., (London), 140, 257-347 (1938); Engineering, 146, 492-4 (1938).
8. Institution of Chemical Engineers and Society of Chemical Industry, Road and Building Materials Groups, Symposium on Particle Size Analysis, London, Feb. 4, 1947 (A collection of eleven papers).
9. Lapple, C. E., Heating, Piping, and Air Conditioning, 16, 410-4, 464-6, 578-81, 635-40 (1944); 17, 611-5 (1945); 18, 108-13 (1946).
10. Schweyer, H. E., and Work, L. T., Am. Soc. Testing Materials, "Symposium on New Methods for Particle Size Determination in the Subsieve Range," pp. 1-23, March 4, 1941.
11. Whytlaw-Gray R. and Patterson, H. S., "Smoke," London, Edward Arnold and Co., 1932.

II. PROPERTIES OF PARTICLE DISPERSOIDS

A. Particle Size: The primary distinguishing feature of a particle is particle size. The most widely used unit of particle size is the micron.

$$1 \text{ micron } (\mu) = 0.001 \text{ mm} = 10^{-4} \text{ cm.}$$
$$= (1/25{,}400) \text{ in.} = 3.28 \times 10^{-6} \text{ ft.}$$
$$1 \text{ millimicron } (m\mu \text{ or } \mu\mu) = 0.001 \text{ micron}$$
$$1 \text{ Angstrom unit } (\text{Å}) = 0.1 \text{ millimicron} = 10^{-8} \text{ cm.}$$

The term "particle size" generally refers to the average or equivalent diameter of a particle though some writers (particularly German) specify particle size by the radius. Another common method of specifying particle size is to designate the screen mesh which has an aperture corresponding to the particle diameter. Since various screen scales are in use, confusion may result unless the screen scale involved is specified. The screen mesh generally refers to the number of screen openings per unit of length or area. The aperture for a given mesh will depend on the wire size employed. The Tyler and the U. S. Standard Screen Scales are the most widely used in the United States.

TABLE I. TYLER AND U. S. STANDARD SCREEN SCALES.

Tyler Mesh	Aperture Microns	U. S. Mesh	Aperture Microns
400	37	400	37
325	43	325	44
270	53	270	53
250	61	230	62
200	74	200	74
170	88	170	88
150	104	140	105
100	147	100	149
65	208	70	210
48	295	50	297
35	417	40	420
28	589	30	590
20	833	20	840
14	1168	16	1190
10	1651	12	1680

Particle sizes of greatest interest in chemical engineering are generally in the range of 0.1 to 1000 microns for gas dispersoids (aerosols) and 0.01 to 100 microns for liquid dispersoids (hydrosols). Colloid chemistry is concerned chiefly with hydrosols finer than 1 micron. It should also be noted that there is at present considerable confusion in specifying particle dispersoids due to a lack of standardization in terminology. The following approximate values should assist in formulating a physical concept of such fine particles:

Limit of resolution with naked eye:	10 to 40 microns
Diameter of large molecules:	0.005 microns
Wavelength of visible spectrum	0.4 to 0.7 microns
Diameter of human hair	50 to 200 microns
Atmospheric dust	0.5 microns
Flour	10 to 100 microns
Pigments	0.2 to 2 microns
Sulfuric acid mist	0.5 to 15 microns
Tobacco smoke	0.2 microns
Talcum powder	2 to 20 microns

B. Particle Shape: In order to define a particle it is necessary to specify its shape as well as its size. For regular particles this can be done by specifying actual or relative characteristic dimensions. However, most particles encountered in practice are irregular. Even in the case of regular particles it is very difficult to measure all characteristic dimensions. Consequently various methods have been devised for assessing particle shape. These are discussed in more detail in References 2, 7, and 8. However, no satisfactory universal method has yet been devised and the method used is dependent on the ultimate purpose of the shape specification. For many practical purposes it is sufficient to assume the particles spherical or to incorporate a shape factor in the expression of particle size by stating an apparent size as defined by the method of size analysis.

C. Particle Surface: While particle surface is determined directly by the size and shape of a particle, the surface is often related more directly to the specific external manifestations exhibited by particles. The creation of additional surface involves a change in intrincic energy which distinguishes many of the characteristics of a particle from those of the same material in solid bulk. The importance of the state of subdivision of a material can be better appreciated when the increase in free surface area is realized as shown in the following tabulation for spherical particles of a specific gravity of 2.0:

Particle Diameter	Specific Surface sq. ft./lb.
1 inch	0.6
1 mm.	15.
100 micron	150.
10 microns	1,500.
1 micron	1.5×10^4
0.1 micron	1.5×10^5
0.01 micron	1.5×10^6

D. Uniformity or Size Distribution: Natural or synthetic particulate systems rarely consist of particles of a given size. Instead, a range of particle sizes is generally encountered. Thus to specify a particulate system, it is necessary to define not only the size and shape of the individual particles but also the relative amounts of each type particle. This is known as a particle size distribution and represents a measure of the uniformity of the system from a size standpoint.

E. Physical, Chemical, and Physiological Properties: The reduced size and extended surface of particulate materials bring into prominence manifestations which are normally negligible in bulk materials. Some of these properties become more and more pronounced as particle size decreases. Others, such as some of the optical properties, reach a peak at sizes in the neighborhood of the wavelength of light. Some properties, such as particle inertia (as evidenced by settling velocity, for example), become increasingly less significant as particle size is reduced and may be entirely negligible for very fine particles. Particulate systems may also present definite engineering problems that may not be encountered in the bulk materials such as health and explosion hazards. Substantially all combustible materials present explosion potentialities in finely divided state. Sand is not considered a health hazard. In finely divided state (less than 10 microns diameter), however, it presents a serious health hazard.

The resultant pulmonary disease known as silicosis has been the subject of extensive studies and legislation. The properties of particulate substances are discussed in detail in References 2, 3, 4, 9, and 11.

III. METHODS OF PARTICLE SIZE REPRESENTATION

As previously mentioned, actual particulate systems are composed of a distribution of sizes. Various methods have been proposed for representing particle size distribution.

A. Frequency Distribution: The most common method is the frequency curve in which the number or weight of particles in a given incremental size range is plotted against the average particle size of the range as shown in the following sketch:

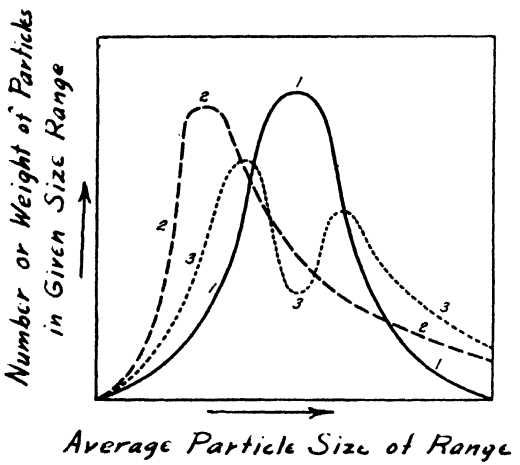


Figure 1. Typical Frequency Particle Size Distribution Plots

Physical laws controlling the formation of particulate systems, whether by comminution or otherwise, tend to form a preferential particle size. As a result particle size frequency distributions tend to approximate a probability relationship with a peak at the preferential size. A normal probability distribution (Curve 1) is approximated by some systems having relatively uniform particle size distributions. Most systems, however, yield a skewed frequency distribution (Curve 2). Some particulate materials may show more than one peak or preferential size, (Curve 3). This is common where particulate materials formed in separate natural or industrial processes are blended, especially where a wide difference in size exists, or in a mixture of physically heterogeneous particles.

In frequency distributions it is essential that a uniform system of selecting the extent of the incremental size range be adhered to in order to obtain an interpretable distribution plot. This fact is not usually stated in publications on the subject, but is generally implied. For a given particulate material an infinite number of frequency distribution curves can be obtained depending on the method of selecting the incremental size range. The most common method is to select equal arithmetic increments of diameter for making the count. In one method the frequency is divided by the size increment involved and the quotient is plotted against some function of the size. This is what is often termed a "per cent per micron" frequency and is, in effect, the equivalent of using an increment of one micron throughout. This method has the advantage that no strict system of selecting increments need be adhered to. In the log-probability type of frequency, which will be discussed below, equal increments of the logarithm of diameter are taken. This is the equivalent of splitting the particle size range into increments bounded by diameters having the same ratio to each other. This is automatically the case where a standard Tyler screen analysis is made since successive sieve apertures increase in the ratio of the square root of 2, or the fourth root of 2, depending on the screen series employed.

B. Cumulative Distribution: A second method of representing particle size distribution which is generally more convenient in application is the cumulative curve, in which the fraction of the total number or weight of particles which have a diameter greater (or less) than a given size is plotted against the size.

C. Analytical Relationships: In order to facilitate interpretation, manipulation, extrapolation, or interpolation, various analytical relationships have been proposed to represent both frequency and cumulative particle size distributions. The more outstanding relationships are those proposed by Gaudin, Roller, Griffith, Rosin, and Rammler, and the arithmetic and log-probability frequency distributions. These are discussed in detail in Ref. 9. While all these have special merit in particular applications, none is completely satisfactory or universally applicable. While most materials will follow one or the other of these relationships over a specific size range, they usually tend to deviate, sometimes very widely, at the extreme ends of the particle size range. (See Figure 2). This is essentially an integrated form of the frequency curve.

p. 270 - The last sentence on the page and the phrase (see Fig. 2) are misplaced. They should be at the end of the second last paragraph. (The original manuscript shows it correctly).

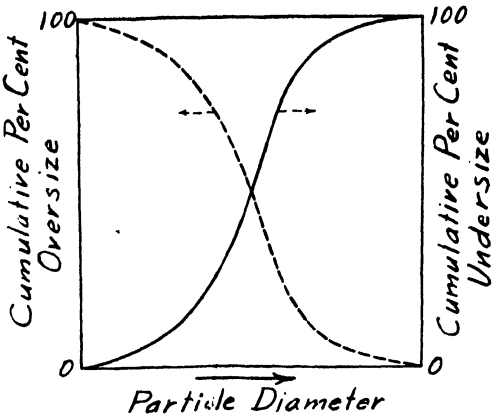


Figure 2. Typical Cumulative Particle Size Distribution Plot

D. Log-Probability Plot: Many materials will tend to approximate a normal probability curve when number or weight frequency is plotted against the logarithm of diameter. Such a frequency distribution can be represented analytically and can be integrated to obtain a cumulative curve by use of tables of the probability integral (9). A graph paper based on this relationship is commercially available (Codex Book Co., Norwood, Mass., Catalog Number 3228) and presents particle diameter on a log scale vs. cumulative per cent larger or smaller than the size on a suitable probability scale as shown in Figure 3.

If a particulate material follows a log-probability frequency distribution, it will plot as a straight line on this graph paper. The distribution can then be completely defined by the geometric mean diameter, corresponding to the 50% cumulative size, and the standard deviation, which is a number greater than unity and numerically equal to the ratio (or inverse ratio as required to give a value greater than unity) of the 50% cumulative size to the 84.13 or 15.87% cumulative undersize or oversize. A distribution plotted on this paper on both a number and a weight basis will yield straight parallel lines. These lines have the same standard deviation and the geometric mean diameters for the two bases are related by a simple analytical expression (5). Other particle properties, such as specific or total particle surface can be computed directly from the geometric mean diameter and standard deviation by simple analytical expressions as discussed in detail in Reference 6.

If the particulate material does not follow a log-probability frequency distribution, it will plot as a curve on this paper. However, this graph still offers a convenient means for representation since the curvature is generally not very great. While analytical conversion to other particle properties cannot be made in a strict sense, it is frequently possible to do so with reasonable accuracy by using straight line approximations for the distribution.

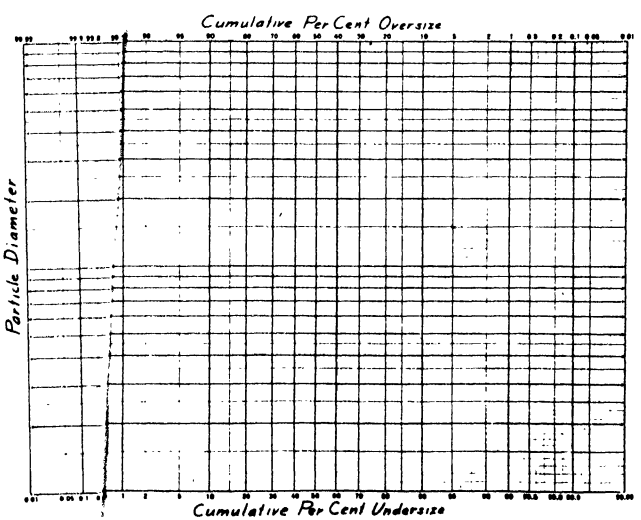


Figure 3. Log - Probability Graph Paper

IV. SAMPLING OF DISPERSOIDS

The sampling of dispersoids differs from ordinary sampling of homogeneous fluids in the provisions that must be made to allow for the differences in the inertia of the dispersed and dispersing phases to avoid segregation or classification of the phases. Usually this is only a major problem with gas dispersoids and most techniques have been developed specifically for such applications. Where liquid dispersoids or suspensions involve relatively large particles, however, the same problems will arise and the same principles will apply.

A. Atmospheric Pollution Measurements: A wide variety of techniques and instruments have been developed for measurement of atmospheric dispersoids. Most of these furnish only empirical and relative evaluations. The simplest

is the dust fall measurement in which a receptable of specified size and shape is located above the roof of a building and allowed to accumulate settled dispersoids over a specified time period. Another method often specified in smoke abatement legislation is the Ringelmann chart which consists of a series of six grids of varying blackness density. The smoke nuisance rating of a stack is determined by visual comparison of the stack discharge with the chart. Atmospheric dust concentration measurements are made by four general types of equipment: the impinger, the hot-wire or thermal precipitator, the alternating current precipitator, and the thimble or filter. A number of variations of instruments in each of these categories is available. A more detailed discussion of this specialized phase of gas dispersoid sampling is given in References 3 and 9.

B. Process Gas Sampling: In sampling process gases either to determine dust concentration or to obtain a representative dust sample, it is necessary to take special precautions to avoid inertial segregation of the particles. To prevent such classification a traverse of the duct must be made and at each point the sampling nozzle must face directly into the gas stream with the velocity in the mouth of the nozzle equal to the local gas velocity at that point. If the sampling velocity is too high, the dust sample will contain a lower concentration of dust than the main stream with a greater percentage of fine particles; if the sampling velocity is too low, the dust sample will contain a higher concentration of dust with a greater percentage of coarse particles. Sampling nozzles have been constructed in which velocity balancing is achieved automatically. Details of sampling nozzles and sampling techniques are discussed in References 1 and 9.

V. PARTICLE SIZE ANALYSIS

The term "particle size analysis" as applied in practice is misleading since most methods of particle size analysis do not measure particle size. Instead they usually measure other properties of the particle which are then converted to an apparent or effective particle size by means of analytical or empirical relationships, many of which incorporate various assumptions in order to permit such a conversion. For extreme particle shapes the particle size analysis can be widely different depending on the method employed. For this reason the method for making a size analysis should be carefully considered in terms of the purpose for which the size analysis is required.

In Table II is given an outline of available methods for particle size analysis. Where feasible, this table also indicate the approximate size range of applicability of each method together with the names of some of the outstanding apparatus in each category. Further detail or sources of detail for most of these methods are given in References 2, 7, 8, 9, and 10.

Table II. Outline of Methods for Particle Size Analysis

I. Sieving Methods - Range over 40 μ
   A. Dry - Tyler Ro-Tap
   B. Wet
II. Microscopic Methods
   A. Light Microscope - Range 0.1 to 50 μ
   B. Ultramicroscope - Range 0.005 to 0.1 μ
   C. Electron microscope - Range 0.005 to 15 μ
III. Settling Velocity Methods
   A. Elutriation - Range 5 to 100 μ
      1. Single Fractionation
         a. Air - Roller, Federal Pneumatic
         b. Water - Schöne
      2. Series Fractionation
         a. Air - Gonell, Haultain "Infrasizer"
         b. Water - Andrews
   B. Decantation - Cummings - Range 1 to 100 μ
   C. Sedimentation
      1. Point Source Methods
         a. Gravity - Palo Travis, Werner
         b. Centrifugal - Layer method
      2. Dispersion Methods
         a. Gravity - Range 1 to 40 μ
            1) Integral
               a) Sedimentation Balance - Oden
               b) Manometer - Wiegner

(Continued on next page)

p. 272 - line 27 (2nd line in 4th paragraph): the word "indicate" should be "indicates".

Table II. Outline of Methods for Particle Size Analysis

- 2) Differential
  - a) Pipette - Andreasen
  - b) Hydrometer
  - c) Manometer
  - d) Turbidimeter
- 3) Photographic - Carey and Stairmand

b. Centrifugal
- 1) Centrifuge - Range 0.05 to 10 μ
- 2) Supercentrifuge - Range 0.03 to 1 μ
- 3) Ultracentrifuge - Range 0.001 to 1 μ

IV. Surface Area Methods
- A. Turbidimetric
- B. Permeability
  - 1. Gas
  - 2. Liquid
- C. Adsorption
  - 1. Gas
  - 2. Liquid
  - 3. Dyes
  - 4. Radioactive materials
- D. Energy
  - 1. Heat of solution
  - 2. Heat of wetting
  - 3. Coercive force

V. Miscellaneous Methods
- A. Light Diffraction and Scattering
- B. X-Ray Diffraction
- C. Spectral Transmission
- D. Electrostatic Fields
- E. Ultrafilters
- F. Brownian Movement
- G. Electronic Count - Guyton

Sieving is one of the oldest and most direct methods of size analysis but is limited to relatively large particles. A sieve analysis generally involves placing a dry sample into the top or coarsest screen of a nest of screens and shaking by hand or by a mechanical device such as the Tyler Ro-Tap. Where considerable fines are present, it may be advantageous to first perform a wet screening to wash out the fines.

In the light or electron microscope, a size analysis is obtained by counting and measuring particles in a given field. The method is quite direct but is laborious and limited to relatively closely-sized particle fractions. The ultramicroscope does not show the particles directly, only the beams of light scattered or refracted from the particles. Considerable technique is required in its use and it yields only an average particle size.

In settling velocity methods use is made of the fact that small particles settle at constant velocity in a fluid according to known laws. Particle size is generally reported as the size of spherical particle of the same density which has the same settling velocity as the particle in question. In elutriation analyses, particulate materials are separated into sized fractions, analogous to those obtained with screens, by the upward motion of a fluid stream which carries with it those particles that are too fine to settle against the upward fluid velocity. In single fractionation elutriators, the particulate material is treated in a single chamber to obtain a single fine fraction. The remaining course fraction is then successively treated in a different chamber or at different fluid flow rates to obtain successively coarser fine fractions. The most widely used instrument in this category is the Roller particle size analyser in which air is used as the elutriating fluid. In a series fractionation elutriator, the fines are carried continuously to successively larger chambers in series so that at the end of the elutriation all of the material is distributed as sized fractions of successively finer size at the base of each chamber. The lower limit of particle size for which elutriators may be used is determined by the time required to effect a separation at the relatively low velocities required with small particles.

In the decantation method, a suspension is allowed to settle for a specified time period, whereupon the liquid above a fixed level is rapidly withdrawn. The sediment is redispersed and the process repeated numerous times. The solids filtered from all the decanted portions of fluids represent the material finer than a predetermined size whereas the final sediment represents the material larger than this size.

In sedimentation analyses, the particles are allowed to settle through a still fluid under the action of gravity or a centrifugal field and differ from elutriation in that the fluid is at rest. Sedimentation methods are inherently capable of a sharper fractionation than elutriation methods due to the difficulty of obtaining a completely uniform fluid velocity across the cross-section of the elutriation tube. Practically, however, equally reliable size analyses can be obtained by both methods due to a compensating effect in the degree of overlap of the fractions obtained by elutriation. Sedimentation analyses are limited almost exclusively to settling in liquids. Sedimentation methods, as well as liquid elutriation methods, require the addition of a dispersion agent to achieve proper dispersion of the particulate material. Failure to secure proper dispersion is the most frequent source of error and this phase must always be carefully checked before attempting an analysis. The lower particle size limit of sedimentation analyses is determined by the point at which thermal eddy currents, Brownian movement, and colloidal properties become appreciable with respect to the particle settling velocity.

The most elementary type of sedimentation analysis is that in which a liquid suspension of particles is introduced in the top of a column of clear liquid and the amount of sediment at the bottom of the column is observed at given time intervals. This method is not very accurate and is limited to routine control work due to the difficulty in obtaining complete particle dispersion and the large eddy currents set up in the initial introduction of the suspension. A centrifugal "layer" method employing dilute suspensions in a less dense liquid layer above the sedimentation liquid has overcome some of these objections.

The more reliable methods of sedimentation analysis are those in which an initially homogeneous dispersion is allowed to settle out. In the integral method either the total weight of solids between two levels, usually between the liquid surface and some point near the bottom of the sedimentation tube, or the total weight of solids settled out, is measured at given time intervals after sedimentation has commenced. The size distribution is obtained from the slopes of the weight-time curve obtained. In the differential methods the solid concentration is measured at some point above the bottom of the tube at various times after sedimentation has started. The concentration-time curve obtained gives a direct measure of the size distribution. Due to the errors inherent in obtaining slopes, the differential methods are generally more accurate than the integral methods. Of the differential methods, the pipette method is probably the most reliable. In this, a sample is withdrawn from a given level at specified time intervals by means of a pipette and analyzed gravimetrically or otherwise for solids content. The hydrometer method is probably the simplest and some available data indicate it to be substantially as reliable as the pipette method. In the hydrometer method, the average concentration of solids in a fixed increment of depth is measured directly by means of a hydrometer at specified time intervals. The use of turbidimetric (or photometric) methods to measure concentration at a given level offers promise of a method which is still simpler than the hydrometer. However, except for cases where sufficient calibration data are available, its accuracy is questionable since the basic relationships between optical properties and particle size have not yet been fully developed.

Carey and Stairmand have developed a photosedimentation method in which the tracks of particles, falling under the action of gravity, are photographed. The size distribution is obtained by counting and measuring the length of the tracks. This method, while capable of great accuracy, is quite laborious and requires relatively expensive equipment.

The sedimentation methods of size analysis have been extended to very fine particles by employing a centifugal field in place of gravity to increase the settling rates of the particles. The ultracentrifuge developes centrifugal fields as high as 750,000 times gravity and has been employed to measure the particle size or size distribution of large molecules.

There are a wide variety of methods which involve essentially a measure of the total surface of a particulate substance. These methods do not yield a size distribution although some have been used in conjunction with sedimentation methods for this purpose. Instead they yield only a single average particle size for the sample as defined by the total particle surface. This information is adequate, however, for many purposes. The permeability method has recently received much prominence and is very simple and rapid. It depends on the measurement of the resistance of a bed of particles to the flow of a fluid through it. This measurement can be translated in terms of total surface by established relationships.

A large number of miscellaneous methods exist, some of the more common of which are listed in Table II. Most of these methods are applicable for special purposes and usually yield only an average particle size, not a size distribution. The electronic count method of Guyton is a very recent development for measuring size distribution which offers promise of a rapid method of size analysis but still requires considerable development work before it is available for general application.

VI. PROBLEMS

1. Given the following microscopic particle count of a powder:

Range of Size Microns	Number of Particles in Range	Range of Size Microns	Number of Particles in Range
0-1	416	12-16	3
1-2	201	16-20	1
2-4	124	20-25	0
4-6	34	25-30	1
6-8	13	30-35	1
8-10	6	35-40	0
10-12	3	>40	0

Convert this count to a cumulative weight size distribution by: (1) numerical calculation; and (2) by conversion of the cumulative count analysis by means of the Hatch algebraic method using log-probability paper.

2. In the above example, calculate the specific surface of the powder in sq.ft./lb. of powder by: (1) numerical calculations; and (2) by algebraic calculation from the cumulative count analysis using log-probability paper.

3. Calculate and compare the particle size distribution curves which would be obtained for a powder in which 70% of the particles on a weight basis are larger than 2 microns in diameter and 10% are larger than 10 microns if the size distribution followed the following relationships: (1) log-probability; (2) arithmetic probability; (3) the Rosin-Rammler relationship; (4) the Roller equation; (5) the Gaudin-Schuhmann relationship. (Note: See pp. 108-113 of Reference 9.)

4. Discuss the important factors to be considered in sampling suspensions of particulate materials and show how these are taken into account in available sampling instruments.

5. Why will air elutriation and liquid sedimentation particle size analyses usually be incompatible for cellular or porous particles?

Chapter 13

PARTICLE DYNAMICS

by

C. E. Lapple*
Engineering Research Laboratory
Engineering Department
E. I. du Pont de Nemours & Co., Inc.
Wilmington, Delaware

TABLE OF CONTENTS

		Page
I.	References	279
II.	Nomenclature	279
III.	Mechanism of Drag on Submerged Objects	281
IV.	Method of Presenting Drag Data	281
V.	Terminal Settling Velocity	282
VI.	Motion of Spherical Particles	283
	A. General Conditions	283
	B. Stokes's Law	284
	C. Newton's Law	284
	D. Intermediate Law	284
	E. Wall Effect	284
	F. Cunningham Correction	285
	G. Brownian Movement	285
VII.	Motion of Disks and Cylinders	286
VIII.	Motion over Flat Plates	286
IX.	Motion of Miscellaneous-Shaped Particles	288
X.	Motion of Irregular Particles	288
XI.	Motion of Fluid Particles	288
XII.	Hindered Settling	289
XIII.	Particle Flocculation and Dispersion	289
XIV.	Application	290

*Present address: Associate Professor, Dept. of Chem. Engineering, Ohio State University, Columbus, Ohio.

XV. Numerical Example 291

XVI. Problems 293

LIST OF FIGURES

Figure 1. Terminal Velocities of Spherical Particles of Different Density Settling in Air and Water at 70°F. under the Action of Gravity 292

LIST OF TABLES

Table I. Values of the Drag Coefficient and Stokes's Law Correction Factors for Spherical Particles 283
Table II. Values of a_m 285
Table III. Values of k_m for Air at Atmospheric Pressure 285
Table IV. Comparison of Brownian and Gravitational Displacements for Spherical Particles Suspended in Air and Water 286
Table V. Comparative Summary of Equations of Motion of Spheres, Disks, and Circular Cylinders 287

I. REFERENCES

1. Davies, C. N. Symposium on Particle Size Analysis, Inst. Chem. Engrs. & Soc. Chem. Ind., London, Feb. 28, 1947.
2. Dryden, H. L., Murnaghan, F. D., and Bateman, H., "Hydrodynamics," National Research Council Bulletin 84, 1932.
3. Francis, A. W., Phsyics, 4, 403-6 (1933).
4. Heywood, H., Proc. Inst. Mech. Engrs. (London), 140, 257-347 (1938).
5. Lamb, H., "Hydrodynamics," 5th Ed., Cambridge, 1924.
6. Lapple, C. E., and Shepherd, C. B., Ind. Eng. Chem., 32 605-17 (1940).
7. Nottage, H. B., and Boelter, L. M. K., Heating, Piping, and Air Conditioning, 12, 326-32 (1940).
8. Perry, J. H., "Chemical Engineers' Handbook," 3rd Ed., New York, McGraw-Hill Book Co., 1950.
9. Prandtl, L., and Tietjens, O. G. (transl. by J. P. Den Hartog), "Applied Hydro- and Aeromechanics," Chap. II and V, New York, McGraw-Hill Book Co., 1934.
10. Rouse, H., "Fluid Mechanics for Hydraulic Engineers," New York, McGraw-Hill Book Co., 1938.
11. Schiller, L., "Handbuch der Experimentalphysik,"Vol. IV, Part 2, pp. 337-87, Leipzig, Akademische Verlagsgesellschaft, 1932.
12. Schiller, L., and Naumann, A., Z. Ver. deut. Ing., 77, 318-20 (1933).
13. Squires, L., and Squires, W., Jr., Trans. Am. Inst. Chem. Engrs., 33, 1-12 (1937).
14. Steinour, H. H., Ind. Eng. Chem., 36, 618-24, 840-7, 901-7 (1944).
15. Vennard, J. K., "Elementary Fluid Mechanics," New York, John Wiley & Sons, Inc., 1940.
16. Wadell, H., Physics, 5, 281-91 (1934); J. Franklin Inst., 217, 459-90 (1934); Pan-American Geologist, 61, 187-220 (1934).
17. Whytlaw-Gray, R., and Patterson, H. S., "Smoke," London, Edward Arnold & Co., 1932.
18. Anon. (Bosanquet, C. H. Carey, W. F., and Stairmand, C.J.) Engineering (London), 150 441-4 (1940).

II. NOMENCLATURE

Any consistent system of units may be used. Since they are more convenient for work in particle dynamics, c.g.s. units are given by way of example.

a_m = constant in Cunningham's correction to Stokes's law, dimensionless

Aa = area of airfoil projected along plane of chord, sq.cm.

A_f = area of plate projected on plane parallel to direction of flow or motion, sq. cm.

A_p = area of particle projected on plane normal to direction of flow or motion, sq.cm. = $(\pi D_p^2/4)$ for spherical particles

B = width or breadth of flat plate, cm.

C = over-all drag coefficient, dimensionless

C_D = airfoil drag coefficient (in direction of motion), dimensionless

C_f = skin friction drag coefficient, dimensionless

C_L = airfoil lift coefficient (normal to direction of motion), dimensionless

C_p = profile drag coeffieient dimensionless

C_∞ = over-all drag coefficient in an infinite fluid, dimensionless

d = "derivative of"

D_p = diameter of sphere, circular cylinder, or disk, cm.

D_{ps} = equivalent Stokes's law diameter, cm.
$= \sqrt{18 u_t \mu / g_L (\rho_p - \rho)}$

D_w = diameter of cylindrical container, cm.

F_D = drag force acting on airfoil (in direction of motion), dynes

F_f = drag force due to skin friction, dynes

F_g = gravitational force acting on body, dynes

F_L = lift force on airfoil (normal to direction of motion), dynes

F_p = drag force due to profile drag, dynes

F_r = total drag force acting on body, dynes

g_L = local acceleration due to gravity, (cm./sec.)/sec.

k_c = correction factor to Stokes's law for proximity or concentration of particles, dimensionless

k_m = Cunningham correction factor to Stokes's law for approach to mean free molecular path, dimensionless

k_n = constant in Newton's law, dimensionless

k_s = correction factor to Stokes's law for surface slip with fluid particles, dimensionless

k_w = correction factor to Stokes's law for proximity of container walls, dimensionless

K_s = flocculation constant in Smoluchowski's equation, cu.cm./sec.

L = length of flat plate along direction of flow or motion; length of rod or cylinder; thickness of disk; cm.

M_p = mass of particle, grams = $(\pi \rho_p D_p^3/6)$ for spherical particles

N = number of molecules in a gram mole (Avogadro's number), 6.064×10^{23} molecules/gram mole

N_p = particle concentration; particle concentration after time t; number of particles per cu. cm. of suspension

N_{po} = initial particle concentration (at t = 0); number of particles per cu.cm. of suspension

N_{Re} = Reynolds number, dimensionless, = $D_p u \rho/\mu$ for spherical or circular particles, = $Lu\rho/\mu$ for flat plates

p = fluid pressure, dynes/sq.cm.

p_p = partial (effective) particle pressure, dynes/sq.cm.

R = gas constant, 8.314×10^7 erg/(°C.)(gram mole)

Δs = average linear amplitude or displacement of particle in time t, cm.

S = surface of body or particle, sq.cm.

t = time, sec.

T = absolute fluid temperature, °K. or °C. abs.

u = relative velocity between main body of fluid and particle or body, cm./sec.

u_t = terminal gravitational settling velocity of body or particle relative to fluid, cm./sec.

u_{ts} = terminal gravitational settling velocity as calculated from Stokes's law, cm./sec. = $g_L D_p^2 (\rho_p - \rho)/18\mu$

ρ = density of dispersion medium or fluid, grams/cu.cm.

ρ_p = true (not bulk) density of particle, grams/cu.cm.

μ = viscosity of dispersion medium or fluid, poises or (grams)/(cm.)(sec.)

μ_p = viscosity of particle fluid, poises or (grams)/(cm.)(sec.)

δ = boundary layer thickness, cm.

ϵ_v = fractional volume of dispersion medium in a suspension of particles, dimensionless

α = angle between tangent to body or particle surface and direction of flow or particle motion, radians

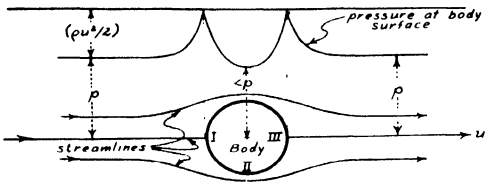
β = "surface viscosity," grams/sec.

τ_o = local sheer stress on body or particle surface, dynes/sq.cm.

p. 280, last line: change "sheer" to shear".

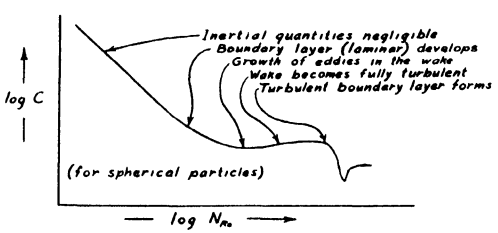
III. MECHANISM OF DRAG ON SUBMERGED OBJECTS

When an ideal fluid flows around an object, the velocity drops to zero at the center of the leading edge but accelerates around the sides. Considering a streamtube for which Bernculli's theorem must hold, the acceleration is accompanied by a decreased pressure. For an ideal fluid (one with zero vixcosity) the fluid in passing around the object again decelerates at the rear with a corresponding increase in pressure as shown below:



Since there can be no friction, the velocity and pressure pattern is symmetrical in front of and behind the body, the excess velocity at Point II being converted back to pressure energy. In a real fluid, however, a surface drag or friction occurs as the fluid passes from Point I to Point II. This friction occurs in a so-called arbitrary boundary layer which, for small Reynolds numbers, will be laminar in character and will cause a dissipation at the expense of kinetic energy. However, after Point II, the general flow pattern indicates a deceleration along the boundary, but such a decrease in velocity must be accompanied by a corresponding increase in pressure. Since energy has been dissipated by friction, such a pressure rise cannot occur. Consequently, a change in flow pattern which requires no deceleration must take place. This involves separation from the surface where deceleration becomes appreciable, with a region of discontinuity beyond that point. Where a laminar layer exists, a reverse flow will take place on the side of the discontinuous layer. As the Reynolds number increases, instability will set in and the vortex formed in the zone of reverse flow will be swept downstream, and a new vortex quickly forms. The speed of such vortex formation increases with increasing Reynolds number, and eventually the interaction of these vortices results in true turbulence in the wake. The pressure in such a turbulent wake is substantially that of the surrounding fluid, which is at a low pressure since separation occurred at a point of low pressure. Thus, the part of the body in contact with the wake will be subjected to a low pressure which, in conjunction with the high (impact) pressure on the leading face of the body, will exert a pressure drag on the body in addition to tangential shear drag.

At high Reynolds numbers, the boundary layer will become turbulent with a very thin laminar layer underneath. The energy transfer within such a turbulent layer will reduce the tendency to reversed flow (vortex formation), and the point of separation will shift to the rear. This results in a reduction in the area exposed to the low pressure wake with resultant decrease in drag. These flow patterns are shown below in their relation to the drag coefficient-Reynolds number plot.



The formation of a turbulent boundary layer will be hastened by a disturbance in the degree of turbulence of the surrounding fluid or by roughness on the body surface. A streamlined body is intended to delay the point of separation and thereby reduce pressure drag. However, due to the greater surface of a streamlined body, it will have a greater frictional (skin friction) drag and consequently will have a higher drag than a blunt object at low Reynolds numbers.

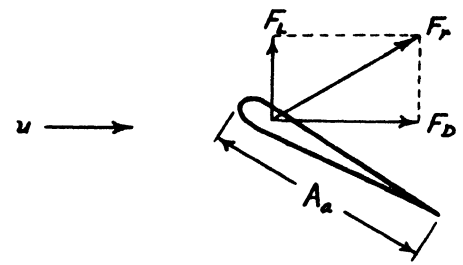
The vortices formed in the wake will result in friction loss in the fluid quite apart from the actual frictional drag of the body on the fluid.

IV. METHOD OF PRESENTING DRAG DATA

Particle drag data can be presented in terms of a plot similar to the friction factor-Reynolds number plot used in presenting pipe-line pressure drop data. The drag coefficient is plotted against the Reynolds number based on a characteristic particle demension and the relative velocity between the particle and the fluid bulk. In aeronautics, the force exerted on a body is generally divided into two parts, a lift and drag, as defined below:

p. 281, line 3: "Bernoulli's" is misspelled.

p. 281, 3rd line from bottom: "dimension" is misspelled.



$$F_L = C_L A_a \rho u^2/2 \quad (1)$$

$$F_D = C_D A_a \rho u^2/2 \quad (2)$$

For general particle motion, as encountered in chemical engineering applications, however, it is generally not necessary to split the drag into separate directional components since the body is usually free to assume its own random orientation, and no permanent lift force can act. The over-all drag coefficient is then defined on the basis of the particle area projected on a plane normal to the direction of relative motion, as given by

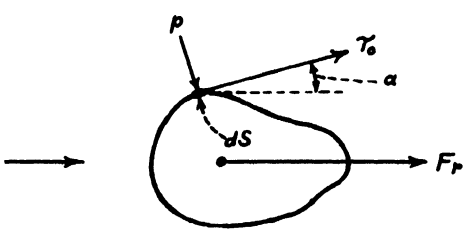
$$F_r = C A_p \rho u^2/2 \quad (3)$$

For analytical purposes, however, the force, F_r, is sometimes split into two separate components, both acting in the same direction in the over-all integrated form. These are the force due to frictional drag on the body (skin friction) and that due to pressure distribution around the body (profile drag). The "skin friction" acts tangential to the surface, while the "form" or "profile" drag acts normal to the surface. Both these forces exert a net force in the direction of motion as given by the surface integrals.

$$F_f = \int^S \tau_o \cos \alpha \, d S \quad (4)$$

$$F_p = \int^S p \sin \alpha \, d S \quad (5)$$

$$F_r = F_f + F_p \quad (6)$$



Skin friction and profile drag coefficients are also defined by

$$F_f = C_f A_p \rho u^2/2 \quad (7)$$

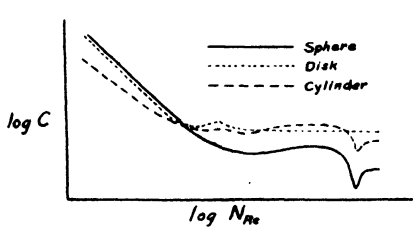
$$F_p = C_p A_p \rho u^2/2 \quad (8)$$

From Equations 3, 6, 7, and 8

$$C = C_f + C_p \quad (9)$$

Where the flow is streamline or laminar, C_p is generally negligible. For fully developed turbulent wakes, C_f is usually negligible except for streamlined bodies.

Plots of drag coefficient data for spheres, cylinders, and disks are given by Heywood (4), Lapple and Shepherd (6), Perry (8), Prandtl and Tietjens (9), Rouse (10), Schiller (11), Squires (13), and Vennard (15). These take the general forms shown in the sketch below:



V. TERMINAL SETTLING VELOCITY

If a body is falling under the action of gravity, the body will attain a constant terminal velocity, u_t, when the net (corrected for buoyancy) gravitational accelerating force, F_g, equals the resisting upward drag force, F_r, acting on the body. Thus

$$F_g = g_L M_p \left[(\rho_p - \rho)/\rho_p \right] \quad (10)$$

$$F_r = (\rho u^2/2) A_p C \quad (11)$$

when $F_r = F_g$, $u = u_t$, and from Equations 10 and 11

$$u_t = \sqrt{2\, g_L\, M_p\, (\rho_p - \rho)/\rho\ \ \rho_p\, A_p\, C} \tag{12}$$

VI. MOTION OF SPHERICAL PARTICLES

A. General Conditions: The following definitions follow from the specification of spherical particles.

$$A_p = \pi D_p^2/4 \tag{13}$$

$$M_p = \rho_p\, \pi D_p^3/6 \tag{14}$$

$$F_r = \pi D_p^2\ C\ \rho\ u^2/8 \tag{15}$$

$$u_t = \sqrt{4\, g_L\, D_p\, (\rho_p - \rho)/3\ \rho\ C} \tag{16}$$

$$N_{Re} = D_p\, u\, \rho/\mu \tag{17}$$

Values of the drag coefficient, C, are given in Table I as a function of N_{Re}. For values of N_{Re} less than 0.1,

$$C = 24/N_{Re} \tag{18}$$

These values of the drag coefficient apply to the motion of particles in an infinite fluid.

TABLE I. VALUES OF THE DRAG COEFFICIENT AND STOKES'S LAW CORRECTION FACTORS FOR SPHERICAL PARTICLES

N_{Re}	C	(u_t/u_{ts})	(D_{ps}/D_p)	$D_p u_{ts}\, \rho/\mu$	$D_{ps} u_t\, \rho/\mu$
0.1	240.0	1.000	1.000	0.10	0.10
0.2	120.0	1.000	1.000	0.20	0.20
0.3	80.0	1.000	1.000	0.30	0.30
0.5	49.5	0.968	0.984	0.52	0.49
0.7	36.5	0.937	0.968	0.75	0.68
1.0	26.5	0.905	0.951	1.10	0.95
2.0	14.6	0.822	0.906	2.43	1.81
3.0	10.4	0.769	0.876	3.90	2.63
5.0	6.9	0.695	0.834	7.20	4.17
7.0	5.3	0.647	0.804	10.83	5.63
10.0	4.1	0.585	0.765	17.08	7.65
20.0	2.55	0.471	0.686	42.5	13.72
30.0	2.00	0.400	0.633	75.0	19.00
50.0	1.50	0.320	0.566	156.2	28.3
70.0	1.27	0.270	0.520	260.0	36.4
100.0	1.07	0.224	0.473	446.0	47.3
200.0	0.77	0.156	0.395	1.28×10^3	79.0
300.0	0.65	0.123	0.351	2.44	105.3
500.0	0.55	0.0872	0.295	5.75	147.6
700.0	0.50	0.0686	0.262	10.20	183.5
1,000.00	0.46	0.0522	0.2283	19.2	228.3
2,000.00	0.42	0.0286	0.1692	70.0	338.0
3,000.00	0.40	0.0200	0.1414	150.0	424.0
5,000.00	0.385	0.0125	0.1118	400.0	559.0
7,000.00	0.390	0.00879	0.0937	796.0	656.0
10,000.00	0.405	0.00592	0.0770	1.69×10^4	770.0
20,000.00	0.45	0.00267	0.0516	7.50	1,032.0
30,000.00	0.47	0.00169	0.0411	17.7	1,233.0
50,000.00	0.49	0.000980	0.0313	51.2	1,565.0
70,000.00	0.50	0.000685	0.0262	102.0	1,835.0
100,000.00	0.48	0.000500	0.0224	200.0	2,240.0

B. Stokes's Law: For streamline flow of a fluid around a sphere, Stokes has shown mathematically that when inertial terms are negligible.

$$F_r = 3 \pi \mu u D_p \tag{19}$$

Substitution of this relation in Equation 15, gives the drag coefficient-Reynolds number relationship for this region

$$C = 24 \mu / \rho u D_p = 24/N_{Re} \tag{20}$$

When the particle attains its free settling velocity, $u = u_t$ and a combination of Equations 16 and 20 gives the equation for the settling velocity

$$u_t = g_L D_p^2 (\rho_p - \rho)/18\mu \tag{21}$$

This is known as Stokes's law for the free-falling velocity of a body in streamline motion. This law has been shown to be valid for Reynolds numbers less than 0.1 and is still a good approximation up to a Reynolds number of 2. For larger values of the Reynolds numbers, inertial terms become important and Oseen and Goldstein have offered modified equations which, however, extend only over a slightly larger range of the Reynolds number.

C. Newton's Law: For conditions of turbulent flow around a particle when viscous forces are negligible, Newton derived the following expression for the terminal velocity of a freely falling particle:

$$u_t = \sqrt{\pi g_L D_p (\rho_p - \rho)/6 k_n \rho} \tag{22}$$

where k_n is a constant indeterminate from theoretical consideration. Equation 22 is identical with Equation 16 for a constant value of C when $k_n = (\pi/8)C$. Experimental data indicate that this law is a good approximation for the region of Reynolds numbers between 1,000 and 200,000 for which region C is substantially constant with an average value of 0.44. For this region Equation 22 then becomes

$$u_t = 1.74 \sqrt{g_L D_p (\rho_p - \rho)/\rho} \tag{23}$$

D. Intermediate Law: For a Reynolds number range between 2 and 1,000, the drag coefficient relationship for spheres can be approximated by the equation.

$$C = 18.5/N_{Re}^{0.6}$$

and by substitution in Equation 16

$$u_t = 0.153 g_L^{0.714} D_p^{1.142} (\rho_p - \rho)^{0.714} / \rho^{0.286} \mu^{0.428} \tag{25}$$

E. Wall Effect: When the diameter of a particle becomes appreciable with respect to the diameter of the container in which it is settling, the container wall will exert an additional retarding effect. This can be allowed for by introducing a factor in Stokes's equation for frictional drag

$$F_r = 3 \pi \mu u D_p k_w \tag{26}$$

The settling velocity as calculated by Stokes's law (Eq. 21) should be divided by the factor k_w to correct for wall effect. Ladenburg (11) has proposed the following value of k_w as modified by Faxen:

$$k_w = 1 + 2.1 (D_p/D_w) \tag{27}$$

Francis (3) has shown experimentally that Ladenburg's correction applies only for values of (D_p/D_w) less than 0.1. His experimental values, covering a range of (D_p/D_w) from 0.13 to 0.97 and N_{Re} from 0.000015 to 6.9, can be empirically correlated by

$$k_w = \left[1 - (D_p/D_w) \right]^{-2.5} \tag{28}$$

This expression fits the data with the following precision:

(D_p/D_w)	Precision
<0.2	± 3%
0.5	±15%
0.95-0.97	±25%

No data on wall effect in other than streamline flow are available, but it is suggested that for other flow regions the same factor be used by multiplying the value of C for flow in an infinite fluid by k_w to obtain the actual value of C,

$$C = k_w C_\infty \tag{29}$$

Schiller (11) summarizes correction factors for other than cylindrical boundaries. In general, wall effect correction factors are rarely of practical importance when dealing with particles finer than 100 mesh.

F. Cunningham Correction (Stokes's Law Lower Limit): Where the size of a particle approaches the same order of magnitude as the mean free path of the molecules of the fluid medium, the settling velocity will be somewhat greater than calculated from Stokes's law. From theoretical considerations, Cunningham has proposed a correction factor to Stokes's law for particles settling in gases,

$$F_r = 3 \pi \mu u D_p / k_m \tag{30}$$

where

$$k_m = 1 + a_m (\lambda / D_p) \tag{31}$$

The value of a_m has been experimentally determined to lie between 1.3 and 2.3 for different gases, particle sizes, and materials. Values of a_m calculated from the data of Millikan are given in Table II.

TABLE II. VALUES OF a_m (CALCULATED FROM MILLIKAN'S DATA)

(λ/D_p)*	a_m
0.01	1.644
0.05	1.644
0.10	1.645
0.3	1.706
0.5	1.792
1.0	1.931
10.0	2.161
∞	2.196

* The value λ as used herein is the value obtained from the viscosity by the kinetic theory of gases and is not the value corrected for the persistence or distribution of velocity. For most common gases, λ is on the order of 0.1 micron.

The settling velocity as calculated by Stokes's law should be multiplied by the factor, k_m, to obtain the actual settling velocity. This correction is of importance only for particles smaller than 3 microns for settling in gases. A comparable effect does not arise for settling in liquids until the particle diameter becomes less than 0.01 micron. Values of k_m for various sized particles settling in air at atmospheric pressure are given in Table III.

TABLE III. VALUES OF k_m FOR AIR AT ATMOSPHERIC PRESSURE

(Based on a_m values given in Table II)

Particle Diameter, microns	Value of k_m at Temperature of 70°F.	212°F.	500°F.
0.1	2.88	3.61	5.14
0.25	1.682	1.952	2.528
0.5	1.325	1.446	1.711
1.0	1.160	1.217	1.338
2.5	1.064	1.087	1.133
5.0	1.032	1.043	1.067
10.0	1.016	1.022	1.033

G. Brownian Movement: Due to bombardment by fluid molecules, particles suspended in a fluid will be subjected to a random molecular motion known as Brownian movement in addition to any net motion in a given direction due to the action of external forces such as gravity. The following relationship expresses the average amplitude or displacement of a spherical particle due to Brownian movement:

$$\Delta s = \sqrt{4\ RT\ k_m\ t/3\ \pi^3\ \mu\ N\ D_p} \tag{32}$$

The value Δs is a scalar quantity representing the statistical average linear displacement or amplitude of a particle in a given direction (regardless of sign) in time t. The algebraic average displacement of all particles is zero at all times; however, and the actual path taken by a given particle consists of a large number of irregular and zig-zag jumps.

Table IV gives a comparison of the magnitude of Brownian movement displacement with that due to gravity settling. It is apparent that Brownian movement becomes appreciable compared to gravity settling for particles smaller than 3 microns diameter and is entirely predominant for particles smaller than 0.1 micron.

TABLE IV. COMPARISON OF BROWNIAN AND GRAVITATIONAL DISPLACEMENTS FOR SPHERICAL PARTICLES SUSPENDED IN AIR AND WATER

	Displacement in 1.0 sec., microns			
	In Air at 70° F., 1 atm.		In Water at 70° F.	
Particle Diameter, microns	Due to Brownian Movement*	Due to Gravitational Settling**	Due to Brownian Movement*	Due to Gravitational Settling**
0.1	29.4	1.73	2.36	0.005
0.25	14.2	6.30	1.49	0.0346
0.5	8.92	19.9	1.052	0.1384
1.0	5.91	69.6	0.745	0.554
2.5	3.58	400.0	0.471	3.46
5.0	2.49	1550.0	0.334	13.84
10.0	1.75	6096.0	0.236	55.4

* This is the mean displacement along an axis for t = 1 sec. as given by Equation 32.

** This is the distance settled in 1 sec. by a particle of sp. gr. = 2.0, including the Cunningham correction factor, k_m, for settling in air.

Brownian movement represents a diffusional characteristic of fine particles which is entirely analogous to the diffusion of gases. Particles suspended or dispersed in a fluid will exert a pressure that is proportional to their concentration as determined by kinetic theory

$$p_p = N_p\ RT/N \tag{33}$$

VII. MOTION OF DISKS AND CYLINDERS

Comparative equations for spheres, disks, and cylinders are given in Table V. In streamline motion a particle will generally retain its initial orientation while settling (1). In the turbulent region it will assume a position of maximum resistance.

VIII. MOTION OVER FLAT PLATES

For flow parallel to thin flat plates, the drag must all be due to skin friction. For such a plate with a sharp leading edge, the boundary layer gradually increases in thickness with distance downstream from the leading edge. Surface shear correspondingly decreases. The drag coefficient in this case is defined by

$$F_r = C\ A_f\ \rho\ u^2/2 \tag{34}$$

If only one side of the plate is exposed to the fluid, A_f = BL; if two sides are exposed (i.e., for an immersed plate), A_f = 2 BL.

The drag coefficient in this case is a function of the Reynolds number based on the length of the plate

$$N_{Re} = L\ \rho\ u/\mu \tag{35}$$

P. 286 - line 4 - correct punctuation as follows:
"...at all times, however, and ..."

TABLE V. COMPARATIVE SUMMARY OF EQUATIONS OF MOTION OF SPHERES, DISKS AND CIRCULAR CYLINDERS

	Sphere Any Direction*	Thin Disk Normal to Face*	Thin Disk Parallel to Face*	Infinite Circular Cylinder Normal to Axis*
General Definitions				
N_{Re} =	$D_p\ u\ \rho/\mu$	$D_p\ u\ \rho/\mu$	$2\ L\ u\ \rho/\mu$	$D_p\ u\ \rho/\mu$
A_p =	$(\pi/4)D_p^2$	$(\pi/4)D_p^2$	$D_p\ y$	$D_p\ L$
M_p =	$(\rho_p\ \pi/6)D_p^3$	$(\rho_p\ \pi/4)D^2\ L$	$(\rho_p\ \pi/4)D_p^2\ L$	$(\rho_p\ \pi/4)D_p^2\ L$
Drag Relationships Streamline Flow ($N_{Re} < 0.2$)				
F =	$3\ \pi\ \mu\ u\ D_p$	$8\ \mu\ u\ D_p$	$(16/3)\ \mu\ u\ D_p$	$(4\ \pi/K)\ \mu\ u\ L$
$C\ N_{Re}$ =	24	$(64/\pi)$	(64/3)	$(8\ \pi/K)$ [where $K = 2.002 - \log_e N_{Re}$]
Turbulent Flow				
Average Value of C (Corresponding N_{Re} range)	0.44 (1,000-200,000)	1.12 (>1,000)	-- --	1.2 (100 - 200,000)
Gravitational Terminal Settling Velocity General				
u_t =	$\sqrt{\left(\frac{g_L(\rho_p - \rho)}{\rho C}\right)\left(\frac{4}{3}\right)D_p}$	$\sqrt{\left(\frac{g_L(\rho_p - \rho)}{\rho C}\right)2\ L}$	$\sqrt{\left(\frac{g_L(\rho_p - \rho)}{\rho C}\right)\left(\frac{\pi}{2}\right)D_p}$	$\sqrt{\left(\frac{g_L(\rho_p - \rho)}{\rho C}\right)\left(\frac{\pi}{2}\right)D_p}$
Streamline Flow ($N_{Re} < 0.2$)				
u_t =	$\left(\frac{1}{18}\right)\left(\frac{g_L(\rho_p - \rho)}{\mu}\right)D_p^2$	$\left(\frac{\pi}{32}\right)\left(\frac{g_L(\rho_p - \rho)}{\mu}\right)DL$	$\left(\frac{3\pi}{64}\right)\left(\frac{g_L(\rho_p - \rho)}{\mu}\right)DL$	--
Wall Effect Factor (For Streamline Flow: ($N_{Re} < 0.2$)				
k_w =	$\left[1 + 2.1(D_p/D_w)\right]$ (Ladenburg-Faxen)	$\left[1 + 1.7(D_p/D_w)\right]$ (Squires)	$\left[1 + 6.5(D_p/D_w)^{1.5}\right]$ (Squires)	--

*Direction of flow or motion.

A. For N_{Re} Less Than 100,000: For a Reynolds number, based on the length of plate, less than 100,000 the drag coefficient is given by (9) (10)

$$C = 1.328\ N_{Re}^{-1/2} \tag{36}$$

The boundary layer thickness is given by

$$\delta = 5.2\ L\ N_{Re}^{-1/2} \tag{37}$$

The value δ is approximate due to difficulties in obtaining a precise definition of this term (9) (10) (15).

The local shear stress at any point on the plate is given by

$$\tau_o = 0.332\ \sqrt{\mu\ \rho\ u^3/L} = 0.664\ (\rho\ u^2/2)N_{Re}^{-1/2} \tag{38}$$

Here L is the distance from the leading edge to the point in question. N_{Re} is also based on this length. The value τ_o gives the actual shear stress at the point in question.

The above equations also hold for flow parallel to the axis of a cylindrical rod (hollow or pointed) provided the boundary layer thickness is small compared to the diameter of the rod. Since the boundary layer thickness increases with length, the length of rod over which the above expressions can be applied is limited. Rewriting Equation 37 and dividing both sides by D_p,

$$(L/D_p) = (D_p\ u\ \rho/\mu)(\delta/5.2\ D_p)^2 \tag{39}$$

Thus the length of rod, expressed as number of rod diameters, for which the above expressions hold as an approximation, is limited to a value on the order of

$$(0.01\ D_p\ u\ \rho/\mu).$$

For this length, (δ/D_p) at the downstream end of the rod or pipe would be 0.5 as can be seen from Equation 39. In flow past such a rod, the straightness of the rod and its method of mounting, however, will probably be important factors in determining the magnitude of drag actually experienced.

B. For N_{Re} Greater Than 10,000,000: The drag coefficient in this range is given by the following empirical expression (15):

$$C = 0.455/(\log_{10} N_{Re})^{2.58}$$

In this range the boundary layer becomes turbulent, and its thickness is given approximately by

$$\delta = 0.37\ L\ N_{Re}^{-0.2} \tag{41}$$

The region of N_{Re} between 10^5 and 10^7 is a critical region in which transition from one law to the other occurs. The value of C in this region may range from 0.003 to 0.006, probably 0.003 to 0.004. While the transition usually starts at a Reynolds number of about 500,000, it is very sensitive to general fluid turbulence and the character of the leading edge of the plate.

IX. MOTION OF MISCELLANEOUS-SHAPED PARTICLES

Drag coefficients have been determined either theoretically or experimentally (or both) for various shaped bodies, such as ellipsoids of revolution, cylinders of circular, cupped, elliptical, rectangular, or triangular cross section, and flat plates. These are discussed in References 1, 2, 5, 9, 10, 11, and 15.

X. MOTION OF IRREGULAR PARTICLES

The data on settling velocity of irregular shapes are not very complete or conclusive and are further complicated by the variety of methods of expressing particle size. Many such data are summarized by Schiller (11). In general, the relationship for spheres hold fairly well (within about ±20%) for irregular particles for values of N_{Re} less than 50 where the particle shapes are not extreme and where the diameter as measured by screens, elutriation, microscope, or otherwise is taken as the diameter of an equivalent sphere. For a Reynolds number greater than 50, however, the drag coefficient curve levels off rapidly to a constant value averaging about 1.2, and the settling velocity of irregular particles of not too extreme shapes will average approximately 60% of that of a spherical particle of the same nominal size and may run as low as 40%. These are very crude conclusions but should serve practical purposes in the absence of better data. Where very extreme shapes, such as hollow particles, thin disks, or needles, are encountered, an attempt should be made to obtain a more reliable estimate of settling velocity by the application of methods previously presented for shapes other than spherical or by experimental determination where this is not feasible.

Heywood (4) has proposed a correlation for irregular particles in terms of particle volume coefficient defined as the ratio of the volume of the irregular particle to the volume of a sphere having the same projected area as the irregular particle. Wadell (16) has proposed a correlation in terms of a sphericity coefficient defined as the ratio of the total surface area of a sphere of the same volume as the particle to the total surface area of the particle.

XI. MOTION OF FLUID PARTICLES

Fluid particles differ from solid particles in that the fluid is not rigid, and the surface layers are free to move with respect to the rest of the particle, and the particle may undergo a change in shape. Various theories have been proposed to modify Stokes's law allowing for surface slip. The most general one is that of Boussinesq (2)

$$F_r = 3\ \pi\ \mu\ u\ D_p\ k_s \tag{41}$$

where

$$k_s = \frac{2\beta + (2\mu + 3\mu_p)\ D_p}{2\beta + (3\mu + 3\mu_p)\ D_p} \tag{42}$$

Here β is a "surface viscosity" arising from the action of surface tension. The settling velocity as calculated from Stokes's law (Equation 21) must be divided by k_s to obtain the actual settling velocity.

p. 288 - 3rd line under X, "relationship" should be "relationships"

For very small particles k_S would approach unity. This means that small drops or bubbles would follow the simple Stokes's law. For solid particles, μ_p is effectively infinite and k_S also approaches unity. For bubbles of a gas in a fluid of low viscosity, like water, the term β is predominant and k_S approaches unity. For large gas bubbles in a very viscous fluid, k_S will approach a value of 2/3 which means that the bubbles will rise 1.5 times as rapidly as if they were solid particles. Data are too meager, however, to permit any accurate prediction of conditions for which k_S will change from 1 to 2/3.

Data on the velocity of rise of air bubbles in water are quite conflicting. In general it appears as though the bubbles follow Stokes's law up to a Reynolds number of 1.0. The bubbles remain spherical up to a Reynolds number of approximately 500 which corresponds to a bubble of 1/16 in. diameter. Larger bubbles begin to deform, assuming a flattened shape normal to the direction of motion. The particle motion is unstable, subject to fluctuations, and may trace a helical course. Indications are that bubbles 1 in. in diameter or larger will reach a maximum velocity of about 1.25 ft./sec., the larger bubbles being flattened to a greater extent or ruptured. For air bubbles larger than 1/4 in. diameter, fluid viscosity (at least up to 100 cp.) appears to have little effect on the velocity of rise.

Liquid droplets falling in gases appear to remain spherical and follow the same drag relationships as solid spherical particles up to a Reynolds number of about 500, corresponding to a 1/16-in. water droplet falling in air. Larger droplets will deform or shatter. In the range of Reynolds numbers of 4,000 to 5,000, a water droplet in air will be ruptured into smaller droplets. The largest water droplet which will fall in air at its terminal velocity corresponds to a 5/16-in. diameter particle and will fall with a velocity of approximately 30 ft./sec. This is the reason why rainfall from high clouds never contains droplets larger than approximately 5/16 in. Very large raindrops generally originate close to the ground and have not attained their terminal settling velocity. Nottage and Boelter (7) have presented calculated trajectories for the motion of water droplets in air.

XII. HINDERED SETTLING

Previous discussions have dealt with the motion of particles present in relatively dilute concentration. When the concentration becomes high, the particles will approach close to each other and exert a mutual retarding effect on the settling. This condition is often termed "hindered" settling.

The effect of concentration for streamline flow may be allowed for as follows:

$$F_r = 3 \pi \mu u D_p k_c \tag{43}$$

where k_c is a factor dependent on particle concentration. Thus the settling velocity as calculated from Stokes's law (Equation 21) must be divided by factor k_c to obtain the actual settling velocity. One of the most recent and complete series of tests to evaluate k_c are those of Steinour (14). His data for spheres of almost uniform size were empirically correlated by

$$k_c = \epsilon_v^2 \, 10^{-1.82 \, (1 - \epsilon_v)} \tag{44}$$

These data covered a range in ϵ_v of 0.5 to 0.95. Burgers (1), in a theoretical study for relatively dilute suspensions, finds

$$k_c = 1 + 6.875 \, (1 - \epsilon_v) \tag{45}$$

These two relationships check well for the range of ϵ_v greater than 0.95.

Steinour has also studied the effect of concentration on the behavior of suspensions of uniform angular particles as well as of highly concentrated flocculated suspensions.

XIII. PARTICLE FLOCCULATION AND DISPERSION

Particles suspended in a fluid partake of molecular motion and as a result will collide with each other. Flocculation results when colliding particles adhere.

For an initially complete dispersion of particles of uniform size, the degree of flocculation, as given by the simple Smoluchowski equation, is

$$(N_p/N_{po}) = 1/(1 + K_S N_{po} \, t) \tag{46}$$

where

$$K_S = 4 \, RT/3 \, \mu N \tag{47}$$

This equation essentially assumes that the particles as well as the flocs are spherical and that all particles adhere upon collision. Various modifications (17) have been proposed to allow for the mean free path of the fluid molecules, electrical charge, heterogeneity of the dispersion, and failure of colliding particles to adhere.

In general, for aerosols, the simple form of Smoluchowski's equation has been found to hold reasonably well, indicating that adhesion generally results in collision. Heterogeneity and mean free path effects for small particles will both tend to give a somewhat higher value of K_s than obtained from Equation 47, and aerosols consisting of very small, heterogeneous particles will flocculate more rapidly than calculated from Equations 46 and 47. In the case of hydrosols, or liquid dispersions, the probability of adhesion upon collision may be very low due to the stabilizing effect of electric double layers or protective colloids or solvated adsorbed liquid layers. Thus it is possible to completely stabilize (i.e., prevent flocculation) a liquid dispersion. No comparable stabilization of aerosols has been observed.

Flocculation can also result from collision arising as the result of fluid turbulence. However, no quantitative study of this phenomena has been made.

The degree of dispersion of particles suspended in a fluid may be regarded as an equilibrium proposition controlled by relative rates of flocculation and dispersion. Dispersion can be achieved by mechanical action either from an external source or by fluid turbulence. No general study of dispersion appears to have been made. Dispersion should be distinguished from stabilization. So-called "dispersing agents" are really stabilizing agents, their function being to reduce the probability of adhesion upon collision. They may be regarded as dispersing agents insofar as they make the mechanical problem of dispersion simpler by reducing adhesive forces between particles.

XIV. APPLICATION

Previous paragraphs have considered particle dynamics in terms of drag force and settling velocity. Settling velocity is an equilibrium condition in which the gravity force on a particle just balances the drag on a particle. In many problems in practice, conditions of accelerated motion are encountered. The application of general drag relationships to such problems is discussed in Reference 6.

Chemical engineering applications are rarely concerned with Reynolds numbers greater than 10,000. Higher Reynolds numbers are concerned chiefly with aircraft, surface craft, and subsurface craft design and with external ballistics.

In order to calculate settling velocities directly from the drag coefficient-Reynolds number relationships, a trial-and-error solution is required, since both drag coefficient and Reynolds number include a velocity term. The terms $C\ N_{Re}^2$ and (C/N_{Re})do not include u or D_p, respectively. To eliminate trial-and-error solutions, values of these terms can be calculated and plotted against N_{Re} (12). Then, depending on whether u_t or D_p is unknown, the value of $C\ N_{Re}^2$ or (C/N_{Re}), respectively, can be calculated and the corresponding value of N_{Re} obtained from such a plot. The value u_t or D_p can then be calculated from the value of N_{Re} obtained. For spherical particles,

$$(C\ N_{Re}^2) = 4\ g_L\ \rho\ D_p^3\ (\rho_p - \rho)/3\ \mu^2 \tag{48}$$

$$(C/N_{Re}) = 4\ g_L\ \mu\ (\rho_p - \rho)/3\ \rho^2\ u_t^3 \tag{49}$$

as obtained by combining Equations 16 and 17.

An alternate method (18) is to calculate the desired value, u_t or D_p, according to Stokes's law and then to apply a correction factor for regions where Stokes's law does not actually apply. It may be shown that the correction factors are functions of a fictitious Reynolds number based on the value calculated from Stokes's law. The correction factors and fictitious Reynolds numbers are related to the actual C and N_{Re} values by the following relationships for spherical particles:

$$(u_t/u_{ts}) = 24/C\ N_{Re} \tag{50}$$

$$(D_{ps}/D_p) = \sqrt{24/C\ N_{Re}} \tag{51}$$

$$D_p\ u_{ts}\ \rho/\mu = C\ N_{Re}^2/24 \tag{52}$$

$$D_{ps}\, u_t\, \rho/\mu = \sqrt{24\, N_{Re}/C} \qquad (53)$$

Plots of (D_{ps}/D_p) vs. $(D_{ps}\, u_t\, \rho/\mu)$ and (u_t/u_{ts}) vs. $(D_p\, u_{ts}\, \rho/\mu)$ can be made from the values given in Table I.

Figure 1 gives the terminal settling velocities of spherical particles of different density settling in air and water at 70°F. under the action of gravity. These curves should be useful for ready reference in practical applications. They are based on the principles previously discussed and were calculated from the drag coefficient values given in Table I.

XV. NUMERICAL EXAMPLE

Problem: Calculate the free settling velocity, in ft./sec., of a 20-mesh (0.0328-in. diameter) spherical sand particle in water at 20°C. Perform the calculation: 1) using the C vs. N_{Re} trial-and-error method, 2) using the $C\, N_{Re}^2$ vs. N_{Re} method, 3) assuming Stokes's law to apply, 4) assuming Newton's law to apply, 5) assuming the Intermediate Law, 6) applying a correction factor to Stokes's law. Tabulate the answer obtained by each method. True sp. gr. of sand is 2.64.

Solution: For the conditions of the problem:

D_p = 0.00273 ft.

ρ = 62.3 (lb.mass)/cu.ft.

ρ_p = 164.5 (lb.mass)/cu.ft.

$(\rho_p - \rho)$ = 102.2 (lb.mass)/cu.ft.

μ = 1.00 cp. = 0.000672 (lb.mass)/ft.)(sec.)

Method 1:

From Equation 16

$$u_t = \sqrt{(4)(32.17)(0.00273)(102.2)/(3)(C)(62.3)}$$
$$= 0.438\, \sqrt{1/C}$$

$$N_{Re} = (D_p\, u_t\, \rho/\mu) = (0.00273)(u_t)(62.3)/(0.000672)$$
$$= 253.0\, u_t = 110.9\, \sqrt{1/C}$$

By assuming values of C the correct value of C can be found by trial-and-error:

Trial No.	Assumed Value of C	Value of N_{Re} Corresponding to C (from curve of C vs. N_{Re})	Calculated Value of N_{Re}
1	1.00	115	110.9
2	1.07	100	107.0
3	1.02	110	109.9

Hence correct value of C is 1.02 and

$$u_t = 0.438\, \sqrt{1/1.02} = \underline{0.434 \text{ ft./sec.}}$$

Method 2:

From Equation 48

$$C\, N_{Re}^2 = (4)(32.17)(62.3)(0.00273)^3\,(102.2)/(3)(0.000672)^2$$
$$= 12{,}300$$

From plot of $C\, N_{Re}^2$ vs. N_{Re}

$$N_{Re} = 110.$$
$$u_t = (110)(0.000672)/(0.00273)(62.3)$$
$$= \underline{0.434 \text{ ft./sec.}}$$

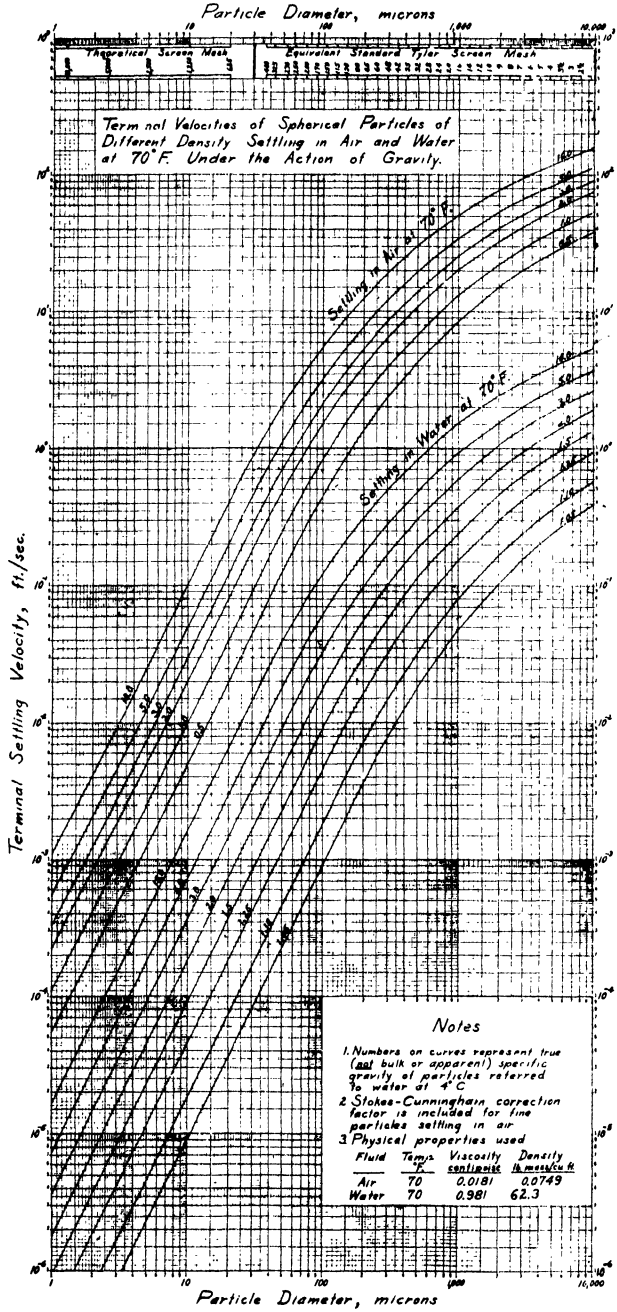


Figure 1. (See page 291.)

Method 3:

From Equation 21

$$u_t = (32.17)(0.00273)^2(102.2)/(18)(0.000672)$$
$$= \underline{2.02 \text{ ft./sec.}}$$

Method 4:

From Equation 23

$$u_t = 1.74\sqrt{(32.17)(0.00273)(102.2)/(62.3)}$$
$$= \underline{0.660 \text{ ft./sec.}}$$

Method 5:

From Equation 25

$$u_t = \frac{(0.153)\ (32.17)^{0.714}\ (0.00273)^{1.142}\ (102.2)^{0.714}}{(62.3)^{0.286}\ (0.000672)^{0.428}}$$
$$= \underline{0.400 \text{ ft./sec.}}$$

Method 6:

From Method 3

$$u_{ts} = 2.02 \text{ ft./sec.}$$
$$D_p\, u_{ts}\, \rho/\mu = (0.00273)(2.02)(62.3)/(0.000672)$$
$$= 511.$$

From plot of (u_t/u_{ts}) vs. $(D_p\, u_{ts}\, \rho/\mu)$

$$(u_t/u_{ts}) = 0.215$$

Hence $u_t = (0.215)(2.02) = \underline{0.434 \text{ ft./sec.}}$

Summary

Method	Free Settling Velocity, ft./sec.
1. C vs. N_{Re} (trial-and-error)	0.434
2. C N_{Re}^2 vs. N_{Re}	0.434
3. Stokes's Law*	2.02*
4. Newton's Law*	0.660*
5. Intermediate Law	0.400
6. Stokes's Law Correction Factor	0.434

*These are apparently not applicable for these conditions since N_{Re} is in range of Intermediate Law.

XVI. PROBLEMS

1. Calculate the free settling velocity of a 60-mesh (0.0097-in. diameter) spherical particle of specific gravity 2.0 in air at 300° C. Perform the calculation using the drag coefficient—Reynolds number curves, Stokes's law, and Newton's law, and tabulate the answers obtained by each method.

2. Calculate the free gravitational settling velocity of a circular aluminum disk, 40 microns diameter and 2 microns thick, (1) when settling horizontally (face normal to direction of motion) in water at 20°C. and (2) when settling vertically (face parallel to direction of motion). What is the diameter in microns of an aluminum sphere that would have the same settling velocity as the disk in each case?

3. How many miles will 5-micron diameter fly ash particles of specific gravity 2.0 be carried by a 10 mi./hr. wind if they are emitted from a 200-ft. high stack with negligible upward velocity? Neglect atmospheric eddy or turbulence effects.

4. Calculate the terminal settling velocity, in ft./sec., of a 48-mesh (Tyler) spherical pellet of sodium hydroxide in hydrogen at 50 atmospheres absolute pressure and 70°F.

5. A mist contains a concentration of 10 grams of water/cu.ft. of air, the water being present as 2-micron diameter droplets. Assuming an air temperature of 70° F., estimate the time, in minutes, required for 90% of the mist particles to coalesce. What time would be required if the droplet diameter was initially 10 microns?

6. In an elutriation-type classifier of a continuous crystallizer, the flow rate is adjusted to produce 20 Tyler-mesh particles. What particle diameter, in microns, should be produced if the flow rate is reduced to one-tenth of its original value? If the flow rate is increased to twice its original value? Assume that the particles are spherical of true specific gravity 2.10 and that the mother liquor has a specific gravity of 1.18 and a viscosity of 2.3 centipoises at operating conditions.

7. The products from an emulsion polymerization process are washed batchwise by pouring the charge into a vessel consisting of an inverted cone in which water is circulated into the bottom and allowed to overflow at the top. The material has a specific gravity of 1.052 and the smallest particles present in appreciable quantity are just retained on a 20-mesh Tyler screen (0.0328 in. aperture). What is the minimum allowable vessel diameter at the overflow point to avoid excessive loss of material for a water circulation rate of 100 gal./min? Assume water temperature is 20°C.

8. What is the average linear displacement in a given direction due to Brownian motion of a 0.1-micron diameter silica particle suspended in air at 200°C. in a period of 1 sec.? In a period of 1 min.?

9. Prove that a plot of $(24/CN_{Re})$ vs. $(CN_{Re}^2/24)$ is identical to a plot of (u_t/u_{ts}) vs. $D_p\ u_{ts}\ \rho/\mu$.

Chapter 14

DUST AND MIST COLLECTION

by

C. E. Lapple*
Engineering Research Laboratory
Engineering Department
E. I. du Pont de Nemours & Co., Inc.
Wilmington, Delaware

TABLE OF CONTENTS

		Page
I.	References	297
II.	Nomenclature	298
III.	Purpose of Dust and Mist Collection	301
IV.	Factors in Dust and Mist Collection Equipment Design	301
V.	Gravity Settling Chambers	303
VI.	Impingement Separators	304
VII.	Cyclone Separators	305
VIII.	Mechanical Centrifugal Separators	309
IX.	Miscellaneous Inertial Separators	309
X.	Packed Bed Collectors	309
XI.	Cloth Collectors	310
XII.	Scrubbers	312
XIII.	Electrical Precipitators	314
XIV.	Air Filters	319
XV.	Miscellaneous Collectors	319
XVI.	Numerical Examples	320
XVII.	Problems	321

LIST OF FIGURES

Figure 1. Typical Cyclone Design Proportions and Performance 307

*Present address: Associate Professor, Dept. of Chem. Engineering, Ohio State University, Columbus, Ohio.

LIST OF TABLES

Table I. Dust and Mist Collection Equipment — Classification of Types and High-Spot Performance Characteristics 302
Table II. Charge and Motion of Spherical Particles in an Electrical Field. 315
Table III. Performance Data on Typical Single-Stage Electrical Precipitator Installations. 316

I. REFERENCES

A. General

1. Anderson, E., Trans. Am. Inst. Chem. Engrs., 16, Part I, 69-86 (1924).
2. Knowles, E. R., Trans. Am. Soc. Heat. & Vent. Engrs., 24, 165-216 (1918).
3. Larcombe, H. L. M., Mining Magazine, 66, 143-50, 206-15, 256-60 (1942); Ind. Chemist, 18, 433-8, 477-83 (1942), 19, 25-8 (1943).
4. Meldau, R., "Der Industriestaub," V. D. I. Verlag, Berlin, 1926
5. Miller, C. E., Chem. & Met., 45, 132-5 (1938).
6. Perry, J. H., "Chemical Engineers' Handbook," New York, McGraw-Hill Book Co., 2nd Ed., pp. 1850-84, 1941; 3rd Ed., pp. 1013-1050, 1950.
7. Powers, E. D., Rock Products, 45, 58-60 (1942) Feb.; 46-8 (1942) Apr.; 48, 49, 51 (1942) Sept.; 46, 66-8 (1943) Mar.; 70, 72 (1943) June; 47, 74, 94-5 (1944) May; 50-1 (1944) July; 48, 92, 94 (1945) June; 84, 94 (1945) July.
8. Roberts, R. T., Power, 83, 345-8, 392-5 (1939).
9. Anon., Sheet Metal Worker, 31, 51-4 (1940) Jan.; 22-4 (1940) Feb.; 29-31 (1940) May; 24, 25, 38 (1940) June; 30-2 (1940) Aug.

B. Impingement Separators

10. Albrecht, F., Physik. Z., 32, 48-56 (1931).
11. Fairs, G. L., Chem Trade J., 115, 571-3 (1944); Ind. Chemist, 20, 637-42 (1944).
12. Houghton, H. G., and Radford, W. H., Trans. Am. Inst. Chem. Engrs., 35, 427-33 (1939).

12a. Langmuir, I., and Blodgett, K. B., U. S. Army Air Forces Technical Report No. 5418, Feb. 19, 1946. (U. S. Dept. of Commerce, Office of Technical Services PB 27565).

13. Sell, W., Forsch. Gebiete Ingenierw., 2, Forschungsheft No. 347 (1931) Aug.
14. Witzman, H., Kolloid Z., 95, 102-119 (1941); Z. Electrochem., 46, 313-21 (1940).

C. Cyclone Separators

15. Alden, J. L, "Design of Industrial Exhaust Systems," Chap. VI, Industrial Press, New York, 1940.
16. Parent, J. D., Trans. Am. Inst. Chem. Engrs., 42, 989-99 (1946).
17. Pollak, A., and Work, L. T., Trans. Am. Soc. Mech. Engrs., 64, 31-41 (1942).
18. Rosin, P., Rammler, E., and Intelmann, W., Z. Ver. dent. Ing., 76, 433-7 (1932).
19. Shepherd, C. B. and Lapple, C. E., Ind. Eng. Chem., 31, 972-84 (1939); 32, 1246-8 (1940).
20. Van Tongeran, H., Mech. Eng., 57, 753-9 (1935).
21. Whiton, L. C., Trans. Am. Soc. Mech. Engrs., 63, 213-18 (1941); Mech. Eng., 65, 885-8 (1943); Power Plant Eng., 47, 92-5 (1943) Dec.; Power, 88, 20-1 (1944); 75, 344-6 (1932); Chem. & Met., 39, 150-2 (1932).

D. Packed Bed Collectors

22. Wells, A. E. and Fogg, D. E., U. S. Bureau of Mines, Bulletin 184, pp. 159-64, 1920.
23. Anon. (Lynch, G. E.), Fuel Economist, 12, 47-8 (1936) Oct.

E. Cloth Collectors

24. Carman, P. C., Trans. Inst. Chem. Engrs. (London), 15, 150-66 (1937).
25. Manegold, E., Kolloid Z., 81, 269-94 (1937).
26. Mumford, A. R., Markson, A. A., Ravese, T., Trans. Am. Soc. Mech. Engrs., 62, 271-81 (1940).
27. Weischaus, L. J., Chem. Eng., 54, 113-5 (1947) Aug.
28. Williams, C. E., Hatch, T., and Greenburg, L., Heating, Piping, Air Conditioning, 12, 259-63 (1940).

F. Scrubbers

29. Bransky, D. W. and Diwoky, F. F., Ref. & Nat. Gasoline Mfg., 19, 191-5 (1940).
30. Collins, T. T., Jr., Seaborne, C. R., and Anthony, A. W., Jr., Paper Trade Journal, 124, 45-49 (1947) June 5, No. 23; 125, 45-49 (1948) Jan. 15.
31. Harmon, R. R., J. Inst. Fuel, 12, 514-36 (1938).

32. Kinney, S. P., Blast Furnace and Steel Plant, 31, 113-6 (1943) Jan.
33. Kleinschmidt, R. V., Chem. & Met., 46, 487-90 (1939).
34. Kleinschmidt, R. V., and Anthony, A. W., Jr., Trans. Am. Soc. Mech. Engrs., 63, 349-57 (1941).
35. Pearson, J. L., Nonhebel, G., and Ulander, P. H. N., J. Inst. Fuel, 8, 119-56 (1935); Combustion, 6, 10-14 (1935) Apr.

G. Electrical Precipitators

36. Anderson, E., Physics, 3, 23-8 (1932) July.
37. Beaver, C. E., Trans. Am. Inst. Chem. Engrs., 42, 251-61 (1946).
38. Deutsch, W., Ann. Physik (4), 68, 335-44 (1922); (5), 9, 249-64 (1931); (5), 10, 847-67 (1931).
39. Ladenburg, R., Ann. Physik (5), 4, 863-97 (1930).
40. Ladenburg, R., and Tietze, W., Ann. Physik (5), 6, 581-621 (1930).
41. Mierdel, G., Z. tech. Physik, 13, 564-7 (1932).
42. Mierdel, G., and Seeliger, R., Trans. Faraday Soc., 32, 1284-90 (1936).
43. Penney, G. W., Electrical Engineering, 56, 159-63 (1937).
44. Schmidt, W. A. and Anderson, F., Electrical Engineering, 57, 332-8 (1938).

H. Air Filters

45. American Railroads Association, Mechanical Division, Report on "Relative Performance of Air Filters," Jan. 15, 1938, Chicago.
46. Am. Soc. Heat. Cent. Engrs., Heating, Ventilating, Air Conditioning Guide, Chap, 33, pp. 595-606 (1947).
47. Carrier, W. H., Cherne, R. E., and Grant, W. A., "Modern Air Conditioning, Heating, and Ventilating," Chap. XI, Pitman Publishing Co., New York, 1940.
48. Rowley, F. B., and Jordan, R. C., Heating, Piping, Air Conditioning, 7, 293-9 (1935); 10, 539-48 (1938); 11, 388-98, 633-8 (1939); 12, 61-7, 669-702 (1940); 13, 99-101, 246-55, 304-6, 524-29 (1941); 14, 19-22, 438-47 (1942); 15, 487-494 (1943).
49. Ziel, H. E. and Sleik, H., Heating, Piping, Air Conditioning, 15, 367-72 (1943).

I. Miscellaneous Collectors

50. Blacktin, S. C., J. Soc. Chem. Ind., 58, 334-8 (1939).
51. Gottschalk, V. H., and St. Clair, H. W., Mining and Metallurgy, 18, 244-7 (1937).
52. Howard, H., Fume Arrestor, U.S. Patent No. 896,111 (1908).
53. St. Clair, H. W., U. S. Bureau of Mines, Rept. Invest. 3400, May, 1938.
54. Watson, H. H., Trans. Faraday Soc., 32, 1073-84 (1936).
55. Anon., Power Plant Engineering, 48, 90-1 (1944) Dec.

II. NOMENCLATURE

Except where special units are specifically indicated in the text, any consistent system of units may be employed. The metric and English units are given below merely by way of example. Where special units are called for in the text, only those units specified below, in the column "Special Units," may be employed In equations employing electrical quantities, only the metric system may be used since there are no comparable electrical units in the English system.

Symbol	Description	System of Consistent Units: Metric(c.g.s).	System of Consistent Units: English	Special Units
A_c	Cyclone inlet area	sq. cm.	sq. ft.	--------
A_e	Area of collecting electrode (side on which particles collect, only)	sq. cm.	sq. ft.	--------
B_c	Width of rectangular cyclone inlet duct	cm.	ft.	--------
B_e	Spacing between wire and plate, or rod and curtain, or between parallel plates in electrical precipitators	cm.	ft.	--------

Symbol	Description	System of Consistent Units: Metric(c.g.s.)	System of Consistent Units: English	Special Units
B_s	Width of gravity settling chamber	cm.	ft.	--------
c_d	Dust concentration in inlet or approach gas stream	--------	--------	grains/cu.ft.
D_b	Representative dimension or diameter of body impinged upon	cm.	ft.	--------
D_c	Cyclone diameter	cm.	ft.	--------
D_e	Cyclone gas exit duct diameter	cm.	ft.	--------
D_p	Diameter of particle	cm.	ft.	--------
$D_{p\mu}$	Diameter of particle	--------	--------	microns
D_{pc}	Cut size, diameter of particles of which 50% of those present are collected	cm.	ft.	--------
D_{pL}	Diameter of drops	cm.	ft.	--------
$D_{p,min}$	Minimum diameter of particle which is completely collected	cm.	ft.	--------
D_{px}	Diameter of particle which settles through a distance x	cm.	ft.	--------
D_t	Inside diameter of collecting tube of concentric cylinder-type electrical precipitator	cm.	ft.	--------
e	Natural or Naperian logarithmic base	2.718...	2.718...	--------
F_{cv}	Cyclone friction loss expressed as number of cyclone inlet velocity heads	dimensionless	dimensionless	dimensionless
g_L	Local acceleration due to gravity	(cm./sec.)/(sec.)	(ft./sec.)/(sec.)	--------
H_s	Height of gravity settling chamber	cm.	ft.	--------
k_m	Stokes-Cunningham correction factor	dimensionless	dimensionless	dimensionless
k_{pc}	Proportionality factor for cloth pressure drop	--------	--------	$\left(\frac{\text{(in.water)}}{\text{(cp.)(ft.min.)}}\right)$
k_{pd}	Proportionality factor for pressure drop through collected dust	--------	--------	$\left(\frac{\text{(in.water)/(ft.min.)}}{\text{(cp.)(grains/sq.ft.)}}\right)$
K_e	Electrical precipitator constant	(sec./cm.)	(sec./ft.)	--------
L_e	Length of collecting electrode in direction of gas flow	cm.	ft.	--------
L_s	Length of gravity settling chamber in direction of gas flow	cm.	ft.	--------
m_s	Mass of solids per unit of cloth area	--------	--------	grains/sq.ft.
N_e	"Effective" number of turns made by gas stream in a cyclone separator	dimensionless	dimensionless	--------
N_o	Number of elementary electrical charges acquired by a particle	dimensionless	--------	--------
N_s	Number of shelves parallel to gas flow in gravity settling chamber	dimensionless	dimensionless	--------
N_t	Number of turns made by gas stream in a cyclone separator	dimensionless	dimensionless	--------

Symbol	Description	System of Consistent Units: Metric(c.g.s.)	System of Consistent Units: English	Special Units
Δp_{cv}	Pressure drop, expressed as number of cyclone inlet velocity heads	dimensionless	dimensionless	--------
Δp_i	Pressure drop	--------	--------	in. water
q	Gas flow rate	cu.cm./sec.	cu.ft./sec.	--------
r_{av}	Average radius of gas stream in cyclone separator	cm.	ft.	--------
t	Time	sec.	sec.	--------
t_m	Time			min.
T	Absolute gas temperature	°K.or°C.abs.	°R. or °F. abs.	--------
u_e	Velocity of migration of particle toward collecting electrode	cm./sec.	ft./sec.	--------
u_t	Gravitational terminal settling velocity of particle	cm./sec.	ft./sec.	--------
u_{tg}	Gravitational settling velocity of minimum particle completely settled out in gravity settling chamber	cm./sec.	ft./sec.	--------
u_{tx}	Gravitational settling velocity of particle of size D_{px}	cm./sec.	ft./sec.	--------
V_c	Average cyclone inlet velocity based on area A_c	cm./sec.	ft./sec.	ft./sec.
V_e	Average velocity of gas flowing through electrical precipitator	cm./sec.	ft./sec.	--------
V_f	Superficial velocity of gas through cloth	--------	--------	ft-/min.
V_o	Average velocity of dust-laden gas	cm./sec.	ft./sec.	--------
V_s	Average gas velocity in gravity settling chamber	cm./sec.	ft./sec.	--------
x	Distance normal to gas stream through which particle moves in cyclone	cm.	ft.	--------
x_L	Distance normal to gas stream through which drops are sprayed	cm.	ft.	--------
y	Ratio of volumetric liquid circulation rate to volumetric gas flow rate	$\left(\frac{\text{cu.cm./sec.}}{\text{cu.cm./sec.}}\right)$	$\left(\frac{\text{cu.ft./sec.}}{\text{cu.ft./sec.}}\right)$	--------
η_f	Fractional collection efficiency, weight fraction collected of entering dipersoid of specific size	dimensionless	dimensionless	dimensionless
η_t	Target efficiency, fraction of disper. soid in swept volume collected on target	dimensionless	dimensionless	dimensionless
ρ	Fluid density	g./cu.cm.	lb.mass/cu.ft.	lb.mass/cu.ft.
ρ_p	True (not bulk) density of particle	g./cu.cm.	lb.mass/cu.ft.	g./cu.cm.
μ	Fluid viscosity	poise	(lb.mass)/(ft.)(sec.)	--------
μ_c	Fluid viscosity	--------	--------	centipoise

p. 300 - Units for V_f should read: "ft./min." in place of "ft-/min."

Symbol	Description	System of Consistent Units: Metric(c.g.s.)	English	Special Units
ϵ	Elementary electrical charge	4.80×10^{-10} e.s.u.	--------	--------
ϵ_v	Fraction voids in bed	dimensionless	dimensionless	dimensionless
ϕ	Cumulative weight fraction in dispersoid larger than given particle size	dimensionless	dimensionless	dimensionless
ϕ_s	Particle shape factor (number less than 1.0)	dimensionless	dimensionless	dimensionless
λ_p	Particle mobility = u_e/ϵ	$\left[\frac{(cm./sec.)}{(statvolt/cm.)}\right]$	--------	--------
$\mathcal{E}$	Electrostatic potential gradient	statvolts/cm.	--------	--------
$\mathcal{E}_i$	Average electrostatic potential gradient in ionization stage	statvolts/cm.	---------	--------
$\mathcal{E}_p$	Average electrostatic potential gradient in collection stage	statvolts/cm.	--------	--------
δ	Dielectric constant	dimensionless	--------	--------
ζ	$\left[1+2(\delta-1)/(\delta+2)\right]$	dimensionless	--------	--------

(ζ ranges from a value of 1 for materials with a dielectric constant of 1 to 3 for conductors.)

III. PURPOSE OF DUST AND MIST COLLECTION

A. Nuisance Elimination - as in cleaning of ventilation air or fly ash removal from power plant combustion gases. The increased interest on the part of civic associations as the result of increased industrialization of metropolitan areas has been responsible for enactment of local ordinances in many areas.

B. Equipment Maintenance Reduction - as in filtration of engine-intake air or pyrites furnace gas treatment prior to its entry to a sulfuric acid system.

C. Safety or Health Hazard Elimination - as in collection of siliceous and metallic dusts around grinding and drilling equipment and in some metallurgical operations and flour dusts from milling or bagging operations.

D. Product Quality Improvement - as in air cleaning in the production of pharmaceutical products and photographic film.

E. Recovery of a Valuable Product - as in collection of dusts from dryers and smelters.

F. Powdered Product Collection - as in pneumatic conveying, the spray drying of milk, eggs, and soap, and the manufacture of high purity zinc oxide and carbon black.

IV. FACTORS IN DUST AND MIST COLLECTION EQUIPMENT DESIGN

The forces or mechanisms utilized for dust collection may be classified as: (1) gravitational, (2) inertial, (3) filtration, (4) electrostatic, (5) physicochemical, (6) thermal, and (7) sonic. Since many forms of dust collection equipment utilize more than one of these forces, it is more convenient to classify dust collection equipment according to type rather than according to the underlying operating principle.

The performance of a dust collector is termed collection efficiency and is generally expressed as a weight ratio of dust (or mist) collected to dust entering the apparatus. Some prefer to evaluate collection efficiency entirely by the dust concentration in the exit gases regardless of inlet concentrations. In either case collector efficiency is in itself not a specific characteristic of a given collector, depending on operating conditions as well as on the physical properties of the particular dust (or mist) handled.

p. 301 - change " $= u_e/\epsilon$ " to "$= u_e/\mathcal{E}$" in definition λ_p

TABLE I. DUST AND MIST COLLECTION EQUIPMENT CLASSIFICATION OF TYPES AND HIGH-SPOT PERFORMANCE CHARACTERISTICS

Type Collector	Approximate Minimum Particle Diameter Collectable, microns	Approximate* Purchase Cost $/(cu. ft./min.)	Outstanding Characteristics or Application
1. Gravity Settling Chamber	40	---	Simple, large, low Δp; precleaner; natural draft exhausts.
Howard Type	10	---	Difficult to clean.
2. Impingement Separators	10	0.10-0.20	Adaptable to existing flues.
Calder Fox	2	---	Sulfuric acid mist removal.
3. Cyclone Separators	5	0.04-0.08	Simple, inexpensive most widely used.
Multiple Units	2	0.15-0.50	
4. Mech. Centrifugal Separators	5	0.10-0.30	Compact: ventilation booths
5. Misc. Inertial Separators			May be adaptable to existing flues.
6. Packed Beds			
Coke Box	0.5	2.00-5.00 (special)	Sulfuric acid mist removal.
7. Cloth Collectors	0.1		High collection efficiency; temp. and moisture limitations.
Baghouse		0.50-2.50	Simple, large.
Unit Filter		0.15-1.50	For small capacities (< 1000 cu.ft./min.)
Mechanical Filter		0.10-0.70	For high capacities.
Automatic Filter		0.50-2.00	For high dust concentrations (> 20 grains/cu.ft.)
8. Scrubbers	0.1-1		Dust wetted; sludge disposal and corrosion problems.
Chamber Type		0.15-1.50	Simple
Cyclone Type		0.30-1.00	
Inertial Type		0.30-1.00	
Mechanical Type		1.00	
Packed Type			
Film Type			
Miscellaneous			
9. Electrical Precipitators	0.01	0.30-1.50	For process gases; heavy duty; expensive on first cost and operation
Single-Stage (Cottrell)		2.00-10.00 (special)	
Plate Type			
Pipe Type			
Two-Stage		0.10-0.30	Small, compact; air conditioning applications
Alternating Current			Laboratory instrument.
10. Air Filters			High capacity, low resistance, low dust concentration; air conditioning.
Viscous	5	0.005-0.030	
Dry	2	0.005-0.050	
Automatic		0.05-0.10	
Misc.			
Wetted Cells			
Electrostatic		0.10-0.30	
Pipe-Line			
Activated Carbon		0.10-0.20	Odor removal.
11. Miscellaneous			
Sonic			Only recently of industrial importance.
Thermal			Not developed industrially.

*For steel construction except where otherwise noted; includes only directly chargeable and necessary auxiliaries; not installed. Based on prices in period 1945-1946.

Note: The above are order-of-magnitude values only applying to the majority of units in each category and do not necessarily apply to all the commercially available types of equipment in each category. In cases where values are very diverse for the specific types or applications in each category, values are not listed.

p. 302 - In Table I under "9. Electrical Precipitators": The items "0.30 - 1.50" and "For process gases .." should both be lowered to correspond to "Single-Stage (Cottrell)." The item "2.00 - 10.00" and "(special)" also correspond to "Single-Stage (Cottrell)" as printed.

The following summarizes the outstanding characteristics of a dust, gas, and system which must be considered in designing a dust collection system. Any one or several of these factors may determine or limit the equipment design for a specific application.

A. Dust or Mist Characteristics

1. Particle size distribution, shape, and density; settling velocity
2. Physicochemical properties; "stickiness"; hygroscopic nature; acidity or alkalinity; flocculating tendencies; electrical conductivity; explosiveness; fusion point
3. Dust or mist concentration

B. Gas Characteristics

1. Temperature and pressure
2. Composition: chemical and physical
3. Humidity
4. Volumetric rate

C. System Characteristics

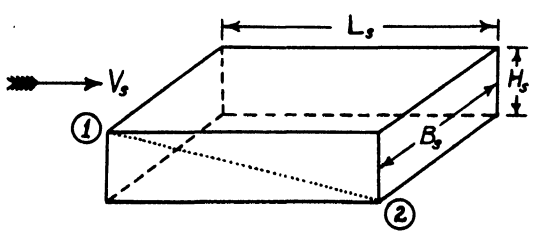
1. Collection efficiency required
2. Allowable pressure drop
3. Headroom and floor space requirements
4. Operating requirements: continuity of operation; maintenance requirements
5. Product quality requirements: wet vs. dry collection; contamination

In Table I is given a classification of dust and mist collection equipment together with a high-spot approximation of range of application, equipment cost, and outstanding characteristics. The subsequent paragraphs will consider each type in more detail and will present underlying performance principles wherever possible.

V. GRAVITY SETTLING CHAMBERS

The gravity settling chamber is probably the simplest and earliest type of dust collection equipment, consisting of a chamber in which the gas velocity is reduced to enable dust to settle out by the action of gravity. Its simplicity lends it to almost any type of construction. Practically, however, its industrial utility is limited to removing particles larger than 325 mesh (43 microns diameter) since the required chamber size for removing smaller particles is generally excessive. The pressure drop through a settling chamber is small, consisting almost entirely of entrance and exit losses. The most frequent application is on natural draft exhausts from kilns and furnaces due to its low pressure drop and structural simplicity.

Gravity collectors are generally built in the form of long, empty, horizontal, rectangular chambers with an inlet at one end and an outlet at the side or top at the other end.



A particle will be completely settled out if it can settle from 1 to 2, a height of H_S, in the time, t, it takes the carrier gas to pass from one end to the other.

$$t = H_S/u_{tg} = L_S/V_S = L_S/(q/B_S H_S) \quad (1)$$
(consistent units)

Hence
$$u_{tg} = q/B_S L_S \quad (2)$$
(consistent units)

Thus a particle with a terminal velocity of $(q/B_S L_S)$ will be completely settled out. It should be observed that this velocity is the same as that of the fluid if it passed vertically through the area, $B_S L_S$. Thus the performance of a gravity settling chamber depends on its horizontal projected area and is independent of its height. The height need be made only large enough so that the gas velocity, V_S, in the chamber is not so high as to cause re-entrainment of separated dust. For this reason, V_S, should not exceed about 10 ft./sec. It is important that the gas be well distributed laterally upon entering the chamber; the vertical distribution is not so important. This distribution can be achieved by gradual inlet transitions, guide vanes, or distributing screens or perforated

plates. The outlet can be abrupt without appreciable effect on performance. Curtains, rods, or screens are sometimes suspended in the chamber to minimize eddy currents. They also serve to increase collection by impingement and may be equipped with rappers.

While alternately arranged vertical baffle plates have been used in settling chambers on the theory of subjecting particles to changes of direction, their use in the simple gravity settling chamber is detrimental since inertial forces are generally small at the velocities encountered in such chambers. Horizontal plates arranged as shelves within the chamber, however, will give a marked improvement in collection. This arrangement is known as a Howard dust chamber and, by a derivation similar to that above, it can be shown that

$$u_{tg} = q/N_S B_S L_S \qquad (3)$$

(consistent units)

A Howard chamber can be used to remove particles as small as 10 microns diameter. Its chief disadvantage is in the difficulty of cleaning due to the close shelf spacing and warpage at elevated temperatures. This is particularly serious at dust loadings over 1 grain/cu.ft.

VI. IMPINGEMENT SEPARATORS

When a dust-laden fluid impinges on a body, the fluid will be deflected around the body whereas the dust particles, by virtue of their greater inertia, will tend to be collected on the surface of the body. The basic principles of impingement separators can be presented in terms of the so-called "target" efficiency which represents the fraction of particles in the fluid volume swept by the body which will impinge on the body. As shown in References 10 and 13, the target efficiency, η_t, should be a function of the dimensionless group $(u_t V_o/g_L D_b)$. For spherical and cylindrical collecting bodies, the following values are given in the literature:

$(u_t V_o/g_L D_b)$	Target Efficiency, η_t			
	For Spheres		For Cylinders	
(consistent units)	Sell(13)	Langmuir(12a)	Sell(13)	Langmuir(12a)
10.0	----	0.95	----	0.93
5.0	----	0.90	----	0.86
2.0	----	0.77	----	0.72
1.0	0.41	0.62	0.66	0.56
0.5	0.28	0.43	0.51	0.39
0.2	0.13	0.20	0.26	0.13
0.1	0.066	0.081	0.14	0.02
0.0625	----	----	----	0.00*
0.05	0.033	0.012	0.070	0.00
0.042	----	0.000*	----	0.00
0.0	0.000	0.000	0.000	0.00

* Value of 0.000 is just attained

While the relationships given by these investigators are conflicting, the values reported by Langmuir are believed to be the more reliable. Langmuir's values were derived from hydrodynamic theory and indicate a limiting value of the group $(u_t V_o/g_L D_b)$ below which no particles are collected to any extent. Sell indicates no such limiting value. Albrecht (10) confirms the form of Langmuir's relationship although he differs in the exact numerical values.

Impingement separators are designed for a pressure drop in the range of 0.1 to 1.5 in. water depending on type and application and are limited to removing dusts that are predominantly larger than 10 to 20 microns diameter. The chief advantage of such units lies in their greater adaptability to existing flues or ducts than some other types of collectors.

The Calder-Fox scrubber (11) is a British development frequently used for removing sulfuric acid mist. It is essentially an impingement separator employing two groups of perforated plates in series. The first "agglomerator" group consists of an "orifice" plate followed by an "impact" plate with staggered orifices and separated by a spacer. This group is followed by a group of three "collector" plates with aligned orifices. The holes in the orifice plate are about 1/8 in. diameter on 3/8 or 1/2 in. centers, square pitch, while the impact plate contains 1/4-in. holes on the same centers and is set 1/8 in. away from the orifice plate. A glass unit has also been developed in which the perforated plates are replaced with strips of glass with 1/16-in. wide orifice slots and 1/8-in. impact slots.

These plates are set 1/16 in. apart and no collector plates are used. In a third modification for use with wax mists the impact plate is replaced with a cooled imperforate rotating drum. The Calder-Fox unit is only effective for mist particles larger than 2 microns diameter. Orifice velocities are generally on the order of 50 to 100 ft./sec., but should not exceed 150 ft./sec. at atmospheric pressure to avoid excessive re-entrainment. The pressure drop is approximately 2.0 to 2.5 orifice velocity heads.

VII. CYCLONE SEPARATORS

A. Fields of Applications: The most widely used type of dust collection equipment is the cyclone, in which dust-laden gas enters a cylindrical or conical chamber tangentially at one or more points and leaves through a central opening. The dust particles, by virtue of their inertia, will tend to move toward the outside separator wall, from which they are led into a receiver. At operating conditions commonly employed, the centrifugal separating force or acceleration may range from 5 times gravity in very large diameter, low-resistance cyclones, to 2,500 times gravity in very small, high-resistance units.

Cyclone collectors offer one of the least expensive means of dust or mist collection from both an operating and investment viewpoint. Cyclones have been employed to remove solids and liquids from gases and solids from liquids, and have been operated at temperatures as high as 1000°C. and pressures as high as 500 atm. Cyclones for removing solids or liquids from gases are generally applicable when particles of over 5 microns diameter are involved. Unless very small cyclones are used, the efficiency will be low if much of the suspended material is finer than 5 microns. In special cases where the dust shows a high degree of agglomeration, or where high dust concentrations (over 100 grains/cu.ft.) are involved, cyclones will remove dusts having a much smaller particle size. In certain cases efficiencies as high as 98% have been realized on dusts having an ultimate particle size of 0.1 to 2.0 microns due to the predominant effect of agglomeration.

B. Flow Pattern: In a cyclone the gas path involves a double vortex with the gas spiraling downward at the outside and upward at the inside. Upon entering the cyclone, the gas velocity undergoes a redistribution so that the tangential component of velocity increases with decreasing radius. The spiral velocity in a cyclone may reach a value several times the average inlet gas velocity. At the wall the gas velocity approaches zero, whereas it reaches a maximum at a certain radius, decreasing rapidly at smaller radii (19).

Superimposed on the "double spiral," there may be a "double eddy" similar to that encountered in pipe coils. However, such double eddy velocities are small compared to the spiral velocity.

C. Pressure Drop: The pressure drop or friction loss in cyclones may be expressed as a certain number of inlet velocity heads (19). The cyclone friction loss is a direct measure of the static pressure and power that a fan must develop and is related to the pressure drop by

$$F_{cv} = \Delta p_{cv} + 1 - (4\ A_c/\pi\ D_e^2)^2 \qquad (4)$$

(consistent units)

The friction loss through cyclones encountered in practice may range from 1 to 20 inlet velocity heads, depending on the geometric proportions (15) (19). For a cyclone of specific geometric proportions, however, F_{cv} and Δp_{cv} are substantially constant, independent of the actual cyclone size. For the cyclone of the proportions shown in Figure 1, F_{cv} is approximately 8.

D. Collection Efficiency: The performance of a cyclone can be calculated in a manner similar to that used for gravity settling chambers. In the following simplified development, following the method presented by Rosin, Rammler, and Intelmann (18), it is assumed that the gas moves through the cyclone as a rigid spiral having a spiral velocity equal to the average velocity at the cyclone inlet. Equating the time of retention of the gas in the cyclone to the time required for a particle to settle radially through a distance, x,

$$t = (x/u_{tx}) = 2\pi\ r_{av}\ N_t/V_c \qquad (5)$$

(consistent units)

Applying Stokes's law for a centrifugal field

$$u_{tx} = V_c^2\ D_{px}^2(\rho_p - \rho)/18\ \mu\ r_{av} \qquad (6)$$

(consistent units)

From Equations 5 and 6

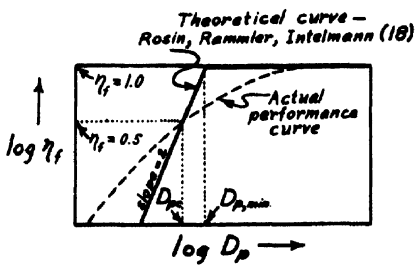
$$D_{px} = \sqrt{9\ \mu\ x/\pi\ V_c\ N_t\ (\rho_p - \rho)} \qquad (7)$$
(consistent units)

A particle, to be completely separated out, must settle across the width of the gas stream, B_c. Thus

$$D_{p,min.} = \sqrt{9\ \mu\ B_c/\pi\ V_c\ N_t\ (\rho_p - \rho)} \qquad (8)$$
(consistent units)

$$D_{px} = D_{p,min.}\ \sqrt{x/B_c} \qquad (9)$$
(consistent units)

It is apparent that a fraction (x/B_c) of particles of size D_{px} will be separated out in the cyclone. It can also be shown that the over-all collection efficiency of a cyclone is given by the mean ordinate of a plot of ϕ as ordinate against (x/B_c) as abscissa over the range (x/B_c) from 0 to 1 where ϕ is the cumulative weight fraction of dust entering the cyclone larger than size D_{px}.

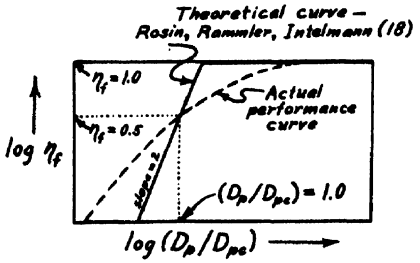


Actually the flow pattern, as described above, is considerably more complex than assumed in this derivation. It is also known that particles larger than $D_{p,min.}$ will pass a cyclone whereas a collection of finer particles greater than anticipated is obtained. If the fractional collection efficiency, η_f (i.e., fraction of particles of size D_p entering the cyclone which are collected in the cyclone), is plotted against the particle size D_p, the above derivation yeilds the solid curve shown at the left.

The actual curve obtained is of the form shown by the dashed curve. Nevertheless, due to compensating effects, the above method of calculation serves as a fairly good approximation for purposes of estimating cyclone collection efficiency provided a proper value of N_t is used. The term N_t in this case may be regarded as an equivalent effective value and does not represent an actual number of gas revolutions.

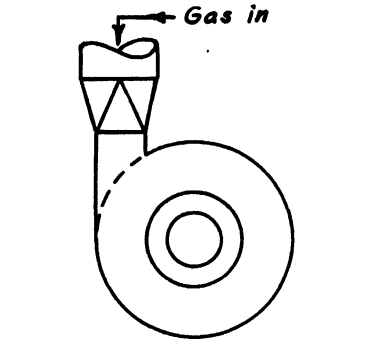
Where the actual fractional collection efficiency curve for a given type of cyclone is known, the following method can be used to obtain a more accurate estimate of cyclone collection efficiency. The above fractional efficiency curves can be presented in terms of particle size, expressed as a ratio to the cut size, D_{pc}, where D_{pc} is defined by

$$D_{pc} = \sqrt{9\ \mu\ B_c/2\pi\ N_e\ V_c\ (\rho_p - \rho)} \qquad (10)$$
(consistent units)



This type of plot is essentially a generalized form of the "fractional" efficiency plot frequently found in commercial literature. For the Rosin, Rammler, and Intelmann curve, the term N_e is identical with N_t. The value of N_e as obtained from experimental data should be unique for a cyclone of given proportions in the absence of re-entrainment. The value of N_e may be regarded as an approximate measure of the effectiveness of a given type of cyclone design. For the cyclone design proportions shown in Figure 1, the value of N_e has been found to be approximately 5.0. For this cyclone the fractional efficiency values are given in the table on Figure 1.

The table on Figure 1 gives the separation efficiency to be expected for a given particle size. The over-all collection efficiency for dusts containing a range of particle sizes is a summation of the efficiency on each particle size prorated according to the fraction of the total dispersoid in that size range. If the particle size distribution is known, the over-all collection efficiency can be calculated graphically by plotting values of η_f and ϕ, corresponding to the same particle size, as ordinate and abscissa, respectively, on arithmetic paper. The over-all
of the plot as shown in Figure 1.



Summary of Performance Equations:

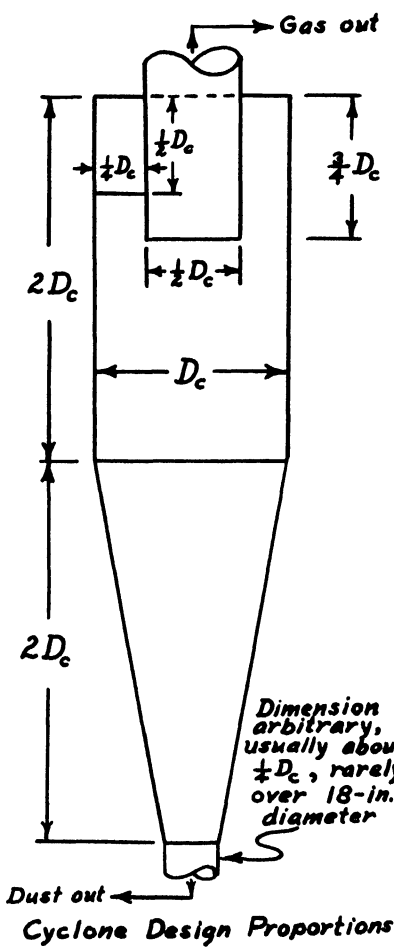
$$D_{pc} = \sqrt{9\mu B_c / 2\pi N_e V_c (\rho_p - \rho)}$$

$$N_e \cong 5.0$$

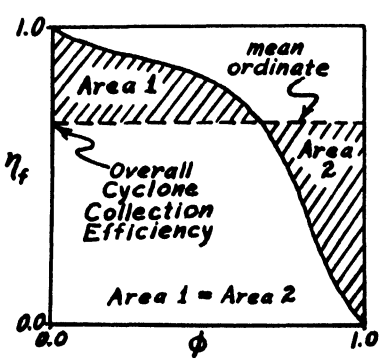
$$\Delta F_{cv} = 8.0$$

Values of η_f:

D_p/D_{pc}	η_f
0.2	0.04
0.3	0.08
0.5	0.20
0.7	0.33
1.0	0.50
1.5	0.69
2.0	0.80
3.0	0.90
5.0	0.96
7.0	0.98
10.0	0.99



Cyclone Design Proportions



Method of Calculating Overall Collection Efficiency

Figure 1. Typical Cyclone Design Proportions and Performance

E. Cyclone Design Factors: Cyclones are generally designed to meet specified pressure drop limitations. For ordinary installations operating at approximately atmospheric pressure, fan limitations generally dictate a maximum allowable pressure drop corresponding to a cyclone inlet velocity in the range of 20 to 70 ft./sec. Consequently cyclones are usually designed for an inlet velocity of 50 ft./sec., though this need not be strictly adhered to.

In the removal of dusts, the collection efficiency can be changed to only a relatively small amount by a variation in the operating conditions. The primary design factor that can be utilized to control collection efficiency is the cyclone diameter, a smaller diameter unit operating at a fixed pressure drop having the higher collection efficiency but requiring a multiple of units in parallel for a specific gas handling capacity. The final design involves a compromise between collection efficiency and complexity of equipment. It is customary to design a single cyclone for a given capacity, resorting to multiple units only if the predicted collection efficiency is inadequate for a single unit. Cyclones in series are generally not justified. Exceptions to this are cases where the dust is fine and has a relatively uniform particle size distribution, and where the dust is present in a highly flocculated state. In the latter case efficiencies predicted on the basis of ultimate particle size distribution will be highly conservative. Also, while normally efficiency is increased by increasing the gas throughput, in such cases the reverse may be the case due to the deflocculating effect of higher velocities.

Reducing the gas outlet duct diameter will increase both collection efficiency and pressure drop. Increasing the length of a cyclone is generally believed to increase collection efficiency though there are no reliable supporting data. There is also no reliable information on the effect of inlet proportions or cone angle on collection efficiency.

A cyclone will operate equally well on the suction or pressure side of a fan if the dust receiver is air-tight. Probably the greatest single cause for por cyclone performance, however, is the leakage of air into the dust outlet of the cyclone. A slight air leak at this point can result in a tremendous drop in collection efficiency, particularly with fine dusts. For a cyclone under pressure, air leakage at this point is objectionable primarily from the local dust nuisance created. For batch operation an air-tight hopper or receiver may be used. For continuous withdrawal of collected dust, a rotary star valve, a double-lock valve, or a screw conveyor may be used, the latter only with fine dusts; a liquid seal leg is sufficient for mist or spray collectors. In any case, it is essential that sufficient unloading and receiving capacity be provided to avoid collected material from accumulating in the cyclone cone.

Generally cone and disk baffles, helical guide vanes, straightening vanes, etc., placed inside a cyclone, will have a detrimental effect on performance. A few of these devices have merit under special circumstances. An inlet vane, formed by extending the inner side of the inlet duct past the cyclone wall to the gas outlet duct, has been found to reduce the friction loss through the cyclone by over 50% (15) (19). However, a correspondingly greater reduction in collection efficiency results. The N_e value for this arrangement is approximately 2 for cyclone inlet velocities on the order of 50 ft./sec. Such a vane is only recommended (a) where collection efficiency is normally so high as to be of secondary importance, (b) where it is desired to decrease the resistance of an existing cyclone system for purposes of increased air handling capacity, or (c) where floorspace or headroom requirements are controlling factors. If an inlet vane is used, it is advantageous to increase the gas exit duct length inside the cyclone chamber. A disk or cone baffle located beneath the gas outlet duct may be beneficial if air inleakage at the dust outlet cannot be avoided. A heavy chain suspended from the gas outlet duct has been found useful in minimizing dust buildup on the cyclone walls. At present there are no known devices which will recover the velocity energy of gas spiralling in the gas outlet duct. Substantially all devices which have been reported to reduce pressure drop do so by reducing spiral velocities in the cyclone chamber and consequently result in a reduced collection efficiency.

Increased dust loading will result in both decreased pressure drop and increased collection efficiency. At dust loadings of over 200 grains/cu.ft., the pressure drop may be as low as half of that calculated in the absence of dust.

F. Commercial Units: Cyclones are available in a wide variety of shapes ranging from long slender units to short squatty units. The bodies may be conical or cylindrical; entrances may be involute or tangential, and round or rectangular.

The following are some of the common manufacturers of cyclones:

a. Simple Cyclones - Bartlett & Snow; Buffalo Forge; Clarage; Day Co.; Gruendler; Gump; Hardinge; Pangborn; Sturtevant; Williams; Wolf.

p. 308 - 4th paragraph, line 2: should be "poor" in place of "por".

b. Complex Cyclones - Clark, American Blower Corp.; Buell (Van Tongeran); American Foundry.

c. Multiple Cyclones - Western Precipitation Corp. (Multiclone); Aerotec Corp.; Prat-Daniel Corp. (Multicyclone, Thermix Tube).

G. Entrainment Separation: Cyclones may also be used to separate liquid droplets from gases. In this connection they find their most frequent application in the removal of mechanical entrainment from such equipment as evaporators and distillation and absorption columns. The collection efficiency on mists formed by vapor phase reaction or condensation will generally be low due to the small particle size involved. In the case of mechanical entrainment, the particles are predominantly larger than 100 microns diameter and complete separation is a simple problem. Any inefficiency in such service is not due to a failure to collect all the spray on the wall but to re-entrainment or wall creep of the liquid film after the spray has been deposited on the cyclone wall. The liquid film may be carried across the cyclone roof to the gas outlet by the action of the "double eddy." The film will then run down the outside of this duct and be carried out of the cyclone. In the case of dusts such action will not occur since the dust cannot adhere to the exit duct as a mobile film. Liquid entrainment separators are discussed further in Reference 17.

VIII. MECHANICAL CENTRIFUGAL SEPARATORS

There are commercially available a number of collectors in which the centrifugal field is supplied by a rotating member (American Air Filter Co., American Blower Corp., Prat-Daniel Corp.). While no comparative data are available, the collection efficiency of such units is probably comparable to that of the single unit, high pressure drop cyclone installation. The chief advantage of these units lies in their compactness, which may be a prime consideration for large installations or plants requiring a large number of individual collectors. Caution should be exercised, however, when attempting to apply this type of unit to a dust that shows a marked tendency to build up on solid surfaces due to the high maintenance costs that may be encountered from plugging and rotor unbalancing.

IX. MISCELLANEOUS INERTIAL SEPARATORS

There are available several types of collectors of the inertial type which do not specifically fall into any of the previous classes. These range from a simple, high-velocity gas reversal chamber (Western Precipitation Corp. Impax Separator) to a rotary unit containing closely-spaced, parallel sinusoidal plates (By-Products Recoveries, Inc.). Other units in this class are put out by Hudson H. Bubar and Buell Engineering Corp.

Most steam or compressed-air entrainment separators are of the inertial type and are intended for the removal of droplets larger than 20 microns diameter. They are available in a wide variety of forms though most of them employ impingement elements or zig-zag parallel plates. Some are cyclonic in action while a few contain rotating members driven by the gas velocity.

X. PACKED BED COLLECTORS

Although practically no dust collectors employing beds of granular solids are available as standard commerical units, such equipment has been designed for specific applications. The most common type in the chemical industry is the coke box (22) frequently used in the manufacture of sulfuric acid. These collectors consist of a tile, brick, or lead-lined chamber packed with closely-sized coke, with horizontal, upward, or downward gas flow. Coke sizes range from 1/40 in. to 1/2 in. diameter, the finer sizes being used in large boxes operating at low superficial velocity to remove very fine mist.

In one common type, the boxes are circular with either upflow or downflow of gas through a 2- to 6-ft. depth of graded coke supported on a tile or brick grid. The effective portion of the bed consists of 1/40-in. to 1/20-in. coke with thin layers of coarser grades above and below the fine coke for support. Superficial velocities may range from 2 to 10 ft./min. with pressure drops in the range of 1 to 10 in. water. For a 30-ton/day sulfuric acid plant, such a box will be on the order of 30 ft. diameter. The cost will be on the same order as that of a Cottrell in this service but maintenance costs will be less. However, it is subject to gradual plugging, depending on the amount of dust in the gas stream. The sulfuric acid mist handled in such a box has a particle size in the range of 0.5 to 3 microns, and collection efficiencies as high as 99.9% have been obtained with the finer coke sizes operated at low superficial velocity. Increased coke depths and decreased gas velocity or coke particle size will result in increased collection efficiency.

p. 309 - line 1: replace comma after "Clark" with a semicolon.

Coarse coke operated at higher superficial gas velocities has been employed for applications involving a coarser mist. Granite, quartz, and sand also have been used as packing materials.

A relatively recent development is the Lynch Granular Filter (23), which utilizes a bed of gravel. The gravel is withdrawn from the bottom of the bed continuously and passed over a screen to remove collected dust and then returned to the top of the bed. Superficial velocities are on the order of 3 ft./sec. with bed depths of 1 to 4 ft. The gravel ranges from 1/2 to 1 in. diameter and the pressure drop is on the order of 1 in. of water.

The separation of dust or mist by packed solids is due to (1) gravity settling, (2) Brownian movement, (3) impingement, (4) interception, and (5) electrostatic separation. It is doubtful whether the latter effect, resulting from electrification of the particles due to the relative gas motion, is an appreciable factor. With beds of small particles operated at low velocities, gravity settling and Brownian movement are the predominant effects and collection efficiency would be expected to increase with decreased gas velocity. With coarse packing, operated at high gas velocities, separation by impingement is controlling and increased gas velocities would be expected to give increased collection provided the gas velocity is not so high as to result in re-entrainment.

XI. CLOTH COLLECTORS

In cloth collectors (also known as bag filters), the dust-laden gases are passed through a woven fabric which "filters" out the dust, allowing the gases to pass on. Actually the separation is not a simple filtration since the pores in the cloth are usually many times the size of the particles separated. When the dust-laden gases first pass through the cloth, the separation efficiency will be low until enough particles have been collected to form a "precoat" in the fabric pores. With conditions for which cloth collectors are usually employed, this precoat will form in a few minutes, usually only a matter of seconds. Once this layer has formed, the separation efficiency will be well over 99%. Failure to achieve a very high collection efficiency with cloth collectors is due entirely to improper equipment maintenance, from such sources as torn bags, poorly installed bags, or stretched bags.

For conditions encountered in practice, the flow through both the cloth and collected dust will be streamline in character. The pressure drop through the cloth can be expressed by

$$\Delta p_i = k_{pc}\, \mu_c\, V_f \qquad (11)$$

(special units)

The value of k_{pc} is a constant dependent on the nature of the cloth and may range from 0.1 to 2.0 for cloths apt to be encountered. Usually a cotton sateen cloth is used with approximately 96 x 60 threads/in. and with a nominal weight on the order of 1.3 yards/lb. For such a cloth, k_{pc} is on the order of 1.0

When the pores of the cloth become filled with dust, the value of k_{pc} may be over 10 times that for the clean cloth. For dry dusts, however, if the dust layer on the cloth is deeper than about 1/16 in. (on the order of 0.1 lb. of dust per sq.ft. of cloth), the over-all pressure drop across the dust-laden cloth will usually be that across the dust layer, the drop across the cloth, including the dust in the pores, being comparatively negligible.

The pressure drop through the separated dust layer may be expressed as

$$\Delta p_i = k_{pd}\, \mu_c\, m_s\, V_f = k_{pd}\, \mu_c\, c_d\, V_f^2\, t_m \qquad (12)$$

(special units)

The last equality gives the pressure drop increase due to the accumulation of dust in time t_m. The resistance factor k_{pc} can be calculated from Carman's (24) equation and may be expressed as

$$k_{pd} = 2.56\,(1 - \epsilon_v)/\phi_s^2\, D_p \mu^2\, \rho_p\, \epsilon_v^3 \qquad (13)$$

(special units)

Unfortunately, sufficient data are not normally available to permit utilization of Equation 13, and an experimental determination of k_{pd} is required. Approximate average values of k_{pd} as a function of particle size based on the data in References 26 and 28 are given below:

Particle Diameter, microns	k_{pd} Experimental Ref. 26, 28	Calculated (Equation 13)* ϵ_v=0.40	ϵ_v = 0.60	ϵ_v = 0.90	ϵ_v = 0.95
0.1	0.3	4800.	950.0	70.0	30.0
1.0	0.2	48.	9.5	0.70	0.30
10.0	0.15	0.48	0.095	0.0070	0.0030
100.0	0.010	0.0048	0.00095	0.00007	0.00003

*Based on ρ_p = 2.0 grams/cu.cm. and ϕ_s = 0.5.

The value of k_{pd} depends on the dust handled, and the above average experimental values are subject to a variation of as much as five-fold in either direction. Values of k_{pd} calculated from Equation 13 for various values of ϵ_v are also shown above. It is apparent from these values that with smaller particles much looser beds are obtained (i.e., higher values of ϵ_v). It should also be noted that Equation 13 is not applicable for particles smaller than 1 micron diameter since other factors allowing for the mean free path of gas molecules must be included. These factors result in a somewhat lower value of k_{pd} than would be calculated from Equation 13.

The older baghouses were usually placed on the pressure side of the fan and contained relatively large bags, a typical size being 18 in. diameter by 30 ft. long, mounted vertically over a receiving hopper and the air discharging through the cloth directly to the atmosphere. Ratings on these units are generally in the range of 0.2 to 1.0 cu.ft./min. per sq.ft. of cloth area, and the bags are manually shaken every 2 to 12 hr.

The more recent trend has been toward mechanical filters which are available as standard commercial units. These comprise two general types: one utilizes cloth envelopes supported by screens; the other uses either oval or round vertically-mounted bags, usually 5 to 8 in. diameter and 8 to 17 ft. long. Access platforms for bag maintenance are usually provided on the clean air side. These units may be shaken manually although motor shaking is generally provided. Complete automatic operation is also possible by providing a timer, shaker motor, and air-or motor-operated gas discharge valves. The small sizes (under 1000 sq.ft. of cloth area) are available as "unit" filters and are shipped completely assembled. Large units are built up of standardized rectangular sections in parallel. Each section contains on the order of 1000 to 2000 sq.ft. of cloth, and the sections are assembled in the field to form a single filter housing. In this manner, the filter can be partitioned so that one or more sections at a time can be cut out of service for shaking or general maintenance. For heavy duty, pressure, or vacuum service, circular, fully automatic units are available.

Mechanical filters generally have a pressure drop of 2 to 6 in. water and are rated at 1 to 8 cu.ft./min. per sq.ft. of cloth area. For very fine dusts or high dust loadings, the rating should not exceed 3 cu.ft./min. per sq.ft. of cloth, and it may be desirable to reduce the rating to 1/2. When dust loadings are high, cyclone precleaners may be employed to reduce the load on the filter.

Ordinary mechanical filters may be shaken every 1/4 to 8 hr., depending on the service. A manometer connected across the filter is useful in determining when the filter should be shaken. Fully automatic filters may be shaken every 2 min. It is essential that the gas flow through the filter be stopped when shaking in order to permit the dust to fall off. With very fine dust, it may even be necessary to equalize the pressure across the cloth (26). In practice, this can be accomplished by cutting one section out of service at a time. In automatic filters, this operation involves closing the dampers, shaking the filter units, either pneumatically or mechanically, sometimes accompanied by a reverse flow of cleaned gas through the filter, and, lastly, reopening the dampers. For compressed air-operated, automatic filters this entire operation may take only 2 to 10 sec. For the ordinary mechanical filters equipped for automatic control, the cycle may run as high as 3 min.

In the recently developed Hersey filter (Pulverizing Machinery Co.), dust is removed from the cloth without shaking and without taking the unit out of service. This is accomplished by admitting high pressure air from a slot in a ring fitted around the outside of the bag. This ring is moved up and down on the bag either periodically or continuously. It is claimed that ratings as high as 30 cu.ft./min. per sq.ft. of cloth can be achieved.

Filter fabrics are generally cotton sateens. For other services, wool, glass, asbestos, or metal may also be used. The maximum recommended operating temperatures are 190, 235, 650, and 650°F. for cotton, wool, glass, and asbestos, respectively, and it is generally advisable to stay well below these limits for good bag life. Bag life varies widely depending on frequency of shaking, the nature of the dust, and the gas characteristics. For mechanical filters, it is generally 6 months to 2 years. Wool is

used for mildly acidic atmospheres whereas cotton is used for neutral or slightly alkaline conditions. Whereas both glass and asbestos have been used for higher temperature service, results have not been very satisfactory due to excessive bag failure. A recent development is "Orlon" acrylic fiber which is expected to provide a cloth resistent to acidic atmospheres at temperature as high as 350°F.

It is generally economical to be conservative in specifying cloth area since incremental cloth costs are relatively small, particularly in small installations. In operation, it is essential that the gas be kept above its dewpoint to avoid plugging of the pores. Cloth filters, however, have been successfully used in steam atmospheres such as are encountered in vacuum dryers. In such cases the housing is steam-chased.

The following are some of the better known manufacturers of mechanical filters: Allis Chalmers; American Foundry Equipment Co.; Dracco Corp.; Ducon Co.; Northern Blower Co.; Pangborn Corp.; Parsons Engineering Corp.; Pulverizing Machinery Co.; Ruemelin Mfg. Co.; W. W. Sly Mfg. Co. Units for special applications are manufactured by American Air Filter Co. (Dust Arrestor), S. Howes Co., and Prinz & Rau Mfg. Co.

XII. SCRUBBERS

Scrubbers may be defined as equipment in which a liquid is employed to achieve or assist in the removal of dispersoids from gases. Water is generally employed as the scrubbing agent although other liquids may be employed. The mechanisms by which a liquid serves to remove a dispersoid from a gas may be summarized as follows:

1. Impingement. When a dust-laden gas is swept by liquid drops, dust particles will be impinged upon the drops according to the principles given on page 12. For the case where a liquid is sprayed radially through a rotating gas, Kleinschmidt (33) has derived an equation which, in more general form, may be written as

$$\eta_f = 1 - e^{-(3\eta_t\, x_L y/2\, D_{pL})} \qquad (14)$$

(consistent units)

Kleinschmidt assumed the factor, η_t, to be unity for cases where the droplet is less than 200 times the particle diameter. The value η_t may be computed from the work of Sell (see page 12) for specific cases and may be less than 0.1 for particles smaller than 5 microns diameter for conditions encountered in practice. While Equation 14 would indicate higher collection efficiency for smaller liquid droplets, there is no advantage in going to drops smaller than about 30 to 50 microns diameter since for smaller drops the value η_t will decrease to a compensating extent due to rapid frictional deceleration of such droplets.

2. Diffusion. Dust particles interdispersed amongst liquid droplets in a gas stream will be deposited on the liquid drops by Brownian diffusion or motion. This mechanism will be predominant in the collection of submicron particles and may be appreciable for dust particles in the range up to 5 microns diameter. Diffusion as the result of fluid turbulence may also be a significant factor in dust deposition. Diffusion is claimed to be the controlling action in the recently developed venturi dust and mist scrubber.

3. Humidification. Humidification may result in a flocculation of suspended particles, making them easier to separate. Details of this mechanism are not yet understood in any detail.

4. Condensation. If the liquid spray causes the gas to pass through its dewpoint, condensation will take place with the dust particles acting as nuclei, thus increasing the effective size of the particles. This mechanism is important for initially hot gases containing relatively small dust concentrations (less than 1.0 grains/cu.ft.).

5. Wetting. Contrary to prevalent beliefs, the wetting characteristics of the liquid do not necessarily play a major role in the actual process of dust collection. Wetting agents, however, may serve to avoid re-entrainment of dust particles once they have been impinged on liquid droplets.

6. Gas Partition. If a gas is passed through a liquid or foam, the gas is segregated into small elements in which the particles can more readily be deposited on the liquid surface by gravitational or Brownian displacements. The mere bubbling of a gas through a liquid is not usually very effective, even with high columns, unless the gas is maintained highly dispersed.

7. Dust Disposal. In some so-called scrubbers, the liquid flows as a film over collecting surfaces and acts to dispose of the dust to avoid re-entrainment aside from humidification or condensation effects.

p. 312 - line 26 (2nd line after Eq. 14): at end of line change "page 12" to "page 304".

8. Electrostatic Precipitation. The rupture and impact of liquid streams may result in electrical charging of the liquid droplets. The role of this mechanism in dust collection is not understood in any detail.

Commercial equipment is available which combines scrubbing with almost every other method of dust and mist collection. Unfortunately, however, there are very few comparative performance data available. In general, the simpler types of scrubbers are not very effective in collecting particles finer than about 5 microns diameter. The more effective scrubbers, however, will permit collection of particles as small as about 1 to 2 microns but collection efficiency drops off very rapidly for finer particles unless flocculation or condensation is a controlling factor. In the following paragraphs are described a few of the common currently-available commercial units.

Chamber Scrubbers: In the conventional air washer the gas is passed horizontally through banks of sprays which may be directed downward, upward, into the gas stream or with the gas stream. A set of zig-zag eliminator plates is provided at the outlet and frequently such plates are placed between banks of sprays. The pressure drop is generally between 0.1 and 0.5 in. water; the water consumption, 0.5 to 2 (gal./min.)/(1000 cu.ft./min.) of gas handled; and superficial gas velocities are on the order of 5 ft./sec.

The water jet scrubber, as represented by the Schutte & Koerting obnoxious vapor condenser, may be considered a modified form of this class. Units of this type are capable of developing a draft up to 8 in. water and have a water consumption on the order of 50 to 100 (gal./min.)/(1000 cu.ft./min.) of gas handled for a draft of 1 in. water. In addition to the jet, a water-gas separating device, which may be a simple gas reversal chamber, must be provided on the outlet side. Such units are available as standard items in cast iron, steel, lead, lead-lined steel, rubber-lined cast iron, stoneware, and Haveg.

A recent development that may be placed in this category is the Pease-Anthony venturi scrubber (30). This unit involves the introduction of water at low pressure (5 lb./sq.in.) at the throat of a venturi. Throat gas velocities are on the order of 200 ft./sec. and the pressure drop is in the range of 10 to 15 in. water; water rates are in the range of 3 (gal./min.)/(1000 cu.ft./min.) of gas handled. Very high collection efficiencies on very fine dusts have been reported.

Cyclone Scrubbers: Typical units in which scrubbing is combined with cyclonic action are the standard Pease-Anthony scrubber, the Hydroclone (Whiting Corp.), and the Multiwash (Claude B. Schneible). In the first unit, gas is admitted tangentially at the base of a vertical cylinder and water is introduced at high pressure (100 to 200 lb./sq.in.) from a vertical central manifold containing radially-directed spray nozzles. In the other two types, liquid dispersion is achieved by the passage of the gas through so-called "disintegrator" plates. In cyclone scrubber units, superficial tower velocities are generally in the range of 4 to 8 ft./sec.; pressure drops range from 2 to 8 in. water; and water circulation rates are in the range of 3 to 10 (gal./min.)/(1000 cu.ft./min.) of gas handled.

Inertial Scrubbers: In this category may be placed those types in which gas velocity is utilized to secure liquid contact and which do not conveniently fall into any of the other classes. Typical units are the Peabody scrubber (Peabody Engineering Corp.), the Brassert disintegrator (S.P. Kinney Engineers, Inc.), the bubble cap scrubber (C.O. Bartlett & Snow Co.), and the vortex contactor (Blaw-Knox Co.). The Peabody scrubber is similar to the Calder-Fox scrubber (page 12). Dust-laden gases are passed through a perforated plate over which water is circulated, a back-up or impingement plate being mounted above each perforation.

Mechanical Scrubbers: A large variety of units are available in which water is sprayed into a rotating member. In the Theisen disintegrator (Freyn Engineering Co.), widely used in blast furnace gas cleaning, the dust-laden gas and scrubbing liquid are passed outward through a series of rotating and stationary arms. Very high collection efficiencies have been reported but power consumption is on the order of 10 hp./(1000 cu.ft./min.) of gas handled. Other mechanical scrubbers are the Type W Rotoclone (American Air Filter Co.), The Bian washer, the Piazza scrubber, and the Centri-Merge Rotor scrubber (Schmieg Industries).

Packed Scrubbers: The conventional tower packed with ceramic rings, tile, etc., has been employed for dust collection. When operated in the normal manner at capacities well below the flooding point, however, it is not very effective for removing particles finer than about 5 microns diameter unless dust flocculation occurs due to humidification or condensation. The action to be expected is primarily one of impingement on the packing with the liquid serving to keep the dust washed off and to avoid re-entrainment of separated dust. Another serious limitation is the possibility of blockage due to dust build-up. A grid-packed tower is not very subject to the latter limitation and results of successful operation have been reported (35).

Film Scrubbers: This group includes those units in which the sole contact between the gas and liquid is through a liquid film on the collecting surface. Except for collection due to humidification and condensation, the liquid serves merely to keep the collecting surface free of solids and prevent re-entrainment of collected dust. In one type the dust-laden gases are passed horizontally across inclined threaded tubes down which water is circulated. In another water is allowed to flow down vertical rectangular impingement elements with concave sides.

Miscellaneous Scrubbers: Simple bubbling of a gas through a bed of liquid is generally not very effective for the removal of fine dust because liquid contact is not very good, gas dispersion is poor, and retention time is relatively short. Good gas dispersion can be obtained by mechanical means or by use of a proper gas sparger. Bransky and Diwoky (29) have reported successful collection of sulfuric acid mist by passing the mist-laden gases up through a deep bed of frothing liquid.

There are commercially available a wide variety of spray booth scrubbers. These consist of a hooded entrance followed by a liquid contacting section, comprising baffles or rotor sprays.

The number and variety of available scrubbers is so great and performance data so meager that it is extremely difficult to give any specific design recommendations at the present time. Scrubbers are specifically limited to applications where the gases may be cooled and where it is permissible to collect the dust as a slurry, the latter being a particularly important point in the chemical industry. Where these are possible, the proper selection and design of a wet scrubber can give very high collection efficiencies on very fine dust. Wet collection alleviates possibilities of local atmospheric nuisance in disposing of the collected dust but generally complicates the final disposition problem unless the sludge can be returned to the process or sent to a ditch. Wet collection may also intensify corrosion problems.

XIII. ELECTRICAL PRECIPITATORS

Theory: When particles suspended in a gas are exposed to gas ions in an electrostatic field, they will become charged and migrate under the action of the field. The fundamental steps and mechanisms in the process of electrical precipitation may be listed as follows:

1. Gas Ionization
2. Particle Collection
    a. Production of electrostatic field to cause charging and migration of dust particles.
    b. Gas retention to permit particle migration to a collecting surface.
    c. Prevention of re-entrainment of collected particles.
    d. Removal of collected particles from the equipment.

There are two general classes of electrical precipitators: (1) single stage, in which ionization and collection are combined; (2) two stage, in which ionization is achieved in one portion of the equipment, followed by collection in another. Various types in each class differ essentially in the details by which each function is accomplished.

In order to obtain gas ionization, it is necessary to exceed, at least locally, the electrical breakdown strength of the gas. Corona is the name applied to such a local discharge which fails to propagate itself. Sparking is essentially an advanced stage of corona in which complete breakdown of the gas occurs along a given path. Since corona discharge represents a local breakdown, it can only occur in a non-uniform electrical field. In order to form an appreciable number of gas ions either corona discharge or sparking is required. However, corona discharge is accompanied by a relatively small flow of electrical current, whereas sparking involves a large flow or power surge, and cannot be tolerated for electrical precipitation equipment. Besides disruptive effects on the electrical equipment and electrodes, sparking will result in low collection efficiency due to reduction in applied voltage, redispersion of collected dust, and current channelling.

In practice, precipitators are usually operated at the highest voltage practicable without sparking since this increases both the particle charge and electrical precipitating field. The sparking potential is generally higher with a negative charge on the discharge electrode and is less erratic in behavior than a positive corona discharge. It is the general concensus, however, that ozone formation with a positive discharge is considerably less than with a negative discharge although there are some reports to the contrary. For these reasons, negative discharge is generally used in industrial precipitators while a positive discharge is utilized in air conditioning applications. The following table gives typical

values for the sparking potential for the case of small concentric wires in pipes of various sizes (Ref. 6, page 1873) for negative polarity:

Diameter of Pipe, in.	Sparking Potential, v.	
	Peak	Root Mean Square
4	59,000	45,000
6	76,000	58,000
9	90,000	69,000
12	100,000	77,000

The sparking potential varies approximately directly as the density of the gas but is very sensitive to the character of any material collected on the electrodes. Even small amounts of poorly conducting material on the electrodes may markedly lower the sparking voltage. For positive polarity of the discharge electrode, the sparking voltage may be very much lower.

By virtue of the momentum transfer from gas ions moving in the electrical field to the surrounding gas molecules, there is set up a gas circulation between the electrodes, known as the "electric" or "ionic" wind. For conditions encountered in electrical precipitators, the velocity of this circulation is on the order of 2 ft./sec.

There are three forces acting on a gas ion located in an electrostatic field in the vicinity of a particle (38) (39) (41): attractive forces due to the field strength and the ionic image: and repulsive forces due to the Coulomb effect resulting from charges on the particle. For spherical particles larger than 1 micron diameter, the ionic image effect is negligible and charging will continue until the other two forces balance. The ultimate charge acquired by the particle is given by

$$N_o = \zeta \mathcal{E} D_p^2 / 4\epsilon \qquad (15)$$

(metric units)

and is very nearly attained in a fraction of a second. For particles smaller than 1 micron diameter, the initial charging will occur according to the same mechanism. However, owing to the ionic image effect the ultimate charge will be considerably greater due to penetration as a result of the kinetic energy of the gas ions. For charging times of the order encountered in electrical precipitation, the ultimate charge acquired by spherical particles smaller than about 1 micron diameter may be approximated by the empirical expression

$$N_o = 3.4 \times 10^3 D_p T \qquad (16)$$

(metric units)

Values of N_o for various sized particles are listed in Table II for 70 F., $\zeta = 2$, and $\mathcal{E} = 10$ statvolts/cm.

TABLE II. CHARGE AND MOTION OF SPHERICAL PARTICLES IN AN ELECTRICAL FIELD

(For 70°F.; $\zeta = 2$; $\mathcal{E} = \mathcal{E}_i = \mathcal{E}_p = 10$ statvolts/cm.)

Particle Diameter, microns	Number of Elementary Electrical Charges N_o	Particle Migration Velocity* u_e ft./sec.
0.1	10	0.27
0.25	25	0.15
0.5	50	0.12
1.0	105	0.11
2.5	655	0.26
5.0	2,620	0.50
10.0	10,470	0.98
25.0	65,500	2.40

*Includes Stokes-Cunningham correction factor.

By equating the electrical force acting on a particle to the resistance due to air friction, as expressed by Stokes's law, the particle velocity or mobility may be expressed by

(a) For particles larger than 1 micron diameter:

$$\lambda_p = (u_e/\mathcal{E}_i) = \zeta D_p \mathcal{E}_p k_m/12\pi\mu \quad \text{(metric units)} \tag{17}$$

(b) For particles smaller than 1 micron diameter:

$$\lambda_p = (u_e/\mathcal{E}_i) = 360\, k_m\, \epsilon\, T/\mu \quad \text{(metric units)} \tag{18}$$

For single-stage precipitators, $\mathcal{E}_i$ and $\mathcal{E}_p$ may be considered essentially equal. It is apparent from Equation 18 that the mobility in electrical field will be almost the same for all particles smaller than about 1 micron diameter, and hence, in the absence of re-entrainment, collection efficiency should be almost independent of particle size in this range. Very small particles will actually have a greater mobility due to the Stokes-Cunningham correction factor. Values of u_e are listed in Table II for 70°F., $\zeta = 2$, and $\mathcal{E} = 10$ statvolts/cm.

While the actual particle mobilities may be considerably greater than would be calculated on the above basis due to the action of the electric wind in single-stage precipitators, the latter acts in a compensating fashion and the over-all effect of the electric wind is probably to provide an equalization of particle concentration between the electrodes similar to the action of normal turbulence (41). On this basis Deutsch (38) has derived the following equations for collection efficiency, the form of which had previously been suggested by Anderson on the basis of experimental data:

$$\eta_f = 1 - e^{-(u_e A_e/q)} = 1 - e^{-K_e u_e} \quad \text{(consistent units)} \tag{19}$$

For concentric cylinder (or wire-in-cylinder)-type precipitators, $K_e = 4\, L_e/D_t\, V_e$; for rod-curtain or wire-plate types, $K_e = L_e/B_e\, V_e$. Strictly speaking, Equation 19 applies only for a given particle size and over-all efficiency must be obtained by an integration process for a given dust distribution. However, over limited ranges of performance conditions, Equation 19 has been found to give a good approximation of over-all collection efficiency with the term for the particle migration velocity representing an empirical average value. Such values, calculated from over-all collection efficiency measurements, are given in Table III for specific installations.

TABLE III. PERFORMANCE DATA ON TYPICAL SINGLE-STAGE ELECTRICAL PRECIPITATOR INSTALLATIONS (RESEARCH CORPORATION)

Type of Precipitator	Type of Dust	Gas Volume cu.ft./min.	Average Gas Velocity, ft./sec.	Collecting Electrode Area, sq./ft.	Over-All Collection Efficiency, %	Average Particle Migration Velocity, ft./sec.
Rod Curtain	Smelter fume	180,000	6	44,400	85	0.13
Tulip Type	Gypsum (Kiln)	25,000	3.5	3,800	99.7	0.64
Perforated Plate	Fly Ash	108,000	6	10,900	91	0.40
Rod Curtain	Cement	204,000	9.5	26,000	91	0.31

For two-stage precipitators with close collecting plate spacings, the gas flow is substantially streamline and no electric wind exists. Consequently, neglecting re-entrainment, collection efficiency may be expressed as (43)

$$\eta_f = u_e\, L_e/V_e\, B_e \quad \text{(consistent units)} \tag{20}$$

which holds for values of $\eta_f \leq 1.0$. In practice, however, extraneous factors may cause the actual efficiency to approach a relationship of the type given by Equation 19.

In general, increased pressure increases precipitation efficiency, although a somewhat higher potential is required, because it reduces ion mobility and hence increases the potential required for corona

and sparking. Increased temperature reduces collection efficiency because ion mobility is increased, lowering critical potentials, and because gas viscosity is increased, reducing migration velocities.

Application: The theoretical considerations expounded above should be used only for order-of-magnitude estimates since there are a number of extraneous factors which may enter into the actual performance. Corona discharge actually takes place from local but mobile points rather than in an even distribution along the discharge electrode. In actual installations, rectified a.c. current is used thus giving a continuously variable electrical field depending on the wave form of the rectifier. The presence of dust in high concentration will affect the electrical discharge conditions as well as the electrical field. If the collected dust is not a good conductor, a high potential may develop across this dust layer. This not only reduces the potential across the gas stream but may result in spark discharge with resultant back-ionization and re-entrainment of dust (37) (42) (44). Beaver (37) indicates that the critical resistivity above which such difficulties may be anticipated is on the order of 10^{10} ohm-cm. Steam, sodium chloride, and ammonia have all been successfully used as conditioning agents to increase conductivity in specific cases. In the majority of applications, however, the resistivity of the dust and the water vapor content of the gases is such that good precipitation is obtained without addition of such agents. Thick dust accumulations are also often avoided by using perforated or slotted collecting electrodes.

Single-Stage Precipitators: The single-stage type of unit, commonly known as a Cottrell precipitator, is most generally used for dust or mist collection from industrial or process gases. The corona discharge is maintained throughout the precipitator and, besides providing initial ionization, also serves to prevent redispersion of precipitated dust and recharges neutralized or discharged particle ions. These units may be divided into two main classes: (1) the so-called plate type in which the collecting electrodes consist of a nest of parallel pipes which may be square, round, or any other shape. The discharge or precipitating electrodes in each case are wires or rods, either round or edged, which are placed midway between the collecting electrodes. The pipe-type precipitator is usually used for the removal of liquid particles and volatilized fume while the plate type is used mainly on dusts.

Collected dust is generally dislodged from the electrodes either periodically or continuously by mechanical rapping or scraping, which may be performed mechanically or manually. Perforated plate or rod-curtain precipitators are frequently rapped without shutting off the gas flow and with the electrodes energized. To minimize re-entrainment tendencies sectional or composite collecting electrodes (also known as hollow, pocket, or tulip electrodes) may be used for free flowing material. In these, the collected dust is guided into dead air spaces.

Semi-conductors, such as reinforced concrete, are sometimes used where there is a tendency to disruptive discharge at voltages below that required for efficient precipitation. This type is known as a "graded resistance" precipitator. The resistance of the electrode tends to suppress the discharge and stabilizes the electrical field. While collecting electrodes are usually metallic, carbon has been used for corrosive conditions and, where the collected material is a conducting liquid, insulators such as glass, terra cotta, or wood have also been used.

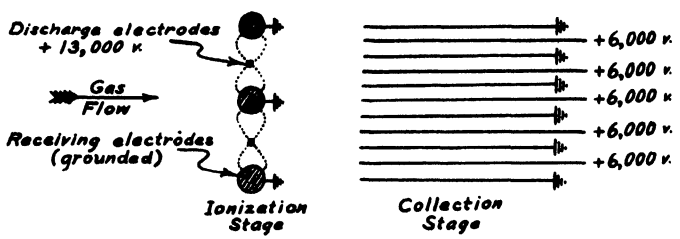
The choice of size, shape, and type of electrode is based on economic considerations and is usually determined by the characteristics of the gas and the suspended matter, mechanical considerations, such as flue arrangement, the available space, and previous experience with similar problems. The spacing between collecting electrodes in plate-type precipitators and the pipe diameter in the pipe types usually ranges from 6 to 15 in. Smaller spacings result in smaller equipment size and permit lower voltages to be used but accentuate difficulties in maintaining alignment and in disturbances from collected material. For very high dust concentrations, such as those encountered in fluid catalyst plants, the first half of a precipitator may involve large spacings followed by a section of closer spacing. Collecting electrodes are generally 3 to 6 ft. wide and 10 to 18 ft. high in plate types and 6 to 15 ft. high in pipe types. It is essential for proper operation that the gas be evenly distributed across the various electrode elements. For this purpose, guide vanes, perforated plates, or screens are frequently located on the upstream side of the electrodes.

Electrical precipitators are generally energized by rectified, alternating current of commercial frequency. Synchronous motor-driven mechanical, electronic, mercury-arc, and contact rectifiers have all been used. The electrical equipment is usually housed in a separate station either remote from or adjacent to the precipitator. Electrode insulators must also be designed for the specific service conditions. Conducting mists require special provisions such as oil seals, energized shielding cups, or air bleeds. With saturated gases, steam coils may be used to prevent condensation on the electrodes.

Electrical precipitators are probably the most versatile of all types of dust collectors. Very high collection efficiencies can be obtained regardless of the fineness of the dust provided they are given proper maintenance. They can be used with moist or wet gases and have been used at temperatures as high as 1200°F. and at pressures as high as 10 atm. The chief disadvantages are in the high initial cost and, in some cases, high maintenance costs. Also combustability of the dust or carrier gas must be considered in design.

Electrical precipitators are generally designed for collection efficiencies in the range of 90 to 99.9%. It is essential, however, that the units be properly maintained in order to achieve the required collection efficiency. Electrical power consumption is generally 0.2 to 0.6 kw./(1000 cu.ft./min.) of gas handled, while the pressure drop is in the range of 1/4 to 1 in. water, consisting primarily of distributor and inlet-exit losses. Applied potentials generally range from 30,000 to 100,000 v. and gas velocities are in the range of 3 to 10 ft./sec. with retention times in the range of 1 to 6 sec. Single-stage precipitators in the United States are manufactured by Koppers Co., Research Corp., and Western Precipitation Corp. Typical applications in the chemical field include de-tarring of manufactured gas, removal of acid mist and impurities in sulfuric acid plants, recovery of phosphoric acid mists, removal of dusts in gases from roasters, sintering machines, calciners, cement and lime kilns, blas furnaces, carbon-black furnaces, regenerators, chemical recovery furnaces, and gypsum kettles. In the carbon-black industry the collection is unique in that the electrical precipitator serves primarily as a flocculator, final collection being accomplished in a cyclone.

Two-Stage Precipitators: In two-stage precipitators, corona discharge takes place in the first stage between two electrodes having a non-uniform field.



The corona discharge is generally obtained by a fine wire discharge electrode and a large diameter receiving electrode. In this stage, the potential difference must be above that required for corona discharge. The second stage involves a relatively uniform electrostatic field in which charged particles are caused to migrate to a collecting surface. This stage usually consists of either alternately charged parallel plates or concentric cylinders with relatively close clearance compared to their diameters. The only voltage requirement in this stage is that no sparking occur, though the higher voltages will result in increased collection efficiency for a given capacity. Since collection occurs in the absence of corona discharge, there is no way of recharging re-entrained and discharged particles. Consequently some means must be provided for avoiding re-entrainment of particles from the collecting surface.

The large-scale application of two-stage precipitators is primarily a comparatively recent development that has taken place in the air conditioning field. There are on the market several units of the same general type (Westinghouse Electric Co.; American Air Filter Co.; Raytheon Mfg. Co.; Aerotic Corp.) (see also sketch above). In these units the ionizing and collecting stages are built in separate sections of standardized size, and multiple units of each size are assembled in parallel to meet a specific capacity. The ionizer receiving electrodes are approximately 1-1/4 in. nominal diameter spaced 3-1/2 in. apart. Between these tubes are the discharge electrodes of 0.008-in. diameter tungsten wire charged to +13,000 v. d.c. The collecting unit consists of plates arranged parallel to the gas flow, with alternate plates grounded and the others charged at +6,000 v. d.c. These plates are spaced 5/16 in. apart and are about 12 to 18 in. deep. Both ionizer and collector sections are generally made in 24 and 36 in. wide units, the heights being variable depending on the specific type or make. The high voltage d.c. potential is obtained from a compact, self-contained vacuum tube rectifier unit operated directly off of a 110-v. a.c. supply line. For air conditioning applications, the plates are coated with a viscous oil to avoid dust re-entrainment. When the dust buildup exceeds a depth of approximately 1/16 in., the plate sections must be taken out, washed, and re-oiled. Automatic means for cleaning and re-oiling in place are also available. Depending on dust concentrations, cleaning may be required every two weeks to three months. Installations are usually provided with guarded doors which automatically cut off the power when the unit is entered. Where poor approach conditions are involved, perforated-plate air-distributors may be employed. The units are rated at 85 to 90% efficiency (U. S. Bureau of

P. 318 - line 16: "blas" should read "blast".

Standards Discoloration Test Method) at superficial velocities in the range of 300 to 500 ft./min. Electrical power consumption is approximately 0.02 kw./(1000 cu.ft./min.) and pressure drops range from 0.1 to 0.2 in. water. There are also available units in which electrostatic precipitation is combined with a dry air filter or with an automatic viscous-coated air filter.

While intended primarily for air conditioning applications, these units have been successfully applied to the collection of relatively non-conducting mists such as oil. The large cost advantage of these units over the Cottrell precipitator lies in the smaller equipment size made possible by the close plate spacing, the lower power consumption due to the two-stage operation, and primarily in the mass production of standardized units. In process applications, the close plate spacing is objectionable due to the relatively high dust concentrations involved.

High-voltage alternating current may be employed for electrical precipitation. The equipment capacity for a given efficiency is considerably less than for direct current operation, however, and difficulties due to induced high-frequency currents may be encountered. The a.c. system has been very satisfactory for laboratory and sampling purposes.

XIV. AIR FILTERS

The equipment previously described, with the exception of two-stage electrical precipitators, is intended primarily for the treatment of process dusts. Air filters are employed in the elimination of atmospheric dust. The difference in application is not so much one of quality of dust as it is of quantity. Process dust concentrations may run as high as several hundred grains per cubic foot of gas, although usually not exceeding 20 grains. Atmospheric dust concentrations are generally below 5 grains/1000 cu. ft., as indicated in the following table giving typical dust concentrations that may be expected in various districts:

District	Dust Concentration,* grain/1000 cu.ft.
Rural or suburban	0.2 - 0.4
Metropolitan	0.4 - 0.8
Industrial	0.8 - 1.5
Dusty factories or mines	4.0 - 80.0

*1 grain/1000 cu.ft. = 2.3 mg./cu. m. = 0.065 mg./cu.ft.

In the elimination of atmospheric dust, no attempt to recover the dust is usually made. Air washers may also be employed for cleaning air, but these are installed primarily for humidifying or cooling the air, and dust removal is only of secondary importance.

Air filters are generally available as standard units to be arranged in parallel for any desired air handling capacity. They are usually designed for face velocities on the order of 300 ft./min. and a maximum pressure drop in the range of 0.2 to 0.5 in. water. They may be classified as (1) viscous filters, (2) dry filters, (3) automatic filters, and (4) miscellaneous types. The latter includes wetted cells, electrostatic precipitators (previously described above), pipe-line filters, and activated carbon filters. The description, design, and performance of these units is considered in detail in References 6 and 47.

XV. MISCELLANEOUS COLLECTORS

High-intensity acoustic vibrations will tend to flocculate fumes and mists whereupon they can be readily collected in conventional apparatus. There is an optimum frequency, generally in the range of 1,000 to 10,000 cycles/sec., below which effective flocculation will not occur, depending on the size and density of the particle and the viscosity and density of the medium. While the Bureau of Mines has sponsored extensive investigations (51) (53), no full-scale commercial applications have been made until recently due to the lack of an economical source of acoustic energy. The recent development of a gas-siren generator (Ultrasonics Corp., Cambridge, Mass.) has, however, permitted the conversion of compressed gas energy into acoustic energy at 50 to 70% efficiency in units developing up to 100 kw. acoustic output. A total range in frequency from 1,000 to 200,000 cycles/sec. can be covered in several stages. With this type of generator compressed gas pressures of 6 lb./sq.in. ga. are normally used for atmospheric pressure application and frequency can be varied continuously within a specified range. The power consumption for aerosol agglomeration is normally in the range of 2 to 5 kw./(1,000 cu.ft./min.)

of gas handled and the cost of a complete installation is on the order of $1.00/(cu.ft./min.) for installations in the range of 50,000 cu.ft./min. capacity. Sonic precipitation is limited to cases where the particle concentration is greater than 1 grain/cu.ft. For cases involving a lower concentration, sonic precipitation is only feasible if the particle concentration is raised by the introduction of additional particles as with the injection of steam. Pilot plant and field tests are in progress on the collection of carbon black and kraft pulp mill fume, and on the precipitation of fog from airport atmospheres.

Molecular impacts tend to repel dispersoids away from a heated body. In thermal precipitation, this principle is utilized to clean gas of suspended particles by passing the gas through or over a heated grid at low velocity (50) (54). While this method has not yet been applied to industrial dust collection, it has been used for atmospheric dust sampling.

XVI. NUMERICAL EXAMPLES

A. Gravity Settling Chamber: It is proposed to install a Howard gravity collector, 12 ft. wide x 10 ft. high x 20 ft. long with a 1-in. shelf pitch to remove 62° Be′ sulfuric acid mist from 1000 cu.ft./min. of converter gases (substantially air) at 70°C. Estimate the smallest diameter, in microns, of mist droplet that should be completely removed by this chamber.

Solution: From conditions of the problem

$$\rho_p = 62° \text{ Be}' = (1.747)(62.3) = 108.8 \text{ lb./cu.ft.}$$

$$\rho = 0.0644 \text{ lb./cu.ft.}$$

$$\mu = 0.0204 \text{ cp.} = 1.37 \times 10^{-5} \text{ (lb.)/(ft.)(sec.)}$$

$$N_S = (10)(12)/(1) = 120$$

$$q = (1000)/(60) = 16.67 \text{ cu.ft./sec.}$$

$$B_S = 12 \text{ ft.}; \; H_S = 10 \text{ ft.}; \; L_S = 20 \text{ ft.}$$

From Equation 3

$$u_{tg} = (16.67)/(120)(12)(20) = 0.000579 \text{ ft./sec.}$$

From Stokes's law

$$D_{p,min.} = \sqrt{(18)(1.37 \times 10^{-5})(0.000579)/(32.17)(108.8)}$$

$$= 0.638 \times 10^{-5} \text{ ft.} = \underline{1.94 \text{ microns}}$$

B. Cyclone Separator: Design a cyclone to handle 1900 cu.ft./min. of ventilation air from a talc dusting booth at a friction loss of 3 in. water. Estimate the collection efficiency assuming the dust to have the following Roller analysis based on a true particle specific gravity of 2.6. Assume an air temperature of 70°F.

Particle Diameter, microns	Cumulative Per Cent Larger Than
5	79.7
10	60.2
20	25.5
40	1.8

From the conditions of the problem

$$q = 1900 \text{ cu.ft./min.} = 31.7 \text{ cu.ft./sec.}$$

$$\rho = 0.0749 \text{ lb./cu.ft.}$$

$$\rho_p = (2.6)(62.3) = 162.0 \text{ lb./cu.ft.}$$

$$\mu = 0.0181 \text{ cp.} = 1.22 \times 10^{-5} \text{ (lb.)/(ft.)(sec.)}$$

$$\text{Inlet velocity} = \sqrt{(3)/(0.003)(0.0749)(8)} = 40.8 \text{ ft./sec.}$$

$$\text{Inlet width} = \sqrt{(31.7)(144)/(2)(40.8)} = 7.5 \text{ in.}$$

Required cyclone dimensions (from Figure 1):

Inlet: 7-1/2 in. wide x 15 in. high
Diameter: 30 in.
Cylinder height: 60 in.
Cone height: 60 in.
Gas exit duct diameter: 15 in.
Gas exit duct length: 22 in.
Dust outlet diameter: 6 in.

$$\text{Inlet area} = (7.5)(15)/(144) = 0.781 \text{ sq.ft.}$$

$$\text{Inlet velocity} = (31.7)/(0.781) = 40.6 \text{ ft./sec.}$$

From Equation 10

$$D_{pc} = \sqrt{(9)(1.22 \times 10^{-5})(7.5)/(12)(2)(3.14)(5.0)(40.6)(162.0)}$$

$$= 1.823 \times 10^{-5} \text{ ft.} = 5.56 \text{ microns}$$

The following tabulation can be prepared from the values given in Figure 1 used in conjunction with a plot of the particle size analysis given above:

D_p/D_{pc}	η_f	D_p microns	ϕ
0.2	0.04	1.11	0.950
0.3	0.08	1.67	0.927
0.5	0.20	2.78	0.882
0.7	0.33	3.89	0.840
1.0	0.50	5.56	0.772
1.5	0.69	8.34	0.667
2.0	0.80	11.1	0.560
3.0	0.90	16.7	0.350
5.0	0.96	27.8	0.103
7.0	0.98	38.9	0.021
10.0	0.99	55.6	0.001

Plotting η_f as ordinate against ϕ as abscissa, the over-all collection efficiency is found from the mean ordinate to be 70.3%.

XVII. PROBLEMS

1. Calciner gases at 500°F., containing particles of calcium oxide, are passed through a settling chamber 20 ft. long, 3 ft. high, and 8 ft. wide at a rate of 5,760 cu.ft./min. (actual volume at 500°F.). What is the smallest size particle that the settling chamber would be expected to separate out completely? Assume that the particles are spherical and that the calciner gases have the same physical properties as air.

2. Design a cyclone to handle 1500 cu.ft./min. of ventilating air (25°C.) from a sodium nitrite dumping booth at a friction loss of 4.4 in. water. The dust picked up by the air at the dumping booth has the following particle size analysis as determined by a Roller analyzer:

Particle Diameter Microns	Cumulative Per Cent Larger Than
5	90.0
10	55.9
15	30.5
20	16.4
40	1.8

3. Design a cyclone installation for handling 6000 cu.ft./min. of combustion gases (essentially air) at 305°F. at a friction loss of 2 in. water. Multiple cyclones of 6-in. diameters are to be used. What dust collection efficiency is to be expected if the dust particles are all substantially 6 microns in diameter and have a true specific gravity of 2.3?

Gas viscosity = 0.023 cp.

4. Design a cyclone to handle 11,500 cu.ft./min. of dryer gases at 240°F. with a friction loss of approximately 2.5 in. water. The dryer discharge gases are essentially air and contain dust at a concentration of 2.2 grains/cu.ft. at operating conditions. Estimate the annual dust values lost in the cyclone discharge gases if the dust is worth $2.50/100 lb. and if the dust entering the cyclone has the following Roller analysis based on a true particle specific gravity of 1.62:

Particle Diameter Microns	Cumulative Per Cent Larger Than
5	95.3
10	84.8
20	56.8
40	14.9

Assume 8000 operating hours per year.

5. If 12-in. diameter cyclones are to be installed in parallel to give the same over-all friction loss as the single cyclone in Problem 4, specify the number of cyclones required and estimate the annual dust values lost with this multiple cyclone installation.

6. A bag filter, having 1050 sq.ft. of cloth, handles 3300 cu.ft./min. of air at 70°F. If the air contains a dust dispersoid of approximately 10 microns average particle diameter at a concentration of 4.3 grains/cu.ft., estimate how often it must be shaken to keep the pressure drop under 2 in. water.

7. A 1/4-in. diameter rod projects across a diameter of a 14-in. i.d. duct in which 3,000 cu.ft./min. of mist-laden air is flowing at 70°F. The mist consists of 60° Be' sulfuric acid drops of 5.0 micron diameter and is present in a concentration of 10 milligrams/cu.ft. Assuming a uniform gas velocity across the entire duct cross-section, estimate the amount of mist, in grams, which will be deposited on the rod in 1 hr.

8. In a closed-circuit system for grinding fluorspar (sp.gr.=3.0), solids are swept out of the mill by 11,000 cu.ft./min. of air at 70°C. The air then goes to an air classifier in which coarse particles are removed and returned to the mill. The fine product, carried out of the classifier by the air, is then collected in a cyclone collector, the air being recycled to the mill through a fan. In order to compensate for air in-leakage at the mill, a bleed-off line, handling 10% of the circulated air, is located on the discharge side of the fan. For purposes of dust recovery, this bleed-off air is passed through a bag filter before going to the atmosphere. The fluorspar production rate (rate of solids discharge from the cyclone) is 6.5 tons/hr. The particle size analysis of the fines leaving the classifier in the air stream was determined by a Roller analyzer to be:

Particle Diameter, microns	Cumulative Per Cent Larger Than
5	93.1
10	76.8
20	40.0
40	3.7

On account of headroom limitations, the cyclone is to consist of four individual cyclones operating in parallel.

On the basis of the above information:

(a) Design the cyclone collectors for a friction loss of 2.5 in. water.
(b) Estimate the collection efficiency of the cyclones.
(c) Estimate the bag area required in the bleed-off air filter, if the shaking cycle is to be on the order of 5 min. for a pressure drop of 2.0 in. water.

In all cases, neglect the effect of dust concentration on cyclone friction loss and collection efficiency.

9. The following cases illustrate some common types of dust collection or nuisance elimination problems encountered in practice. What type or types of dust collection equipment would most probably be used for the following cases and why? A brief statement is sufficient in each case and no details as to equipment size are required.

Case	Dust or Mist*	Carrier Gas		
		Rate, cu.ft./min.	Temp., °C.	Dust Conc., grains/cu.ft.
1	Dyestuff, $< 5\ \mu$ from dumping booth ventilation air	2,000	25	1.0
2	90% H_2SO_4 mist, $< 3\ \mu$, from contact plant system	5,000	40	2.5
3	Fly ash, 85% $> 20\ \mu$, 30% $> 40\ \mu$, from power plant	20,000	300	2.0
4	Atmospheric dust, $< 10\ \mu$ from room ventilation air	100,000	25	0.002
5	Zinc ore, 90% $> 5\ \mu$, 10% $> 40\ \mu$, from ball mill	5,000	65	120

* μ is symbol used to designate "microns."

Chapter 15

FIXED AND FLUIDIZED BEDS OF GRANULAR MATERIALS

by

Rollin D. Morse
Engineering Research Laboratory
Engineering Department
E. I. du Pont de Nemours & Co., Inc.
Wilmington, Delaware

TABLE OF CONTENTS

	Page
I. References	327
II. Nomenclature	327
III. The Fluidized-Solid Technique	328
1. General Description and Definitions	328
2. Description of the "Boiling Bed"	329
3. Advantages	329
4. Disadvantages	331
5. Applications	331
IV. Fluid Flow in a Fixed Bed.	332
1. Blake	332
2. Burke and Plummer	333
3. Furnas	333
4. Chilton and Colburn	333
5. Carman	334
6. Leva	335
7. Other Work	336
V. Fluid Flow in a Fluidized-Solid Bed	336
1. General	336
2. Uniformity of Fluidization	337
3. Segregation Tendency	337
4. Generalized Fluid Flow in a Fluidized-Solid Bed	338
a. Leva and Associates	338
b. Wilhelm and Kwauk	339
c. New Analysis of Data	340

5. Summary 342

Illustrative Problem 347

Problem Exercise 348

LIST OF FIGURES

Figure 1. Fixed Beds—Wilhelm and Kwauk Data 343
Figure 2. Fluidized Beds 343
Figure 3. Leva's Uniform Round Sands 344
Figure 4. Leva's Uniform Sharp Sands 344
Figure 5. Comparison of Round and Sharp Sands 345
Figure 6. Comparison of Size Mixtures with Uniform Sizes 345
Figure 7. Fluidization with Water—Wilhelm and Kwauk 346
Figure 8. Fluidization with Air—Wilhelm and Kwauk 346

I. REFERENCES

1. Alden, R. C., Oil Gas J. 45, 27, November 9, 1946.
2. Anon, Oil Gas J. 45, 47, March 30, 1946.
3. Blake, F. C., Trans. Am. Inst. Chem. Engrs. 14, 415 (1922).
4. Brownell, L. E. and Katz, D. L., "The Flow of Fluids through Porous Media," Ph.D. Thesis, Univ. of Michigan, February 8, 1946.
5. Burke, S. P. and Plummer, W. B., Ind. Eng. Chem. 20, 1196 (1928).
6. Carman, P. C., Trans. Inst. Chem. Eng. (British) 15, 150-66, Part 1 (1937).
7. Chilton, T. H. and Colburn, A. P., Ind. Eng. Chem. 23, 8, 913-9 (1931).
8. Dolch, Paul, "Technique of the Water-Gas Processes," Chap. VIX, "The Winkler Generator." (In German - publisher and date unknown)
9. Furnas, C. C., Bur. Mines Bull. 307 (1929).
10. Golumbic, N. R., "Review of Fischer-Tropsch and Related Processes for Synthetic Liquid Fuel Production," Bureau of Mines Circular IC 7366, August 1946.
11. Hall, C. C., Engineering 163, 30, (1947) No. 4226 Jan. 10; 4227, Jan. 17; 4228, Jan. 24.
12. Keith, P. C., Oil Gas J. 45, 6, June 15, 1945.
13. Kite, R. P. and Roberts, E. J., Chem. Eng. 54, 12, 112-115 (December 1947).
14. Kozeny, Ber. Wien Akad. 136a, 271, (1927).
15. Lane, J. C. and Weil, B. H., Petroleum Refiner 25, 8, August 1946; 25, 9, September 1946; 25, October 1946; 25, 11, November 1946.
16. Leva, M., Chem. Eng. Prog. 43, 10, 549-54, October 1947.
17. Leva, M. and Grummer, M., Chem. Eng. Prog. 43, 633-8, November 1947.
18. Leva, M. and Grummer, M., Chem. Eng. Prog. 43, 713, December 1947.
19. Leva, M., Grummer, M., et al, Chem. Eng. Prog. 44, 511, (1948).
20. Leva, M., Grummer, M., et al, Chem. Eng. Prog. 44, 619, (1948).
21. Leva, M., Grummer, M., et al, Chem. Eng. Prog. 44, 720, (1948).
22. Murphree, E. V., et al, Trans. Am. Inst. Chem. Engrs. 41 (1) 19-33, (1945).
23. Oman, A. O. and Watson, K. M., Nat. Pet. News, Nov. 1, 1944.
24. Roberts, G. and Phinney, J. A., Oil Gas J., 45, 45, March 15, 1947.
25. Rose, H. E., Inst. Mech. Eng. 153, 1945.
26. Sullivan, R. R. and Hertel, K. L., J. Appl. Physics 11, 761-5, December 1940; 12, 503-8, June 1941; 13, 725-30, November 1942.
27. Wilhelm, R. H. and Kwauk, M., Chem. Eng. Prog. 44, 3, 201-18, March 1948.
28. Parent, J. D., Yagol, N., and Steiner, C. S., Chem. Engr. Prog. 43, 8, 429-37, August 1947.
29. Various authors, "Symposium on Fluidization" Ind. Eng. Chem. 41, 6, 1099-1250, June 1949.

II. NOMENCLATURE

p. 327 - In reference 8 should read Chapter XIV.

a	surface area of particles per unit volume of packed space, sq.ft./cu.ft.
a_o	surface area per unit volume of particles (i.e., not including void volume), sq.ft./cu.ft.
a_p	surface area per unit packed space of spheres of equal volume, sq.ft./cu.ft.
a'	constant in equation for loss of head in contraction of flow.
A	cross-sectional area of bed, sq.ft.
A_p	surface area of the average particle of diameter D_p, sq.ft.
b	empirical exponent in Furnas' correlation, dimensionless.
D	diameter of the bed, ft.
D_p	diameter of sphere of the same volume as that of the particle, ft.
f'	modified Fanning friction factor.
g_c	conversion factor, 32.17 (ft.) (lb.)/(lb.force) (sec.)^2
g	local acceleration due to gravity, (ft./sec.)/sec.
G_o	interstitial mass velocity, lb./(sec.)(sq.ft.).
G	superficial mass velocity (based on gross cross-sectional area of empty tube), lb./(sec.)(sq.ft.).

k = empirical correlation factor, dimensionless.

$K_{\Delta p}$ = Wilhelm and Kwauk's (27) correlating factor based on friction factor in granular beds, dimensionless.

$K_{\Delta \rho}$ = Wilhelm and Kwauk's (27) correlating factor based on drag coefficient, dimensionless.

L_s = height of fixed or settled bed (or length of pipe), ft.

L_e = height of expanded bed, ft.

L_f = height of fluidized bed, ft.

L_t = length of tortuous flow passage through a granular bed, ft.

L_a = height of hypothetical bed containing no voids, ft.

L_1 = length of flow path between segregating zones, ft.

m = exponent on $\frac{\epsilon^3}{1-\epsilon}$ in Leva's (20) fluidization correlation, dimensionless.

n = exponent on Reynolds number to correlate with friction factor, dimensionless.

N_V = expansion ratio $= \frac{\text{actual bed volume}}{\text{settled bed volume}}$

$= (1 - \epsilon_s)/(1 - \epsilon)$

$N_{Re,C}$ = Reynolds number, $= \frac{\phi_s D_p G}{\mu(1-\epsilon)}$, dimensionless

$N_{Re,W}$ = Reynolds number, $= \frac{D_p G}{\mu}$, dimensionless

Δp = pressure difference, lb. force/sq.ft.

$\Delta p_{K.E.}$ = pressure drop equivalent to the kinetic energy lost by the particles by collision, lb. force/sq.ft.

u_o = superficial velocity of fluid through the bed, ft./sec.

D_p = volume of the average particle with diameter V_p, cu.ft.

V_T = volume of the bed, cu.ft.

α = fractional free cross-sectional area, dimensionless.

ϵ = fraction of voids in the bed of particles, dimensionless.

ϵ_s = fraction of voids in the settled bed, dimensionless.

μ = fluid viscosity, absolute, lb.mass/(ft.)(sec.)

ψ = "a function of"

ϕ_s = Carman's shape factor for securing the specific surface of non-spherical particles.

ρ_F = fluid density, lb.mass/cu.ft.

ρ_S = true (not bulk) particle density, lb.mass/cu.ft.

III. THE FLUIDIZED-SOLID TECHNIQUE

1. General Description and Definitions. The term "fluidized-solid technique" is used to designate the gas-solid contacting process in which a bed of finely-divided solid particles is lifted and agitated by a rising stream of process gas. At the lower end of the velocity range, the amount of lifting is slight, the bed behaving like a boiling liquid, hence the term "boiling bed." At the other extreme, the particles are fully suspended in the gas stream and are carried along with it; the terms "suspension," "suspensoid," and "entrainment" contact have all been used to designate this action.

The related operations of elutriation and hindered settling, which are methods for the classification of particles by size and density, are not included in the restricted scope of this definition.

p. 328 - The symbol D_p should be V_p, and in the same line the symbol V_p should be D_p.

In processes using the fluidized-solid technique, it is common to handle the solid material in one or more stages or steps, and to transfer it from step to step through pipelines in much the same manner as with a liquid. To raise the material to a higher level, it is carried as a suspension in a gas stream at 20 - 40 ft./ sec. velocity. To take it to a lower level, or to a region of higher pressure, the settled material is allowed to flow vertically down a pipeline to the desired point, the weight of material in the pipe more than equalling the differential pressure.

The fluidized-solid technique has several unique advantages, and some disadvantages; these will be discussed below.

2. Description of the "Boiling Bed". Consider a bed of granular particles through which a stream of gas is slowly flowing upward. Friction produces a pressure drop which increases with velocity in a manner that may be expressed by the Carman-Kozeny fixed-bed correlation (See paragraph IV-5.) Finally, as the velocity is increased, a point is reached where the pressure drop becomes equal to the sum of the weight of the bed per unit cross-sectional area, plus the friction of the bed against the walls. When this point is reached, one of two things may happen: either the bed expands and assumes a more open arrangement so that the gas can flow without the pressure drop exceeding the unit bed weight, or the entire bed is lifted by the gas stream and rises like a piston. The latter occurs with materials which are not free-flowing and can, therefore, form an arch from wall to wall. In the majority of cases the arch will break away, and the under side will fall down in clumps, or aggregates. If the clumps fall so as to form an open stable channel of sufficient size, most of the gas will flow through this channel, and although the bed has expanded its expansion will be far from uniform.

With a further increase in gas velocity, the pores and channels enlarge and the particles become more widely separated. For free-flowing materials the pore spaces eventually become so large that no stable arrangement can exist, and the particles vibrate or circulate locally, in a semi-stable arrangement; this is the point at which fluidization begins.

Another increment of velocity results in over-all circulation of the bed, often with transient upward-flowing gas streams in channels that contain relatively few particles, and downflow of clumps of particles.

The type of fluidization described above has been call "aggregative" by Wilhelm and Kwauk (27). For a variant of it, consider the phenomenon known as "slugging." In small-diameter vessels many materials show a tendency to slug when fluidized; that is, the gas pocket grows until its diameter is equal to that of the vessel, and then it pushes ahead of itself a slug of the material. During this time the under side of the arch is continuously breaking away, the various-sized pieces falling out until the slug decomposes entirely and the gas pocket moves up by flow of its contents past the falling clumps.

Quite a different situation exists when a liquid instead of a gas is used to fluidize a material. In this case the individual particles remain comparatively well dispersed throughout the fluid. The fluid rises at relatively uniform velocity throughout the cross section. The turbulence is primarily fine-grain and local, showing much less general circulation of the bed than in the previous cases. This type of fluidization Wilhelm and Kwauk have termed "particulate."

3. Advantages: a. Temperature Control. The ability of the fluidized-solid bed to maintain an isothermal condition is the outstanding advantage of that method over other methods of carrying out reactions. This factor is vital to nearly all applications of the fluidized-solid technique, the other advantages generally being of far less importance.

Close control of chemical reaction variables is well known to be important in obtaining maximum yields of desired products. Of the several variables, temperature is commonly the most important, for reaction rates change exponentially with temperature (often doubling or trebling for a 10 C. change). In the common case in which several competing reactions may occur, a temperature change of a few degrees may shift the balance between the several rates from a favorable one to an unfavorable one.

The unusually close control of temperature which is possible in a fluidized-solid bed is due to a combination of the following three factors, in the order of their importance:

1. Turbulence within the fluidized mass, which breaks and disperses any hot or cold spots throughout the bed before they grow to significant size. It should not be inferred from this statement that the temperature of every solid particle in a given fluidized-catalyst bed is the same. The catalytic activity will differ somewhat from particle to particle, and those with greater activity will accelerate the reaction in their neighborhood to a greater extent; as a consequence, their temperature will be different from that of the surrounding particles of lower activity. However, the departure of the individual particle temperature from the mean value for the bed will be much less than in a fixed-bed converter, because of the turbulent mixing, plus the factors discussed in the following paragraphs.
2. High heat capacity of the bed relative to the gas within it. This factor stabilizes the

p. 329 - 15th line from the bottom should read: "..For a 10°C. change".

temperature of the bed, permitting it to absorb relatively large heat surges with only small temperature change. For example, a bed of ordinary sand fluidized with air, at a solids concentration of about 70 lb./cu.ft., would contain only about 0.05 lb. of air/cu.ft., corresponding to a mass ratio of 1400 to 1.

3. High heat-transfer rates, which are possible because of the large amount of transfer surface per unit volume of the fluidized bed.

The high transfer rates permit rapid leveling of any temperature surges either from the incoming gas or from reaction within the bed. Although the heat transfer coefficients are not unusually high, the amount of surface per unit volume is very large; in the example of the previous paragraph, the surface area of the sand would be in the range of 1000 to 5000 sq.ft./cu.ft. of bed.

The remarkable uniformity of temperature in a fluidized bed has been noted in many references. Temperature traverses in large fluidized-catalyst beds indicate that the point-to-point variation is less than 10°C. when the feed-gas temperature is not greatly different from that of the bed. Even if the feed gas is considerably hotter or colder than the bed, the high transfer rates possible commonly produce a close approach to thermal equilibrium within a few inches from the beginning of contact.

b. Continuity of Operation. The ability to handle the fluidized solid like a liquid permits the technique to be easily adapted to many continuous operations, thereby obtaining the advantages of such operations, such as lower labor requirements, precise and automatic control of process variables, and uniformity of product quality.

c. Heat Transfer. The fluidized-solid technique is a convenient method for transferring heat, either alone, or in conjunction with other operations, such as catalysis, gas-solid reactions, and transport of solids and fluids incidental to these operations.

The advantages of the fluidized-solid technique for heat transfer are as follows:

1. The possibility of combining heat transfer with other operations.
2. For large heat-transfer units, the equipment volume can be smaller than with conventional heat exchangers, because so much transfer surface is available in the fluidized bed.
3. Corrosion resistance and extreme-temperature resistance can be easily obtained by using ceramic materials for vessels and for granular solid.
4. The transfer can be effected in two stages, the fluidized solid acting as the heat reservoir to carry the heat from one fluid to the other; the stages may be physically close together or far apart.
5. The transfer may be effected with extreme rapidity, because of the large surface available; this is important when undesirable reactions would occur at intermediate temperatures.
6. Similarly, a liquid may be heated and vaporized in a small fraction of a second by direct contact with hot solid.

d. Catalysis. Fluidized-solid technique is adaptable to the contacting of free-flowing, non-sticky, granular solids with gases. It may therefore be applied in catalytic gas reactions in which solid catalysts are used. The technique has been widely applied to the catalytic cracking of petroleum, because of the unique combination of advantages which are inherent in fluidized-solid processing:

1. Control of reaction temperature.
2. Maintenance of uniform catalyst activity (and continuous catalyst regeneration).
3. Continuous removal of solid by-products.
4. Supply of heat to endothermic reaction.
5. Simple equipment with few moving parts.
6. Continuous operation with automatic control.

Most catalysts gradually lose their activity during use, because of poisoning or coating of the active surface with by-products. Replacement or regeneration is therefore eventually required. As the activity decreases, operating conditions in conventional catalyst contactors must be altered in order to maintain operating rate. Use of higher temperature is one expedient, but this may increase the amount of by-product formation with consequent loss in yield and increase in cost of product. Use of lower operating rate is another expedient, but this also results in increased costs through higher investment, because the plant must be large enough to manufacture at an average rate sufficient to compensate for the low-rate period.

In contrast to the above, the fluidized-solid technique makes possible the maintenance of a definite level of catalyst activity, because partially spent catalyst can be continuously withdrawn and fresh catalyst added. The level of activity is proportional to the ratio of the rate of loss of catalyst activity and the rate of withdrawal of the catalyst. A stable catalyst will require a lower catalyst withdrawal rate

than would one which loses activity rapidly; correspondingly, a higher level of activity would require a larger withdrawal rate. The activity in any actual bed must be a compromise based on economic considerations, taking into account the following factors:

1. Relationship between yields and catalyst activity.
2. Value of incremental yield.
3. Rate of catalyst degradation.
4. Costs of handling and regenerating the catalyst.
5. Catalyst losses during handling and regenerating.
6. Cost of catalyst.

e. Gas-Solid Reactions. Advantages of the fluidized-solid technique for carrying out gas-solid reactions are the isothermal reaction bed, the easily varied time of contact, the effective contact (as compared with rotary kilns or tray-type reactors), the simple methods of handling solids (no moving parts) and transferring heat, and the ease of continuous, automatic operation.

4. Disadvantages. Parallel or countercurrent flow cannot be secured in the simple fluidized bed; modifications which permit an approach to these types of action complicate the process, increase the investment or reduce the other advantages.

Solids which do not flow freely or which tend to agglomerate cannot be processed in a fluidized-solid reactor; rotary kilns and tray-type reactors are not thus limited.

As the reaction proceeds, fine solid particles may be formed which will become entrained in the gas leaving the fluidized bed; recovery means must usually be included in the design.

The pressure drop in the gas system of a fluidized-solid boiling-bed-type reactor may be larger than in kilns or tray-type reactors, because the gas supports and fluidizes the solid; this pressure drop may sometimes be a serious objection on account of the larger compressors required.

Occasionally it is desirable to obtain a temperature gradient in a catalytic process; for example, a higher temperature may be desired at the upper part of a reactor in order to effect a cleanup of residual reactant. In the single boiling-bed fluidized-solid reactor this is not possible; however, by proper design, to include baffles or other staging or zoning means plus internal heat exchangers, or by the use of series reactors, temperature gradients may be secured.

The pressure drop through a fluidized bed may be large as compared with that through an ordinary heat exchanger. If the fluidized bed is used solely for heat transfer, this high pressure drop would be detrimental.

The observation that gas bubbles rising through the fluidized solid often contain but little of the solid, indicates that the efficiency of contact in a boiling bed may be much less (in terms of the continuous availability of the active surface of the solid) than in a fixed bed reactor; this disadvantage is at least partially overcome, however, by the fact that the fluidized catalyst can be of much smaller particle size (and therefore much greater surface) than that used in fixed bed reactors.

5. Applications. a. "Fluid Cat Cracker" for Petroleum. This process is the one in which the fluidized-solid technique has received its greatest development. There are now many large plants in the United States (of 64 wartime cracking plants (1), 31 used the fluidized-solid technique). Their capacities are mostly high, of the order of 10,000 to 15,000 barrels per day (22, 1). It has been stated that economic considerations do not in general favor small-size fluidized-solid cracking plants as compared with other methods; details of these considerations have not been found. Recently, the Universal Oil Products Company has developed a 1000-bbl./day unit which is claimed to be economically justified.

A fluidized-solid petroleum-cracking plant consists of a reactor in the form of a closed, vertical, cone-bottom tank perhaps with one or more perforated plate baffles; a regenerator of similar form; and a distillation system for product separation. In the reactor, the catalyst, which is a natural or synthetic silica-alumina composition in the form of fine particles, causes the petroleum vapor, a gas-oil fraction, to crack into lighter compounds in the gasoline range. The cracking takes place at about 800°F. and essentially atmospheric pressure. The vapor leaves the reactor through catalyst-recovery cyclones and passes to the distillation system. The catalyst gradually accumulates carbon and loses activity. It is therefore continuously withdrawn, falling into a stream of air, which carries it to the regenerator. Here, at a temperature of about 1000°F., the carbon is burned off, regenerating the catalyst. The hot catalyst is withdrawn, drops into the liquid-oil feed line to the reactor, vaporizes the oil, and is carried by the vapor into the reactor. The catalyst still contains sufficient sensible heat to supply the heat needed by the endothermic cracking reaction.

b. "Hydrocol" Process. The "Hydrocol" process, also known as the "Synthine" process, is the American improvement of the Fischer-Tropsch process for reacting carbon monoxide with hydrogen to

produce hydrocarbons, particularly those in the gasoline range. The complete process extends from facilities for preparation of "synthesis gas" (CO plus H_2 from partial combustion of methane with oxygen) to product separation and purification facilities.

The catalytic reactions between carbon monoxide and hydrogen are very complex and not thoroughly understood. The American process has an iron catalyst that is said to be rugged and inexpensive.

Catalysis is carried out in a fluidized-solid bed, in which the iron catalyst (75 - 80% less than 325 mesh) operates at 300°C. and 20 atm. The reaction is very exothermic (4000 P.c.u./lb. of product) and requires close control of temperature in order to prevent loss of yield. Therefore, the reactor contains many closely spaced tubes in which water is evaporated at 650 lb./sq.in. pressure in order to remove the heat of reaction. The fluidized catalyst is not circulated outside the reactor. Details of the reactor and operation are not given.

At the present time, one pilot plant with a capacity 10 bbl./day has been operating. From this basis a large-scale plant is being constructed at Brownsville, Texas (for Carthage Hydrocol, Inc.). This plant will consume 64,000,0000 cu.ft./day of natural gas, and will produce 5800 bbl./day of motor fuel, 1200 bbl./day of diesel fuel, and 150,000/day of crude alcohols. The plant investment is said to be $15,000,000. The estimated total cost of gasoline from this plant, including capital costs, and after credit for value of other products, is 5.25¢/gal.

(References: 1, 10, 11, 12, 15, 24)

c. Winkler Process. The Winkler water-gas generator (8) is basically a shaft kiln in which friable brown coal, lignite, or lignite coke, naturally available in Germany, is consumed to produce water gas. The operation is semi-continuous; fuel is fed continuously into the reactor, but the gas flow is cyclic. In the first part of the water-gas cycle, the bed is fed with air, burning part of the fuel and heating the bed highly; in the second part, the hot bed is fed with steam, producing water gas, until the temperature drops so far as to require reheating.

The first full-scale Winkler generator was put into operation at Oppau in 1924; it had a diameter of 7.5 ft. The success of the first one inspired the construction of another, this time at Leuna, in 1926, with a diameter of 12.5 ft., and a height of 43 ft. From this scale, the next expansion was to four units 18 ft. in diameter, each of which produced 10,500,000 cu.ft./hr. of water gas.

Efforts to make the Winkler generator fully continuous seem to have been aimed at doing so in a single vessel; these efforts were based on the use of oxygen to replace part of the air, a mixture of oxygen, air, and steam being fed simultaneously. Partial success was achieved, but it is believed that the cost of oxygen prevented general use of this method.

d. Dorr Company's Multi-Stage Lime Burner (13). The Dorr Company, Westport, Connecticut, has been developing applications of the fluidized-solid technique to gas-solid reactions, primarily calcinations of ores. Among these developments, the calcination of limestone in a continuous, multi-stage reactor has been carried through the stage of an 11-ton/day pilot plant, and a 100-ton/day plant is being built. The pilot plant reactor operates in a countercurrent manner, ground lime stone being fed to the top stage for preheating with gas rising from the second stage. The preheated lime stone overflows into the second stage where it is calcined with Bunker C fuel oil. The oil is injected as a liquid into the bed and burned with preheated air rising from the third stage. The calcined lime stone overflows to the third stage where it is cooled with air, the air being simultaneously preheated before passing to the calcination stage above.

IV. FLUID FLOW IN A FIXED BED

It is believed desirable to review the main work leading up to correlations of fluid flow variables in a fixed bed before proceeding to the discussion of the fluidized-solid bed.

1. Blake (3). Blake on the basis of a dimensional analysis arrived at a grouping of variables which has been the starting point for several later investigators. Blake considered that a bed of granular particles was equivalent to a set of parallel pipes. His resulting equation is therefore analogous to that for flow in pipes:

$$\frac{\Delta p\, g_c\, F\, D_p}{L_S\, G^2} = \psi\left(\frac{G\, D_p}{\mu}\right) \qquad (1)$$

In deriving this relationship, Blake assumed that the diameter of the channels through the bed was about the same as the particle diameter.

p. 332 - 14th line should read: 64,000,000 cu.ft. per day.

p. 332 - Equation 1 should insert the Greek letter rho before the subscript F.

Blake checked his equation experimentally by determining the pressure drop through beds of broken pumice and of small glass rings. A fair correlation was secured for the data obtained with pumice, but a curve of a different slope resulted from the glass ring data.

Blake then decided that the specific surface of the solid represented a better measure of the channel character than did particle diameter, and he also recognized the fact that the velocity of the fluid through the interstices of the bed would be greater than the open-tube velocity. He corrected his relationship by dividing G by ϵ and replacing D_p with $\frac{\epsilon}{a}$, and obtained:

$$\frac{\Delta p}{L_S}\frac{g_c \rho_F \epsilon^3}{G^2 a} = \psi\left(\frac{G}{\mu a}\right) \tag{2}$$

This relationship was found to correlate better with the data for glass rings and for hollow packings.

2. Burke and Plummer (5). These investigators regarded the total resistance of a bed to be made up of the sum of the resistances of the individual particles, calculating these resistances from the rate of free fall of the particles. This approach would not be expected to correlate well with experimental facts, for the conditions are far from those of free fall. Their relationship took the form:

$$\frac{\Delta p}{L_S}\frac{g_c \rho_F \epsilon^3}{G^2 (1-\epsilon) a} = \psi\left(\frac{G(1-\epsilon)}{\mu a \epsilon}\right) \tag{3}$$

A fair correlation was secured, but the range of experiment was narrow.

3. Furnas (9). The approach taken by this writer was wholly empirical, and did not consider all of the variables. The resulting relationship

$$\frac{\Delta p}{L_S}\cdot\frac{\rho_F}{G^2} = k\, G^b \tag{4}$$

contains two empirical constants (k and b) and cannot be considered generally useful.

4. Chilton and Colburn (7). These investigators considered the flow through a bed of particles to be similar to flow through parallel conduits of irregular cross section. With this type of flow, the resistance under isothermal conditions will then be made up mainly of the frictional resistance at the particle surfaces and the losses in head caused by expansion and contraction.

They start with the Fanning equation for frictional resistance through conduits. For the frictional resistance, this is then modified by substituting particle diameter for channel diameter, and the product of superficial velocity by "fractional effective free area" for channel velocity. Fractional effective free area is used rather than fraction void because it is said to correct the open-tube velocity more accurately to the interstitial velocity. The fractional effective free area is smaller than the fraction void, being only 9 to 21% for spheres, where fraction void would be 4 to 2 times higher.

For the loss in head caused by the expansions and contractions, the Fanning equation was further modified to include A_1/A_2 factors, where A_1 and A_2 are the "upstream area" (a zone of small free cross-sectional area) and the "downstream area" (a zone of large free cross-sectional area) respectively.

Since A_1, A_2, and fraction-free cross-sectional area are not easily determined, they were not included in correlating the experimental data. The final theoretical forms are:

$$\frac{\Delta p}{L_S}\frac{g_c \rho_F}{G^2}\frac{D_p}{} = 2f' \tag{5}$$

where, for viscous flow,

$$f' = \frac{\mu}{D_p G}\left[\frac{16}{\alpha} + \frac{25}{\alpha}\left(\frac{A_1}{A_2} - \frac{A_2}{A_1}\right)\right] \tag{6}$$

and, for turbulent flow,

$$f' = \frac{.06}{\alpha^{1.8}}\left(\frac{\mu}{D_p G}\right)^{0.2} + \frac{a\left(\frac{A_1}{A_2}\right)^2 + \frac{A_1}{A_2} - 1}{4\alpha^2} \tag{7}$$

For correlation, the form used was

$$\frac{\Delta p}{L_S}\frac{g_c \rho_F}{G^2}\frac{D_p}{} = k\left(\frac{D_p G}{\mu}\right)^n \tag{8}$$

p. 333 - Equation 7 should contain a space between the second $\frac{A_1}{A_2}$ and the minus sign.

Experimental results were determined for pellets, granules, pebbles, and balls, the Reynold's numbers extending well into the turbulent range. In addition, much data of other investigators was replotted. From these combined data, the constant and exponent for the above equation were found to be:

$$\text{For } D_pG/\mu < 40 \quad : \quad k = 1700., \text{ and } n = -1$$

$$\text{For } D_pG/\mu > 80 \quad : \quad k = 76., \text{ and } n = -.15$$

5. Carman (6). Carman reviewed the work of Blake (3), Kozeny (14), and others, demonstrated the general applicability of Blake's method of dimensional analysis, and for the special case of streamline flow, its reduction to the form which Kozeny derived independently. Carman assembled the available data, demonstrating how well most of the data correlate.

Blake's equation is as follows:

$$\frac{\Delta p}{L_s} \frac{g_c \rho_F \epsilon^3}{G^2 a} = \psi \left(\frac{G}{\mu a} \right) \tag{2}$$

Carman's correlation of the data showed that for streamline flow

$$\frac{\Delta p}{L_s} \frac{g_c \rho_F \epsilon^3}{G^2 a} = 5 \left(\frac{G}{\mu a} \right)^{-1} \tag{9}$$

Kozeny (14) arrived at this same equation, starting with the assumption that the granular bed is equivalent to a group of parallel, similar channels, such that the total internal surface and the total internal volume are equal to the particle surface and the pore volume, respectively, in the bed itself. He assumed further that the tortuous passage is longer than the depth of the bed, and the channel velocity correspondingly higher than if a straight vertical channel existed.

For the region of turbulent flow, $\left(\frac{G}{\mu a} > 100 \text{ or } \frac{\phi_s D_p G}{\mu (1 - \epsilon)} > 600 \right)$, Carman found that

$$\frac{\Delta p}{L_s} \frac{g_c \rho_F \epsilon^3}{G^2 a} = 0.4 \left(\frac{G}{\mu a} \right)^{-0.1} \tag{10}$$

For spheres, Carman transforms specific surface to particle diameter by the use of the following geometrical relationship:

$$a = \frac{6 (1 - \epsilon)}{D_p} \tag{11}$$

For non-spherical particles, he introduces the factor ϕ_s in the following manner:

$$a = \frac{6 (1 - \epsilon)}{\phi_s D_p} \tag{12}$$

Inspection will show that ϕ_s may be defined as:

$$\phi_s = \frac{a_p}{a} \tag{13}$$

ϕ_s is therefore unity for a sphere, and since a sphere has minimum specific surface, is less than unity for all other shapes.

Carman's table of the values of ϕ_s for various materials is reproduced below:

Material	Values of ϕ_s Nature of Grain	ϕ_s
Sand - average	--	0.75
Flint sand	jagged	0.65
Flint sand	jagged flakes	0.43
Ottawa sand	nearly spherical	0.95
Sand	angular	0.70 - 0.75
Sand	rounded	0.83
Cork	--	0.69

(Continued on next page)

p. 334 - Equation 13 should read Greek letter $\phi_s = \frac{a_p}{a}$ with the second s now appearing after ϕ_s deleted.

Material	Values of ϕ_s Nature of Grain	ϕ_s
Pulverized coal	--	0.73
Natural coal dust	up to 3/8 in.	0.65
Flue dust	fused aggregates	0.55
Flue dust	fused, spherical	0.89
Mica	flakes	0.28
Fusain fibers	--	0.38

Carman's correlating curve is shown on most of the attached figures. Several useful forms of Carman's equation are listed in the footnote below.*

In the correlations for spherical particles, the only serious deviations found by Carman were for large lead shot at high Reynolds numbers, where the pressure drops were found to be about twice those expected from Carman's curve. This deviation casts some doubt on the validity of the Blake dimensional-analysis correlation for large values of the Reynolds number. It is found, however, that the curve effects correlation for wire spirals and Berl saddles, which are not only non-spherical but also are of different orders of size and porosity.

For rings, on the other hand, the correlating curve starts in coincidence with Carman's general curve, but as Reynolds number increases, does not drop as rapidly, indicating a higher pressure drop for the rings (or hollow particles) than for solid particles at the same Reynolds number. Carman ascribes this effect to the eddy currents and dead spaces within the rings.

6. Leva (16, 17, 18). Leva, in a series of three papers, disclosed a correlation for the flow of fluids through packed beds, included the effect of surface roughness, and investigated the effect of vessel diameter on voidage of a bed.

The first paper deals with the general equation relating pressure drop to fluid and particle properties. The equation is based on an analogy to flow in empty pipes. The final equation develops from a consideration of pore velocity, the modified hydraulic radius of the pores, and a particle shape factor for non-spherical particles, in much the same manner as Blake's (3) equation as extended by Carman (6). The final general equation can be algebraically rearranged to become identical with Carman's equation, even to the point that Leva's shape factor is the reciprocal of Carman's shape factor, ϕ_s.

Leva's main contribution in this paper is to extend Carman's correlation into the range of Reynolds numbers to 40,000

$$\text{using} \quad N_{Re,C} = \frac{\phi_s D_p V \rho_f}{\mu(1-\epsilon)} .$$

*1. For the streamline flow region, where

$$N_{Re,C} = \frac{G \phi_s D_p}{\mu(1-\epsilon)} = \frac{6G}{\mu a} = < 20:$$

$$u_o = \frac{\epsilon^3 \Delta p g_c}{5\mu a^2 L_s} = \frac{\epsilon^3 \phi_s^2 D_p^2 \Delta p g_c}{180 (1-\epsilon)^2 \mu L_s} \tag{14}$$

$$G = \frac{\rho_F \epsilon^3 \Delta p g_c}{5\mu a^2 L_s} = \frac{\rho_F \epsilon^3 \phi_s^2 D_p^2 \Delta p g_c}{180 (1-\epsilon)^2 \mu L_s} \tag{15}$$

2. For the turbulent flow region, where

$$N_{Re,C} = > 100:$$

$$u_o^{1.9} = \frac{\epsilon^3 \Delta p g_c}{0.4\mu^{0.1} a^{1.1} \rho_F^{0.9} L_s} = \frac{\epsilon^3 \phi_s^{1.1} D_p^{1.1} \Delta p g_c}{2.9 (1-\epsilon)^{1.1} \mu^{0.1} \rho^{0.9} L_s} \tag{16}$$

$$G^{1.9} = \frac{\rho_f \epsilon^3 \Delta p g_c}{0.4\mu^{0.1} a^{1.1} L} = \frac{\rho_f \epsilon^3 \phi^{1.1} D_p^{1.1} \Delta p g_c}{2.9 (1-\epsilon)^{1.1} \mu^{0.1} L} \tag{17}$$

p. 335 - Just above the footnote, in the Reynolds number equation the term ρ_f, should read ρ_F.

p. 335 - Equations 16 and 17, in all cases ρ should be ρ_F and L should be L_s.

For one case, brass rings with a calculated $\phi_s = 0.46$, a fair correlation was secured with the line representing particles with shape factors near 1.0.

Leva's line representing his experimental data has been plotted along with Carman's curve on Figure 4, and will be noted to give values of the pressure drop factor 0 - 40% higher than Carman's curve in the range of Reynolds number from 400 to 10,000.

Leva in his second paper attempts to bring out the effect of surface roughness of the particles. The approach was to take nine different materials increasing in roughness from celite spheres and cylinders to aloxite granules, and to plot the friction factor-Reynolds number correlation, including in the friction factor the shape factor

$$\phi_s = \frac{36\pi^{1/3} V_p^{2/3}}{A_p}$$

that relates the surface and volume of the particle. However, the shape factor was calculated from the gross geometry of the individual particles, not from their true surface area and volume. The roughness of the surfaces would tend to increase the surface area, and, since pits and depressions would be overlooked in calculating the particle volumes, to subtract from the particle volumes. As Leva indicates the combined effects would produce a true shape factor which conceivably might be much smaller than that calculated from the gross geometry.

Leva's correlation showed three reasonably distinct zones in the turbulent range with higher friction factors for the "rougher" particles, the roughest ones having a friction factor about twice that of the smoothest with the intermediate zone about 30% higher than the smoothest. The correlation enables a somewhat improved estimate of pressure drop through a bed of particles whose gross geometry permits calculation of a "gross" shape factor. The over-all procedure should be considered empirical, however, since the specific effects attributed to shape and roughness are probably interrelated and are probably not a true representation of the magnitude of each.

In his third paper (18), Leva discusses the relationship of bed diameter to the voidage of the bed. Furnas (9) and Carman (6) had already done this for uniform spheres. Leva extended the work to include cylindrical pellets, Raschig rings, and mixtures of spheres.

The presence of a wall around the bed tends to prevent the particles moving into their positions of closest packing and minimum voidage: The effect is most prominent near the wall and results in an increased voidage of the bed. The voidage will be influenced considerably for particles whose diameter is of the same order as that of the tube containing them. Carman's data indicate that for particles smaller than about 1/15 of the tube diameter the over-all effect on the bed is negligible. Leva's data did not extend sufficiently to permit this limiting point to be determined.

Leva's graphical correlation (18) contains useful general information about voidages of various materials, the effect of surface roughness, and the effect of mixing of particles of various sizes upon the voidage. Leva's mixtures were mostly limited to a particle-size range of less than threefold. Carman (6) had shown that the effect on voidage of mixing of sizes is even more pronounced where the size ratio is 5 or greater.

7. Other Work. Among the other recent investigators in the field of pressure drops in granular beds are Oman and Watson (23), Rose (25), Sullivan and Hertel (26), and Brownell and Katz (4).

V. FLUID FLOW IN A FLUIDIZED-SOLID BED

1. General. The present high cost of buildings and equipment makes it imperative that new reaction equipment be designed to secure maximum conversion and yield. The factors which must be controlled in order to secure such good performance are reasonably well understood for fixed-bed reactors. Even the factor of temperature distribution is amenable to calculation if sufficient data are available.

The situation in the boiling bed reactor is more complex because of the boiling action. Prior to analysis of the action of a boiling bed, a brief review of the factors involved in reactor performance is considered desirable.

Conversion, defined as the fraction of a specified feed material reacted, measures the over-all effect of all the reactions that take place. Yield, defined as the fraction of the specified feed converted into specified products, when compared with conversion, measures the balance between desirable and undesirable reactions. In many reaction systems a complex network of parallel and consecutive reactions is possible, so that optimum performance requires consideration of many factors. One of the most important factors is that of uniformity of treatment, for a by-product once formed because of a

deviation from optimum conditions cannot normally be recovered by a subsequent opposite deviation. The result is that in such complex systems (and they constitute the majority of systems in practice) any deviation from the optimum conditions causes a lowering of reactor performance.

The fluidized-solid bed has been acclaimed as a reaction bed where uniform reaction conditions are secured. Actually, however, the irregular boiling action makes conditions in the boiling bed less uniform in many respects than in the fixed bed. The main advantage still is the one originally claimed: namely, the great reduction in the duration of hot spots because of the mixing.

2. Uniformity of Fluidization. This term is defined to mean the combination of uniformity of particle dispersion and uniformity of gas velocity in a boiling bed. The more uniform are both these factors, the higher the uniformity of fluidization. Water-fluidized beds of sand may be extremely uniform. The bed which slugs or channels badly is at the other extreme of uniformity. The bed in which the fluid pockets remain small and well distributed, with a steady, even, over-all boiling of the bed, is intermediate. The author's observations indicate that most materials fluidized with gases are at the low end of the quality range.

In the previous section the dependence of reactor performance upon uniformity of treatment was developed. In most fluidized beds the treatment is far from uniform, and the performance is correspondingly affected. At least three effects are produced by the non-uniform treatment: 1) the time of contact of the gas in the pockets is less than that of the gas within the clumps; 2) the amount of particle surface available to the gas is much more in the clumps than in the pockets; 3) when several types of reaction are possible, the gas which passes initially through pockets can react differently than the gas which has adequate contact surface initially available.

To put it simply, optimum reactor performance requires maximum uniformity of contact, which for the fluidized bed defines the maximum uniformity of fluidization.

Since a boiling bed is produced by agitation of the particles in a rising fluid stream, it should be possible to describe its action quantitatively by the usual parameters of fluid flow, such as pressure drop, length of flow path, cross section of path, amount of contact surface and its roughness, fluid velocity, density, and viscosity, with the addition of factors to take into account the special characteristics of the small moving particles. Fortunately, a large amount of the basic work has been done already in connection with the flow of fluids through fixed beds.

3. Segregation Tendency. The basic difference between the above-mentioned gas- and liquid-fluidized beds is one of degree of segregation of the particles from the fluid. The other differences observed are believed to arise from the difference in degree of segregation. A highly segregated bed contains comparatively long channels and large clumps of only slightly separated particles. The fluid rushing through the channels tears particles from the lower clumps and deposits the particles at subsequent low-velocity pockets or at the surface of the bed. The upper clumps descend as the lower ones are torn apart, thereby completing the circulation path of the bed.

In the bed of slight segregation, on the other hand, the channels are small, short, and well distributed throughout the bed; the particles in the surrounding clumps are separated from one another to such an extent that the path of flow through the clumps is not much higher in resistance than the path through the channels; therefore, the fluid flow is more uniformly distributed, the range of velocities is much smaller, and the particle circulation is primarily local.

It will be understood that these differences are of degree only--both situations commonly occur simultaneously, but in the case of "aggregative" fluidization, the first situation predominates, and in the case of "particulate" fluidization, the latter situation predominates.

It was stated that both situations could be referred to a common basis, the degree of segregation. The degree of segregation is the result of a dynamic balance between two tendencies: (1) the segregation tendency, or rate of separation of fluid from particles, and (2) the remixing tendency, or rate of gravity-flow of particles into fluid pockets.

The remixing tendency is a function of the so-called "free-flow" quality of the particles, and would be expected to be related to their angle of repose. Further work is required to relate these properties.

The segregation tendency is inherent in any fluidized bed, as will be shown below, and varies with the properties of the fluid and particles, and the shape of the containing vessel. A bed of free-flowing particles, with a high segregation rate, will exhibit predominantly "aggregative" fluidization, but with a low segregation rate, will exhibit mainly "particulate" fluidization. The rate of segregation is a fluid-flow problem and can be approximately related to the physical properties of the components by the application of the Carman-Kozeny correlation to the segregation taking place between two small adjacent zones in a fluidized bed, in the following manner:

It will be assumed that the rate of segregation is small enough to fall in the viscous flow range, thereby permitting the use of equation (14) in the following slightly modified form

$$u_0 = \frac{\epsilon_3^3 \, \Delta p g_c}{5 a^2 \, L_1} \tag{14a}$$

in which ϵ_3 is the fraction of voids in the flow path from zone to zone and L_1 is the length of this flow path. For the present purpose, evaluation of ϵ_3 and L_1 is unnecessary. Δp can be related to the differing concentrations of particles above the two zones and reduced algebraically to the following form:

$$\Delta p = L_f \, (\rho_S - \rho_F)(\epsilon_2 - \epsilon_1) \tag{18}$$

in which L_f is the height of fluidized bed above the two zones under consideration, and ϵ_1 and ϵ_2 are the fractions void in the columns above the two zones.

Substituting this expression in equation (14a), the following form is obtained:

$$u_0 = \frac{L_f \, (\rho_S - \rho_F)(\epsilon_2 - \epsilon_1) \, g_c \, \epsilon_3^3}{a^2 \, 5 L_1} \tag{19}$$

From this equation several useful conclusions can be drawn:

(1) The segregation tendency is inherent in any fluidized bed, and is self-accelerating. This conclusion is drawn from the dependence of u_0 on $\epsilon_2 - \epsilon_1$; as segregation proceeds, ϵ_2 increases, and ϵ_1 decreases, consequently their difference increases also, and thereby the segregation rate, u_0, increases. The limit is reached if ϵ_2 becomes 1.0 and ϵ_1 becomes the voidage of the settled bed; when this situation exists, stable channels pass through a stagnant bed, and segregation has proceeded to completion. This situation normally occurs only with materials which are not free-flowing.

(2) The segregation rate is greatest at the bottom of the bed, since u_0 is proportional to L_f. As a corollary, deeper beds should exhibit greater segregation, and correspondingly poorer quality of fluidization.

(3) Liquid-fluidized beds have much smaller segregation rates than do gas-fluidized beds, because of the roughly 50-fold higher viscosity, and the smaller density difference. This is believed to be the principal reason for "particulate" fluidization in Wilhelm and Kwauk's water-fluidized beds and aggregative" fluidization of the air-fluidized beds.

(4) High-density particles have correspondingly high segregation rates. As a corollary, decreasing the effective particle density by using hollow or vesicular particles, or by using porous flocs, should decrease the segregation rate.

(5) The smaller the particle, the larger is its specific surface, and consequently, the smaller its segregation rate. Unfortunately, decrease of particle size is often accompanied by decrease in the free-flow quality of a powder, which may offset the advantage of lower segregation rate.

4. Generalized Fluid Flow in a Fluidized-Solid Bed. Quantitative information on fluid flow in the fluidized-solid bed is scarce. Extensive published investigations are those by Wilhelm and Kwauk (27), by Leva and associates (19, 20), and by Parent, Yagol, and Steiner (28). (The reader is referred also to the recently published A.C.S. symposium on Fluidization (29)).

a. Leva et al (19, 20). Leva worked with round and with sharp sands in the range of 0.002 to 0.015 in. diameter, (270 to 35 mesh) using 2-1/2-in. and 4-in. columns. His sands were studied as narrow size cuts, and also as mixtures of widely distributed sizes. His gases were air, carbon dioxide, and helium. Various bed depths were used.

Leva's correlation was based on Carman's equation for laminar flow, modified by assuming a constant pressure drop for the fluidized bed, and rearranged in the following steps:

$$G = \frac{\rho_F \epsilon^3 \, \phi_S^2 \, D_p^2 \, \Delta p \, g_c}{180 \, (1 - \epsilon)^2 \, \mu \, L_s} \tag{15}$$

For the fluidized bed, L_s was replaced by L_f:

$$G \cdot \frac{\mu L_f}{\rho_F} = \frac{\epsilon^3}{(1 - \epsilon)^2} \cdot \frac{\Delta p \, g_c \, \phi_S^2 \, D_p^2}{180} \tag{20}$$

$$G \cdot \frac{\mu}{\rho_F} \cdot L_S N_V = \frac{\epsilon^3}{(1-\epsilon)^2} \cdot \frac{\Delta p\, g_c\, \phi_s^2\, D_p^2}{180} \tag{21}$$

$$G \cdot \frac{\mu}{\rho_F} \cdot \frac{1-\epsilon_s}{1-\epsilon} = \frac{\epsilon^3}{(1-\epsilon)^2} \cdot \frac{\Delta p\, g_c\, \phi_s^2\, D_p^2}{180 L_s} \tag{22}$$

$$G \cdot \frac{\mu}{\rho_F}\, N_V = k \left(\frac{\epsilon^3}{(1-\epsilon)^2} \right)^m \tag{23}$$

Since all the other terms on the right hand side are assumed to be constant, m = 1.0 if the fluidized bed follows Carman's equation. Leva correlated his data on the basis of Equation 23 and conclusions must, therefore, originate with it. Leva found that m was as large as 4.5 for the smallest particles (0.002 in.) decreasing gradually as particle size increased, and did not reach 1.0 until the particle size reached 0.016 in., the largest size studied.

Inspection of Equation 23 indicates that (if the items grouped in the constant k are really constant) the values for m above 1.0 require correspondingly higher values for velocity than would be required by Carman's equation. From this fact and his data, Leva concludes that the smaller particles require an extra amount of energy for fluidization. He terms the ratio of this "extra energy" to the total energy supplied the "fluidization efficiency" and correlates it with particle size. "Fluidization efficiency" is then zero when no "extra energy" is required over that calculated from Carman's equation and increases as the exponent m increases.

Leva's term "fluidization efficiency" may be misleading since the most efficient operation would be that in which no energy is required in excess of that indicated by Carman's equation. A better term might be "deviation factor" signifying the deviation from Carman's equation and defined as the difference between the actual velocity and that called for by Equation 15, divided by the actual velocity.

b. Wilhelm and Kwauk (27). In a comprehensive investigation, Wilhelm and Kwauk studied the fluidization characteristics of sand, glass beads, lead shot, crushed stone, and Socony catalyst beads, over a particle size range of 0.011 to 0.21 in. Columns of 3-in. and 6-in. diameter were used. (Column size and depth of bed were found to be unimportant.) In addition to air, water was also used as a fluidizing medium.

In correlating their data, Wilhelm and Kwauk chose to use four dimensionless groups, as shown by the following equations:

$$N_{Re,W} = \frac{D_p G}{\mu} = N_{Re,C}\, (1-\epsilon)/\phi_s \tag{24}$$

$$\epsilon = \frac{L_f - L_a}{L_f} \tag{25}$$

$$K_{\Delta p} = \frac{\Delta p\, D_p\, g_c\, \rho_F}{L_a\, 2G^2} \times \left(\frac{D_p G}{\mu} \right)^2 = \frac{\Delta p\, D_p^3\, \rho_F g_c}{L_a\, 2\mu^2} \tag{26}$$

$$K_{\Delta \rho} = \frac{(\rho_s - \rho_F)\, D_p\, g\, \rho_F}{2G^2} \left(\frac{D_p G}{\mu} \right)^2 = \frac{(\rho_s - \rho_F) D_p^3 \rho_f\, g}{2\mu^2} \tag{27}$$

The term $K_{\Delta p}$ is essentially the product of a friction factor and the square of a Reynolds number. By choosing this combination of functions, the velocity or flow rate term is eliminated. It will be noted that the friction factor and Reynolds number as defined by Wilhelm and Kwauk are identical with the corresponding terms used by Carman with the exception that Wilhelm and Kwauk left out all voidage terms and shape factors. The term $K_{\Delta \rho}$ is the same as $K_{\Delta p}$ with the weight of the bed per unit of bed area substituted for the pressure drop. The effect of voids is later included as parametric curves in plots of $K_{\Delta p}$ and $K_{\Delta \rho}$ against the Reynolds number.

Wilhelm and Kwauk noted that $\frac{(\rho_s - \rho_F)\, D_p\, g\, \rho_F}{2G^2}$ is related to the drag coefficient, the only difference being the numerical factor which in the drag coefficient is 4/3 instead of 1/2. In their experiments on fluidization with water, available drag coefficient relationships were used to calculate the points for 100% voids on the curve of $K_{\Delta p}$ vs. Reynolds number.

As was earlier mentioned, Wilhelm and Kwauk noted an important difference between fluidization with water and fluidization with air. In the former case, the bed is made up of agitated, well-dispersed

p. 339 - Equation 27, the third section, ρ_f should be ρ_F.

p. 339 - Third line from bottom $K_{\Delta p}$ should read $K_{\Delta \rho}$.

particles, the water rising between the individual particles. In the latter case, however, the particles are not well dispersed, but tend to agglomerate into clumps or aggregates, which tend to move to one side and allow the gas to pass as a "bubble" (better termed a pocket) relatively free of particles, or else are carried upward as slugs by the gas. The first case Wilhelm and Kwauk called "particulate" fluidization and the second, "aggregative."

c. New Analysis of Data. Carman's equation was based on a theoretical mechanism for flow at low Reynolds number in fixed granular beds. The resistance considered major under this condition was that of fluid friction. The voidage function accordingly has this basis. Carman's equation is presented again below, with specific surface replaced by the particle size equivalent:

$$\frac{\Delta p\ g_c\ \rho_F \phi_s\ D_p\ \epsilon^3}{L\ G^2\ (1-\epsilon)} = k' \left(\frac{G\ \phi_s\ D_p}{(1-\epsilon)\mu} \right)^n \tag{28}$$

This equation was found by Carman, and by Leva (16), to apply also to fixed beds at higher Reynolds numbers, the value of the exponent and the constant being different for these Reynolds numbers. For the higher Reynolds numbers, kinetic energy losses in the sinuously flowing streams constitute the major resistance, and fluid friction a minor factor. In spite of this change in mechanism, the voidage function apparently fits available fixed-bed data reasonably well. Therefore, it appeared worthwhile to compare the data for fluidized beds with Carman's curve for fixed beds. This has been done in Figure 2 - 8 inclusive. The dotted line is Carman's correlating curve. The ordinate is twice the friction factor; for convenience, it is set up both in Carman's form, using specific surface, and in the form of Equation 28, which is equivalent. The abscissa is the Reynolds number, defined to include specific surface or its equivalent in terms of particle diameter.

Leva's data have been recalculated into Carman's coordinates, and the results plotted in several forms for comparison with the Carman-Kozeny curve. In Figure 2 all of the recalculated Leva data fall in the upper left portion of the plot (Reynolds numbers below 10). The points fall almost entirely below the Carman-Kozeny curve. The left hand portion of the heavy line on Figure 2 represents the best general correlation of the data. (The balance of this line represents Wilhelm and Kwauk data, discussed below.) However, the data for all but the coarsest of the materials studied by Leva do not plot parallel to this heavy line, as reference to Figures 3, 4, 5, and 6 will show. In all cases except the largest particles, the data fall on straight lines with a considerably larger negative slope than the Carman-Kozeny line (slope = -1. at low Reynolds numbers). In Figure 3 the data for uniformly-sized round sands are presented and, in Figure 4, for uniformly-sized sharp sands. In Figure 5 round sands are compared with sharp sands of similar sizes. In Figure 6 mixtures of sizes are compared with uniformly-sized particles of similar equivalent diameter.

It will be noted that (1) the sharp-sand data are in close agreement with the round-sand data, and (2) the uniform-size data agree with the mixed-size data. The minor differences may well be due to wrongly assumed values for the shape factors, ϕ_s, (0.70 for sharp sands, 0.82 for uniform and for mixed sizes of round sands).

Nearly all of the data obtained by Leva indicate lower friction factors than for the corresponding fixed bed of the same voidage. In other words, the pressure drop through the fluidized bed is smaller than through the corresponding fixed bed at the same gas velocity; put another way, at equal pressure drops more gas would flow through the fluidized bed.

Leva's explanation of this phenomenon was that fluidization of the bed requires extra energy above that required in the fixed bed; however, this appears to be in direct opposition to the observed lower friction factor for Leva's fluidized bed of very small particles.

A better explanation is believed to be that flocculation of the very small particles, because of the surface forces present, causes these particles to act not as individuals but as transient porous agglomerates or flocs. The specific surface of these agglomerates effective in causing pressure drop of the flowing fluid would depend upon the separation of the agglomerates from one another. When the agglomerates are close together as in a fixed or only slightly expanded bed, the size and resistance of the paths for fluid flow through the flocs would be of the same order as the size and resistance of the paths around them. On the other hand, when the bed is highly expanded, the majority of the fluid would flow via the large open channels around the flocs rather than via their pores, thereby largely by passing the internal surface of the agglomerates. The effectively smaller specific surface would result in larger real Reynolds numbers and smaller real friction factors than those calculated from the total surface; the correction for a given bed would be larger at higher velocities because of the greater bed expansion. The correction would move the friction factor - Reynolds number curve toward the Carman-Kozeny curve, decreasing its slope simultaneously. The fact that Leva's data for the larger

particles are in better agreement with Carman's curve is confirmatory evidence, for it is known that flocculation for a given material varies inversely with particle size.

Inspection of the plots of Leva's data (Figures 3, 4, 5, and 6) indicates that an effective specific surface 1/2 to 1/3 times the total bed surface will serve to bring into line with Carman's equation those points which deviate most widely.

Direct visual evidence of flocculation has been observed in the fluidization of extremely fine, widely sized, precipitated silicas such as Santocel. Large agglomerates (1/64 - 1/8 in. in diameter) are easily visible through the column walls.

Inasmuch as the surface forces which are presumed to cause the flocculation tendency probably vary from material to material, the data which Leva has secured must be considered specific to the materials studied. It may be that other equally fine materials on which the surface forces are much less will show close agreement with the Carman-Kozeny relationship.

The data of Wilhelm and Kwauk (27) have also been recalculated and the results compared with the Carman-Kozeny correlation. The comparisons are presented in several groups.

In the first group are all of the Wilhelm-Kwauk data for the beds before fluidization, that is, fixed beds. These data, both for air flow and water flow, are plotted in Figure 1. Generally good agreement with the Carman-Kozeny line is evident. It will be noted, however, that all of the data for air-flow fall slightly above the curve, while the majority of the data for water flow fall slightly below the curve. There is no obvious reason for this slight discrepancy.

In the second group (Figure 7), are the Wilhelm-Kwauk data for fluidization with water. It will be noted that the slopes are the same as the Carman-Kozeny curve, but that the best line for the Wilhelm-Kwauk data would fall slightly lower, the disagreement being slightly larger than in the previously mentioned fixed-bed correlation, Figure 1.

In the third group are the Wilhelm-Kwauk data for fluidization with air. These data are the basis for the "Fluidized Beds" line on Figure 2, which also includes Leva's data.

In Figure 8 the Wilhelm-Kwauk data for air fluidization at high Reynolds numbers have been plotted; this time, however, the curves for each of the materials have been drawn in for comparison with the Carman-Kozeny curve. It is evident that some additional factor is now involved, for there is a complete lack of correlation. The curves show near the left hand end an increase of friction factor with Reynolds number, followed by a flattening out and then a decrease of friction factor with further Reynolds number increase.

In the gas-fluidized beds that Wilhelm and Kwauk studied, the large Reynolds numbers were secured only with relatively large or heavy particles. Both the Wilhelm and Kwauk observations and those of the author indicate a difference between the fluidization of beds of such large or heavy particles, and the fluidization of small or low-density particles. The difference in appearance is much the same as the difference between what Wilhelm and Kwauk call "aggregative" fluidization with gases and what they call "particulate" fluidization with liquids. Parent, Yagol, and Steiner (28) confirm this observation about the difference of fluidization between large and small particles.

The explanation here proposed for the deviations at high Reynolds numbers from the Carman-Kozeny relationship is based on the previously outlined mechanism of fluidization and the consequent inherent segregation tendency of the fluidized bed. Beds of large or heavy particles fluidized with gas are inherently extremely unstable, with a strong tendency to segregate. This segregation tendency results in the formation of a non-uniform bed which contains strong rising currents of expanded solid and strong descending currents of concentrated solid. Some of these currents are localized, others extend over the entire bed. The particles being elevated in these currents absorb from the gas stream the required kinetic energy, which is eventually lost by collisions among particles and against the walls.

The order of magnitude of the loss in kinetic energy of the particles and its effect on the bed circulation may be estimated as follows:

Assume a fluidized bed, 1-ft. high and 1 sq.ft. in cross section, of particles which show a fluidization curve like those on Figure 8, with an ordinate, 2f', of 7. at a Reynolds number of 200, and a linear superficial gas velocity of 1 ft./sec. The ordinate for the Carman-Kozeny line is about 2.6. Such a bed, if of sand, might have an expanded bed density of about 80 lb./cu.ft., equivalent to a pressure drop of 80 lb./sq.ft. for the 1-ft. height. The pressure drop ($\Delta p_{K.E.}$) equivalent to the kinetic energy of the particles would be

$$\Delta p_{K.E.} = 80 \times \frac{7. - 2.6}{7} = 50 \text{ lb./sq.ft.}$$

The power consumption would be

$$\Delta p_{K.E.} \; Au_o = 50 \times 1 \times 1 = 50 \text{ ft.-lb./sec.}$$

If this energy be presumed to elevate the particles from the bottom to the top of the bed (which from visual observations is not unreasonable), a distance of 1 ft., turnover rate will be 50 lb./sec., equivalent to 50/80 = 0.63 times/sec. This rate is qualitatively similar to actual bed turnover rates.

The few items of Wilhelm and Kwauk data for fluidization at low Reynolds numbers do not show these large friction factor deviations. Part of this lack of deviation may be due to some flocculation tendency, but their data are mainly at Reynolds numbers at or above those at which Leva's data indicate no more flocculation. A more logical reason is that in this Reynolds number region (the higher end of the "streamline flow" region) the large magnitude of the "viscous" forces as compared with the "inertia" forces obscures the losses of particle kinetic energy in the fluidized bed.

In the high Reynolds number region, the "viscous" forces are much lower, the "inertia" forces much larger, and the portion of energy used in accelerating the particles, therefore, is much more significant.

5. Summary. A mechanism of fluidization is hypothesized, based on the simple packed bed to which has been added a further variable, freedom of movement of the particles because their weight is supported in an expanded bed by a fluid stream. The following phenomena derive from the existence of this variable:

(1) The particles can change their degree of flocculation in response to surface or other attractive forces.
(2) The particles can be moved around by the drag of the fluid streams and by their own weight. It was demonstrated qualitatively that this ability results in an inherently unstable expanded bed, the fluid tending to segregate from the particles by flowing in channels or pockets, thereby promoting non-uniformity and turbulence. This tendency would be expected to increase with difference in density between particle and fluid, and to decrease with increase in the specific surface of the solid and with increase in the fluid viscosity.

The quantitative data of Leva et al. for the fluidization of fine sand particles in gases, with modified Reynolds numbers below 10, show negative deviations from the Carman-Kozeny fixed-bed correlation. These deviations are explainable by the flocculation or clustering which has been observed to occur with fine particles.

The quantitative data of Wilhelm and Kwauk extending from modified Reynolds numbers of 10 (streamline flow) to 10,000 (turbulent flow) show increasingly large positive deviations for the rough, non-uniform, "aggregative" fluidization secured with gases. These deviations are interpreted as evidence of the large amounts of energy transferred from the fluid stream into kinetic energy of the turbulently moving particles and then dissipated by collisions.

The absence of these positive deviations for the smooth, "particulate" fluidization secured with water at similar high Reynolds numbers correlates well with the observation that in such beds there is only local circulation of the particles, and consequently only small kinetic energy losses by particle collisions.

Positive deviations from the Carman-Kozeny correlation are, therefore, evidence of non-uniform dispersion of fluid and particles, that is, of poor quality of fluidization, and steps taken to reduce the magnitude of these deviations would be expected to improve the quality of fluidization. Through its effect on conversion and yield, high quality of fluidization is important in obtaining the best performance of fluidized-solid reactors.

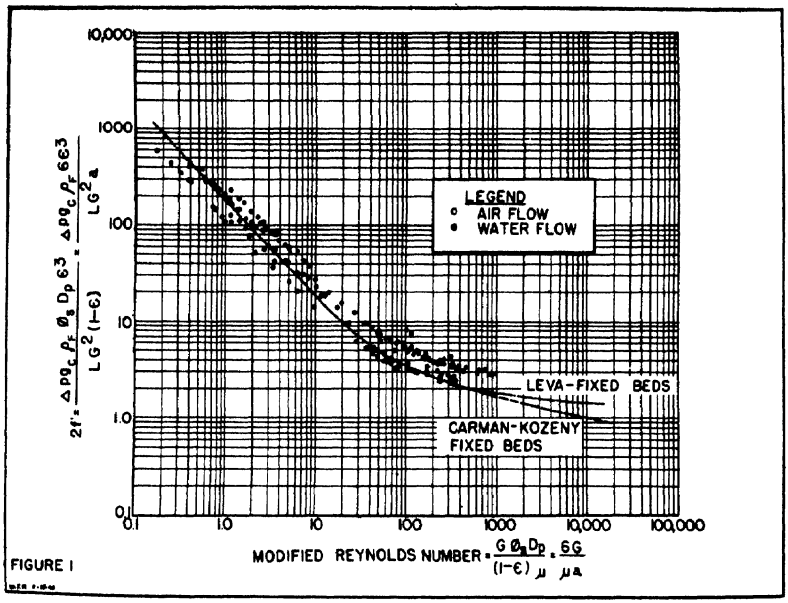


Figure 1. Fixed Beds - Wilhelm and Kwauk Data.

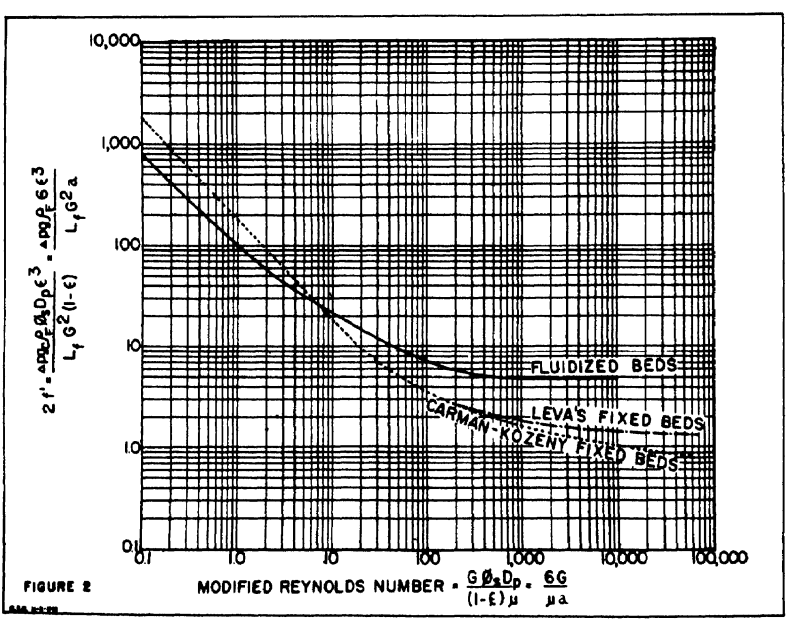


Figure 2. Fluidized Beds.

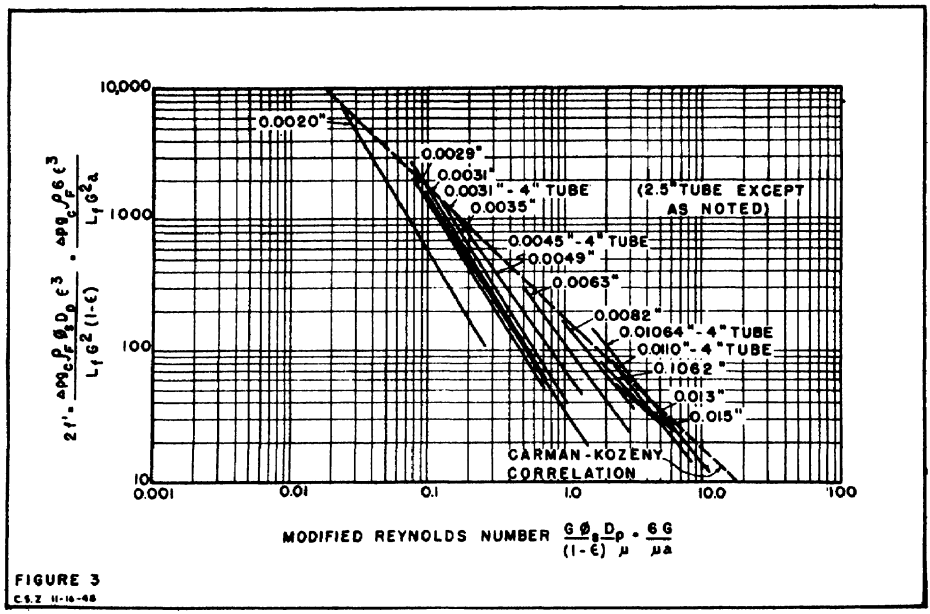


Figure 3. Leva's Uniform Round Sands

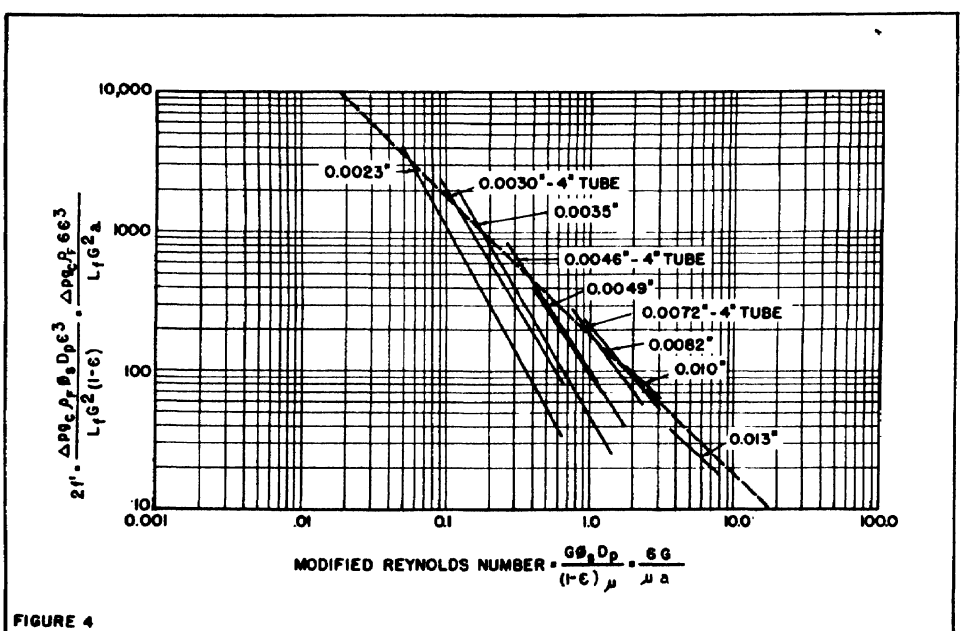


Figure 4. Leva's Uniform Sharp Sands

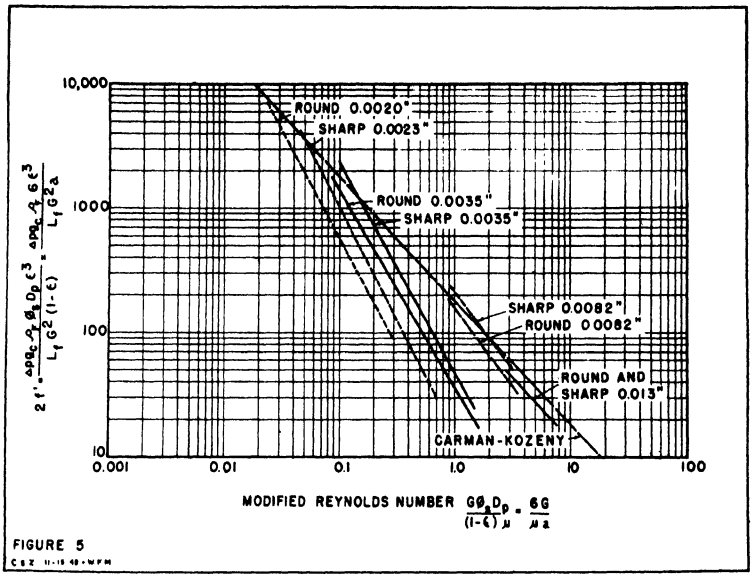


Figure 5. Comparison of Round and Sharp Sands.

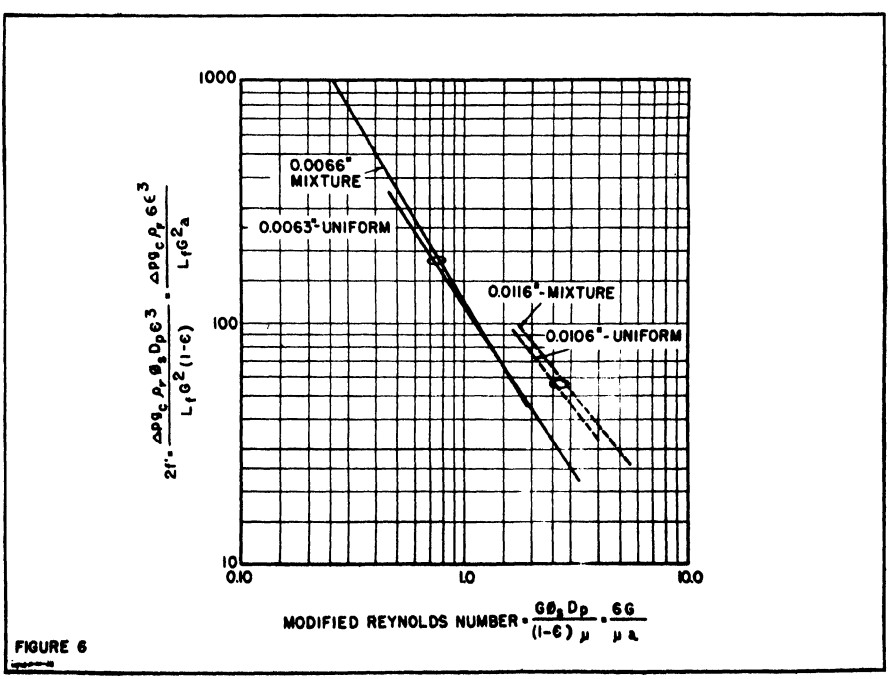


Figure 6. Comparison of Size Mixtures with Uniform Sizes.

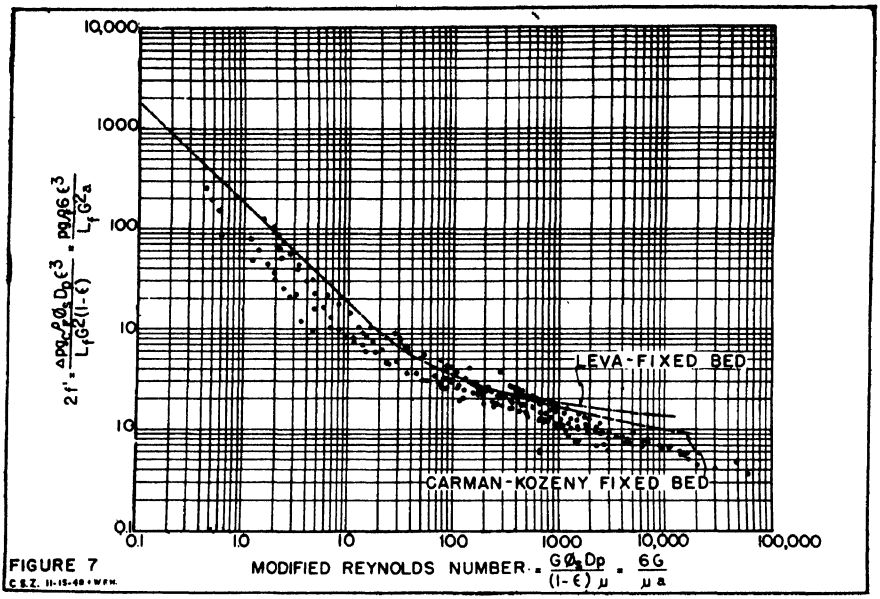


Figure 7. Fluidization with Water - Wilhelm and Kwauk.

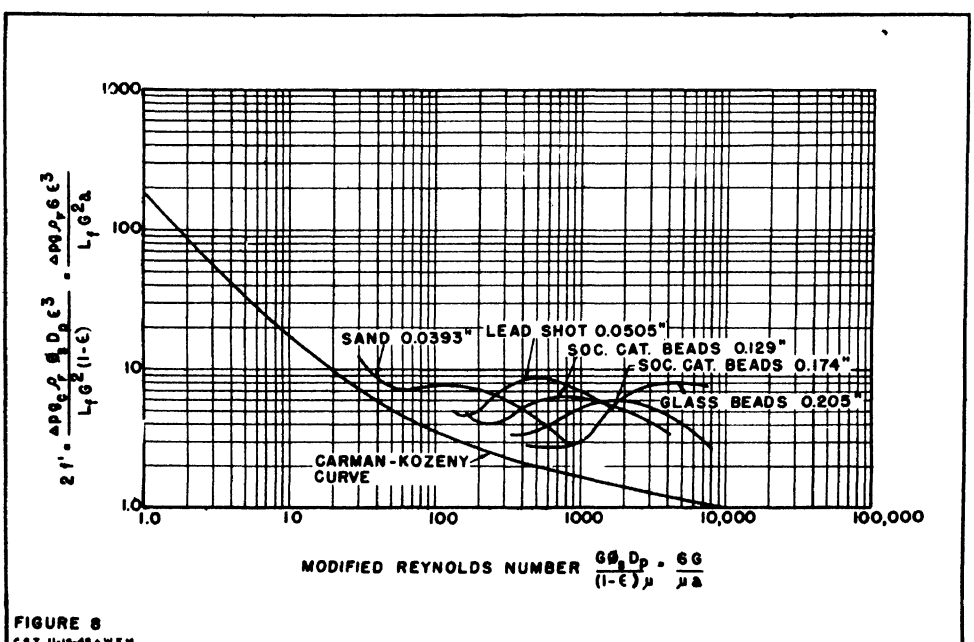


Figure 8. Fluidization with Air - Wilhelm and Kwauk.

Illustrative Problem

A bed of uniform spherical particles of 75 micron average diameter is to be fluidized with air at approximately atmospheric pressure and 250°C. Physical properties of the material and other data are given in the table below.

Data

Air:	Viscosity	- 0.027 centipoises
	Density	- 0.042 lb./cu.ft.
Particles:	Size	- 75 micron
	Bulk Density	- 100 lb./cu.ft.
	Particle Density	- 162 lb./cu.ft.
	Shape Factor	- 1.0

Estimate the gas velocity required (a) to initiate fluidization and (b) the velocity at which the bed will be fluidized with 50% expansion, assuming that Carman's correlation holds.

Solution: (a) Because of the small size of the particles, it will be tentatively assumed that operation will be in the viscous flow region, $N_{Re} < 20$, and equation (14) will be applied.

Voidage: Volume of solid per cu.ft. of bed = $\frac{100}{162}$

$= 1 - \epsilon_s = 0.617$ cu.ft./cu.ft.

Volume of voids = 1.0 - 0.617 = 0.383

p. 347 - The equation $\mathcal{E} = 0.383$ $\epsilon = 0.383$ should be $\mathcal{E}_s = 0.383$.

Bed will become fluidized when pressure gradient is equal to weight of bed per sq.ft., per foot of height.

Pressure gradient: Δp = (bulk density) x L_s In the second line under Pressure Gradient

p. 347 - or $\Delta p/L$ = bulk density = 100 lb./(sq.ft.)(ft.) Δ_p/L should be Δ_p/L_s.

Velocity: $$u_o = \frac{\epsilon^3 \phi_s^2 D_p^2 \Delta p \, g_c}{180 (1-\epsilon)^2 \mu L}$$ p. 347 - Under Velocity, (14)

$$= \frac{(0.383)^3 \times 1^2 \times [3.28 \times 75 \times 10^{-6}]^2 \times 100 \times 32.2}{180 \times (0.617)^2 \times 0.027 \times 0.672 \times 10^{-3}}$$

$= 0.0883$ ft./sec. the answer now reading 0.0883 should be 0.00883.

Flow Condition: $$N_{Re} = \frac{D_p u_o \rho_F}{\mu(1-\epsilon)}$$ p. 347 - Under Flow Conditions, the answer now reading

$$= \frac{75 \times 10^{-6} \times 3.28 \times 0.0883 \times 0.042}{0.027 \times 0.672 \times 10^{-3} \times 0.617}$$ 0.0814 should be 0.00814.

= 0.0814 - This Reynolds number is evidently in the range for viscous flow, and the original assumption is valid.

(b) Velocity for 50% expansion if Carman's correlation holds

Voidage: Volume of settled bed: $\frac{1}{100}$ cu.ft./lb.

Volume of fluidized bed: 150% x $\frac{1}{100} = \frac{1.5}{100}$ cu.ft./lb.

Volume of particles in either bed: $\frac{1}{162}$ cu.ft./lb. = 0.00617 cu.ft./lb.

Volume of pores in expanded bed: 0.015 - 0.00617 = 0.00883

Voidage, $\epsilon = \frac{0.00883}{0.015} = 0.588$

$1 - \epsilon = 0.412$

Pressure Gradient: $\Delta p = 100 \text{ lb./cu.ft.} \times \frac{1 \text{ ft.}}{1.5 \text{ ft.}} \times L_f$

$\Delta p / L_f = 66.7 \text{ lb./(sq.ft.)(ft.)}$

Velocity from equation (14): p. 348 - Under Velocity From Equation 14,

$$u_0 = \frac{(0.588)^3 \times 1^3 \times [3.28 \times 75 \times 10^{-6}]^2 \times 66.7 \times 32.2}{180 \times (0.412)^3 \times 0.027 \times 0.672 \times 10^{-3}}$$

$= 0.47$ ft./sec. the answer now reading 0.47 should be 0.048.

Flow condition: p. 348 - In the computation under Flow Condition,

$$N_{Re} = \frac{D_p \, u_0 \, \rho_F}{\mu(1 - \epsilon)}$$

the term 0.41 should be 0.048

$$= \frac{75 \times 10^{-6} \times 3.28 \times 0.41 \times 0.042}{0.027 \times 0.672 \times 10^{-3} \times 0.412}$$

and the term 10^3 should be 10^{-3},

$= 0.0658$ - This Reynolds number is also in the viscous flow range, and the original assumption is still valid.

Problem

Given the same data as used in the illustrative problem, what velocity will be required to secure 15% bed expansion if the material (a) follows the Carman correlation, or (b) behaves similarly to those evaluated by Leva?

INDEX

Adiabatic flow 54
Air change 249
Air filters 242, 319
Anemometer:
    hot-wire 156
    vane 155
Annular orifice 148
Apparent viscosity 125
Aspect ratio 230
Bag filters 310
Bernoulli's theorem 36, 53, 74
Bingham plastic 120, 123
Boiling bed 329
Boiling liquid 104
Boundary layer equations:
    laminar 27
    turbulent 28
Brownian movement 285
Catalysis 330
  Cat cracker 331
Cavitation 206
Centrifugal pumps 191, 210, 212
Centrifugal separators 309
Choking velocity 109
Coke box 309
Coefficient:
    drag 282
    jet 65
    orifice 12, 60, 148
Collection efficiency 301, 305, 306, 316, 317
Compressibility 53
Condensing vapor 15, 104
Continuity, equation of 5
Contraction, abrupt 13, 43
Convergent-divergent nozzle 57
Convergent nozzle 55
Conversion 336
Corrosion 215
Cottrell precipitator 317
Critical flow 54, 144
Cunningham correction 285
Cut size 306
Cyclone 305
Decantation 273
Diameter, geometric mean 271
Differential head:
    nozzle 45
    orifice meter 45
    pitot tube 45
    venturi meter 45
Diffusers 249
Dilatancy 121
Dispersing agents 132, 290
Dispersion 289

Draft tube 11, 64, 76
Drag 281
coefficient 282
Ducts 225, 234
Dust collection 301
Efficiency:
collection 301, 305, 316, 317
fluidization 339
isothermal 108
target 304
volumetric 206
Ejector 11, 63, 72
draft tube 76
effect of solids 78
venturi type 76
Elbows:
losses in 229
Elutriation 273
Energy balance:
mechanical 6, 7, 14
overall 5
Expansion, abrupt 9, 43
False body suspension 122
Fans 242
Filters:
air 242, 319
bag 310
Flanges 169
Flashing liquid 103
Flocculation 289, 340
Flow nozzle 143
Fluidization:
aggregative 329, 337
efficiency 339
particulate 320, 337
Fluidized solid 328
Friction factor 26, 27
Friction loss 7, 36, 46
abrupt contraction 43
abrupt expansion 43
granular beds 43
pipes 37
tube banks 36
Gas lift 106, 109
Geometric mean diameter 271
Granular beds 43
Grilles 246
Hindered settling 289
Hoods 259
Hot wire anemometer 143
Hydrocol process 331
Ideal fluid 281
Impingement Separators 304
Injector 77
Intermediate law 284
Isothermal efficiency 108
Isothermal flow 54
Jet:
coefficients 65
deflected by fixed surface 9

deflected by moving surface . . . 9
deflected by series of moving vanes . . . 10
impact . . . 9
Laminar layer . . . 24
Lift:
gas . . . 106, 109
isothermal efficiency . . . 108
suction . . . 199
water-air . . . 107
Liquid-gas flow:
horizontal pipes . . . 100
vertical pipes . . . 106
Mach number . . . 55
Mechanical energy balance . . . 6, 7, 14
Mesh, screen . . . 268
Mixing length . . . 21
Momentum balance . . . 8
Net positive suction head, NPSH . . . 199
Newtonian liquids . . . 119
Newton's law . . . 8, 284
Non-Newtonian suspensions . . . 120
Nozzle . . . 45, 74
convergent . . . 55
convergent-divergent . . . 52
flow . . . 143
Orifice:
annular . . . 148
coefficients . . . 12, 50, 148
compressible flow . . . 59
differential head . . . 45
metering assembly . . . 13, 45, 145
segmental . . . 148
Overall energy balance . . . 5
Particles:
distribution . . . 270, 271
fluid . . . 288
log-probability plot . . . 271
motion . . . 286
shape . . . 269
size . . . 268
size analysis . . . 272
surface . . . 270
Piping:
design . . . 169
dimensions . . . 167
economic size . . . 170
industrial . . . 163
manufacture . . . 166
specifications . . . 171
supports . . . 171
tolerances . . . 168
Pitot tube . . . 45, 149
Pneumatic conveying . . . 109
Precipitators:
electrical . . . 314
Cottrell . . . 317
sonic . . . 319
Pressure drop:
calculation for flow system . . . 7, 36, 46
in pneumatic conveying . . . 110

through fittings and valves, table . . . 40
(see also under individual equipment)
Pseudoplasticity . . . 120
Pulsating flow . . . 152
Pumps:
centrifugal . . . 191, 210, 212
controlled volume . . . 216
deep well . . . 198
mixed flow . . . 202
reciprocating . . . 206
rotary . . . 203
turbine . . . 200
Reciprocating pumps . . . 206
Rheology . . . 119
Rheopexy . . . 122
Ringelmann chart . . . 271
Rotameter . . . 150
Sampling:
dispersoids . . . 271
process gas . . . 272
Schedule number . . . 167
Screen mesh:
Tyler scale . . . 268
U. S. Standard scale . . . 268
Scrubbers . . . 312
Sedimentation . . . 274
Segmental orifice . . . 148
Segregation . . . 337
Separators:
centrifugal . . . 309
impingement . . . 304
Settling:
chamber . . . 303
hindered . . . 289
velocity . . . 282
Shape factor . . . 334
Shock, compression . . . 57
Sieving . . . 273
Slip . . . 205
Slip velocity . . . 109
Slugging . . . 329
Specific speed . . . 202
Standard deviation . . . 271
Stokes's law . . . 284
Submergence . . . 106
Suction lift . . . 199
Supersonic velocity . . . 59
Suspension:
false body . . .
non-Newtonian . . . 120
Target efficiency . . . 304
Terminal velocity . . . 282
Thermo-compressor . . . 77
Thixotropic breakdown . . . 125
Thixotropy . . . 121
Tube banks . . . 30
Tubing . . . 167
Turbulence theory:
Boundary layer equations . . . 27
Prandtl . . . 20

Reynolds 19
Stanton 21
von Karman 21
Tyler screen mesh 268
Valves 169, 171
Vane anemometer 153
Velocity:
choking 109
deficiency 23
slip 109
supersonic 59
terminal 282
Velocity distribution:
in laminar layer 25
in rough pipes 26
in smooth pipes 23
Velocity head concept 32
Venturi:
ejector 76
meter 45, 151
Viscometers 126
Viscosity:
apparent 125
Volumetric efficiency 206
Wall effect 284
Weirs:
Cipolletti 158
rectangular 157
triangular-notch 132
Winkler process 332
Yield 336